National Academy of Sciences of Ukraine (NASU)
Frantsevich Institute for Problems of Materials Science of NASU
Ukrainian Materials Science Association "Composites"
INTEM LTD (Ukraine)

Under auspices of

# INTERNATIONAL CONFERENCE

## "Science for Materials in the Frontier of Centuries: Advantages and Challenges"

20030106 032

# PROCEEDINGS OF CONFERENCE

**Editor: Academician, Professor Valery V. Skorokhod**

4-8 November 2002
Kyiv, Ukraine

# REPORT DOCUMENTATION PAGE

Form Approved OMB No. 0704-0188

Public reporting burden for this collection of information is estimated to average 1 hour per response, including the time for reviewing instructions, searching existing data sources, gathering and maintaining the data needed, and completing and reviewing the collection of information. Send comments regarding this burden estimate or any other aspect of this collection of information, including suggestions for reducing the burden, to Department of Defense, Washington Headquarters Services, Directorate for Information Operations and Reports (0704-0188), 1215 Jefferson Davis Highway, Suite 1204, Arlington, VA 22202-4302. Respondents should be aware that notwithstanding any other provision of law, no person shall be subject to any penalty for failing to comply with a collection of information if it does not display a currently valid OMB control number.
**PLEASE DO NOT RETURN YOUR FORM TO THE ABOVE ADDRESS.**

| 1. REPORT DATE *(DD-MM-YYYY)* | 2. REPORT TYPE | 3. DATES COVERED *(From – To)* |
|---|---|---|
| 19-11-2002 | Conference Proceedings | 4 November 2002 - 8 November 2002 |

**4. TITLE AND SUBTITLE**

Science for Materials in the Frontier of Centuries: Advantages and Challenges

Vol. I

**5a. CONTRACT NUMBER**
F61775-02-WF042

**5b. GRANT NUMBER**

**5c. PROGRAM ELEMENT NUMBER**

**6. AUTHOR(S)**

Conference Committee

**5d. PROJECT NUMBER**

**5d. TASK NUMBER**

**5e. WORK UNIT NUMBER**

**7. PERFORMING ORGANIZATION NAME(S) AND ADDRESS(ES)**

Institute for Problems of Materials Science
3 Krzhyzhanovsky Str.
Kyiv 03142
Ukraine

**8. PERFORMING ORGANIZATION REPORT NUMBER**

N/A

**9. SPONSORING/MONITORING AGENCY NAME(S) AND ADDRESS(ES)**

EOARD
PSC 802 BOX 14
FPO 09499-0014

**10. SPONSOR/MONITOR'S ACRONYM(S)**

**11. SPONSOR/MONITOR'S REPORT NUMBER(S)**
CSP 02-5042

**12. DISTRIBUTION/AVAILABILITY STATEMENT**

Approved for public release; distribution is unlimited.

**13. SUPPLEMENTARY NOTES**

**14. ABSTRACT**

The Final Proceedings for Science for Materials in the Frontier of Centuries: Advantages and Challenges, 4 Nov 02 - 8 Nov 02

I. Fundamental problems of materials science including phase transformations, reaction kinetics, deformation of materials, materials modeling, and surface phenomena.
II. Prospective materials for functional and structural purposes as composites, ceramics, amorphous and nano-crystalline materials, quasi-crystals, fullerenes, nano-tubes, intermetallics, eutectic materials, hard alloys and cermets.
III. Materials processing routes including materials synthesis in the bulk and dispersed states, self-propagating high-temperature synthesis, powder formation, sintering, joining, and coating.
IV. Characterization of materials properties using non-destructive methods, microscopy, spectroscopy, acoustics, and X-ray

**15. SUBJECT TERMS**
EOARD, Materials, Metals & alloys, Polymers, Ceramics

| 16. SECURITY CLASSIFICATION OF: | | | 17. LIMITATION OF ABSTRACT | 18. NUMBER OF PAGES | 19a. NAME OF RESPONSIBLE PERSON |
|---|---|---|---|---|---|
| a. REPORT | b. ABSTRACT | c. THIS PAGE | | | Charles H. Ward, Lt Col, USAF |
| UNCLAS | UNCLAS | UNCLAS | UL | 793 | 19b. TELEPHONE NUMBER *(Include area code)* +44 (0)20 7514 3154 |



AQ F03-03-0434

# This conference is dated to 50th Anniversary of Frantsevich Institute for Problems of Materials Science of National Academy of Sciences of Ukraine

Copies Furnished to DTIC
Reproduced From
Bound Originals

Reproduced From
Best Available Copy

DISTRIBUTION STATEMENT A
Approved for Public Release
Distribution Unlimited

# VOLUME I

AQ F03-03-0434

# LIST OF ABBREVIATIONS

NASU – National Academy of Sciences of Ukraine

RAS – Russian Academy of Sciences

NASB – National Academy of Sciences of Belarus

NSAU – National Space Agency of Ukraine

PAS – Polish Academy of Sciences

BAS – Bulgarian Academy of Sciences

SB – Siberian Branch of RAS

KSC FEB – Khabarovsk Science Center of Fast East Branch

NTUU "Kiev Polytechnical Institute" – National Technical "University of Ukraine "Kiev Polytechnical Institute"

**EXTENDED ABSTRACTS ARE PUBLISHED IN ORIGINAL PRESENTED BY THEIR AUTHORS**

**ORGANIZING COMMITTEE DOES NOT RESPONSIBLE FOR QUALITY AND CONTENT OF THESE MATERIALS**

*Scientific Secretary of Conference*
*L. CHERNYSHEV*

# INTERNATIONAL PROGRAMME COMMITTEE:

Paton B. – honorary chairman, Ukraine

Skorokhod V. – co-chairman, Ukraine

Lyakishev N. – co-chairman, Russia

Glasow P. – IUMRS, President

Siffert P. – E-MRS, General Secretary

Ciach R. – E-MRS, Poland

# MEMBERS OF COMMITTEE:

Antsiferov V. (Russia)

Effenberg G. (Germany)

Froes S. (USA)

Gogotsi Yu. (USA)

Haberko K. (Poland)

Kieback B. (Germany)

Manukyan N. (Armenia)

Millers T. (Latvia)

Naidich Yu. (Ukraine)

Miracle D. (USA)

Novikov N. (Ukraine)

Ortner H. (Germany)

Panin V. (Russia)

Parilak L. (Slovakia)

Pokhodnya I. (Ukraine)

Roman O. (Belarus)

Rogl P. (Austria)

Ristich M. (Yugoslavia)

Seminozhenko V. (Ukraine)

Sheleg V. (Belarus)

Shevchenko V. (Russia)

Shveikin G. (Russia)

Stankowskj Ya. (Poland)

Taran-Zhovnir Yu. (Ukraine)

Uskokovich D. (Yugoslavia)

Yastrabik L. (Czech Republic)

# NATIONAL ORGANIZATION COMMITTEE:

Skorokhod V. – chairman
Kostornov A. – deputy chairman
Firstov S. – deputy chairman
Chernyshev L. – scientific secretary

# MEMBERS OF COMMITTEE:

Arsenyuk V.
Bondarenko V.
Chebunin A.
Glinchuk M.
Gnesin G.
Grinev B.
Ivasishin O.
Kartuzov V.
Koval Yu.
Kovaltchenko M.
Kurdyumov A.
Milman Yu.
Nesterenko L.
Paustovskii A.
Poznyak L.
Velikanova T.
Yutchenko K.
Zavorotnyi M.

## INTRODUCTION

Contemporary materials science is extensive and multi-disciplinary field of knowledge, which accumulates the progress in both a number of fundamental sciences: solid state physics, physical chemistry, mechanics of deformable solids, and the technology in the broadest sense of that word. Enormous and continuously increasing worldwide interest to the science of materials is caused by extraordinary role which play new materials in technological revolution taking place before our eyes during last decades.

In XX century, especially in its second half, the material scientists made outstanding progress together with technologists in discovering and developing production of a number of truly unique materials. Suffice it to say about synthesis under high pressure a diamond and cubic boron nitride, ferroelectrics and piezoelectrics, supermagnets, ultra-heat-resistant and radiation stable alloys, alloys having shape memory, metal glasses, quasicrystals, high-temperature superconductors, foamed metals, viscous ceramics, nanostructured materials, including fullerenes and nanotubes, and many others. It became real high technologies for production materials as ultra-fine powders, thin films, single crystals, directed eutectics, laminated and gradient structures. We are now close to directed engineering of materials with specified structure and necessary set of properties.

However, XXI century presents to material scientists more grandiose problems. The requirements increase abrupt to structural materials with respect to their strength, work temperatures, ability to perform in aggressive media. There is the necessity in materials, which can adapt to hazard, often extreme performance conditions. An electronics requires superminiaturization that is possible only upon development super-conductors, semi-conductors and dielectrics of new generation. The medicine requires materials of new generation with principally new properties: bio-compatibility and bio-activity. An important role must play various sensors, which respond to the change of external conditions. The scientists are seriously engaged in creating "intelligent" and "smart" materials.

Present conference makes it its aim to discuss both progress in contemporary materials science, and those problems — challenges, which have to be solved in nearest future.

The conference topics cover wide range of problems: modeling of production processes and behavior of materials under various conditions; experiments directed to obtaining materials with new level of properties; high technologies; new testing methods and material characterization.

With respect to problems under discussion and number of participants our conference is one of the largest materials-science forums which have been held at the beginnig of current century at the territory of the former Soviet Union.

Of course, it is impossible to embrace all problems, which are under solution in contemporary materials science. Our conference is devoted mainly to up-to-date inorganic — metal and ceramic — materials and composites base on them.

I hope that the interest to that conference is due the fact that it is dated to 50th anniversary of one of the largest materials science center in Europe — the Frantsevich Institute for Problems of Materials Science of Ukraine National Academy of Sciences.

The most important papers of leading Ukrainian and foreign specialists, which cover main conference topics are collected in chapter "plenary sessions" in 1st volume of our issue. This volume contains also the materials of sections "Fundamental problems of materials science" and "Specific technologies". The 2nd volume include materials from two sections: "Perspective materials of functional and structural purposes: possibilities of obtaining new level properties" and "Characterization of materials properties". The materials published reflect to a great extent the tendencies in development contemporary materials science, and I hope will be discussed with large interest at conference.

I would like to express my sincere gratitude to the sponsors of our conference, which financial support allows for to hold conference at proper level and to publish current issue. These are: Ukraine National Academy of Sciences, State Administration in Kiev, Science and Technology Center in Ukraine, and also our old friends and colleagues from European Office of Aerospace Research and Development of US Air Forces.

We also appreciate very much the respected materials science organizations, EMRS and UIMRS, and personally their managers Dr. Paul Siffert and Dr. P.Glasow for agreement to hold conference under patronage of those organizations.

In conclusion I would like to wish the conference participants great success in work, and pleasant and fruitful way of spending time in one of the most beautiful European cities — Kiev.

V. Skorokhod,
Editor,
Academician of Ukraine National Academy of Science,
Chairman of Conference Organizing Committee,
Director of Frantsevich Institute for Problems of Materials Science
of Ukraine National Academy of Science

# Институту проблем материаловедения им. И.Н.Францевича НАН Украины — 50 лет

Д.А. Левина, Л.А. Чернышев

История Института проблем материаловедения многообразна и сложна. К сожалению, пока не проведена работа по ее достаточно полному описанию с полной и объективной оценкой всех тех, кто внес вклад в становление и развитие Института. Авторы этой небольшой заметки, проработавшие в Институте более 35 лет, осмелились дать свою трактовку его творческого пути, представить свой взгляд на тех, чье имя навсегда будет внесено в его летопись. Мы это делаем для того, чтобы участники нашей конференции смогли представить себе тот путь, что прошел наш Институт. Мы понимаем, что может быть и несколько иной взгляд на нашу историю, расставлены иные акценты и выделены иные доминанты его творческого развития. Мы заранее приносим извинения тем, о ком мы упомянули недостаточно или вовсе не упомянули. Объем этого материала невелик и обо всех сказать не представилось возможным. Итак, в путь.

В послевоенные годы в Институте черной металлургии АН УССР существовал отдел физико-химии металлургических процессов, который проводил разработки материалов с высокими показателями жаростойкости, жаропрочности и эрозионной стойкости с широким использованием методов порошковой металлургии. В 1952 году на его основе была организована Лаборатория спецсплавов, откуда и ведется летоисчисление Института. В 1955 году эта Лаборатория была реорганизована в Институт металлокерамики и спецсплавов АН УССР. С 1965 года он носит название Институт проблем материаловедения.

Основными направлениями научной деятельности Института являются разработка научных основ создания новых материалов с заданными свойствами на базе результатов фундаментальных исследований в области физики твердого тела, физического материаловедения, физической и неорганической химии, механики деформированного тела; синтез новых металлических сплавов и тугоплавких соединений, новых порошковых, композиционных и керамических материалов, разработка новых и усовершенствование существующих процессов их производства и соответствующего оборудования, разработка разнообразных материалов для покрытий и процессов обработки и соединения материалов.

Одним из основателей и первым директором Института (до 1973 г.) был академик АН Украины Иван Никитич Францевич (1905-1985 гг.) – известный ученый в области физической и неорганической химии, порошковой металлургии и твердого тела, человек выдающихся способностей, большой эрудиции и широкого кругозора, много сделавший для становления Института как крупного материаловедческого центра, который с 1985 года носит его имя.

Под руководством И.Н.Францевича были созданы и внедрены разнообразные композиционные материалы на основе черных и цветных металлов и тугоплавких соединений, сформулированы научные принципы для разработки ударостойких и сверхтвердых композиций, разработаны методы электрозащиты от коррозии магистральных газопроводов. В 1961 г. по инициативе И.Н.Францевича основан научный журнал "Порошковая металлургия", который является одним их немногих отечественных журналов, который переводится на английский язык и пользуется популярностью за рубежом. За высокие достижения И.Н.Францевичу были

присуждены Государственные премии СССР и Украины и присвоено самое высокое по тем временам звание Героя Социалистического Труда.

С 1973 г. на протяжении 28 лет директором Института был академик НАН Украины и АН СССР (впоследствии Российской АН) Виктор Иванович Трефилов (1931-2001 гг.). Он является одним из авторов разработки физических основ теории прочности и пластичности тугоплавких материалов, теории деформационного упрочнения и разрушения поликристаллических металлических материалов. Впервые в материаловедении В.И.Трефилов с коллегами разработали основы технологии производства так называемой "вязкой" керамики и алмазоподобных керамик. В.И.Трефилов - дважды лауреат Государственной премии Украины. В.И.Трефилов был крупным государственным деятелем, членом парламентов УССР и СССР, вице-президентом АН УССР. Он выступил инициатором создания и руководителем многочисленных национальных и международных программ, направленных на обеспечение современной техники новыми материалами с необходимыми эксплуатационными характеристиками.

С 2001 года Институтом руководит академик НАН Украины Валерий Владимирович Скороход, чья деятельность посвящена разработке научных основ процессов порошковой металлургии, теории физико-механических свойств материалов, которые изготавливаются спеканием порошков, в связи с их структурой и технологией изготовления. Им создана строгая количественная теория процессов деформирования порошковых материалов при спекании, горячем прессовании и обработке давлением, которая позволяет осуществлять инженерные расчеты оптимальных технологических режимов, созданы методы расчетов электропроводности, модулей упругости, скорости распространения ультразвуковых волн в гетерофазных материалах; экспериментально исследованы и теоретически обоснованы разнообразные физико-химические методы активирования и интенсификации процессов восстановления оксидов является инициатором и исполнителем работ, направленных на создание новых керамических материалов, в частности, керамик на основе интерметаллидов, наноструктурной керамики на основе нитрида и титаната бора. В.В.Скороход является одним из ведущих специалистов в области исследований и разработки функциональных материалов, в т.ч. гидридных и с памятью формы.

Здесь мы считаем уместным вспомнить тех, кто, будучи членом руководства Института в течение прошедших лет, внес существенный вклад в его развитие (к сожалению, многих из них уже нет среди нас). Это Г.В.Самсонов, В.Н.Еременко, И.М.Федорченко, А.Н.Пилянкевич, В.Н.Клименко, Л.Ф.Колесниченко, Л.А.Позняк, В.Р.Бранцевич, Г.В.Исаханов, В.И.Ковпак, А.И.Райченко, М.Д.Синявская, Г.Г.Сердюк, А.В.Паустовский.

В Институте работали такие выдающиеся ученые, как Г.В.Самсонов - физико-химическое материаловедение тугоплавких соединений; И.М.Федорченко - материаловедение порошковых материалов и порошковые технологии; В.Н.Еременко - физико-химия неорганических материалов; Г.С.Писаренко (один из основателей ИПМ, в дальнейшем на основе отдела ИПМ организовал Институт проблем прочности НАН Украины) - проблемы прочности материалов; М.П.Арбузов - структурные исследования материалов; А.Н.Пилянкевич - разработка современных методов структурного анализа материалов, в т.ч. сверхтвердых керамик; С.Г.Тресвятский - материаловедение оксидных материалов; Г.А.Виноградов - передовая технология прокатки порошков; И.Д.Радомысельский - разработка и

реализация новых материалов и технологий порошковой металлургии в промышленности; П.С.Кислый и Т.Я.Косолапова - физико-химия и технология тугоплавких соединений; Д.М.Карпинос - разработка и внедрение новых композиционных материалов.

Сейчас в Институте трудится творческий коллектив, в составе которого 2 академика, 8 членов-корреспондентов НАН Украины, 69 докторов и около 300 кандидатов наук. Широко известны в мире научные труды активно работающих сегодня ученых - М.Д.Глинчук (фазовые превращения в сегнетоэлектриках, радиоспектроскопия твердого тела, теория неупорядоченных сегнетоэлектриков), Г.Г.Гнесина (исследования широкого класса керамических материалов, разработка износо- и ударостойких материалов на их основе), А.Г.Косторнова (исследования структуры и свойств материалов, изготовленных методами порошковой металургии, создание порошковых и волоконных материалов широкого назначения), А.В.Курдюмова (структурные исследования широкого класса материалов, создание материалов на основе фаз высокого давления), Ю.В.Мильмана (разработки в области теории термоактивационных процессов деформации, материаловедения тугоплавких металлов, сплавов на основе алюминия, аморфных и квазикристаллических материалов), Ю.В.Найдича (исследования в области капиллярных явлений, адгезии и смачивания, физико-химические основы создания композиционных материалов, разработка технологии пайки разнородных материалов), Л.А.Позняка (исследования в области металургических процессов, разработки высокопрочных и инструментальных сталей), К.Д.Товстюка (исследования процессов интеркаляции полупроводниковых материалов, разработки материалов для новых высокоэффективних источников тока и высокоемкостных конденсаторов), С.А.Фирстова (изучение гранично упрочненных материалов и материалов с высокой удельной прочностью и жесткостью, структурный анализ материалов и микромеханизмов пластичности и разрушения).

Благодаря работам ученых Института созданы всемирно известные научные школы, которые плодотворно развиваются.

Среди наиболее важных работ, выполненных в Институте, необходимо отметить разработку теоретических основ процессов порошковой металлургии и создание порошковых и композиционных материалов разного назначения. Важное значение имеют физико-химические исследования взаимодействия жидких фаз с твердыми поверхностями, капиллярных свойств и контактных явлений, фазовых равновесий и термодинамики металлических сплавов и тугоплавких соединений; разработанная в Институте теория пластической деформации и разрушения тугоплавких материалов позволяет связать механические свойства с реальной кристаллической структурой. В мире хорошо известны работы сотрудников Института по материаловедению порошковых металлов, сплавов, псевдосплавов, интерметаллидов, тугоплавких соединений, слоистых структур, материалов на основе углерода, вюрцитоподобного нитрида бора.

По заказам народного хозяйства созданы материалы для новой техники - конструкционные (жаропрочные и жаростойкие), электротехнические, (контактные и электродные), для тонко- та толстопленочной электроники, инструментальные (в т.ч. ударостойкий сверхтвердый гексанит-Р), пористые проницаемые металлические, керамические и полимерные материалы из порошков и волокон для фильтрации и капиллярного транспорта, полупроводниковые материалы для использования в высокоемкостных накопителях энергии, фото- и термоэлектрических

преобразователях солнечной энергии; разработаны технологии и оборудование для электроэрозионного упрочнения деталей и инструмента, разработаны технологические схемы горячей обработки порошковых материалов и получение экономно-легированных сталей с использованием порошковой проволоки и многое другое.

Наряду с активной научной деятельностью Институт на протяжении всего периода своего существования проводил интенсивную научно-организационную и координационную работу. В течение более 10 лет Институт был головной организацией в СССР, которая координировала научную и научно-техническую деятельность в области порошковой металлургии. Им были инициированы правительственные постановления, которые в значительной мере способствовали развитию науки и промышленности порошковой металлургии в Украине и в других республиках СССР. Для улучшения координации работ в этой области и ускорения реализации научных разработок в промышленности на базе ИПМ был создан межотраслевой научно-технический комплекс (МНТК) "Порошковая металлургия", ядро которого составили собственно Институт, его особое конструкторское бюро, информационно-вычислительный центр и опытное производство. В деятельности МНТК принимали участие около 20 крупных институтов, проектных организаций и предприятий СССР. В 1990 году в МНТК "Порошковая металлургия" работал коллектив из 4500 человек, усилия которого были направлены на развитие фундаментальных материаловедческих исследований и внедрение новых материалов и технологий в передовые области народного хозяйства - прецизионное машиностроение, электронику, энергетику, авиационную и космическую технику, наземный транспорт и др. Много работ Институт выполнял по военным заказам, чем способствовал укреплению обороноспособности страны. Достижения Института заслужили высоких правительственных отличий.

И.Н.Францевич, В.И.Трефилов, Д.М.Карпинос, Ю.Л.Пилиповский и Л.А.Позняк с сотрудниками были отмечены Государственными премиями СССР и УССР.

Государственные премии УССР и Украины были присуждены также таким ведущим ученым Института, как В.В.Скороход, А.Н.Пилянкевич, Г.В.Самсонов, В.Н.Еременко, И.М.Федорченко, И.Д.Радомысельский, Ю.В.Найдич, М.С.Ковальченко, Ю.В.Мильман, А.Г.Косторнов, М.Д.Глинчук, К.Д.Товстюк, А.В.Паустовский, И.В.Гриднева, И.А.Лавриненко, Г.М.Лукашенко, Т.Я.Косолапова, В.Д.Ковалюк, В.Я.Петровский, В.В.Паничкина, Л.Н.Тульчинский, Г.В.Лашкарев, Г.Г.Гнесин, В.Х.Кадыров, В.Г.Ткаченко, Т.В.Дубовик, Л.А.Дворина, Г.Г.Карюк, В.Н.Буланов, В.М.Крячек, В.Н.Клименко, А.С.Болгар и др.

Многие сотрудники Института удостоены звания лауреатов премий имени выдающихся ученых.

Институт был награжден Орденом Трудового Красного Знамени, неоднократно завоевывал переходящее Красное Знамя ЦК КПСС, Совета Министров, ВЦСПС и ЦК ВЛКСМ, что в 80-х годах в СССР было одной из наиболее престижных оценок деятельности организаций.

В эти же годы Институт возглавил два направления Комплексной программы научно-технического сотрудничества стран-членов Совета Экономической Взаимопомощи (КП НТП СЭВ) - "Порошковая металлургия" и "Техническая керамика". Были разработаны и успешно выполнялись планы по этим направлениям программы, участниками которых были более 60 организаций из 8 стран.

К сожалению, сегодня Институт переживает не лучшие свои времена:

недостаточное финансирование исследований, практически полное отсутствие заказов от промышленности, устаревшее научное и технологическое оборудование, отток научных кадров, отсутствие поступлений в библиотеки научных монографий и периодических изданий, отсутствие средств на научные командировки, низкая заработная плата, плохие условия быта и труда ученых- все это не способствует развитию их творческой активности. Тем не менее сотрудники Института используют все возможности для получения средств для проведения исследований. Среди них участие в выполнении конкурсных работ по приоритетному для Украины направлению "Новые вещества и материалы", по тематике, которая поддерживается национальным фондом фундаментальных исследований, по европейским программам INTAS, INCO COPERNICUS, программам NATO , CRDF, грантами Научно-технологического центра в Украине и т.п.. В эти непростые годы Институт старается поддерживать связи с иностранными учеными и специалистами, систематически проводя международные конференции и семинары по материаловедческой тематике. Много энергии для поддержки научных направлений деятельности Института отдает директор ИПМ В.В.Скороход и его заместители по научной работе А.Г.Косторнов, А.В.Рагуля, С.А.Фирстов, ученый секретарь В.В.Картузов. Хотя и не в такой степени, как было бы желательно, в Институте идет омоложение научных кадров. Приходят на работу выпускники вузов, коллектив пополняется аспирантами.

Да, нам сейчас трудно. Но нам удалось сохранить научные школы, и поэтому мы смотрим в будущее с оптимизмом. Кроме того, добавляет оптимизма вера в то, что наука в нашей стране снова станет востребованной, а промышленности станут необходимы новые материалы, без которых невозможно создавать технику будущего.

Этот текст мы написали на трех языках. И сделали это с определенным умыслом. Это символично. Наш Институт возник и развивался в стране, где официальным языком был русский, сейчас наш государственный язык - украинский. Мы написали также на английском, потому что мы устремлены в мировое научное сообщество и надеемся найти там свое место.

# Інституту проблем матеріалознавства ім. І.М.Францевича НАН України - 50 років

Д.А. Левіна, Л.І. Чернишев

Історія Інституту проблем матеріалознавства різноманітна та складна. На жаль, поки не проведена робота з її повного опису, який би містив повну та об'єктивну оцінку всіх тих, хто вніс внесок до становлення та розвитку Інституту. Автори цього невеликого допису, які пропрацювали в Інституті більше за 35 років, насмілилися дати своє тлумачення його творчого шляху та свій погляд на тих, чиє ім'я назавжди буде внесене до його літопису. Ми це робимо для того, щоб учасники нашої конференції змогли б уявити той шлях, що пройшов наш Інститут. Ми розуміємо, що може існувати декілька інший погляд на історію Інституту, розподілені інші наголоси та виділені інші домінанти його творчого розвитку. Ми заздалегідь просимо вибачення у тих, про кого ми згадали недостатньо або зовсім не згадали. Обсяг цього матеріалу невеликий і тому про всіх сказати просто не було можливим. Отже, в дорогу.

В повоєнні роки в Інституті чорної металургії АН УРСР діяв відділ фізико-хімії металургійних процесів, який проводив розробки матеріалів з високими показниками жаростійкості, жаротривкості та ерозійної стійкості з широким застосуванням методів порошкової металургії. В 1952 році на його основі була організована Лабораторія спецсплавів, від якої ведеться родовід Інституту. В 1955 р. ця Лабораторія була реорганізована в Інститут металокераміки та спецсплавів. З 1965 р. він носить назву Інститут проблем матеріалознавства.

Основними напрямами наукової діяльності Інституту є розробка наукових засад створення нових матеріалів із заданими властивостями на базі результатів фундаментальних досліджень у галузях фізики твердого тіла, фізичного матеріалознавства, фізичної та неорганічної хімії, механіки деформованого тіла; синтез нових металевих сплавів і тугоплавких сполук, нових порошкових, композиційних і керамічних матеріалів; розробка нових і вдосконалення існуючих процесів їх виробництва і відповідного устаткування; розробка численних матеріалів для покриттів та процесів з'єднання матеріалів, в тому числі з теплофізичними та хімічними властивостями, що значно відрізняються одні від других.

Одним з засновників та першим директором Інституту (до 1973 р.) був академік АН України Іван Микитович Францевич (1905-1985 рр.) – відомий вчений в галузі фізичної та неорганічної хімії, порошкової металургії та твердого тіла, людина видатних здібностей, великої ерудиції та широкого кругозору, багато зробивший для становлення Інституту як крупного матеріалознавчого центру. Під керівництвом І.М. Францевича були створені та запроваджені у життя численні композиційні матеріали на основі чорних і кольорових металів та тугоплавких сполук, створені наукові підстави для розробки ударостійких та надтвердих композицій, розроблені методи електрозахисту від корозії магістральних газопроводів. У 1961 р. за ініціативою І.М. Францевича засновано науковий журнал "Порошкова металургія", один з небагатьох українських наукових журналів, який перекладається на англійську і користується великою популярністю за кордоном. За високі досягнення І.М. Францевичу була присуджені Державні премії СРСР і України та присвоєне найвище за тих часів звання Героя Соціалістичної Праці. Нині Інститут носить його ім'я.

З 1973 на протязі 28 років директором Інституту був академік НАН України та РАН Віктор Іванович Трефілов (1930-2001 рр.). Він є одним з авторів розробки фізичних основ теорії міцності та пластичності тугоплавких матеріалів, теорії деформаційного зміцнення та руйнування полікристалічних металевих матеріалів. Вперше в матеріалознавстві В.І. Трефілов з колегами розробили основи технології виробництва так званої "в'язкої" кераміки та алмазоподібних керамік. В.І. Трефілов - двічі лауреат Державної премії України. Він був ініціатором створення та керівником численних національних та міжнародних програм, спрямованих на забезпечення новітньої техніки сучасними матеріалами з необхідними експлуатаційними характеристиками.

З 2001 року Інститутом керує академік НАН України Валерій Володимирович Скороход, чия діяльність присвячена розробці наукових основ процесів порошкової металургії, теорії фізико-механічних властивостей матеріалів, що виготовлюються спіканням порошків, в зв'язку з їх структурою та технологією вироблення. Ним створена строга кількісна теорія процесів деформування порошкових матеріалів при спіканні, гарячому пресуванні та обробці тиском, яка дозволяє здійснювати інженерні розрахунки технологічних режимів, необхідних для досягнення заданої густини та структури матеріалу, створені методи розрахунків електропровідності, модулів пружності, швидкості поширення ультразвукових хвиль в гетерофазних матеріалах; експериментально досліджені та теоретично обґрунтовані різноманітні фізико-хімічні методи активування та інтенсифікації процесів відновлення оксидів металів з метою одержання високодисперсних порошків. Він є ініціатором та виконавцем робіт, спрямованих на створення нових керамічних матеріалів, зокрема кераміки на основі інтерметалідів, наноструктурної кераміки на основі нітриду та титанату бору. В.В. Скороход є одним з провідних спеціалістів в галузі досліджень та розробки функціональних матеріалів, в т.ч. гідридних та з пам'яттю форми

Ми вважаємо за доцільне згадати тих, хто на протязі минулих років вніс значний внесок в розвиток Інституту, перебуваючи на керівних посадах. Це Г.В. Самсонов, В.Н. Єременко, І.М. Федорченко, О.М. Пілянкевич, В.М. Клименко, Л.Ф. Колесніченко, Л.О. Позняк, В.Р. Бранцевич, Г.В. Ісаханов, В.І. Ковпак, О.І. Райченко, М.Д. Синявська, Г.Г. Сердюк, О.В. Паустовський.

В Інституті працювали такі визначні вчені, як Г.В. Самсонов - фізико-хімічне матеріалознавство тугоплавких сполук; І.М. Федорченко - порошкові матеріали та порошкові технології; В.Н. Єременко - фізико-хімічні основи матеріалознавства; Г.С. Писаренко (один з засновників ІПМ, який в подальшому на базі відділу ІПМ організував Інститут проблем міцності НАН України) - проблеми міцності; М.П. Арбузов - структурні дослідження матеріалів; О.М. Пілянкевич - розробка методів структурного аналізу для дослідження матеріалів, зокрема, надтвердих керамік; С.Г. Тресвятський - розробка та впровадження оксидних матеріалів;. Г.А. Виноградов - передові технології прокатування порошків; І.Д. Радомисельський - створення та впровадження матеріалів та технологій порошкової металургії в промисловість; П.С. Кислий та Т.Я. Косолапова - фізико-хімія та технологія тугоплавких сполук; Д.М. Карпінос - розробки та впровадження нових композиційних матеріалів.

Тепер в Інституті працює творчий колектив, до складу якого входять 2 академіки, 8 членів-кореспондентів НАН України, 70 докторів та біля 300 кандидатів наук. Широко відомі наукові роботи активно працюючих сьогодні вчених - М.Д. Глинчук (фазові перетворення в сегнетоелектриках, радіоспектроскопія

твердого тіла, теорія неупорядкованих сегнетоелектриків), Г.Г. Гнесіна (дослідження широкого класу керамічних матеріалів, розробка зносо- та ударостійких матеріалів на їх основі), А.Г. Косторнова (дослідження структури та властивостей порошкових матеріалів, створення порошкових і волокнових матеріалів широкого призначення), О.В. Курдюмова (структурні дослідження широкого класу матеріалів, створення матеріалів на основі фаз високого тиску), Ю.В. Мільмана (розробки в галузі теорії термоактиваційних процесів деформації, матеріалознавства тугоплавких металів, сплавів на основі алюмінію, аморфних та квазикристалічних матеріалів), Ю.В. Найдича (дослідження в галузі капілярних явиш, адгезії, змочування, фізико-хімічні основи створення композиційних матеріалів, розробка технології паяння різнорідних матеріалів); Л.О. Позняка (дослідження в галузі металургійних процесів, розробка високоміцних та інструментальних сталей), К.Д. Товстюка (дослідження процесів інтеркаляції напівпровідникових матеріалів, розробка матеріалів для високоефективних джерел струму та високоємних конденсаторів); С.О. Фірстова (вивчення гранично зміцнених матеріалів та матеріалів з високою питомою міцністю та жорсткістю, структурний аналіз матеріалів і мікромеханізмів пластичності та руйнування).

Завдяки роботам вчених Інституту створені всесвітньо відомі наукові школи, які плідно розвиваються.

Серед найбільш важливих робіт, виконаних в Інституті, слід відзначити розробку теоретичних основ процесів порошкової металургії та створення порошкових і композиційних матеріалів різного призначення. Важливе значення мають фізико-хімічні дослідження взаємодії рідких фаз з твердими поверхнями, капілярних властивостей та контактних явищ, фазових рівноваг та термодинаміки металевих сплавів і тугоплавких сполук; розроблена в Інституті теорія пластичної деформації та руйнування тугоплавких матеріалів, яка дозволяє пов'язати механічні властивості з реальною кристалічною структурою, дослідження з хімічної термодинаміки. В світі добре відомі роботи в галузі матеріалознавства порошкових металів, сплавів, псевдосплавів, інтерметалідів, тугоплавких сполук, слоїстих структур, матеріалів на основі вуглецю, вюрцитоподібного нітриду бору.

На замовлення народного господарства створені матеріали для нової техніки - конструкційні (жароміцні та жаростійкі), електротехнічні, (контактні та електродні), для тонко- та товстоплівкової електроніки, інструментальні (в т.ч. ударостійкий надтвердий гексаніт-Р), напівпровідникові матеріали для використання у високоємних накопичувачах енергії, фото- і термоелектричних перетворювачах сонячної енергії; розроблені технології та устаткування для електроерозійного зміцнення деталей та інструменту; розроблені технологічні схеми гарячої обробки порошкових матеріалів і отримання економно-легованих сталей з застосуванням порошкового дроту тощо.

Поряд з активною науковою діяльністю Інститут на протязі всього свого існування проводив інтенсивну науково-організаційну та координаційну діяльність. На протязі більше 10 років Інститут був головною організацією, в СРСР, та координувала наукову та науково-технічну діяльність в галузі порошкової металургії. Ним ініційовані урядові постанови, які значною мірою сприяли розвитку науки та промисловості порошкової металургії в Україні і в багатьох республіках. Для покращання координації робіт в цій галузі та полегшення запровадження наукових розробок в промисловість на базі ІПМ був створений міжгалузевий науково-технічний комплекс МНТК "Порошкова металургія", ядро якого створили власне інститут, його

Особливе конструкторсько-технологічне бюро, інформаційно-обчислювальний центр та дослідне виробництво. У 1990 році в МНТК "Порошкова металургія" працював творчий колектив з 4500 осіб, зусилля якого були спрямовані на розвиток фундаментальних матеріалознавчих досліджень та запровадження нових матеріалів та технологій в передові галузі народного господарства - прецизійне машинобудування, електроніку, енергетику, авіаційну та космічну техніку, наземний транспорт та ін. Багато робіт Інститут виконував на військові замовлення, чим сприяв зміцненню обороноздатності країни. Досягнення колективу та його членів заслужили високих урядових відзнак.

І.М. Францевич, В.І. Трефілов, Д.М. Карпінос, Ю.Л. Пилиповський одержали Державні премії СРСР.

Державні премії УРСР та України одержали також такі провідні вчені Інституту, як В.В. Скороход, О.М. Пілянкевич, Г.В. Самсонов, В.Н. Єременко, І.М. Федорченко, І.Д. Радомисельський, Ю.В. Найдич, М.С. Ковальченко, Л.О. Позняк, Ю.В. Мільман, М.Д. Глинчук, А.Г. Косторнов, К.Д. Товстюк, О.В. Паустовський, І.В. Гриднєва, І.О. Лавриненко, Г.М. Лукашенко, Т.Я. Косолапова, В.Д. Ковалюк,, В.Я. Петровський, В.В. Панічкіна, Л.Н. Тульчинський, Г.В. Лашкарьов, Г.Г. Гнесін, В.Х. Кадиров, В.Г. Ткаченко, Т.В. Дубовик, Л.А. Дворина, Г.Г. Карюк, В.М. Буланов, В.М. Крячек, В.М. Клименко, О.С. Болгар та ін. – всього біля 50 чоловік. Багато співробітників Інституту удостоєні звання лауреатів премій імені визначних вчених.

Інститут був нагороджений Орденом Трудового Червоного Прапору, багаторазово виборював перехідний червоний прапор ЦК КПРС, Ради Міністрів ВЦРПС та ЦК ВЛКСМ, що у 80-х роках в СРСР було однією з найбільш престижних оцінок діяльності організації.

В ці ж роки Інститут очолив два напрями Комплексної науково-технічної програми співробітництва країн - членів Ради економічної взаємодопомоги "Порошкова металургія" та "Технічна кераміка". Були розроблені і успішно виконувалися програми за цими напрямами, учасниками яких були більше 60 організацій з 8 країн.

На жаль, сьогодні Інститут переживає не кращі свої часи: недостатнє фінансування досліджень, практично повна відсутність замовлень від промисловості, застаріле наукове і технологічне обладнання, відтік наукових кадрів, відсутність надходжень до бібліотек наукових монографій та періодичних видань, відсутність коштів на наукові відрядження, погані умови життя та праці вчених - все це не сприяє розвитку їх творчої активності. Співробітники Інституту використовують всі можливості одержання коштів для проведення досліджень. Серед них участь в виконанні конкурсних робіт за пріоритетним для України напрямом "Нові речовини та матеріали", за тематикою, що підтримується національним фондом фундаментальних досліджень, за європейськими програмами INTAS та INCO COPERNICUS та програмами NATO, CRDF, грантами Науково-технологічного центру в Україні (УНТЦ), тощо. В ці непрості роки Інститут намагається підтримувати зв'язки з іноземними вченими та фахівцями, систематично проводячи міжнародні конференції та семінари за матеріалознавчою тематикою.

Багато вчених Інституту стажуються за кордоном та виконують в закордонних організаціях роботи за спільними науково-технічними проектами.

Багато енергії для підтримки наукових напрямів діяльності Інституту віддає директор ІПМ В.В. Скороход, та його заступники з наукової роботи А.Г. Косторнов, А.В. Рагуля, С.О. Фірстов, учений секретар В.В. Картузов. Хоча і не в такій мірі, як

було б бажано, в Інституті йде омолодження наукових кадрів. Приходять на роботу випускники вузів, поповнюється колектив аспірантами.

Так, нам зараз важко. Але нам вдалося зберегти наукові школи і тому ми дивимося в майбутнє з оптимізмом. Крім того, додає оптимізму віра в те, що наука в нашій країні знову стане востребуваною, а промисловості стануть потрібні нові матеріали, без яких неможливо створювати техніку майбутнього.

Цей текст ми подаємо трьома мовами. І це символічно. Наш Інститут виник та розвивався в країні, де офіційною мовою була російська, наразі наша державна мова - українська. Ми написали також англійською через те, що ми націлені до світового наукового співтовариства й маємо надію знайти там своє місце.

# 50th Anniversary of Founding the Frantsevich Institute for Problem of Materials Science (IPMS)

D. Levina, L. Chernyshev

The history of the IPMS is versatile and complicated. Unfortunately, up to now it has not been described comprehensively and the input of persons who promoted the foundation and development of IPMS has not been evaluated. The authors of this paper having worked at the IPMS more than 35 years made an attempt to express their opinion about persons whose names will store the IPMS history. We do this in order to help the conference participants to view the path covered by IPMS. We recognize that another glance to our history can exist. Another accent can be given, and another dominants in its development can be pointed out. We apologize in advance to those whose input was not sufficiently pointed or missed. The paper volume is restricted and it is impossible to tell in detail about everybody. So, let's go.

After world war II physica' and chemistry of metallurgical processes division of existed in the Institute of ferrous metallurgy of Academy of Science of UkrSSR, which dealt with the development of highly heat resistant and erosion resistant materials with making use of powder metallurgy techniques. Based on that division, the Laboratory of special alloys was founded in 1952, and just from that moment the history has begun. In 1955 the Laboratory was transformed into the Institute of Metal Ceramics and Special Alloys of Academy of Science of UkrSSR. Starting from 1965 it is named as Institute for Problem of Materials Science.

The main areas of scientific activity of IPMS are following: development of scientific bases for designing new materials with specified properties through fundamental researches in solid state physics, physical materials science, physical and inorganic chemistry, mechanics of deformed body; synthesis of new metal alloys and refractory compounds, new powders, composite and ceramic materials; developing new and improving available processes of production them as well and corresponding equipment; development of various materials for coating and processes for machining and joining of materials.

Founder and the first Director of IPMS (till 1973) was Academician of Academy of Sciences of Ukraine Ivan Nikitovich Frantsevich (1905-1985) – famous scientist in the field of physical and inorganic chemistry, powder metallurgy and solid state physics, an outstanding broad-minded person of great learning who made much for development of the IPMS to a large materials science center, which bears his name from 1985.

Under leadership of I.N.Frantsevich various composite materials based on ferrous and non-ferrous metals and refractory compounds have been designed and introduced in industry, scientific principles for development ofimpact-stable and superhard compositions have been formulated, the methods of electrical protection of gas pipelines against corrosion have been developed. In 1961 I.N.Frantsevich initiated the scientific journal «Powder Metallurgy». It is one of few native journals, which is translated in English and is known abroad. I.N.Frantsevich was awarded with premiums of USSR and Ukraine and the highest in those time title of Hero of Socialist Labour.

From 1973 an Academician of Ukrainian National Academy of Sciences and Academy of Sciences USSR (later of Russia) Victor Ivanovich Trefilov (1930-2001) became the

Director of IPMS and he was in this position for 28 years. V.I.Trefilov was one of authors of the physical fundamentals for the theory of deformation of strengthening and fracture of polycrystalline refractory materials. For the first time in materials science V.I.Trefilov and his colleagues had developed the basis of technologies for production of so called «tough» ceramics and diamond-like ceramics. V.I.Trefilov was twice awarded with the State Premium of Ukraine. He was an outstanding governmental person, member of UkrSSR and USSR parliaments, vice-president of AS of UkrSSR. He initiated and managed various international and national scientific programs aimed to creating new materials with necessary service properties.

Starting from 2001 the Academician of UNAS Valery Vladimirovich Skorokhod is the director of IPMS. He is engaged in development of scientific fundamentals for powder metallurgy processes, theory of physical and mechanical properties of powder materials produced with sintering with relation to their structure and production processes. He created regular quantitative theory of deformation of porous materials upon sintering, hot pressing and pressure treatment, which makes it possible to perform technical calculation of optimal technological regimes; developed the methods for calculation of electrical conductivity, elastic modules, velocity of supersonic waves propagation in heterophase materials. He has developed various experimental and theoretic physical and chemical methods for activating and intensifying the processes of metal oxides reduction in order to obtain highly-disperse metal powder. Recently he initiated and performed the works considering the creating new ceramic materials, in particular based on intermetallics, as well as nanostructural ceramics based on boron nitride and titanate. V.V.Skorokhod is one of the leading specialists in the field of investigation and development of functional materials, including hydrides and having the shape-memory ones.

We consider it to be appropriate to mention those who were involved in the management of IPMS and promoted its development (unfortunately many of them deceased): They are G.V.Samsonov, V.N.Yeremenko, I.M.Fedorchenko, A.N.Pilyankevich, B.N.Klimenko, L.F.Kolesnichenko, L.A.Poznyak, V.R.Brantsevich, G.V.Isakhanov, V.I.Kovpak, A.I.Raychenko, M.D.Sinyavskaja, G.G.Serdyuk, A.V.Paustovskij.

Many outstanding scientists worked at the IPMS, such as G.V.Samsonov – physicochemical materials science of refractory compounds; I.M.Fedorchenko – materials science of powders and powder metallurgy technologies; V.N.Yeremenko – physicochemistry of inorganic materials; G.V.Pisarenko (one of founder of IPMS; later organized the Institute for strength problems of UNAS on the base of IPMS division) – problems of materials strength; M.P.Arbuzov – investigation of materials structure; A.N.Pilyankevich – development of contemporary methods of analysis of materials structure, including superhard ceramics; S.G.Tresvyatskij – materials science of oxides; G.A.Vinogradov – advanced technology for powder rolling; I.D.Radomysel'skij – development and realization new materials and powder metallurgy technologies in industry; P.S.Kislyi and T.Ja.Kosolapova – physicochemistry and technologies of refractory compounds; D.M.Karpinos –development and application of new composite materials.

To-day a creative staff works in IPMS comprising 2 academicians and 8 correspondence-member of UNAS, 70 doctors of science and about 300 candidates of science. Known worldwide are scientific achievements of present working scientists: M.D.Glynchuk – phase transformations in ferroetoelectrics, radiospectroscopy of solids, theory of

unordered ferroelectrics; G.G.Gnesin - investigation of various ceramic materials, development of wear-resistant and impact-stable materials based on those ceramics; A.G.Kostornov – theoretical and experimental study of structure and properties of materials obtained by the powder metallurgy methods, development of powder and fibrous materials of wide application; A.V.Kurdyumov – study of structure of superhard and ceramic materials, development of materials based on the high-pressure phases; Yu.V.Mil'man - theory of thermoactivated deformation processes, materials science of refractory metals, alloys based on aluminum, amorphous and quasicrystalline materials; Yu.V.Naidich – capillary fenomena, adhesion and wettability, physicochemical base for designing composite materials, technology for brazing different materials; L.A.Poznyak – study of metallurgical processes, development of strength and tool steels; K.D.Tovstyuk – intercalation processes in semiconductive materials; S.A.Firstov – study the strengthened materials and those with high specific strength and stiffness, structure analysis of materials and micromechanisms of plastisity and fracture.

Owing to the works of the scientists of IPMS there have been created worldwide known scientific schools, which have developed fruitfully.

Among the most important works carried out in IPMS the development of theoretical basis for powder metallurgy processes and designing powder metallurgy and composite mateerials of various application should be pointed out. Greatly important are physicochemical studies of reaction of liquid phases with solid surfaces, capillary properties and contact fenomena, phase equilibria and thermodynamics of metal alloys and refractory compounds. The theory of plastic deformation and fracture of refractory materials, which was developed in IPMS, makes it possible to relate mechanical properties to real crystal structure. The works of scientists of IPMS in the field of materials science of powder metals, alloys, pseudoalloys, intermetallics, refractory compounds, layered structures, carbon- based materials, wurzite-like bboron nitride are well known worldwide.

For the need of economics the materials for new technics have been designed: structural heat resistant, electrotechnical (contact and electrod), for thin-film and sick-film electronics, tool (including impact-resistant superhard hexanite-R), porous permable metal, ceramic polymeric materials from powder and fibers for filtration and capillar transportation, semiconductive materials for high-capacity accumulators of energy, photoelectrical and thermoelectrical transformers of solar energy; the technologies and equipment for electroerosion of strengthening of parts and tools, as well as technological schemes for hot processing powder materials and production of low-alloyed steels with the usage of powder wire and many others have been developed and designed.

Along with scientific activity the IPMS an intensive scientific-organizing and coordination works were carrying out during all the period of the Institute's existence. For more than 10 years the IPMS was leading institution in the former USSR, which coordinated scientific and scientific-technical activity in the field of powder metallurgy. The IPMS initiated governmental resolutions, which to a great extent promoted the development of science and industry of powder metallurgy in Ukraine and other Republics of the USSR. In order to improve coordination of works in that field and accelerate realization of scientific development in industry, the interdepartmental scientific-technical complex «Powder Metallurgy» comprising IPMS, its Special Design Bureau, Information-Computational Center and experimental production plant. About 20 large institutes, design organizations and enterprises of the USSR took part in activity of this complex. In 1990 the staff of

«Powder metallurgy»complex amounted to 4500 employees whose activity was directed to the development of fundamental materials-scientific researches and introduction of new materials and technologies in leading branches of native economics – precise machine-building, electronics, energetics, aviation and space technics, transport etc. Many works have been performed by military orders thus promoting defense potential of state.

The achievement of IPMS won many governmental awards. I.N.Frantsevich, V.I.Trefilov, D.M.Karpinos, Yu.L.Pilipovskij and L.A.Poznyak were awarded the State premiums of USSR.

State premium of UkrSSR and Ukraine were awarded such leading scientists, as V.V.Skorokhod, A.N.Pilyankevich, G.V.Samsonov, V.N.Yeremenko, I.M.Fedorchenko, I.D.Radomysel'skij, Yu.V.Naidich, M.S.Koval'chenko, L.A.Poznyak, Yu.V.Mil'man, A.G.Kostornov, M.D.Glynchuk, K.D.Tovstyuk, A.V.Paustovskij, I.V.Gridneva, I.A.Lavrinenko, G.M.Lukashenko, T.Ya.Kosolapova, V.D.Kovalyuk, V.Ya.Petrovskij, V.V.Panichkina, L.N.Tul'chynskij, G.V.Lashkaryov, G.G.Gnesin, V.Kh.Kadyrov, V.G.Tkachenko, T.V.Doubovik, L.A.Dvorina, G.G.Karyuk, V.N.Bulanov, V.M.Kryachek, V.N.Klimenko, A.S.Bolgar and etc – approximately 50 scientsts.

Many specialists of IPMS were awarded the premiums named in honor of outstanding scientists.

The IPMS was rewarded the Order of Labor Red Banner, many times won the prize The Red Banner of the Central Committee of CPSU, the Council of Ministers, the All-Union Central Council of Trade Unions, and Leninist Young Communist League of the USSR, which was in the former USSR one of the most prestige assessment of organization activity.

In 1980 the IPMS headed two scientific-technical programs of Complex Program of Cooperation between Countries-members of Council of Economical Mutual Assistance (former Socialist European Countries) –«Powder Metallurgy» and «Advanced Ceramics». The plans were drawn and fulfilled concerning these programs in which more than 60 organizations from 8 countries participated.

Unfortunately, to-day the IPMS experiences are not in their best times: insufficient financing of researches, almost full absence of orders from industries, the scientific and technological equipment became obsolete, many scientists left Institute, lack of scientific monographs and journals in library, as well as funds for scientific trips – all this does not promote increase of creative activity of IPMS' scientists. Nevertheless, our scientists use all opportunities to get funding for researches. One should mention the participation in program «New Substances and Materials», which is one of high priorities for Ukraine; various programs supported by State Fund for Fundamental Research; European programs INTAS, INCO COPERNICUS, programs NATO, CRDF, SCTU etc.

To-day the IPMS trays to hold up the links with foreign scientists and specialists by regularly holding international conferences and seminars on materials science topics. Much energy apply Director of IPMS V.V.Skorokhod, deputy-directors S.A.Firstov, A.G.Kostornov, A.V.Ragulya, scientific Secretary V.V.Kartuzov for support scientific activity of Institute. Now young specialists graduated institutes and universities come to IPMS.

We recognize that to-day it is hard to work. But we preserved scientific schools and thus we look in future with optimism. We trust that our society will get better, the science be necessary for our state, and the industries will require new materials, without which it is impossible to create the technics for future.

We have written this text in three languages. We did it intentedly. Our Institute was founded and developed in the country, where official language was Russian. At present our official language is Ukrainian. We wrote also in English because we are striving for world scientific community and hoping to find there our place.

# CONTENT

# VOLUME I


| | Pages |
|---|---|
| **INTERNATIONAL PROGRAMME COMMITTEE** | i |
| **NATIONAL ORGANIZATION COMMITTEE** | ii |
| **INTRODUCTION** | iii |
| **ИНСТИТУТУ ПРОБЛЕМ МАТЕРИАЛОВЕДЕНИЯ ИМ. И.Н.ФРАНЦЕВИЧА НАН УКРАИНЫ — 50 ЛЕТ**<br>Д.А. Левина, Л.А. Чернышев | v |
| **ІНСТИТУТУ ПРОБЛЕМ МАТЕРІАЛОЗНАВСТВА ІМ. І.М.ФРАНЦЕВИЧА НАН УКРАЇНИ — 50 РОКІВ**<br>Д.А. Левіна, Л.І. Чернишев | x |
| **50TH ANNIVERSARY OF FOUNDING THE FRANTSEVICH INSTITUTE FOR PROBLEM OF MATERIALS SCIENCE (IPMS)**<br>D. Levina, L. Chernyshev | xv |
| ***PLENARY SESSION*** | 3-36 |
| **P369 DESIGNING AND ENGINEERING OF MATERIALS STRUCTURE AS A METHOD OF OPERATING BY THEIR PROPERTIES: ACHIEVEMENTS AND PROBLEMS**<br>Skorokhod V.V. | 3 |
| **P346 ELECTRON BEAM TECHNOLOGY OF INORGANIC MATERIALS DEPOSITION FROM THE VAPOUR PHASE IN VACUUM (EB-PVD) - STATE OF THE ART**<br>Movchan B. | 5 |
| **P125 STRUCTURAL LEVELS OF PLASTIC DEFORMATION AND FRACTURE OF SOLIDS**<br>Panin V.E. | 7 |
| **P127 SEARCH FOR NOVEL SUPERHARD MATERIALS**<br>Novikov N.V. | 9 |
| **P49 PRODUCTION TECHNOLOGY HIGH-TEMPERATURE CARBON/CARBON-SILICON CARBIDE COMPOSITES**<br>Kostikov V.I., Chernenko N.M. | 11 |
| **P362 METALLIC AEROSPACE MATERIALS WITH EXCEPTIONAL STRUCTURAL EFFICIENCY**<br>Miracle D. B., Firstov S.(1), Milman Yu.(1) | 12 |
| **P354 NEW HEAT RESISTANT Ti-BASED EUTECTIC COMPOSITE**<br>Firstov S., Mazur V.(1), Miracle D.(2), Kapustnikova S.(1), Kulak L. | 14 |
| **P172 HIGH-STRENGTH ALUMINUM-BASED ALLOYS**<br>Milman Yu.V. | 15 |
| **P136 INFLUENCE OF PYRAMID ENERGY ON STRUCTURE AND PROPERTIES OF ALUMINIUM ALLOYS**<br>Antsiferov V., Ragozin Y.(1), Porozova S., Tichonov A.(1) | 17 |
| **P375 STRUCTURAL HYDRODYNAMICS OF POROUS METAL MATERIALS**<br>Kostornov A.G. | 18 |
| **P143 PRINCIPLES OF ADAPTIVE CONTROL OF ELECTRIC PULSE SINTERING**<br>Belyavin K.E., Sheleg V.K., Minko D.V., Kuznechik O.O. | 20 |
| **P261 THE MOST RECENT INVESTIGATION OF THE PROCESSES OF PRODUCTION OF TUNGSTEN AND TUNGSTEN CARBIDE POWDERS**<br>Bondarenko V.P., Martynova L.M. | 21 |
| **P169 PHASE TRANSFORMATIONS IN LAYERED STRUCTURES UNDER HIGH PRESSURES AND CONTROLLED SYNTHESIS OF DIAMOND-LIKE PHASES**<br>Britun V.F., Kurdyumov A.V. | 23 |

**P347 NANOSTRUCTURED MATERIALS: BASIC CONCEPTS, SCIENTIFIC PROBLEMS AND PERSPECTIVES**
Andrievski R.A. 25

**P377 NEW GENERATION OF THE MATERIALS FOR SENSORS, ACTUATORS AND ULTRASOUND TECHNIQUE ON THE BASE OF FERROELECTRIC RELAXORS**
Glinchuk M.D., Laguta V.V., Bykov I.P. 26

**P148 PHYSICOCHEMICAL ASPECTS OF THE DEVELOPMENT OF FUNCTIONAL MATERIALS BASED ON ALIOSUBSTITUTED OXIDES AND THEIR APPLICATION**
Belous A.G. 28

**P190 HYDROGEN ABSORBING INTERMETALLICS FOR CHEMICAL CURRENT SOURCES**
Solonin Yu.M. 30

**P15 BORON-RICH SOLIDS AND THEIR AUSPICIOUS ASPECTS IN MATERIAL SCIENCE AND TECHNOLOGY**
Werheit H. 32

**P86 TOUGHNESS AS CHARACTERISTIC OF MECHANICAL STATE OF STRUCTURAL MATERIAL**
Kotrechko S., Meshkov Yu. 34

**P7 HYDROGEN-INDUCED PHASE TRANSFORMATIONS AND THEIR USE IN HYDROGEN TREATMENT OF MATERIALS**
Goltsov V.A. 35

***SECTION I. FUNDAMENTAL PROBLEMS OF MATERIALS SCIENCE*** 39-238

**I22 QUASICRYSTALS AND RELATED PERIODIC PHASES IN ALLOYS OF ALUMINUM WITH TRANSITION METALS - FORMATION AND STABILITY (A REVIEW)**
Grushko B., Velikanova T.Ya.[1] 39

**I207 PHASE EQUILIBRIA IN REFRACTORY OXIDES SYSTEMS**
Lopato L.M., Shevchenko O.V. 40

**I208 PHASE DIAGRAMS FOR THE $ZrO_2$-$Y_2O_3$-$Ln_2O_3$ SYSTEMS AND FIELDS OF ITS APPLICATION**
Andrievskaya E.R., Lopato L.M. 42

**I35 INTERACTION IN PHASES OF TERNARY Fe(Co, Ni)-B-C SYSTEMS**
Makara V.A., Kudin V.G. 44

**I331 COMPUTER MODELLING OF GAS EUTECTIC RE**
Shapovalov V.I. 46

**I305 COMPUTER STRUCTURE-IMITATING MODEL OF SPHERICAL PARTICLES SINTERING**
Alievsky V.M., Kadushnikov R.M., Nurkanov E.Y., Skorokhod V.V. 48

**I322 CORRELATION EFFECTS IN MATERIALS AND MODELS FOR THEIR DESCRIPTION**
Shpak A.P., Ristic M.M.[1], Kunitsky Yu.A.[2], Pryadko L.F.[3] 50

**I329 MATERIAL SCIENCE ASPECTS OF PROPERTIES AND STRUCTURES DEGRADATION OF BOILER ELEMENTS AFTER LONG OPERATION**
Piskalenko V.V., Gromov V.E., Tsellermaer V.Ya. 52

**I320 KINETICS OF DIAMOND SPONTANEOUS CRYSTALLIZATION**
Turkevich V.Z. 54

**I355 PHASE COMPOSITION OF THE PRODUCTS OF INTERACTION BETWEEN EUROPIUM (III) FLUORIDE AND CERIUM (III) FLUORIDE**
Zinchenko V.F., Efryushina N.P., Markiv V.Ya.[1], Eryomin O.G., Bilyavina N.M.[1], Mozkova O.V.[2] 56

**I133 PROBLEMS AND PERSPECTIVES OF THE STUDIES OF DEFECT FORMATION IN SEMICONDUCTING SILICON**
Talanin V.I., Talanin I.E., Levinson D.I.[1] 58

**I258 PHYSICOCHEMICAL FUNDAMENTALS OF CREATING MATERIALS WITH ELEMENTS OF SELF-ORGANIZATION**
Skorokhod V.V., Solntsev V.P., Solntseva T.A. 60

**I139 SELF-ORGANIZED CRITICALITY IN FRACTURE PROCESS OF MATERIALS**
Hilarov V.L. 62

**I61 INSERTION OF RARE EARTH AND OTHER METALS INTO AgI**
Despotuli A. L., Levashov V.I. 64

**I93 TRIPLE JUNCTION MOTION IN ALUMINUM TRICRYSTALS**
Protasova S.G., Sursaeva V.G. 66

**I380 EFFECT OF RANDOM FLUCTUATING POTENTIAL ON ORDER PARAMETER AND PHASE TRANSFORMATION TEMPERATURE**
Dmitriev A.I., Radchenko M.V., Lashkarev G.V., Butorin P.E. 68

**I108 THEORETICAL AND EXPERIMENTAL BASIS FOR DEVELOPING STRUCTURAL MATERIALS FOR GLASSMOULDING TOOLS**
Kolotilkin O. 70

**I52 VISCOELASTIC PROPERTIES OF INHOMOGENEOUS MEDIA**
Novikov V.V., Wojciechowski K.W.[1] 72

**I65 COATING OF A NEW FOAMING AGENT FOR ALUMINIUM**
Nakamura T.[1], Byakova A.V.[2], Gnyloskurenko S.V.[1],[5], Sakamoto K.[3], Ishikawa R.[4], Raychenko O.I.[5] 74

**I166 THEORY OF THE THERMAL AND DYNAMIC EFFECTS IN A CURRENT-CARRYING MELT SURROUNDING A FIBRE**
Raychenko O.I. 76

**I111 THE INTERFACE FENOMENA BETWEEN ALUMINA FIBRES AND PHOSPHATE BINDER**
Ulyanova T.M., Krutko N.P., Feodorova I.L.[1] 78

**I184 STRUCTURAL FOUNDATIONS OF THE FORMATION OF COVALENT TYPE CERAMICS UNDER HIGH PRESSURES AND AT HIGH**
Oleynik G.S. 80

**I215 MODELLING OF INTERACTION AT INTERFACES DURING POWDER COMPOUNDS FOR CERMET FILMS SINTERING**
Shulishova O.I., Shevchyk N.V., Shcherbak I.A. 82

**I85 CRACK NUCLEUS AND BRITTLE FRACTURE OF METALS AND ALLOYS**
Kotrechko S., Meshkov Yu. 84

**I103 METHODOLOGY OF ESTIMATION OF STRENGTH RELIABILITY OF STRUCTURAL MATERIALS AT ALL STAGES OF LIFE CYCLE**
Mileshkin M., Biblik I. 85

**I211 PHYSICAL-MACROMECHANICAL MODELLING INFLUENCE OF STRUCTURE ON MECHANICAL PROPERTIES OF COMPOSITE AND HIGH-POROSITY MATERIALS**
Lugovskoi Y.F. 87

**I349 RESIDUAL STRESSES AND PROBLEMS OF STRENGTH OF THE AXIALLY SYMMETRIC METAL ARTICLES**
Kolmogorov G.L., Kuznetsova E.V., Kovalev A.E. 89

**I295 CHEMICAL TREATMENT OF SEMICONDUCTOR SURFACES AT THE BEGINNING OF THE THIRD MILLENNIUM**
Tomashik V.M., Tomashik Z.F., Bilevych Ye.O., Gumenyuk O.R., Kusiak N.V.[1] 91

**I114 EQUILIBRIUM DAMAGE ACCUMULATION PROCESSES, POSSIBILITIES OF INCREASE OF DEFORMATION RESOURCES AND MACROFAILURE CONDITIONS OF COMPOSITE MATERIALS**
Wildemann V.E. 93

**I180 THE STRUCTURAL HEREDITY AT A CRYSTALLIZATION AND THE NATURE OF OVERCOOLING OF IRON**
Maiboroda V.P., Kunitskiy Yu.A.[1] 95

**I6 WARM COMPACTION OF GREEN POWDER BLANKS: COMPUTER MODELLING AND EXPERIMENT**
Gorokhov V.M., Sevastyanov E.S., Ustinova G.P., Zvonarev E.V. 97

**I10 PHASE TRANSFORMATION, STRUCTURE AND PROPERTIES OF MULTICOMPONENT Ti-Si-BASED ALLOYS AS FUNDAMENTAL BACKGROUND FOR ELABORATION OF HIGH-TEMPERATURE TITANIUM MATERIALS**
Bulanova M., Firstov S., Kulak L., Miracle D.[1], Tretyachenko L., Velikanova T. 99

**I12 ALLOY PHASE DIAGRAMS IN Ti CORNERS OF TERNARY AND QUATERNARY TITANIUM-BORIDE SYSTEMS AS A BASE FOR DEVELOPMENT OF IN-SITU METAL-MATRIX COMPOSITES**
Velikanova T.Ya., Bondar A.A., Artyukh L.V., Bilous O.O., Firstov S.A., Miracle D.[1] 100

**I13 ALLOY CONSTITUTION AND PROPERTIES OF METAL-BORIDE ALLOYS IN THE Ti-Al-Nb-B SYSTEM**
Tsyganenko N.I., Artyukh L.V., Bilous O.O., Bondar A.A., Borysov D.B., Burka M.P., Martsenyuk P.S., Shapoval T.O. 101

**I14 PHASE EQUILIBRIA IN THE TERNARY SYSTEM Ti-Al-B AND HIGH-TEMPERATURE STRENGTH OF ALLOYS**
Artyukh L.V., Bilous O.O., Bondar A.A., Burka M.P., Martsenyuk P.S., Tsyganenko N.I., Shapoval T.O. **102**

**I23 SOLIDUS SURFACE PROGECTION OF THE Al-Rh-Ti SYSTEM IN THE RANGE OF COMPOSITIONS 0-50 AT. % Rh**
Korniyenko K.Ye., Khorujaya V.G., Martsenyuk P.S. **103**

**I31 CONDUCTANCE OF DIRECTIONALLY CRYSTALLIZED EUTECTIC ALLOYS OF $B_4C$-$Me^{IV}B_2$ SYSTEMS**
Loboda P.I., Bogomol Yu.I. **104**

**I34 THERMODYNAMIC RESEARCHES FOR THE DECISION OF TECHNOLOGICAL PROBLEMS OF METALLURGY AND WELDING PRODUCTION**
Stukalo V.A., Sudavtsova V.S., Bieloborodova O.A. **106**

**I36 THERMODYNAMICAL PROPERTIES OF Ni-Nb-Al SYSTEM**
Sudavtsova V.S., Vovkotrub N.E. **108**

**I37 THERMODYNAMICAL PROPERTIES OF BINARY Al (IV-ELEMENT)-3D METAL**
Sudavtsova V.S., Podarevskaya O.V.[(1)], Zhuravlev V.S.[(2)] **110**

**I38 A NEW APPROACH TO QUANTITATIVE EVALUATION OF DANGER OF SHALLOW CRACKS**
Kotrechko S.O., Meshkov Yu.Ya., Popovych V.O. **112**

**I40 SPREADING OF CONDUCTIVE DROP OF METALLIC MELT IN MAGNETIC FIELD**
Kanchoukoev V.Z., Karamurzov B.S., Sozaev V.A. **114**

**I43 CALORIMETRIC RESEARCH OF MIXING ENTHALPIES In LIQUID ALLOYS OF Al-Ga-Y TERNARY SYSTEM**
Dubyna V.M., Zinevich T.M., Kotova N.V., Bieloborodova O.A. **116**

**I58 INFLUENCE OF ULTRASONIC TREATMENT ON STRUCTURE OF ROLLED Mo SINGLE CRYSTALS**
Pronina L.N., Mazilkin A.A., Aristova I.M. **117**

**I59 SINGULARITIES OF A INTERPLAY KINETICS FROM CO-GASES WITH IRON CATALYSTS**
Kirichenko A.G., Berenda V.V, Kolesnik N.F. **119**

**I62 AB-INITIO STUDY OF THE IMPURITY EFFECTS IN NIAL: FROM ELECTRONIC AND CRYSTAL STRUCTURE TO MECHANICAL PROPERTIES**
Medvedeva N.I. **121**

**I66 COMPUTER SIMULATION OF THE CRACK NUCLEUS ORIENTATION EFFECT ON THE VALUE OF BRITTLE FRACTURE OF POLYCRYSTALLINE METALS**
Kotrechko S., Stetsenko N., Kucher O. **123**

**I67 CRITERION OF THE CRACK NUCLEUS UNSTABLE EQUILIBRIUM**
Kotrechko S., Meshkov Yu., Ovsyannikov O. **124**

**I72 ABOUT DENSIFICATION AND HARDENING OF POROUS BLANKS DURING AXIAL COMPRESSION**
Ryabicheva L.A., Kravtsova J.V. **125**

**I78 InSe SOLAR CELLS**
Katerynchuk V.M., Kovalyuk Z.D., Zaslonkin A.V., Sidor O.M. **127**

**I79 RADIATION STABLE PHOTODETECTORS BASED ON LAYERED III-VI COMPOUNDS**
Drapak S.I., Kovalyuk Z.D., Netyaga V.V., Orletskii V.B. **129**

**I84 PHASE COMPOSITION & INTERFACE DESIGN OF HIGH COERCIVE SINTERED PERMANENT MAGNETS OF $SmCo_5$–TYPE**
Andreeva A.V.[(1)], Talijan N.M.,. Milutinovic-Nikolic A, Static-Trosic J., Jovanovic Z.D. **131**

**I87 EFFECT OF GRAIN SIZE AND PLASTIC STRAIN ON WEIBULL PARAMETERS**
Zimina G., Kotrechko S. **133**

**I94 THE INFLUENCE OF DISPERCED NANOCARBON ON THE KINETICS OF MESOPHASE COAL TAR PITCH TRANSFORMATIONS**
Rimbu G.A., Banciu C., Bondar A.M., Stamatin I. **135**

**I98 THE HEALING OF CRACK IN TRANSPARENT DIELECTRICS UNDER INFLUENCE OF ELECTROMAGNETIC RADIATION**
Feodorov V.A., Plushnikova T.N., Tjalin Yu. I., Chivanov A.V. **136**

**I100 DENSIFICATION OF COMPACTS DURING LIQUID-PHASE SINTERING**
Romanov G.N., Tarasov P.P.[(1)], Tsypandin P.P.[(1)], Mestnikov N.S.[(1)], D'yachkovsky P.K.[(1)], Savitskii A.P.[(2)] **138**

**I102 EFFECT OF A SMALL AMOUNT OF BORON ON STRUCTURE AND PROPERTIES IN MOLYBDENUM ALLOYS** 140
Morito F., Noda T., Krajnikov A.(1)

**I107 LOCALIZED PLASTIC SHEAR PROPAGATION IN A METAL LAYER** 141
Stepanov G.V., Shirokov A.V.

**I109 THE DESCRIPTION OF THE SILICON MELT MOVEMENT AT THE FZ PROCESS** 143
Egorov S.G., Chervonyi I.F., Kolobov G.A., Nikonenko A.P.

**I116 THE INFLUENCE OF INITIAL POWDERS DISPERSIVITY, ACTIVATING AGENTS AND HOT PRESSING TEMPERATURE ON $Si_3N_4$-SiC CERAMICS DENSITY** 145
Goloubtsova E.S., Kaledin B.A., Malkevich N.G.

**I117 INVESTIGATION OF THE INTERACTION IN THE Cu-Mg-C SYSTEM UNDER HIGH PRESSURE AND TEMPERATURE** 147
Turkevich V.Z., Kulik O.G., Osipov A.S., Garan A.G.

**I119 SHORT-SAMPLE MODELLING OF STRESS EFFECTS IN SUPERCONDUCTING COMPOSITES** 149
Kislyak I., Dotsenko V.(1), Tikhonovsky M.(2), Shkilko A.(3), Zagoruiko L.(3)

**I135 BEHAVIOUR FEATURES OF QUARTZ CERAMICS WHEN CONTACTING WITH ALKANOTROPHIC RHODOCOCCI** 151
Antsiferov V.N., Ivshina I.B.(1), Porozova S.E., Ritchkova M.I.(1)

**I137 EFFECT OF HARDENING ON INTERNAL FRICTION IN Ti-ALLOY** 153
Konstantinova T.E., Ryumshina T.A.(1), Nosolev I.K., Pilipenko N.P.

**I142 ABOUT NANOSIZABLE STRUCTURES UNDER THE ELECTROPLASTIC DEFORMATION** 155
Petrunin V.A., Tzellermaer V.Ya.,Gromov V.E.

**I144 ALUMINUM ALLOYS HARDENING BASED ON PHASE TRANSFORMATIONS OF PERITECTIC TYPE** 156
Zinkovsky G., Spiridonova I., Litvin B.

**I147 EFFECT OF LOW-ENERGY ELECTRON AND ION IRRADIATION ON THE COMPOSITION OF THE ZnS SINGLE CRYSTAL SURFACE** 158
Ivanishina I.M., Mischuk O.A.(1), Telemko A.V.(1)

**I154 POSSIBILITIES OF INDEPENDENT GASEOUS ATMOSPHERE IN STRUCTURAL ENGINEERING OF FUNCTIONAL MATERIALS** 160
Slys I.G.

**I165 MACROSCOPIC TURN OF SOLID CYLINDRICAL PARTICLE UNDER ELECTRIC CURRENT ACTION** 161
Derev'yanko O.V., Popov V.P., Raychenko O.I., Pavlenko T.P.

**I179 THE INVESTIGATION OF STABILITY OF COMPOSITE SCREENS ON THE BASIS OF ALUMINIUM TO EFFECT BY A LASER IMPULSE** 163
Maiboroda V.P., Revo S.L.(1), Ivanenko K.O.(1), Molchanovskaya G.M., Sckolniy V.K.

**I181 STRUCTURAL CHANGES IN A CRYSTALLINE FILM OF Co AT HEATING** 165
Maiboroda V.P., Maksimiva G.M., Molchanovskaya G.M.

**I182 STRUCTURAL CHANGES IN ALLOY OF A CHROMIUM AT LOW TEMPERATURE PHASE TRANSFORMATION** 167
Maiboroda V.P., Adeev V.M., Maksimiva G.M., Molchanovskaya G.M.

**I185 INFLUENCE OF ROLLING ON THE STRUCTURAL STATE OF 2H BN PARTICLES** 169
Volkogon V.M., Oleynik G.S., Avramchuk S.K.

**I186 THE INVESTIGATION OF ELECTRONIC FRAME In AND Sn IN SOLID AND LIQUID CONDITION BY A METHOD OF X-RAY-PHOTOELECTRON SPECTROSCOPY** 171
Maiboroda V.P., Sinelnichenko A.K.

**I191 PHASE EQUILIBRIA IN THE TERNARY SYSTEMS $Al_2O_3$-$ZrO_2$ - RARE EARTH ELEMENTS OXIDES** 173
Lakiza S.M., Red'ko V.P., Lopato L.M.

**I213 COMPLEX MODELLING OF THE PHASE EQUILIBRIA IN Al-Ti SYSTEM AND SEGREGATION IN THE GRAIN BOUNDARY PHASE OF ITS POLYCRYSTAL ALLOYS** 175
Danylenko V.M., Yagodkin V.V.

**I217 HIGH-PERFORMANCE MATERIALS BASED ON $ZrO_2$** 177
Shevchenko A.V., Ruban A.K., Dudnik E.V., Lopato L.M.

**I218 THE PHYSICO-CHEMICAL BASES OF MELTING THE HIGH PURE ALLOYS OF Ti, Zr, Cr AND DEVELOPMENT OF PERSPECTIVE TECHNOLOGIES FOR ITS PURPOSE** 179
Kyznetsova T.L., Jakimenko I.L.

**I233 RESEARCH OF STRUCTURE AND MECHANICAL PROPERTIES OF CHROMIUM FILM CONDENSATES IN AN INTERVAL AT TEMPERATURES 20-1100°C**
Pisarenko V.A., Rakitsky A.N., Rogul T.G., Sameluk A.V., Pavlov V.S.[(1)] 181

**I235 THERMOELASTIC MARTENSITIC TRANSFORMATION IN Fe-Co-Ni-Ti ALLOYS AND STRUCTURE OF MARTENSITE**
Shevchenko O.M., Kozlova L.E.[(1)] 182

**I237 PHYSICAL ASPECTS OF ACTIVATED SINTERING OF METAL POWDERS BY HIGH-RATE ELECTRIC CONTACT HEATING**
Andrushchik L.O., Oschkaderov S.P. 184

**I244 SOME ASPECTS OF PLASTICITY OF FINE-GRAINED TITANIUM**
Kotko A.V., Malashenko I.S.[(1)], Moiseev V.F., Ulshin S.V.[(2)] 186

**I250 INVESTIGATION OF PHASE TRANSFORMATIONS IN THE $Al_3(Ti_{1-x}Zr_x)$ INTERMETALLIC BY IN SITU X-RAY DIFFRACTION METHOD**
Karpets M.V., Milman Y.V., Miracle D.B.[(2)], Barabash O.M.[(1)], Korzhova N.P., Legkaya T.N.[(1)], Voskoboinik I.V., Senkov O.N.[(2)] 188

**I252 PHASE EQUILIBRIA AND SOME PROPERTIES OF PHASES IN TI-CORNERS OF THE Ti-Zr-Si AND Ti-Zr-Si-Al SYSTEMS**
Bulanova M.V., Tretyachenko L.A., Meleshevich K.A., Samelyuk A.V., Saltykov V.A. 190

**I253 PHASE EQUILIBRIA AND THERMODYNAMICS OF THE PHASES IN THE R-Pb BINARY SYSTEMS**
Bulanova M.V., Buyanov Y., Sidorko V. 191

**I255 THERMODYNAMIC PROPERTIES OF BISMUTH SELENIDES AND TELLURIDES AND QUASIBINARY SYSTEM $Bi_2Se_3$-$Bi_2Te_3$**
Gorbachuk N., Sidorko V., Bolgar A., Goncharuk L. 192

**I256 THERMOCHEMISTRY OF LIQUID Co-Ce AND Co-Sm ALLOYS**
Ivanov M., Berezutski V., Usenko N. 193

**I257 INFLUENCE OF IRON FAMILY ADDITIONS FOR ADHESIVE CHARACTERISTICS AND FORMATION INTERPHASE BOUNDARIES IN THE SYSTEM Cr-Cu**
Lesnik N.D., Minakova R.V., Homenko E.V. 194

**I263 SYNTHESIS OF POROUS MATERIALS, BASED ON SILICON CARBIDE IN ULTRA-DISPERSED REACTIVE SYSTEM**
Antsiferov V.N., Gilev V.G., Sung J.S.[(1)] 196

**I273 NEW TRENDS IN SUPERHARD MATERIALS SCIENCE**
Ilyasov V. 198

**I277 STRUCTURAL TRANSFORMATIONS IN SURFACE LAYERS OF GRANITES IN DYNAMIC CONTACT ZONE**
Paschenko E., Shilo A., Lazhevska O. 200

**I280 CALCULATION OF INTERNAL STRESSES IN THE COATINGS COHERENT WITH A SUBSTRATE**
Kosenko N.S.[(1)], Ustinov A.I.[(1,2)], Kosenko P.N.[(3)] 202

**I282 THERMOMAGNETIC ANALYSIS OF TRANSFORMATIONS DURING THE HEATING OF AMORPHOUS FOILS OF THE ALLOY $Fe_{80}Si_6B_{14}$**
Gryhoryeva O.V. 204

**I304 EFFECT OF POWDER PARTICLES' SIZE DISPERSION ON SYNTERING KYNETICS AND STRUCTURAL GENESIS OF A SINTERED POWDER BODY**
Nurkanov E.Y., Kadushnikov R.M., Alievsky V.M. 206

**I311 PHASE TRANSFORMATIONS IN ELASTICS-CRYSTALS OF THE STRUCTURE $G5_1$**
Matysina Z.A., Zaginaichenko S.Yu.[(1)], Eremenko A.M. 208

**I314 DIFFUSION WAY OF STRUCTURE AND PROPERTIES FORMATION IN Fe-BASED ALLOYS UNDER DEFORMATION EFFECT AND DOPING WITH N AND C**
Demchenko L.D. 210

**I324 AB INITIO INVESTIGATIONS OF THE EFFECT OF CHEMICAL BONDING ON THE SPIN STATE OF HYDROGEN ATOM IN $ZrH_2$**
Yuryeva E.I., Pletnev R.N. 212

**I334 TECHNIQUE OF PARAMETR'S DEFINITION OF DYNAMIC PHASE TRANSITIONS IN METALS**
Usherenko S.M., Ovchinnikov V.I., Koval O.I. 213

**I336 CALCULATION OF FORCE OF INTERPLANE INTERACTIONS AND STRENGTH CHARACTERISTICS OF TITANIUM AND CERAMIC MATERIALS AT HIGH RATE LOADING**
Zakarjan D.A., Kartuzov V.V. 215

**I339 A NOVEL BORON-BASED SUPERHARD MATERIAL PRODUCED AT HIGH PRESSURES AND TEMPERATURES**
Shulzhenko A.A., Sokolov A.N., Belyavina N.N.(1), Markiv V.Ya.(1) 217

**I340 THE ROLE OF IMPURITY STATE IN SILICON CRYSTALS AND THEIR ELECTRONIC EXCITATION IN THE FORMATION OF MECHANIC-AND-PLASTIC PROPERTIES**
Makara V.A., Steblenko L.P., Rudenko O.V., Naumenko S.M., Kravchenko V.M. 219

**I341 INVESTIGATION OF HOT STRETCHING PROCESS OF THIN-WALLED TUBES ON CONIC MANDRELS**
Petrosyan G.L., Petrosyan V.G., Hambardzumyan A.F. 221

**I348 THE EFFECT OF TEMPERATURE, PRESSURE, AND ADDITIONS OF ALUMINUM IN SINTERING OF cBN POWDERS ON THE cBN→hBN PHASE TRANSFORMATION**
Shulzhenko A.A., Bezhenar M.P., Bozhko S.A., Belyavina N.M.(1), Markiv V.Ya.(1) 223

**I353 THE INFLUENCE OF BEND – TENSILE STRAINING PARAMETERS ON THE SUBSTRUCTURE OF COLD ROLLED SHEET STEELS**
Vakulenko I.A., Levchenko G.V. 225

**I363 ROLE OF THE CRYSTALLINE ELECTRIC FIELD ON THE PHYSICAL PROPERTIES OF $REB_{12}$ COMPOUNDS**
Czopnik A., Shitsevalova N.(1), Paderno Yu.(1), Krivchikov A.(2), Pluzhnikov V.(2), Bat'ko I.(3), Flachbart K.(3) 227

**I379 MATERIALS AT THE FRONTIER OF CENTURIES**
Levina D.A., Chernyshev L.I. 230

**I395 NEW DEVELOPMENTS IN MATERIALS ENGINEERING: FROM COORDINATION POLYOXOMETALATE COMPOUNDS TO SEMICONDUCTING THIN FILMS AND COVERINGS**
Lisnyak V.V., Stus N.V., Sudavtzova V.S., Popovich P.(1), Slobodyanik N.S. 232

**I24 SYNTHESIS OF SUB-MICRON FILM STRUCTURES UNDER EFFECT OF FRACTAL-MATRIX TRANSPARENCIES**
Serov I.N., Alekseitsev A.V., Bel'skaya G.N., Bonshtedt B.E.(1), Egorova N.B., Margolin V.I.(2), Potsar N.A.(2) 234

**32 FORECAST OF STRENGTH OF IRON POWDERS AND SINTERED MATERIALS**
Bulanov V.Ya. 236

***SECTION III. SPECIFIC TECHNOLOGIES*** 241-355

**III195 A WAYS FOR IMPROVING QUALITY OF POWDER TOOL STEELS**
Poznyak L.A., Ulshin V.I., Tychomyrov S.V., Sorokin U.V. 241

**III126 EVOLUTION OF PRIMARY IRONMAKING TO THE UNTRADITIONAL COKE-LESS TECHNOLOGY WITH POWER GENERATION**
Tovarovskiy I.G. 243

**III206 INFLUENCE OF MELTING CONDITIONS AND OF ALLOYING WITH TRANSITION AND RARE-EARTH METALS ON STRUCTURE AND PROPERTIES OF HIGH-STRENGTH ALUMINUM ALLOYS**
Patsyna R.V., Voropaev V.S., Goncharuk V.A., Danylenko M.I., Zakharova N.P., Lotsko D.V., Milman Yu.V., Samelyuk A.V., Sirko O.I. 245

**III238 PRESSURE WELDING OF DISSIMILAR METALS**
Zamkov V.N., Kireev L.S., Sabokar V.K. 247

**III251 ELABORATING OF THE MULTILAYER BRAZED JOINT OF NONMETALLIC CERAMIC PLATE TO METALLIC ROD**
Zhuravlev V.S., Naidich Y.V., Grigoriev O.N., Prokopenko A.A., Mosina T.V., Koval A.Y. 248

**III134 THE DEVELOPMENT OF THE TECHNOLOGY OF THE PRODUCING OF THE CHEMICALLY STABLE POROUS POLYMERIC MEMBRANES FOR THE BAROMEMBRANE MIXTURE SEPARATION**
Goncharenko V.V., Gvozd G.V., Churpita Ya.V., Gleevoi Yu.V., Ponirko E.F. 249

**III16 LOW TEMPERATURE SYNTHESIS OF MICROPOROUS SILICON CARBIDE MEMBRANES**
Antsiferov V.N., Gilyov V.G., Sung J.S.(1), Kim T.W.(1), Choo K.Y.(1) 250

**III3 MMT-PROCESS INCREASES THE LIFE OF CEMENTED CARBIDE ARTICLES**
Lisovsky A.F. 252

**III90 USE OF PROCESSES OF BURNING FOR RECEPTION OF MATERIALS ON A BASIS TUNGSTEN AND ZIRCONIUM BORIDES**
Verchoturov A.D., Nikolenko S.V., Lebuchova N.V., Gostishev V.V.[1] **254**

**III275 A NEW MODEL OF PHASE AND STRUCTURE FORMATION IN SELF-PROPAGATING HIGH-TEMPERATURE SYNTHESIS**
Khina B.B., Rabinovich O.S.[1], Formanek B.[2] **256**

**III287 MECHANOCHEMICAL SYNTHESIS OF NANOCOMPOSITES IN METAL-OXIDE SYSTEM**
Grigorieva T.F., Ivanov E.Yu.[1], Barinova A.P., Boldyrev V.V. **258**

**III28 MODELLING HOT-WIRE CHEMICAL VAPOUR DEPOSITION OF NANOCRYSTALLINE SILICON THIN FILMS**
Bruehne K., Rakhlin M., Schubert M. **259**

**III223 STRUCTURE AND PROPERTIES OF COATINGS FROM THE CHROMIUM-BASED ALLOYS OBTAINED AT SUPERSONIC PLASMA SPEED**
Gorban V., Grechishkin E., Petrov S.[1] **260**

**III344 INVESTIGATION OF CONDITIONS FOR FORMATION OF INTERMETALLIC PHASES DURING DETONATION SPRAYING OF CLAD Ni-Al POWDERS**
Astakhov E.A., Mitz I.V., Kildiy A.I., Kokorina N.N., Kaplina G.S. **262**

**III27 EVALUATION OF SERVICEABILITY OF PLASMA COATINGS ON BODIES OF ROTATION**
Shevchenko V., Belchikov E. **264**

**III367 GRANULAR SILICON TECHNOLOGY OF MONOSILLANE IN A FLUIDIZED BED REACTOR**
Borodulia V.A., Vasilevich V.P.[1], Vinogradov L.M., Rabinovitch O.S., Stepanenko V.N.[2], Akulitch A.V. **266**

**III366 FLUORIDE HYBRIDE TECHNOLOGY OF POLYCRYSTALLINE SOLAR SILICON PRODUCTION FROM THE RECYCLE PRODUCT OF APATITE RECYCLING**
Khitko V.I., Stepanenko N.V.[1], Vasilevich V.P.[1] **268**

**III1 EFFECT OF DOPING ON THE RESISTIVITY AND MICROSTRUCTURE OF CARBON FILMS**
Onoprienko A., Artamonov V.[1], Yanchuk I.[1] **270**

**III5 OUTLOOKS OF MANUFACTURING OF COMPOSITE MATERIALS USING ULTRASONIC TECHNOLOGIES**
Kozlov A.V., Mordyuk B.N., Prokopenko G.I. **272**

**III9 EFFECTIVE METHODS OF SYNTHESES OF PRODUCTS FROM COMPOSITE MATERIALS WITH USE OF FOUNDRY TECHNOLOGIES**
Zatulovsky A.S., Lakeev V.A. **274**

**III39 EVOLUTION OF STRUCTURE OF COPPER AFTER TORSION EXTRUSION**
Varyukhin V.N., Pashinskaya E.G., Domareva A.S., Tkachenko V.M., Pashinskaya O.V. **275**

**III44 SYNTHESIS OF SILICON CARBIDE POROUS MATERIALS BASED ON ULTRA-DISPERSED REACTIVE SYSTEM**
Antsiferov V.N., Gilyov V.G., Sung J.S.[1], Kim T.W.[1] **277**

**III48 TWO-STAGES SCHEME OF CARBONLESS IRON POWDER PRODUCTION**
Khovavko O.I., Svyatenko O.M., Semenyuk N.I., Bondarenko B.I. **279**

**III51 SYNTHESIS OF THE MODIFIED BIOACTIVE CALCIUM HYDROXYAPATITE**
Zaslavskaya L.V., Belousova E.E, Rosantsev G.M. **281**

**III60 THE ANODE DISSOLUTION OF La (III) IN WATERLESS SOLVENT**
Kostyuk N.N., Dick T.A., Tereshko N.V. **283**

**III68 THE THERMAL PROPERTIES OF THE TRIS-PIVALOYLTRIFLUOROACETONATE RARE EARTH METAL COMPLEXES**
Kostyuk N.N., Dick T.A., Trebnikov A.G. **285**

**III71 THE ION IMPLANTATION FOR IMPROVEMENT OF THE PROTECTIVE NITRIDE LAYERS PROPERTIES FOR APPLICATION IN BIOCOMPATIBLE ENVIRONMENT**
Fedirko V., Pohreliuk I., Yaskiv O., Mynyk S. **287**

**III73 TECHNOLOGY OF PRODUCING THE SMOOTH POWDER BUSHES WITH HIGH DENSITY**
Ryabicheva L.A., Tsirkin A.T., Khichenko V.F. **289**

**III74 DIE FORGING OF COPPER FIBRES**
Ryabicheva L.A., Tsyrkyn A.T., Losiev U.A. **291**

**III106 DESIGNING AN AUTOMATIC MACHINE FOR ELECTROSPARK ALLOYING OF STEEL**
Nikolenko S.V., Verchoturov A.D., Kovalenko S.V. **293**

**III110 THE METHODS OF COMBUSTION CHAMBER WALL PROTECTION FROM INFLUENCE OF HIGH-INTENSIVE HEAT FLOW**
Arinkin S.M. 295

**III151 SYNTHESIS OF TERNARY GRAPHITE-LIKE PHASES IN THE B-C-N SYSTEM**
Lyashenko V.I., Tomila T.V., Zelyavskii V.B., Krushinskaya L.A., Kurdyumov A.V. 296

**III152 DEVELOPMENT OF METHODS OF DEPOSITION OF DISCONTINUOUS NICKEL COATINGS ON POWDERS OF $AB_5$ TYPE ALLOYS**
Slys I., Shcherbakova L., Rogozinskaya A., Shchur D., Rogozinskii A. 298

**III157 DIFFUSION BONDING APPLICATION FOR MANUFACTURING OF OXIDE CERAMICS JOINTS IN AIR ATMOSPHERE WITH THE USE OF PLATINUM OR PALLADIUM GASKETS**
Naidich Yu.V., Gab I.I., Stetsyuk T.V., Kurkova D.I. 300

**III167 ANTIFRICTION COMPOSITION MATERIALS WITH ULTRADISPERSE DIAMOND POWDERS OBTAINED BY CONVENTION AND ELECTRODISCHARGE SINTERING**
Istomina T.I., Dubrova O.E.(1), Volkogon V.M., Raychenko O.I., Pavlitchuk T.V., Kostenko A.D. 302

**III171 MODERN METHODS OF SYNTHESIS OF A SUPERCONDUCTIVE MATERIAL AND ITS PROPERTIES**
Flis A.A. 304

**III188 MELT-SINTERING PROCESSING OF HYDROXYAPATITE BIOCOMPOSITES**
Ivanchenko L.A., Fal'kovs'kaja T.I.(1), Pinchuk N.D., Blyznuk O.V.(1) 306

**III192 FEATURES OF THE FORMATION OF SOLID SOLUTIONS OF TITANIUM CARBIDE WITH CARBIDES OF SOME TRANSITION METALS**
Prilutskiy E.V., Makarenko G.N., Kud' I.V., Fedorus V.B., Likhoded L.S., Eremenko L.I. 308

**III193 FINE BORON CARBIDE POWDERS AND WHISKERS FOR CERAMIC**
Prilutskiy E.V., Liashenko V.I., Tkachenko Yu.G. 310

**III198 THE APPLICATION OF CONCENTRATED LIGHT RADIATION FOR DEVELOPMENT OF TECHNOLOGICAL METHODS OF THE HIGH-TEMPERATURE MELTING OF OXIDE COMPOUNDS**
Frolov A.A., Andrievskaja E.R., Lopato L.M. 312

**III209 THE USAGE OF TITANIUM HYDRIDE FOR THE PREPARATION WEAR RESISTANCE COMPOSITE COATING**
Guslienko Y.A., Luchka M.V., Kostenko V.K., Meduch R.M. 314

**III243 STRUCTURE AND PROPERTIES OF MAGNETRON FILMS USING ADVANCED COMPOSITE AlN-$TiCrB_2$ CERAMICS**
Teplenko M.A., Panasyuk A.D., Podchernyaeva I.A., Boltovets N.S.(1), Ivanov V.N.(1) 316

**III246 STUDY OF INFLUENCE OF BORON STATE AS INITIAL REAGENT ON MODE OF BORON SUBOXIDE SYNTHESIS AND ITS PROPERTIES**
Kharlamov A.I., Khotynenko N.G., Kirillova N.V.(1), Trapalis Ch.(2), Fomenko V.V.(3), Goydina S.V., Shatscikh C.K., Gubareni N.I. 317

**III268 STRUCTURE AND PROPERTIES OF RAPIDLY COOLED FIBRES PRODUCED BY EXTRACTION FROM A MELT OF METALS**
Smetkin A.A., Haidarshin A.F. 319

**III284 SYNTHESIS OF NANOCRYSTALLINE $ZrO_2$-X MOL.% $Y_2O_3$ POWDER**
Kobylinska O.V., Labunets T.F., Karpetz M.V., Ragulya A.V. 321

**III289 COMBINATION OF SHS AND MECHANOCHEMICAL ACTIVATION FOR NANOPOWDER TECHNOLOGIES**
Grigorieva T.F., Korchagin M.A., Lyakhov N.Z. 323

**III290 STAGE SEQUENCE IN MECHANOCHEMICAL SYNTHESIS OF NANOMETRIC SOLID SOLUTIONS IN METAL SYSTEMS**
Grigorieva T.F., Barinova A.P., Boldyrev V.V. 324

**III291 PROPERTIES OF ULTRAFINE SUPERSATURATED SOLID SOLUTIONS OBTAINED BY MECHANICAL ALLOYING**
Grigorieva T.F., Barinova A.P., Belykh V.D., Boldyrev V.V., Lyakhov N.Z. 325

**III299 FUSIBLE UNDERLAYERS DURING DEPOSITION OF THERMAL COATINGS**
Kuprianov I.L. 326

**III300 ELECTRODEPOSITION OF MOLYBDENUM CARBIDE ON THE SUFACE OF SEMICONDUCTORS FROM IONIC MELTS**
Gab A.I., Uskova N.N., Malyshev V.V.(1) 327

**III301 CHARACTERIZATIONS OF THERMAL SPRAYED BRONZE COATINGS FOR BEARING APPLICATIONS**
Ilyuschenko A.Ph., Koval V.A., Beliaev A.V. 329

**III318 STRUCTURE AND PROPERTIES OF $Al_2O_3$ AND $Al_2O_3$+$Cr_2O_3$ COATINGS DEPOSITED TO STEEL 3 (0.3wt.%C) SUBSTRATE USING PULSED DETONATION TECHNOLOGY**
Pogrebnjak A.D.[1], Tyurin Y.N., Zadkevich M.L. 331

**III321 INVESTIGATION OF IMPULSE-PLASMA TREATMENT PROCESSES FOR THERMAL SPRAYED PROTECTIVE COATINGS**
Ilyuschenko A., Shevtsov A., Okovity V., Astashynski V.[1], Chivel Yu.[1], Steinhauser S.[2] 333

**III326 FORMATION OF GRADIENT STRUCTURE-PHASE STATES AT CRYSTALLIZATION OF FERRITE STEEL DURING WELDING**
Gagauz V.P., Kovalenko V.V., Tsellermaer V.Ya., Gromov V.E., Kozlov E.V.[1], Konovalov S.V. 335

**III330 FORMATION OF GRADIENT STRUCTURE–PHASE STATES AT ROLLING OF BIG DIAMETER ARMATURES**
Yuriev A.B., Gromov V.E., Kovalenko V.V., Kozlov E.V.[1], Plevkov A.V.[1], Konovalov S.V. 337

**III338 THE EFFECT OF MECHANICAL ACTIVATION ON THE PHASE FORMATION PROCESSES DURING SELF-PROPAGATING HIGH-TEMPERATURE SYNTHESIS OF BARIUM HEXAFERRITE**
Vityaz P.A., Talako T.L., Okatova G.P., Beliaev A.V., Letsko A.I., Kuznetsov M.V.[1], Morozov Yu.G.[1] 339

**III345 SOME FEATURES OF FORMING THE DETONATION COATINGS VK-15 IN ROTOR PARTS OF HIGH-DUTY GTES**
Sergeyev V.V., Spiridonov Yu.L., Lunyov A.N.[1] 341

**III351 DENTAL IMPLANTS FABRICATED BY SELECTIVE LASER PROCESSING OF TITANIUM POWDERS**
Tolochko N.K., Savich V.V.[1], Artushkevich A.S.[2], Laoui T.[3], Froyen L.[4], Kruth J.-P.[4], Onofrio G.[5], Signorelli E.[5] 343

**III352 SYNTHESES OF NEW COMPOSITE CERAMIC AND METAL-CERAMIC MATERIALS IN COMBUSTION MODE**
Okrostvaridze O., Tavadze G., Khvadagiani A., Lekishvili K., Sahvadze D. 345

**III364 ZIRCONIUM DODECABORIDE SINGLE CRYSTAL GROWTH**
Paderno Yu.B., Layshchenko A.B., Filippov V.B., Duhnenko A.V. 347

**III381 OBTAINING OF MONO- AND BIMETAL DISPERSE POWDERS BY ELECTROLYSIS AND SEGMENTATION**
Kunty O.I., Sribny V.M.[1], Minakova R.V.[2], Kozak S.I. 349

**III388 DEVELOPMENT OF TECHNOLOGY OF COHESION OF METALLIC DENTAL BODY WITH POLYMERS AND CERAMICS**
Besov A.V. 351

**III359 ON PRODUCTION OF SEMICONDUCTIVE SILICON: ANALYSIS OF WASTE AND METHODS OF RECYCLING THEM**
Galieva J.N., Stepanenko N.V.[1], Bondaruk O.N. 353

# VOLUME II

Pages

## *SECTION II. PERSPECTIVE MATERIALS OF FUNCTIONAL AND STRUCTURAL PURPOSES: POSSIBILITIES OF OBTAINING NE LEVEL OF PROPERTIES* 359-646

**II308 UNMIXED SYSTEMS AS THE NEW CLASS OF PERSPECTIVE MATERIALS FOR MODERN TECHNIQUE**
Bashev V.F., Dotsenko F.F., Ryabtsev S.I., Beletskaya O.E., Kutseva N.A., Balyuk Z.V. 359

**II239 ELECTRON BEAM WELDING OF γ-TITANIUM ALUMINIDE**
Zamkov V.N., Sabokar V.K., Vrzhyzhevsky E.L. 361

**II162 ADVANCED LIGHT ALLOYS METALLIC SYSTEMS FOR THE FUTURE: PROGRESS IN HIGH-CURRENT ELECTRONICS AND DYNAMIC (STRUCTURAL) APPLICATIONS**
Tkachenko V.G. 363

**II175 POWDER TITANIUM INTERMETALLIDES**
Ivanova I.I., Demidik A.N. 365

**II29-30 AN INFLUENCE OF COOLING RATE AND OVERHEATING OF A MELT ON STRUCTURE AND MECHANICAL BEHAVIOR OF Ti-Si CAST ALLOYS**
Mazur V., Miracle D.[(1)], Kapustnikova S., Shportko A., Podrezov Yu.[(2)], Bega N.[(2)], Levitsky M.[(3)], Miroshnichenko V.[(3)] 367

**II225 HIGH-STRENGTH ALUMINUM-BASED ALLOYS HARDENED BY QUASICRYSTALLINE NANOPARTICLES**
Lotsko D.V., Milman Yu.V., Miracle D.B.[(1)], Sirko O.I., Yefimov M.O., Bilous A.M., Danylenko M.I., Neikov O.D., Voropayev V.S. 371

**II91 LOW TEMPERATURE MECHANICAL PROPERTIES OF BULK NANOSTRUCTURED TITANIUM PROCESSED BY SEVERE PLASTIC DEFORMATION**
Bengus V.Z., Tabachnikova E.D., Natsik V.D. 373

**II307 HIGHLY EFFECTIVE DISPERSION STRENGTHENED MATERIAL BASED ON COPPER POWDER OF DISCOM® TRADE MARK FOR CURRENT REMOVING INSERTS OF PANTOGRAPHS OF HIGH SPEED ELECTRIC TRAIN**
Shalunov E.P., Lipatov Ya. M., Wendland St.[(1)], Shalunova N.B. 375

**II183 HIGH-STRENGTH RAPIDLY SOLIDIFIED P/M ALUMINUM ALLOYS**
Neikov O.D., Milman Yu.V., Sirko A.I., Lotsko D.V., Zakharova N.P., Danylenko M.I., Laptev A.V., Patsyna R.V., Tokhtuev V.G., Voropaev V.S., Samelyuk A.V. 377

**II390 COMPACTING DYNAMICS OF THE WC-Co CEMENTED CARBIDES DURING HOT IMPULSE PRESSING IN VACUUM**
Kovalchenko M.S., Laptev A.V. 379

**II373 GLASS-COMPOSITE ABRASIVE-CONTAINING MATERIALS OF TOOL ASSIGNMENT**
Shilo A., Bondarev E., Kukharenko S. 381

**II343 SUPERHARD CARBON FILMS WITH PREDOMINANTLY $SP^2$ BONDS**
Kulikovsky V., Bohac P.[(1)], Kurdyumov A., Jasrabik L.[(1)] 382

**II342 PERSPECTIVES OF NANOSTRUCTURE MATERIALS APPLICATION FOR CUTTING AND PRODUCTION OF A WIRE**
Panov V.S., Malochkin O.V. 384

**II365 STRUCTURAL ENGINEERING OF NANOCRYSTALLINE MATERIALS FOR CONSTRUCTION APPLICATION**
Podrezov Yu.N. 385

**II104 MULTISTAGE HIGH STRAIN RATE SUPERPLASTICITY OF MICROCRYSTALLINE ALLOYS**
Kamalov M.M., Myshlyaeva M.M., Medvedev A.S., Myshlyaev M.M.[(1)] 387

**II156 DEVELOPMENT OF HIGH-HARDNESS WEAR RESISTANT BORON-CONTAINING COMPOSITE MATERIALS**
Makarenko G.N., Timofeeva I.I., Bykov A.I., Gridneva I.V., Fedorus V.B., Buzhenets E.I., Isaeva L.P. 389

**II245 WEAR-RESISTANT COMPOSITE MATERIALS AND PARTS, MANUFACTURED BY HOT PRESSURE TREATMENT**
Serdyuk G.G., Sakhnenko A.V., Pavligo T.M., Svistun L.I.[(1)], Plomodyalo R.L.[(1)], Plomodyalo L.G.[(2)] 391

**II174 NONCARBON NANOTUBES AND THEIR 2D CRYSTALS. REVIEW.**
Pokropivny V.V. 393

**II41 FERRITIC STEEL INTERCONNECT FOR REDUCED TEMPERATURE SOFC**
Shemet V., Pirón Abellán J., Singheiser L., Quadakkers W.J. 395

**II370 ANALYSIS STRESS-STRAIN STATE OF DIAMOND-SiC COMPOSITE MATERIAL**
Grygoryev O.M., Stepanenko A.V., Bega M.D. 397

**II230 HIGHLY TEXTURED POLYCRYSTALS OF DIAMOND-LIKE PHASES OF BN**
Britun V.F., Kurdyumov A.V., Petrusha I.A.[(1)] 399

**II319 THE STRUCTURE AND PROPERTIES OF A HARD ALLOY COATING DEPOSITED BY HIGH-VELOCITY PULSED PLASMA JET ONTO A COPPER SUBSTRATE**
Tyurin Yu.N., Pogrebnyak A.D.[(1)], Zadkevich M.L., Kolisnichenko O.V. 401

**II17 HYDROGEN-OXYGEN INTERPLAY IN HYDRIDES OF OXYGEN-STABILIZED Zr- AND Ti-BASED INTERMETALLIC COMPOUNDS**
Zavaliy I.Yu. 403

**II26 ADVANCE CERAMIC: SELF STRENGTHENING EUTECTIC REFRACTORY COMPOUND COMPOSITES, PRESENT AND FUTURE**
Paderno Yu.B., Paderno V.N., Filippov V.B. 404

**II297 HIGH-PRESSURE SYNTHESIZED $MgB_2$ WITH HIGH CRITICAL CURRENT DENSITY AND IRREVERSIBLE FIELD, POSITIVE INFLUENCE OF Ta ON SUPERCONDUCTIVE CHARACTERISTICS**
Prikhna T.A.[(1)], Gawalek W.[(2)], Savchuk Ya.M.[(1)], Sergienko N.V.[(1)], Moshchil V.E.[(1)], Dub S.N.[(1)], Wendt M.[(2)], Melnikov V.S.[(3)], Surzhenko A.B.[(2)], Litzkendorf D.[(2)], Nagorny P.A.[(1)], Schmidt Ch.[(2)] 406

**II196 SILVER-CARBON COMPOSITE MATERIALS HIGH IN CARBON. STRUCTURE AND PROPERTIES**
Minakova R.V., Zatovskiy V.G., Kryachko L.A., Lukovich V.V., Kartuzov V.V., Golovkova M.E., Yenevich V.G., Susidko V.L.[(1)] 408

**II46 ORGANIC-INORGANIC NANOSTRUCTURAL COMPOSITE COATINGS PREPARED BY SOL-GEL PROCESSING**
Shilova O.A., Tarasyuk E.V., Shevchenko V.V.[(1)], Klimenko N.S.[(1)], Hashkovsky S.V., Shilov V.V[(1)] 410

**II205 THE MODERN TENDENCIES OF R&D IN THE FIELD OF BIOCERAMICS BASED MATERIALS**
Dubok V.A., Shevchenko E.A., Shinkaruk A.V. 412

**II149 LITHIUM-CONDUCTING SOLID ELECTROLYTES BASED ON SOLID SOLUTIONS $La_{2/3-x}Li_{3x4/3-2x}Me_2O_6$ (Me=Nb; Ta)**
Gavrilenko O.N., Belous A.G., Pashkova Y.V. 414

**II260 DIELECTRIC CERAMICS BASED ON COMPLEX NIOBATES $La_{2/3-x}Na_{3x}Nb_2O_6$ AND $Nd_{2/3-x}Na_{3x}Nb_2O_6$**
Ovchar O.V., Mischuk O.D. 416

**II294 INVESTIGATION OF PROPERTIES OF CASTED METALLIC COMPOSITE MATERIALS**
Kondratenko V., Kasakov S.[(1)], Knokhin V.[(1)], Vinoviy V.[(2)] 418

**II129 NEW LEVEL OF MATERIAL PROPERTIES FOR AUTOMOBILE AND TRACTOR FRICTION ASSEMBLIES**
Dmitrovich A.A. 420

**II212 MAGNETIC PROPERTIES OF CONDENSED MATTER**
Lashkarev G.V. 422

**II69 NANOCRYSTALS OF SEMICONDUCTORS IN ORDERED ORGANIC MATRICES: GROWTH AND PROPERTIES**
Savin Yu.N., Tolmachev A.V. 423

**II64 DEVELOPMENT OF MULTILAYERED $Si_3N_4$–BASED CERAMIC COMPOSITES HAVING AN ABILITY TO ARREST CRACKS**
Gogotsi G.A., Lugovy M.I.[(1)], Slyunyayev V.N., Orlovskaya N.A.[(2)] 425

**II99 CREATION OF HEAT-INSULATION OF INTERNAL SURFACES OF ELEMENTS OF INTERNAL-COMBUSTION ENGINES WASTEGATE LINE**
Ved V. 427

**II113 SYNTHESIS AND INVESTIGATION OF COMPLEX REFRACTORY OXIDES WITH SPHENE AND PSEUDOBROOKITE STRUCTURE**
Grigoryan R., Grigoryan L.[1] 429

**II47 SOME ASPECTS OF THERMOEXFOLIATED GRAPHITE PRODUCTION AND ITS APPLICATION**
Kozhan O.P., Bondarenko B.I., Kurganskyi M.P., Sergienko O.A., Korsak Yu.V., Strativnov V. 431

**II4 ASSESSMENT OF THE STATE OF THE BINDER PHASE OF WC-Co CEMENTED CARBIDES BY THEIR FRACTURE TOUGHNESS**
Loshak M.G., Alexandrova L.I. 433

**II8 ECONOMICALLY REINFORCED CAST COMPOSITE MATERIAL (CCM) - SUCCESSFUL TECHNOLOGICAL DECISION FOR MASS MACHINE BUILDING**
Zatulovsky S.S., Kostornov A.G.[1], Zatulovsky A.S., Kosinskaia A.V., Kostenco A.D.[1], Sharai E.V. 435

**II11 MECHANICAL PROPERTIES OF THE COMPOSITES IN-SITU BASED ON TITANIUM-BORIDE EUTECTIC**
Velikanova T.Ya., Bilous O.O., Bondar A.A., Artyukh L.V., Firstov S.A., Miracle D.[1] 437

**II18 EFFECT OF OXYGEN MODIFICATION AND HDDR-PROCESS ON ELECTROCHEMICAL CHARACTERISTICS OF METAL HYDRIDE ELECTRODES BASED ON TITANIUM–NICKEL ALLOYS**
Saldan I.V., Zavaliy I.Yu. 438

**II19 WORK UP OF A NEW POWDERED MATERIAL FOR SUPPORTS OF SUBMERGED ELECTRIC MOTORS**
Kurilov G.V. 439

**II32 SOME PECULIARITIES OF TITANIUM ALUMINIDE PRODUCING BY THE METHOD OF ELECTROSLAG REMELTING**
Ryabtsev A.D., Troyansky A.A., Pashynsky V.V., Mastepan V.Yu. 441

**II33 DEVELOPMENT OF ADVANCED TECNOLOGIES FOR PRODUCTION OF HARD ALLOY ROLLS FOR MODERN ROLLING MILLS**
Pashynsky V.V., Sydorenko D.G.[1], Kulik A.I.[1], Kashyryn V.P.[1] 443

**II42 INFLUENCE OF HIGH PRESSURE AND NITROGEN ON STRUCTURAL KINETIC MODIFICATIONS IN AUSTENITE OF Fe-Cr-Mn-Ni ALLOY**
Bilousov M.M. 445

**II45 UNIDIRECTIONAL SOLIDIFICATION AND COLD-ROLLING OF NON-STOICHIOMETRIC TWO PHASE Ni-RICH SUPERALLOYS**
Borodians'ka H.Yu., Kotko A.V., Hirano T.[1] 447

**II53 BIOMIMETIC RECEPTION OF HYDROXYAPATITE COATINGS**
Kryshanovska A.S., Korovnikova N.I., Savin Yu.N., Tolmachev A.V. 451

**II54 NANOCRYSTALLINE DIAMOND-SiC CERAMICS**
Ekimov E.A., Palosz B.[1], Lojkowski W.[1], Gierlotka S.[1], Filonenko V.P., Antanovich A.A., Kuzin N.N., Slesarev V.N. 452

**II70 LOW TEMPERATURE PLASTIC BEHAVIOR OF THE $Zr_{46.8}Ti_{8.2}Cu_{7.5}Ni_{10}Be_{27.5}$ BULK AMORPHOUS ALLOY**
Tabachnikova E.D., Bengus V.Z., Natsik V.D., Macht M.[1], Miskuf J.[2], Csach K.[2] 454

**II76 COPPER DOPED BISMUTH SELENIDE AS ACTIVE CATHODE MATERIAL FOR LITHIUM BATTERIES**
Zaslonkin A.V., Kovalyuk Z.D., Mintyanskii I.V., Savitskii P.I. 456

**II77 PROTON INTERCALATES: OPTICAL PROPERTIES AND THERMALLY STIMULATED DEINTERCALATION OF HYDROGEN**
Boledzyuk V.B., Kovalyuk Z.D., Pyrlya M.M. 458

**II81 FORMATION AND CONDUCTIVITY OF OXIDES IN THE SYSTEM $La_{2-x}NiO_4$**
Nedilko S., Kulichenko V., Dziazko A. 460

**II82 EFFECT OF STRUCTURAL FEATURES OF $Sm_{1+x}Ba_{2-x}Cu_3O_y$ HIGH-TEMPERATURE SUPERCONDUCTORS ON CRITICAL TEMPERATURE**
Drozd V.A., Baginsky I.L., Nedilko S.A., Nischenko M.M.[1], Likhtorovich S.P.[1] 462

**II83 STRUCTURAL ANALYSIS OF NON-CRYSTALLINE POLYMER FOLLOWING EXAMPLE OF POLYVINILTRIMETHYLSILANE**
Polikarpov V.M., Korolev U.M.[1] 464

**II88 SYNTHESIS AND PHASE TRANSITIONS OF AMORPHOUS $C_3N_4$ POWDERS UNDER HIGH PRESSURE**
Khabashesku V.N.[1,2], Brinson B.[2], Margrave J.L.[2], Davydov V.A.[3], Kashevarova L.S.[3], Rakhmanina A.V.[3], Yakovlev E.N.[3], Filonenko V.P.[3] 465

**II89 OXYGEN PACKING IN HIGH PRESSURE OXIDES OF W, Ta, Nb**
Filonenko V.P., Zibrov I.P.[1] 467

**II97 COMPARATIVE ANALYSIS OF BRITTLENESS OF ANNEALED METALLIC GLASS BY BOTH MICROINDENTATION AND U – METHOD**
Ushakov I.V., Feodorov V.A., Permyakova I.J. 469

**II105 RECEPTION AND RESEARCH OF PROPERTIES OF HEAT RESISTING CERAMICS ON A BASIS ZIRCONIUM DIOXIDE'S, STABILIZED OXIDES ALKALI-EARTH METALS OF METALS**
Nikolenko S.V., Verchoturov A.D., Vlasova N.M. 471

**II112 PRINCIPLES FOR CREATION OF NEW ADVANCED HIGH-STRENGTH CAST EUTECTIC ALUMINUM ALLOYS**
Barabash O.M., Milman Yu.V.[1], Korzhova N.P.[1], Legkaya T.N.[1], Podrezov Y.N.[1], Voskoboinik I.V.[1] 473

**II115 REFRACTORY PERMEABLE THERMAL INSULATION: PRODUCTION AND APPLICATION**
Gorin A.I. 475

**II121 NEW EUTECTIC MATERIALS OF THE TERNARY SYSTEM Al-Ti-Cr BASED ON THE INTERMETALLIC $Al_3Ti_{1-x}Cr_x$**
Barabash O.M., Milman Y.V.[1], Miracle D.B.[2], Karpets M.V.[1], Korzhova N.P.[1], Legkaya T.N., Mordovets N.M.[1], Podrezov Y.N.[1], Voskoboinik I.V.[1], Voynash V.Z. 476

**II122 HOT DEFORMATION OF HOT-RESISTANCE SILICIDE-HARDENED TITANIUM-BASED ALLOY**
Kuzmenko N.N., Kulak L.D., Baglyuk G.A. 478

**II123 PROPERTIES AND THE STRUCTURAL CONDITION OF COMPOSITES WC-Ni WITH THE ULTRAHIGH MAINTENANCE OF THE SHEAR OBTAINED BY THE METHOD OF ELECTRON BEAM ZONED SINTERING**
Bondarenko V.P., Zankevich A.B., Jurchuk N.A., Asnis E.A.[1], Zabolotin S.P.[1] 480

**II124 EFFECT OF ZIRCONIA(+CaO) CONTENT AND SINTERING TIME ON DENSIFICATION AND MECHANICAL STRENGTH OF ALUMINA-ZIRCONIA COMPOSITE**
Gavriliu G., Diaconescu M., Ţârdei C. 482

**II131 INFLUENCE OF NANOSTRUCTURE STATES ON MAGNETIC PROPERTIES OF FINE POWDES OF ALLOYS BASED ON CUPPER**
Chuistov K.V., Efimova T.V., Zalutskiy V.P., Perekos A.E., Ruzhitskaya T.V. 483

**II138 THE FORMATION OF THE SUPERHARD MATERIALS BASED ON NANODIAMOND**
Senyut V. 485

**II141 NEW CERAMIC $ABO_3$–MATERIALS FOR FABRICATION OF FUEL CELLS AND HEATING DEVICES COMPONENTS**
Gorbunova V.A.[1], Gorbunov A.V., Novikov G.I.[1], Gamanovitch N.M.[1] 487

**II145 HARD ALLOYS WITH STRUCTURAL GRADIENT FOR DRILLING TOOLS EDGES**
Florea C., Florea A. 489

**II146 PREPARATION OF BENZENE-STABILIZED COBALT NANOPARTICLES IN HYDROGEN ATMOSPHERE**
Normatov I.Sh. 490

**II150 SOLID-STATE CONSOLIDATION OF WC-Co HARDMETALS. PECULIARITIES AND PROSPECTS**
Laptev A.V. 491

**II153 STUDY OF HEAT RESISTANCE SOME INTERMETALLIDES, CONTAINING A CHROMIUM**
Oryshich I.V., Poryadchenko N.E., Brodnikovskij N.P., Krapivka N.A. 493

**II155 FEATURES OF THE BEHAVIOR OF TITANIUM NITRIDE NANOPOWDERS DURING SINTERING UNDER THE CONDITIONS OF HIGH PRESSURES**
Bykov A.I., Timofeeva I.I., Klochkov L.A., Ragulya A.V., Gridneva I.V. 495

**II158 THERMODYNAMIC PROPERTIES OF $LaNi_{4.5}Cu_{0.5}$ AND $LaNi_{4.5}Mn_{0.5}$ IN THE WIDE TEMPERATURE RANGE**
Gorbachuk N.P., Skrypai A.A., Muratov V.B., Bolgar A.S. 496

**II163 INFLUENCE OF TEMPERATURE ON FORMATION OF TRIBOTECHNICAL PROPERTIES OF REFRACTORY COMPOUNDS**
Tkachenko Yu.G. 498

**II164 MATERIAL SCIENCE ASPECTS OF MATERIALS FOR SPARK HARDENING**
Bovkun G.A., Tkachenko Yu.G., Laptev A.V. 500

**II168 ENERGETIC CHARACTERISTICS OF FULLERENES AND FULLERENE-LIKE SUBSTANCES**
Goryachev Y.M., Dekhteruk V.I., Siman M.I., Fiyalka L.I., Shvartsman O.Y. 502

**II170 WEAKENING OF POROUS TITANIUM-SILICEOUS CARBIDE $Ti_3SiC_2$ AT ACTIVE AND STATIC LOADING**
Firstov S.A., Ivanova I.I., Pechkovsky E.P. 504

**II177 INFLUENCE OF TRIBOSYSTEM COMPONENTS ON THE FRICTION BEHAVIOR OF Al-Cu-Fe QUASICRYSTAL**
Grinkevych K.E., Lotsko D.V., Milman Yu.V., Bykov O.I., Shurygina Z.P., Ponomarev S.S., Bilous A.M., Yefimov M.O. 506

**II178 THE OPTIMAL DESIGN OF IMPLANTS CONTENT AND SHAPE ON THE COMPUTER MODELLING BASE**
Mikhailov O.V., Tkachenko L.N., Shtern M.B., Dubok V.A. 508

**II189 STRUCTURE OF THIN FILMS AND EXTREMELY GRINDED POWDERS OF FULLERENE $C_{60}$**
Solonin Yu.M., Grayvoronskaya E.A. 509

**II194 THE AFFECT OF CONCENTRATED SOLAR RADIATION INTO THE SIALON CERAMICS IN THE AIR**
Neshpor I.P., Panasiyuk A.D., Liydvinskaya T.A. 511

**II197 INFLUENCE OF SILICONORGANIC ADDITIONS ON COMPOSITION MATERIALS PROPERTIES**
Kostornov A.G., Beloborodov I.I., Sukhostavets S.V. 512

**II199 THE SEMI-DRY CERAMIC POWDER ROLLING**
Radchenko A.K. 513

**II200 PERFORMANCES OF ELECTRODES FROM Ag AND COMPOSITION Ag-C FOR SHAPING ELECTROSPARK LAYERS**
Kryachko L.A. 514

**II201 ON THE POSSIBILITY OF THE $Pb(Ti, Zr)O_3$ THIN FILMS PRODUCING BY THE REACTION SYNTHESIS**
Andreeva A.F., Kasumov A.M., Utkin S.V., Frenkel O.A. 516

**II202 THE USAGE PERSPECTIVES OF THE THIN FILMS OF THE RARE-EARTH METALS OXIDES**
Andreeva A.F. 517

**II203 THE STRUCTURE AND THE PROPERTIES OF THE THIN IRON FILMS PREPARED BY MAGNETRON SPUTTERING**
Andreeva A.F., Dvoynenko O.K., Kasumov A.M., Statsenko V.M. 518

**II204 WEAR- AND CORROSION RESISTANT POWDER MATERIALS ON THE BASE OF TUNGSTEN-FREE HARD ALLOYS AND CARBIDE STEELS**
Maslyuk V.A., Napara-Volgina S.G. 519

**II214 STUDY OF THE EFFECT OF THERMAL TREATMENT ON THE STRUCTURE AND PROPERTIES OF Ti-Al-Si-Zr SYSTEM ALLOYS**
Datskevich O., Kulak L., Miracle D.[(1)], Senkov O.[(1)], Firstov S. 521

**II216 INVESTIGATION OF THE HEAT CAPACITY AND ENTHALPY OF $Bi_2Se_3$ AND $Bi_2Te_3$ IN THE TEMPERATURE RANGE 58-1012 K**
Gorbachuk N.P., Bolgar A.S., Sidorko V.R., Goncharuk L.V. 523

**II219 STRUCTURE-PHASE TRANSFORMATION IN THE CONTACT WORKING LAYER MATERIALS AND EROSION STABILITY OF THEM**
Minakova R.V., Chomenko E.V., Kryachko L.A. 525

**II220 DEFORMATION AND FRACTURE OF HIGH-STRENGTH ALLOYS BASED ON Al-Zn-Mg-Cu SYSTEM**
Lotsko D.V., Milman Yu.V., Ivashchenko R.K., Sirko O.I., Samelyuk A.V., Sarzhan G.F. 527

**II221 PROPERTIES OF CERAMIC COMPOSITES BASED ON $Si_3N_4$-TiN**
Sartinska L.L., Gnesin G.G., Osipova I.I. 529

**II222 THE STRUCTURE AND MECHANISM OF WEAR OF COMPOSITES ON THE BASE OF TITANIUM NITRIDE IN DRY FRICTION IN AIR**
Evtushok T.M., Kostenko A.D., Grigorev O.N., Zhunkovskii G.L., Kotenko V.A., Shaposhnikova T.I. 531

**II224 STRUCTURE OF RAPIDLY SOLIDIFIED Al-13at.%Sc ALLOYS**
Yefimov M.O., Miracle D.B.[(1)], Milman Yu.V., Lotsko D.V., Slipenyuk A.N., Kuprin V.V., Danylenko M.I. 533

**II226 EFFECT OF SMALL ADDITIONS OF TRANSITION METALS ON THE STRUCTURE of Al-Zn-Mg-Zr-Sc ALLOYS**
Lotsko D.V., Milman Yu.V., Yefimov M.O., Mordovets N.M., Rachek O.P., Trofimova L.M.[(1)] 535

**II227 INFLUENCING OF PLASTIC DEFORMATION ON MECHANICAL BEHAVIOR OF Ti-Al-Si-Zr ALLOYS**
Kuzmenko M.M., Verbylo D.G., Koval' O.Yu. 537

**II228 FEATURES OF FORMING OF INTERMETALLIC COMPOUNDS IN A ZONE OF CONTACT CHROME - COATING FROM METAL OF IV GROUP**
Zykova E.V., Dubikovsky L.F., Brodnikovskyy M.P., Sameluk A.V., Dub S.N.[(1)] 539

**II229 RESEARCH OF DIFFUSION MOBILITY ON THE INTERFACE BETWEEN ELEMENTS OF SYSTEM Cr-Ti(Zr, Hf) AT THE TEMPERATURES 1373-1473 K**
Pisarenko V.A., Zubets Y.E., Sameluk A.V., Dub S.N.[(1)] 541

**II231 EFFECT OF CRYSTALLIZATION ON DEFORMATION OF ZrTiCuNi METALLIC GLASS INVESTIGATED BY NANOHARNDNESS TECHNIQUE**
Dub S.N.[(1)], Slipenyuk A.N., Milman Yu.V., Danylenko M.I. 543

**II232 STRUCTURE AND PROPERTIES OF THE WC+8 MASS % Ni CEMENTED CARBIDE FABRICATED BY PRESSURE FREE SINTERING AND HOT IMPULSE PRESSING IN VACUUM**
Kovalchenko M.S., Yurchuk M.O.[(1)] 545

**II234 RESEARCH OF IMPACT OF TECHNOLOGY OF RECEIVING FRAGILE MATERIALS ON THEIR STRENGTH UNDER UNI-BIAXIAL PRESSURE**
Okhrimenko G.[(1)], Dubikiwsky L. 547

**II240 THE INFLUENCE OF METAL-LUBRICANT ON COPPER BASIS ON THE STRUCTURE AND TRIBOTECHNICAL CHARACTERISTICS OF THE COMPOSITE ANTI-FRICTIONAL MATERIAL THAT WORKS IN THE VACUUM**
Kostomov A.G., Ficshich O.I., Chevychelova T.M., Kostenko A.D., Simeonova Y.[(1)] 549

**II241 MICROSTRUCTURAL MODIFICATION OF AS-CAST HYPOEUTECTIC Ti-Al-Si-Zr ALLOYS BY MICROALLOYING WITH ADDITIONAL ELEMENTS**
Gornaya I., Kulak L., Miracle D.[(1)], Senkov O.[(2)], Firstov S. 550

**II242 ACID RESISTANT CERAMICS ON THE BASE OF SLAG WASTES OF THE METALLURGY INDUSTRY AND WALL BRICK WASTES**
Vlasova M., Kakazey M., Gonzales-Rodriguez J.G., Dominguez G., Tomila T.[(1)], Kilimnik A.A.[(2)] 552

**II247 SIMPLEST SYNTHESIS OF FULLERENES USING ECONOMIC ARC DISCHARGE POWER SOURCE**
Chujko A.A., Dymenko V.V.[(1)], Kasumov M.M., Malashenkov S.P., Ogenko V.M., Paton B.E.[(1)] 554

**II248 PECULIARITIES OF PLASTIC DEFORMATION OF WC SINGLE CRYSTAL**
Milman Yu.V., Luyckx S.[(1)], Chugunova S.I., Goncharova I.V., Dub S.N.[(2)] 556

**II254 STRUCTURE AND PROPERTIES OF AL-8%Fe-3.4%Cr ALLOY PREPARED FROM RAPIDLY SOLIDIFIED MELT FLAKES**
Gornaya I., Kusmenko N., Kulak L., Miracle D.[(1)], Sarzhan G., Senkov O.[(1)], Firstov S. 558

**II259 DISTRIBUTION OF MANGANESE IONS AND ITS INFLUENCE ON THE PROPERTIES OF PTCR CERAMICS BASED ON BARIUM TITANATE**
V'yunov O., Kovalenko L., Belous A. 560

**II262 CARBIDE STEELS OF METASTABLE AUSTENITE STRUCTURE**
Latypov M.G. 562

**II265 FORMATION OF FULLERENES DURING SINTERING OF POWDER STEELS**
Antsiferov V.N., Grevnov L.M. 563

**II266 LIQUID-PHASE SINTERED SILICON CARBIDE BASED ON COMMERCIAL POWDERS**
Antsiferov V.N., Gilev V.G. 564

**II267 WEAR – RESISTANT POWDER MATERIALS WITH METASTABLE AUSTENITE STRUCTURE**
Antsiferov V.N., Smyshlyaeva T.V.[(1)] 566

**II269 CONCERNING DENTAL COATINGS ON TITANIUM SURFACE**
Kulmetyeva V.B., Porozova S.E., Belyaeva O.V.[(1)] 568

**II270 COMPUTER-AIDED DESIGN OF COMPOSITION AND STRUCTURE OF WC-Co CEMENTED CARBIDES – CANDIDATES FOR SOLID-PHASE HIGH-PRESSURE APPARATUSES**
Novikov N.V., Shestakov S.I. 570

**II271 THE IMPROVEMENT IN THE EFFICIENCY OF THE USE OF ENGINEERING CERAMICS FOR IMPACT-RESISTANT BARRIERS**
Shestakov S.I., Maystrenko A.L., Kulich V.G. 572

**II272 ON PHASE COMPOSITION OF ALUMINUM SURFACE TREATED IN THE ELECTROLYTIC PLASMA**
Fedorenkova L. 573

**II274 DEVELOPMENT OF SCIENTIFIC APPROACHES OF DERIVING OF COMPOSITE METAL MATERIALS BY A METHOD AT EXPLOSIVE ALLOYING**
Sitalo V.G., Usherenko S.M.[1], Gubenko S.I.[2], Bunchuk J.P. 575

**II276 COMPOSITES WITH ACTIVE COMPONENTS, IMMOBILIZED IN FILLER'S CRYSTALLINE LATTICE: THE NEW CONCEPT MATERIALS FOR ZONE OF FRICTION**
Paschenko E., Shilo A., Kukharenko S., Klimenko N. 577

**II278 IMPULSE THERMOSTABILITY OF COMPOSITE MATERIALS ON POLYMERIC BINDING**
Paschenko E., Silchenko Ya., Chernenko A. 579

**II279 GLASS-COMPOSITE ABRASIVE-CONTAINING MATERIALS OF TOOL ASSIGNMENT**
Shilo A., Bondarev E., Kukharenko S. 581

**II281 INFLUENCE OF VARIABLE MAGNETIC FIELD ON FORMATION OF SOLID SOLUTION DURING MECHANICAL ACTIVATION OF PURE Cu, Ni AND Fe POWDER MIX**
Prokopenko G.I., Mordyuk B.N., Efimova T.V., Perekos A.E., Ruzhitskaya T.V. 582

**II285 PECULIARITIES OF THE STRUCTURE OF QUASICRYSTALLINE Al-Cu-Fe COATINGS, PRODUCED BY EBPVD**
Ustinov A.I.[1,2], Movchan B.A.[1], Polischuk S.S.[2] 584

**II286 MECHANICAL AND THERMAL-PHYSICAL PROPERTIES OF DISPERSIBLE HARDENED MATERIALS ON THE BASIS OF POWDER COPPER**
Kolmogorov G.L., Mokretzov A.S., Gorokhov V.U., Ulrikh T.A. 586

**II288 SOME FEATURES OF THE MECHANICAL ALLOYING IN THE SYSTEMS Cu-Bi AND Fe-Bi**
Grigorieva T.F., Barinova A.P., Lyakhov N.Z. 588

**II292 MULTILAYER COMPOSITE STEEL FOR MODERN MACHINE-BUILDING**
Kondratenko V.M., Stovpchenko A.P.[1], Knohin V.N.[2], Kazakov S.S.[2] 589

**II293 METALLURGICAL METHOD FOR ADVANCED COMPOSITE WELDING WIRE MANUFACTURE**
Stovpchenko A.P., Panin V.N.[1], Polyakov V.A.[2] 591

**II296 ELECTRICAL CONDUCTIVITY OF POLYMERIC FILMS FILLED WITH Ni-CARBON FIBRES**
Shpilevskaya L.E., Safonova A.M. 593

**II298 SOLDERING OF MELT-TEXTURED YBCO USING Tm123 POWDER**
Prikhna T.A.[1], Gawalek W.[2], Moshchil V.E.[1], Sergienko N.V.[1], Surzhenko A.B.[2], Sverdun V.B.[1], Litzkendorf D.[2], Kordyuk A.A.[3], Melnikov V.S.[4], Dub S.N.[1], Alexandrova L.I.[1] 595

**II302 QUANTUM CHEMICAL SIMULATION OF NEW HYBRID NANOSTRUCTURES: SMALLER FULLERENES $C_{20}$ AND $C_{28}$ ENCAPSULATED INTO BORON-NITROGEN NANOTUBES**
Ivanovskaya V.V., Sofronov A.A., Enyashin A.N., Makurin Yu.N., Ivanovskii A.L.[1] 597

**II306 HEAT RESISTANT AND HEAT- AND WEAR-RESISTANT DISPERSION STRENGTHENED COMPOSIT MATERIALS ON A COPPER POWDER BASE OF DISCOM® TRADE MARK FOR VALVE GUIDES AND VALVE SEATS FOR DIESEL AND PETROL ENGINES**
Shalunov E.P., Orlov S.A.[1], Slavoljubov V.S.[2] 599

**II309 FEATURES OF MICROSTRUCTURE FORMATION AND MECHANICAL PROPERTIES OF Ti-B As-CAST ALLOYS**
Bankovskiy O., Beha N., Kulak L, Miracle D. [1], Senkov O. [1], Firstov S. 601

**II310 ADVANCED NANOSTRUCTURED MATERIALS BASED InN FILMS: PREPARATION, PROPERTIES AND POTENTIAL APPLICATION**
Goryachev Yu. M., Malakhov V.Ya., Rud B.M. 603

**II312 WEAR-RESISTANT W-C AND Cr-Ti-C PARTICULATE COMPOSITES**
Spiridonova I., Sukhova O., Butenko V. 605

**II315 THE INFLUENCE OF LITHIUM- AND ALUMINUM-CONTAINING ADDITIVES ON THE PROCESSES OF PHASE FORMATION DURING THE SILICON NITRIDE-BASED MATERIAL SINTERING**
Grigoriev O.N., Rogozinskaya A.A., Klochkov L.A., Krushinskaya L.A., Dubovik T.V., Zyatkevich N.S. 607

**II316 THE INFLUENCE OF VIBRO-MILLING ON THE PROPERTIES OF AIN-BN SYSTEM MATERIALS**
Kovalchenko M.S., Dubovik T.V., Rogozinskaya A.A., Panashenko V.M., Zyatkevitch N.S. 609

**II317 INTERACTION OF PULSED PLASMA WITH SURFACE LAYERS; PROCESSES OF IMPLANTATION AND MASS TRANSFER**
Tyurin Y.N., Pogrebnjak A.D.[1], Kshnjakin V.S.[1], Kolisnichenko O.V. 611

**II323 FORMATION OF COMPOSITE METAL MATERIALS IN CONDITIONS OF SHOCK-WAVE LOADING**
Usherenko S.M., Zel'dovich V.I.[1], Homskaja I.V.[1], Ovchinnikov V.I., Koval O.I. 613

**II325 SURFACE ALLOYING OF METALS BY IMPULSED HETEROGENEOUS PLASMA JETS**
Budovskikh E.A., Martusevich E.V. 615

**II335 HIGH-TEMPERATURE ANTIFRICTIONAL COMPOSITES**
Shevchuk U.F., Roik T.A.(1) 617

**II337 COMPOSITE MATERIALS FOR EROSION-CORROSION APPLICATIONS**
Ilyuschenko A.Ph, Belyaev A.V., Talako T.L., Formanek B.(1) 619

**II350 CERAMIC COMPOSITE MATERIALS FOR MICRO-ELECTRODES PRODUCED**
Sudnik L.V., Ananitch G.V.(1), Gorelik P.N.(1) 621

**II358 STRUCTURE AND MECHANICAL PROPERTIES OF Ti-Si-X IN-SITU COMPOSITES**
Firstov S., Koval' O., Kulak L., Kuzmenko M., Miracle D.(1), Podrezov Yu., Vasylyev O. 623

**II361 OXIDE CERAMIC MATERIALS ON THE BASIS OF COMPOSITIONS WITH LOW THERMAL EXPANSION**
Pavlikov V.N., Garmash E.P., Tkachenko V.D., Pleskach I.V., Maroresku I.I. 625

**II368 MECHANICAL BEHAVIOR OF $LaCoO_3$ PEROVSKITES FOR SOLID OXIDE FUEL CELL CATHODES**
Gogotsi G. A., Orlovskaya N.(1), Einarsrud M.-A.(2) 627

**II371 OPTIMISATION OF STRUCTURE OF ALLOYS OF THE SYSTEM Cu-Al-Ni-Me HAVING MARTENSITE TRANSFORMATION FOR WORK IN CONDITIONS OF SLIDING FRICTION**
Shcheretsky O.A., Novytskyy V.G., Lakhnenko V.L., Shumikhin V.S., Havryliuk V.P. 629

**II374 IMPULSE THERMOSTABILITY OF COMPOSITE MATERIALS ON POLYMERIC BINDING**
Paschenko E., Silchenko Ya., Chernenko A. 630

**II376 THE DEVELOPMENT OF THE STRUCTURAL-PHYSICAL BASES OF STRENGTH AND PLASTICITY OF LAMINATED MATERIALS AND HYBRID COMPOSITIONS ON THEIR BASIS**
Kolomiets A.T., Firstov S.A., Rogul T.G., Usakov E.I. 632

**II382 DEPOSITION OF a-C:H FILMS ON NON-CONDUCTING SUBSTRATES BY TWO DIFFERENT PACVD TECHNIQUES**
Varshavskayal.G., BukhovetsV.L., Ravi N.(1) 633

**II383 MICROSTRUCTURAL FEATURES AND MECHANICAL PROPERTIES OF Ti-Si AS-CAST ALLOYS**
Bankovskiy O., Beha N., Vasylyev O., Kulak L., Miracle D.(1), Senkov O.(1), Firstov S. 634

**II384 PROCESSES OF PHASE FORMATION IN SPARK COATINGS WITH UTILIZATION OF ELECTRODES ON BASE OF INTERMETALLIDES, NITRIDES AND CARBIDES**
Paustovsky A.V., Alfintseva R.A., Kirilenko S.N., Kurinnaya T.V., Gubin Yu.V., Novikova V.I. 636

**II392 PECULIARITIES OF MECHANICAL ACTIVATION OF TITANIUM IN THE PRESENCE OF WATER AND ALCOHOL**
Kharlamov A.I., Antonova M.M., Bobet J.L.(1), Khomko T.V., Ushkalov L.N., Fomenko V.V.(2), Kosourukov P.A. 638

**II393 MECHANOCHEMICAL TREATMENT AS AN EFFICIENT MEAN TO MODIFY SUBSTANCE TEXTURE**
Kharlamov A.I, Ushkalov L.N., Bobet J.L.(1), Gubareni N.I., Bondarenko M.E., Shipovskiy V.Yu. 640

**II80 REGULATION IN FORMATION OF STRUCTURE AND PROPERTIES IN DISPERSION-HARDENED COMPOSITE COPPER-BASED MATERIALS**
Plekhanov K.A., Danilov N.V., Mkrtychev Yu.G. 642

**II128 FORMATION OF NANOSTRUCTURE OF AMORPHOUS FILMS $As_xSe_{100-x}$ AND $Ge_xSb_{100-x}$ AT DISCRETE THERMAL COVERING**
Dubrovskaya G., Kolin'ko S., Kovtunenko V. 643

**II360 GLUE MATERIALS FOR CONVEYER ASSEMBLING**
Malysheva G.V. 645

***SECTION IV. CHARACTERIZATION OF MATERIALS PROPERTIES*** 649-728

**IV372 "SELF-ORGANIZATION" OF HEATING OF MATERIALS AT HEAT DESTRUCTION OF ITS SURFACE**
Frolov A.G. 649

**IV176 NANOMANIPULATION, NANOLITHOGRAPHY AND NANOASSEMBLING BY PROBE MICROSOCOPY. REVIEW**
Pokropivny A.V., Pokropivny V.V., Skorokhod V.V. 651

**IV327 DISLOCATION SUBSTRUCTURES EVOLUTION DURING FATIGUE TESTS OF AUSTENITIC STEEL**
Konovalov S.V., Kovalenko V.V., Sosnin O.V., Tsellermaer V.V., Gorlova S.N., Gromov V.E., Kozlov E.V.(1) 653

**IV328 EVOLUTION OF DISLOCATION SUBSTRUCTURE STAINLESS AUSTENITE STEEL DURING ELECTROSTIMULATED LOW-CYCLE FATIGUE**
Kovalenko V.V., Sosnin O.V., Gromov V.E., Konovalov S.V., Efimova I.E., Tsellermaer V.V., Ivanov Yu.F.[1], Kozlov E.V.[1] 655

**IV333 NEW METHODS AND MACHINE FOR TRIBOLOGICAL TESTS OF MATERIALS**
Shipitsa N.A., Zharin A.L., Saroka D.I. 657

**IV96 ACCOUNT OF ACOUSTIC EMISSION FEATURES AT STRENGTH DIAGNOSTICS OF POLYMERIC COMPOSITE MATERIALS**
Mileshkin M., Biblik I. 659

**IV21 DIAGNOSTICS OF FATIGUE DESTRUCTION OF MAGISTRAL PIPELINES**
Ovchinnikov I.N., Ermishkin V.A., Lepeshkin Y.D. 661

**IV50 EXOEMISSION DIAGNOSIS OF SURFACE LAYERS ON CONSTRUCTION MATERIALS**
Skilko A.M. 662

**IV55 FEATURES OF RESEARCHING STRUCTURE AND COMPOSITION OF THE THIN GLASSY FILMS PREPARED BY THE SOL-GEL METHOD**
Shilova O.A., Moshnikov V.A.[1], Maximov A.I.[1], Rumyantseva A.I.[1], Koscheev S.V.[1], Bubnov Yu.Z.[2], Zhabrev V.A. 664

**IV394 FRACTURE INDENTATION PHENOMENON: APPLICATION FOR CERTIFICATION AND CONTROL OF CERAMIC COATINGS**
Byakova A.V. 666

**IV173 ELECTRONIC STRUCTURE OF METASTABLE AND NONSTOICHIOMETRIC PHASES BASES BASED ON TUNGSTEN AND MOLYBDENUM TRIOXIDES**
Khyzhun O.Yu., Solonin Yu.M., Graivoronskaya E.A. 668

**IV120 SCANNING TUNNELING SPECTROSCOPY: A NANOMETER RESOLUTION PROBE OF ELECTRONIC PROPERTIES**
Roditchev D., Sacks W., Klein J., Cren T., Giubileo F.[1], Bobba F.[1], Lamy R. 670

**IV92 FURTHER ADVANCE IN USAGE OF THE COMPOSITE PIEZOELECTRIC VIBRATOR METHOD: NONDESTRUCTIVE ACOUSTIC SPECTROSCOPY OF MATERIALS AT HIGHER HARMONICS**
Smirnov S.N., Natsik V.D., Pal-Val P.P. 672

**IV210 ACOUSTIC MATERIALS SCIENCE TODAY**
Bezimyanniy Y.G. 674

**IV313 HIGH-TEMPERATURE RAMAN SPECTROSCOPY OF DEFECT STRUCTURE IN COMPOSITE OXIDE PHASES**
Koviazina S.A., Pereliaeva L.A., Leonidova O.N., Leonidov I.A., Strekalovsky V.N.[1] 676

**IV159 APPLICATION OF GLOW DISCHARGE MASS SPECTROMETRY FOR ANALYSIS OF ADVANCED MATERIALS**
Kurochkin V.D. 677

**IV391 HIGH-TEMPERATURE X-RADIOGRAPHY IN PHYSICAL METALLURGY**
Belots'ky O.V., Yurkova O.I. 679

**IV236 STM STUDY OF THE SURFACE MICROSTRUCTURE OF MAGNETIC GRANULAR THIN FILMS**
Gorobetz Yu.I., Silantiev V.I., Bondarkova G.V., Kravets A.F. 681

**IV95 EVOLVING HETEROGENEOUS DISTRIBUTION AND ANISOTROPY OF FACTUALITY OF SURFACE ROUGHNESS IN SINGLE CRYSTAL FOILS UNDER CONSTRAINED CYCLICAL TENSION**
Gordienko Yu.G., Zasimchuk E.E. 683

**IV75 STATISTICAL ANALYSIS OF PLASTIC INSTABILUTY: UNIVERSAL SCALING**
Lebyodkin M.A., Dunin-Barkowskii L.R., Lebedkina T.A. 685

**IV118 A NEW METHOD OF THE ANALYSIS OF RELAXATION RESONANCES: BROADENING AND SHIFT CAUSED BY RANDOM DISPERSION OF THE PARAMETERS OF THE ELEMENTARY RELAXATORS**
Natsik V.D., Semerenko Yu.A. 687

**IV2 THERMAL CONDUCTIVITY INVESTIGATIONS OF POWDER AND SUPERHARD MATERIALS BY SOLVING OF HEAT CONDUCTION INVERSE PROBLEMS**
Isayev K.B. 689

**IV20 COMPLEX APPROACH TO ASSESSMENT OF FAILURE MECHANISMS OF STRUCTURAL MATERIALS CONTACTING WITH VISCOUS AGGRESSIVE MEDIUM**
Kolotilkin O. 691

**IV56 COMBUSTION SYNTHESIS OF STABILIZED ZIRCONIUM OXIDE IN SYSTEM $ZrO_2$-$Y_2O_3$-MgO**
Hashkovsky S.V., Shilova O.A. 693

**IV57 STRUCTURAL - PHASE TRANSFORMATIONS AND DIFFUSION OF NITROGEN IN SUBSURFACE AREAS OF ION ALLOYED MOLYBDENUM**
Bodnar O.B., Bdikin I.K.[1], Aristova I.M.[1], Mazilkin A.A.[1], Zamalin E.Yu., Pronina L.N.[1] 695

**IV63 STUDYING MATERIAL DEGRADATION IN THE COURSE OF OPERATION BY THE METHOD OF LM-HARDNESS**
Lebedev A.A., Muzyka N.R., Voltchek N.L. 697

**IV101 VISUALIZATION OF BORON DISTRIBUTION IN MOLYBDENUM ALLOYS BY PARTICLE-TRACKING AUTORADIOGRAPHY**
Morito F., Krajnikov A.[1], Saito H.[2] 699

**IV130 SIMULATION OF THE CONCENTRATION PROFILES USING AUGER ELECTRON-SPECTROSCOPY AND SECONDARY ION MASS_SPECTROMETRY**
Vasylyev M.A., Sidorenko S.I.[1], Voloshko S.M.[1], Vilkova N.Yu.[1], Tkachuk A.A. 700

**IV160 DISTINCTIONS OF ANALYSIS OF NEW ALUMINUM ALLOYS BY AES, X-RAY AND GDMS METHODS**
Kravchenko L.P., Kurochkin V.D., Romanenko O.M., Tsurpal L.A. 702

**IV161 ELIMINATION OF STRUCTURAL EFFECTS AT SILICON DETERMINATION IN ALUMINUM ALLOYS USING GD-MS AND X-RAY METHODS**
Kravchenko L.P., Kurochkin V.D. 704

**IV187 CERAMIC SOLID ELECTROLYTE DEVICES TO CONTROL AND MAINTAIN OXYGEN PARTIAL PRESSURE**
Dubok V.A., Lashneva V.V. 706

**IV249 PRECISION MEASUREMENT OF LATTICE PARAMETERS IN HIGH-TEMPERATURE X-RAY DIFFERACTOMETRY**
Karpets M.V. 708

**IV264 INFRARED SPECTROSCOPIC RESEARCH OF STRUCTURAL CHANGES WHEN GRINDING A SILICON CARBIDE**
Gilev V.G. 710

**IV283 AN OPTICAL METHOD OF INVESTIGATING THE VISCOSITY OF POLYMER SOLUTIONS**
Kasheuski S.B., Prokhorov I.V. 712

**IV303 CATHODOLUMINESCENCE SRECTRA OF DOPED CUBIC BORON NITRIDE CRYSTALS**
Gameza L.M. 714

**IV332 INVESTIGATION OF METAL SURFACE BY SCAN KELVIN PROBE**
Shipitsa N.A., Zharin A.L., Saroka D.I. 716

**IV378 THE INVESTIGATION OF FERROELECTRIC MATERIALS BY RADIOSPECTROSCOPY METHODS**
Bykov I.P., Glinchuk M.D., Laguta V.V., Slipenyuk A.M., Yurchenko L.P. 718

**IV385 ATOMIC FORCE MICROSCOPY OF THICK FILM RESISTORS ON THE BASE OF METAL BORIDES**
Paustovsky A.V., Rud` B.M., Shelud`ko V.E., Tel`nikov E.Ya., Tsukruk V.V.[1], Luzinov I.A.[1] 720

**IV387 AUTOMATIC DEVICE FOR DETERMINATION OF POWDER FLOWABILITY AND CALIBRATION OF FUNNELS**
Vinnitchenko V.D. 722

**IV389 PECULIARITIES OF THE ELECTRON SPECTRUM FOR $Zr_xHf_{1-x}V_2$**
Nemoshkalenko V.V., Shevchenko A.D. 724

**IV140 THE USAGE OF SCANNING ELECTRONIC AND ATOMIC-POWER MICROSCOPY METHODS FOR RESEARCH OF THE STRUCTURE OF THIN COMBINED COATINGS**
Andreyev M., Markova L., Kuznetsova T., Chekan V. 728

***INDEX OF AUTHORS*** 731-736

***LIST OF PARTICIPANTS*** 739-788

# *PLENARY SESSION*

# DESIGNING AND ENGINEERING OF NANOPHASE MATERIALS STRUCTURE AS A METHOD OF OPERATING BY THEIR PROPERTIES: ACHIEVEMENTS AND PROBLEMS

**Skorokhod V.V.**
Frantsevich Institute for Problem of Materials Science, Ukraine National Academy of Sciences, Kiev, Ukraine

In late decades of 20th century the nanostructured materials have found their application in contemporary high technologies as fundamentally new class of functional materials with specific, sometimes unique useful properties, as well their unusual combinations. Nanophase materials (or nanocomposites) form a very important group of nanostructured materials which are characterized by heterogeneous structure. This structure is formed by phases with mean linear dimensions of structural elements less than 100 nm, which do virtually not interact each other. It is actual and complicated problem to apply the methods of structure designing and engineering to these materials which have been developed in the second half of 20th century and are successively used for laminated and reinforced macrocomposites. We dwell on the general description of metal, ceramic-metal, and ceramic nanocomposites. Both grains of predominant phase (matrix) and second phase inclusions should be considered as structural elements in these systems. With respect to the nature of chemical bonding, both above phases could be not only metal (metals, alloys, intermetallics, metal-like refractory compounds), but also non-metal (oxides, halkohenides, covalent nitrides and carbides).

Therefore, the regarded composites can be by both dielectrics (semi-conductors) and conductors from the viewpoint of their electrical properties, depending on the volume fraction of conductive phase in composite. As to mechanical properties, the metal nanophase composites have the most often limited plasticity while ceramic-metal have very low plasticity with sufficiently high fracture toughness. Finally, the ceramic composite in a whole is, as a rule, brittle material and the parameters of its fracture toughness can considerably depend on properties and morphology of the second phase inclusions.

The designing of composites structure, including nanophase ones, has to be carried out taking into account the technological processes in which the structure engineering is performed. Four main groups of technological processes for manufacturing bulk nanocomposites should be pointed out:

a) mechanical mixing of initial nanodisperse powders followed by consolidation (pressing and controlled sintering, hot pressing, sintering under high pressure etc.);
b) preliminary synthesis of composite nanostructured powders of nanophase particles by mechanical-chemical, plasmochemical, colloidal-chemical and other methods followed by hot pressure treatment;
c) reactive sintering of heterophase nanodisperse system, which is accompanied by considerable change in phase composition of system;
d) synthesis of complex compounds and subsequent decomposition of them in selective chemical reactions (oxidation, reduction, formation of hydrides, carbides, nitrides etc.) with formation of nanodispersed mixtures and sintering of them.

Obviously the above mentioned typical schemes for technological processes for preparation nanocomposites can be divided into two groups, one of which corresponds to principle of **joining** particular phases into composites, and another to **separation** of initially monophase system into two or more phases. The principal qualitative characteristics of nanocomposite structure are linear dimensions (size distribution) of grains, morphology and linear dimensions of inclusions, extent of coherency between them. To those can be related also the degree of perfection grain and interphase boundaries, which is dependent on their effective thickness, and also the purity and fractal dimension. Just those parameters which greatly depend on the choice and optimization of technology for composite production, determine the extent of occurrence of so-called **dimensional effect** which has to be accounted in designing on optimal nanophase structure. However, the properties of nanocomposite are determined by not only the properties of particular phases (taking

into consideration the dimensional effect) and volume content of them, but also the geometric parameters of heterophase structure of a system as a whole. The most typical classes of heterophase structures are matrix and statistic (stochastic) ones. These differs first of all by topological characteristics, i.e., degree of connection of structural elements. The classification of nanocomposites by the geometry of structural elements. and also proper choice of microstructure integral parameters favor the structure designing. Here it have to be taken into account that the equations which put the basis for such designing and describe the dependence of effective physical properties (conductivity, permeability) of macrocomposites on volume content of phases and parameters governing microstructure type must be essentially corrected upon transition to nanophase systems.

If phases in a composite differ considerably in their properties (for example, conductivity, dielectrical permeability or hardness), the differences in system properties even within one structure type (for instance, matrix) with the same volume content of phases, can be large depending on form factor of inclusions. These differences become especially large when comparing systems with matrix and statistical structure. The structure of real composites most often is intermediate between matrix (i.e., ordered in a some way) and statistical ones. To determine effective properties of such systems it is necessary to know a number of complementary special parameters of heterophase structure - the extent of matricity or stochasticity and the characterictic of coherency (contiguity) for phases, and for nanophase systems also the relative portion of "boundary" phase. In stochastic structures with some critical difference in phase properties (conductivity, permeability, hardness) the percolation and fractal effects become of importance. In such systems the complementary parameters of geometrical structure appear, in particular the percolation threshold and fractal dimension for each phase.

From these positions it is discussed the nanostructured functional composites of "paramagnet-ferromagnet", "conductor-dielectric", "conductor-superconductor" types, and the degree of influence of directed change in technological factors (correlation between sizes of phase particles, wetting angle for refractory phase by melt, texture in packing of non-equiaxial particles etc.) on the critical macrostructure parameters, their stability and the nature of change in principal property (permeability, conductivity) near percolation threshold is analyzed. It can be claimed that effective methods for designing and engineering microstructure have been developed for this class of nanophase composites. The forecasting of mechanical properties of nanocomposites (hardness, strength, fracture toughness, plasticity) and designing in general case the structure which corresponds to optimum combination of those properties is more complicated and unresolved up new problem. However, there is information that the methods based on optimization heterophase structure have been successively applied to increase strength and fracture toughness of matrix nanocomposites "plastic phase-highly-hard nondeformable phase". In conclusion, the prospects are discussed for wide use of designing and engineering the structure of nanophase materials aimed to purposeful application them in various branches of techniques and technology.

# ELECTRON BEAM TECHNOLOGY OF INORGANIC MATERIALS DEPOSITION FROM THE VAPOUR PHASE IN VACUUM (EB-PVD) - STATE OF THE ART

**Movchan B.**
International Center for Electron Beam Technologies of the E.O.Paton Electric Welding Institute of the NAS of Ukraine, Kiev, Ukraine*

The 30ties of the XXth century marked the start of application of electron beam heating for material evaporation in vacuum and deposition of thin films, i.e. the start of electron beam technology of physical deposition of the vapour phase in vacuum (EB-PVD).

The processes of evaporation (atomisation) and subsequent condensation of various substances form a unique technological package, allowing development of advanced materials. Materials, being in the vapour phase, «do not know» the laws of solubility. Therefore, simultaneously evaporating several materials, mixing their vapour flows and then condensing them on a substrate, allows producing such structures that are very difficult or impossible to implement by other methods.

In mid-60ties equipment for high-rate evaporation of materials in vacuum was developed on the base of powerful electron beam guns, and systematic studies of the structure and properties of thick condensates of 1 to 2 mm thickness were begun [1]. Experimental data accumulated so far confirm the ability to produce from the vapour phase advanced inorganic materials with the specified structure and properties: amorphous and nanocrystalline materials with a non-equilibrium structure, including diamondlike carbon-based phases: dispersion-strengthened, microlaminate, microporous and functionally-graded materials, based on metals, alloys and ceramics. Synthesis of intermetallics, refractory compounds and quasi-crystals on the condensation surface is also possible [2-6].

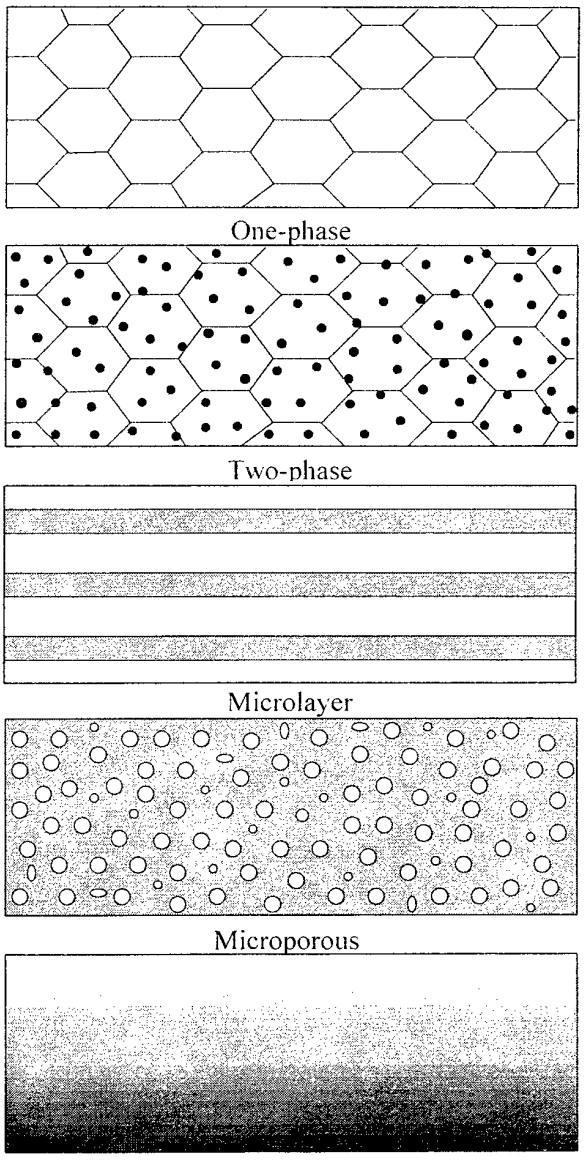


SCHEMATICS OF STRUCTURES OF EB-PVD MATERIALS AND COATINGS

* Web-site: http://www.paton-icebt.kiev.ua

The efficiency of the modern electron beam evaporators, consisting of 3 to 4 sources (crucibles), is 10 - 15 kg of vapour per hour. The achieved average rates of metals and alloys are equal to 50 to 100 μm/min.

Characteristically, the processes of evaporation and condensation allow combining material synthesis in deposition on a substrate with other technological requirements. For instance, depositing the vapour flow onto a surface of a specified configuration, it is possible to shape the condensed material as required. Controlling the condensate adhesion to the substrate allows achieving a good physical contact (adhesion) on the interface, or, contrarily, creating the conditions for separation of the produced material from the substrate.

Condensed materials can be obtained in the form of relatively thin (10 - 150 μm) coatings on finished items, for instance, gas turbine blades; thick (1 - 2 mm) structural coatings, having the function of a load-carrying structural element; semi-finished products (foil, strip, sheet); blanks and items of a complex shape (for instance, bodies of revolution); billets of 100 to 200 kg weight for subsequent thermoplastic treatment and shaping them as required [5, 6].

It should be also noted that the processes of evaporation and condensation, implemented in vacuum ($10^{-3}$ - $10^{-2}$ Pa) are perfect in terms of ecology, as they practically eliminate harmful evolutions into the environment.

Aviation, microelectronics, power engineering and instrument- making, chemical and tool industry, medicine are the current and future users of these materials and coatings.

The International Center for Electron Beam Technologies of the E.O.Paton Electric Welding Institute conducts systematic studies and development in the field of EB-PVD. The Center has designed and is manufacturing laboratory, pilot production and commercial EB-PVD units.

References:


1. Bunshah R.F. Vacuum Evaporation – History, Recent Developments and Applications,
   Zeitschrift für Metallkunde. **75**, N11, (1984), p.840 – 846.
2. Movchan B.A. Structural Conditions for Maximum Ductility of Two-phase Polycrystalline Materials.
   Mater. Sci. and Eng. **72**, (1985), p.109 – 117.
3. Movchan B.A. Dimensional-structural Relationships of the Strength of Two-phase Polycrystalline Inorganic Materials.
   Mater. Sci. and Eng. **A138**, (1991), p.109 – 121.
4. Movchan B.A. Composite materials deposited from the vapour phase under vacuum.
   Surface and Coatings Technology **46**, (1991), p.1 – 14.
5. Movchan B.A. EB-PVD Technology in the Gas Turbine Industry: Present and Future.
   JOM, (J. Metals. Miner. Mater. Soc.) **48**, (1996), p.40 – 45.
6. Movchan B.A. Functionally Graded EB-PVD Coatings.
   Surface and Coatings Technology **149**, (2002), p.252 – 262.

# STRUCTURAL LEVELS OF PLASTIC DEFORMATION AND FRACTURE OF SOLIDS

**Panin V.E.**
Institute of Strength Physics and Materials Science, SB, RAS, Tomsk, Russia

A conventional description of the relationships governing the plastic deformation and fracture of solids is based on two approaches:

a) Continuum mechanics (macroscale level);

b) Dislocation theory (microscale level).

The continuum mechanics and physics of plasticity and strength using the dislocation theory make use of the force-model methodology, Fig. 1. It is generally agreed that the yield strength and work hardening of the material above the yield point should be calculated to describe the stress–strain relation. However, the plastic deformation and fracture of a solid under load are due to its shear-stability loss in local regions of stress concentrators of different scales. These processes are inherently relaxational in character and give rise to quite another scheme of plastic deformation represented in Fig. 2.

High-nonequilibrium states of the crystal lattice occur in stress-concentrator regions. The lattice no longer obeys Hooke's law. It undergoes a local structural transformation, and its motion towards equilibrium occurs as a synergetic process. The methodology of describing plastic deformation and fracture must be built upon synergetic laws [1]. This idea was first formulated in [2]. In the last two decades the Institute of Strength Physics and Materials Science of Siberian Branch of the Russian Academy of Sciences has been developing a new approach based on the concept of the structural levels of deformation and fracture of solids.

Qualitatively new propositions are put forward within this concept [2–5]:

1. Shears found in a solid under load are due to the local shear-stability loss suffered by the material medium and may occur at the micro-, meso-, and macrolevels as a local change in the original internal structure, Fig. 3.

a) Microlevel: the local structural transformation of the original crystal lattice at the microlevel shows itself as nucleation of dislocation cores and their motion in a stress-gradient field.

b) Mesolevel: the local stability loss suffered by the internal structure occurs both at the micro- and mesoscale levels; this effect shows up as mesoscale localized-deformation bands propagating within individual conglomerates of internal-structure elements whose self-organization causes fragmentation of a strained specimen at the mesolevel.

c) Macrolevel: a loaded solid as an entity suffers a global shear-stability loss, which is evident as the formation of one macroband or two parallel (in the dipole form) or conjugate macrobands propagating across the testpiece; this process ends with the specimen being broken down into two parts.

2. Shears at any scale level may occur only in local regions of stress concentrators of the scale involved, since the structure of a loaded solid, on the whole, retains its shear stability when acted upon by mean applied stresses.

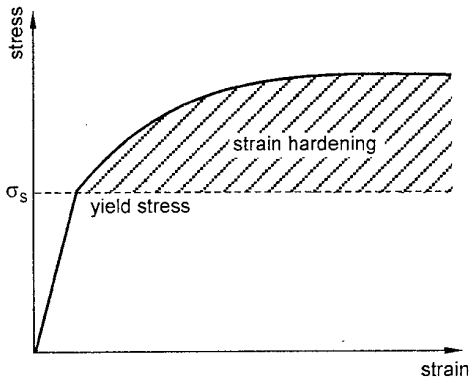


Fig. 1. A conventional approach to describe the stress-strain curve in the force-model methodology

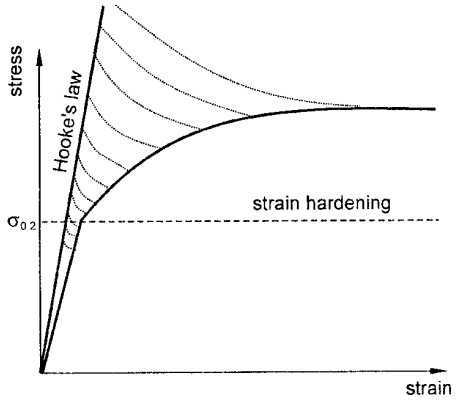


Fig. 2. Stress-strain curve within the methodology of local shear-stability loss at different structural levels

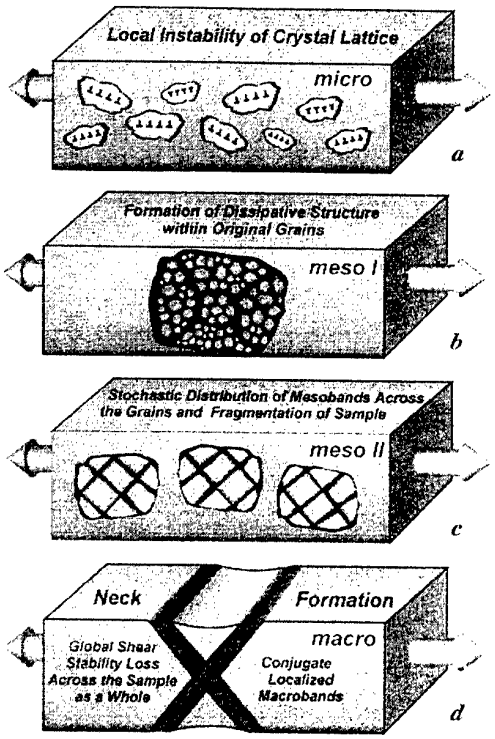


Fig. 3. Schematic of scale levels of shear stability loss in deformed solid.

3. The lowest shear stability in a loaded solid is found within its free surface. Because of this, the primary elastoplastic shears originate within surface layers and spread along the direction of maximum tangential stresses. The primary stress concentrator is the grip of a testing machine (or an external load point). The secondary stress concentrators caused by elastoplastic shears in the surface layers of the material undergo relaxation due to generation of strain-induced defects of varying scale. The latter penetrate into the bulk of the specimen giving rise to its plastic flow and fracture.

4. Shear of a continuous medium with a constrained material rotation would generate a bending-torsion zone. This creates another stress concentrator.

5. Being a relaxational process in a finite elastoplastic medium, shear generates damped elastic (acoustic emission) and elastoplastic (damped inelastic oscillations of adjacent shears) self-oscillations.

6. Plastic deformation is developed according to the following steps: primary stress concentrator, relaxation shear with a constrained rotation responsible for the formation of a local bending-torsion zone, relaxational shear with self-excited elastic or elastoplastic self-oscillations, etc. The self-excited wave process is most conspicuous when it is localized at the macroscale level alone. In the general case, it develops at several interacting scale levels. This accounts for the multiple-scale pattern of localized deformations.

7. Self-organization of shears is related to the self-consistency of shear-induced elastoplastic rotational modes and bending-torsion zones. For a given axis of loading, the sum of rotation and bending torsion is zero for the hierarchy of shears at self-consistent structural levels involved in plastic deformation. Violation of this condition gives rise to cracking as rotational modes of deformation.

8. The global shear-stability loss and fracture are observed locally at a macroscale stress concentrator and determined by the mechanics controlling the development of macroscale bands of localized deformation associated with meso- and microscale relaxational processes.

9. The mechanisms of plastic flow, its carriers and corresponding stages of stress-strain curves follow the law of similarity or scale invariance principle.

The concept of the structural levels of deformation and fracture of solids has proved to be successful in the cases of high-temperature creep, cyclic loading, friction-couple wear, shock loading, surface-hardening and coating deposition technologies, design and degradation of thin films and multilayer materials for electronics etc. The approach under consideration gives rise to establish the natural relations between the physics of dislocation-induced deformation, continuum mechanics of solids, and fracture mechanics.

## References

1. G. Nikolis, I. Prigogin, Self-organization in Non-equilibrium Systems, Wiley, New York, 1989.
2. V.E. Panin, V.A. Likhachev, and Yu.V. Grinyaev, Structural Levels of Deformation in Solids, Nauka, Novosibirsk, 1985.
3. V.E. Panin, Yu.V. Grinyaev, V.I. Danilov et al., Structural Levels of Plastic Deformation and Fracture, Nauka, Novosibirsk, 1990.
4. V.E. Panin (Ed.), Physical Mesomechanics of Heterogeneous Media and Computer-Aided Design of Materials, Cambridge Interscience Publishing, Cambridge, 1998.
5. V.E. Panin, Synergetic principles of physical mesomechanics, Theor. Appl. Fract. Mech. 37 (2001) 261–298.

# SEARCH FOR NOVEL SUPERHARD MATERIALS

**Novikov N.V.**
Institute for Superhard Materials of the Ukrainian National Academy of Sciences, Kiev, Ukraine

At present diamond and cubic boron nitride are the most efficient superhard materials for abrasive machining and cutting of a wide spectrum of inorganic and organic materials. Their application areas can be essentially expanded due to the structural composite superhard materials recently developed at the ISM. At the same time a search for novel superhard materials, which combine high hardness and strength, chemical inertness to the workpiece materials and relatively low cost, remains urgent. On the other hand, an expensive new superhard material can also find its niche in the market if its unique properties offer better performance and the workpiece material cannot otherwise be economically machined

The paper reviews the fundamentally new superhard materials developed by the researchers of the Institute for Superhard Materials of the National Academy of Sciences of Ukraine for the last two years and discusses the prospects of producing novel superhard materials.

## NEW SUPERHARD PHASE, CUBIC $BC_2N$

Phase transitions of graphite-like BN–C solid solutions (g-$BC_xN$) were studied up to 32 GPa and 3000 K using a laser heated diamond anvil cell and angle-dispersive X-ray diffraction at ESRF (Grenoble) [1]. At 25.8 GPa, the heating of g-$BC_2N$ up to 1600 K is not accompanied by any change in the diffraction patterns which exhibit only a broad line in the region of 111 reflections of diamond-like phases. At higher temperatures, the profile of this broad line changes to a rather complicated fine structure, and two new weak lines with $d_{hkl}$ = 1.26 and 1.09 Å (at ambient temperature) also appear. Finally, above 2200 K a drastic change in the spectrum is observed (Fig. 1, top pattern), which clearly points to the formation of a new phase. The diffraction pattern of the quenched sample exhibits only 111, 220, and 311 lines of the cubic lattice, which indicates that the sample is single-phase.

Laser heating experiments at different pressures have shown that the formation of c-$BC_2N$ is observed only at pressures above 18 GPa. At 14.5 GPa and temperatures above 2000 K g-$BC_2N$ decomposes to form a mixture of cubic boron nitride (cBN) and diamond. On further decrease in pressure down to 11.0 GPa, the thermal decomposition of g-$BC_2N$ proceeds to form cBN and disordered graphite.

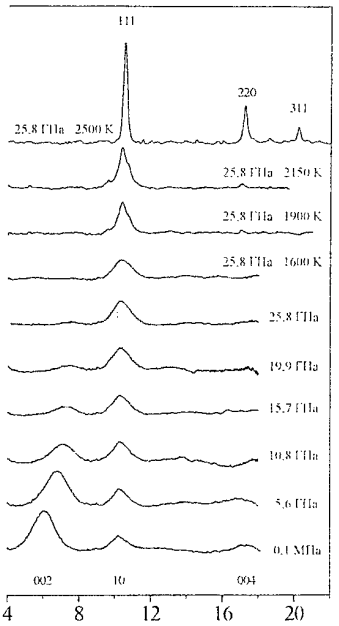


Fig. 1. Laser heating sequence of diffraction patterns at several pressures and temperatures.

The lattice parameter of c-$BC_2N$ at ambient conditions is $a$ = 3.642±2 Å, which is larger than those of both diamond and cBN.

The hardness, Young's modulus, fracture toughness and structure of this phase have been examined using micro- and nanoindentation and transmission electron microscopy. The hardness and elastic modulus values (E, G) of the c-$BC_2N$ are intermediate between diamond and cubic boron nitride, which makes this phase the hardest known solid after diamond (Table 1) [2].

Table 1
Hardness, Young's modulus and fracture toughness of superhard cubic phases of the B–C–N system at room temperature

| Material | $H_V$ (GPa) | $H_K$ (GPa) | $H_N$ (GPa) | E (GPa) | $K_{Ic}$ (MPa $m^{1/2}$) |
|---|---|---|---|---|---|
| c-$BC_2N$ | 76(4) | 55(2) | 75(3) | 980(40) | 4.5(4) |
| Cubic BN | 62(3) | 44(3) | 55(2) | 909 | 3.0(3) |
| Diamond | 115 | 63 | | 1141 | 5 |

## COMPOUNDS OF THE B–$B_2O_3$–BN AND Mg–Al–B SYSTEMS.

The electronic structure of a boron atom is responsible for special features of this element and its properties as well as for its ability to form high-hardness compounds. In the last few years the compounds of boron with oxygen have attracted considerable interest. At the Institute for Superhard Materials, the conditions of formation, crystalline structure and properties of individual phases in the $B–B_2O_3–BN$ system have been studied at high temperatures and pressures (1300 – 2300 K, 4.0 – 7.0 GPa). It has been found that the preparation of a new superhard phase of the $B_6O_xN_y$ composition with hardness $H_{V0,491}$ that may be as great as 47 GPa.

A possibility of obtaining a novel ceramic superhard material by hot pressing has been shown by the AMES Laboratory (USA). The chemical composition of the resultant material approximately corresponds to the $AlMgB_{14}$ + X formula, where X is BN, AlN, Si and some other additives, which greatly increase the material hardness [3]. The production technology requires specific particle size and quality of the initial materials, and for protective medium. Sintering time is 60 min [4]. Depending on the production conditions and additives, the resultant material hardness ranges from 35 to 42 GPa.

At the Institute for Superhard Materials of the National Academy of Sciences of Ukraine, an $AlMgB_{14}$-based superhard material has been developed under high pressures and temperatures. The material is characterized by an orthorhombic structure and the following crystal lattice parameters: $a$ = 5.8368 Å, $b$ = 8.1176 Å and $c$ = 10.3073 Å [4]. The use of high-pressure technique has allowed us to essentially simplify the technologies of preparation of the initial mixture and making the material as well as to intensify the synthesis. The optimization of the chemical composition and conditions of making has ensured stable-in-quality samples of the new superhard material. Table 2 compares the hardness of the novel material with that of other superhard materials.

Table 2
Hardness of superhard materials

| Material | Hardness, $H_V$ (GPa) | Note |
|---|---|---|
| $AlB_{12}$ | 25–26 | |
| $AlMgB_{14}$ | 32–35 | |
| $AlMgB_{14}$ + X | 35 – 42 | hot pressing, 60 min. |
| $AlMgB_{14}$ (ISM) | 39–43 | 6.5 GPa, 1800 K, 5 min. |

Superconductive (SC) properties of $MgB_2$ have been revealed in January 2001. The influence of Ta addition on critical current density ($j_c$) and irreversible field ($H_{irr}$) of high-pressure (HP) synthesized and sintered $MgB_2$ has been first studied in the ISM. 2 – 10 wt.% addition of Ta allowed us to synthesize nanostructure multiphase $MgB_2$-based material (at 2 GPa, 800-900 °C for 1h) with highest SC characteristics ($j_c$ and $H_{irr}$) that have been ever reported for bulk $MgB_2$. $j_c$ in 1 T field were: 570 kA/cm$^2$ at 10 K, 350 kA/cm$^2$ at 20 K and 40 kA/cm$^2$ at 30 K and in 10 T field – 650 A/cm$^2$ at 10 K. In synthesis and sintering processes, Ta plays the role of an absorbent of impurity gases (H, N, O etc.) and forms $Ta_2H$, TaH, $TaN_{0.1}$, Ta-O compounds etc., thus promotes the reduction of $MgH_2$ in Mg-B-O-matrix phase as well as of the impurity N and O in $MgB_2$ single crystals distributed over the matrix. For the first time have been estimated the hardness of $MgB_2$ single crystals $H_B$= 35.6± 0.9 GPa, that occurred to be higher than that of sapphire $H_B$=31.1±2.0 GPa

## CARBON NITRIDE $C_3N_4$

A material produced by using a Na flux method and chemical reaction between sodium azide and hexachlorobenzene and having a structure consisting of a three-dimensional network of covalently bonded C and N atoms is experimentally demonstrated at NIMS (Tsukuba) to exist as a single crystalline phase at high pressure (7.7 GPa) and temperature (700 °C). Experimental lattice constants of the observed crystalline phase (a = 6.58±0.05 Å and c = 2.49±0.02 Å) are in good agreement with ab-initio calculations for $C_3N_4$. The bulk modulus of the hard phase produced was estimated to be 460 GPa, which is comparable with that of diamond (443 GPa). These results open new possibilities for study of real carbon nitride properties and comparison with diamond properties.

Thus, there is a good reason to aim the further search for superhard materials at both developing new compounds in the B–C–N–O quaternary system of light elements and at synthesizing borides of magnesium and aluminum as well as silicon, phosphorus and sulfur compounds.

**References**

[1] V.L. Solozhenko, D. Andrault, G. Fiquet, M. Mezouar and D.C. Rubie, Appl. Phys. Lett., **78** (2001) 1385-1387.

[2] V.L. Solozhenko, S.N. Dub, N.V. Novikov, Diamond and Related Materials. **10** (2001) 2228-2231.

[3] Пат. 6099605 США, МКИ C04B 035/58; C09K 003/14. Superabrasive boride and a method of preparing the same by mechanical alloying and hot pressing, B.A. Cook, J.L. Harringa, A.M. Russell, 08.08.2000.

[4] A.A. Shulzhenko and A.N. Sokolov, Journal of Superhard Materials, **4** (2001) 74-75.

# PRODUCTION TECHNOLOGY HIGH-TEMPERATURE CARBON/CARBON-SILICON CARBIDE COMPOSITES

**Kostikov V.I., Chernenko N.M.**
Federal Governmental Unitarity Enterprise "The State Research Institute of Graphite-Based Structural Materials" – FGUE "NIIGrafit", 2 Electrodnaya Str., Moscow 111141, Russia;
E-mail: grafit@aha.ru; Tel./Fax: 7 (095) 176-2988

A production technology has been developed for high-temperature heat-resistant composites based on a carbon-silicon carbide matrix reinforced with carbon fibers. The process of obtaining the composite is realized via a successive thermochemical conversion of a polymeric coke-forming matrix of a starting carbon plastic into a carbon matrix with an open porosity of transport type which in its turn, is trans-formed into a carbon-silicon carbide matrix by capillary impregnation with liquid silicon and conversion of carbon into silicon carbide. To prevent the interaction between the liquid silicon and the reinforcing fiber, onto the internal surface of a carbon-carbon preform there is applied a silicon carbide film, a diffu-sion barrier against diffusion of carbon into liquid silicon which ensures the selectivity of interaction of liquid silicon with carbon-carbon preform components through varying their chemical reactivity.

For the bulk infiltration of a carbon matrix of the carbon-carbon preform with liquid silicon, there are suggested a novel principle and a production process based thereon for obtaining a carbon matrix the pore structure whereof is characterized by prevailing open porosity of transport type. And pyrolized is a coke-forming matrix (mixture) in the form of interpenetrating polymer networks of its components, at least, one whereof is gasified under carbonization without forming a carbon residue and forms in the carbon matrix being produced intercommunicating channel pores of open type.

The resulting structural carbon/carbon-silicon carbide composite has high physicomechanical proper-ties in an oxidizing medium up to the temperature of 1700 °C at which its high-temperature strength is 1,5 times as high as the corresponding indices at room temperature.

# METALLIC AEROSPACE MATERIALS WITH EXCEPTIONAL STRUCTURAL EFFICIENCY

**Miracle D. B., Firstov S.[1], Milman Yu.[1]**
Air Force Wright Laboratory, Materials and Manufacturing Directorate, Wright-Patterson AFB, OH USA
[1] Frantsevich Institute for Problems of Materials Science of NAS of Ukraine, Kiev, Ukraine

Research and development in the aerospace industry has displayed revitalized interest in structural metals with high specific strength and stiffness. Specific strength and stiffness are the two most pervasive material characteristics in the design of aerospace systems, controlling the system configuration as well as the size and spacing of nearly every structural component. Metallic materials with increased specific properties can provide performance improvements by decreasing system weight through reduced component mass and more efficient system design. Since system weight often controls the ability to achieve advanced aerospace missions (as in hypersonic and trans-atmospheric missions), structural weight is sometimes an enabling consideration. Thus, metallic materials with high structural efficiency can provide enabling mission capabilities by enabling structural minimization, which may be achieved by advanced methodologies of systems design and construction. Highly unitized construction is one such example that has been accomplished with expensive graphite/epoxy systems, but has not been widely practiced with current metallic materials due to their lower specific properties. Metallic materials with high specific properties are also enabling for the expanding US Air Force emphasis on access and utilization of space. In addition to improvements in system capabilities, these materials will also impact affordability by reducing the number of parts, and hence the significant cost associated with system assembly. The number of parts is reduced by increased component spacing and by unitized construction. By adding good strength retention at moderate temperature (up to 200°C, and in some cases up to 300°C) to high specific strength in candidate Al-based materials, replacement of Ti structures can become feasible, with further reductions in system weight and cost.

Metallic composites offer significant increases in specific stiffness relative to the matrix alloy (Figure). Discontinuously reinforced Al (DRA) possesses specific stiffness values more than double those of conventional Al alloys. Although a high volume fraction of reinforcements are required to achieve these levels of stiffness, more modest reinforcement levels still provide an increase of up to 50% in stiffness, while retaining good ductility and toughness. DRA relies upon age-hardenable Al alloys, and the maximum use temperature is limited to ~150°C, similar to conventional Al alloys. Amorphous and nanocrystalline Al alloys provide significant improvement in specific strength, but provide no improvement in specific stiffness. DRA is now a commercial material with a wide range of applications, while amorphous and nanocrystalline Al alloys are still in the research and development stage.

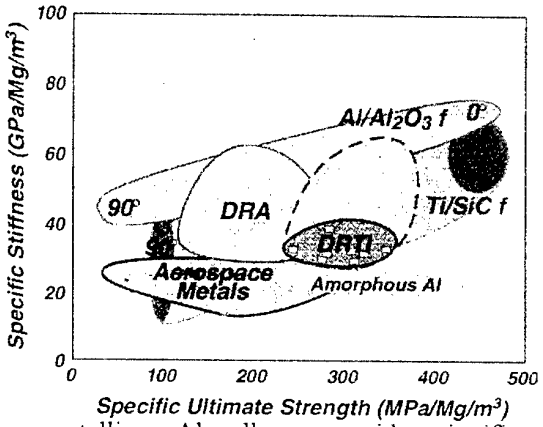


Efforts to develop structural materials with specific strength and stiffness higher than conventional metals and DRA are now being undertaken as a joint activity between scientists at the Frantsevich Institute for Problems of Materials Science (IPMS) and the Materials and Manufacturing Directorate of the US Air Force Research Laboratory (AFRL). The objectives are to increase the maximum operating temperature of Al-based metals from the current limit of ~150°C to ~200°C. Approaches include the introduction of thermodynamically stable, coherent precipitates in Al alloys. Additions of Sc produce coherent $Al_3Sc$ particles that range in size from 5-25 nm, and are very effective in strengthening Al alloys. In addition, Sc is a potent grain-refining agent, and also inhibits recrystallization. Hypo-eutectic additions of Sc are being pursued to provide dramatic improvements in strength below 150°C, due to the formation of

secondary $Al_3Sc$ particles, and hyper-eutectic levels of Sc are added to provide obtaining fine grain polyhedral structure in as cast conditions due to primary $Al_3Sc$ particles.

The very effective way to increase the mechanical properties of Al alloys is the complex alloying by Sc and transition metals (Zr, Ti, Hf, V, Nb etc.). The addition of Sc to alloys of Al-Zn-Mg system made possible to increase the concentration of Zn in these alloys (up to 10%) and to increase strength without decreasing plasticity. It was shown that these alloys may be welded.

The increase of the high temperature strength of Al alloys was achieved by using the PM technology that makes possible to obtain a non-equilibrium state of material. The quasicrystalline particle of 50-100 nm in diameter were introduced to Al matrix by this way. These particles are stable up to 400°C, and Al alloys of such type may used at elevated temperatures to 300°C.

Other approaches to produce improved properties in Al-based materials include the exploration and characterization of novel Al-based intermetallic eutectic alloys.

This way makes possible to increase both specific stiffens and specific ultimate strength.

Important efforts to establish joining technologies are being pursued through collaboration with the E.O. Paton Electrowelding Institute.

As shown in Figure, discontinuously reinforced Ti (DRTi) can provide simultaneous improvement in both specific strength and specific stiffness. Only limited data is available in the literature for this new class of materials. The joint program between IPMS and AFRL is focusing on in-situ eutectic Ti-based alloys. The Ti-Si and Ti-B systems are both being investigated. A deep eutectic reaction in the Ti-Si system produces an in-situ microstructure containing alpha and/or beta Ti reinforced with Ti-silicide phases. A similar eutectic reaction in the Ti-B system produces TiB reinforcements in a Ti alloy matrix. The eutectic reactions provide the possibility of a refined cast microstructure, so that subsequent ingot breakdown and thermomechanical processing is more easily accomplished. Cast, wrought, and powder metallurgy approaches are all being pursued on the joint IPMS/AFRL collaboration.

The overall objectives, approaches and results from this joint collaboration will be presented and discussed. Both Al-based and Ti-based technologies will be described.

The authors would like to acknowledge funding of this project from the US Air Force Office of Scientific Research, and the assistance of the Science and Technology Center of Ukraine.

# MICRO- AND NANOSTRUCTURED METAL – BASED MATERIALS AND THEIR ULTIMATE MECHANICAL PROPERTIES

**Firstov S.**
Frantsevich Institute for Problems of Material Science, NASU, Kyiv, Ukraine

Up-to-date technologies allow controlling the size of structural elements (grains, subgrains, cells, blocks, fragments etc.) in a wide range including nano-size and transition in amorphous state as a limit. In particular it is possible to realize with severe plastic deformation or deposition from gaseous phase. Strengthening at severe plastic deformation may be expressed as

$$\Delta\sigma(e) = Kd^{-m}(e)$$

Where m is ½ or1 in dependence on temperature of deformation, size of structural elements в and their disorientation.
At big plastic deformationб a change of "d" is not controlled by Taylor-Polany law and may be determined (for $e \geq e_0$) as

$$d(e)=d_0/1+\alpha(e-c_0),$$

Where $e_0$ is deformation that corresponds to beginning of linear stage of hardening, $d_0$ is a size of deformation cells at $e_0$.

It has been also demonstrated that the severe plastic deformation results not only in the high strain hardening of the bcc metals, but also in decreasing of the temperature of the brittle-ductile transition. This effect is based on the formation of the disoriented cell structure (practically superfine-grained structure).

It has been found that the theoretical strength can be reached at the d=0,02μm assuming that the mechanism of plastic deformation remains changeless with the cell refining.

Some specific values of structural elements corresponding to changes of mechanisms of deformation or hardening may be determined. Namely, at sizes d≥1μm m=1/2 hardening is described by the Hall-Petch equation. At d< 1 μm hardening is intensiver at the "d " decreasc and m=1.

Obviously, the next critical size must be in area of nanosizes ( d≤ 50 nm). Here the stress when dislocation source could be switched on is close to theoretical strength at shear. As it was shown in a few works, weakening at grain size decrease may be noted in the area of sizes named. As the possible reason is an increase of volume of "bad" material ( volume of interfaces, triple points, etc.) as well as transition to intergranular mechanisms of deformation and fracture.

Meanwhile polycomponent materials (consisting of two and more kinds of atoms) can be strengthened with increase of interface strength. For this hardening both difference of atomic sizes of basic and alloying elements and possibility of introducing of "useful" admixtures creating strong interatomic ties with atoms of basic materials are recommended.

# HIGH-STRENGTH ALUMINUM-BASED ALLOYS

**Milman Yu.V.**
I.M.Frantsevych Institute for Problems of Material Science,
Ukrainian Academy of Sciences, Kiev, Ukraine

The pure aluminum is the very soft metal with hardness 210 MPa and yield stress 10-15 MPa. But the modern methods of alloying made possible to increase hardness of Al alloys to 2200 MPa, yield stress to 700 MPa and ultimate tensile stress to 800 MPa. High strength characteristics of these alloys are combined with plasticity to fracture 5-15 % that is enough for the practical use. This dramatic increase of strength has been possible due to very high plasticity of pure Al (which has FCC structure) and due to fundamental theoretical and experimental investigations in the theory of alloying and physics of strength and plasticity.

The alloys of Al-Zn-Mg-Cu system have the higher strength characteristics among wrought Al alloys. These alloys are the basic structural materials for aerospace engineering. Their strengthening is due to a very fine precipitation of $\eta'$-phase, which is enriched with Zn and Mg. The strength of these alloys increases when the concentration of Zn increases. However, an increase in the concentration of Zn above 7% leads to a dramatic decrease in fracture-related properties as well as deterioration of weldability and corrosion resistance. It was recently found that mechanical properties of these alloys containing up to 6-7%Zn can be improved considerably by addition of small amounts of Sc and Zr [1-3].

A diverse effect of alloying with Sc and Zr is stipulated by specific properties of the $Al_3(Sc_{1-x}Zr_x)$ intermetallic phase that forms fine coherent precipitates in the Al matrix. These coherent particles are very stable upon heating due to low solubility and diffusivity of Sc and Zr in the Al matrix and low interface energy. Combined alloying with Sc and Zr in the amount as low as 0.2% refines microstructure of casting and welding [2], improves workability and deformability of castings [3, 4], leads to formation of a very uniform and fine cellular dislocation structure in wrought products, and impedes recrystallization during heat treatment due to the obstacle action of the coherent particles. The last two factors facilitate an increase in strength and ductility of these wrought alloys in T6 or T7 conditions.

It has been shown that alloying by additions of Sc and Zr made possible to increase concentration of the main alloying element Zn [5].

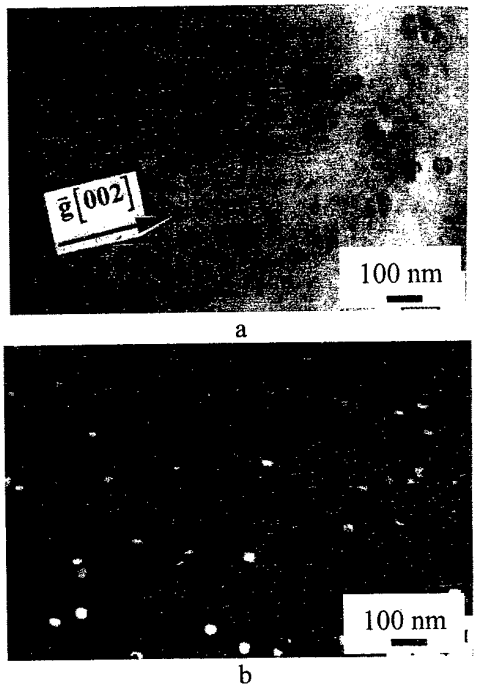


Figure 1. Image in a transmission electron microscope of $Al_3(Sc_{1-x}Zr_x)$ particles in as-cast Al-6.8Zn-1.3Mg-0.12Zr-0.05Sc (wt.%) alloy subjected to the homogenisation at 470°C during 3h: a) light-field image, foil plane (110), the forming reflection $\bar{g}$ = [002]; b) dark-field image, foil plane (110), $\bar{g}$ = [001] $Al_3Sc$

For example, in the alloy Al-12.0Zn-3.3Mg-1.2Cu-0.13Zr-0.4Mn-0.49Sc high mechanical properties were obtained, i.e. YS = 790 MPa and UTS = 820 MPa. This high strength was achieved due to additional combined alloying with transition metals, such as Sc, Zr, Cr and Mn, which retard recrystallization during heat treatment and retain cellular dislocation structure of deformed material, with a dislocation cell size of 1-2 μm. This non-recrystallized structure is more ductile, because brittle fracture along grain boundaries is not developed. An addition of Sc in combination with Zr, Mn and Cr increases the size of $\eta'$-particles, leading to an increase in ductility. A decrease in strength accompanying this growth is compensated and even exceeded by contribution

of small $Al_3(Sc_{1-x}Zr_x)$ coherent particles to hardening.

The main beneficial effect of alloying with Sc in combination with Zr is the possibility of increasing the concentration of Zn without loss in ductility. An additional alloying with Cr was shown to decrease the size of $\eta'$-particles to about 3 nm, which was not accompanied by a drop in ductility.

It was shown [6] that additions of Sc increase the resistance of Al and its high-strength alloys against general and pitting corrosion in the sea water.

Al-Zn-Mg-Cu alloys containing Sc may be used even at cryogenic temperatures where these alloys have good combination of strength and ductility [7].

The high-strength Al-Zn-Mg-Cu alloys may be produced not only by casting, but by PM technology as well. The special equipment for water atomization of Al alloys by high-pressure water (up to 200 kbar) has been elaborated. Cooling rate during producing powders by this technology may be up to $10^6$ K/c. The PM technology makes possible to increase plasticity of high-strength Al-Zn-Mg-Cu alloys without Sc additions [8-10].

The best Al wrought alloys for elevated temperature application were obtained using dispersion strengthening by quasicrystalline particles 15-50 nm in diameter with volume fraction 70-90 % in Al matrix (Fig.2) [11].

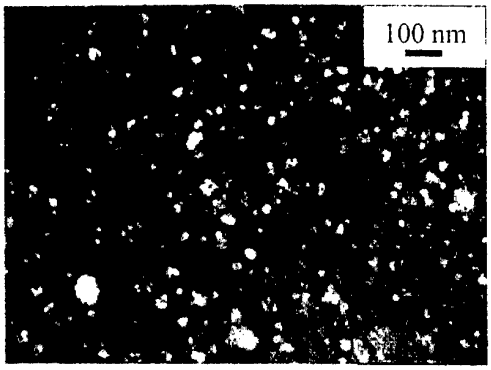


Figure 2. Quasicrystalline particles in $Al_{93}Fe_3Cr_2Ti_2$ melt-spun ribbon, dark field image

We have used in our experiments quasicrystalline phase $Al_{84.2}Fe_7Cr_{6.3}Ti_{2.5}$. For the alloy of Al-Fe-Cr-Ti system obtained by rapid solidification technique with the following compacting of powders the strength at 300 °C was more than 300 MPa, that corresponds to the air-force goal level. The structure and mechanical properties of these alloys are stable up to 400 °C.

Our investigations have shown that quasicrystalline phases may be formed in the processing of different Al alloys, especially containing Sc.

The high-strength cast alloys with good castability and increased mechanical properties were elaborated on the base of eutectic composition Al-13vol.%$Mg_2Si$ with additional alloying by transition and rare-earth metals [12, 13].

The development of this direction is the elaboration of cast eutectic alloys in the system Al-Ti-Cr, containing $L1_2$ phase. These alloys have higher melting point (1275 °C), essential ductility in compression tests and high hardness and strength up to 800 °C [14].

1. Senatorova O.G., Uksusnikov A.N., Legoshina S.F., Fridlyander I.N. and Zhegina I.P.// Mater. Sci. Forum, 2000. – **331-337.** – P.1249.

2. Davydov V.G., Yelagin V.I., Zakharov V.V. and Rostova T.D.// Metallovedenie i Termicheskaya Obrabotka Metallov, 1996. – **8.** – P.25.

3. Milman Yu.V., Lotsko D.V. and Sirko O.I.// Mater. Sci. Forum ICAA7, 2000. – **331-337.** – P.1107.

4. Eskin G.I.// Technologia Legkikh Splavov, 2000. – **2.** – P.17.

5. Milman Y.V., Sirko A.I., Lotsko D.V., Senkov O.N. and Miracle D.B.// Mater.Sci.Forum ICAA8, 2002. – **396-402.** – P.1217.

6. Vyzovikina N., Milman Yu., Sirko A.// Problems of Corrosion and Corrosion Protection of Materials, Physico-chemical Mechanics of Materials, special issue No.3, Lviv, 2002. – P.554.

7. Senkov O.N., Miracle D.B., Milman Y.V., Scott J.M., Lotsko D.V. and Sirko A.I. // Mater.Sci.Forum ICAA8, 2002. – **396-402.** – P.1127.

8. Neikov O.D. // Proc. of 2000 Powder Metallurgy World Congress, Kyoto, Japan, 2000. – Part 1. – P.464.

9. Neikov O.D., Milman Yu.V., Miracle D.B., Lotsko D.V., Sirko A.I., Yefimov N.A. // Proc. of PM2001, Nice, France, 2001. – **2.** – P.219.

10. Neikov O.D., Lotsko D.V., Sirko A.I., Sameljuk A.V., Thompson G.E., Zakharova N.P., Yefimov N.A. // Mater.Sci.Forum ICAA8, 2002. – **396-402.** – P.1223.

11. Milman Yu.V., Lotsko D.V., Neikov O.D., Sirko A.I., Yefimov N.A., Bilous A.N., Miracle D.B. and Senkov O.N. // Mater.Sci.Forum ICAA8, 2002. – **396-402.** – P.723.

12. Barabash O.M., Legkaya T.N., Sylzhenko O.V., Korzhova N.P.// Metallofiz. Noveishie Tekhnol., 1999. – **21.** – No.5 – P.24.

13. Barabash O.M., Milman Yu.V., Voskoboinik I.V., Korzhova N.P., Legkaya T.N. // Functional Materials, 2001. – **8.** – No.1. – P.159.

14. Milman Yu.V., Miracle D.B., Chugunova S.I., Voskoboinik I.V., Korzhova N.P., Legkaya T.N., Podrezov Yu.N.// Intermetallics, 2001. – **9.** – P.839.

# INFLUENCE OF PYRAMID ENERGY ON STRUCTURE AND PROPERTIES OF ALUMINIUM ALLOYS

**Antsiferov V., Ragozin Y.[1], Porozova S., Tichonov A.[1]**
Research Center Powder Materials Science, Perm, Russia
[1]Perm State Technical University, Russia

Academician P.Capitsa said "Science relates to that is impossible, while the possible is just a technology". It is "impossible" this work is devoted toresearch of pyramid field (energy) influence on a structure and properties of aluminium alloys.

Today number of studies has sharply grown, in which the attention is focused on unusual properties of pyramids. And though a modem hardware fails to determine the characteristics of pyramid energy, numerous phenomenal effects on both organized matter and abiotic environment were discovered. To the last objects are belonging those which are undoubtedly to be of interest for specialists. For example, polluted jewelry and coins are self-cleaned, the shaving edges become as new (this method of sharpening even was patented), the common salt crystals of unusual shape grow under pyramid, also, colloid solutions are unusually separated, spontaneous charge of condensers occurs, the temperature threshold of superconductivity changes and so on. Is it astonishing? Yes! But another is also surprising: this exotics did not become commonly accepted, "effect" of pyramid still has no trust. Apparently, further in-depth researches using modem methods and hardware are required. Such investigations started in several research organizations, including in Perm.

In this work the influence of aging conditions on microstructure of B 124 cupriferous silumin, filtered through various filters, was studied. Aging of the hardened alloy was carried out according to three-case studies: 1st case - aging for 1 month in natural conditions, 2nd case - aging for 1 month in conditions of pyramid influence, and 3d case - aging for 3 hours at 250 °C. Study of samples microstructure and photosynthesis was conducted with Neophot-21 optical microscope. Microradiographic spectral analysis was performed with MAP-2, and X-ray structure analysis with ДРОН-3M diffractometer in cobalt radiation. The analysis of results of the performed research has shown that the aging in conditions of pyramid influence is accompanied with: a) sharp decrease of copper content in an aluminium solid solution; b) increase of dissolved iron and manganese; c) reduction of free silicon; d) more coarse microstructure with formation of extended lamellar and branched skeletal phases, which are composed, according to the data of microradiographic spectral analysis, of silicon and copper without iron and manganese.

So deep change of structure when aging in the pyramid field should be accompanied with respective alteration of mechanical properties. This assumption was tested by research ofД16 aluminium alloy - after a hardening it was subjected to a natural aging under usual conditions and in a field of pyramid. It was established that in the first case of aging the mechanical characteristics, having reached the optimum value (after some time of aging), further do not change, while at aging in a pyramid field a process occurs similar to a process observable at artificial aging.

Strength properties, having reached a maximum at optimum time ofaging-100 hours, further essentially decrease (~1.3 times). And the deformation process of the samples having the maximal strength is accompanied with unusual effects: deformation curve has the steps of loading (increments) and several yielding teeth.

From the above data it can be concluded that the pyramid field influences in most extent the long-time processes, hi this connection, research of pyramid energy influence on so-called quasi-relaxation processes is of interest, hi the sample loaded up to the initial tension, after switching off me drive, a spontaneous drop of tension begins. As the sample length during the test with rigid machines after switching off the drive does not remain constant, this process is named as quasi-relaxation. It is supposed that this process is connected with the change of dynamic dislocation density. Quasi-relaxation curve for AK8 aluminium alloy under usual and pyramid energy conditions was plotted. Comparative analysis has shown that pyramid energy influence on a quasi-relaxation process of AK8 alloy is rather essential: under pyramid field just in several hours the relaxation limit is achieved which under usual conditions would require 5000 hours to achieve.

Summarizing the results of the research, it is necessary to note that, apparently, despite of the numerous skeptics, we are on a threshold to create the new nonconventional alternative technologies of materials processing.

# PRINCIPLES OF ADAPTIVE CONTROL OF ELECTRIC PULSE SINTERING

**Belyavin K.E., Sheleg V.K., Minko D.V., Kuznechik O.O.**
Powder Metallurgy Research Institute, Minsk, Belarus

The perfecting technologies enabling to produce porous powder materials (*PPM*) with improved complex of physical-mechanical and hydrodynamic properties is an actual problem for powder metallurgy. The method of electric pulse sintering (*EPS*) based on pulse advancing of electric current through powder bulk at discharge of a high-voltage capacitor bank allows simultaneously to sinter and compact powder materials different from conventional technologies where these operations are separated. The *EPS* method provides high speed of heat exchange in contact zones ($\sim 10^6 \div 10^8$ K/s) at small duration ($\sim 10^{-4} \div 10^{-3}$ s) [1].

For obtaining a *PPM* with a given complex of physical-mechanical and hydrodynamic properties the adaptive control system is developed which enables to transform *EPS* technological modes automatically.

The supervisory circuit couples feedback between performance curve of the *EPS* installation, which is indicated as *R* on the skeleton diagram of control (fig. 1) and parameters of powder bulk indicated as *OC*. It consists of a measuring unit and an intellectual module allowing to realise the following algorithm of activity:

the measurement unit, due to sensors and device of their interrogation, determines initial state of *OC*;

1) the measurement unit determines an initial state of *OC* due to sensors and device of their interrogation;

2) the intellectual module, the core thereof is a control electronic computer, calculates the necessary technological mode for *R* and represents it as defined values of the control voltage ($u$) to the executive unit;

3) the executive unit transforms values obtained from the intellectual module to a controlling voltage for actuators *R*. After that the electric pulse discharge of the capacitor bank through powder takes place.

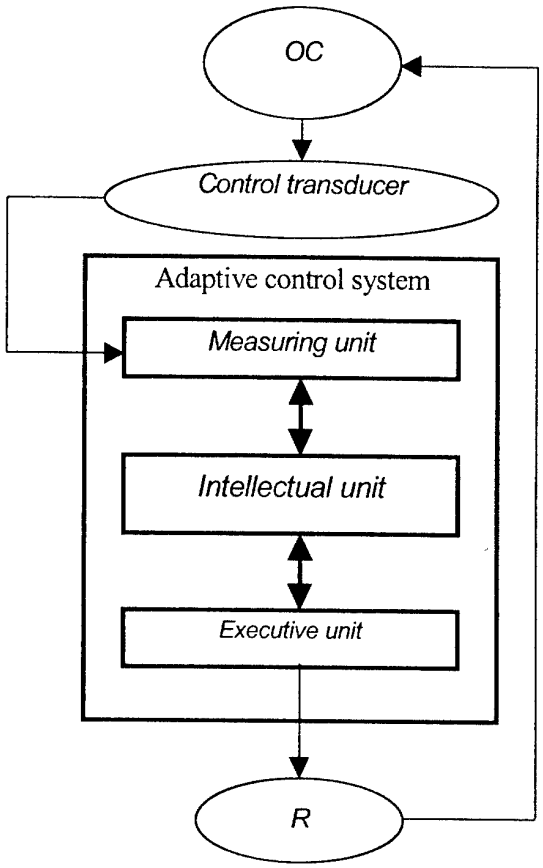


Fig.3. Structural scheme of adaptive control

For a supervisory circuit the technique of the control is developed, which includes a method of obtaining the information about processes taking place in powder bulk, a method of processing the latter and a method of selecting performance parameters for *EPS* installation.

The method of obtaining the information is based on the principle of joint measurements [2], based on combination of direct and indirect measurements and containing problem solving on definition:

– dispersion of a random variable at direct measurement taking into account deviation of devices transmitting signals;

– dispersion of a random variable at indirect measurement considering the value of a methodical error in the mathematical calculation program;
– the main instrument error of the monitoring system, which is the lower threshold of the monitoring system sensitivity.

The method of processing the observed data is directed to construction of hardware system on recognition of an image of a mathematical model of *EPS* process and includes [3-4]:
– order of data processing coming from primary converters;
– way of control of the device specifying parameters of process;
– a computational method permitting indirectly judge condition *OC* by results of direct measurements.

When developing algorithm of selecting values for the executive unit of the supervisory circuit the following was taken into account:
– the *EPS* process for the supervisory circuit represents analytical relation as some $F^0$ functional between $Y^0$ vector, compounded considering output values of the intellectual *OC* module, and vector $X^0$, compounded considering drawn up values obtained from the measurement unit [5].

By $F^0$ selection the *EPS* peculiarities were taken into consideration from which follows[6]:
– the output parameters of an intellectual module describing $Y^0$, change with the lapse of time, i.e. $Y^0=Y^0(t)$;
– the process of changing input parameters of the intellectual module description $X^0$, is non-liner one.

Technique and supervisory circuit have allowed to realise the scheme (fig.2) in which parameters of deviation and disturbance are used for *EPS* process control. It has allowed to fulfil the following principle of its activity:

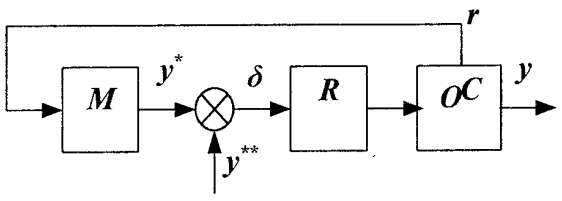


Fig. 2 Scheme of adaptive control

– *R* through parameters *u* set environment of effect on *OC*, then values for *y* and *r* appear on exits of controlling sensors.

The first of them (*y*) characterises condition of an object and the second (*r*) - condition of the environment affecting it.

Parameter *r* is an input value for analytical model of *M* which establishes relation between condition of the affecting environment and *OC* condition. This connection is determined by the value of response ($y^*$), which is compared with setting ($y^{**}$) parameter. The difference between them as $\delta$ deviation goes on an *R* input and depending on its value the regulator changes *u* values.

Cycle of control continues till $\delta$ is equal to zero point.

The developed adaptive control system allows to lower considerably discard during production of a *PPM* by *EPS* method and to reduce costs for improvement of technological modes at transition from one kind of articles to another.

References.

1. K.E. Belyavin, D.V. Minko, V.V. Mazyuk, O.O. Kuznechik The Main Pecularities of Heat Change in Powder Particles During Electric Pulse Sintering // Engineering.- «Technoprint» Publishers, Minsk, issue #17, 2001, p. 157-161 (in Russian).

2. K.L. Kulikovsky, A.Y. Kuper Methods and Devices for Measuring // «Energoatomizdat» Publishers, Moscow, 1986, p.29 (in Russian).

3. L.B. Zazhigaev, A.A. Kishyan, Y.I. Romanov Methods for Planning and Processing Results of Physical Experiment // «Atomizdat» Publishers, Moscow, 1978, p.12 (in Russian).

4. K. Werchagen, R. Dein, F. Grun et all. Patterns Recognition: Status and Prospects // «Sovetskoye Radio» Publishers, Moscow, 1985, p.104.

5. A.L. Khudolei, O.O. Kuznechik, G.A. Presnyakov Control and Adaptive Technique during Electro-Thermal Sintering of Porous Powder Materials // «Welding and Allied Sciences Technologies» issue #2, Welding Research Institute, Minsk, 1999, p.119-123 (in Russian).

6. K.E. Belyavin, V.V. Mazyuk, D.V. Minko, V.K. Sheleg Theory and Practice of Electric-Impulse Sintering of Porous Powder Materials // «Remico» Publishers, Minsk, 1997, p.180 (in Russian).

# BORON-RICH SOLIDS AND THEIR AUSPICIOUS ASPECTS IN MATERIAL SCIENCE AND TECHNOLOGY

**Helmut Werheit**
Solid State Physics Laboratory, Gerhard Mercator University, D-47048 Duisburg, Germany

The boron-rich solids are characterized by complex crystal structures containing polyhedra like octahedra, icosahedra, dodecahedra, and their derivatives together with single boron or foreign atoms.

Their outstanding properties, including in general high melting temperatures, extraordinary hardnesses, small extension coefficients, and high chemical resistivity, predestine them for technical application under conditions that are hardly accessible for most other materials. Moreover, the high absorption cross-section for neutron radition is important. The large variety of structures and their modification by the change of chemical composition within specific structure groups or within sometimes large homogeneity ranges, by forming ternary compounds, and by the substitution or interstitial accommodation of foreign atoms offer a large spectrum for tayloring boron-rich solids for specific applications, while the general proprties largely remain unchanged.

In the same way the structural variety of the boron-rich solids offers excellent prerequisites for the scientific investigation of interrelations between structural and electronic properties of solids with complex crystal structures. In particular, the generation of structural defects immediately correlated with the electronic properties has been proved. Accordingly, there are diverse possibilities to improve electronic properties that are favourable for according technical use.

Actual properties of specific boron-rich solids promising future technical applications are for example the high Seebeck coefficients of both signs (boron carbide, positive; some metal hexaborides, negative), high-temperature superconductivity ($MgB_2$), nanostructures.

# THE MOST RECENT INVESTIGATION OF THE PROCESSES OF PRODUCTION OF TUNGSTEN AND TUNGSTEN CARBIDE POWDERS

**Bondarenko V.P., Martynova L.M.**
V. Bakul Institute for Superhard Materials of the National Academy of Sciences of Ukraine,
2, Avtozavodskaya Str., Kiev, Ukraine

It is known that the properties of tungsten powder depend on many factors. Among them are: temperature, feed rate of a boat, thickness of the oxide layer, the number of stages of the reduction process, methods of the $WO_3$ preparation for the process of reduction, shape and sizes of $WO_3$ compacts, methane content of hydrogen, methods of packing the W powder in a boat for carbidization. We have studied the effect of a number of new factors on the properties of the W powder.

Through the use of the sieve classification of the $WO_3$ powders we obtained powders of the fractions: 250/200, 200/160, 160/125, 125/100, 100/80, 80/63, 63/50, and 50/40 μm, and a fine class - 40 μm. The content of the first two coarse fractions in the $WO_3$ powder is rather low, i.e. 0.2%. The content of the other coarse fractions (160/125-50/40 μm) is from 2.2 to 15.9%, and grains of the fine class (-40 μm) constitute 37.5%. Analysis of the grain composition of the resulting fractions has shown that the sieve classification yields the $WO_3$ powders uniform in grain size. As to the morphology they are individual large-sized particles, aggregates of particles of isomorphous and pseudomorphous types, and plates.

One-stage reduction of coarse fractions of $WO_3$ (160/125 and 125/100 μm) yields the medium-grained W powder with $\bar{d}_w$ = 3.5-3.8 μm. The reduction of the $WO_3$ powder of the 100/80, 80/63, 63/50, and 50/40 μm fractions allows the W powder with $\bar{d}_w$, respectively, of 6.2, 3.4, 7.7, and 2.8 μm to be obtained. This powder consists of isometric faceted particles, plates, and aggregates. The $WO_3$ powder of the fine class (-40μm) yields the high-temperature tungsten powder with $\bar{d}_w$= 7.5 μm.

By crushing $WO_3$ we managed to produce high-temperature W powder with $\bar{d}_w$ = 1.0 μm. The results we obtained allow the conclusion that there is no strict relation between dispersion and morphology of starting $WO_3$ powders and W powders prepared from $WO_3$.

X-ray diffraction analysis of the resulting W powders exhibits only slight widening of X-ray lines. The line width is $(6.3\text{-}6.9)\times10^{-3}$ rad. This points to a high degree of perfection of crystal lattice of particles of high-temperature W powder even in the case of using $WO_3$ crushed to 0.08 μm.

To increase the $WO_3$—$H_2$ contact surface and to decrease the path of $WO_3$ diffusion in the powder, we compacted $WO_3$ powder to prepare variously shaped and sized compacts: plates and cylinders. The cylinders were made of various masses m (g), diameter d (mm) and heighth (mm) (d=12.5, h=20.1, m=9.5; d=15.0, h=22.0, m=14.5; d=25.0, h=3.8, m=72.0; d=37.5, h=38.0, m=160) and reduced in a GP-130 stationary electrical furnace with a graphite tube at 1200±20 °C for two hours. The compacts were spaced 2 mm apart. The plates pressed from $WO_3$ were of the following sizes and weights: 200x32x75 mm, 2000 g; 200x39x75 mm, 2500 g; 200x42x75 mm, 2700 g; 200x49x75 mm, 3000 g. The cylinders ( $\bar{d}$=50 mm, h=80 mm, m=600 g) were placed in the boat in tens, the plates in twos (each weighing 3000 g) and in threes (each weighing 2000 g ) so that the total weight of the compacts in the boat was 6000 g. In all the cases the compacts were placed into molybdenum boats and the latter were inserted into a graphite container. The compacts were reduced in a pusher-type electric resistance furnace at the boat feed rate = 2 mm/min, $H_2$ consumption = 2.0 $m^3$/h, dew point of $H_2$ = 52°C, T = 1200±20 °C. It has been found that the W powder properties, all other things being equal, depend to a large extent on both the value of free specific surface of $WO_3$ compacts which is in contact with hydrogen ($F_{sp}$) and the shape of a compact.

As $F_{sp}$ increases, so does the specific surface of the W powder ($S_{sp}$), while the mean diameter of particles ( $\bar{d}_w$) decreases. For the case of reduction of the compacts in the form of large plates this dependence is given as $S_{sp} = 25.6 \cdot F_{sp}^{2.38}$, while in the case of cylinders $S_{sp}=5.04 \cdot F_{sp}^{2.38}$. Also, with increasing $F_{sp}$ of the plates from 0.064 to 0.086 1/mm the value of

$\bar{d}_w$ decreases from 9.2 to 3.6 mm, while with increasing $F_{sp}$ of the cylinders from 0.09 to 0.37 1/mm the value of $\bar{d}_w$ decreases from 13.5 to 0.7 mm .

In the case of free charging of $WO_3$ in a graphite boat (weight of a charge = 6000 g, the layer thickness = 45 mm ) and one-stage reduction at 1200± 20°C, we obtained the coarse-grained W powder with $\bar{d}_w$ = 19.5 μm, for the weight of a charge = 800 g $\bar{d}_w$ = 4 μm. The powder consists of highly symmetrical polyhedrons, large-sized cuboids, isometric particles, elongated particles on which the stages of the reconstruction of whiskers into rounded form are observed.

X-ray diffraction analysis of the W powders reduced from pressed compacts has shown that they have perfect crystalline structure as well: the width of X-ray line is $(6.0–6.3)x10^{-3}$ rad.

The relations we obtained have made it possible to devise processes for the production of W powders which differ in $d_w$ and particle-size distribution with temperature and holding time being unchanged, i.e. unchanging the furnace operating conditions. The capacity of an one-muffle furnace was 6-7 kg/h.

When studying the process of gas carbonization of the W powders we have found that some of them sinter strongly. This generated a need for additional power-intensive operations of crushing and grinding of the WC sintered compacts. The use of the Agte criteria [1] did not allow a logical explanation of the phonemenon. To study the factors which affect the sinterability of W powders, the latter were carbidized in the loose state following the selected test conditions of carbidization: temperature 2000±20°C, holding time 2h, methane-hydrogen medium containing 2 vol% $CH_4$.

When carbidizing W powders fabricated in Ukraine, Russia, Germany, WC compacts of different compression strength ($\sigma_{comp}$), were obtained (from 1.0 to 66.0 MPa). At $\sigma_{comp} \leq 7.0$ MPa the WC sintered compacts were easily pulverized. At $\sigma_{comp} \geq 25$ MPa the sintered compacts have to be crushed.

The degree of sinterability of W powders was investigated as a function of specific surface $S_{sp}$ ($m^2/g$), apparent density ρ ($g/cm^3$), specific magnetic susceptibility χ ($m^3/kg$), mass fraction of particles of the powder of -40 μm class *f*, and mean particle size $\bar{d}_m$ (μm) of this class (the division of the W powder was perfomed by sieving it on a 40 μm mesh sieve), adsorpsion potential and content of metal impurities in W powders.

The treatment of experimental results has allowed the following equation of regression:

$$\sigma_{comp} = -35.45+104.7 \cdot S_{sp} + (4.7-4.98\ S_{sp})\ \rho + 5.94\ 10^8 \chi_{sp} + 3.09f \cdot d_m, \text{ MPa.}$$

The values of the adsorpsion potential and the impurity content have appeared insignificant. The regression model is characterized by a rather high degree of adequacy: the coefficient of determination $R^2 = 0.995$, the sum of squares of regression residuals $\Delta\sigma = 0.454$ $MPa^2$ and the Darbin-Watson coefficient DW = 2.3 [2].

The obtained dependence of $\sigma_{comp}$ on a set of properties of tungsten powders forms the basis of the method of an incoming inspection of W powders to define the possibility of their use to produce slightly sintering compacts of WC when carbidzing in a gas medium.

Thus, numerous studies related to the production of W and WC powders have shown that the use of only some technological procedures (sieving of the starting raw material to yield narrow fractions, size reduction, pressing compacts of varions shapes and sizes, variation of the $WO_3$ charge mass, and the use of a methane-hydrogen medium of an eguilibrium composition) have allowed us to devise a number of advanced technologies of W and WC production [3].

References

1. K. Agte and I. Watsek, Tungsten and Molybdenum, Izd-vo Energiya, Moscow, 1964.
2. V. Bondarenko, L. Martynova and V. Golovchan, Method of the production of tungsten carbide powder, Patent of Ukraine № 36958, Publ. 16 April 2001, Bullet. no. 3.
3. V. Bondarenko, E. Pavlotskaya, L. Martynova, and I. Epik. Advanced technologies of production of cemented carbides and composite materials based on them. Proc. 15th Int. Plansee Seminar Austria, vol. 2: P/M Hard Materials, pp.189—203, 2001.

# PHASE TRANSFORMATIONS IN LAYERED STRUCTURES UNDER HIGH PRESSURES AND CONTROLLED SYNTHESIS OF DIAMOND-LIKE PHASES

**Britun V.F., Kurdyumov A.V.**
Frantsevich Institute for Problems of Materials Science, National Ukrainian Akademy of Sciences, Kiev, Ukraine

The majority of synthesis methods of super hard diamond-like phases (DP) are based on transformations of graphite-like phases (GP) under high pressures. These transformations as well as those in other substances can occur by two basic different mechanisms: diffusion or martensitic. At the so-called "catalytic synthesis" of DPs, the diffusion mechanism is usually realized while the GP → DP direct transformations can proceed by both mechanisms (Fig.1).

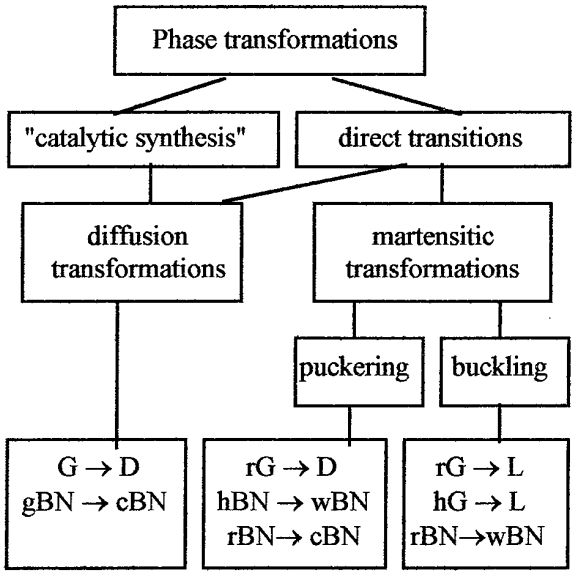


Fig.1. The dependence of the resulting DP on transformation mechanism. Phase designations: G - graphite, D- diamond, L - lonsdaleite, g - graphite-like phasees, h and r - hexagonal and rombohedral modifications, w and c wurtzite and cubic BN.

The objective of the present report is to discuss the peculiarities of the direct phase transformations in carbon and boron nitride and to analyze the dependence of the structure of the resulting DPs on the transformation mechanism. The peculiarity of the GP → DP transformations is related to their high volume effect and to variety of possible structural states of carbon and boron nitride. A great quantity of investigations the results of which are summarized, e.g. in [1], have established that: - at high pressures, diamond and cBN are stable diamond-like phases, while lonsdaleite and wBN are metastable diamond-like phases, - metastable DPs are formed only by martensitic transformations (MT), while stable DPs can be formed by both martensitic and diffusion transformations.

The following experimentally found regularities point to the reality of martensitic transformations in carbon and boron nitride: 1. Rates of transformations to form lonsdaleite and wBN are very high (under static compression the transformations manage to occur in a matter of thousandths of second, while under shock compression in millionths of a second). 2. These transformations can proceed at temperatures at which diffusion processes are impracticable (these transformations have been experimentally observed down to room temperature). 3. Diamond-like phases formed by MT are regularly oriented with respect to the initial graphite-like phases. 4. The degree and the mere possibility of the transformations like graptite → lonsdaleite and gBN → wBN essentially depend on the structure perfection of the initial GPs. 5. Martensitic diamond-like phases have highly imperfect structures and the type of defects is directly related to the crystallographic mechanisms of MT.

Figure 2 is a schematic representation of the *p-T* diagram of GP → DP direct transformations by different mechanisms [2]. The initial GPs are assumed to have an ordered structure, as the MT cannot occur in turbostratic GP. In this diagram below the $p_m$ line but above the $p_0$ line only diffusion transformations are allowable in terms of thermodynamics, however they are practically not recorded in the region of low temperatures. Above the $p_m$ line both diffusion and martensitic transformations are allowable. In this case, in low-temperature region, virtually only MTs are realized, while at rather high temperatures martensitic and diffusion transformations compete with one another. The decisive role in the competition is played by the structure ordering of initial GPs. GP → DP martensitic transformations always involve such deformation processes as a lattice compression along the a1 c a0 axis and splitting of flat basal lay-

ers. Here, there are two principal modes of spliting: layer puckering and layer buckling [3]. Under high pressures MT of hBN is carried out only by puckering mechanism, while all other GPs of carbon and BN can undergo the MT via both mechanisms. For these GPs the realization of one or another martensitic mechanism depend, first of all, on the degree of the hydrostatic nature of compression conditions. It has been found experimentally that under hydrostatic conditions puckering mechanism is realized, while under nonhydrostatic conditions the buckling mechanism occurs mainly [4].

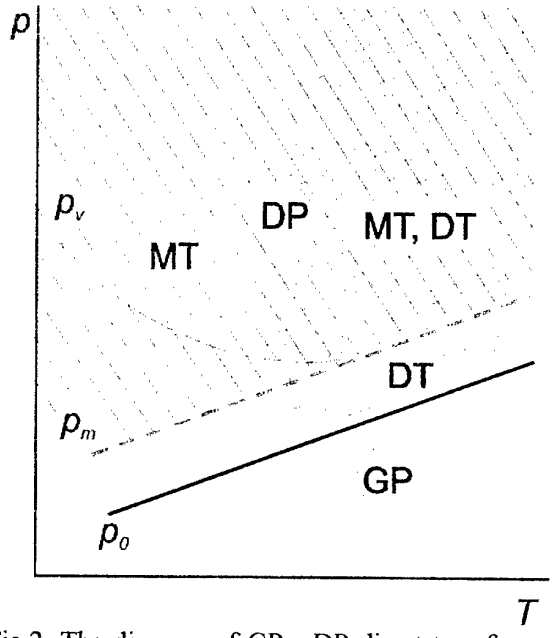


Fig.2. The diagram of GP - DP direct transformations by different mechanisms; MT and DT are the regions of martensitic and diffusion transformations. $p_0$ - equilibrium line between stable GP and DP; $p_m$ - barrier for termally activated MT; $p_v$ - a line of equal nucleation rates.

The mechanism of GP → DP transformations determines both the crystallographic nature of resulted diamond-like phases (see Fig.1) and their real structure. Diffusion transformations, as a rule, give rise to the equaxial grains with a small number of defects, while due to martensitic transformations, a wide variety of structures form that differ in type and concentration of defects. So, in the structure of wBN formed from hBN, defects develop due to the effect of the puckering mechanism: if the atoms of the same name within the same initial grain displace into opposite directions, then at the interfaces between these nuclei growing in radial directions, inversion boundaries (IB) arise in prismatic planes of wBN [5]. Such planar defects hinder the transformation of metastable wBN into stable at high pressures the cBN. A distinguishing feature of wBN produced from rBN by alternative MT mechanism of buckling is a high concentration of basal stacking faults (BSF). These defects are developed due to the nonuniform shear that accompanies buckling MT. Unlike IB, BSF do not hinder but favor the layer-by-layer lattice change in the course of wBN-zBN transformation (as well as the lonsdaleite → diamond transformation; that's why to produce lonsdaleite without diamond impurities is a very difficult task [1]).

Thus, the above peculiarities of GP →DP martensitic transformations by different mechanisms allow us to vary the real structure of the resulting DP over a wide range. Of special interest is the use of textured CVD graphite-like phases: the realization of MT in these phases gives a basic possibility of producing crystal-oriented superhard polycrystals of the diamond-like structure.

1. A.V.Kurdyumov. The structural aspect of high pressure superhard phase synthesis // Powder Metallurgy and Metal Ceramics.- 1995.-V.34, N7.- P.409.
2. V.F.Britun, A.V.Kurdyumov. Martensitic transformations in carbon and boron nitride // J. Superhard Mater.- V.22, N2.- P.3.
3. A.V.Kurdyumov, V.F.Britun, I.A.Petrusha. Structural mechanisms of the rhombohedral BN transformations into diamond-like phases // Diamond and Relat. Mater.- 1996.- V.6.-P.1229.
4. V.F.Britun, A.V.Kurdyumov. Mechanisms of martensitic transformations in boron nirtide and conditions of their development // High Press. Res.- 2000.- V.17.-P.101.
5. V.B.Britun, A.V.Kurdyumov. Crystal defect generation during diffusionless transformations in boron nitride by puckering mechanism // J.Mater.Sci- 1999.- V.34.-P.5677.

# NANOSTRUCTURED MATERIALS: BASIC CONCEPTS, SCIENTIFIC PROBLEMS AND PERSPECTIVES

**Andrievski R.A.**
Institute of Problems of Chemical Physics, Russian Academy of Sciences
Chernogolovka, Moscow Region, Russia

In recent 15-20 years, the development of nanomaterials (nanostructured, nanocrystalline nanophase, nanosize and so on materials (NMs)) has emerged as an important step in creating a new generation of materials. Because of their very fine microstructure (a grain size is usually below 100 nm) NMs potentially revolutionize the traditional material design in many applications via atomic-level structural tailoring of the physical, chemical, mechanical, and biological properties. Note at least three reasons accompanying with the burst of research work in the field of NMs. First, the interest is connected with the hope to realize a high level of properties in the nanocrystalline state. Second, this topic is really an interdisciplinary problem for physicists, chemists, material science specialists, biologists, engineers, and specialists in the Earth Sciences. Third, this topic has revealed many gaps in both our understanding of the nature of the nanocrystalline state and its practical realization. It is not accidentally that the researches of NMs are important parts in the National Nanotechnology Programs such as NNI (USA), NEDO (Japan) and others [1-4]. These Programs are briefly discussed.

There are many types of NMs such as consolidated ones, nanosemiconductors, nano-polymers, nanoglasses, carbon nanostructures, nanoporous solids, nanobiomaterials, catalysts, and supramolecular structures which can be produced by many preparation methods. Some of NMs such as nanostructured Ni foil, magnetic alloy Finemet, superhard multilayer nitride films are successfully produced on an industrial scale. The features of their technology methods, structure and properties are discussed in detail. Some forward-looking NMs such as thermal barriers, sensors, thermally sprayed wear resistant coatings, and new superhard materials are considered also.

The development of new effective NMs is closely linked with decision of many fundamental problems of materials science, physics, mechanics and chemistry of condensed matter. An examples are a nature of crystalline state, regularities of size effects, thermal stability of nanostructures and so on. Presently some preparation methods permit to obtain NMs with very low grain size of about 1-2 nm and lower [5]. The understanding of nature of such peculiar cluster consolidated solids (in contradiction to cluster assemblies) seems to be also very important for the future progress of NMs. The quantum size effects seem to be very likely in these NMs with very small grain size.

**References**

1. Nanotechnology Research Directions, eds. M.C. Roco, R.S. Williams, P. Alivisatos (Klu-
wer Acad. Publ., Dordrecht, 2000) (Russian Translation, ed.R.A.Andrievski, MIR, Mos-cow, 2002)
2. Y. Yamaguchi, H. Komiyama, J. Nanoparticle Research, **3** (2001) 105.
3. M.C. Roco, J. Nanoparticle Res., **3** (2001) 353.
4. R.A. Andrievski, Advanced Materials, №6 (2001) 5.
5. R.A.Andrievski, G.V.Kalinnikov, A.E.Oble-zov and D.V.Shtanskiy, Doklady of Russian Academy of Sciences, **384** (2002) №1.

# STRUCTURAL HYDRODYNAMICS OF POROUS METAL MATERIALS

**Kostornov A.G.**
Frantsevich Institute for Problems of Materials Science NAS of Ukraine, Kyiv, Ukraine

Porous metal materials are widely used as capillary structures in heat-exchange systems of evaporation-condensation and transpiration types.

In operation of above systems the capillary forces have key influence, which govern both transfer of working liquid over pore channels and foraing out of it by pressure or temperature gradient.

In the absence of pressure gradient the liquid in porous body moves under effect of a capillary pressure which in general case is balanced by losses in pressure due to friction in pores and difference of pressure in liquid due to gravity.

Neglecting the inertia effects at low flow rates one can obtain from the equation of pressure balance the following relationtship for average flow rate of liquid.

$$\overline{V} = \frac{Д_{эф}^2}{32\mu LB^2}\left(\frac{4\sigma|\cos\alpha|}{Д_{эф}} - \rho g L \sin\tau\right), \quad (1)$$

from which the maximum rate of capillary absorption under the conditions of full wetting of material is

$$V_{max} = \frac{Д_{эф}\sigma}{8\mu LB^2}, \quad (2)$$

and the maximum heigh of capillary rising is

$$H_{max} = \frac{4\sigma}{Д_{эф}\rho g}. \quad (3)$$

In above expressions $D_{eff}$ is average effective size of pores in material, which is equal to equilibrium value of average hydraulic diameter $D\frac{eq}{h}$ of pore channels in the case of regular porous structures, for which the coefficient of sinuosity is B; $\sigma$, g and $\mu$ are surface tension, density and absolute viscosity of working liquid at wetting angle $\alpha$, respectively; q is gravitational acceleration; L is distance to which the liquid front displaced in material (its ultimate value equals to the specimen length Lo), which is located at the angle $\tau$ with respect to horizontal.
Based on traditional quantity which determines the structural characteristic of permeable material, namely general porosity $\theta$, one can derive the following expression for average flow rate of liquid in pores

$$\overline{V} = \frac{2\sigma}{\mu}\frac{1}{S_0^2}\frac{1}{B^3 Lo}\frac{1}{Д_{гидр}^{равн}}\left(\frac{\theta^2 \ln\theta}{1-\theta}\right)^2, \quad (4)$$

where So is specific surface of the unit volume of porous body.

High-porous specimens made from powders of copper PMS, bronze BrOF10-1, steels H18N10 and H18N15, titanium PTE, PTEM-2, PTM, PTOM and its alloy VT9 with varions dispersity and particle shape; discrette fibers of copper M1 and titanium alloy VT6 with different diameter, and also grid-like specimens made from steel H18H9T were used for experimental study of the kinetics of capillary transport of ethanol, distilled water and acetone.

All determining characteristics for the pore structure of materials under study were preliminary determined in the specimens-whitnesses.

Wide possibilities have been demoustrated concerning the forcast control of the capillar effects in powder structures by technological methods: pressing via elastic film; by adding pore-forming and agents; by vibroforming with both continuous and discrette variation in pore size; by precipitation of fine-grained particles in porous sceleton; by deformation of billets with wedge shape; by cyclic oxidation-reduction; by electric deposition.

The most promissing capillar structures were shown to be materials from monodisperse fibers which capillar potential can be essentially varied through the control of adhesion work with the aid of high-temperature oxidation and vacuum treatment.

In such structures the most effect on the rate of capillar transport in horizontal location has the variation in specific surface of pores and then in porosity and effective pore size.

Upon movement of liquid against gravitational force, porous materials having the most value of parameter of capillar pump $K/O_h^{eq}$ showed the highest capillar rising.

For correct calculation of transport properties of capillar structures in various pore materials, we present the data about wetting them with different liquids (benzine, acetone, ethanol, methanol, water). The equilibrium wetting angles were determined by the methods of lying drop, photographine of shadow image of free meniscus upon wetting of vertically placed specimen with liquid and capillar rising.

Some examples of practical use of capillar mass transfer and its lows are shown for the resolving of methodical and technological tasks (determination of closed porosity in specimens, preparation of composite materials by impregnation, forecasting of service parameters of heating tubes and optimization of their mass and dimensions for different service conditions.

# NEW GENERATION OF THE MATERIALS FOR SENSORS, ACTUATORS AND ULTRASOUND TECHNIQUE ON THE BASE OF FERROELECTRIC RELAXORS

**Glinchuk M.D., Laguta V.V., Bykov I.P.**
I.N.Frantsevich Institute for Problems of Materials Science, NASc of Ukraine, Kiev, Ukraine

1. Piezoelectric and electrostrictive ferroelectric materials lie in the heart of most actuators, sonar transducers and sensors, performing the essential role of electromechanical conversion. Among the modern piezoelectrics and electrostrictors relaxor ferroelectrics are the most important due to giant electrostriction and high electromechanical coefficients ($k \sim 0{,}95$), while in the conventional piezomaterials $k \sim (0{,}5–0{,}6)$. In the last years much attention of the scientists and engineers was paid to inorganic relaxors $PbMg_{1/3}Nb_{2/3}O_3$ (PMN), $PbSc_{1/2}Nb_{1/2}O_3$ (PSN), $PbSc_{1/2}Ta_{1/2}O_3$ (PST), $Pb_{1-x}La_xZr_{0,35}Ti_{0,65}O_3$, $0{,}6 \le x \le 0{,}9$ (PLZT), to their composites like $(PMN)_{1-x}(PbTiO_3)_x$ (PMN-PT), $(PSN)_{1-x}(PST)_x$ and to organic relaxors on the base of illuminated by fast electrons polymeric ferroelectrics P(VDF/TrFE).

The scientists of our Institute are working in the field of the relaxor ferroelectrics during 15 years. They developed the scientific concept that made it possible to find out the fundamental mechanisms which are in response on unusual properties of the relaxor based ferroelectrics. In particular it was shown that the high level of useful properties is related to the appearance of mixed ferro-glass phase with coexistence of long and short range polar order. The absence of conventional type of domain structure in this phase results in high dielectric permittivity ($\varepsilon \sim 10^5$), giant electrostriction, high coefficient of electromechanical coupling with small hysteresis and small dielectric losses, the mechanical distortions ($s \sim 5$ %) being more than an order of magnitude larger than the level achieved in the conventional piezoelectric ceramics.

Since in the disordered ferroelectrics like relaxors the local structure plays the decisive role in this material properties we performed the local properties investigations by ESR [1] and NMR methods (see [2–4] and ref. therein).

The brief review of these results as well as those related to aforementioned concept for the relaxor based material properties explanation [5–9] is given in this report.

2. In the NMR studies of solids the nucleus is used as a probe to investigate local structure via its coupling with the lattice. The coupling the most frequently involved is the interaction of the nuclear quadrupole moment with the electric field gradient (EFG) which is known to be very sensitive to local structure. In the case of disordered ferroelectrics, such as PMN, substitutional disorder in the B-site lattice (e.g. $Nb^{5+}$ substituted for $Mg^{2+}$ and vice versa) and the ions shifts from their positions in the ideal cubic crystal lead to appearance of nonzero random EFG. The randomness of EFG has to result in inhomogeneous broadening of NMR line. The theoretical analysis of the observed line shape [2] made it possible to obtain information about the values and the directions of the ions shift.

In Fig.1 one can see the observed NMR spectrum of $^{93}Nb$ (transition $+1/2 \leftrightarrow -1/2$) shown by points and calculated shape shown by solid line for the case when there are the microregions with the Nb ions shifts along ⟨001⟩, ⟨011⟩ and ⟨111⟩ type of directions, their volume being respectively 60 %, 20 % and 20 % of the sample volume. The mean values of shifts were estimated in nm as $d_{\langle 001\rangle} = 0{,}032$; $\Delta d_{\langle 001\rangle} = 0{,}005$; $d_{\langle 011\rangle} = 0{,}03$; $\Delta d_{\langle 011\rangle} = 0{,}01$; $d_{\langle 111\rangle} = 0{,}02$; $\Delta d_{\langle 111\rangle} = 0{,}01$; where $\Delta d$ is the dispersion so that there are the distribution of the ions shift values and directions.

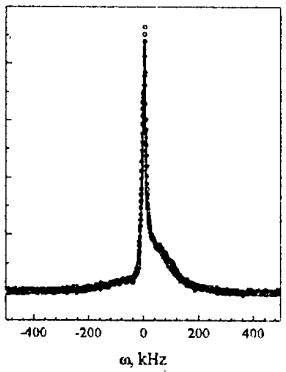


Fig.1. Comparison between the experimental $^{93}Nb$ $1/2 \leftrightarrow -1/2$ NMR and calculated line shape in PMN for $\mathbf{B} \| [001]$, $d \| \langle 001\rangle, \langle 011\rangle, \langle 111\rangle$.

3. This distribution as well as the vacancies of lead and oxygen, the random excess charges related to the ions substitutional disorder results in the distribution of random electric field, that influence all the properties of the relaxors, including its phase diagram (see Fig.2), where $dE_0 = k_B T_{cmf}$

is mean field related to indirect interaction of the shifted ions via Burns phase soft mode and $\Delta E$ its dispersion. The condition $E_0 >> \Delta E$ corresponds to conventional transition between ferroelectric (FE) and paraelectric (PE) phase which could be in Burns phase, so that $T_{cmf} = T_{Burns}$ that is known to be about 600–650 K in most the relaxors. But the strong random field gives $\Delta E \approx E_0$ or $\Delta E > E_0$ that leads to FE long range order destruction so that only nonergodic mixed ferro-glass phase (FG) or dipole glass state (DG) with short range order polar clusters appeared to be possible [5].

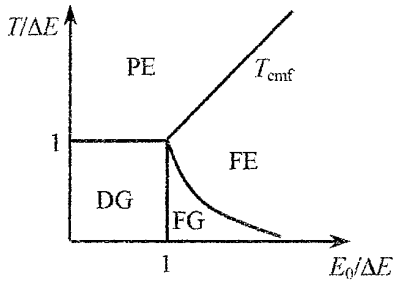


Fig. 2. Schematic phase diagram of relaxor.

The physical concept developed in the random field theory framework [5] made it possible to explain the dependence of dielectric susceptibility maximum position on concentration of La ions in PLZT, the peculiarities of nonlinear susceptibility of the PMN and PMN-PT relaxors [6], the origin of Vogel-Fulcher law in the relaxation time behaviour [7], the anomalies of correlation radius temperature dependence in PMN [8].

In what follows we shall describe briefly the results of PMN-PT phase diagram calculations performed in the random field theory framework [9]. The electric polarization of $(PMN)_{1-x}(PT)_x$ composite was written as

$$\vec{P} = x\frac{\beta_1 \vec{d}_1^{\,*} L_1}{a_1^3} + (1-x)\frac{\beta_2 \vec{d}_2^{\,*} L_2}{a_2^3}, \qquad (1)$$

where $L_i$, $a_i$, $\beta_i$ and $\vec{d}_i^{\,*}$ $(i = 1, 2)$ are respectively the number of coherently oriented dipoles, lattice constants, fraction of unit cells in which dipoles exist and $\vec{d}^{\,*}$ is effective dipole moments related to the ions shift. The directions of $\vec{d}_1^{\,*}$ and $\vec{d}_2^{\,*}$ reflect the tetragonal symmetry of PT and rhombohedral symmetry of PMN.

For the case of two orientable dipoles one can write

$$L_i = \int \tanh\left(\frac{d_i^* E}{k_B T}\right) f_i(E, L_i) dE, \qquad (2)$$

where the random field $E$ distribution function $f_i(E,L_i)$ was calculated in the statistical theory approach and for conventional ferroelectrics like PT it has the form of $\delta$-function $f(E,L) = \delta(E - E_0 L)$.

The phase diagram gives the dependence of temperature $T_c$ on concentration $x$ at which polarization arises. The calculated $T_c(x)$ dependence is depicted in Fig.3. One can see that the theory (solid line) describes pretty good the experimental points.

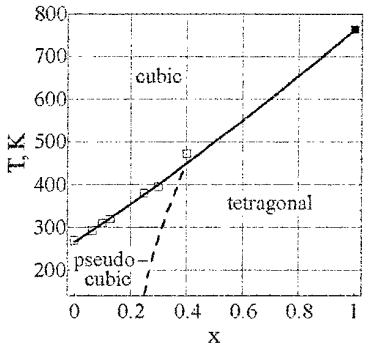


Fig. 3. Phase diagram of $(PMN)_{1-x}(PT)_x$: points – experiment, solid line – theory

The calculations have shown that maximal contribution of pseudo-cubic (rhombohedral) component takes place at $x = 0{,}135$. Because of pseudo-cubic symmetry the maximal value of dielectric response, piezoelectric and electromechanical coefficient can be expected at $x = 0{,}135$. This concentration a little bit larger than $x = 0{,}1$ where the aforementioned properties high values were observed.


1. M.D.Glinchuk, V.V.Skorokhod, I.P.Bykov et al., J.Phys.:Condens.Matter, **6**, 3421 (1994).
2. M.D.Glinchuk, V.V.Laguta, I.P.Bykov et al., J.Appl.Phys., **81**, 3561 (1997).
3. R.Blinc, A.Gregorovic, B.Zalar, R.Pirc, V.V.Laguta, M.D.Glinchuk, Phys.Rev. B, **63**, 024104 (2000).
4. M.D.Glinchuk, S.N.Nokhrin, I.P.Bykov, V.V.Laguta et al., Phys.Stat.Sol.(b), **228**, 757 (2001).
5. M.D.Glinchuk, R.Farhi, J. Phys.: Condens. Matter, **8**, 6985 (1996).
6. M.D. Glinchuk, V.A. Stephanovich, J. Phys.: Condens. Matter, **10**, 11081 (1998).
7. M.D. Glinchuk, V.A. Stephanovich, J. Appl. Phys., **85**, 1722 (1999).
8. M.D.Glinchuk, V.A.Stephanovich, E.A.Eliseev, et al., Appl.Phys.Lett., **80**, 646 (2002).
9. M.D.Glinchuk, E.A.Eliseev, V.A.Stephanovich, B.Hilczer, Ferroelectrics, **254**, 13 (2001).

# PHYSICOCHEMICAL ASPECTS OF THE DEVELOPMENT OF FUNCTIONAL MATERIALS BASED ON ALIOSUBSTITUTED OXIDES AND THEIR APPLICATION

**Belous A.G.**
V.I.Vernadskii Institute of General and Inorganic Chemistry, Kyiv, Ukraine

The progress in the development of new functional materials substantially determines the evolution in frontrank areas of engineering. When developing these materials the search for effective ways in the simulation of their properties already at the synthesis stage is the strategic direction of the research. In this connection the investigation of aliovalent substitution in the structural sites, which may result in the lattice distortions, formation of structural channels and vacancies, varying charge of crystal sublattices are of a great scientific and practical interest. This investigation could evidently result in the synthesis of new compounds as well as in the development of new materials based on them with the important engineering properties.

Therefore, the research in the field of the chemistry of aliosubstituted oxides - in particular, those of elements of III-V groups - directed to the synthesis, investigation into their structure and properties, as well as the development of new materials with promising applications in engineering is the problem of a topical interest.

In this work the compounds have been synthesized with various crystal structures including those of the perovskite, defect perovskite, layered perovskite, tetragonal tungsten bronze, spinel. It has been synthesized the series of the ferrites, aluminates, titanates, zirconates, niobates, and tantalates.

In consequence of the complex research the number of new regularities common for the aliovalent substitution have been revealed.

When using as the example the systems $(La,Li)(Ti,Nb,Ta)O_3$, where the ions of lithium substitute for the lanthanum ions, it has been shown that aliovalent substitution may result in certain conditions when the ions residing crystallographic sites do not meet structural requirements. The ions of lithium and lanthanum, whereas residing in one sublattice, act contrary: the lanthanum ions promote the formation of the perovskite structure while the lithium ions reduce the total number of "structural vacancies" and consequently contribute to the stabilization of the perovskite structure at higher temperature.

In the systems $(La,M)(Ti,Nb,Ta)O_3$, where M is Li, Na, K, the permittivity magnitude in optical band has been shown to depend only on the matrix structure whereas the alkaline ions affect the dielectric properties only in radiofrequency range. In this case the lithium ions reside in the crystallographic channels characterized by the lack in the filled sites, and, as the consequence, they have not rigid bonds with the matrix. This allowed the development of new lithium conducting materials with the record-high characteristics [1-5].

In the parallel systems -where the ions of rare-earth elements are replaced by alkaline ions with larger ionic radii (sodium or potassium ions)- microwave (MW) dielectrics have been shown to form. They simultaneously combine high dielectric permittivity, low dielectrics loss and high temperature stability of physical properties in the MW frequency range. Whereas the presence of one low-frequency oscillation in the phonon spectrum (soft mode), which is responsible for the low temperature stability of physical properties, is typical for the perovskites the aliovalent substitution may result in another low-frequency oscillation. It noticeably contributes to the permittivity and provides high temperature stability of electrophysical properties. Similar trends have been found out also in the materials with both the structures of the defect perovskite and tetragonal tungsten bronze [6-8].

The "structural vacancies" have been shown to be the additional scattering centers of electromagnetic energy. Therefore, it is possible to control the scattering degree when reducing total amount of the vacancies by aliovalent substitution when sites corresponding to "structural vacancies" are filled up by different ions [9].

When using the aliovalent substitution in the crystal sublattices it is possible to obtain the nonlinear materials with PTCR properties. It has been shown that amongst the intermediate phases of the synthesis of these materials there is the phase, which is not stable at high temperatures in air. However, its interaction with other intermediate phases results in the formation of materials with PTCR properties [10-12].

Thus, by means of aliovalent substitution within the range of certain structural type and close chemical compositions it is possible to control the properties of complex oxide systems varying them from those of MW dielectrics to those of cation conductors and semiconductors – ferroelectrics.

The synthesis technique should ensure high chemical homogeneity of the materials to provide the highest potential level of their electrophysical properties. To this goal the chemical methods of synthesis are required. Regarding the functional materials the precipitation from solutions could be considered as the most generalized technique. However, this method is characterized by significant lacks. In particular, the precipitates formed at the synthesis stage require prolonged both flushing and filtering stages. Moreover, after preheating the precipitates form the conglomerates, which require long-time mechanical milling. It is possible to show that when carrying out the precipitation these lacks originate in the high speed of the formation of crystallization centers in comparison to that of the diffusive grain growth. In order to overcome the above lacks the ways of the enhancement of the precipitation technique have been developed. The results allowed the production of the precipitates with high filtering and flushing rates, which form soft powders after the thermal treatment and do not require any additional milling. This also allowed the production of the powders with nanosize particles characterized by narrow size distribution [13].

As an outcome of the investigation carried out new functional materials and elements based on them for the applications in radio communication and mechanical engineering have been developed [14].

## References


1. A.G.Belous, L.G.Gavrilova, S.V.Polyanetskaya, Z.Ya.Makarova, V.P.Chalyi. Stabilization of the perovskite structure of lanthanum titanate // Soviet Progress in Chemistry. 1984, v.50, No.5, pp.12-14.
2. A.G.Belous, G.N.Novitskaya, S.V.Polyanetskaya, Yu.I.Gorniciv. Crystal-chemicals and electrophysical characteristics of complex oxides $La_{2/3-X}M_{3X}TiO_3$ //Zh.Neorg.Khim. 1987, v.32, No.2, pp.283-286.
3. A.G.Belous. Synthesis and electrophysical properties of novel lithium ion conducting oxides// Solid State Ionics. 1996, v.90, pp.193-196.
4. A.G.Belous. Propertis of Lithium Ion-Conducting Ceramics based on Rare-Earth Titanates // Ionics, 1998, v.4, No.5-6, pp.360-363.
5. A.G.Belous. Lithium ion conductors based on the perovskite $La_{2/3-X}Li_{3X}TiO_3$ // Journal of the European Ceramic Society. 2001, v.21, pp.1797-1800.
6. A.G.Belous, O.V.Ovchar. MW Ceramic Dielectrics Based on the System BaO-$(Nd,Sm)_2O_3$-$TiO_2$//Key Engineering Materials. 1997, v.132-136, pp.1191-1194.
7. A.G.Belous, O.V.Ovchar. Solid-state reaction mechanism for the formation of $Ba_{6-X}Ln_{8+2X/3}Ti_{18}O_{54}$ (Ln = Nd, Sm) solid solutions //Materials research Society. 2001, v.16, No.8, pp.2350-2356.
8. A.G.Belous. Physicochemical aspects of the development of MW dielectrics and their use //Journal of the European Ceramic Society. 2001, v.21, pp.2717-2722.
9. A.G.Belous. Physicochemical Aspect of the Development of new functional materials based on heterosubstituted titanates of rare-earch elements with the perovskite structure //Theoretical and Experimental Chemistry. 1998, v.34, No6, pp.301-318.
10. L.L.Kovalenko, O.I.V'ynov, A.G.Belous. Semiconducting Barium Titanate Doped with Oxygen-free Compounds // Journal of the European Ceramic Society. 1999, v.19, pp.965-968.
11. O.I.V'ynov, A.G.Belous. Phase Transformation in the Synthesis of $Ba(Ti_{1-X}M_X)O_3$-based PTCR Ceramic. 1999, v.19, pp.935-938.
12. A.G.Belous, O.I.V'yunov, L.L.Kovalenko. (Ba,Y)(Ti,Zr,Sn)-Based PTCR Materials //Ferroelectrics. 2001, v.254, pp.91-99.
13. A.G.Belous, E.V.Pashkova, A.N.Makarenko, B.S.Khomenko, I.Ya.Pishchai. Effect of Synthesis Procedure on the Crystallization of Yttria-stabilized Zirconia //Inorganic Materials, 1997, v.33, No12, pp.12461250.
14. V.G.Tsykalov, A.G.Belous, O.V.Ovchar, Y.D.Stupin. Monolithic filters and frequency-separation devices based on the ceramic resonators // 27 European microwave Conference-Exhibition, Jerusalem, September 8-12, 1997, pp.544-549.

# HYDROGEN ABSORBING INTERMETALLICS FOR CHEMICAL CURRENT SOURCES

**Solonin Yu.M.**
Frantsevich Institute for the Problems of Materials Science, NAS of Ukraine, Kyiv, Ukraine

During last 10-15 years the new perspective direction of the hydride-forming alloys application appeared. These materials may be used for the substitution of the poisonous cadmium in very popular nickel-cadmium rechargeable batteries. The new nickel- metal hydride (Ni-MH) batteries possess enhanced characteristics and are ecologically safe. An electrode which can quasi-reversibly store a large quantities of hydrogen is of interest as a construction material for high energy density batteries. Secondary batteries using a hydrogen rechargeable electrode operate in a different manner than lead/acid, nickel/cadmium or other battery systems. Upon application of an electrical current to the anode, the anode material (Me) is charged by the absorption of hydrogen:

$$Me + xH_2O + xe^- \rightarrow MeH_X + xOH^-$$

Upon discharge the stored hydrogen is released to provide an electric current:

$$MeH_X + xOH^- \rightarrow Me + xH_2O + xe^-$$

The MH electrodes are still posed essentially on the rare earth-based $AB_5$-type alloys with an electrochemical capacity of less than 300mAh/g. Zr-based $AB_2$-type hydrogen-absorbing alloys propose 30% higher capacity. But these alloys require very strong conditions or a lot of cycles for activation and their extreme characteristics are not stable during cycling. The most perspective materials for battery application are Mg-based alloys. The research on Mg-based alloys-hydrogen systems has increased because of its promising characteristics (3,6 wt. % H for $Mg_2NiH_4$) for the use in vehicles, which is demanding a lower material cost and higher hydrogen storage capacity than in the conventional secondary nickel-metal hydride batteries, based on $AB_5$ –type alloys. However the kinetic properties of Mg-based alloys are poor and the hydrides formed are too stable to release hydrogen at low temperatures. It has been reported that amorphous and nanocrystalline Mg-Ni alloys prepared by ball-milling and mechanical alloying can electrochemically absorb and desorb hydrogen even at room temperature (theoretically discharge capacity may achieve 900 mAh/g), but the cycle life of these alloys is very short [1].

The microstructure of the hydrogen forming alloys strongly effects their electrochemical characteristics. Electrode materials with disordered and amorphous structures have become of interest due to their unique combinations of mechanical, chemical and electrical properties. Hydrides of the disordered metal alloys are capable of absorbing larger amounts of hydrogen than their ordered counterparts and possess of high cycle-life. Method of the Braked Diffusion Interaction (BDIM) based on the precise sintering have been realized [2,3], which allows to obtain the $LaNi_{4.5}Al_{0.5}$ and $LaNi_{2.5}Co_{2.4}Al_{0.1}$ alloys with controlled disordered and inhomogeneous structure. Such structure consists of small deviation from average correlation of different B-type elements in alloy with strictly invariable correlation between B- and A- type constituents according formula $AB_5$. The alloys $LaNi_{4.5}Al_{0.5}$ with such structure possess the enhanced cycle life during electrochemical hydriding-dehydriding.

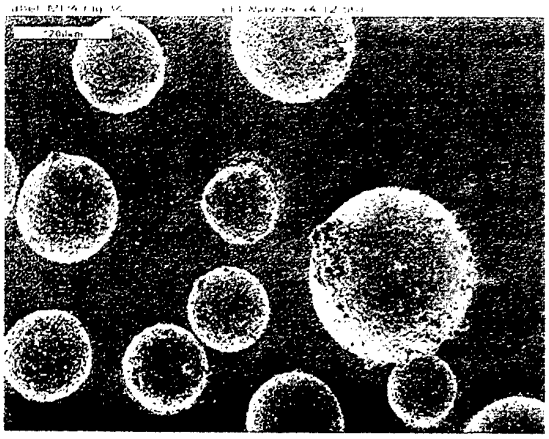

Fig.1.

During gas atomization of liquid metals very high cooling rate up to $10^6$K/s can be achieved and the peculiar structure of the powders with fine grains and amorphous component obtained. Powders of the hydride-forming alloys with such structure possess enhanced corrosion resistance and seem to be promising materials for the negative electrodes of the nickel/metal hydride batteries. The gas atomized powders of $LaNi_{4.5}Al_{0.5}$, $LaNi_{2.5}Co_{2.4}Al_{0.1}$, $(Mm,La)Ni_{3.5}Co_{0.7}Al_{0.35}Mn_{0.4}Zr_{0.05}$ alloys were prepared [3-5] and separated into fractions with different particle sizes (Fig.1.) The morphology,

oxygen content, crystal structure of the powders depending on particle size have been analyzed by means of XRD, SEM, EDS. The hydriding and electrochemical properties of different fractions were evaluated too. The fractions with particle size less than 50μm have a poor activity at both gaseous and electrochemical hydriding. On the DTA curve of the fraction of small particles the additional exothermal peak was observed, which could be attributed to the thermal induced crystallization of the more developed amorphous component of the small particles structure. Gas atomized powders of large particles sizes display a similar hydrogen and electrochemical capacity as arc melt alloys.

The alloys type $La(Mm)Ni_{5-x}Me_x$, where Me are Co, Mn, Zr, Al and other metals, are most widely used material for the production of the negative electrodes of the nickel/metal hydride batteries [3]. The use of the mishmetal instead of pure La allows to lower the alloy cost. The mishmetal produced in Ukraine have the composition: La - 20-25%; (Nd+Pr) - 10-15%; Ce - 48-55%; Dy - 0,5-1,0%; Y - 4-5%; Sm - 1-1,5%. It is known that such content of the La in mishmetal is not enough to provide the high level of hydriding and electrochemical properties. The La and Co have been added to improve the electrochemical activation and cycle life characteristics. The alloy with additions of La and Co is more active during hydriding and needs less time for activation [6]. This alloy also forms hydride with higher content of hydrogen up to 1,5 weight.% and electrochemical capacity about 240 mA.h/g.

For the preparations of the scandium containing $AB_5$ alloy we used the Al-Sc primary alloy, which contains 4 weight % of Sc. After 5 cycles of charge-discharge the alloy $LaNi_{2,5}Co_{2,4}Al(Sc)_{0,1}$ demonstrates the electrochemical discharge capacity on the level of 300mA.h/g. The conventional alloy type $LaNi_{2,5}Co_{2,4}Al$ without Sc addition have electrochemical capacity - 240mA.h/g. So, the small additions of the scandium can improve the characteristics of hydride-forming alloys of electrochemical application.

Zirconium-based alloys are perspective materials for negative electrodes of nickel-metal hydride batteries. At the same time, these alloys have a number of lacks, which prevent their wider use. The basic lacks are, firstly, a necessity of additional processing for alloys activation and, secondly, the insufficient cycle life of the alloys with really high specific capacity (more than 400 mAh/g). We studied structure and electrochemical properties (Fig.2) of $ZrMn_{0.5}Cr_{0.2}V_{0.1}Ni_{1.2}$(1), $ZrMn_{0.5}Cr_{0.18}Al_{0.1}Ni_{1.2}$(2) and $Zr_{0.59}Ti_{0.41}V_{0.53}Cr_{0.22}Fe_{0.20}Co_{0.27}Ni_{0.78}$(3) alloys [7].

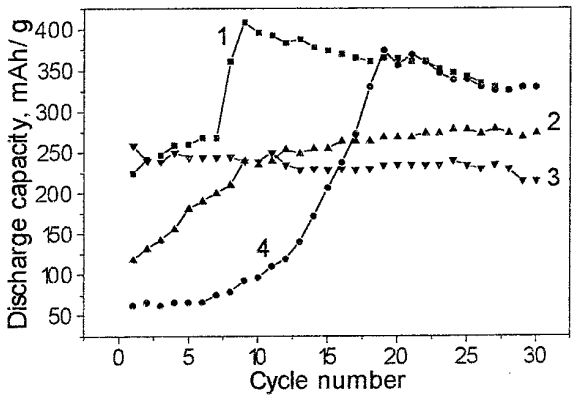


Fig.2.
1,2,3 – corresponding alloy in composite with Ni,
4 – pure alloy N1

For the determination of the electrochemical properties, such as discharge capacity and its dependence on cycle number, the mixtures of the alloys powders with nickel powder in mass proportion 1:1 were prepared. The electrochemical measurements were carried out in sealed cells. The alloy $ZrMn_{0.5}Cr_{0.2}V_{0.1}Ni_{1.2}$ mixed with nickel already in first cycles demonstrated discharge capacity up to 400 mAh/g. At the same time, without Ni this alloy needs about 20 cycles to reach the nominal capacity.

**References**

[1] Yu.M. Solonin. et al., Extended Abstracts of ICHMS'2001,ADEF-Ukraine, Kiev-2001,114-115.
[2]Yu.M.Solonin et al., Functional Materials,**6**,#2(1999), pp. 1-5.
[3] Yu.M. Solonin et al., Poroshkovaja Metallurgija, 2002 (in Russian) in press.
[4] Yu.M. Solonin et al., J. Alloy and Comp., **253-254** (1997), pp. 594-597.
[5] Yu.M. Solonin et al., Int. J. Hydrogen Energy, **24**(1999), pp. 277-282.
[6] Yu.M. Solonin et al., Hydrogen Materials Science and Chemistry of Metal Hydrides, NATO Science Series publ., 2002, in press.
[7] M.V.Karpets et al., Extended Abstracts of ICHMS'2001, ADEF-Ukraine, Kiev-2001,106-107.

# TOUGHNESS AS CHARACTERISTIC OF MECHANICAL STATE OF STRUCTURAL MATERIAL

**Kotrechko S., Meshkov Yu.**
G.V.Kurdyumov Institute for Metal Physics, National Academy of Sciences of the Ukraine, Kyiv

Toughness is one of the most important mechanical properties of structural materials because of their mechanical stability under the conditions of loading. Toughness nature is not quite simple since this property appears in different ways, namely: ductility at fracture; residual ductility in the presence of crack (it is fracture toughness $K_{IC}$); energy of fracture; resistance to impact loading *KCV*; resistance to embrittlement at cooling of metal (it is cold-resistance).

All these characteristics have a common feature – resistance to transition to brittle state i.e. resistance to brittleness. Therefore, the most general definition of toughness may be given as follows: it is the measure of resistance to transition to brittle state (toughness parameter) $p_T$:

$$p_T = R_{MC} / \sigma_1(e) \qquad (1)$$

where $R_{MC}$ is critical stress of brittle fracture of metal (it "brittle strength"); $\sigma_1(e)$ is maximum tensile principal stress at the value of strain that is equal to *e*. If $p_T > 1$ then metal is tough; at $p_T < 1$ and $\sigma_1(e) > \sigma_{02}$ ($\sigma_{02}$ is proof stress at $e = 0.002$ (0.2%)) metal is brittle.

Principal stress $\sigma_1(e)$ depends on the value of strain hardening, on overstress $j$ caused by the crack, on loading rate $\dot{\varepsilon}$ and temperature $T$. All these factors affect metal and result in certain overstress $E_m$ over proof stress $\sigma_{02}$:

$$\sigma_1(e) = \sigma_{02} \cdot E_m \qquad (2)$$

So

$$p_T = R_{MC} / \sigma_{02} \cdot E_m = K_T / E_m \qquad (3)$$

Here $K_T = R_{MC} / \sigma_{02}$ is toughness index.

For structural concentrator expression for $E_m$ is the following [1]:

$$E_m = (j / K_{SS})(\alpha_\sigma \sigma_N / \sigma_{02})^{2n/(1+n)} \qquad (4)$$

where $\alpha_\sigma$ is Neuber stress concentration factor; $\sigma_N$ is nominal (average) stress; $n$ is Hollomon strain hardening index; $K_{SS}$ is parameter accounting for the strain gradient within the local plasticity region near concentrator.

Toughness parameter $p_T$ of material with stress concentration factor $\alpha_\sigma$ in approximation of small plastic region ($j \sim 1.15$, $K_{SS} \sim 1$) may be written:

$$p_T = (K_T / 1.15)(\alpha_\sigma \sigma_N / \sigma_{02})^{2n/(1+n)} \qquad (5)$$

Ductile metal ($K_T > 1$) with stress concentration factor $\alpha_\sigma$ may be tough ($p_T > 1$) or brittle ($p_T < 1$). This depends not only on its structure ($K_T$, $n$) but also on environment ($\alpha_\sigma$) and just on the level of applied stresses $\sigma_N$.

Formula (5) expresses local toughness parameter $p_T$ ahead of concentrator with stress concentration factor $\alpha_\sigma$ only if local plastic deformation started i.e. conditions required for fracture have now arisen. Consequently, material's state characterising by parameter $p_T = 1$ means, by (5), realisation of fracture criterion i.e. for material with stress concentration factor $\alpha_\sigma$, condition $p_T = 1$ is sufficient condition for its fracture because stress $\sigma_N$ guarantees required condition of yielding ahead of concentrator.

It results from formula (5) that one has an important possibility to select safe stress level $[\sigma_N]$ for material with specified structure ($K_T$, $\sigma_{02}$, $n$) and concentrator characterising by $\alpha_\sigma$ (for given toughness parameter $p_T = 1.30$) (see Table 1).

Parameter $p_T$ control according to (5) enables to realise an optimal combination of strength ($\sigma_{02}$) and toughness ($K_T$) in steels in which overbalance of toughness ($K_T \sim 2.5 \ldots 3.0$) may be decreased to safe level owing to increase in strength ($\sigma_{02}$) by proper heat treatment.

Unlike conventional characteristics of toughness (*KCV*, $K_{IC}$, $\psi$), toughness parameter $p_T$ allows to differentiate influence of structure ($K_T$, $\sigma_{02}$, $n$) and mechanical state ($\alpha_\sigma$, $j$, $\sigma_N$) on metal toughness. Besides, such approach to toughness permits to combine optimally main characteristics of metal – its strength $\sigma_{02}$ and toughness $p_T$.

Table

| Steel | $\sigma_{02}$, MPa | $K_T$ | $p_T$ | $[\sigma_N]$, MPa |
|---|---|---|---|---|
| 15ГС | 380 | 2.45 | 1.64 | 190 |
| 30ХГСА | 1360 | 1.58 | 1.30 | 272 |
| 40Х | 700 | 2.24 | 1.59 | 350 |
| 18Х2Н4ВА | 1060 | 1.73 | 1.31 | 115 |

# HYDROGEN-INDUCED PHASE TRANSFORMATIONS AND THEIR USE IN HYDROGEN TREATMENT OF MATERIALS

**Goltsov V.A.**
Donetsk National Technical University, Donetsk, Ukraine

Hydrogen treatment of materials [1] is based on specific peculiarities of hydrogen giving a possibility of a *strong and controllable* action on materials. This action is *reversible* in the sense that hydrogen can be removed from a material up to very low temperatures. Hydrogen action on materials comprises physical, chemical, physico-chemical and mechanical components [2].

Hydrogen action causes a disturbance of thermodynamic conditions of a material existence. As a result there appears a thermodynamic necessity in hydrogen-induced phase transformations. This is the so-called 'artificial' hydrogen-induced polymorphism. Hydrogen-induced phase and structural transformations are classified [2] into three large classes: hydride (diffusive–cooperative), diffusive and intermediate phase and structural transformations.

*Hydride (diffusive–cooperative) phase transformations* [3] take place in hydrogen–material systems at low temperatures ($T$<(0.2–0.45)$T_m$). They have a diffusive–cooperative synergetic mechanism, which includes two different, but interconnected and mutually conditioned sub-mechanisms: diffusive rearrangements in the hydrogen interstitial subsystem, and a cooperative, martensite-like sub-mechanism of structural rearrangements in a material matrix.

Another significant feature of hydride transformations is that hydrogen stresses play an absolutely important role in material–hydrogen systems. Near a critical point of a transformation, hydrogen concentration stresses are first generated by small hydrogen inhomogeneities (for instance, those caused by hydrogen fluctuations). Elastic coherent nuclei of a hydride phase are produced on supercooling or some elevation of hydrogen pressure. In metallic materials during the process of a nuclei growth hydrogen stresses grow too, coherency is lost at some time and *plastic deformation of matrix takes place*. In turn, this gives rise to a mutual redistribution of hydrogen, evolution of hydrogen stresses, *etc*. In other words, the loss of coherency and a further growth of hydrogen precipitates trigger the mechanisms of hydrogen phase naklep (cold work).

So, the appearance and relaxation of very strong internal 'hydrogen' stresses induced by hydrogen gradients and differences in the specific volumes of transforming phases are very important to understand the nature of this class of phase transformations. A thermo(baro)–elastic–diffusive braking of the transformation or even equilibrium of transforming phases are realized during hydride transformations. A synthesis of the knowledge of hydride transformations is given in [2]. Kinetics and morphology of hydride $\alpha \rightarrow \beta$ and $\beta \rightarrow \alpha$ phase transformations can be found in [3].

Hydrogen treatment based on this class of transformations permits the preparation of stronger metals, the production of fine structure metallic materials, superstrong materials with a high TRIP plasticity, materials with a memory shape effect, the production of an intermetallic material powder, and makes the powdering easier (HD process).

*Hydrogen-induced diffusive phase transformations* [4] take place at elevated temperatures ($T$>(0.2–0.45)$T_m$). They have a mechanism of nucleation and diffusion-controlled growth. The kinetics of a hydrogen-induced phase transformation in the $Nd_2Fe_{14}B$-type alloys was studied in [4].

At all temperatures (600-750°C) there was a transformation incubation period (30–90 *sec*). Analysis of the mechanism of the transformation was carried out [4] using the Avrami theory, according to which a phase transformation can be described by:

$$k = 1 - \exp(-dt^n),$$

where $k$ is a degree of transformation, $t$ is time, $d$ and $n$ are constants.

The results were plotted in coordinates: $\ln\ln[1/(1-k)]$-$\ln t$. The curves were parallel straight lines, the slope of which gave $n$=1.06. By the Avrami theory, if $n$ = 1–1.5, a transformation has a nucleation and growth mechanism with diffusion-controlled growth of particles of new phases. This result is very important and it confirms that hydrogen-induced phase transformations at elevated temperatures ($T$ >(0.2–0.45)$T_m$) have a classical mechanism of nucleation and growth and are controlled by a long-range diffusion of material atoms. Therefore, they may be classified as hydrogen-induced *diffusive* phase transformations.

Processes based on transformations of this class permit the production of materials with a changed phase structure, with the finest grain and sub-grain structure, *etc.* For example, this transformation is the basis of a very well-known HDDR process permitting the production of high coercive magnetic materials of the Nd–Fe–B type.

*Hydrogen-induced intermediate transformations* [2] take place at moderate temperatures ($0.2T_m<T<0.45T_m$). The main peculiarity of this class of transformations is that only short-range (atomic scale) rearrangements of atoms – components of a material – take place. Dissolved hydrogen changes the interaction of atoms – components of a material. Thus, if under the action of hydrogen the interaction of atoms of different species becomes stronger, there might be an atomic ordering transformation. On the contrary, if the interaction of the same atoms becomes stronger, there might be an atomic segregation transformation. Hydrogen-induced amorphization (HIA) is a transformation of the same class. Common conditions of HIA taking place *in solid state* materials were formulated in the middle of the 1980s [2]:

1. Initial intermetallic alloys of the $A_nB_m$ ($A_{n-x}C_xB_{m-y}D_y$)-type must consist of atoms having a large difference in their affinity for hydrogen. Atom A must be a potent hydride-forming element (Zr, Ti, *etc.*) and B must be a non-hydride forming element (Fe, Co, Ni, Rh, Al, Ga, *etc.*).

2. This intermetallic alloy in a homogenized crystal state should be able to absorb hydrogen at low to moderate temperatures and *form a hydride which is less stable than the hydride of element A.*

3. Such an alloy as a $A_nB_mH_x$ hydride alloy is thermodynamically unstable. At elevated temperatures, when an enhancement of diffusivity takes place, the $A_nB_mH_x$ hydride alloy will undergo a diffusive phase transformation and will be transformed from a mono-phase state to a poly-phase state. Usually, one of these phases is the hydride of element *A*, or a phase based on it. The other phase without hydrogen or with a low hydrogen content is based on the crystal phase of element *B*. As mentioned above a hydrogen-induced diffusive phase transformation needs a long-range diffusion of metal atoms. Therefore, *for kinetic reasons they cannot be fulfilled at low and moderate temperatures.*

4. Under the above conditions there must exist some moderate or low to moderate temperature interval where a short (atomic)-range diffusion only is possible. At this moderate temperature under the same thermodynamic driving force, short-range diffusive rearrangements of the structure might be realized, and unstable (but frozen) or metastable structural states will be formed. Therefore, *HIA is one of those intermediate transformations leading to the formation of an amorphous structure.*

Many investigations have been conducted (see, for example, Refs. [2]) and an understanding of HIA is now much deeper. More than 70 intermetallics have been already amorphized by the HIA treatment [2]. They are intermetallics of the following types: $A_3B$ with $L1_2$ (f.c.c.) crystal structure ($Zr_3Rh$, *etc.*) and with $D0_{19}$ crystal structure ($Ti_3Ga$, *etc.*); $A_2B$ with $C_{23}$ crystal structure ($Y_2Al$, *etc.*) and with $B8_2$ crystal structure ($Zr_3Al$, *etc.*); $AB_2$ with C15 crystal structure ($CeFe_2$, *etc.*).

The transformations of this class provide great possibilities of improving the structure and properties of metallic and intermetallic materials.

From the kinetic viewpoint, it is very important that hydrogen accelerates greatly material atom diffusion. Therefore, a hydrogen-induced diffusive rearrangement of the atomic, micro and macrostructure of materials might be achieved at much lower temperatures than it was conceived before.

*Hydrogen-controlled phase transformations* [2] in polymorphic metals and alloys may be considered as a special, very wide class of transformations. This class of transformations is rather well studied in titanium alloys. They are the basis of many HTM-technologies permitting the improvement of the structure and properties of many titanium alloys, the improvement and creation of industrial technologies to produce deformed and cast articles and constructions.

**References**

1. Progress in Hydrogen Treatment of Materials, V.A. Goltsov, Editor. Donetsk–Coral Gables: Kassiopeya, 2001.–543 pp.

2. Goltsov V.A. Fundamentals of hydrogen treatment of materials//Progress in Hydrogen Treatment of Materials, V.A. Goltsov, Editor. Donetsk–Coral Gables: Kassiopeya, 2001.–P. 3–36.

3. Goltsova M.V., Artemenko Yu.A., Zhirov G.I. Hydride transformations: nature, kinetics, morphology//Progress in Hydrogen Treatment of Materials, V.A. Goltsov, Editor. Donetsk–Coral Gables: Kassiopeya, 2001.–P. 161–184.

4. Goltsov V.A., Rybalka S.B., Fruchart D., Didus V.A. Kinetics and some general features of hydrogen-induced diffusive phase transformations in $Nd_2Fe_{14}B$ type alloys//Progress in Hydrogen Treatment of Materials, V.A. Goltsov, Editor, Donetsk–Coral Gables: Kassiopeya, 2001.–P. 367–390.

# SECTION I.
# FUNDAMENTAL PROBLEMS OF MATERIALS SCIENCE

# QUASICRYSTALS AND RELATED PERIODIC PHASES IN ALLOYS OF ALUMINUM WITH TRANSITION METALS - FORMATION AND STABILITY (A review)

**Grushko B., Velikanova T.Ya.[1]**
Institut für Festkörperforschung, Forschungszentrum Jülich, D-52425 Jülich, Germany
[2]Frantsevich Institute of Problems for Materials Science, Ukrainian National Academy of Science, Kyiv, Ukraine

Quasiperiodic phases or quasicrystals (QC) with "noncrystallographic" symmetries five, ten and others have been found in numerous alloy systems. In several systems they exhibit remarkable thermal stability at elevated temperatures, which permits them to be classified as equilibrium phases at these temperatures. Apart from QCs, related periodic phases with complicated structures containing hundreds of atoms in their unit cells are known in these alloy systems.

QC phases, discovered in 1984, become more and more popular for the basic and applied research. To date a wide spectrum of QC modern materials including large single-crystal QCs are produced and studied in a number of leading laboratories in Europe, USA and Far East. Some interesting peculiarities in their thermal, wear, electronic properties and mechanical behavior were observed [1]. The discovery of QCs stimulated also structural investigation of crystalline phases forming at adjacent compositions. Progress in the investigation of these novel materials depends on the good knowledge of the corresponding phase diagrams. Moreover, the study of phase equilibria also has a basic scientific interest for the understanding of the phase formation rules in these alloy systems.

Among the alloy systems containing QCs those of Al with the d-transition metals (TM) are most widely investigated. In these systems QCs are usually formed in Al-rich regions, their compositions vary from one alloy system to another but are still in the limits between 60 and 80 at.% Al. In binary Al-TM systems (TM = V, Cr, Mn, Fe, Co, Ni; Mo, Ru, Rh, Pd; W, Re, Os, Ir, Pt) they are metastable and can be produced by rapid solidification. With addition of a third element (also TM) they can be stabilized in a number of alloy systems as Al-Ni-(Fe, Co, Ru, Rh), Al-Cu-(Fe, Co, Ru, Rh), Al-Pd-(Mn, Re) [1-3].

In order to clarify the thermodynamic stability of a phase one need to investigate a reasonable part of the corresponding phase diagram. The current information concerning many alloy systems, even the above mentioned list is not systematic and reliable. More investigations are necessary.

In this contribution we present the state of the art of the physical chemistry of the binary and ternary alloy systems of Al with TM containing QCs and related periodic phases, including the recent original data of authors ([4-12], for example).

**References**

[1] Physical properties of quasicrystals, Ed. by Z. Stadnik. Springer. 1999, 434 p.
[2] B. Grushko, Heterogeneous Chemistry Rev. 1, 255-269 (1994).
[3] B. Grushko and T. Ya. Velikanova. In preparation.
[4] B. Grushko, K. Urban, Phil. Mag. **70**, No. 5, 1063-1075 (1994).
[5] B. Grushko, M. Yurechko and N. Tamura, J. Alloys Comp., **290**, 164-171 (1999).
[6] B. Grushko, J. Gwóźdź and M. Yurechko, J. Alloys Comp. **305**, 219-224 (2000).
[7] B. Grushko, Mater. Sci. Eng. **A294-296**, 45-48 (2000).
[8] M. Yurechko, A. Fattah, T. Velikanova and B. Grushko, J. Alloys Comp. **329**, 173-181 (2001).
[9] M.Yu. Yurechko, B.S. Grushko, K.W. Urban and T.Ya. Velikanova, Poroshkovaia metallurgia (in Russian). No.7/8, 75-81 (2001). *English translation in:* Powder metallurgy and metal ceramics. **40**, 374-379 (2001).
[10] B. Grushko, S. Mi and J.G. Highfield, J Alloys Comp. **334**, 187-191 (2002).
[11] M. Yurechko, B. Grushko, T. Velikanova and K. Urban, J. Alloys Comp. **337**, 172-179 (2002).
[12] M. Yurechko, T. Velikanova and B. Grushko, Report of the National Academy of Science of Ukraine (in Russian). No.4, 168-172 (2002).

# PHASE EQUILIBRIA IN REFRACTORY OXIDES SYSTEMS

**L.M.Lopato, O.V.Shevchenko**
I.N.Frantsevich Institute for Problems of Materials Science, Kiev, Ukraine

Phase equilibria investigations in the systems including oxides with the melting points above 2000 °C were initiated in IPMS NAS of Ukraine by Prof. S.G.Tresviatsky in 1962. At the beginning of these investigations the interaction of oxides of rare-earth elements (REE) with highly refractory oxides of II-IV groups elements of the periodic system was one of the less-studied areas of high-temperature chemistry. The literature data concerned mainly some binary REE-oxides systems with silica and alumina.

The first investigation subjects were the phase diagrams of the binary REE-oxides-MgO and $Cr_2O_3$ systems. These investigations revealed that in the systems studied a number of phases formed at high temperature were not retained at room temperature at the cooling rates less than $10^2$ deg/sec that were common in the laboratory practice. So a number of investigation methods were developed and improved in the department, as well as such apparatus for:

- DTA in reducing and inert environment up to 2500°C using the principle of string thermocouple by Yu.O.Kocherghinsky.
- Thermal (TA) and derivative thermal analyses (DrTA) in air using a solar furnace up to 3000 °C, that determine phase transitions temperatures from the radiation of a turning cavity and a surface of the samples partially fused in the focus of a solar furnace;
- Realization of rapid quenching from the liquid state at different cooling rates varying from $10^4$ to $10^5$ deg/sec using concentrated solar radiation.
- Synthesis and melting of the samples at the equilibrium partial oxygen pressure conditions using radiant heating to avoid sample contamination.

The developed methods allowed not only to raise the investigation temperature, but also to study such systems as:
oxide systems with cations to have the ability to change the oxidation grade depending on oxidizing potential of a media ($Eu^{3+}$, $Eu^{2+}$, $Ti^{4+}$, $Ti^{3+}$, $Tb^{4+}$, $Tb^{3+}$ etc.) and the systems with slightly volatite components like magnesium, strontium, barium, chromium oxides because it was possible to melt the samples and quench them in several seconds without noticeably upsetting the stoichiometry.

The crystal growing method from solution in the melt for some compounds was developed for the detailed investigation of compounds structure especially useful in practice such as lanthanum and yttrium chromites. It allowed to explain the properties changes when proceeding from lanthanum chromite to lutecium chromite.

Phase composition of the melted and annealed samples was studied by microstructurial, petrographic and X-ray analyses. The samples were also examined by means of scanning electron microscopy and electron microprobe X-ray analysis.

As a result DTA and TA methods allowed to investigate high temperature reversible polymorphic transitions of the lanthanide pure oxides (>1800 °C) and to determine their melting temperatures.

Phase diagrams of the binary systems composed of REE-oxides and alkali-earth oxides, zirconia, hafnia, titania, alumina, REE-oxides and others were explored. Altogether over 60 binary systems were studied first and over 30 binary systems were reinvestigated. It was found that the modification of phase diagram type in the ranks of system studied took place mainly at the Nd – Sm and Ho – Er elements like in the ranks of other compounds classes, where one of the components was the appropriate RE-compound. The systems including yttria are similar to the systems with lanthanoidas from yttrium subgroup. The scandia including phase diagrams along with certain similarities with lanthanoid series end phase diagrams revealed some differences concerned with specific features of scandium, which is on the one hand a transition element and on the other hand the group lanthanoid analogue.

In the middle of 80-ties the investigation of ternary oxide systems began. The binary systems we had studied before were the basis of these investigations. Last years nearly 30 phase diagrams have been studied first in temperature range 1250-2800 °C: $Hf(Zr)O_2 - MgO - Y_2O_2$, $Hf(Zr)O_2 - CaO - Y_2O_3$, $ZrO_2 - Al_2O_3$ – REE-oxides, $Hf(Zr)O_2 - Y_2O_2$ – REE-oxides, $Hf(Zr)O_2 - CeO_2 - Y_2O_2$, $Hf(Zr)O_2 - TiO2 - Al_2O_3$, $HfO_2 - ZrO_2 - Al(Sc,Y)_2O_3$, $HfO_2 - ZrO_2 - TiO_2$.

The common feature of the studied systems is the absence of ternary compounds, i. e. the

interaction character in boundary binary systems defines the phase equilibria in ternary systems. The most typical feature of the systems including titania, hafnia, zirconia, magnesia, calcia, REE-oxides is the formation of solid solution regions of different extension on the base of different crystal modifications of initial components and intermediate compounds of the binary systems. In $Al_2O_3$–containing systems ternary solid solutions actually were not found. The existence and absence of solid solutions defines the design of different materials types, especially structural ceramics.

The studied systems became the base for creating of high-performance materials for engineering industry, medicine, power engineering, metallurgy and other branches. Just so – from phase diagram study to materials design – Prof. S.G.Tresviatsky saw the evolution of these researches when starting them in the department.

The following candidates of chemical sciences: Pavlikov V.M., Lugin L.I., Kuschewsky A.E., Ogorodnikova A.A., Maister I.M., Gerasimjuk G.I., Nigmanov B.S., Obolonchik T.V., Red'ko V.P., Andrijevskaya O.R., Lakiza S.M., Zajtseva Z.J. and others took part in these investigations.

# PHASE DIAGRAMS FOR THE $ZrO_2$-$Y_2O_3$-$Ln_2O_3$ SYSTEMS AND FIELDS OF ITS APPLICATON

**Andrievskaya Elena R., Lopato Lidiya M.**
Institute for Problems of Materials Science NAS of Ukraine, Kiev,Ukraine

The systems $ZrO_2$-$Y_2O_3$-$Ln_2O_3$ (where Ln= La, Sm, Eu, Gd, Er) are perspective from the standpoint of creation high refractory materials and ones with increased strength characteristics in which the composition of both matrix and strengthening phase is the same. Zirconia-based materials are used in high-temperature thermal barrier coatings, solid electrolytes, oxygen and chemical sensors, fuel cell membrane, rods for nuclear reactors etc.

However, phase equilibria in the mentioned ternary systems were not studied. First, the phase equilibria in the systems were studied on melted and annealed samples in the wide range of temperatures (1250-3000 °C) and concentrations by experimental methods: X-ray diffraction, thermal analysis in air using a solar furnace at temperatures to 3000 °C, differential thermal analysis in He at temperatures to 2500 °C, microstructural and petrographic analyses, electron microscopy and theoretical means: development of a mathematical models for the liquidus surfaces by a reduced polynomial method.

Isothermal sections of these phase diagrams at 1900, 1600, 1550, 1500 and 1250 °C were created. No new phases were found. Phase equilibria are determined by the constitution of the boundary binary systems. Solid solutions are based on hexagonal (H and A), monoclinic (B), cubic (C and X) polymorphous forms of the rare earth oxides, monoclinic (M), tetragonal (T), cubic (F) $ZrO_2$ as well as ordered phases crystallizing in perovskite-type structure with rhombic distortions $LaYO_3$ (R) in the system $ZrO_2$-$Y_2O_3$-$La_2O_3$ and cubic pyrochlore-type compound $Ln_2Zr_2O_7$ (Py) in the systems $ZrO_2$-$Y_2O_3$-$Ln_2O_3$ (Ln= La, Sm, Eu).

Phase equilibria in these systems correspond to relatively high thermodynamic stability of the lanthanum zirconate ($\Delta H$=80-126 kJ/mol), which reacts with the all phases of the system. Third component dopant ($ZrO_2$) was stated to expand the temperature interval of R-phase existence. Mutual dopant effect of the component on the polymorphous transformations is analyzed. The variation of the homogeneity field boundaries for the pure components and intermediate compounds $Ln_2Zr_2O_7$ and $LaYO_3$ as well as their thermal stability is depended on the relation between ion radii of the cations. These regularities are experimentally revealed and discussed in view of spatial model of the substitution-type solid solutions.

The liquidus and solidus surfaces of the systems $ZrO_2$-$Y_2O_3$-$Ln_2O_3$ (Ln= La, Sm, Eu, Er) are described.

The liquidus surface of the lanthana system consists of five fields of phase-primary crystallization based on F-$ZrO_2$, C and H-$Y_2O_3$, X-$La_2O_3$, $La_2Zr_2O_7$ (Fig. 1). It also includes three four-phase invariant equilibria, there are peritectic types. The coordinates of the invariant points: 29 mol % $ZrO_2$, 42 mol % $Y_2O_3$ at 2250 °C ($U_1$), 12 mol % $ZrO_2$, 66 mol % $Y_2O_3$ at 2200 °C ($U_2$) and 24 mol % $ZrO_2$, 24 mol % $Y_2O_3$ at 2070 °C ($U_3$).

Four fields of primary crystallization of C-, H-$Y_2O_3$, F-$ZrO_2$ and X-$Sm_2O_3$ phases form the liquidus surface of the $ZrO_2$-$Y_2O_3$-$Sm_2O_3$ system (Fig. 2). There are two four-phase invariant points of peritectic-type reactions with the coordinates 15 mol % $ZrO_2$, 50 mol % $Y_2O_3$ at 2330 °C ($U_1$) and 13 mol % $ZrO_2$, 70 mol % $Y_2O_3$ at 2360 °C ($U_2$).

The liquidus surface of the $ZrO_2$-$Y_2O_3$-$Eu_2O_3$ system is consisted of four fields of phase primary crystallization based on the $ZrO_2$ phase with the fluorite-type of structure and H, C forms of $Y_2O_3$ as well as X-$Eu_2O_3$ (Fig. 3). There are two invariant points four-phase equilibria of peritectic-type on the liquidus with the coordinates 20 mol % $ZrO_2$, 50 mol % $Y_2O_3$ at 2340 °C ($U_1$) and 20 mol % $ZrO_2$, 40 mol % $Y_2O_3$ at 2310 °C ($U_2$).

The system $ZrO_2$-$Y_2O_3$-$Er_2O_3$ is characterized by the formation of extended solid solutions based on the fluorite-type form of $ZrO_2$ and cubic and hexagonal forms of $Y_2O_3$ and $Er_2O_3$ (Fig. 4). The boundary curves of these solid solutions have the minima at 2350 °C (18.0 mol % $ZrO_2$, 39.0 mol % $Y_2O_3$) and 2330 °C (12.5 mol % $ZrO_2$, 41.0 mol % $Y_2O_3$).

The phase diagrams evolution of the ternary oxide systems $ZrO_2$-$Y_2O_3$-$Ln_2O_3$ is under consideration ($Ln_2O_3$ is the rare earth oxides).

Such evolution originates from ion radius decrease in the row of sesquioxides from $La^{3+}$ (0.114 nm) to $Lu^{3+}$ (0.084 nm). The phase diversity in these systems is defined by the relation between ion radius of $Ln^{3+}$ and that of $Zr^{4+}$ (0.083 nm) or $Y^{3+}$(0.092 nm).

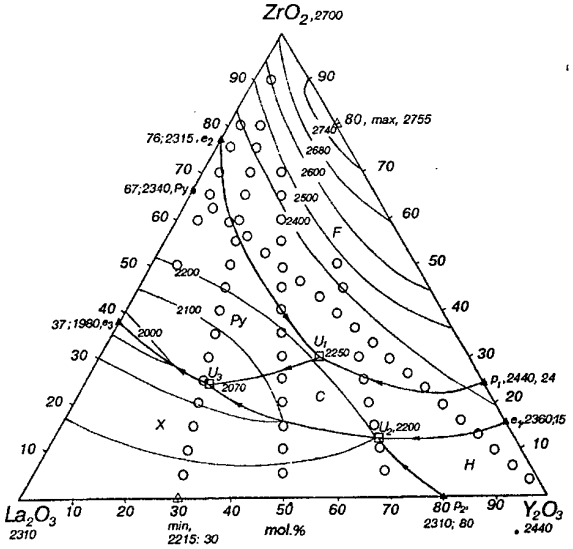


Fig. 1. Projection of the liquidus surface for the $ZrO_2$-$Y_2O_3$-$La_2O_3$ system (O - experimental points).

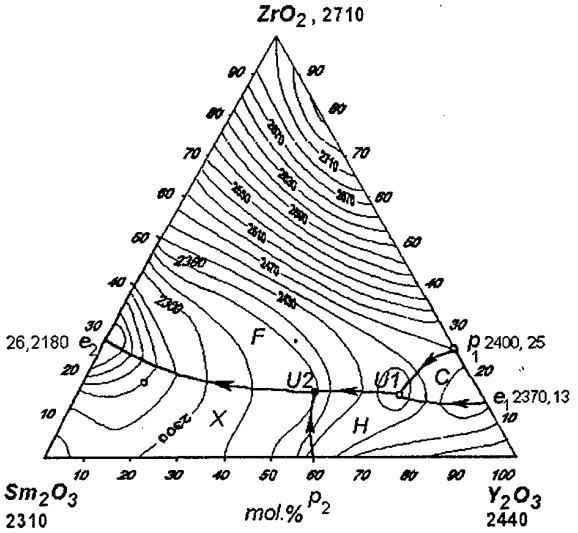


Fig. 2. Projection of the liquidus surface for the $ZrO_2$-$Y_2O_3$-$Sm_2O_3$ system (calculated).

The closer are $r_{Ln3+}$ and $r_{Zr4+}$ the simpler is the diagram constitution. For instance, the liquidus and solidus surfaces become simpler from $La_2O_3$ to $Er_2O_3$.

The minimal melting temperature for the $ZrO_2$-$Y_2O_3$-$Eu_2O_3$ system is 2130 °C ($e_2$), maximum temperature of the liquidus surface is equal to 2750 °C, which corresponds to the melting point of 80 mol % $ZrO_2$-20 mol % $Y_2O_3$.

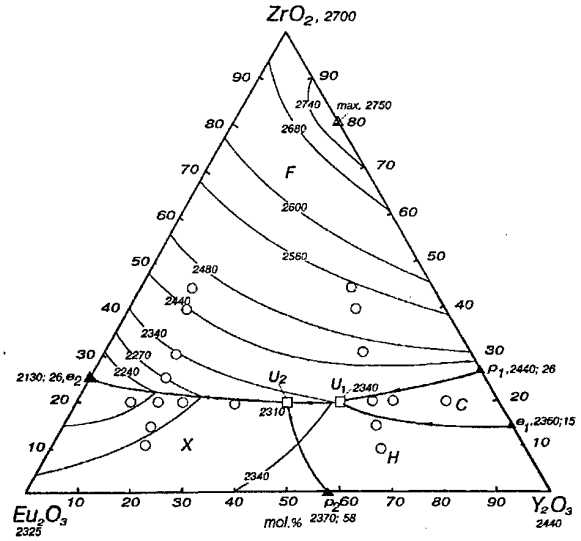


Fig. 3. Projection of the liquidus surface for the $ZrO_2$-$Y_2O_3$-$Eu_2O_3$ system (O - experimental points).

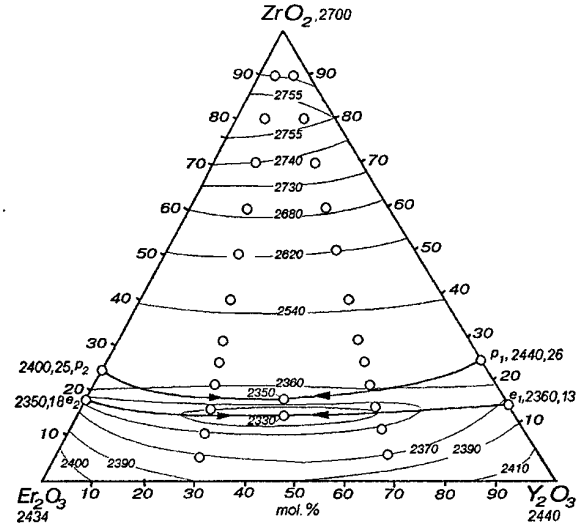


Fig. 4. Projection of the liquidus surface for the $ZrO_2$-$Y_2O_3$-$Er_2O_3$ system (O - experimental points).

ACKNOWLEDGEMENTS

Authors thanks A.V. Shevchenko, V.P. Red'ko, I.E. Kiryakova, Z.A. Zaitseva, and V.P. Smirnov for their helpful advices and assistance in experimetal study of presented phase diagrams.

# INTERACTION IN PHASES OF TERNARY Fe(Co, Ni)-B-C SYSTEMS

**Makara V.A., Kudin V.G.**
Phisical Department of Kyiv National Taras Shevchenko University, 64 Volodymyrska Str., 01033 Kyiv, Ukraine

The materials on a basis of carbides, borides, carboborides of metals have wide application in various spheres of a national economy. But their use has the large prospects, as the modifying by their various additives essentially changes their properties. In this respect urgent there are items of information on thermal properties both phase equlibrium of compounds and compositions on their basis, which should be investigated experimentally, and also to simulate because of this refractory and high hardness.

The purpose of the present work was to investigate interaction in quasibinary $FeB_2$($Ni_3B$,$Co_3B$)-C in a solid and liquid condition, and also to predict character of interaction in a wide interval of composition of ternary alloys of Fe(Co,Ni)-B-C systems. Samples for study phase equilibrium prepared by hot-pressing well crushed powders of compounds $Co_3B$, $Ni_3B$, $FeB_2$ of the mark "pure" and spectral-pure with pure graphite, then melted in the arc-furnace. The obtained alloys alloed at 1500 and 2000 K during 8 h and 1 h, accordingly. X-ray, metallographic and differential-thermal studies have shown, that all three systems are eutectics one. The temperatures and composition for proposed eutectics are given below:

| | | |
|---|---|---|
| $FeB_2$-C | 1815 K. | 26 weights % |
| $Co_3B$-C | 1739 K. | 34 weights % |
| $Ni_3B$-C | 1700 K. | 45 weights % |

The alloys of these sections also were investigated by a high temperature isoperibolic calorimetry at 1900 K. Samples from graphite heated up to 1600 K, and in liquid bath was placed remelted alloys. Determined enthalpies of mixing have appeared small values, that is visible from the given below data.

ΔH, kJ/mol

| System $x$ | 0.05 | 0.1 | 0.15 | 0.2 |
|---|---|---|---|---|
| $FeB_2$-C | 2.3 | 3.6 | 4.4 | 5.9 |
| $Ni_3B$-C | 3.8 | 5.2 | 6.3 | 7.8 |
| $Co_3B$-C | 3.3 | 4.2 | 5.1 | 6.2 |

From known thermochemical properties of binary boundary systems [2] by use Toop equation and non-symmetrical Bonier-Caboz method the same parameters for ternary Fe(Co,Ni)-B-C systems in wide composition interval (fig. 1) are predicted.

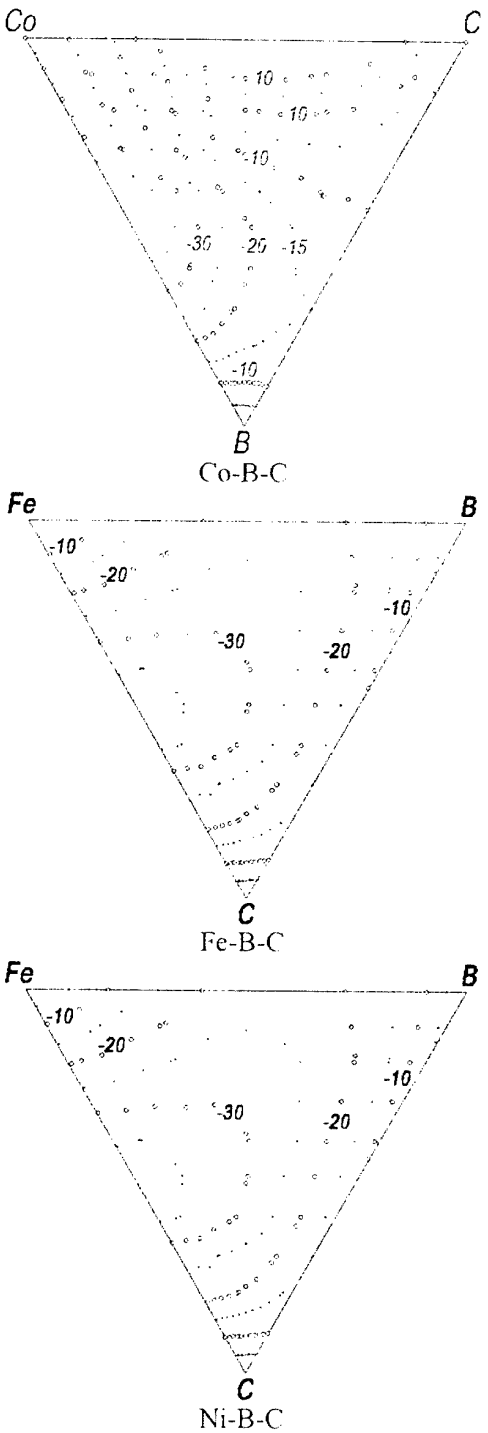


Fig. 1. Isoenthalpy of mixing in ternary melts Fe(Co, Ni)-B-C.

It is visible, that the strongest interparticle interaction is characteristic for threefold system Fe-B-C, which can predict formation of new compounds.

Using all set of the thermodynamic data and the known items of information about phase equilibrium have been simulated state diagrams of ternary systems, i.e Fe(Co,Ni)-B-C. The received data in the form of isothermal sections are given in a fig. 2.

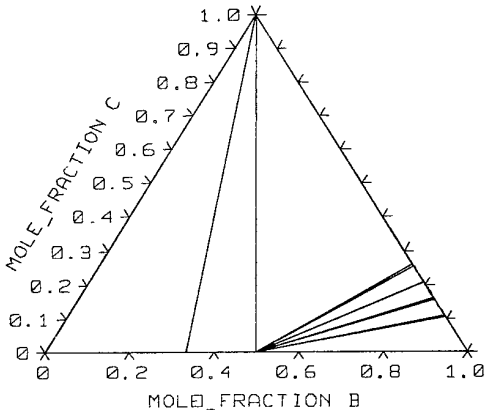


Fe-B-C

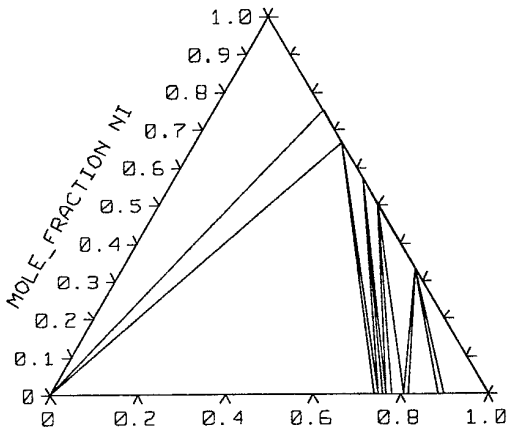


Ni-B-C

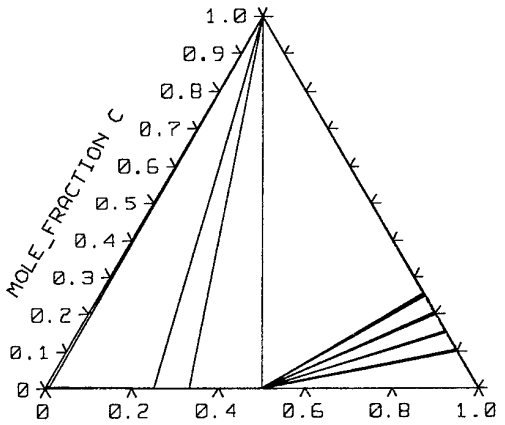


Co-B-C

Fig. 2. Isothermal sections of ternary Fe(Co, Ni)-B-C systems at 1000 K.

It is necessary to note, that agrees of the determined state diagrams in them the ternary compounds are not formed. It has been confirms character of interaction in a number of ternary Me-B-C systems, but will not completely be coordinated to diagram of state for Fe-B-C, given in Ref.[2].

Reference

1. Witusiewicz V.T. Thermodynamic Properties of liquid Alloys of 3d-Transition Metals with Metalloids: generalization // J. Alloys and Comp. – 1995. – v. 221. - №1. – P.74-85.
2. Kuzma Ju.B., Tchaban N.F. Diagrams of states of binary and ternary systems, containing B and C, 1990. – M.:"Metallurgiya". – 321 p.

# COMPUTER MODELING OF GAS EUTECTIC REACTION

**Shapovalov V.I.**
Sandia National Laboratories, Department of Energy, USA
National Metallurgical Academy of Ukraine, Dnepropetrovsk, Ukraine

## Introduction

Simultaneous formation of solid and (hydrogen) gas from the liquid takes place in M-H alloys having gas-eutectic compositions. This reaction was named gas eutectic reaction [1-3].
An ordered combination of phases termed gasarite may arise from a gas eutectic reaction. It is comprised of a polycrystalline solid matrix and continuous oriented pores filled with hydrogen.
The gasarite forms at solidification velocities ranging from 0.05 to 5 mm/s. The hydrogen content and the gas pressure largely determine its morphological characteristics over the solidifying melt.
Short-range order of pores with a coordination number of about 6 is observed in a plane normal to the direction of solidification.
The pore size distribution is dependent on gasarite formation conditions and is nonuniform, because concurrent growth of large and small pores is possible.
As the solidification front advances, the average pore diameter is increased and neighboring pores may coalesce now and again. No branching of pores ever occurs.
A pore may have periodic necks over its length.
Pore growth arrest and nucleation of new pores may occur all through the solidification.
No gasarite pores are nucleated on the mold surface. A nonporous metal skin 0.05-5 mm thick forms first.
In what follows, an attempt is made to explain mechanisms of phase nucleation and growth in gas eutectic reaction on the basis of experimental data.

## Major Results

**Nucleation.** It is believed that nucleation of a gaseous phase in a liquid is heterogeneous, i.e. occurs on existing discontinuities in the liquid bulk or at the liquid/solid interface. The discontinuities may vary in nature, like

- gas bubbles entrained from the atmosphere during melt pouring or stirring,
- bubbles formed in passing a gas through the melt,
- small bubbles caused by cavitation,
- small pits on the surface of high-melting particles suspended in the melt,
- small pits on the mold walls,
- regions where the liquid does not contact the solidification front.

The gaseous phase nucleation in formation of ordered gas-solid structures may occur at the solidification front or on high-melting particles suspended in the liquid ahead of the front. The first mechanism would seem more viable. The critical radius of bubble nuclei is shown to hyperbolically decrease with pressure. The bubble nucleation rate is increased accordingly.

**Gasarite growth**. In the gasar process, solid metal precipitates from the liquid simultaneously with gas. No decrease in pressure is necessary for this to happen. Moreover, increasing pressure is commonly needed to produce an ordered structure.

Gasar pore formation follows a mechanism distinct from that of evolution of gas in carbonated beverages or bubbling in a boiling liquid. Furthermore, the ellipsoidal pore growth cannot be ascribed to stretching of gas bubbles by the advancing solidification front.
The gasar pore growth proceeds by hydrogen transverse diffusion ahead of the solidification front and concurrent advancement of the solid and the gaseous phase into the melt. When the growth rates of the two phases are equal, an "ideal" structure including cylindrical channelways in a nonporous matrix should form.
Unlike in solid-solid eutectics, the gasarite pore spacing is determined not only by diffusional self-adjustment. Rather, it is a function of the nucleation conditions and the solidification pressure

A pore may be terminated by any of the following causes:

- nucleation of a new pore in a space between the growing pores,
- supplementary removal of heat from the bubble tip via thermal radiation into the channelway, and pressure reduction in the pore due to the gas average temperature declining as the pore extends.

**Pore coarsening** in growth of a gas eutectic may be caused by wedging (see Figure on top) or pore coalescence (see Figure on bottom). Wedging is mainly observed at low, and coalescence at high void fractions.

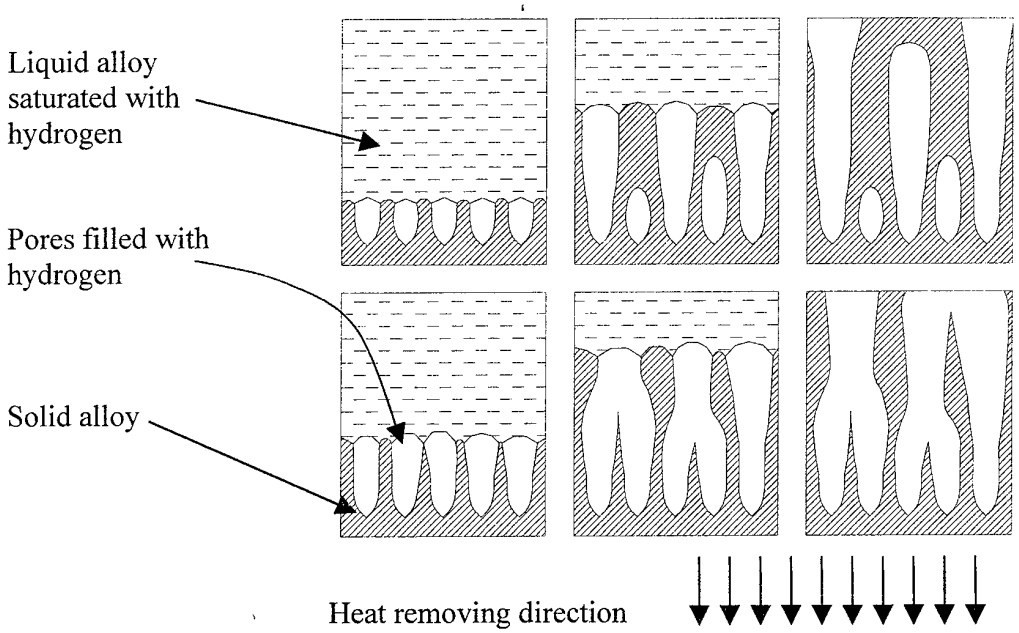


**Some conical pores result** from wedging while their massive formation is due to pressure changes in solidification.

**Corrugated pores** may form due to periodical changes of pressure above the melt. Similar effects are caused by repeated detachment of bubbles from the solidification front.

**Pore orientation** in gasarite is determined by the shape of the solidification front, because the growth vector direction of a pore is always normal to the front at its location.

References

1. Shapovalov V.I., Porous Metals, MRS Bull., 19(4), 24(1994).
2. Shapovalov V.I., Method of manufacturing porous articles, US Patent 5,181,549 (26 January, 1993).
3. Shapovalov V.I., Metal and Casting of Ukraine, 1995, No. 2, 2-10.
4. Shapovalov V. Formation of Ordered Gas-Solid Structures Via Solidification in Metal-Hydrogen Systems. Porous and cellular materials for structural applications. Symposium held April 13-15, 1998, San Francisco, California, USA. MRS Symposium Proceedings Volume 521, p. 281-290.
5. Shapovalov V. and Boyko L. Anisotropic Porous Metals Production by Melt Processing, Proceedings of the 1997 International Symposium on Liquid Metal Processing and Casting, Santa Fe, New Mexico February 16-19, 1997, p.p.417-426 (USA)
6. Shapovalov V. Metal-Hydrogen Phase Diagrams in the Vicinity of Melting Temperatures. Proceedings of the 1999 International symposium on Liquid Metal Processing and Casting, Santa Fe, New Mexico, Februaty 21-24, 1999, p.330-343

# COMPUTER STRUCTURE-IMITATING MODEL OF SPHERICAL PARTICLES SINTERING

**Alievsky V.M., Kadushnikov R.M., Nurkanov E.Y., Skorokhod V.V.**
Urals State Technical University, Ekaterinburg, Russia

Computer structure-imitating model of spherical particles sintering is used for computational experiments, representing the sintering process from a viewpoint of its representation in three stages: filling, sintering, recrystallization and normal grain growth.

Initial green compact is formed during the filling stage. Random close packing (RCP) of spherical particles represents initial unordered structure of powder body. To create RCP from spheres with different sizes in a bunker with flat-walls we use an algorithm based on the following physical idea. The spheres are generated according to the chosen law of size distribution and are dropped to the bunker either from one point, or from randomly chosen positions. As soon as the dropped sphere encounters an obstacle - the bunker wall or an already packed sphere - it sticks to it (without impact) and begins to slide on its surface in the direction of the minimum of the potential energy to the following obstacle. (This direction is a projection of the free fall direction on the surface of the obstacle.) The movement of the sphere stops, obviously, at a point of intersection of 3 surfaces (3 spheres, 2 spheres and 1 plane and etc.) or on a surface situated perpendicular to the direction of the free fall of the sphere (for example, on the bottom of the bunker).

The constructed random close packing of spheres represents the initial data for the second stage - simulation of the evolution of the spheres during sintering. For deriving the equations of movement and dynamics of the sizes of the sintered spheres, the main incentive was to satisfy the equations of sintering kinetics for each pair of contacted spheres in the system. Initial powder body is represented by the random close packing of $N$ spherical particles: $S_i(R_i,\mathbf{r}_i,\mathbf{v}_i)$, $i=1,N$; $R_i$ – radii of the spheres, $\mathbf{r}_i$ – coordinates of their centres, $\mathbf{v}_i$ – velocities of the spheres, located in a bunker limited by flat walls.

It needs to take into account the interaction of the contacted spheres, resulting in sintering, in case of contact presence or appearance. Distance between the centers of contacting spheres is the following:

$$|\mathbf{r}_{ij}| = |\mathbf{r}_i - \mathbf{r}_j| < R_i + R_j$$

Equations of sintering kinetics for all pairs of incident (contacting) spheres can be written down in the following form:

$$\mathbf{v}_{ij} = \dot{\mathbf{r}}_{ij} = f\left(|\mathbf{r}_{ij}|\right)\mathbf{r}_{ij}, i = 1, N; j \to i, \quad (1)$$

(the last entry means, that "j is incidental to i"). To use clause (1) as a "tendency" of movement for the spherical particles system let us construct the deviation functional

$$Q = \sum_{i,j:\, j\to i} \mathbf{v}_{ij} - f\left(\mathbf{r}_{ij}\right)\mathbf{r}_{ij}^{\,2}, \quad (2)$$

and add the antigradient $Q$ with a weight multiplier $\mu$ in the right part of the equations of Newton

$$\begin{cases} \dot{\mathbf{r}}_i = \mathbf{v}_i \\ m_i \dot{\mathbf{v}}_i = \mathbf{F}_i \end{cases}, \quad (3)$$

The conservation of weight means that during movement and sintering the volume $V$ of the geometrical union of spheres remains constant:

$$\dot{V} = \sum_i \left( \frac{\partial V}{\partial \mathbf{r}_i} \dot{\mathbf{r}}_i + \frac{\partial V}{\partial R_i} \dot{R}_i \right) = 0, \quad (4)$$

Let us balance the change in volume $V$ of the union of spheres connected with movements of some sphere $S_i$ with the change in the radius $R_i$ of this sphere [1]:

$$\frac{\partial V}{\partial \mathbf{r}_i} \dot{\mathbf{r}}_i + \frac{\partial V}{\partial R_i} \dot{R}_i = 0, \quad (5)$$

Thus, we receive the following equations of dynamics of the radii of the spheres:

$$\dot{R}_i = |\dot{\mathbf{r}}_i| \Xi_i / |S_i|. \quad (6)$$

So the resulting equations of movement (3) should look as follows:

$$\begin{cases} \dot{\mathbf{r}}_i = \mathbf{v}_i - \mu \sum_{j\to i} \left( \mathbf{v}_{ij} - f\left(|\mathbf{r}_{ij}|\right)\mathbf{r}_{ij} \right) \left( f\left(|\mathbf{r}_{ij}|\right) + f'\left(|\mathbf{r}_{ij}|\right)|\mathbf{r}_{ij}| \right) \\ \dot{\mathbf{v}}_i = \frac{\mathbf{F}_i}{m_i} - 3\frac{\mathbf{v}_i |\dot{\mathbf{r}}_i|}{R_i |S_i|} \cdot \Xi_i - \mu \sum_{j\to i} \left( \mathbf{v}_{ij} - f\left(|\mathbf{r}_{ij}|\right)\mathbf{r}_{ij} \right) \\ \dot{R}_i = \frac{|\dot{\mathbf{r}}_i| \cdot \Xi_i}{|S_i|} \end{cases}, \quad (7)$$

where $m_i = 4/3\pi\rho R_i^3$, $\rho$ – density of spheres' material, $\mathbf{F}_i$ – sum of the external forces, affecting each sphere, $\mu$ - weight multiplier, actually responsible for the degree of sintering affecting the movement of the system of spheres, $|S_i| = \iint_{\Phi_i} ds = \frac{\partial V}{\partial R_i}$ - area of the free surface $\Phi_i$ of the $i$-th sphere, $\frac{\partial V}{\partial r_i} = \Xi_i = \iint_{\Psi_i} \frac{\dot{\mathbf{r}}_i}{|\dot{\mathbf{r}}_i|}\mathbf{n}ds$ can be interpreted as an area of projecting the occupied surface $\Psi_i$ of the $i$-th sphere on the plane, normal to $\dot{\mathbf{r}}_i$ ($\mathbf{n}$ – solitary vector of normal to the surface), $V$ – volume of spheres' union.

The third stage is totally determined by movement and sintering of the spheres, that is why it is necessary to continue integrating system of equations (7). Effects of the normal grains' growth are reflected only in equations for dynamics of spheres' sizes, exactly, for spheres with the surface, totally closed by the neighbours (not causing effect on conservation of the mass), equations of dynamics of normal grain growth are used:

$$\dot{R}_i = \lambda \sum_{j \to i} \left( \frac{1}{R_j} - \frac{1}{R_i} \right), \qquad (8)$$

Hereby, in some moment of time $t$ the state of a physical system is described by a set of positions and velocities of the particles $\{\mathbf{r}_i(t), \mathbf{v}_i(t), i=1,N;\}$. Cycle of a time step is recalculating these values, using forces of interaction and movement equations to obtain the state of a system in a later moment of time $t+dt$.

It is necessary to specially bring attention to the function $f(|\mathbf{r}_{ij}|)$, that is determined as follows:

$$\mathbf{v}_{ij} = f\left(|\mathbf{r}_{ij}|\right)\mathbf{r}_{ij}, \quad f\left(|\mathbf{r}_{ij}|\right) = \frac{B}{m\varepsilon(1-\varepsilon)^{m-1}}, \quad \varepsilon = \frac{|\mathbf{r}_{ij}|}{|\mathbf{r}_{ij}^{(0)}|}, \qquad (9)$$

It is possible to get expression (9) if differentiating by time the known phenomenological formula [2] describing kinetics of initial stage of spherical grains' sintering

$$\left( \frac{|\mathbf{r}_{ij}^{(0)} - \mathbf{r}_{ij}|}{|\mathbf{r}_{ij}^{(0)}|} \right)^m = Bt$$

where $\mathbf{r}_{ij}$, $\mathbf{r}_{ij}^{(0)}$ - the current and the initial distance between the centres of contacting particles, $B$ and $m$ are the constants, determined by the matter type, and a mechanism mass transportation. For the mechanism of viscous flow

$$m = 1, \quad B = \lambda / |\mathbf{r}_{ij}^{(0)}|, \quad \lambda = 3\sigma / 4\eta$$

where $\eta$ - viscosity coefficient, $\sigma$ - surface tension (specific surface energy), $\lambda$ - actual initial speed of approach for the centres of contacting spheres.

Integrating of equations (7) results in a complete description of structure genesis and the spherical particles ensembles evolution while sintering (pic. 1).

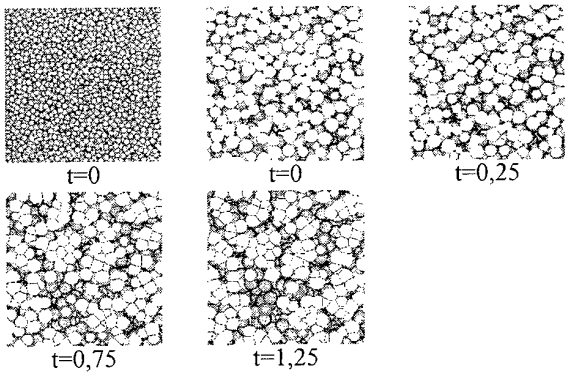


Pic. 1. Stages of sintering of the spherical particles packing. Stage (t=0) is presented by view both of initial packing and its cross-section.

### References

1. Kadushnikov R.M., Skorohod V.V., Nurkanov E.Yu., Kamenin I.G., Alievsky V.M., Alievsky D.M. Computer modelling of of sintering of spherical particles. Powder metallurgy. - № 3/4. 2001. pp. 71-82.
2. Geguzin Ya.E. Physics of sintering. Moscow: Nauka. 1984.

# CORRELATION EFFECTS IN MATERIALS AND MODELS FOR THEIR DESCRIPTION

**Shpak A.P., Ristic M.M.[(1)], Kunitsky Yu.A.[(2)], Pryadko L.F.[(3)]**
Kurdumov Institute of Metal Physics of Ukrainian AS, Kyiv
[(1)]Institute of Technical Science of Serbian ASA, Belgrade
[(2)]Technical Centre of Ukrainian AS, Kyiv
[(3)]Francevich Institute for Problem of Materials Science of Ukrainian AS, Kyiv

New paradigm of Materials Science appeal to the first principles of quantum statistical physics [1]. Structure and properties of substances and materials from the objects of evolution (geochemistry, biochemistry) to advanced technologies (nanotubes, fullerens) can be described in terms of the axiomatical Shredinger equation and it solutions [2].

The one-electron approach in this sence is the first succeful project of the mentioned paradigm. It conceptual apparatus cover the models of Bohr atoms and chemical interatomic bond, insulating, metallic and semi-conductor crystals, impure, disordered and many other types of condensed systems. The development of Materials Science depends upon the progress of computing physics now, and it is frequently reduced to the mathematical modeling; the databanks about band structure and the Fermi-surfaces catalogues have turned to the technologist`s tool [3].

Today the conception of the Hartree-Fock independent electrons has become "zero approach" for more exact analysis of the Shredinger equation [4]. This new project is intended to develop conceptual apparatus concerned to the description of the correlated electrons systems including superconductive and magnetic materials, intermediate valence, heavy-fermions, Kondo-system [5].

By definition, the correlation interactions describe the variety of the effects with different physical origin and are incorporated by common property of "nonelectron nature". Their study was set up by "the points of growth" arising from the critical needs of technology and new opportunities of the electron theory. Variety of investigated correlation effects requires systematization, classification of materials, which they are shown in, typing of "batch behaviour" of system-complex of their properties [6].

The most important correlation states have been submitted schematically in space of their fundamental contributions relatively to the mean energy (per electron) **E**: 1) kinetic energy (T); 2) evectron-ion interaction; 3) electron electron-electron interaction (Fig.1).

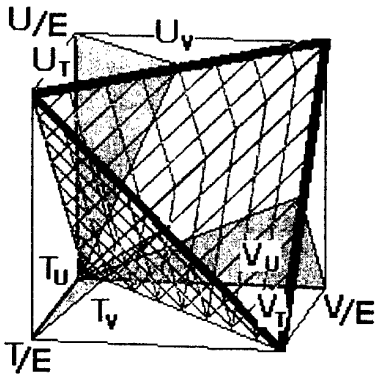


Fig.1. The areas of the various correlation behaviour of condensed system in **T-V-U**-space

It corresponds to the use of basic qualitative criteria in plasma–systems - degree of compression, relative interparticle interaction and propensity of formation of the localized states. The basic plane **T-V** will be transformed to the Hartree-Fock area by means of the screening effects. Further it is possible to separate the areas of weak-binding electron behaviour ($\mathbf{T_V}$) from its tight-binding behaviour ($\mathbf{V_T}$). Plane **T-U** corresponds to the correlation behaviour in free electron gas, and area $\mathbf{T_U}$ represents the field of applicability of random phase approximation while $\mathbf{U_T}$ area is the field of the Wigner crystallization. In the similar way $\mathbf{U_T}$ area is the Hubbard crystall with strong electron correlation. The most interesting area **T-V-U**-body (inside the traced

triangle), sory to say, is not yielded to a simple quasiparticle interpretation.

Generelly, the structure of the correlation terms **U**, is complicated, but at **T>V** they may be sorted in the Bloch representation, and their most important part is taken into account in approach of "correlation hole". In case of **T<U** it is expedient to use the Wanier basis and to allocate from intraatomic (**U**) and interatomic (**U`**) parts, each of them, in turn, includes the Coulomb (**K**) and exchange (**J**) components.

The universal character of such division assumes unity of laws of the alternation of phases in **T-V-U**-space, both for different materials, and for one material at the variation of the external conditions (pessure, temperature, electrical and magnetic fields).

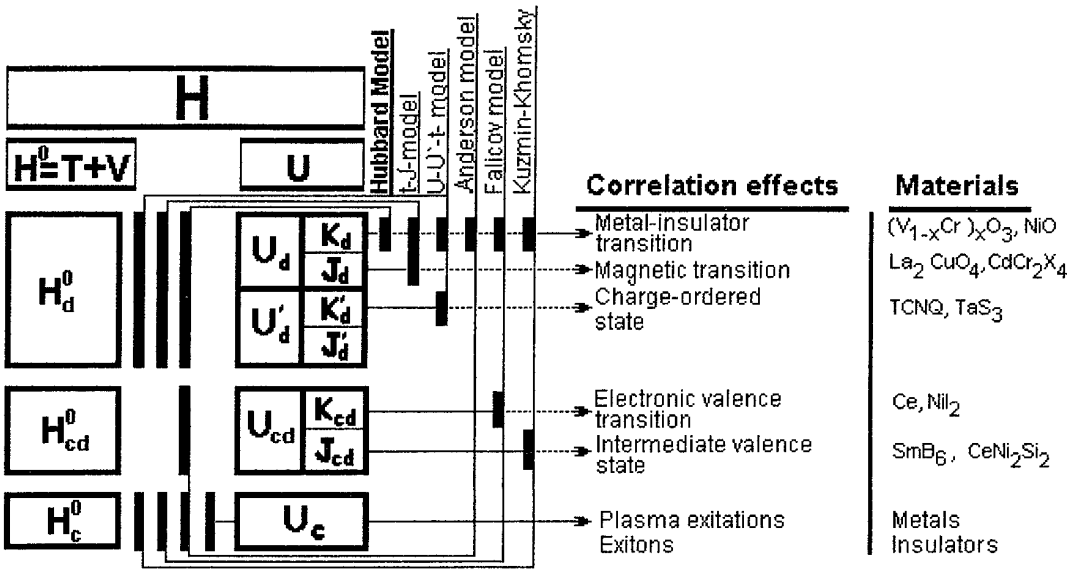


Fig.2. The correlation effects in Materials containing localized and collectivized electrons

The body of this structure is represented on Fig.2. Here the most typical exemples of changing phase materials states correspond to principle types of interaction between collectivized (c-) and localized (d-) electrons. The effects of c-d-interaction in transition and rare-earth materials with variable atom valece have been discussed in oyher paper [7].

[1] Сучасне матеріалознавство XXI сторіччя / Ред. І.К.Походня. - Київ: Наукова думка, 1998

[2] Шпак А.П., Куницкий Ю.А., Карбовский В.Л.. Кластерные и наноструктурные материалы. - Киев: Академпериодика, 2001

[3] Ergebnisse in elektronentheorie der Metall/ Unter Leitung P.Zishe und G.Leman.- Berlin: Akademie-Verlag, 1983

[4] Kreft W.D., Kremp D., Ebeling W., Ropke G. Quantum Statistics of Charged Par-ticle Systems. - Berlin: Academie-Verlag, 1986

[5] Дидух Л.Д., Прядко Л.Ф., Стасюк И.В. Корреляционные эффекты в узкозонных материалах. - Львів: Вища школа, 1983.

[6] Ристич М.М., Прядко Л.Ф., Куницкий Ю.А. и др. Прогноз физико-химических свойств материалов.- Белград: Центр мультидисциплинарных исследований при Белградском университете, 1996

[7] Pryadko L.F., Pryadko I.F. A configuration model of matter ant the problem of the valence factor in the theory of the constuction of d-, f-electronic system.- Powder metallurgy and ceramics. - 1998.- N 1-2.- p.15

# MATERIAL SCIENCE ASPECTS OF PROPERTIES AND STRUCTURES DEGRADATION OF BOILER ELEMENTS AFTER LONG OPERATION

**Piskalenko V.V., Gromov V.E., Tsellermaer V.Ya.**
Siberian State University of Industry, Novokuznetsk, Russia

The steam boilers elements are exposed to the intensive and long operation in difficult conditions of thermal and mechanical loadings. Therefore the requirements produced to materials of which details of heat power installations are made, are always very high.

New express methods of an estimation of serviceability of the equipment and system of the continuous control of material condition are necessary. Such problems can not be solved without deep understanding of physical and chemical processes of metal characteristics change. In the given situation the comparative researches of structure and properties of materials after various long periods of boiler installations work are rather useful.

In this work the change of mechanical properties and structures of boiler pipes from steel 10 (0.13%C; 0.44%Mn; 0,23%Si; P, S ≤0,02 %) after 50 years of operation at working pressure ≤ 1.5MPa and temperature ≤250$^0$C were investigated.

The measurement of acoustic waves velocity by autocirculation pulses method was applied to an estimation of structure stress-strain state of a material.

As a result of operation there was a change of all basic mechanical characteristics. The yield stress and tensile stress have decreased accordingly on 27,5 % and 16,5 %, and specific elongation before break and reduction of area – have increased by 15,7 % and on 9 %.

Table 1.

| Material | $\sigma_т$, MPa | $\sigma_в$, MPa | $\delta$, % | $\psi$, % | Velocity of ultrasound, m/s |
|---|---|---|---|---|---|
| Steel 10 in a condition of delivery | 364 | 510 | 25,4 | 56 | 2851±2 |
| Steel 10 after operation (50 years) | 264 | 426 | 29,4 | 61 | 2865±0,2 |

In an initial condition steel has the ferrite-pearlite structure where the pearlite volume fraction does not exceed 15%. The boundaries of the ferrite grains are thin and precise. The precipitations of carbide phases are absent both in the body of ferrite grains, and on the boundaries. After the long operation the structure becomes very non-uniform. The alongside with sites where it has remained practically former, there are the zones of local recrystallization where the average size of a grain has increased from 17,6 microns up to 22,2 microns. In these zones there is no the pearlite component. On the other hand, the increased content of pearlite is observed on the edges of such zones. Obviously, the strong disorder of microhardness from 1430 up to 1700 MPa is connected with these facts. Also it is important to note, that the fracture of the samples took place in area of such recrystallization zones.

The two competing points of view exists concerning the reasons of decrease of constructive strength of metal of the heat power equipment. According to the first [1-3] there is an ageing, isolation of the carbide phase and its transformation to the complex one and, then, in chromic. It also proves to be true by our researches executed on steel 12Х1МФ [4]. However the result of such processes is the metal embrittlement and the occurrence of thermal crack during long operation.

In steels, without carbide forming elements the processes structures degradation proceed in another way [5]. First, the decarburization of steel occurs very slowly. Second, there is the decay and the redistribution of pearlite component. The recrystallization processes are definitely took peace at last. All these processes results in decrease of strength characteristics and to growth of plasticity of metal. In the present case as a result of long operation there were described above phenomena (growth of a grain, pearlites redistribution and the decrease of microhardness due to decarburization).

***Conclusions:***

1. It is established, that as a result of long (50 years) operation boiler pipes (steel 10) there was a decrease of yield stress on 27 %, tensile stress – on 16 % and increase specific elongation before fracture – on 15 %.
2. These changes of mechanical characteristics were consequence of steel structures degradation due to redistribution and partial decay of pearlite component, growth of ferrite grains in separate zones and, apparently, in decarburization.
3. Processes of degradation of mechanical properties and structure of a material were accompanied by regular changes of velocity of distribution of ultrasonic waves that opens prospect of use of an acoustic method for diagnosing of the heat power equipment state.

References

1. Bogdanov V.I., Vladimirov S.A., Galdshtejn L.I., Goritskij V.M.//Problems of strength. 1976. - No7. – pp.65-73.
2. Berezina T.G., Judina A.G.//Physics of Metalls and Physical Metallurgy. 1980. - V. 49, 1. - pp. 90-99.
3. Goritskij V.M., Galdshtejn L.I., Shnejderov G.R.// Proceeding of AS USSR. Metals. 1982. - No2. - pp. 150-156.
4. Danilov V.I., Podboronnikov S.F., Cats H.H., Gromov V.E., Zuev L.B.// Proceeding of High Schools. Ferrous metallurgy. - 1993. - No8. - pp.50-51.
5. Kats S.N.//Power systems. - 1955. - No11. - pp.13-17.

# KINETICS OF DIAMOND SPONTANEOUS CRYSTALLIZATION

**Turkevich V.Z.**
Institute for Superhard Materials of the Ukrainian National Academy of Sciences, Kiev, Ukraine

Synthetic diamond powders are produced at high pressures and temperatures by crystallization from a carbon solution in melts of carbon-metal solvents multicomponent systems. The kinetic regularities of diamond spontaneous crystallization define the quantity of nuclei, the rate of their growth, the presence of defects and inclusions of the growth medium in crystals, and, hence, their strength and thermostability. Away from the graphite-diamond equilibrium line deep in the diamond thermodynamic stability region, a great quantity of low-strength crystals with a considerable concentration of inclusions can be produced at a high rate and in a short time [1, 2]. Close to the equilibrium line, a lesser amount of high-strength crystals with a small number of defects nucleates and grows, and the time of crystallization is two orders of magnitude increased [3]. Of great importance is also the type of a metal solvent as the key quantities, which define the kinetics of crystallization, like the melt-crystal interfacial energy and the coefficient of carbon diffusion in the melt vary as a function of it. A rate of diamond spontaneous crystallization is observed to decrease in the following series of systems: Ni–Mn–C, Fe–Ni–C, Fe–Al–C, Cu–Mn–C, the p,T-parameters being approximately the same [4, 5].

The diamond spontaneous crystallization from melt solution of the Mn–Ni–C and Fe–Ni–C systems starts at high pressures immediately after melting of the Solid solution + Carbide + Graphite ternary eutectic. The diamond crystallization from the melt solution of the Mn–Ni–C and Fe–Ni–C systems is limited by thermally activated diffusion. For this reason, a rise in temperature considerably speeds up crystallization. The activation energy of the diamond crystallization in the above systems is evaluated to be 150±70 kJ·mol$^{-1}$ [6].

For the diamond crystallization in the Fe–Co–C and Fe–Al–C system, the overheating by 100 – 150 K above the temperature of ternary eutectic is needed [7, 8]. Due to relatively low rates of diamond crystal growth, the Fe-Al-C system is used only to grow large diamond crystals by the temperature gradient method. For the efficient diamond spontaneous crystallization from the melt of this system, *p,T*- parameters, which are deep in the diamond stability region, are required. This, however, presents no technical problems for a toroid-type high-pressure apparatus. The results obtained at 6.5 GPa and the temperatures of 1720, 1820 and 1920 K using a cubic anvil type high pressure apparatus at the SPring-8 are shown in Fig. 1 as the degree of the graphite-to-diamond conversion (α) vs. time [8].

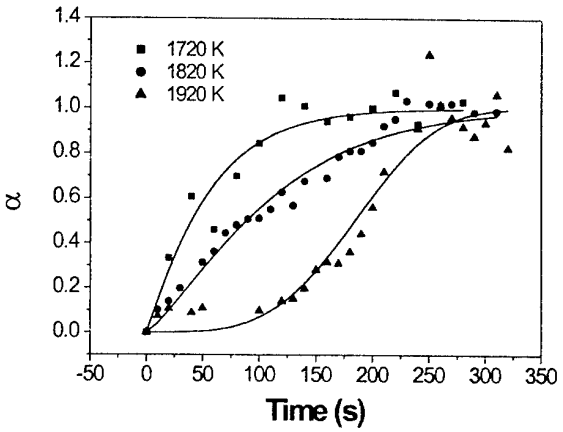


Fig. 1. Degree of graphite-to-diamond conversion versus temperature plot for the diamond crystallization from the Fe–Al–C melt at 6.5 GPa and temperatures 1720, 1820, 1920 K. Solid lines are calculated kinetic curves.

To process the kinetic data, we have used the Avrami relation [9]:

$$-\ln(1-\alpha) = k \cdot t^{r}$$

The Avrami relation best describes experimental data at the following values of the equation order: r = 1.08 (1720 K), r = 1.277 (1820 K), r = 3.709 (1920 K). The r = 1.08 and r = 1.277 values indicate that diamond crystallization in the Fe–Al–C system is characterized by an instantaneous nucleation and is controlled by the carbon diffusion to the surface of a growing diamond crystal. The value r = 3.709 at 1920 K indicates that we are dealing here with the process, which is characterized by nucleation proceeding at a constant rate and controlled by the processes on the surface of a growing crystal. It is obvious that a temperature of 1920 K is sufficiently high both for the new nuclei to form in the course of crystallization and kinetic difficulties due to the carbon diffusion via melt to be overcome.

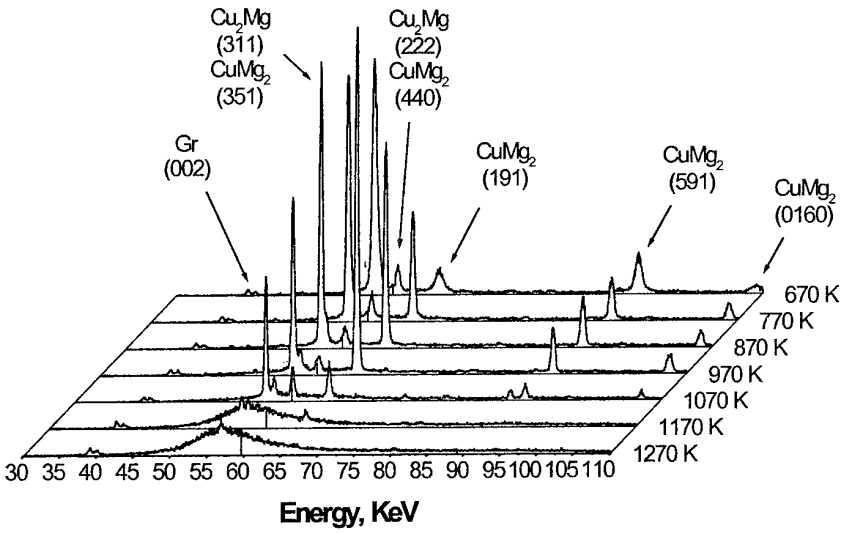


Fig. 2. Diffraction patterns of the Cu–Mg–C system taken at 6.5 GPa and 1370 K

The observed change of the crystallization mechanism in the range from 1820 to 1920 K renders calculation of the activation energy from the available data impossible. The common tendency for a decrease in the crystallization rate with increasing temperature (Fig. 1) is explained by the decrease (with temperature) in the ultimate solubilities of graphite and diamond in the melt, which is a thermodynamic impetus to the graphite-to-diamond recrystallization.

When employing copper, zinc or germanium as a solvent for carbon, the liquid phase appears in these systems at temperatures that do not exceed 1300 K and the parameters of diamond production are 6 GPa and 1870 K [10]. The authors [10] attribute this fact to the insufficient solubility of graphite in the melt at low temperatures. With an increase in temperature, the carbon solubility increases and creates conditions for graphite to recrystallize into diamond via the liquid phase. To this type of unconventional solvents must be added alloys of magnesium with zinc and copper, which offer diamond production at 6 GPa and 1820 K [5].

Diamond crystallization in the Mg–C system is observed at 7.7 GPa and 2100 K, while the liquid phase appears at 1150 K [11]. However, up to 2100 K the melt is in equilibrium with $MgC_2$ carbide and only after melting of the carbide, a stable diamond liquidus is observed. There have been reasons to believe that a similar situation is true for the Cu–Mg–C and Zn–Mg–C systems, i.e. that the equilibrium with a melt of any crystalline phase retards the crystallization of diamond. However, in situ studies by x-ray diffraction with synchrotron radiation using a cubic anvil type high pressure apparatus at the SPring-8 have shown that even at 1200 K (6.5 GPa) the melt is in equilibrium with graphite (Fig. 2). No lines of other crystalline phases have been recorded. Thus, at 6.5 GPa the absence of the diamond crystallization below 1800 K in the Cu–Mg–C and Zn–Mg–C systems is due to the necessity of overcoming kinetic difficulties (a low rate of nucleation, insufficient solubility).

## References

[1] Litvin, Yu.A., Growth of Crystals, vol. 9 [in Russian]. Nauka, Moscow, 1972.
[2] G.N. Bezrukov, V.P. Butuzov, V.A. Laptev, Doklady AN SSSR 200 (1971) 1088.
[3] R.H. Wentorf, J. Phys. Chem. 69 (1965) 3063.
[4] Aleshin, V.G., Andreev, V.D., Bogatyreva, G.P., Synthetic Superhard Materials, vol.1 [in Russian]. Naukova Dumka, Kiev, 1986.
[5] A.V. Andreev, H. Kanda, Diamond Relat. Mater. 6 (1997) 28.
[6] V.L. Solozhenko, V.Z. Turkevich and A.A. Kurakevich, J. Phys. Chem. (in press).
[7] T. Sugano, N. Ohashi, T. Tsurumi, O. Fukunaga, Diamond Relat. Mater. 6 (1997) 28.
[8] V. Turkevich, T. Okada, W. Utsumi, A. Garan, Diamond Relat. Mater. (in press).
[9] Avrami, M., J. Chem. Phys. 7 (1939) 1103; 8 (1940) 212; 9 (1941) 177.
[10] H. Kanda, M. Akaishi, and S. Yamaoka, Appl. Phys. Lett. 65 (1994) 784.
[11] A.A. Shul'zhenko, I.Yu. Ignat'eva, N.N. Belyavina, I.S. Belousov, Sov. J. of Superhard Materials. 6 (1988) 17.

# PHASE COMPOSITION OF THE PRODUCTS OF INTERACTION BETWEEN EUROPIUM (III) FLUORIDE AND CERIUM (III) FLUORIDE

**Zinchenko V.F., Efryushina N.P., Markiv V.Ya.[1], Eryomin O.G., Bilyavina N.M.[1], Mozkova O.V.[2]**

A.V. Bogatsky Physico–Chemical Institute of NASU, Odesa, Ukraine
[1]Taras Shevchenko Kyiv National University, Kyiv, Ukraine
[2]CDO "Arsenal", Kyiv, Ukraine

Phase composition and structure of the phases produced in the system $EuF_3$–$CeF_3$ at equimolar ratio $EuF_3$: $CeF_3$ and various temperatures have been studied. Initial compounds were synthesized from the oxides $Eu_2O_3$ and $CeO_2$ by their dissolving in the hydrochloric acid (in the last case in the presence of $H_2O_2$ as reductor) and subsequent precipitation of fluorides using hydrofluoric acid.

Obtained in such manner fluorides were melted in inert (argon) atmospheres in graphite crucible. Another portion of $EuF_3$ was sintered as a pellet at $1000^0$C in the vitreous carbon crucible.

For studying interaction the samples of initial compounds were stirred, mixed and pressed as pellets of 20-mm diameter and 15-mm thickness. The pellets were inserted into vitreous carbon crucible and sintered consequently at 700, 800, 900, 1000 and $1100^0$C in inert (helium) atmosphere. One of the initial samples was quenched at $1100^0$C in vacuum ~ $10^{-1}$ Pa. Another pellet was evaporated in the vacuum supply VU–1A to form thin film coat on the K 8 optical glass substrate.

The obtained materials as well as deposited coat and refuse after evaporation by X–ray phase and structure analysis using automated DRON–3 diffractometer. X–ray data of the products of interaction in the system $EuF_3$–$CeF_3$ show significant change of the phase composition in comparison with the initial components. Such changes are especially expressive in a case of the samples, which were undergone vacuum treatment; thus the refuse after evaporation is absolutely avoided from $CeF_3$ and contain mainly the phase $EuF_{2+x}$ (Table).

The presence of Eu(II) – based phases has been proved by the diffusion reflectance spectroscopy. Spectral characteristics of the quenched samples contain a wide absorption band in UV and, partly, in the visible interval of wavelengths. Appearance of this band is the result of the presence of Eu in the different valence states. In addition to this, the spectral characteristics show ready weakening up to entire vanishing of the bands of 4f–5d-electron transition of the Ce(III) ions in the UV interval as well as of a narrow peak of 4f–4f transition for the Eu(III) ion at ~ 395 nm.

All these data prove the deep chemical transformations, which take place in the studied system. The mechanism of chemical interaction between Eu(III) and Ce(III) fluorides was proposed. An oxidation-reduction reaction between the components occurs at high temperatures:

$$EuF_3 + CeF_3 \rightarrow EuF_2 + CeF_4$$

The motive force of this reaction is stabilization of the valence states Eu(III) and Ce(IV) due to the donor-acceptor interaction between compounds:

$$EuF_2 + EuF_3 \rightarrow Eu_3F_7,$$

and

$$EuF_2 + CeF_4 \rightarrow EuCeF_6$$

The above-described mechanism clarifies the fact of the significant decreasing of the Ce–phase content with increasing temperature and under the vacuum. The matter of fact that $CeF_4$ is a rather volatile compound and it intensively evaporates at relatively high temperatures and essentially under the vacuum. At the same time the coat consists mainly of β–$EuF_3$ and, partly, of $EuF_{2+x}$, i.e. the phase ratio is reverse to that for the refuse after evaporation.

It worth mentioning that the coat reveals rather high optical and operational characteristics. Optical thickness of the coat was of 1.8 μm. Computer modeling showed surprisingly an increasing of the refractive index ($n$) from 1.56 to 1.61 with the increasing of the thickness of the film, the average value of $n$ being about 1.59.

Scattering coefficient of the coat reaches 0.07÷0.1 % at the wavelength 0.63 μm.

Table – Effect of thermal and vacuum treatment on the phase composition and structural parameters of phases in the system $EuF_3$–$CeF_3$ (50 mol. %)

| # | Character of treatment | Phase composition and parameters of crystal lattices, Å |
|---|---|---|
| 1 | 2 | 3 |
| 1 | 700°C | 60% α–$EuF_3$; $a$=6.6204;$c$=7.0155; $c$=4.3905<br>40% $CeF_3$; $a$=7.1235;$c$=7.2722<br>traces of β–$EuF_3$; $a$=6.9846;$c$=7.1159 |
| 2 | 700°C ($EuF_3$ melted) | 46% $CeF_3$; $a$=7.1321;$c$=7.2661<br>33% α–$EuF_3$; $a$=6.6204;$c$=7.0238; $c$=4.4101<br>21% β–$EuF_3$; $a$=7.0347; $c$=7.2231 |
| 3 | 800°C | 51% α–$EuF_3$; $a$=6.6392; $c$=7.0317; $c$=4.3942<br>36% $CeF_3$; $a$=7.1252; $c$=7.2603<br>13% β–$EuF_3$; $a$=6.9373; $c$=7.2719 |
| 4 | 900°C | 47% $CeF_3$; $a$=7.1296; $c$=7.2855<br>45% α–$EuF_3$; $a$=6.6406; $c$=7.0381; $c$=4.4031<br>7% $EuF_{2+x}$ (β–cub.), x~0.39; $a$=5.7638 |
| 5 | 1000°C | 43% α–$EuF_3$; $a$=6.6803; $c$=7.0762; $c$=4.4014<br>42% $CeF_3$; $a$=7.1180; $c$=7.2770<br>15% $EuF_{2+x}$ (β–cub.), x~0.37; $a$=5.7810<br>traces of β–$EuF_3$; $a$=7.0196; $c$=7.2329 |
| 6 | 1100°C | 37% β–$EuF_3$; $a$=7.0385; $c$=7.1793<br>33% $EuF_{2+x}$ (α–cub.), x~0.10; $a$=5.8285<br>30% $CeF_3$; $a$=7.1668; $c$=7.2970 |
| 7 | 1100°C, vacuum | 44% $EuF_{2+x}$ (tetragonal), x~0.35; $a$=3.9675; $c$=5.6787<br>36% β–$EuF_3$; $a$=7.0043; $c$=7.2820<br>20% $CeF_3$; $a$=7.1068; $c$=7.2820 |
| 8 | Refuse after evaporation | 89% $EuF_{2+x}$ (α–cub.), x~0.09; $a$=5.8230<br>11% β–$EuF_3$; $a$=7.0159; $c$=7.1701 |
| 9 | Coat | 78% β–$EuF_3$; $a$=7.0349; $c$=7.1142<br>22% $EuF_{2+x}$ (β–cub.), x~0.39; $a$=5.7642 |

The coat showed a high mechanical durability (about 18000 cycles without damage).

This work has been supported by Science and Technology Center in Ukraine (STCU), project 1356.

# PROBLEMS AND PERSPECTIVES OF THE STUDIES OF DEFECT FORMATION IN SEMICONDUCTING SILICON

**Talanin V.I., Talanin I.E., Levinson D.I.**[(1)]
Zaporozhye State Engineering Academy, Zaporozhye, Ukraine
[(1)]Zaporozhye Institute of State and Municipal Government, Zaporozhye, Ukraine

The technological level of deriving of semiconducting materials largely determines the development of modern electronic engineering. The dominating tendency of development is the complication and miniaturization of semiconducting devices. With every new generation of semiconductor devices, the complexity and functionality of the devices increases and, hence, more transistors per chip are to be integrated.

The semiconducting silicon is main material in such major areas of electronic industry as a microelectronics and nanoelectronics, force semiconducting electronics, functional electronics, optical electronics, photoelectronics, measuring engineering etc. During production of silicon monocrystals it is necessary to solve the problem of their structural perfection. Therefore the control about the defect formation processes and grown of silicon with a specific defective structure is one from major problems of modern materials sciences.

Now grown the high purity silicon monocrystals at a simultaneous increasing of their diameters in which such structural defects as dislocations are not present (i.e. "dislocation-free" monocrystals). In that case the object of study is a thermodinamically stipulated defects of other nature. These defects are named as "microdefects".

Structural microdefects formed during cooling of crystals after their growth which may include agglomerates of point defects (vacancies or silicon self-interstitials) and impurities. These structural defects can detrimentally affect reliability of semiconducting devices and their performance. Their sizes is 0.003...50 μm. Since only high purity silicon can be used in modern electronic industry knowledge of processes of formation of defects in a semiconducting material is necessary.

According to a modern classification the A-, B-, D-microdefects and also area with simultaneous present so-called I (interstitial) and V (vacancy) of defects are exist [1].

Various theoretical models were suggested to explain the regularities of formation of microdefects in silicon. Main problems were the assumptions about the dominant type of point defects in crystal, their concentration, and interaction among themselves. In some models it was assumed, that the dominating type of point defects in crystal are interstitial atoms of silicon. In other models it was supposed, that the dominating type of defects are the vacancies. In contrast, were suggested simultaneous independent coexistence of both main types of point defects at high temperatures.

The sense of commonly accepted Voronkov model [2, 3] consists of the following: a) existence of recombination between self-interstitials and vacancies for temperatures close to temperature of smelting; b) was supposed that only vacancy nature for primary grown-in microdefects; c) independent existence areas with only interstitial and only vacancy microdefects.

None of these models could explain experimental results, which were obtained later such as Refs. [1, 4-12]. On base of this results the Voronkov model requires a following clarifications:

a) The recombination between vacancies and self-interstitials for temperatures close to temperature of smelting is very hampered.

b) Primary grown-in microdefects are vacancy and interstitial defects.

c) In the "vacancy area" of the crystals which grown in "vacancy" regime of growth contains simultaneously interstitial and vacancy defects in identical concentration.

Thus, on base of numerous experimental results we offer the physical model of microdefects formation and transformation in semiconducting silicon [1, 12]. This model is based on such positions:

a) Approximate equality of concentration of vacancies and silicon self-interstitials at the crystallization front near to smelting temperature.

b) The recombination process of intrinsic point defects at a high temperatures is hampered.

c) The impurities of oxygen and carbon are centres of microdefects nucleation and take the part in process of further growth and transformation of microdefects.

d) Disintegration of oversaturated solid solution of intrinsic point defects on two independent mechanisms: vacancy and interstitial.

The our model is shown in a Fig. 1. The offered model of nucleation, growth and transformation of microdefects can be used for the both of crystal growth methods: floating-zone method and Czochralski-grown method. Thus, irrespective of a method of growth of dislocation-free silicon monocrystals at the their cooling from the crystallization temperature the nucleation of vacancy and interstitial microdefects are happens which will be transformed in interstitial D-microdefects. The further transformation of interstitial microdefects is happens according to following scheme: D-microdefects → B-microdefects → A-microdefects.

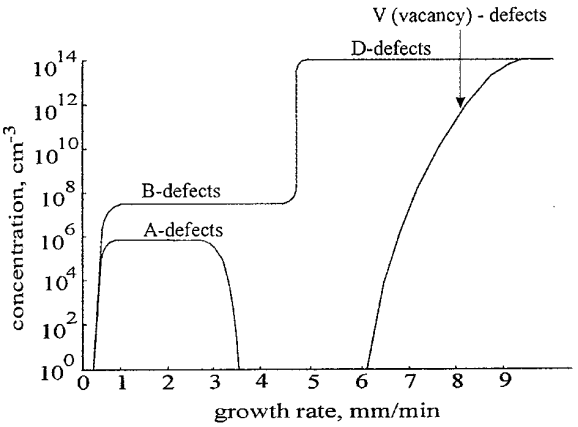


**Fig. 1. The scheme of formation and transformation of microdefects in FZ-silicon (the crystal diameter is 30 mm)**

The identity of processes of microdefects formation in both types of crystals which grown with a various diameters is confirmed by our results. Principal tendencies in Czochralski and floating-zone methods must be considered in reference to the goal of obtaining dislocation-free monocrystals with large diameters and controlled content of microdefects. Significant attention must be paid to the nature of grown-in microdefects in dislocation-free monocrystals and the role of intrinsic point defects in their formation. The defect structure in large-scale silicon monocrystals is not subjected to essential modifications [13]. Thus, offered model [1, 12] with allowance for difference of the growth conditions is applicable for monocrystals of any diameters which have been grown by both methods, float-zone and Czochralski.

Thus, the success in growth of high purity monocrystals and creation of silicon devices considerably depends on possibilities of monitoring of the conduct of intrinsic point defects.

**References**

[1] Talanin V.I., Talanin I.E., Levinson D.I. // Semicond. Sci. Technol. 17 (2002) 104.
[2] Voronkov V.V. // J. Cryst. Growth 59 (1982) 625.
[3] Voronkov V.V., Falster R. // J. Cryst. Growth 194 (1998) 76.
[4] Bublik V.T., Zotov N.M. // Cryst. Rep. 42 (1997) 1033.
[5] Kim Y.K., Ha Tae S., Yoon J.K. // J. Mater. Sci. 33 (1998) 4627.
[6] Nango N., Iida S., Ogawa T.// J. Appl. Phys. 38 (1999) 5695.
[7] Talanin V.I. // Siberian Russ. Workshops on Electron Devices and Materials (EDM'2000). Proc., (NSTU, Novosibirsk, 2000) p. 87.
[8] Iida S., Aoki Y., Okitsu K. et al. // Jpn. J. Appl. Phys. 39 (2000) 6130.
[9] Talanin V.I., Talanin I.E., Levinson D.I. // Proc. of ICSC-01 (Obninsk, 2001) p. 205.
[10] Dornberger E., Von Ammon W., Virbulis J. et al. // J. Cryst. Growth 230 (2001) 291.
[11] Larsen T.L., Jensen L., Lüdge A. et al. // J. Cryst. Growth 230 (2001) 300.
[12] Talanin V.I., Talanin I.E., Levinson D.I. // Cryst. Res. Technol. (2002) in press.
[13] Von Ammon W., Dornberger E., Hansson P.O. // J. Cryst. Growth 198/199 (1999) 390.

# PHYSICOCHEMICAL FUNDAMENTALS OF CREATING MATERIALS WITH ELEMENTS OF SELF-ORGANIZATION

**V.V.Skorokhod, V.P.Solntsev, T.A.Solntseva**
Institute for Problems of Materials Science of NASU, Kyiv, UKRAINE

A possibility of creation of a new generation of materials which are capable under operating conditions to exhibit functions, similar to living organisms, is recently spoken about at rather representative scientific conferences and symposiums. The problem of creating such materials arose as a result of appearance and progressing the ideas of thermodynamics of irreversible processes, as establishing conceptual approach that covered all natural sciences as a whole at the end of the twentieth century. Originally having arisen from a problem of reconciling two diametrically opposite aspects of evolution, in classic thermodynamics (the Carnot -Clausius principle) as the continuous law of disorganization and breaking down the initially created structure, and in biology and sociology objective complicating entities, formation of structure, the thermodynamics of irreversible processes allowed to find out, that the given ways correspond to different edges of physical reality. Thus the basic idea of a non-equilibrium thermodynamics became the concept of arising structures as consequence of originating self-organizing processes far from equilibrium state in open systems. The tendency to self-organizing is a peculiar property of open systems, and the non-equilibrium is a source of ordering and appearance of dissipative structures. The originating of dissipative structures does not suppose existence of the shape, self-isolating the object from an exterior world and scooping from it a building material and energy, that is peculiar to the vegetative and fauna world. However, supervising originating of temporary or time-space structure during auto-oscillating reactions in homogeneous media, where the shape is an inert bulb, some relevant properties of living systems, as for example self-reproduction are discovered, namely capacity of one of matters to be multiplied at the expense of raw materials. This functional property is determined by existence of autocatalytic stage at weep of set of so-called competitive or conjugated reactions.

In modern natural sciences it is supposed, that the set of the elementary shapes and functions of a substance is limited, while the new shapes and functions occur only as a result of a combination and superposition of the elementary ones. Really, the originating mechanism of concentration auto-oscillations in homogeneous reactionary medium demonstrates how during several reactions, the kinetics of every one is described by the exponential laws, owing to a superposition the system as a whole acquires non-monotonous character of kinetic behavior, there is a temporary "chemical clock." The relevant property of such systems is the conservation of an excitability. Physicochemical medium, in which auto-oscillating reaction takes place permanently erethitic in relation to exterior material flow, i.e. in conditions of interchanging with an exterior world it recreates the capacity to stimulation. Such mechanism of self-organization in the majority familiar physicochemical systems is molecular, appropriate to homogeneous media, liquid or gas, and is referred to single-leveled, suspected originating of the structure, and not isolated object having a stable form. Only ,when the dynamic system acquires a stable form enclosing and self-isolating area of space, where the internal processes ensure its conservation, progressing and ordered interchanging with an exterior world within the framework of the conditions, imposed to them, it becomes the material object, in some sense functionally similar to one of a living matter. Speaking about a system, its sizes and behavior as a unit, the founder of modern thermodynamics of irreversible processes I.Prigogine in one way or another set a central problem of the shape stability." For originating dissipative structure usually it is required, that the size of a system should exceed some extreme value- a composite function of arguments. We can argue, that the chemical instabilities set the long-distance order, by means of which one the system operates as a unit "

Thus, the appearance of the shape is related to interaction inside a non-equilibrium physicochemical system, however extra level, above-molecular, supplying self-isolation of dynamic object from a kinetic and diffusion dispersal into an environment. The conservation of the shape is impossible without leap of kinetic parameters of a system on an interface with an

environment and the phase transition is necessary. From the above reasoning creating materials with elements of self-organization is possible alternativlessly by selecting only powder heterogeneous non-equilibrium physicochemical systems, which may be associated with known artificial techniques into the shape, and the internal processes will induce phase transitions, localizing the area course of chemical reactions in kinetic zone and saving it and the object as a unit.

The practical realization of presented principles is obtained at sintering non-equilibrium powder compositions based on transition metals of IУ and УA groups of the Periodic system. As a source of thermodynamic instability dichalcogenides of transition metals of IУ, V and УIA groups.were inputted into composition. The supply of thermodynamic instability may be any compound formed by transition metal with metalloid, giving diatomic gas in an individual state. As it is known, at decomposing of such compounds the liberating gas interacts with an active environment - a metallic matrix, in which the unstable compound is present. Thus topochemical reaction of diatomic gas with transition metal has autocatalytic stage resulting in chemical instability. The auto-oscillating reaction in distributed environment generates concentration and temperature waves. As powder medium is discrete, the interaction of concentration and temperature waves from various sources induces phase transitions scaling the reactionary area. The induced phase transitions as a result of a cascade of instabilities, become the next ones in their hierarchy and close them into a cycle, immediately holding a source of instability. That is, in non-equilibrium physicochemical heterogeneous medium the closed triad of instabilities generates the dynamic nature of stability, in some kind like a living matter representatives.

The compositions with dynamic nature of stability in conditions of affecting of mechanical energy, for example, at its transformation into heat, at dry friction as well as at sintering show non-linear adaptation mechanisms that results in fall-off of a wear intensity. The systems are now found and the materials on their base developed, where physicochemical mechanisms resulting in processes of self-organization and self-healing of structural defects are present at rather low temperatures of about 473K. The effects of self-organization are also found in heterogeneous systems with oxygen, nitrogen and in other physicochemical systems, that will allow in the nearest future to develop materials of a new generation with a broad spectrum of functional properties.

# SELF-ORGANIZED CRITICALITY IN FRACTURE PROCESS OF MATERIALS

**Hilarov V.L.**
A.F. Ioffe Physical Technical Institute of RAS, St. Petersburg, Russia

It is well known since the pioneer works of Bak, Tang and Wiesenfeld [1,2] that nonequilibrium systems with many degrees of freedom may organize themselves into a critical state when they are driven far from thermal equilibrium. Solid states under mechanical stress can be considered as such nonequilibrium systems, trying to relax mechanical stresses by means of their defect structure evolution.

It is also well known that fracture surfaces of materials have clearly pronounced fractal character. During last decade a huge amount of investigations were carried out in order to measure fractal dimension of fracture surfaces for a wide spectrum of materials demonstrating both brittle and ductile fracture (metals, alloys, ceramics, glasses and rock species) [3]. This scale invariant state of fracture surfaces allows assuming that these surfaces appear as a result of some universal fracture mechanism and that this mechanism is related with self-organized criticality.

In order to check this hypothesis we investigated both space and time correlation properties of crack generation process in materials (steel industrial construction and granite laboratory samples) under mechanical loading. Initial experimental data contains acoustic emission information (times, amplitudes and sometimes coordinates of generated cracks) received by piezoelectric receivers on the sample surface. From this data one can construct different space and time correlators. We chose Grassberger-Procaccia correlation function as the space correlator:

$$C(r) = \frac{2}{N(N-1)} \sum_{j=1}^{N} \sum_{i=j+1}^{N} H(r - r_{ij}) \quad (1)$$

Here $H$ is a Heaviside function, $r_{ij}$ are distances between cracks, $N$ is a number of cracks. Thus $C(r)$ is simply the number of pairs of points of the statistical set separated by a distance less than $r$. The calculated correlator (1) displays well pronounced power behavior as function of $r$ with the exponent index close to fractal dimension of fracture surface on the late stage of fracture process. On the earlier stages of the fracture process this index approximately coincides with the dimension of 3d Euclidean space (fig. 1). The data ends when the fracture of the sample occures.

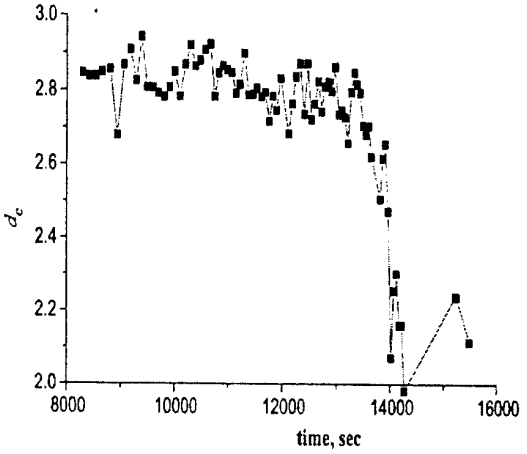


fig. 1 Time dependence of correlation fractal dimension

Thus we see that the process of crack generation shows a clear tendency to evolve towards a space scale invariant state.

As the main time characteristic of the process one can choose the time dependence of acoustic signal amplitudes. Then the time autocorrelation function may be constructed and power spectral density of the process calculated. in the form of:

$$K(t_1,t_2) = < x(t_1)x(t_2) >;$$

$$S(\omega) = \int_{-\infty}^{\infty} K(\tau)\exp(i\omega\tau)d\tau \quad (2)$$

Here $x$ is the stochastic variable (acoustic amplitude), $K(t_1,t_2)=K(t_1-t_2)$ the time correlator, depending on the time difference for the stationary process, $S(\omega)$ power spectral density. However, this procedure leads to significant data scattering in the $S(\omega)$ dependence. To avoid this, one can use wavelet analysis to construct the

scalogram corresponding to $S(\omega)$ smoothed on each scale by the spectrum of analyzing wavelet ("sombrero" wavelet was used). Such scalogram, obtained for the time 14000 in fig.1 shows clearly pronounced *1/f* noise feature for the large scale (low frequency) region in logarithmic coordinates (fig.2).

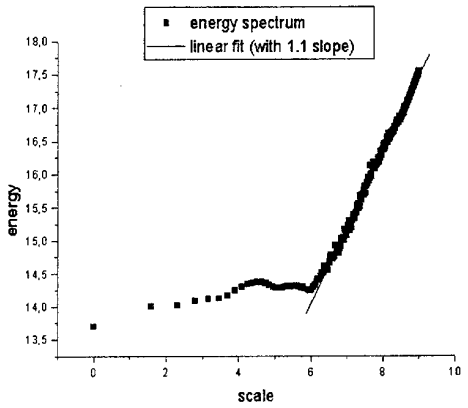


fig.2 scalogram – wavelet energy spectrum

The same scalogram calculated in the beginning of the fracture process also shows the low frequency scale invariant feature, but the slope is about 2. This slope reflects the power spectrum of the step function, caused by each acoustic event.

So the time correlation features also change significantly on last stage of the crack generation process from individual to collective behavior.

Thus both the space and time correlation features show well pronounced scale invariant features on the final stage of fracture process. It allows to assume, that during the fracture process the evolution of the defect structure occurs in such a way that that higher and higher scale levels are involved. On the final stage the material looses the possibilities to relax at all time and space scale levels of defect structure and self-organized critical state is formed. Due to the limited sizes of samples and industrial constructions this situation leads to material fracture.

Literature.

1. P. Bak.,C. Tang, K. Wisenfeld. Phys. Rev. Lett., **59**, 381, (1987).
2. P. Bak.,C. Tang, K. Wisenfeld. Phys. Rev. A **38**, 364 (1988)
3. V. Milman, N. Stelmashenko, R. Blumenfeld. Progr. Materilal Sci., **38**, 425, (1994).

# INSERTION OF RARE EARTH AND OTHAR METALS INTO AgI

**Despotuli A. L., Levashov V.I.**
Institute of Microelectronics Technology and High Purity Materials RAS, Chernogolovka, Russia

Impurity centers determine many properties of technologically important crystals and their optical spectra and relaxation behavior are of diagnostic value (for example, Lanthanide Ion Probe Spectroscopy. The specific features of high impurity concentration areas are the formation of defect associates, superlattice ordering, concentration-dependent structure phase transitions, metal-dielectric transitions, synthesis of new compounds, disordering of parent structures, etc. The variety of properties, types of behavior, and possible application spheres of crystals modified by impurities cause the appearance of new directions in research and technology. Compounds and materials containing rare earth (RE) impurities attract particular attention because of their unique optical, magnetic, and some other properties.

The materials with low maximum phonon energy are having prospects for MID-IR applications. The silver halides possess many interesting properties: nonhygroscopic, the frequency cutoff of the phonon spectrum located at low $\hbar\omega$, < 200 $cm^{-1}$, refractive index is high (2.0 -2.2) and they are highly transparent in a broad spectral interval. Therefore AgHal can be used for fabrication of miniature planar optical waveguaides - the key structures for optoelectronics applications. Another applications AgHal materials doped by RE are NIR and MID-IR optical fiber amplifiers and lasers. The area of such devices - scientific instruments, control, surveillance, remote measurements, systems for laying and aiming of weapon. The known ways of syntheses do not allow to get high concentrations of RE-ions at the systems on the base of AgHal because of separations in samples the phases of highly hygroscopic rare earth halides $REHal_3$.

In our previous work [1], it was suggested that crystal structures with high concentrations of impurity centers and specific properties could be created by inserting certain metals into channels of cation conductivity in solid electrolytes (superionic conductors) where the density of vacant crystallographic sites of various types is higher than $10^{22}$ $cm^{-3}$. At the works [1-3] an insertion Sm and Yb into a solid electrolyte-superionic conductor $RbAg_4I_5$ was discovered by optical absorption method. The experimental samples were prepared by vacuum thermal sputtering (2 x$10^{-6}$ Торг) of Sm or Yb films onto polycrystalline $RbAg_4I_5$ films 100-200 nm thick at 293 K. Then RE-metals dissolved into $RbAg_4I_5$. Materials forming by insertion of RE do not change optical features in humid atmosphere.

The following features were observed in the optical absorption spectra of the samples obtained after the reaction of Sm or Yb films with $RbAg_4I_5$ films: 1) a wide band of strong absorption peaking in the region 2.4 eV. The band was interpreted as due to the F-centers (electron in the I vacancy) with an equilibrium concentration of ~ 3 x$10^{20}$ $cm^{-3}$; 2) a band in the region 3.6-3.8 eV appearing at higher Sm concentrations and interpreted as an edge exciton of a new phase formed in the sample.

According to the mechanism proposed in work [1], the insertion of RE into $RbAg_4I_5$ films proceeds via precipitation of small quantities of AgI on the surface of crystallites and filling the vacancies of silver and iodine in the $RbAg_4I_5$ lattice by RE-ions and electrons, respectively. Assuming that RE form trivalent ions, the composition of the superionic conductor turned out to be $RE_xRbAg_{4-3x}I_{5-3x}$ .

It was found that storage of the samples in dry atmosphere or in air at room temperature (RT) led to the restoration of the initial optical spectra, electrical conductivity and Debye-grams. The observation was explained as due to a reduction of RE-ion and F-center concentrations by the formation of RE oxides ($O_2 \rightarrow 2O^{2-} + 4h^+$) and by returning of silver and iodine ions back into the crystallites.

In the works [4,5], the idea to extend our previous results on all RE metals and some groups of silver (copper) halides is realized. These works based on results Releigh [6] which establish the structural principles for silver halide superionic conductors. According to his results, $RbAg_4I_5$ and many other $Ag^+$- ($Cu^+$-) superionic conductors with a common formula QI nAgI (Q = nitrogenous organic bases such as tetraalkylammonium, pyridinium, quinolinium, etc.), as well as numerous compounds obtained by adding AgI to silver oxy-salts (phosphates, tungstate, molybdate, chromate, vanadate, arsenate, cyanides, polymethonium iodides, sulfonium iodides, tropyllium iodides and mercuric iodochalcogenides) inherit one important feature of the wurtzite structure of β-AgI, namely, faced-shared iodide tetrahedra where each $Ag^+$-filled $I_4$ tetrahedron shares a face with the adjacent empty one. The main function of $Q^+$-modifying ions is to increase the degree of face-sharing by iodide ion coordination polyhedra.

If an essential condition for RE insertion is a pair of faced-shared iodide tetrahedra or simply the availability of a fraction of empty tetrahedra (the size of tetrahedra enough suited for RE), then the results similar to [1-3] should be obtained both for β-AgI and a number of other silver halides differing by the chemical composition and structure. In zinc-blende structure half of the metal positions is not occupied. Because of this structure close related to wurtzite modification, γ-AgI was also included in area of our interest.

In the work [4,5] the rare-earth metals La, Ce, Pr, Nd, Sm, Tb, Dy, Tu, Yb, and Lu as well as Sc and Y were inserted into polycrystalline β- (γ-)AgI films for the first time under the conditions characteristic of topochemical reactions. Sm was also first inserted into films of the superionic conductor $CsAg_4Br_{3-x}I_{2+x}$. The experimental samples were created by deposition of RE metals (a laser ablation method) onto AgI films (100-200 nm) at the vacuum chamber with pressure about 1 $x10^{-6}$ Torr and temperature 293 K. The specific features of the obtained optical spectra were explained by the formation of F-centers, disordering of the initial crystal structures of β-(γ-) AgI, and synthesis of novel nonstoichiometric compounds termed rare earth silver iodides. These compounds with optical band gap 3.6 -3.8 eV at 293 K (a band gap of AgI - 2.9 eV) appear at the approximately 10% concentrations of La, Ce, Pr, Nd, Sm or Dy in the samples. For Tb and more heavier RE then Dy take place disordering of initial structure of AgI at the insertion of RE but the formation of novel phase is not observed. For the novel compounds, the preliminary data of electron and x-ray diffraction indicate the patters which differ from one of AgI.

Recently, the optical absorption data indicating the formation of novel compound under an insertion of Mn into AgI were also obtained at the IMT RAS. The band gap of this compound is more wide than a band gap of AgI and the edge of optical absorption is more complicated than for novel compound forming at the RE-AgI systems.

We also performed few experiments under insertion RE into CuI.

REFERENCES

[1] Despotuli, A. and Despotuli, L. (1997), "Influence of Samarium on Optical Absorption in Thin Films of the Solid Electrolyte $RbAg_4I_5$", *Phys.Solid State* 39, 1374-1377.

[2] Despotuli, A., Matveeva, L. and Despotuli, L. (1998), "UV Absorption of Thin-Film $RbAg_4I_5$ - RE (Sm, Yb) Systems", *Ionics* 4, 383-389.

[3] Despotuli, A. and Matveeva, L. (1999), "UV Absorption of Thin-Film $RbAg_4I_5$ -RE (Sm,Yb) Systems", *Phys.Solid State* 41, 218-222.

[4] Despotuli, A. (in press, 2002), "Insertion of Rare-Earth Metals into Ag-Hal Based Compounds. First Evidence of Disorder and Strong Modification of the Initial Crystal Structure AgI" (in the NATO-ASI series, "New Trends in Intercalation Compounds for Energy Storage", KLUWER ACADEMIC PUBLISHERS).

[5] Despotuli, A. (2002), "INSERTION OF RARE EARTH INTO SILVER HALIDES. I. KEY GENERALIZATION: AgI" (http://preprint.chemweb.com/inorgchem/0203002).

[6] Raleigh, D. (1977), "Structural Principles for Silver Halide Superionic Conductors", *J. Electrochem. Soc.* 124, 1157-1160.

# TRIPLE JUNCTION MOTION IN ALUMINUM TRICRYSTALS

**Protasova S.G., Sursaeva V.G.**
Institute of Solid State Physics, Russian Academy of Sciences, Chernogolovka, Moscow district 142432, Russia

The results of an investigation of the steady state motion of grain boundary systems with triple junctions in high purity Al are presented. Namely, the migration of systems with <111> and <110> tilt boundaries was studied. The experimental results demonstrate that the motion of grain boundary systems with triple junctions in Al can be controlled by slowly moving triple junctions. The influence of triple junctions depends on temperature. It is particularly strong at low temperatures. In the high temperature regime the motion of a connected grain boundary system is less affected by the triple junction, and, therefore, effectively controlled by the grain boundary mobility. The experiments revealed a drastic difference between activation enthalpy of grain boundary and triple junction motion. Therefore, there is a temperature, below which triple junctions govern the motion of the connected boundary system. This temperature was found to depend on the grain boundary and triple junction geometry, used in the experiment.

The motion of three grain boundaries systems with triple junctions (Table 1) was investigated. The investigated triple junctions consisted of two high angle tilt grain boundaries (GBI and GBII) and a low angle tilt boundary (GB III). The most important parameter of the motion of a boundary system with a triple junction in Fig. 1 is the angle $\theta$ in the point where the three boundaries meet. The magnitude of this angle $\theta$ defines the shape of the stationarily moving grain boundary system [1].

Table 1. Misorientation of the investigated tricrystals.

| *Sample* | *GB I* | *GB II* | *GB III* |
|---|---|---|---|
| *S I* | 21°<111> | 18°<111> | 3°<111> |
| *S II* | 27°<110> | 22°<110> | 5°<110> |

The role of the angle $\theta$ becomes clear from the relation between the steady-state value of $\theta$ and the dimensionless criterion $\Lambda = \frac{m_{tj} a}{m_b}$, (1)

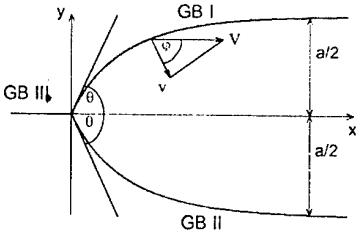


Fig. 1. Geometry of the grain boundary system with triple junction during steady-state motion.

which describes the influence of the triple junction on the motion of the entire boundary system :

$$\Lambda = \frac{m_{tj} a}{m_b} = \frac{2\theta}{2\cos\theta - 1} \qquad (3)$$

When $\Lambda$ is small, i.e. $\Lambda \sim 1$, the angle $\theta$ tends to zero and the steady-state velocity is controlled by the mobility of the junction :

$$V = m_{tj}\sigma \qquad (4)$$

For $\Lambda >> 1$ the junction easily adjusts to the motion of the boundary system, and the angle $\theta$ tends to its equilibrium value $\theta$=p/3.

As it can be seen in Fig. 2, the measurement of the temperature dependency of $\Lambda$ can be utilized as a method to analyze the experimental data and to separate different regimes of motion of the system, i.e. triple junction and boundary controlled kinetics. At relatively low temperatures, up to 430°C for sample *SI* and up to 510 °C for sample *SII*, the value of $\Lambda$ is of the order of unity. Since the criterion $\Lambda$ specifies the ratio of triple junction mobility to grain boundary mobility, low values of $\Lambda$ mean that the triple junction mobility is comparable to the grain boundary mobility. Therefore, the motion of the system in the low

temperature regime can be interpreted as a triple junction controlled motion. The rise of Λ with increasing temperature indicates that the system motion becomes increasingly less affected by the triple junction, and boundary kinetics become predominant. There is a distinct transition from triple junction kinetics at low temperatures to grain boundary kinetics at elevated temperatures and the activation enthalpy for triple junction motion $H_{TJ}$ is considerably higher than that for grain boundary migration ($H_b$). The behavior of the grain boundary controlled branch in Fig. 3 compares well with measurements of the reduced grain boundary mobility obtained from literature data [2] of independent bicrystal experiments. The corresponding evaluation for system *SI* is given in Fig. 3a and yields comparable behavior. Owing to only few triple junction systems investigated so far, it is an open question how the transition range between grain boundary and triple junction control of migration kinetics depends on grain boundary and correspondingly triple junction geometry. In particular grain boundary systems consisting of structurally different grain boundaries (<111> and <110> tilt boundaries in the current study) need to be adressed to probe the influence of triple junctions and their geometry on texture development during grain growth. It is finally noted that the results of the current study again demonstrate that the determination of an average grain boundary mobility by measurement of the mean grain size evolution during grain growth in polycrystals can be deceptive and, in particular, different for measurements in the high and low temperature range.

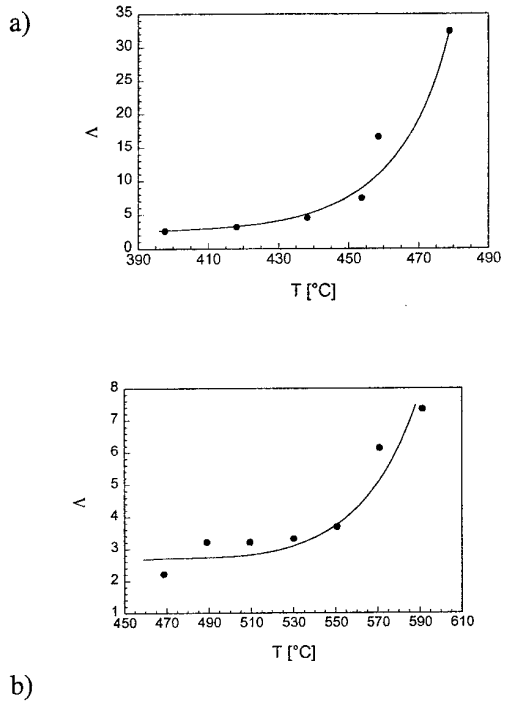


Fig. 2. Temperature dependence of the criterion Λ for triple junctions in samples *SI* (a) and *SII* (b).

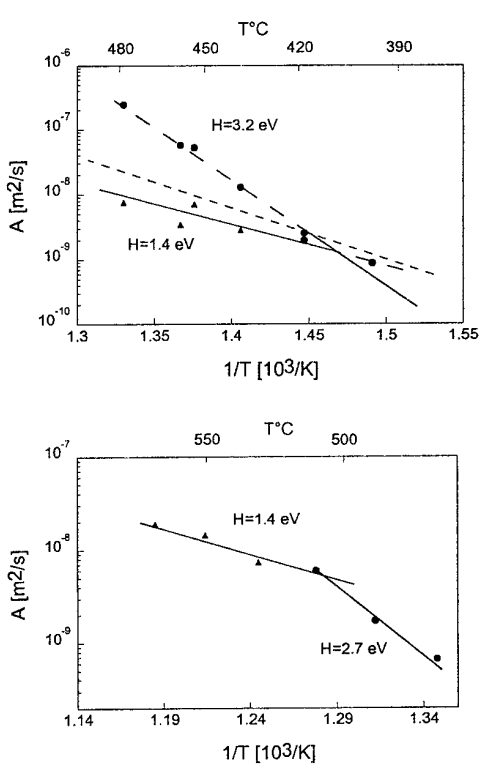


Fig. 3. Temperature dependence of triple junction (●) and grain boundary mobility (▲) in samples *SI* (a) and *SII* (b). Dotted line represents the mobility of a 21°<111> tilt boundary in Al as reconstructed from literature data [2] ($H$= 1.6 eV; $A_0$= $10^3$ $m^2/s$).

References

1. Galina, A.V., Fradkov, V.E., Shvindlerman, L. S., *Phys. Met. Metall.*, 1987, **63**, 165.
2. Gottstein, G. and Shvindlerman, L. S. *Grain Boundary Migration in Metals: Thermodynamics, Kinetics, Applications*, CRC Press, 1999.

# EFFECT OF RANDOM FLUCTUATING POTENTIAL ON ORDER PARAMETER AND PHASE TRANSFORMATION TEMPERATURE

**Dmitriev A. I., Radchenko M.V., Lashkarev G.V., Butorin P.E.**
Department for Functional Materials and Cryogenic Investigations, Institute for Problems of Materials Science National Academy of Sciences of Ukraine, 03680 Kiev-142, Ukraine
E-mail: lashk@ipms.kiev.ua

It is known that instability of crystal lattice occurs for narrow-gap semiconductors $Pb_{1-x}Sn_xTe$ in the composition range $0,18 \le x \le 1,0$ within temperature interval $25 \le T \le 100$K. Discovered the existence of three PT by the help of X-Ray structure analysis. The change of crystal lattice symmetry occurs at two of these phase transition (PT).

Earlier we shown, that temperature dependencies of thermoelectric power and magnetic susceptibility give sufficient information for PT research in A4B6. Therefore in this paper the researches of neutron diffractometry as well as thermoelectric power (TP) $\alpha$, magnetic susceptibility (MS) $\chi$, Hall coefficient $R_x$ in the temperature range 4,2-300K and Shubnikov oscillations in magnetic fields up to 4T are represented.

Random fluctuating potential (RFP) arises owing to defects of a structure, including irregular distribution of components of alloy or chemical compound of complicate composition. In semiconductors RFP results in nonthermal spreading of band edges, what is equivalent to nonthermal spread of a chemical potential level of magnitude $\Delta E \sim \varepsilon^{-1} (Nr)^{1/2}$ ($\varepsilon$- the dielectric susceptibility, N - concentration of defects, r- action radius of perturbation potential). Obviously, the spread of quantum levels has a close value. The latter allows experimentally evaluate the magnitude of perturbing action of RFP corresponding to nonthermal spread of quantum levels, which is described by Dingle temperature - $T_D$, ($\Delta E = kT_D$). In quantum oscillation phenomena $T_D$ determines damping amplitude of oscillations and a degree of crystal imperfection at T= O K. Then in general case one can write the equation for order parameter Q

$$Q = Q_0 + \Delta Q = \alpha (Tc - T)^{\beta} + \gamma T_D$$

where Tc- temperature of phase transition, $\alpha$, $\gamma$ - factors, $\beta$ -critical index of order parameter.

Hence, the temperature reduction of PT at increase of defectivity of crystal lattice connected with RFP can by described by Dingle temperature. The magnitude $T_D$ in multicomponent semiconductors reaches values about 25 K, in metals - 1 K.

The structure phase transitions in semiconductors AIVBVI attract an interest to this phenomenon during series of years.

By method of neutron diffractometry the sequence of phase transformations in solid solutions $Pb_{1-x}Sn_xTe$ (x = 0.2) of high structural perfection was investigated. In accordance with the data of single frequency Shubnikov-de Haas oscillations of thermoelectric power these samples have $T_D = (8 \pm 1,2)$ K.

At temperature reduction from 290 K up to 100 K the interplane distance d along [100] direction fluctuates within 0,342 - 0,344 нм. At $T_{C1} < 100$ K the strong reduction of d size to values 0,336 нм happens, that is probably due to phase transition. In the range T = 90-40 K the top of a diffraction reflex is splitted to three lines, the peak intensity drops up to a minimum value at T = 60 K. The an increase of temperature results in an increase of reflex intensity and vanishing of splitting. In general, temperature changes of reflex intensities and their disposition on the scale of interplane distances in directions [110] and [111] are similar.

Minims on temperature dependence of neutron reflection intensity from a plane (111) are identified as phase transformations at temperatures $Tc_1 = (35 \pm 5)$ K; $Tc_2 = (110 \pm 5)$ K; $Tc_3 = (140 \pm 5)$ K; $Tc_4 = (260 \pm 5)$ K. The comparison of these results with the data on research of temperature dependencies of thermoelectric power, magnetic susceptibility and X-Ray structure analysis, confirms the fact of observation of sequence of four phase transformations in $Pb_{1-x}Sn_xTe$ (x = 0.2).

In the temperature range 6 K< T < 35 K the TP of investigated crystals is linear and displays a break at $Tc_1 = 35$ K. The dependence $\alpha$ (T) at

$(\mu H/c)>>1$ ($\alpha \to \infty$) has such a break also at the same temperature as in the case of $\alpha = 0$. The mentioned fact shows that process of current carriers scattering does not influence on forming of this break. The same feature of $\alpha$ we observed earlier at 20-25 K for the crystals with close concentration of current carriers which manifest PT. At $Tc_2$= 115 K we had observed a peculiarity which we related with the second PT. In the temperature interval $Tc_1 < T < Tc_2$ TP is characterized by hysteresis loop of small square. The hysteresis is related with a creation of the second phase nucleuses and with an energy consumption for increase of their surface.

It is necessary to pay attention to the fact that in the hysteresis region reflection (111) splits and its intensively has a minima at $T \cong 60K$. Then the following temperature decrease leads to an enlargement of its intensively and to disappearance of a splitting. The similar hysteresis loop was observed by us in the case of $Pb_{1-x}Ge_xTe$ also. It seems that the TP hysteresis loop at PT of displacement type had been observed by us for the first time.

At $Tc_1$ the hole gas is degenerated one and one can observe the break of linear dependence of $\alpha$ (T). In the same time at $Tc_2$ where the degeneracy disappears the feature of $\alpha$ (T) seems like a bend. The similar regularities had been noticed by us earlier for the samples $Pb_{0.8}Sn_{0.2}Te$ and $Pb_{0.94}Ge_{0.06}Te$. This fact is an additional argument which testifies to our observation of the PT.

It should by noticed that the temperature of the first PT in $Pb_{0.8}Sn_{0.2}Te$, grown from the vapour phase is sufficiently higher than in the case of crystals grown by Bridgman method (35 K and 20-25 K. respectively).

Earlier we shown that PT in SnTe, $Pb_{0.82}Sn_{0.18}Te$ and $Pb_{1-x}Sn_xTe$ results in the peculiarity of magnetic susceptibility like a splash of paramagnetism on the diamagnetic background. The MS temperature dependence is characterized by two features at $Tc_1$ and $Tc_2$. The temperature of first peculiarity is close to the $Tc_1$ determined from the TP temperature dependence. Therefore we explain it by PT, as we had done earlier.

At PT the fluctuational feature of MS appears which obliged to the fluctuations of order parameter. Indeed a temperature dependent correction to the energy gap $E_g$ appears at PT. Because of the small magnitude of $E_g$ in narrow gap semiconductor $Pb_{0.8}Sn_{0.2}Te$ the renormalization of band spectrum should lead to the changes of its magnetic and kinetic properties: a correction to magnetic susceptibility appears which is obliged to fluctuations of order parameter in the vicinity of PT. The manifestation of the third PT on the temperature dependence of magnetic susceptibility ($Tc_3 = (140 \pm 5)$ K) coincides with the extremum on the dependence on integral intensity of reflection (111) on temperature. There is also weekly expressed change of $\chi$ (T) in the vicinity of $Tc_2 = (110 \pm 5)$ K.

The measurements of Hall effect demonstrated that R is practically independent on temperature and does not have feature at PT. It can be explained by low hole concentration when Fermi level is situated in the light hole band and does not penetrate into heavy hole band . This results in independence of hole concentration at PT.

The combined analysis of the data of neutron diffraction, thermoelectric and magnetic researches testifies to the existence of four phase transitions at Tc1 =(35±5) K, Tc2 =(110 ± 5) K, Tc3 = (140 ±5) K and Tc4 =(260 ±5) K in the single crystals $Pb_{0.8}Sn_{0.2}Te$.

The structural perfection improvement of single crystals of solid solution $Pb_{0.8}Sn_{0.2}Te$ results in the shift of the first phase transition temperature $Tc_1$ from 20-25K to $Tc_1$ = 35K. Again it has lead to the appearance of phase transition at $Tc_2$ = 110K and thermoelectric power hysteresis in the temperature range $Tc_1$ - $Tc_2$ which testifies to the I type of this phase transition. The observed splitting of reflection peaks of the neutron diffraction spectrums in the same temperature interval indicates the lowering of crystal lattice symmetry. Phase transformations at Tc3 and Tc4 are transitions of presumable the II kind.

# THEORETICAL AND EXPERIMENTAL BASIS FOR DEVELOPING STRUCTIRAL MATERIALS FOR GLASSMOULDING TOOLS

**Kolotilkin O.**
The Zaporozhye national technical university, Zaporozhye, Ukraine

Mechanisms of failure of structural materials for glassmoulding tools have been established. New methodology enabling to use standard and newly proposed devices and techniques has been worked out for complex estimation of materials working capacity.

The influence of graphite phase in ferrous-carbon alloy on sensible heat, physical mechanical, and service properties has been studied. It was revealed that with increase of graphite phase quantity from 2,1 up to 18,3 volumetric percent heat conduction increases by 78 %. At the same time surface area of failure with graphite increases from 9±0,5% to 90±0,5%, so alloy failure occurs mainly in graphite inclusions that explains deterioration of mechanical properties and viscosity of failure. It was found that iron wetting with glass mass, roughness and velocity of thermochemical erosion rises respectively to 65%, 412,5% and 292% with an increase of graphite phase quantity.

The analytical task of determining ultimate strength of heterogeneous material (ferrite + graphite) with growing carbon content from 0,48 up to 4,02% has been solved. It was shown that the failure character of ironcarbon alloys at loading is related to concentration of stresses at points of graphite inclusions. Experimentally it was proved, that when loading at points of graphite inclusions microzones of plastic deformation are being formed. Using numerical-analytical method of finite elements, analytical task in frames of theory of plasticity has been solved enabling to determine sizes of plastic deformation zones which are related to size and shape of inclusion, load and elastoplastic characteristics of inclusions and metallic matrix. Relationship between microdeformed metal factor and parameter of inclusion shape has been ascertained.

It is shown that with the increase of parameters of inclusion shape the share of microdeformed metal grows with exponential relationship.

The idea of cast iron failure mechanism on periodic contact with glasmass melt has been widened. It was found that cast iron wetting with glasmass is related to shape and roughness and velocity of thermochemical erosion to shape and sizes of graphite inclusions. The mechanism of damage of cast iron with different degree of alloying has been studied. It is proved that graphite has a dominant role in failure and formation of cast iron properties regardless of alloying degree. On basis of analysis of regressive relationships of proposed criteria of durability to chemical composition of cast iron, optimum combinations of concentration of carbon and silicon providing required level of mechanical and service characteristics for definite conditions of tools parts operation have been found.

It was found that at simultaneous alloying of cast iron with chromium (0,4...0,6%) and aluminum (0,4...0,6%) strength, viscosity of failure and thermal resistance increase that is associated primarily with finer structure of perlite and relatively low graphite participation in failure. Finer structure of perlite and presence on cast iron of oxide films with crome and aluminium base offer minimum values of roughness, wetting, adhesive factor, velocity of thermochemical erosion and better resistance to failure of oxide layers. It has been proved the copper content in cast iron should be within limits of 0,15...0,3% to increase heat conductivity of cast iron for the purpose of extraction of heat from working surface of glassmoulding tool. On basis of results obtained compositions of cast iron for parts of glassmoulding tools working in conditions of thermochemical erosion, thermocyclic and mechanical loads have been obtained.

Relationships describing the influence of chemical composition of cast high speed steel for knives fragment of glassmass to suggested criteria of reliability and durability have been enstablished. It is shown that carbon content of 0,855% provides optimum combination of mechanical, operational and technological properties of steel. It has been proved that increasing content of tungsteen, molibdenium and vanadium by 5% enhances coefficient of adhesion by 117,4%, 183,3% and 157%, breakage of oxide layers – by 135%, 15% and 55% and roughness – by 293,3%, 206,7% and 220,4% respectively. It has been found out that concentration of tungsteen (1%), molibdenium (3%) and vanadium (3%) decrease to maximum the velocity of thermochemical erosion as a consequence of leveling off carbide het-

erogeneity, desintegration of carbide phase and decrease in electrode potential between carbide phase and metal matrix. On the basis of these obtained results steel has been elaborated for manufacturing knives with prolonged operational resource.

Relationships of influence of basic alloying element of copper, self-fluxing elements of boron and silicon as well as calcium and cerium modifiers to regularity of structure formation and creating mechanical, operational and technological properties of built-up metal on a basis of nickel have been enstablished. It has been proved that silicon content in nickel alloys with 0,5...1,5% of B should not exceed 2% that provides for minimum coefficient of adhesion of glassmass to built-up metal. It has been proved that addition of 12...15% of Cu to nickel alloy with boron and silicon enables decreasing in roughness and adhesion factor. Increase of copper content up to 30% improves the adhesive strength of built-up metal with base one and thermal resistance respectively. It has been proved that addition of Ca (0.15...0.3%) and Ce (0.1...0.2%) to copper-nickel alloy with boron and silicon improve thermal resistance and decrease adhesive factor, roughness and velocity of thermochemical erosion at the expense of disintegration of eutectic colonies.

Using results obtained compositions of building-up materials for restoration and hardening the parts of glassmoulding tools of different designation have been developed.

Character of damage of structural materials contacting with aggressive media is influenced by the number of technological factors and contact duration with aggressive media. For the purpose of researching the processes occurring in contacting zone of structural material with media, the model of transferring the viscous smelt on tool surface has been worked out. Calculated scheme is shown in figure.

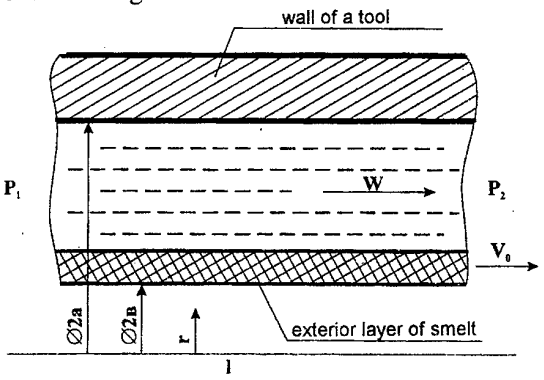


Figure 1 Scheme of transferring viscous smelt on tool surface.
W – velocity of smelt transfer;
$V_0$ – velocity of transferring of outer layer of silicate smelt flow;
$P_1>P_2$ – flow moving force;
2a – inner diameter of tool;
2b – inner diameter of flow;
l – length of system area;
r – flowing radius.

According to developed model the velocity of transferring of viscous silicate smelt on tool surface is determined by relationship:

$$W = -\frac{1}{4}\beta^2 r^2 + C_1 \ln r + C_2, \qquad (1)$$

where $\beta = \frac{P_1 - P_2}{\mu \cdot l}$;

$C_1$ and $C_2$ - factors, considering $\beta$, $V_0$ values and parameters $a$ and $b$ (see computated scheme).

Fogel-Tammans formular relationship of dynamic viscosity of silicate smelt $\mu$ and temperature $T$ is presented as:

$$\lg \mu = A + \frac{B}{T - T_0}; \qquad (2)$$

where $T$ is the temperature of smelt, $A$, $B$, $T_0$ - constants, depending on chemical composition of silicate smelt.

On basis of formulas (1) and (2) the program enabling to determine the velocity of transferring viscous silicate smelt on tool surface with consideration of changing viscosity has been compiled. Design of glassmoulding tools with rational profile of working surface have been worked out on the basis of results obtained. This enabled to increase the velocity of transferring the viscous silicate smelt in most critical areas of working surface of tool and decrease contacting time of surface layers of metal with aggressive smelt.

In whole complex approach in evaluation of thermoerosive failure processes and wear out of tool surface when processing viscous aggressive silicate smelts has enabled to increase the durability of tools by 4 times and decrease its metal consumption by 15% and improve a great number of other technical and economical indices when manufacturing glassmass goods.

# VISCOELASTIC PROPERTIES OF INHOMOGENEOUS MEDIA

Novikov V.V., Wojciechowski K.W.[1]
Odessa National Polytechnical University, 1 Shevchenko Prospekt, 65044 Odessa, Ukraine
e-mail: novikov@te.net.ua
[1]Institute of Molecular Physics, Polish Academy of Sciences, M. Smoluchowskiego 17, 60-179 Poznań, Poland e-mail: kww@man.poznan.pl

In the present communication we report investigations of viscoelastic properties of chaotic, fractal structures in which one of the phases shows negative shear modulus. A phase of negative shear coefficient is a particular case of the Lakes' system [1] of negative stiffness and, as such, is obviously mechanically unstable since the feedback between the stress and deformation favors increase of any deformation. One can stabilize, however, such a phase by immersing it into a matrix of positive stiffness.

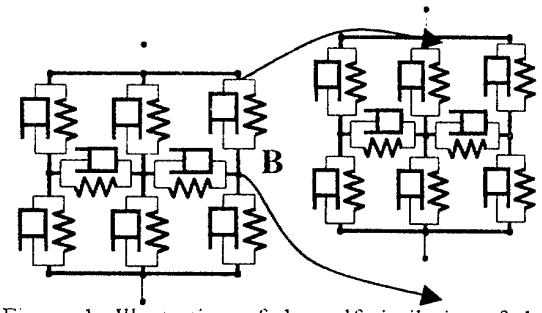


Figure 1. Illustration of the self-similarity of the fractal system $\Omega_n(L_0, p_0=1)$ (where $n\to\infty$) of viscoelastic bonds for $L_0 = 2$. The viscoelastic bonds are, for simplicity, represented by parallelly connected 'pistons' (viscous element) and 'springs' (elastic element).

The analysis was performed on the basis of a hierarchical model of two-component structure and is a generalization of the method of elastic properties calculations described in detail in [2]. In the modeling of chaotic structures presented there, hierarchical lattices of bonds representing random distribution of parameters were applied. In contrast to the case considered in [2], where the bonds of the lattice represented purely elastic properties, the bonds considered here may represent more general, viscoelastic case (see Fig. 1).

The dependencies of the viscoelastic properties on properties and concentrations of phases forming the considered inhomogeneous medium were modeled by a simple generalization of the "blob model" [2,3]. Namely, the results obtained for static elastic properties correspond to results for viscoelastic properties (for arising harmonic vibrations) obtained by replacing the real elastic modules, $K$ (the bulk modulus) and $\mu$ (the shear modulus), by the complex modules $K^*, \mu^*$.

Calculations were performed for a two-component, inhomogeneous medium. For simplicity, it has been assumed that both the phases are isotropic and the first phase is purely elastic whereas the second phase is elastic from the point of view of volume deformations and viscoelastic from the point of view of shear deformations. The concentration of the purely elastic phase is denoted by $p$.

It is convenient to write the shear modulus of the second phase, $\mu^*_2$, in the form

$$\mu^*_2 = \mu'_1 x(1+iy), \qquad (1)$$

where $y=tg(\varphi_2)=\mu''_2/\mu'_2$, $x=\mu'_2/\mu'$, and $\mu^*_1=\mu'_1$ is the (real) shear modulus of the first phase.

In the following we compare the effective shear modulus of an inhomogeneous medium with fractal structure (further referred to as a fractal composite) with a composite material corresponding to the Hashin-Strikman formulae (further referred to as the Hashin-Strikman composite).

In Fig.2, the ratio of the effective shear modulus to the shear modulus of the elastic phase is shown as a function of the concentration of the elastic phase and $x$ for $y=10^{-3}$. It is assumed that the viscoelestic phase in Fig. 2 has a negative shear modulus (i.e. negative real part of the complex shear modulus) and is characterized by $y=tg\varphi_2=0.00$ and the Poisson's ratios of both phases (calculated from real parts of the elastic moduli) are equal to 0.184... . (The latter assumption means that the ratio of the real part of the shear moduls to the bulk modulus is equal to $\mu'_i/K'_i = 0.8$, where $i=1,2$ numerates the phases; in consequence the ratio of the bulk modulus of the second phase to the bulk modulus of the first phase is equal to $x = K'_2/K'_1$.) It can be seen there that for the inhomogeneous fractal medium the shear modulus shows in some *ranges* of concentration a resonance-like behavior similar to that discussed in [1] whereas in the Hashin-Strikman composite there exists only *one* such a resonance in the vicinity of the concentration $p=1$.

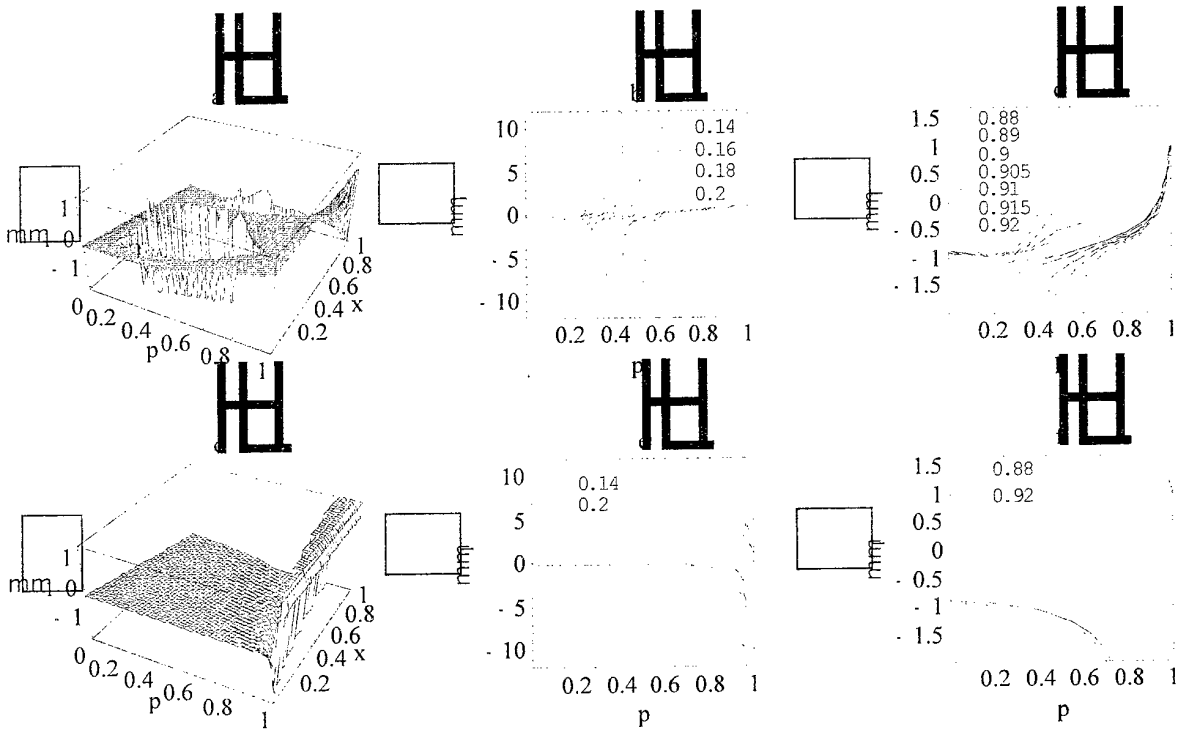


Figure 2. Comparison of the ratio of the effective shear modulus to the shear modulus of the elastic phase at $y$=0.001 as a function of the concentration of the elastic phase and $x$ : (a) in the fractal composite and (b) in the Hashin-Strikman composite. In (c) and (e) some sections of the (a) are presented, whereas in (d) and (f) some sections of (b) are shown; the values of $x$ corresponding to the sections are given in these figures.

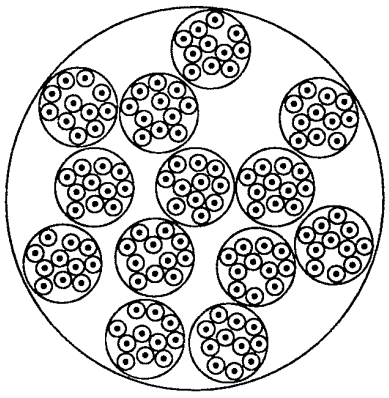

Figure 3. The idea of construction of a material with fractal structure.

The above comparison shows that the viscoelastic properties of the fractal composite differ qualitatively from the properties of the Hashin-Strikman composite. The observed differences can be understood taking into account that the hierarchical model considered takes into account clusters of various length scales and different parameters of their 'resonances' which are formed in the fractal composite whereas the Hashin-Strikman composite is 'uniform' in this aspect. At this point let us notice that a material of fractal structure which should show the viscoelastic properties similar to those obtained by solving the model described can be manufactured in reality by the following scheme. At the first step (the lowest size level) one produces "tablets", e.g. of a polymer with required inclusions. At the next step, the tablets obtained at the preceding level are used as inclusions to larger tablets. The process is continued and a hierarchy shown in Fig.3 is obtained.

This work was supported by the Polish Committee for Scientific Research (KBN) and by the Ukrainian National Academy of Science.

**References**

1. R. S. Lakes, T. Lee, A. Bersie, Y. C. Wang, Nature **410**, 565 (2001).
2. V. V. Novikov, K. W. Wojciechowski, D. V. Belov and V. P. Privalko, Phys. Rev. E**63**, 036120 (2001).
3. V. V. Novikov, K. W. Wojciechowski, Fiz. Tv. Tela **41**, 2147 (1999).

# COATING OF A NEW FOAMING AGENT FOR ALUMINIUM

**Nakamura T.[1], Byakova A.V.[2]*, Gnyloskurenko S.V.[1],[5], Sakamoto K.[3]**, Ishikawa R.[4], Raychenko O.I.[5]**

[1]Institute of Multidisciplinary Research for Advanced Materials, Tohoku University, Sendai, Japan
[2]National Technical University of Ukraine «Kiev Polytechnic Institute», Kiev, Ukraine
[3]Keihin Corporation, Kakuta, Japan
[4]Honda R&D CO., LTD., Tochigi, Japan
[5]Institute for Problems of Materials Science of NAS of Ukraine, Kiev, Ukraine
*Formerly: Visiting Professor, Tohoku University, Sendai, Japan
**Formerly: Graduate student, Tohoku University, Sendai, Japan

## 1. Introduction

Aluminium foams are a new class of lightweight materials attractive for the automotive industry. Molten metal can be processed to a porous material by injecting gas into the melt [1] or by adding a foaming agent (FA) into it [2]. Metal foams currently are not widely used in spite of their excellent properties because of difficult control of the foaming process and high production cost.

To meet the above requirements, a new widely available FA, calcium carbonate, is suggested. A homogeneous distribution of the FA in a melt can be achieved by enhancing the wetting of particles. Applying a surface coating technique solves this problem. In this work, the ion-exchange process was employed for the (novel) purpose of coating calcium carbonate powder with fluoride.

The present study aims to investigate the coating procedure, to compare the foaming ability of the conventional FA ($TiH_2$) with the new candidate ($CaCO_3$), and to elucidate the impact of surface phenomena occurring during melt foaming on the structure of solid foam.

## Materials and Experimental Procedures

**Powder coating technique and surface analysis.** A commercial calcium carbonate powder with particle size of 7.5□m was coated with $CaF_2$ in an aqueous solution containing NaF. The solution was stirred at 40°C to induce the ion exchange reaction: $CaCO_3 + 2NaF = CaF_2 + Na_2CO_3$. After stirring, the solution was filtered and the $CaCO_3$ powder was then dried in an oven at 120 °C.

Particle size and morphology of the powder were examined by scanning electron microscopy (SEM) and X-ray photoelectron spectroscopy (XPS) was used to study the chemical composition of the carbonate surface.

**Preparation of agents.** Instead of $CaCO_3$ powder, a marble plate polished with 1 μm diamond slurry was used in the wetting study. The samples were coated with $CaF_2$ by the technique described above. $TiH_2$ powder with a particle size of 10 μm was compacted into cylindrical tablets and cut, to obtain straight-edged sections.

**Wettability study.** The dipping of a solid plate into pure aluminium (99.9 mass%) was employed to study the wetting behaviour of liquid Al in contact with foaming agents. The contact angle was determined from an image contour of the junction of the three phases, obtained by the X-ray radioscopic visualization technique. Al was melted in a resistance furnace in an argon atmosphere. A solid plate of foaming agent was mounted by steel wire at the lower end of an $Al_2O_3$ tube and introduced vertically into the melt at 690°C. X-ray observation was carried out for 15 min.

**Foaming experiment.** Aluminium foaming tests by both the conventional FA (titanium hydride) and the new FA (calcium carbonate) were carried out using the ALPORAS [2] foaming route. Aluminium alloy A 356 in a stainless steel crucible was melted in a resistance furnace. Ca used as a thickening agent was added into the melt at 750 °C while stirring in an ambient atmosphere. After cooling to the prescribed value (640°C for $TiH_2$, 680°C for $CaCO_3$), the molten aluminium was stirred with the FA powder (1 wt.%). The FA then decomposed, evolving gas and caused the melt to foam. Finally, this foam was cooled by fans.

## Results and Discussion

**SEM and XPS surface analysis of foaming agent coating.** The only difference in surface morphology of uncoated and coated particles was the presence of dissolution traces on the edges of

the coated particles. Apparently this coating couldn't be detected by SEM.

XPS analysis revealed the 1s peak of F, designating F bonded to Ca (F – Ca). This peak occurred throughout a 10 min sputtering period indicating the presence of calcium fluoride on the carbonate surface. The F 1s peak was not detected on uncoated carbonate particles.

**Wettability study.** Analysis of the X-ray images revealed that $TiH_2$ formed a lower contact angle (130°) compared with $CaCO_3$, and coated $CaCO_3$ resulted in a contact angle 15° less than that formed by uncoated $CaCO_3$ ($\theta \approx 140°$ and 155°, respectively). These observations confirm that the surface properties of the coated carbonates promote better wetting by the melt.

The presence of an alumina layer on the melt surface and also gas evolution from the decomposing FA make it difficult to quantify precisely the wetting angles from this type of experiment. Nevertheless, a comparative analysis of wetting behaviour for different FA and molten aluminium can be made.

**Foaming experiments.** The influence of surface coating on foaming ability of the agents was also examined. The coated agent ensured a larger foamed fraction than the uncoated one (Fig. 1), resulting in an increase in sample height and a

Figure 1. Cross–section of the foamed Al samples treated with (a) $TiH_2$, (b) uncoated $CaCO_3$ and (c) coated $CaCO_3$.

decrease in total sample density ($1.0\times10^3$ kg·m$^{-3}$ compared with $1.7\times10^3$ kg·m$^{-3}$). These results can be explained by the contribution made by agent coating.

It is known that solid particles with poor wettability tend to coagulate in a liquid. In contrast, wetted particles can be well distributed in a liquid without formation of large aggregates. If the solid is the source of a gas, the first occurrence results in fewer bubble nucleation centres in a liquid than the second one does. Consequently the liquid fraction containing bubbles is larger when the second occurrence is operating. It is likely that in our experiments the particles of coated carbonate were distributed in the melt more uniformly than the uncoated one did and produced foamier melt with lower density

Most important for practical use of the new foaming agents is that coated carbonates produced metallic foam with a density comparable to that of samples treated by titanium hydride ($\sim1.0\times10^3$ kg·m$^{-3}$) and with pores (cell size = $1.1\times10^{-3}$ m) (Fig. 2) smaller than those produced by conventional hydrides.

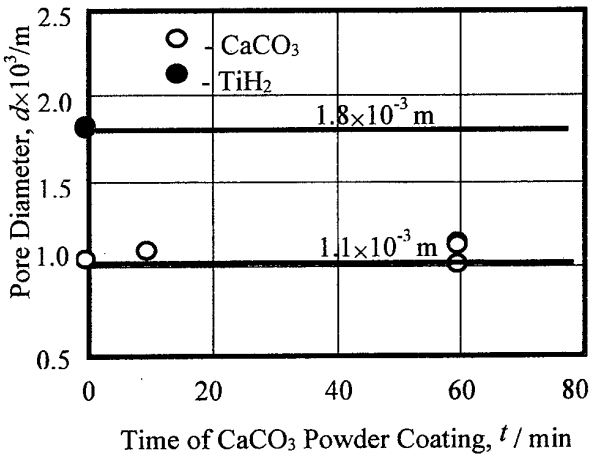


Figure 2. Dependence of pore diameter of the foamed samples on powder coating time for different FA.

## Conclusions

A calcium carbonate coating was prepared by an ion exchange method. The effect of a coating was studied by examining the wetting behaviour of the FA by the Al melt. The coating of $CaCO_3$ by the $CaF_2$ resulted in a decrease in contact angle (~ 15°) in comparison with uncoated carbonate. Coated carbonate produced metallic foam with a density comparable to that of samples treated by titanium hydride ($1.0\times10^3$ kg·m$^{-3}$) and much less then uncoated carbonate ($1.7\times10^3$ kg·m$^{-3}$). For practical use of the new foaming agent, it is important that coated carbonate ensures aluminium foam with smaller pores ($1.1\times10^{-3}$ m) than those produced by the conventional FA, titanium hydride ($1.8\times10^{-3}$ m). The present study shows that calcium carbonate is highly applicable to foamed metal production.

## References

[1] I. Jin, L.D. Kenny and H. Sang: US Patent 5112697 (1992).

[2] S. Akiyama, H. Ueno, K. Imagawa, A. Kitahara, S. Nagata, K. Morimoto, T. Nishikawa and M. Itoh: US Patent 4713277 (1987).

# THEORY OF THE THERMAL AND DYNAMIC EFFECTS IN A CURRENT-CARRYING MELT SURROUNDING A FIBRE

**Raychenko Oleksandr I.**
I.M. Frantsevych Institute for Problems of Materials Science ,
National Ukrainian Academy of Sciences, Kyiv, Ukraine

Some heterogeneous materials contain foreign inclusions of cylindrical and close shapes. They may be reinforcing fibres or pivots. One of extreme examples of such inclusions is a cylindrical pore. If one applys the electric technology for fabrication or thermal processing of such materials then the melting of a binder phase may occur. There is the necessity of understanding of character of interactions between such inclusions and surrounding medium. During passing of electric current the thermal, mechanical, mass-interchange processes arise in materials.

The model of a representative elementary volume of such a heterogeneous material may be imaged as a cylindrical poly-layered medium., for example, a three-layered one. Thus, the object under consideration is following one: a cylindrical conductor unlimited in axial direction is located inside a cylindrical liquid , which, in one's turn, is surrounded by a next solid layer. The electric current that is directed at an arbitrary angle with an axis of the model passes in general case. The current component which is parallel to the axis results in heating and pressure in radial directions to the axis [1].It is expedient to concentrate the main attention on the current component that is directed perpendicularly to an axis (cross current). Since the model is not limited in the axial direction the problem is considered as two-dimensional. The stationary problem was solved. In the first step the electric current density distribution was determined. Such a distribution depends on conductivities of all media materials and geometrical dimensions. Further, the function of the thermal sources density $W(r,\gamma)$ was determined ($r,\gamma$ are the radial and angle coordinates). This heat arises due to the Joule-Lenz effect. The function of the thermal sources density depends on the current density (besides conductivities, heat capacities and densities of the media materials).The following step includes determination of the temperature field $T(r,\gamma)$. It depends on the heat conductivities (besides above properties)[2]. If the temperature dependence of conductivity is taken into account then additional causes of the flows may arise. At stationary regime the temperature and velocity fields are described by the equations (in reduced variables)

$$(\mathbf{V}\nabla)\Theta = \nabla^2\Theta + \frac{\rho_e c_p a^2 W}{k_e \Delta T} \qquad (1)$$

$$(\mathbf{V}\nabla)\mathbf{V} = -\nabla P + \mathrm{Pr}\nabla^2\mathbf{V} + \frac{\rho_e c_p{}^2 a^3 \Delta T}{k_e{}^2}\frac{\partial \mathbf{f}}{\partial T}\Theta \qquad (2)$$

where $V$ is the velocity, $\Theta$ is the ratio of temperature excess over the minimum temperature to the whole temperature range $\Delta T$, $\rho_e$ is the density $c_p$is the heat capacity, $a$ is the radius of the inner boundary of a liquid layer, $k_e$ is the heat conductivity, $f$ is the body Lorentz-force arising due to current, $P$ is the pressure, Pr is the Prandtl number.

Eq. (1) is the equation of heat transfer; Eq. (2) is the modified Navier-Stokes equation.

.The phenomenon predicted –arising of streams due to the term with $(\partial f/\partial T)\Theta$ in Eq. (2) – might be called the electric-resistance-thermal convection. The character of such a velocity field $V$ is determined in the first place by the dimensionless group that plays the similarity criterion

$$R_{em} = \frac{\alpha \mu_0 J_0{}^2 a^4 \Delta T}{\rho_e \nu \chi_e} \qquad (3)$$

where $\alpha$ is the temperature coefficient of resistivity, $\mu_0$ is the magnetic constant, $J_0$ is the current density in outer medium far from the liquid layer, $\nu_e$ is the kinematic viscosity, $\chi_e$ is the thermal diffusivity.

The physical sense of the dimensionless group (3) is such: it matches up the electromagnetic pressure

$\alpha\mu_0 J_0^2 a^4 \Delta T/\rho_e$ born due to a difference of the conductivity with the product $\nu\chi_e$accounting for viscosity and heat conducting ability of fluid. Group (3) resembles in some extent the classical Rayleigh number [3] , the criteria proposed by Bologa, Grosou and Kozhukhar' [4], and Daya, Morris and Bruin [5] The group proposed in the present theory characterizes the events of non-threshold nature (in contrast, for example, with the Rayleigh number). In real situations (for example, in some objects containing liquid metals with solid inclusions) the electric-resistance-thermal convection may coexist with other convection types. These phenomena may influence, in particular, the mass transfer and alloying processes.

## REFERENCES


1. Maninger R.A. In : Exploding Wires. Moscow: "Mir", 1963, p. 142-154.
2. Raychenko O.I., Derev'yanko O.V., Popov V.P. Calculation of two-dimensional temperature field arising at electric heating of a three-layered cylindrical medium. *–Metallofiz. Noveishie Tekhnol.-1999.-V.* ***21, No.7.-P. 69-80.*** (In Russian).
3. Lord Rayleigh. On convection currents in a horizontal layer of fluid when the higher temperature is on under side. – *Phil. Mag.-1916.-V.32, No. 192..-P.529-546.*
4. Bologa M.K., Grosou F.P., Kozhukhar' I.A. *Electroconvection and Heat Exchange.* – Kishinev: Shtiintsa, 1977. (In Russian).
5. Daya Z.A.., Morris S.W., de Bruin J.R. Electroconvection on a suspended fluid film: A linear stability analysis.- *Phys Rev. E.-1977.- V. 55, No. 3A.-P.2682-2692.*

# THE INTERFACE FENOMENA BETWEEN ALUMINA FIBRES AND PHOSPHATE BINDER

**Ulyanova T.M., Krutko N.P., Feodorova I.L.**[(1)]
Institute of General and Inorganic Chemistry of the National Academy of Scienses, Minsk, Belarus
[(1)]State Institute of System Analyses, Minsk, Belarus

Study of an interaction between fibrous filler and liquid binder at a stage of a "green body" forming is an integral part of a complex investigation of ceramic composite materials. Earlier it has been shown, that metal oxide fibres prepared by oxidation of salt-containing polymer materials possess a developed surface, high porosity, and consist of oxide nanograins [1]. When ceramic fibres are used as a filler in composite it is necessary to know their adhesion properties to a liquid binder because their interaction during a composite production influences on technical characteristics of ceramics.

The work described here deals with the interaction between alumina fibres and aluminium cromium phosphate binder (ACPB) at their surface contact.

Alumina fibres were obtained by oxidising hydrated cellulose fibres impregnated with aluminium chloride and additive magnesiun cloride solution. As initial materials cellulose filaments, felt and cord fabric were used. The ACPB was prepared in the form of aqueous solutions, their viscosity changed from $8{,}7\cdot10^{-3}$ up to $145\cdot10^{-3}$ Pa·s.

The investigation of surface phenomena was performed by method based on a continuous recording of the force variations during a wetting process of the cellulose fibre surface with ACPB from a contact moment up to a moment equilibrium [2]. The interaction between alumina fibres and ACPB solutions was characterized relaxation time of wetting $\tau$ (s), an initial velosity of impregnation $\upsilon$ (m/s) and wetting force $f_0$ (N/m). The last parameter was determined as a ratio of the wetting force to the fibres bun perimeter: $f_0 = F_0/P$, when $P=\pi D/4$, and D – diametr of fibres bun.

Alumina filaments, felt and cord fabric remained their matrix forms of initial poplymer materials, and they possessed differential porocity (50-85%), and specific surface values (15-100 $m^2/g$). More over the channels between individual fibres had various forms: parallel, perpendicular, branchy, etc. Therefore, these factors influenced on a velocity of wetting and impregnation too.

In the present research the interaction of alumina fibrous materials with the liqid binder ACPB occured so actively that impregnation – liquid rise in fibrous samples was in advance of wetting meniscus formation at the boundary fibre – liquid ACPB. When values of alumina fibre specific surface were above 30-40 $m^2/g$, impregnation proceeded rapidly, for several seconds and quicker. If values of fibre specific surface 20 $m^2/g$ and less the impregnation velocity was influenced of channel forms, the capillary forces was more in parallel interfibre channels. In felt the interfibre channels were branched, so impregnation rate was slower. A texture of a cord fabric is very complex: filaments are disposed perpendicular to each other. Besides the single fibres form screw-shaped channels because a liquid movement became slower (fig. 1).

During investigation of the fibre – binder inetrface a viscosity, dencity and suface tension of ACPB solutions were taken into account. Normally, increase of salt concentration doesn't tend to cause changes in the surface tension of regular solution. But phosphoric acid and its salts in aqueous solutions form polymolecular structures: cyclic or branched [3]. Due to that a density, viscosity of aqueous phosphate solutions and cohesion interaction in the liquid binder increased as well as a surface tension at the interface liquid – gas. When the solution viscosity of the ACPB binder was changed from $8{,}7\cdot10^{-3}$ to $145\cdot10^{-3}$ Pa·s the wetting relaxtion time became an order of magnitude higher and the impregnation rate decreassed correspondingly (fig. 2).

The investigation established that the alumina fibres prepared by impregnation of polymer fibrous material with aluminium salt solution and by subsequent heat treatment had a high adhesion power to ACPB binder. The main technologycal factors affecting wetting and impregnation were solution viscosity and fibre texture. The role of these factors predominated over another parameters: a composition, fibre specific surface and ACPB surface tension.

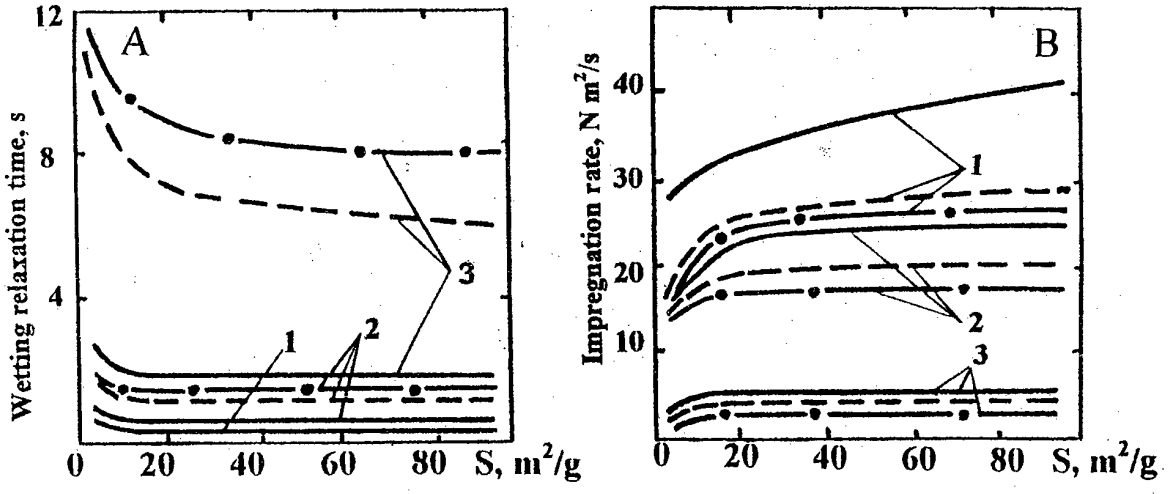


Fig.1. Wetting relaxation time (A) and initial impregnation rate (B) versus spesific surface quantity for alumina materials: filament (solid line), felt (dotted line), cord fabric (dush dot line); ACPB binder viscosity: $8{,}7 \cdot 10^{-3}$ (1), $40 \cdot 10^{-3}$ (2), $145 \cdot 10^{-3}$ Pa·s.

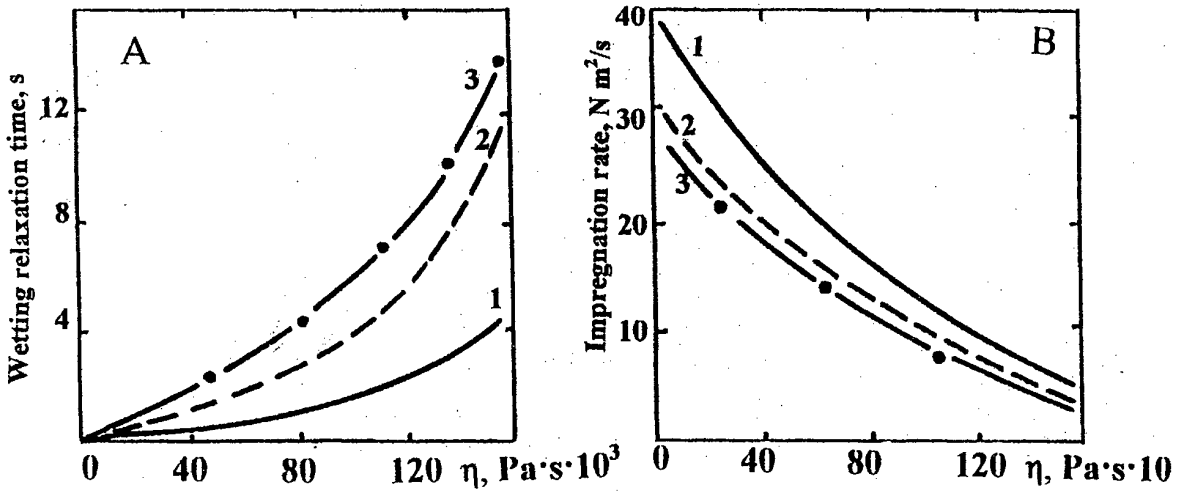


Fig.2. Wetting relaxation time (A) and initial impregnation rate (B) of alumina fibrous materials versus ACPB binder viscosity for various textures: filament (1), felt (2), cord fabric (3).

References:

1. Yermolenko I.N., Vityz P.A., Ulyanova T.M., Fyodorova I.L. – Synthesis and Sintering of $ZrO_2$ Fibres. // Sprechsaal, Vol. 118, No. 4, 1985. P. 323 – 325.
2. Grigoriev G.A., Belyavsky V.S., Lapin V.L., Zhykhovitski A.A. – Dimentional Theory Applied to Describe the Kinetics of Wetting a Solid with Liquid. /In : Wetting and Surface Properties of Melts and Solids. Edd. by Naukova Dumka, Kiev. 1978. P. 80-83.
3. Konstant Z.N., Dindune A.P. - Phosphates of Bivalent Metalls. Edd. by Zinatne, Riga. 1987, 371 p

# STRUCTURAL FOUNDATIONS OF THE FORMATION OF COVALENT TYPE CERAMICS UNDER HIGH PRESSURES AND AT HIGH TEMPERATURES

**Oleynik G.S.**
Frantsevich Institute for Problems of Materials Science, National Academy of Sciences of Ukraine, Kiev, Ukraine

In the modern ceramics science, the following two interconnected urgent problems stand out. 1. Development of new material of engineering application, including materials intended for replacing critical metals. 2. Search for new approaches to the production technology of such materials. From an analysis of the world literature it follows that, in the last years, in production of ceramic materials, deformation treatments, including high-pressure ones, are extensively used. This is the evidence of the tendency to «metallurgization» of ceramic technologies. The preparation of ceramics by thermobaric sintering is an example of employing thermomechanical treatments that are widely used in metallurgical practice for regulating structural states and strength properties of materials. The development of a class of polycrystalline superhard materials on the base of dense diamond and boron nitride phases is a direct corroboration of the high efficiency of the deformation approach in ceramic technologies [1, 2].

Electron microscopy and X-ray studies of superhard materials has shown [2, 3] that sintering of covalent materials under high pressures and at high temperatures is completely controlled by plastic deformation. This has been confirmed by further studies of the structure formation processes in samples of model materials (SiC, AlN, $TiB_2$, $B_4C$, and $Si_3N_4$).

Irrespective of the type of the structure of starting materials, the formation of polycrystalline materials under high pressures and at high temperatures proceeds due to the development of structural transformations in the system of powder particles without high-angle boundaries formed between them. In the case of using starting nanopowders, the major structure formation processes are: formation of centers of collective growth through coalescence, collective recrystallization, and further deformation of grains formed. For large starting particles (from several to hundreds of micrometers in size), the following sequence of structural transformations is realized. 1. Translational (lattice) plastic deformation characterized by the high density of accumulated stacking faults in particles. 2. Plastic deformation and structural transformations in highly defective particles, i.e., under the conditions of suppression of lattice plasticity. 3. Fragmentation of particles as a result of their splitting into disoriented regions (with smooth and discrete disorientations). 4. Primary recrystallization. 5. Collective recrystallization. The structure of starting powder materials exerts a radical influence on the mechanisms of development of the indicated processes, which is caused by different mechanisms of lattice deformation. This is most convincingly confirmed by the example of studies of a group of materials on the base of diamond and diamond-like phases with the wurtzite (2H BN, 6H SiC, 2N AlN) and sphalerite (3C BN, 3C SiC) lattices [4].

In terms of mechanisms of translational deformation, determining the type of a defective substructure, these substances can be divided into three groups. 1. 2H BN and 6H SiC. Deformation is realized by splitted basal dislocations, which determines the high density of stacking faults formed in particles. 2. Diamond, 3C BN, and 3C SiC. The combination of slip and small-scale twinning along the planes (111). 3. 2H AlN. Slip by complete basal dislocations. Based on the dependence of the factor of splitting of dislocations on the energy of a stacking fault, it can be suggested that the value of the latter increases from the first to the last group of materials.

Data on the development of processes of structural transformations in the indicated three groups of materials in the stage of rearrangement of highly defective structures formed as a result of lattice deformation obtained in electron microscopy studies of structure evolution are presented in the Table.The investigated specimens were prepared in a toroid type chamber.The results of a study of deformation-induced substructures in the sections (110) of diamond, 3C BN, and 3C SiC crystals and in the sections $(11\bar{2}0)$ of 2H BN, 6H SiC, and 2H ALN crystals are given.

**Mechanisms of Dynamic Rearrangement of the Deformation-Induced Substructure in Powder Particles.**

| Starting material | A sequence of action of the mechanisms of structure rearrangement with increasing temperature under P = 7,7 GPa and temperature ranges |
|---|---|
| 2H BN | Kinking → dislocation recovery within the boundaries of fragments → primary recrystallization (PR) of the 3C phase → collective recrystallization (CR) (1200–2000°C) |
| 6H SiC | Kinking → dislocation recovery within the boundaries of fragments → PR of the 3C phase → CR of heterophase grains → PR of heterophase grains (1200–2300°C) |
| 2H AlN | Bending deformation → dislocation recovery in the bulk of particles → formation of subboundaries → PR (1000–1600°C) |
| Diamond | Entering of dislocations in the bulk of twins → development of reorientation bands → formation of dislocation pile-ups along the path of twins → destruction of twins → dislocation recovery in the bulk of twins) (1800–2300°C) |
| 3C BN | Entering of dislocations in the bulk of twins → development of reorientation bands → formation of dislocation pile-ups along the path of twins → destruction of twins → PR (1600–2200°C) |
| 3C SiC | Mechanisms analogous to those for 3C BN (1400–2000°C) |

It is seen from the Table that, in the process of evolution of the deformation-induced substructure, fragmentation of particles and their further recrystallization proceeds. For AlN only, fragmentation of crystals is caused by processes of ordering of dislocations in volume (dynamic dislocation recovery). For the other substances, it occurs due to proceeding rotational plasticity, retardation of transverse slip, kinking, and formation of bands of reorientation. The development of this deformation is caused by the action of the following three factors: suppression of transformational plasticity, retardation of transverse slip, which is due to the low energy of stacking faults, and the constraint of deformation processes in the system of differently oriented particles. Further primary recrystallization of the considered materials proceeds due to preliminary fragmentation. In the indicated three groups of materials, the mechanisms of deformation also differ [5]. In the first stage, recrystallization proceeds along grain boundaries, and then in the volume of particles. Only in the stage of primary recrystallization, well-developed grain boundaries form.

On the whole, the formation of the materials under high pressure with increasing temperature proceeds by successive transformation of one structural state into another (see the Table). Depending on sintering conditions (pressure, temperature, the time of isothermal exposure, and the degree of hydrostatics in a pressure chamber), in the material, can be obtained both a structural state (highly strained, fragmented, recrystallized) homogeneous within the whole volume and a heterogeneous one. The rearrangement of the microstructure with increasing temperature proceeds in the direction of decreasing size of starting particles due to fragmentation and primary recrystallization. With using powders of highly strained substances, in materials, nanodisperse states (in the whole volume or in a binding phase) can be obtained as a result of processes of fragmentation and recrystallization. This has been shown by the example of 2H BN synthesized in shock waves and diamond the powders of which were preliminary treated in shock waves.

The results of the structural studies of the materials on the base of diamond and diamond-like phases allow us to conclude that the mechanisms of plastic deformation and further structural rearrangements during thermobaric sintering of covalent materials are determined by such a fundamental characteristic as the energy of a stacking fault.

## References

1. Superhard Materials (edited by Frantsevich I.N.). – Kiev: Naukova Dumka, 1980. –286 p.
2. Synthetic Superhard Materials (edited by Novikov I.N.), – Kiev: Naukova Dumka, 1986. –Vol. 1. – 278 p.
3. Pilyankevich A.N. and Oleynik G.S., Influence of High Pressures on a Substance. – Kiev: Naukova Dumka, 1987. – Vol. 1 – P. 57–77.
4. Oleynik G.S. and Danilenko N.V. Works of IPM NANU. Electron Microscopy and Strength of Materials. – Kiev, 1999. – Issue 10. – P. 106–128.
5. Oleynik G.S. and Danilenko N.V., Poroshkov. Metallurgiya. – 1998. – No. 12. – P. 63–77.

# MODELLING OF INTERACTION AT INTERFACES DURING POWDER COMPOUNDS FOR CERMET FILMS SINTERING

**O.I.Shulishova, N.V.Shevchyk, I.A.Shcherbak**
Institute for Problems of Materials Science of NANU, Kiev, Ukraine

Ultimately composition, structure and peculiar characteristic of sintered compound materials are conditioned by interaction on the boundary between the different phases during sintering. Electrical properties of material, conductivity and its temperature dependence are especially sensitive to composition change in interphases contacts zone.

Thus, the electrophysical properties of cermet films are formed by the physicochemical interaction between the current conducting and the glass binding phases in the process of firing resistive composites. It is just what affects the real microstructure and the electrophysical properties of resistive films.

Investigation the interaction on the boundary between the current conducting and the glass binding phases directly in cermet films by electron microprobe analysis with recording of the intensity of reflected electrons and the intensity of the characteristic x-ray radiation of the elements composing the specimen is complicated by small dimensions of the initial powder particles.

The depth of penetration of the electron probe, amounting to several micrometers, is comparable with the dimensions of the particles of the current conducting phase and with the width of the regions of interactions of the current conducting and glass binding phases, and it was therefore not possible to reveal the peculiarities of the diffusion of each element directly on the sections of the cermet films.

Moreover when sections of the films are studied, the "edge effects" on the boundary of the current conducting phase must also be taken into account: they are due to the fact that the particles have a shape close to spherical, and the electron probe, intersecting them, passes through different thickness at the edge of the particle or at its center. That is why the distribution curves of the intensity of the characteristic x-ray radiation contain the contribution of both the actual diffusion of chemical elements on the phase boundary and of the above-mentioned "edge effect".

To eliminate both, the "edge effect" and the effect of the small dimensions of the particles, we carried out investigations of the physicochemical interaction of the materials of the current conducting phase and the glass phase on model sections. Model specimens was transverse sections consisting of alternative layers of current conducting and glass biding phase subjected to heat treatment by the regime of firing resistive pastes. As objects of the investigation we chose films containing hexaborides of rare-earth elements (REE) $SmB_6$, $PrB_6$, $EuB_6$ and of glass with crystallizing composition and also films based on ordinary ruthenium oxide and glass.

The films were obtained by the standard technology, i.e., applying by stencil printing the respective resistive pastes to a base of ceramics type M7 with subsequent high-temperature firing at $850^0$C in air with holding for 10 min at the maximal temperature. The change of concentration of the chemical elements at the transition across the boundary between the current conducting and glass binding phase was investigated on an x-ray microanalyzes type "Superprobe-733".

It is established that there is considerable interdiffusion of the chemical elements contained in the current conducting and the glass binding phase. The diffusion of most elements into the bulk, across the phase boundary, may amount to several micrometers. Consequently, the composition of the intergranular dielectric interlayers, which play an important role in the mechanism of the passage of electric current in cermet films, differs considerably from the composition of the initial powders of the glass binding phase.

It had been established earlier [1] that in high-temperature firing hexaborides of REE as components of the resistive films are subjected to considerable oxidation. The oxide film forming on the surface of the particles contains boron oxide and borates of REE, and its protects the particles against further oxidation. When hexaborides are used as current conducting phase, this oxide film in the process of high-temperature firing of the resistive pastes interacts with the fused glass phase, and this leads to the formation of the real microstructure of the resistive film. Bearing this in mind, we have to expect that there is a substantial difference between interdiffusion of chemical elements on the phase boundary in specimens fired in air, where the processes of oxidation play a

significant role, and in specimens fired in vacuum where there is no such oxidation. This is bound tj find expression in the working characteristics of the respective resistive films.

The good working characteristics of cermet precious metal films are due tj the absence of oxidation of the electrically conducting phases. It is of interest. too. to study the behavior of resistive boride films also fired under conditions precluding the oxidation of the boride grains, e.g., in vacuum.

To find out to what extent the processes of oxidation affect the scale at interaction on the boundary of the current conducting and glass binding phase in hexaboride films, we investigated the zone of contact of samarium hexaboride single crystal with the glass binder. The use of single crystals made it possible to eliminate the effect of the porosity of the specimens of hexaboride on the intensity of the characteristic x-ray radiation of the elements contained in the model section.

The photomicrographs of sections fired in vacuum and in air show distinctly the difference in the diffusion of chemical on the phase boundary.

For instance, in specimens fired in air there occurs diffusion of samarium into glass and depletion of silicon in the near-boundary layer of glass; this is bound to lower the melting point of glass and the viscosity of its melt. This manifests itself on the working characteristics of the resistive films. The resistivity of films fired in vacuum is almost ten times lover than those fired in air, the resistance temperature coefficients attains in absolute value $3.10^{-3}.K^{-1}$, after moisture resistance tests of resistors the resistance of films increases by a factor of 10÷15. In films fired in air, oxidation of particles of the current conducting phase has the effect that the oxide film forming on the surface interacts intensively with the molten glass phase, and this results in the formation of a compact flawless microstructure of the films. This makes it possible to obtain precise working characteristics of resistors based on hexaborides of REE. For instance, in the range of resistivities $10^2$-$10^5$ they have a resistance temperature coefficient in absolute value not exceeding $1.10^{-1}K^{-1}$, and moisture resistance not poorer than 1%.

In the investigation of the cross section of cermet films based on ruthenium oxide and glass, in which firing is not accompanied by processes of oxidation, we find weak interaction of the current conducting phase with the glass phase with imperceptible diffusion on the boundary, this follows from the more distinct maximum of intensity of the characteristic radiation of ruthenium when the electron probe passes over the boundary of the current conducting phase. The investigation of diffusion zone in different conditions of the firing and its coordination with working characteristics of cermet films fired in the same conditions makes it possible to determine the criterion of the stability and the reproductivity of the working characteristics of cermet films:

Manufacturing of resistive cermet films with stable and reproductive working characteristics it is possible only when maximal dimension of the current conducting particles is smaller than width of the diffusion zone in model sections fired at the same conditions as the firing of the cermet films.

Optimum working characteristics of the resistive cermet films based on $MeB_6$ correspond to the correlation when maximal dimension of the $MeB_6$ current conducting particles 3-5 time smaller than average dimension of the diffusion zone.

It obviously means that during process of the high-temperature firing at 850°C in air with holding for 10 min at the maximal temperature diffusion processes have enough time to occur completely in particles of all dimensions in the cermet film and its composition and property are average for each particle.

For ordinary regime of firing of cermet resistors according to this criterion optimum of the current conducting particles based on $SmB_6$ dimension must be 3-5 μkm, as it is really confirmed experimentally.

For resistor based on noble metals with very narrow diffusion zone current conducting particles dimension must be ten time smaller. That is why better cermet resistors based on noble metals contain current conducting particles of submicrometre dimensions [2].

However it is necessary to notice that the smaller current conducting particles the stronger the influence of electrostatical charge effect upon temperature dependence of eloctroconductivity [3]. That is why cermet resistor based on borides of REE surpass by its working characteristics cermet resistor based on noble metals.

Literature

1. R.K.Islamgaliev, A.V.Zyrin, A.A.Semenov-Kobzar at al. "Poroshk. Metall., №12, 36-39 (1987).
2. K.I.Martyushov "Problems of resistor materials science", Obzory po Electron. Tekh., Ser.5,№2 (1108)6 3-166 (1985).
3. K.L.Chopra, "Electronic phenomenon in thin films", M., Mir, 436 (1972).

# CRACK NUCLEUS AND BRITTLE FRACTURE OF METALS AND ALLOYS

**Kotrechko S., Meshkov Yu.**
G.V.Kurdyumov Institute for Metal Physics, National Academy of Sciences of the Ukraine, Kyiv, Ukraine

Possibility of development of physical theory of fracture of metals and alloys based on a concept of the crack nucleus (CN) as the origin of brittle fracture of crystalline solids is presented in this report. It is shown that CN are of the same importance for brittle fracture of metals as dislocations for plastic deformation. It means that analysis of the CN properties gives the following possibilities:

- to study main regularities of microstructure, substructure and crystallographic texture effect on the level of brittle strength of structural steels;
- to formulate ideas on physical nature of brittle and ductile state of metal;
- to explain stress-strain state effect on the value of brittle fracture stress.

It is shown that interrelation between the CN length and grain size gives rise to increase in brittle fracture stress with grain structure refinement. Specific feature of structural steels is that their fracture is controlled by the CN of two kinds:

- CN that form by dislocation mechanism and have size ~0.01 $d_g$ ($d_g$ is grain size);
- CN which are the result of carbide particle fracture and have respective size.

In such case the level of brittle strength of structural steel, $R_{MC}$, is controlled by those microstructural element in which the CN of maximum length form. It results in existence of certain critical relations between sizes of microstructural elements, which control the level of brittle strength of steel. These relations are key condition for both optimisation of steel structural states and estimation of possibility to raise steel strength and toughness. Physical theory of influence of grain inhomogeneity on the level of brittle strength of metal is given. It is shown that decrease in brittle fracture stress at growth of grain sizes variance is due to CN formation in grains which sizes are situated in "tail region" of distribution. Relation between real grain size variance and $R_{MC}$ level is ascertained. For martensite steels ultimate levels of brittle strength are estimated, and demands to grain structure homogeneity that enables to reach such $R_{MC}$ levels are formulated.

Theoretical analysis of microstress effect on the CN unstable equilibrium is carried out. It is shown that solely microstresses acting at the moment and at the locus of crack nucleation affect essentially the CN. Dislocations of the same sign piled near grain boundaries where the CN usually form are the origin of such microstresses. Influence of these microstresses gives rise to decrease in the value of macroscopic stress required for the CN unstable equilibrium. This effect is the cause for existence of decreasing branch on the curve "brittle fracture stress vs. strain" for metals and alloys. This branch has minimum which determines the value of brittle strength of metal $R_{MC}$. Critical value of residual strain, $e_C$, corresponds to it (for iron and carbon steels $e_C$~0.02-0.08).

Physical nature of influence of great pre-strain on the level of brittle strength of metal and its anisotropy is considered. It is shown that crystallographic determinancy of orientational distribution of CN opening planes is the cause for this effect. Estimations of the maximum value of brittle strength anisotropy are obtained for rolling and drawing textures in iron.

The CN are sensitive to stresses normal to their opening plane. As a result, critical stress of the CN unstable equilibrium depends on its orientation and stress state. It permits both to explain physical nature of the well-known in mechanics effect of fall in the value of brittle fracture stress of metal at transition from uniaxial to bi- or triaxial tension and to give its quantitative description.

In conclusion, theoretical ideas on ductile and brittle state of metal are formulated. It is shown that ductile or brittle state of metal is predetermined by degree of stability in the CN ensemble. Metal is ductile if at the moment of CN formation the level of tensile stresses acting in metal is not enough for the CN unstable equilibrium. Metal may deform plastically without danger of brittle fracture at such state in the CN ensemble. Otherwise, metal is brittle. Such approach has allowed to establish comprehensive characteristic for description of the effect of both structure and loading conditions on metal state. On this basis new comprehensive quantitative characteristic of toughness that includes macroscopic properties of metal as well as conditions of metal loading is formulated

# METHODOLOGY OF ESTIMATION OF STRENGTH RELIABILITY OF STRUCTURAL MATERIALS AT ALL STAGES OF LIFE CYCLE

**Mileshkin M., Biblik I.**
A. Podgorny Institute for Mechanical Engineering Problems of the National Academy of Science of Ukraine, Kharkov, Ukraine

Usually at designing of engineering products from any materials four basic moments are emphasized: development of materials, their estimation, designing of product and prediction of its fracture. It is obviously, that in number of cases this scheme should be supplemented with various tests of materials, and then of products (control-technological, hand-over tests, regulation during operation etc.). The basic task of these tests is estimation of a real level of strength reliability and resource.

It is obviously, that it is necessary to aspire to consideration of strength aspects of the material behaviour at all stages of its life cycle within the bounds of uniform methodology. The difficulties of creation of uniform methodology are connected with several reasons - variety of materials, variety of mechanisms of deformation and fracture and such features of real materials, as dispersion of properties, presence of various technological and operational defects, change of material properties onstream etc. [1].

One of possible approaches to decision of this problem was creation of special design-experiment method (DEM) [2]. This method is realized within the bounds of traditional model of strength reliability, but the realization of model essentially differs from traditional approaches and represents imitating computer modeling per se.

It is known, that the model of strength reliability consists of four particular models – model of material, model of form, model of loading and model of fracture.

We shall consider briefly the basic moments of DEM realization.

Model of a material. The existing models of a material can be divided on physical, engineering-physical and engineering (model of continuum). Namely the engineering models are used in traditional strength analysis most often. However real constructional materials are characterized by structural and (or) mechanical heterogeneity first of all. Heterogeneity of deformation and fracture is characteristic even, for example, for single-phase materials. Therefore creation of adequate model of material in DEM is one of the main tasks. In DEM the model of material represents an array of structural elements, to each of which the value of its limiting mechanical properties (deformability, strength etc.) is set depending on statement of task. This array represents one "layer" of material. Depending on type of material and product the final model of material represents a certain set of arrays.

The models of the form and loading are almost traditional. Based on them the "step of loading", and also "the value of a step" are defined.

The model of fracture represents imitating development of process of deformation and fracture. We shall illustrate it briefly.

Let three neighboring structural elements (Fig. 1) have deformation of fracture 1,0 %, 2,0 % and 3,0 %.

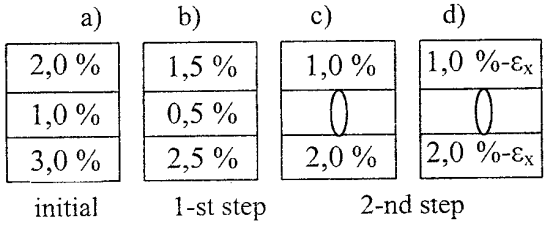


Fig. 1. The schematic sketch of development of fracture process

Let value of "step of loading" is 0,5 %. We make first step. At that the resource of deformability of each structural element is exhausted on this value. Already after second "step of loading" the middle element has exhausted the resource of deformability and has fractured. It is natural, that because of stress and deformation concentration in its tops the arisen crack will lower residual deformability of 1-st and 3-rd elements on certain value $\varepsilon_x$. If value $\varepsilon_x$ is more than 1 %, 1-st element will be fractured also, the crack length will increase etc. According to such scheme the "loading" of computer model of

a material is continuing until its complete fracture will not come and then the strength characteristics of material will be defined. Definition of value $\varepsilon_*$ is made depending on tasks of modeling by means of power or energy approach.

The various examples of method realization are considered in this work. Here are given only some of them.

1. An estimation of strength at the material designing we shall consider on example of composite aluminium - boron. Array size – 300x300. Characteristics of fibres: module of elasticity - 400 GPa, diameter of a fibres – 100 μ, fibre vo-lume - 50 %, distribution of limiting deformations – according to the normal law with a maximum at 0,9 % of deformation; a matrix: module of elasticity - 70 GPa, module of normal plasticity - 1,4 GPa, distribution of limiting deformations – according to normal law with a maximum at 20 % of deformation. Loading - uniaxial tension. Step of deformation in fibre direction - 0,05 %. For realization of fracture model the energy approach is used. The diagram of deformation in line with the reference data is given in Fig. 2.

2. Designing of product and analysis of ways of increasing of its strength are considered on an example of cylindrical shells with the bottoms from glass firer-epoxy composite. The shells consisting of 12 layers (6 ring and 6 spiral) were loaded with internal pressure. The registration of fracture process at the loading was carried out by a method of acoustic emission (AE). The researches have shown, that the early formation of cracks in parallel to fibres in ring and spiral layers is characteristic for such shells. The modeling was carried out on the basis of AE parameters using. After debugging of modeling method the designing new shells has been carried out on the basis of results of test of the reference specimens using AE method also. The results of designing have shown, that the method can be used as well for research of influence of initial properties of components on strength. For example, the increase of matrix deformability results in disappearance of early fractures between fibres and increase of strength [2].

3. Estimation of strength reliability of material with operational defects (Fig. 3). Material - pipe steel. Types of damages - corrosion, cracks, "aging" (reduction of material fracture deformation). Model of material - at thickness of pipe of 10 mm and at grain size of steel of 0,1 mm it is expediently "to create" a model consisting of 100 layers. Distribution of limiting deformations – according to the normal law with a maximum at 30% of deformation. Loading step – 1,0 %, approach to pressure redistribution - power.

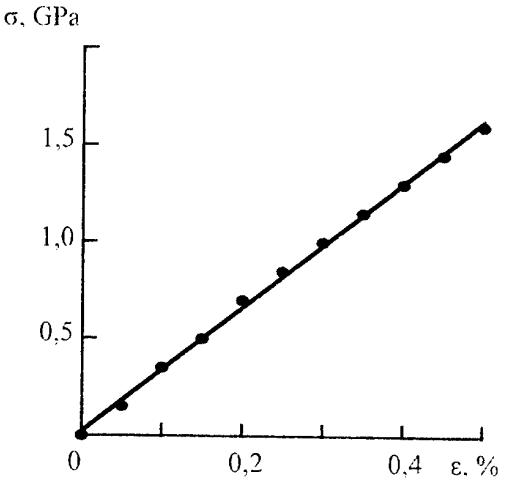


Fig. 2. Diagram of deformation of composite aluminium-boron.

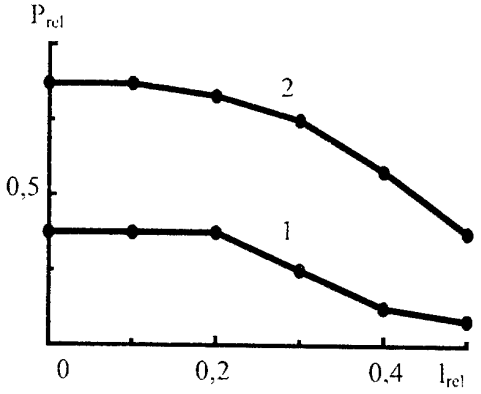


Fig. 3. Change of bearing strength of pipeline element ($P_{rel}$) with surface crack ($l_{rel}$) at various macrodeformability of steel:
1 - ε = 12 %, 2 - ε = 24 %.

References

1. Сопротивление материалов деформированию и разрушению: Справочное пособие / В.Т. Трощенко, А.Я. Красовский, В.В. Покровский, Л.А. Сосновский, В.А. Стрижало: В двух частях. - Часть II.- Киев: Наукова думка, 1994.- 702 с.

2. Mileshkin M.B., Biblik I.V. Diagnostics for strength of fibre-epoxy composite material wares using computer modeling of fracture processes // proceedings 2nd jnt. conf. " computer methods and inverse problems in non-destructive testing And Diagnostics ", Minsk, 1998.- P.123 - 129.

# PHYSICAL-MICROMECHANICAL MODELLING INFLUENCE OF STRUCTURE ON MECHANICAL PROPERTIES OF COMPOSITE AND HIGT - POROSITY MATERIALS

**LUGOVSKOI YURI**

I.N. Francevich Institute of Problems for Materials Science
Ukrainian National Academy of Science, Kiev, Ukraine

The review of the literature shows, that the majority of publications in the field of development of new materials is devoted to an experimental research of those or other mechanical characteristics in connection with technological parameters of their reception and, at the best, with their structure. Only small part of works is directed on construction of structure-property models of a material. In this connection the problem of construction of the above-stated models is actual.

Models of mechanical properties can be divided on mechanical and physical.

The former are based on postulates of the mechanics of a deformable solid body on the homogeneous continuous medium, its indissolubility, linear or more complex dependence between stress and deformation in an allocated element of volume. In a result the mechanical approach gives the equation of a mix for a structural - non-uniform or composite material

$$\sigma_K = \sigma_\phi V_\phi + \sigma_M V_M \qquad (1)$$

where $\sigma_K$ - strength of a composition, $\sigma_\phi$ and $\sigma_M$ - strength of a phase and matrix components. $V_\phi$ and $V_M$ - reletive volume fractions of the appropriate phases. If to enter into (1) such concepts frequently discussed in experimental researches as boundary between phases or intermediate layer, its strength and thickness, and also residual stress which operate mainly in it, researched dependence becomes complicated. For example, with reference to materials of layered structure (microlayer) in work [1] the equation of a mix is offered as

$$\sigma_{-1}^K(N) = \sigma_1(N)(h_1 - 2h_{ПС1})/(h_1 + h_2) + [\sigma_{ПС1}(N) + \sigma_{ост}]\,2h_{ПС1}/(h_1 + h_2) + \sigma_2(N)(h_1 - 2h_{ПС2})/(h_1 + h_2) + [\sigma_{ПС2}(N) - \sigma_{ост}]\,h_{ПС2}/(h_1 + h_2), \qquad (2)$$

where $\sigma_{-1}^K(N)$- cyclic (in particular) strength of a composition, $\sigma_1(N)$ and $\sigma_2(N)$ - cyclic strength of its components, $h_1$ and $h_2$ - thickness of components, $h_{ПС1}$ and $h_{ПС2}$ - thickness of intermediate layers in component, $\sigma_{ПС1}(N)$, $\sigma_{ПС2}(N)$, $\sigma_{ПС2}(N)$ - cyclic strength of intermediate layers and residual stress of the second sort (in components). To calculate strength of a composition in this case it is inconvenient, as all values included in more complexmodel are not known.

Physical models of strength are based on positions of a science about dislolocations or physics of a solid body. It first of all models of the Hall - Petch [2,3] for a yield strength, the Mott- Stroh [4] and Grednev with co-authors [5] for ultimate strength, and also for fatigue strength [6]

$$\sigma_K = \sigma_i + K_i \Delta^{-1/2}, \qquad (3)$$

where $\sigma_i$ and $K_i$ - factors, $\Delta$ - the generalized parameter of structure which can become medium-sized grain D or a dislolocation cell d in polycrystalline, an average free way between particles $\Lambda$ in dispertion-strengthened, thickness of a layer h in layered materials. Within the framework of these models this or that parameter of structure and strength of a structural - non-uniform material, settlement value of the second or experimental value of the first factor (3) are usually known, and the problem is reduced to definition of this or that unknown value.

It is obvious, that the joint decision of the equations (1) - (3) allows to understand mechanisms of destruction of structural - non-uniform materials more deeply to determine strength of separate components of a composition and to reveal thus its weak places.

The given method was applied for research of mechanical properties of microlayer condensed materials Fe/Cu, Cr/Cu, Mo/Cu , Cu (Y)/Mo, and also dispertion-strengthened

materials Cu-Mo, CuAl-Mo, Cu-NbC [7], NiCr-$Al_2O_3$. Thus experimental dependences $\sigma_{-1}$, $\sigma_B$, $\sigma_{0,2}$, $\delta$, $\varepsilon_{-1}$ as functions D, h, $\Lambda$ are obtained, and also micromechanical models of local strength that has allowed to obtain a number of new results are constructed. In particular, it was possible to explain within the framework of quantitative model negative values of the first factor of the equation such as Mott-Stroh for a limit of endurance in system Mo/Cu and to predict initial destruction on an interphase surface, and also to assess thickness and strength of an intermediate layer on border of the unit of phases and residual stress in it.

Another application of the given method is proposed for sintered materials of a different nature and according to various structure. Modelling structure sintered higt-porosity materials on the basis of discrete fibres (such as felt) and cell-porous materials and expecting their elastic deformation it was possible to obtain analytical dependences of the module of elasticity [8], deformations and fatigue strength of researched materials from properties of a firm phase, parameters of structure and porosity. In the practical plan it allows to reveal weak places higt-porosity materials and to offer measures for their strengthening.

References

1. Lugovskoi Y.F. Influence of structure and duration cyclic loading on fatigue resistance of the microlayer condensed materials. II. The analysis of the first factor of dependence such as Mott-Stroh. // Powder metallurgy, 1996, N 5 - 6, - P. 111-118.

2. Hall E.O. The deformation and ageing of mild stell // Proc. Phys. Soc.-1951.-64, N9,- p.747-753.

3. Petch N.J. The clevege strength of polycrystalline // J.Iron and stell Inst.-1953.- 173.p.25-28.

4. Stroh A.N. Proc. Royal Sos. 1954, ser .A, nr.223, p.404-414.

5. Gridnev V.N., Gavriljuk V.G., Meshkov U.J. Strength and plasticity cold-drawn steel. - K.: Sciences dream- 1974. - 232 p.

6. Lugovskoi Y.F., Kuz'menko V.A., Grechanuk N.I. Fatigue strength resistance of dispertion-strengthened and the microlayer condensed materials // Powder metallurgy, 1988, N10. - P. 52-55.

7. Lugovskoi Y.F. Influence of structure and duration cyclic loading on fatigue resistance of the dispertion-strengthened condensed materials on a basis of copper. 2. The analysis of the first factor of dependence such as Mott-Stroh // Powder metallurgy, 1998, N 7/8. - P.101-107.

8. Lugovskoi Y.F. Influence of structure on the module of elasticity higt-porosity materials on a basis copper // Powder metallurgy, 2000, N 6, - P. 112-120.

# RESIDUAL STRESSES AND PROBLEMS OF STRENGTH OF THE AXIALLY SYMMETRIC METAL ARTICLES

**Kolmogorov G.L., Kuznetsova E.V., Kovalev A.E.**
Perm State Technical University, Perm, Russia

*Introduction*

Technological residual stresses define the quality and operating characteristics of metal production During the process of production of axially symmetric articles by means of plastic deformation under the action of residual stresses the scheme of flat elastic deformed state is realized in the articles. One of the typical characteristics of such scheme is the absence of axial deformations ($\varepsilon_z = 0$).

*Definition of residual stresses*

Solving the flat problem of the elasticity theory with regard for boundary conditions, the components of residual stresses tensors may be written in the following form for pipes [1]

$$\left.\begin{aligned} \sigma_r &= -a_0(R_1 - r)(r - R_2), \\ \sigma_\theta &= +a_0[(r - R_1)(r - R_2) + r(2r - R_1 - R_2)], \\ \sigma_Z &= a_0\mu[2(r - R_1)(r - R_2) + r(2r - R_1 - R_2)] \end{aligned}\right\} \quad (1)$$

where $\sigma_r, \sigma_\theta, \sigma_z$ – are radial, peripheral and axial residual stresses respectively, $r$ – is a current radius of article, $a_0$ – is an unknown constant, characterizing distribution of residual stresses along the thickness of the pipe; $R_1$ and $R_2$ – are external and internal radiuses of the pipe respectively, $\mu$ – is a Poisson coefficient;

Knowing the tensor of residual stresses $\sigma_{ij}$ in the wire and pipe stocks, it is possible to define potential energy of elastic deformation in the volume of wire and pipe stocks respectively from actions of residual elastic stresses.

For the known components of the stresses tensor $\sigma_{ij}$ it is possible to find the components of tensor of relative elastic deformations $\varepsilon_{ij}$ by means of the generalized Hook law and to calculate the potential energy of residual stresses, corresponding to the initial strained state

$$U = \frac{1}{2}\int_V \sigma_{ij}\varepsilon_{ij}\, dV, \quad (2)$$

where $V$ – is a stock volume.

After substitution of tensors of stresses and deformations into the expression (2) and after integration along the unit length and transformation we shall obtain expressions for potential energy in the pipe stock

$$U_p = \frac{\pi a_0^2}{60E}\left(1 - \mu^2\right)\left(1 - \overline{R}^2\right)\overline{B}\, R_1^6, \quad (3)$$

where

$$\overline{B} = 7\left(1 + \overline{R}^4\right) + 22\overline{R}^2 - 18\overline{R}\left(1 + \overline{R}^2\right);\ \overline{R} = R_2 / R_1.$$

All existing methods of the residual stresses definition have experimental character in the whole, they are not universal and their application leads very often to the significant errors. In the work [1] the engineering method of definition of technological residual stresses under the plastic deformation of axial symmetric articles on the basis of energetic approach, containing the fact that potential energy of elastic residual stresses is considered as a part of energy required for plastic deformation, is suggested

$$U = \psi U_d, \quad (4)$$

where $U_d$ – is the energy of plastic deformation; $\psi$ – is a parameter, defining the part of plastic deformation energy, required for formation of residual stresses.

The energy of plastic deformation has the following form for the pipe of a unit length:

$$U_d^p = \pi\left(R_1^2 - R_2^2\right)\int_0^{\varepsilon_{av}} \sigma_s\, d\varepsilon \quad (5)$$

where $\sigma_s$ – is a resistance to deformation of the processed material; $\varepsilon_{av}$ – is an average degree of deformation along the stock's cross-section;

Degree of deformation, included in the given relations, has a large value under the technological calculations. It necessary to know the degree of deformation in order to make justified choice of the main technological parameters of concrete processes of metals processing by pressure.

In accordance with the method, suggested in the work [2] it is possible to write down the expressions for definition of deformation degree in the pipe

$$\varepsilon_{av}^{p} = 2 \operatorname{Ln} D_0 / D_1 + \frac{4tg\ \alpha_M \left(1 - a^3\right)}{3\sqrt{3}\left(1 - a^2\right)}, \quad (6)$$

where $D_0$ and $D_1$ are pipe external parameters before and after deformation, $a = R_0' / R_0$, $R_0'$ and $R_0$ – internal and external radiuses of pipe before deformation, $\alpha_M$ – is a slope angle of the generator of conic instrument to the axis of a stock.

It is known that degree of deformation influences the resistance of construction materials to the deformation. For the majority of metals this dependence has the following form:

$$\sigma_S = \sigma_{S_0}\left(1 + m\varepsilon_{av}^{n}\right). \quad (7)$$

where $\sigma_{S_0}$ – is the initial resistance of metal to deformation; $m$, $n$ – are the empirical coefficients, characterizing deformation strengthening.

With regard for the degree of plastic deformation and deformation strengthening of the stock material we shall obtain the expressions for definition of unknown parameters, characterizing the value of residual stresses:

$$a_0 = \frac{2\sigma_{S_0}\psi^*}{R_1^2}\sqrt{\frac{15\varepsilon_{av}^{p}\left(1 + m{\varepsilon_{av}^{p}}^{n}/(n+1)\right)}{\left(1-\mu^2\right)\overline{B}}}, \quad (8)$$

where $\psi^* = \left(\frac{\psi E}{\sigma_{S_0}}\right)^{1/2}$ – is a dimensionless parameter.

By means of the formula (8) in accordance with the known parameters of the plastic deformation process is possible to calculate postdeformation residual technological stresses in pie (1) articles.

*Evaluation of strength of the axially symmetric articles*

The experience of constructions' exploitation shows that residual stresses in the surface layers of a stock can influence the strength of the whole detail and under the action of alternating stresses in particular. The intensity of stresses can be defined in case, if we know the level of residual stresses (1):

$$\sigma_i = \frac{2}{\sqrt{2}}\sqrt{(\sigma_r - \sigma_0)^2 + (\sigma_r - \sigma_z)^2 + (\sigma_0 - \sigma_z)^2}. \quad (9)$$

Radial stresses for the internal and external pipe surfaces – are zero. Having substituted expressions (3) into formula (21) we define the intensity of residual stresses for the internal ($\bar{r} = R_2$):

$$\sigma_i = a_0 R_2 (R_1 - R_2)\sqrt{1 - \mu + \mu^2}, \quad (10)$$

and external surfaces of a pipe stock ($\bar{r} = R_1$):

$$\sigma_i = a_0 R_1 (R_1 - R_2)\sqrt{1 - \mu + \mu^2}. \quad (11)$$

In this connection evaluation of danger of the stock fracture because of residual stresses in accordance with the strength criterion of the specific energy of form measuring

$$\sigma_i = \sigma_B. \quad (12)$$

In some cases it was established that $\sigma_B = \sigma_S$ ($\sigma_B$ – is a strength limit on tension).

Thus, using the above-mentioned method of calculation of technological residual stresses it is possible to define the limiting modes of plastic deformation of axially symmetric articles by the conditions of strength security.

*Conclusion*

The method of calculation of technological residual stresses in axially symmetrical articles, made by plastic deformation. is suggested. Formulas for definition of residual stresses in the rod and pipe stocks have been obtained. The influence of turning of axially symmetrical stocks on the level of potential energy of residual stresses has been shown. The influence of residual stresses on the rods' and pipes' strength is evaluated.

## REFERENCES

[1] Kolmogorov G.L., Kuznetsova E.V. Formation of residual stresses under plastic deformation of pipe stocks // Vestnik PSTU. Dynamics and strength of machines. Perm, 2000. P. 15–19.

[2] Kolmogorov G.L., Kuznetsova E.V. About deformation degree under the axially symmetrical deformation // Izv. Vuz. Ferrous metallurgy. 2000. № 11. P. 31–33.

# CHEMICAL TREATMENT OF SEMICONDUCTOR SURFACES AT THE BEGINNING OF THE THIRD MILLENIUM

**Tomashik V.M., Tomashik Z.F., Bilevych Ye.O., Gumenyuk O.R., Kusiak N.V.**[(1)]
Institute for Semiconductor Physics, National Acadamy of Sciences of Ukraine, 03028, Kyiv-28, Nauki ave., 41
[(1)] Ivan Franko Zhytomyr Pedagogical University, 10001, Zhytomyr, Velyka Berdychivs'ka vul., 44

The development of modern semiconductor material science and semiconductor device manufacturing is tightly connected with advance in processing and preparing of semiconductor surfaces. The receiving of high quality surfaces of semiconductor materials, which have perfect structure and geometry and homogeneous chemical composition, has exceptional importance at the manufacturing of semiconductor devices. Now these problems are successfully resolved by the chemical wet etching. The etchants with different etching velocity, surface roughness, degree of surface contaminations with etchant components and products of chemical interaction of semiconductor with etchant and some other characteristics are worked out for various purpose.

Chemical etching, based on the chemical dissolution processes, is one of the main technological operation at the chemical treatment of semiconductor single crystals and thin films which widely used at the manufacturing of different semiconductor devices, apparatus and integrated circuit. Knowledge of kinetic behavior, mechanism and nature of semiconductor dissolution are the most important condition and measure at the selection of corresponding solution composition for polishing, anisotropic or selective etching and chemical cutting. High resolving power of some etchants allows to use them on the different phases of substrate manufacturing, but for this, it is necessary to develop the etchants with corresponding velocity of material elimination, surface roughness and some other parameters.

The miniaturization of integral circuit and semiconductor devices required the development of new etchant composition with slow etching rate and the possibility to obtain the stoichiometric composition of surface layers for different semiconductor materials. This necessitates the creation of new etchants for different purposes at the chemical treatment of semiconductors.

The velocity of the semiconductor dissolution is the quantitative characteristic of etching process and one of the main etchant properties. Therefore it is necessary to investigate the concentration dependence of semiconductors dissolution for all etchant compositions. Such dependencies for three component etchants can be represented as the surfaces of equal etching rate or Gibbs diagrams.

The diagrams "etching rate of semiconductor (mμ/min) – etchant composition" of the different systems, using nitric acid, hydrogen dioxide, iodine and potassium dichromate as a oxidizing agent were constructed by us with the help of mathematical planning of experiment. Such diagrams provide the possibility of comparison of the different etchant compositions by their etching rates and selection of the best etchant for given semiconductor compound.

The dependence of etching rates of semiconductors on etchant compositions of different etching systems have been studied in reproduced hydrodynamic conditions using rotating disk. The experiments were performed using single-crystal wafers with the surface area of about 0.5 $cm^2$ and thickness 1.5-2 mm, which were cut from ingots. Prior to the etching, the wafers were mechanically polished, and the surface layer of 50 to 80 μm was removed with etchant of the same composition as that subsequently used for studies of the etching process. Etchants were made just prior to use from high purity components. The samples were attached to quartz substrates using pizzeine and then mounted in a holder allowing measurements in the rotating disk mode (with the rotation rate ranging from 36 to 120 $min^{-1}$). After processing the samples were washed off with distilled water.

The etching rate was determined by the wafer thickness reduction using ICh-1 time indicator (accuracy of measurements was 0.5 μm). Two or three samples were etched simultaneously, with difference in the measured thickness not exceeding 5 %. Before etching all etchants were allowed to stand for 40-80 min to ascertainment the equilibrium in the chemical reactions which can take place between etchant components. The solutions were prepared using high-cleans 70 % $HNO_3$, 30 % $H_2O_2$, 13 % $K_2Cr_2O_7$, 34 % HCl, 40 % HBr, 55 % HJ, 100 % acetic, 27 % tartaric, 20 % citric, 9 % oxalic and 40 % lactic acids, 100 % glycol and 100 % dimethylformamide.

Using the Gibbs diagram we have the possibility to study the dopant influence on the etching rate also. Comparing the Gibbs diagram for undoped and doped material one can be concluded that the doping of semiconductors can strongly influence on the etching rate. In the case of tin doped InAs the doping leads to decreasing of the etching rate in all investigated solutions. This can be explain by the retarding of the InAs dissolution velocity in the presence of tin compounds, which can be formed at the chemical etching of such material. Doping of CdTe by Ge leads to small increasing of the etching rate.

The Gibbs diagrams give us the possibility to determine the concentration ranges of polishing solutions in each investigated system. It is possible to choose the etchant composition with necessary polishing rate in given ternary system at the comparing of these two types Gibbs diagrams or to reach a conclusion about impossibility of such etchant composition. In the last case it is necessary to change one of the etchant component and to investigate a new ternary system to obtain the necessary etchant composition.

The Gibbs diagrams provide also the possibility of definition of the mechanism of semiconductor interaction with etchant at the chemical etching. One can conclude that the dissolution of cadmium telluride and solid solutions based on it in the solutions $HNO_3$-HCl-$CH_3COOH$. $HNO_3$-HHal-tatrtaric acid and some others is limited by the interaction of tellurium, which is formed on the surface, with etchant component, if we compare the surfaces of equal etching rates (Gibbs diagrams) of CdTe and Te in such solutions. Such conclusion is based on the similarity of the obtained surfaces of equal etching rate for CdTe, $Zn_xCd_{1-x}Te$ and $Cd_xHg_{1-x}Te$ solid solutions and Te in the investigated etchant compositions.

One can be note that using the surfaces of equal etching rates (Gibbs diagrams) for the interaction of solid solutions with given etchant it is possible also to define the influence of solid solution composition on the mechanism of its dissolution.

It is necessary to indicate that the doping of semiconductors leads not only to changing of etching rate but to changing also the range of polishing solutions in each investigated system. Therefore, at the chemical treatment of semiconductors it is necessary to account the nature of doping element and to develop the polishing etchant compositions for different dopant which can be used for the modification of the semiconducting properties of given semiconductor. The formation of solid solutions based on given semiconductor leads also to the modification both etching rate and range of polishing composition in each investigated system but these modifications are small in comparison of dopant influence. These can be explained by the fact that mainly the similar compounds that have similar chemical and physical properties form the solid solutions and the different chemical elements are used for semiconductor dopings.

However, at the chemical treatment of semiconductor surfaces it is necessary to know not only the etching rate but the surface roughness, degree of surface contamination with etchant components and reaction products, deviation from stoichiometry of the surface layers and some other characteristics. Therefore, the concentration dependencies for all these parameters must be constructed in the form of Gibbs diagrams also. One can chose the best etchant for given semiconductor if we shall construct such diagrams and compare them with each other. The plotting of Gibbs diagrams at the chemical etching of semiconductor compounds is the scientific basis for preparation of the best etchant composition for given technological process. It is necessary to note that the comparison of all etchant properties can be made using the empirical equations for each property, which was obtained at the constructing of corresponding Gibbs diagrams.

Using the Gibbs diagrams the three-components etchants with different etching velocity, surface roughness, degree of surface contamination with etchant components and interaction products and some other characteristics are worked out for the chemical treatment of InAs, InSb, GaAs, CdTe and solid solutions $Cd_{1-x}Hg_xTe$ and $Zn_xCd_{1-x}Te$. The liquid solutions of the $HNO_3$-HCl (HBr, HJ)-organic acid, $H_2O_2$-HBr-organic acid and $K_2Cr_2O_7$-HBr-HCl (organic acid) systems were used for the creation of different etchant compositions (we used the oxalic, acetic, lactic, tartaric and citric acids as the organic acids). Sometimes a part of organic acid was changed by glycol of dimethylformamide.

The proposed method for developing of etchant compositions can be successfully used for the four-component solutions as well as for more complicated system. In the case of such systems it is necessary to use the empirical equations that are obtained at the mathematical planning of experiments.

# EQUILIBRIUM DAMAGE ACCUMULATION PROCESSES, POSSIBILITIES OF INCREASE OF DEFORMATION RESOURCES AND MACROFAILURE CONDITIONS OF COMPOSITE MATERIALS

**Wildemann V.E.**
Perm State Technical University, Perm, Russia

The macroscopic failure of composite materials is preceded by complex multilevel processes accompanied by accumulation and localization of damaged centers and formation of a failure cluster. Therefore, the study of these mechanisms is one of the basic problems for the mechanics of modern composite materials used in aerospace engineering.

A formulation of a quasi-static problem of the mechanics of elastic-plastic bodies with loss-of-strength zones and boundary conditions of contact type is given which enables the properties of the loading system to be taken into account [1]. With certain constraints on the constitutive relation and using a condition for stability of the softening process in a local zone, theorems are proved on the uniqueness of the solution of the boundary-value problem and on the maximum and minimum of the functionals when the kinematically or statically possible and actual fields coincide. The corresponding generalized variational principles are given [2]. The possibility of stabilizing the damage accumulation process at the postcritical deformation stage due to loading system properties control is theoretically proven.

The formation of a theory of the stable postcritical deformation of the work-softening media is considered. The pseudo-plastic deformation affected by structural damage of granular composites is investigated within the framework of the considered two-level structurally phenomenological model of heterogeneous media .

The stable evolution of the interconnected processes is accompanied by stress redistributions, partial or complete unloading, and strain or damage localization that are one of the main causes of implementation of the postcritical deformation stage [3]. The numerical calculation results of inelastic deformation and failure of the periodic unidirectional fiber-reinforced composites are presented under conditions of the displacement-controlled transverse proportional loading mode [4]. The main mechanisms of the work-softening behavior for the indicated type of materials are described in the macro-homogeneous stress-strain states. Macroscopically, the failure of heterogeneous media as a result of postcritical deformation and the loss of stability of damage accumulation depends on the stiffness of the loading system. When a deformable body is fixed on the closed surface with sufficiently but not infinitely large coefficients of stiffness, it is possible to observe the equilibrium development of the localized volumes of work-softening and damage.

The constitutive equations for the work-softening isotropic, transverse isotropic, and orthotropic media are presented. The effect of the loading system on the stability of deformation, damage accumulation, and failure under monotone and nonmonotone triaxial loading was studied. The growth of failure strains with increase in stiffness of the loading system and unequal resistance of heterogeneous body are registered and investigated. A preventive unloading method is offered for the mathematical modeling of the damage accumulation during the testing of the materials on the servo-controlled systems.

The displacement-controlled mode is simulated by a series of soft loading and unloading cycles. The detected phenomenon of failure where the unloading leads to stress-strain diagrams with a negative slope of the descending branch was not found either in the displacement or stress-controlled monotone loading mode.

Realization of the postcritical deformation stage leads to an employment of the stored load-carrying capacity that can be used for optimum design of structures and special materials. For estimating the stability of growth of the equilibrium damage in the postcritical stage, a relation between the energy spend (a sum of the elastic strain energy increment and the work of fracture) and supplied energy (the work of external forces) should be considered at a fictitious small increment of the strain. Stability conditions of the postcritical deformation of the components of granulated, laminated and fibrous composites are given with setting limitation to the relations of the stiffness response and parameters of the descending line of the diagram [4, 5].

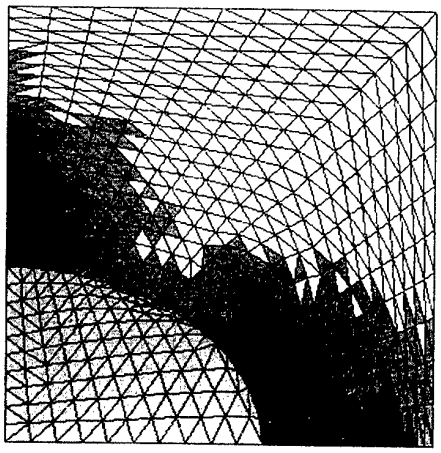

Fig. 1. The finite element model of the unidirectional fiber-reinforced composite

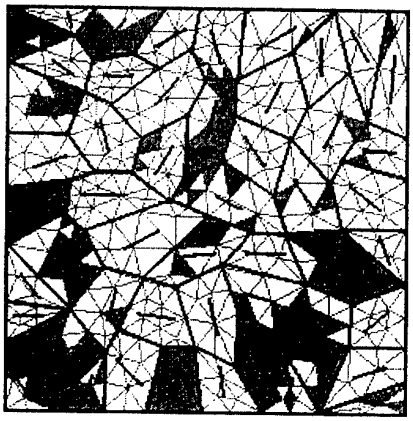

Fig. 2. The model of the granular composite with damage zones

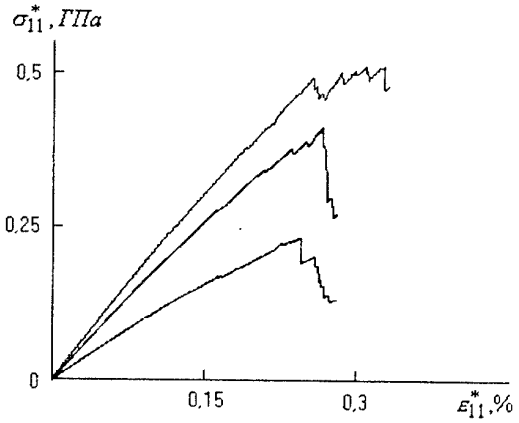


Fig. 3. Calculated macrostress-macrostrain diagrams of granular composites with pores and rigid inserts

Ensurement of realization of the postcritical deformation conditions employs an additional load-carrying capacity, as well as extends the durability of structures to resist external loads at the stage of formation and development of macrocracks.

New experimental data concerning quasistatic deformation of the orthotropic fibrous copper composite materials on postcritical stages after preliminary cyclic loading are analyzed.

Possibility of practical use of the obtained results — optimal choice of structural parameters of new materials and structures with the purpose of increase of deformation resources [6], carrying capacity and survivability on the basis of providing the conditions of stability of dissipative processes necessary for accommodating of materials to requirements of their usage.

The work was supported by Grant of the President of the Russian Federation 00-15-99264 and Grant of the Russian Foundation for Basic Research RFBR-Ural 01-01-96479.

1. Wildemann V.E., Sokolkin Yu.V., Tashkinov A.A. Mechanics of Inelastic Deformation and Failure of Composite Materials, Nauka, Moskow, 1997.
2. Wildemann V.E. On the solution of elastic-plastic problems with contact-type boundary conditions for solids with loss-of-strength zones, J. Appl. Math. Mechs., 62, No. 2 (1998), 281—288.
3. Wildemann V.E., Zaitsev A.V., Gorbunov A.N. Mechanisms and regularities of heterogeneous-solid damage-accumulation at the supercritical stage // Physical Mesomechanics. 1999, V. 2, No. 4, 37–44.
4. Sokolkin Yu.V., Vildeman V.E., Zaitsev A.V., Rochev I.N. Structural damage accumulation and stable postcritical deformation of composite materials. Mechanics of Composite Materials, V. 34, No.2, 1998, 171–183.
5. Sokolkin Yu.V., Vildeman V.E. Postcritical deformation and failure of composite materials, V. 29, No. 2, 1993, 163–170.
6. Antsiferov V.N., Tashkinov A.A., Wildemann V.E., Sevastianova I.G. Pseudoplastic deformation and failure of Y-TZP-$AL_2O_3$ ceramics at high temperature // Fracture Mechanics of Ceramics. V. 12: Fatigue, Composites and High-Temperature Behavior. NY: Plenum Publishing Corparation, 1996, 561–567.

# THE STRUCTURAL HEREDITY AT A CRYSTALLIZATION AND THE NATURE OF OVERCOOLING OF IRON

**Maiboroda V.P., Kunitskiy Yu.A.**[(1)]
I.Franzevich Institute of Materials Sciense Problems of National Academy of Scienses of Ukraine, Kiev, Ukraine
[(1)]The Technical Centre of National Academy of Science of Ukraine, Kiev, Ukraine

Research of value of an overcooling of liquid iron except for one activity [1], do not find out while unified regularity. Is convincingly rotined [2], that the crystallization descends on walls of a steel mold, the roughness by which one always exceeds the critical size of a crystallization centre, and nevertheless the observed values of overcooling of iron make 300-500$^0$C [3]. In quoted activity [1] the overcooling in 300$^0$C, fig.1, was watched at exposure of a melt, in so-called area of molecular-polymorphic transformation of an iron melt 1600-1650$^0$C ($\delta_{liq} \rightarrow \gamma_{liq}$).

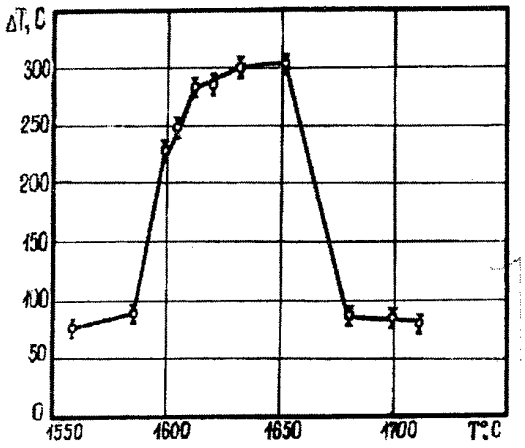


Fig.1

Feature of observed process is that increase of temperature of exposure of a melt above $\geq$1680$^0$C, at preservation of conditions of experiment, results not in apparent preservation, or increase of an overcooling, but to a boomerang effect (descending branch of a curve of a fig.1). The variation by a cooling rate of a melt in an interval 0,75-6,7 K/s does not result in essential changes of value of an overcooling, fig.2. How it is visible from pieces of thermograms, at the melt temperature 1560$^0$C (curve 1), the solidification descends with overcooling ~70$^0$C, and $\delta \rightarrow \gamma$ transformation - with a overcooling ~140$^0$C.

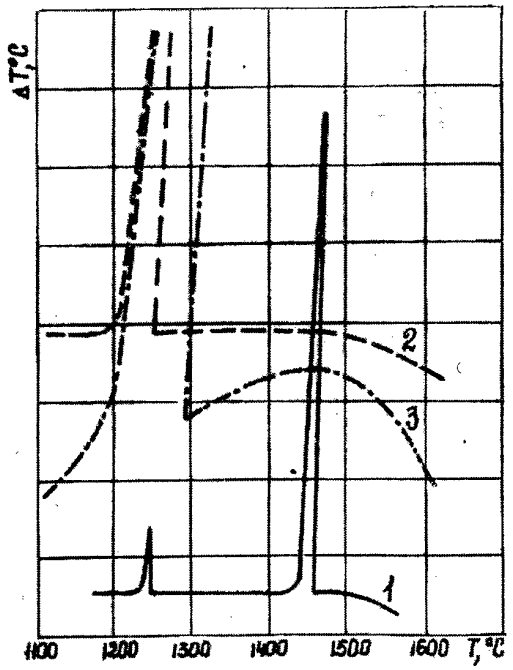


Fig.2 1 and 2– 0,75 K/s, 3 – 6,7 K/s

At research of the nature of a chemical and structural microinhomogeneity of medium-carbon steels [4] the data about modifying influencing of dopes of molten ferrite on a constitution of an ingot and on increase of a plasticity cast and rolled thermo-hardened metal are obtained. In the given report the outcomes of researches about influencing a melt of ferrite on conditions of a solidification and on a constitution of an ingot high-clean are resulted.

For activity the carbonyl refined iron ЧМТУ 1-884-70 with carbon content 0,003; sulfur 0,002; Si, Ni, Cr, Ni, Mn in the sum no more than 0,04 mas % was used. The thermographing conducted on the installation of a hyperthermal differential thermal analysis (HDTA) with the string thermoelectric couple in medium of helium. The measurement accuracy makes $\pm$10$^0$C [1]. The value of a hinge fitting makes 0,15 g and is in alund tumbler. Weight of a dope - 5 mas % from weights of a melt. The installation (HDTA) is

supplied with the manipulator and allows at a selected smelting practice to dope in a melt. In a fig. 3, the pieces of the obtained thermograms are adduced.

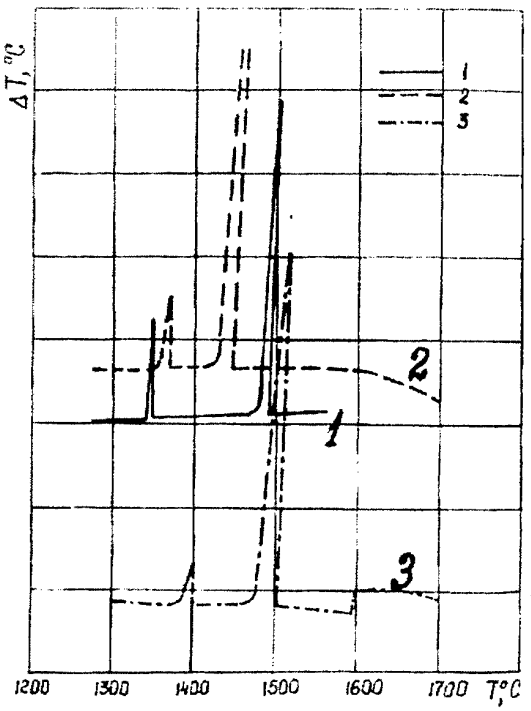


Fig.3

The decreasing of a cooling rate up to 0,25K/s, curve 1, as against a curve 1, the fig. 2, reduces to minimum the overcooling of a melt and $\delta \rightarrow \gamma$ transformaion. From confrontation of curves 1 figures 2 and 3 follow, that the main relaxational processes at a solidification and crystalline modification of iron flows past during $\geq$ 10 minutes. The curve 2, fig.3, corresponds to a descending segment of relation, fig. 1, and is obtained at the same cooling rate (0,75 K/s). For analysis of influencing of molten ferrite in a melt, similar to curve 2, the fig.3, is entered a dope. Thereof the melt temperature is lowered up to ~1600$^0$C, curve 3, and at this temperature the bosh is maintained 15 min. This time has enough for a full melting of a dope and "homogenization" of a melt. On a curve 3, fig.3, this method is indicated by step. How it is visible from a thermogram, the beginning of a crystallization descends at 1510$^0$C, and $\delta \rightarrow \gamma$ transformation descends practically without overcooling. Apparently, such conditions of a solidification should be attributed to ideal. Confrontation of macrostructures 20 -kg castings of iron, fig.4, as well as in a case with steel [4], confirms improvement of the quality of metal at the introducing in a melt of a liquating dope. From the obtained data follows, what the introducing liquating of ferrite dope in overheated up to ~1700$^0$C an iron melt and exposure of a bosh in the field of temperature 1600$^0$C originates $\delta_{liq} \rightarrow \gamma_{liq}$ transformation. Hercinafter this pre-crystalization process provides more equilibrium conditions how solidifications, also and $\delta \rightarrow \gamma$ transformation.

From reduced outcomes follows, that the solidification descends on the gear of ordering of polyfragment elements which are generatrix composite motive of a constitution of a melt and components the basis of crystallization centres.

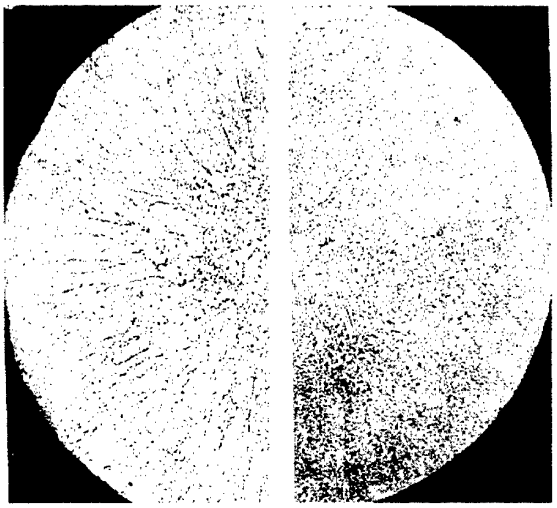

Fig.4. The image is decrease in 1,25 times

Literature

1.V.P.Maiboroda.//Preprint of AS UkSSR, Institute of Materials Sciense Problems of National Academy of Scienses of Ukraine, №11, Kiev, -1987.-17 P.

2. Kostyuchenko V.P., Fedorov O.P.//Physica metallov. - 1986.- 7, №4. – P. 65-69.

3. Duchin A.I.//Problemi metallovedeniya i physica metallov. - Moscow.: Metallurgizdat, 1959. - V.6. – P. 9-34.

4.V.P.Maiboroda//Rasplavi.-1995.- № 5.-P.64-74.

# WARM COMPACTION OF GREEN POWDER BLANKS: COMPUTER MODELING AND EXPERIMENT

**Gorokhov V.M., Sevastyanov E.S., Ustinova G.P., Zvonarev E.V.**
Powder Metallurgy Research Institute, Minsk, Belarus

**INTRODUCTION.** Theoretical substantiation and search of new methods of manufacturing P/M parts are caused by lacks of well known pressing and sintering main of which are high porosity, low accuracy and quality of a part surface and also insufficient level of mechanical properties. In this connection a number of new technological methods provide high density products of the complex shape with high mechanical properties, high accuracy and low roughness of a surface. The most widely used method of pressing and sintering provides density of iron structural parts up to 6.8-7.0g/cm$^3$, that makes 85-90% of theoretical density. Increased density of powder parts assumes the value of 7.3g/cm$^3$ or 93% of theoretical density and is reached by various combinations of pressing and sintering. Higher density is reached essentially by other methods, among which it is necessary to note well known double pressing - double sintering, injection moulding, cold and hot forging. Other methods, such as high-temperature sintering, pressing with lubricating of the die or warm compaction, quickly develop and will find wide application in the future. Especially fast development finds a method of warm compaction of metal powders for producing high density structural parts, basically due to development of the Swedish firm "Hoganas AB" in the area of metal powders and German firm "Dorst" in the field of creation specialized equipment for pressing [1,2]. In this paper peculiarities of densification of iron and low alloyed steel powders are investigated during warm isothermal compaction of green blanks using high polymers as a hard lubricant.

**WARM COMPACTION OF GREEN BLANKS.** Necessity of further increase of mechanical properties, service life and reliability of structural parts produced by methods of powder metallurgy, urgently demands to find new ways of realization of potential opportunities of warm compaction to increase density. One of the versions of warm compaction is the method of warm compaction of green blanks previously pressed at room temperature.

The experiments were executed on annular samples with an outside diameter of 30 mm, internal diameter of 20 mm and height of 9.5 mm. Samples were made of powder iron and powder low alloyed steel with 4%Ni, 2%Cu, 1%Mo with addition of pencil graphite, zinc stearate and polymer with the total contents of the additives 0.6 % (mass). Density of annular samples after cold pressing was about 7.0g/cm$^3$. Warm compaction of green samples was carried out at 120$^0$C with accuracy of measurement to 1$^0$C. The results have shown, that density after pressing at 120$^0$C makes 7.6 $\pm$ 0.01g/cm$^3$. The received density is 0.2g/cm$^3$ higher in comparison with warm compaction of a metal powder.The results of influence of the total contents (S) of carbon, zinc stearate and polymer on density ($\gamma$) during warm compaction of green samples show that the maximal value of density is reached at S = 0.6 %. It is necessary to note, that a similar result we have received during warm compaction of metal powders.

**COMPUTER MODELING OF WARM COMPACTION OF GREEN BLANKS.** At the background of theoretical problem of powder densification there has been undertaken an attempt to take into account real porous structure of a sample. The representative element of structure includes a system of particles and pores interacting with each other. Various schemes of structure are formed with four particles of iron without lubricant material between particles and with it. Rigid bonding of particles with each other simulates densification of a metal powder without lubricant material between the particles. Ideal slip of particles is provided in the scheme, in which the powder particles are divided by finite elements allocated properties of a liquid lubricant material. The intermediate variant includes according to our estimation approximately 30-40% of the surface of contacting particles simulating introduction in the structure of iron powder or low alloyed steel 0.5-1.0% zinc stearate. Average size of iron particles is about 100 micrometers. The calculations has been carried out using elastic-plastic reology, the iron powder with known elastic and plastic properties is chosen as a

modeling material. The finite elements simulating lubricant are assumed incompressible with Young modulus equal to zero.

The calculations of the typical cells under external force during pressing in a rigid die have been carried out using finite element method. They have confirmed expediency of introduction of a lubricant into metal powder that would ensure ideal slip in the zone of contact between particles and high efficiency of densification. We have investigated plastic flow of metal particles and formation of possible destruction zones of a material with a lubricant between particles of a pressed powder and compared the results with similar ones calculated without a lubricant. It should be noted that in both cases the plastic flow does not cover all representative volume at once and in the beginning is located in certain zones closed to the corners of polygon simulating pore section and corners of the representative cell. In the absence of a lubricant the effective process of pore closing begins from the moment when areas of deformation localization being distributed from concentrators of pressure merge and block space between pore and lateral borders of a representative element. The distribution of area of plastic flow occurs approximately in regular intervals in all directions. At the presence of a lubricant the border undressed between particles becomes the area, directing in distribution, of plastic flow from the corners inside metal particles. The plastic elements "advance" in the direction from pore to lateral borders of a representative element, being gradually distributed in the central areas of particles. It is clear that presence of a lubricant provides effective displacement of particles that results in essential increase of density. In the present work there have been carried out calculations of densification curves of samples from powder iron and low alloyed steel during warm compaction of green cylindrical samples with diameter of 10 mm and height of 16 mm with initial relative density of 87%. As the result of calculation dependences "pressure - density" are derived during pressing in various conditions of internal friction between particles.

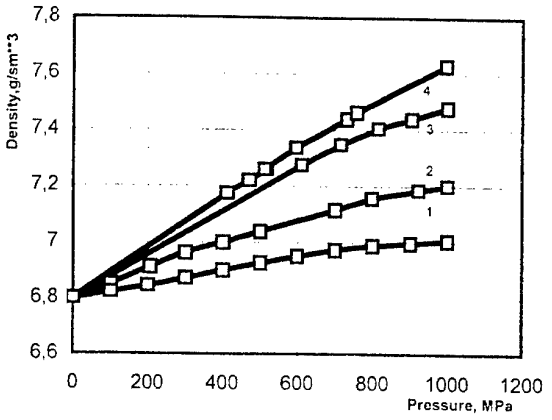


*Influence of pressure on density of powder steel: 1 - numerical experiment (pressing of a powder material without finite elements simulating lubricant on borders between particles); 2 - numerical experiment (pressing of a powder material with a lubricant material between particles) the amount of elements corresponds to the contents of zinc stearate 0.5%; 3 - numerical experiment (warm pressing of a powder material) the borders between particles are filled with finite elements simulating lubricant; 4 - full-scale experiment of warm pressing of a powder material at 120 $^0C$ and contents of zinc stearate 0.5%.*

When pressing without a lubricant (curve 1) density of a powder material changes insignificantly (0.1 - 0.2g/cm$^3$) despite high pressure. The cold pressing of powder materials with a lubricant (curve 2) allows to produce samples with density of 7.1 - 7.2g/cm$^3$, that exceeds a little results received in experiments. Warm pressing allows to get density of 7.4 - 7.5g/cm$^3$ in numerical experiment (curve 3), while in full-scale experiments it was possible to make density of 7.6 - 7.62g/cm$^3$. Divergence of theoretical and experimental results has made 5%, that confirms adequacy to the chosen theoretical model of warm pressing to the real process.

**REFERENCES**

1. Ridgel J. Metal Powder Report. February (1996), 28-31.

2. Unkel R. Metal Powder Report. February (1996), 22-26.

# PHASE TRANSFORMATION, STRUCTURE AND PROPERTIES OF MULTICOMPONENT TI-SI-BASED ALLOYS AS FUNDAMENTAL BACKGROUND FOR ELABORATION OF HIGH-TEMPERATURE TITANIUM MATERIALS

**Bulanova M., Firstov S., Kulak L., Miracle D.[(1)], TretyachenkoL., Velikanova T.**
Frantsevich Institute for Problems of Materials Science NAN Ukraine, Kiev, Ukraine
[(2)]Air Force Research Laboratory, Materials and Manufacturing Directorate, 2230 Tenth Street, Wright-Patterson AFB, OH 45433 USA

Ti-Si is a prospective basic system for high-temperature materials with different hardening mechanisms (solid solution, ageing, *in-situ* composites) which may exist singly or in combination. Silicon is known to increase mechanical characteristics (thermal stability, corrosion and creep resistance etc.) of both titanium, and Ti-Al alloys. Aluminum, as an active α-stabilizer, is usually added to titanium alloys to expand the interval of working temperatures as Al essentially increases the α↔β transformation temperature of titanium (from 882°C in the pure titanium up to ~1500°C in an alloy with ~45 at. % Al). It is known, meanwhile, that in polymorphous metals the highest working temperature occurs near the α↔β-transformation.

This is valid for single-phase materials with solid solution hardening mechanism. In ageing alloys and in *in-situ* composites multiple phases (two, as a rule) coexist. As a result, a number of solid-state transformations in addition to α↔β might occur. In this case, the highest working temperature is defined by the lowest solid-state transformation temperature.

Thus, understanding of phase relationships, especially in the solid state, and of the temperatures of solid-state transformations, is absolutely necessary for the efficient thermomechanical processing of materials.

Many alloying elements are used in titanium alloys to improve their high-temperature strength and room-temperature plasticity, including *d-metals* (Sc, Y, Zr, Hf, V, Nb, Ta, Mo, W etc.), *p-elements* (Al, Si, Sn) and microadditions of *f-metals* (La, Ce, Nd, Dy). Modern alloys are contain up to 8 elements.

However, extremely scarce information is available on phase compositions and the temperatures of phase transformations in these multicomponent systems. Moreover, among the possible boundary ternaries, only a few are studied to some extent. Available data are often inconsistent and insufficient.

Thus, here we summarize our results of the last ten-years of experimental study of phase equilibria in multicomponent Ti-Si-based systems and of some properties of individual phases and phase constituents. Information is considered according to the following scheme:

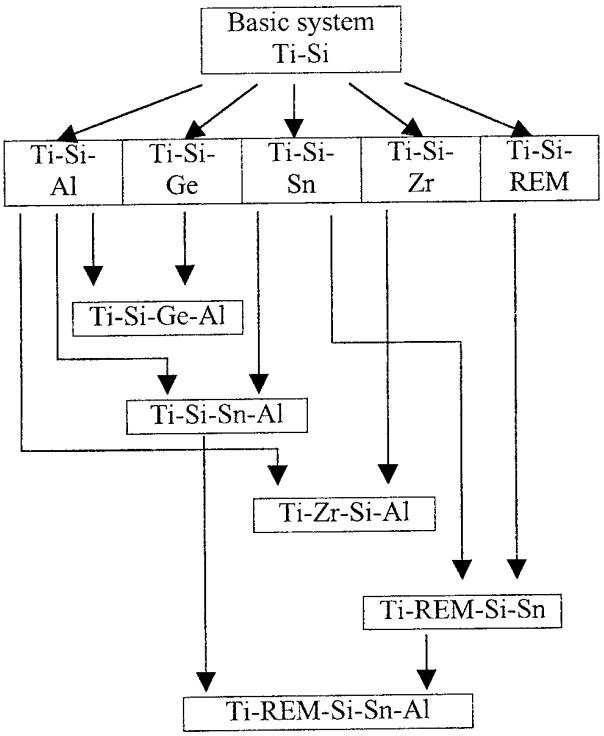


Correlation between the elements of phase diagrams, details of the crystal structure and properties of phases is discussed.

# ALLOY PHASE DIAGRAMS IN Ti CORNERS OF TERNARY AND QUATERNARY TITANIUM-BORIDE SYSTEMS AS A BASE FOR DEVELOPMENT OF IN-SITU METAL-MATRIX COMPOSITES

**Velikanova T.Ya., Bondar A.A., Artyukh L.V., Bilous O.O., Firstov S.O., Miracle D.**[(1)]
Frantsevich Institute for Problems of Materials Science Ukrainian National Academy of Science, Kyiv, Ukraine
[(1)]Air Force Wright Laboratory, Materials and Manufacturing Directorate, Wright-Patterson AFB, OH USA

Titanium-boride metal matrix composites are presently under conclusion as materials for high strength, high temperature applications. In order to realize or extend their full potential, the high-temperature-capable boride reinforcement should be additively introduced into advanced titanium matrix, with the both constituents being in equilibrium. The creative development may be conceivable only through the complex systematic investigation resulting in a scientific background, which includes phase equilibrium data and alloy composition-constitution-properties relationships. The present report is a part of such complex investigations and deals with phase equilibria in Ti corners of Ti-B-*X* and Ti-Al-B-*X* systems, where *X* is Zr, V, Nb, Si, Ge, or Sn.

The alloys were prepared by arc-melting (cooling rates about 100°C/sec) and studied, in states as-cast and annealed at subsolidus temperatures, by light optical and electron scanning microscopy (LOM and SEM), electron probe microanalysis (EPMA), and X-ray diffraction (XRD) technique. Phase transformation temperatures were determined by DTA and pyrometry measurements after Pirani & Alterthum (melting points).

Basing on the data obtained, phase diagrams in the Ti corners of the ternary Ti-Al(V,Nb,Ge,Sn,)-B and quaternary Ti-Al-Zr(V,Nb,Si,Ge,Sn)-B systems were constructed in melting (crystallization) temperature ranges, i.e. melting behavior of alloys, $\alpha \rightarrow \beta$ transformation temperatures, partitions of alloying additives (location of tie-lines on a phase diagram). The systems in the ranges under investigation are characterised by extensive area of eutectic crystallisation of *bcc* metal and boride (TiB) phases. The microstructure of the two-phase (Ti)+(TiB) alloys containing 7.5 at.% B is practically eutectic, i.e. the volume content of the reinforcing phase in the ternary and quaternary eutectic alloys did not changes practically. The results allow to restrict the ranges of two-phase (Ti) + (TiB) fields - up to 10-12 at.% Al, up to 5-6 at.% Ge or Sn, about 12 at.% V or Nb for $\alpha+\beta$ matrix, and ≥20 at.% V or Nb for $\beta$ matrix.

The alloying additives are divided into 2 groups: *p*-elements and *d*-metals. The titanium boride does not practically solve *p*-elements Al, Si, Ge, and Sn. In titanium-boron-*p*-element(s) systems a matrix composition is not affected by adding any amount of reinforcing boride TiB. Partitions of V and Nb between the metal and boride phases are comparable. In the latter, any alloying addition causes changes of the both phases' compositions.

Aluminium, tin, and niobium increase the melting points of the ternary (Ti) + (TiB) eutectic alloys, up to invariant equilibria: $L_e \leftrightarrow$ (Ti,Al) + TiB (taking place at ~1560°C), $L_e \leftrightarrow$ (Ti,Sn) + TiB (~1580°C), and $L_U$ + (NbB) $\leftrightarrow$ (Ti,Nb) + (TiB) (1610°C). In the Ti-Ge(V)-B systems there are drops of melting points for the (Ti) + (TiB) eutectic, up to invariant equilibria $L_E \leftrightarrow$ (Ti,Ge) + TiB + ($Ti_5Ge_3$) at 1315°C and $L_e \leftrightarrow$ (Ti,V) + (TiB) at ~1430°C.

Comparison of ternary and quaternary phase diagrams reveals that the substitution of 10 at.% Ti by Al results in a noticeable influence on alloy properties, increasing the $\alpha \rightarrow \beta$ transus temperatures (by ~100°C) and melting points (by 20 to 50°C).

Basing on obtained phase diagram results, a special approach was developed in order to reveal a role of either matrix and boride phases in deformation testing, as follows: a numbers of alloys were prepared within a certain tie-line, due to the fact that tie-lines were constructed. In the case, hypoeutectic and eutectic alloys were obtained with identical compositions of matrix and boride phases, as well as the alloy of matrix composition without boride.

**Acknowledgement.** This research was suported by the Air Force Office of Scientific Research (USA) under the Project P-060. The authors thank D.B.Borysov, M.P. Burka, P.S. Martseniuk, T.O. Shapoval, N.I. Tsyganenko for technical assistance.

# ALLOY CONSTITUTION AND PROPERTIES OF METAL-BORIDE ALLOYS IN THE Ti-Al-Nb-B SYSTEM

**Tsyganenko N.I., Artyukh L.V., Bilous O.O., Bondar A.A., Borysov D.B., Burka M.P., Martseniuk P.S., Shapoval T.O.**

Frantsevich Institute for Problems of Materials Science Ukrainian National Academy of Science, Kyiv, Ukraine

Titanium boride TiB, Nb, and Al are of obvious interest in reinforcing titanium alloys. Phase equilibria in the Ti–Nb–B system are insufficiently studied, only at 1400°C [1]. In the present work the Ti-Nb-B and Ti-Al-Nb-B alloys were investigated in the Ti corner at melting (crystallization) temperatures.

The alloys were prepared by arc-melting (cooling rates about 100°C/sec) and studied, in states as-cast and annealed at subsolidus temperatures, by melting point determination (pyrometry measurements after Pirani & Alterthum and DTA), light optical and electron scanning microscopy (LOM and SEM), electron probe (EPMA), and X-ray diffraction (XRD) analyses.

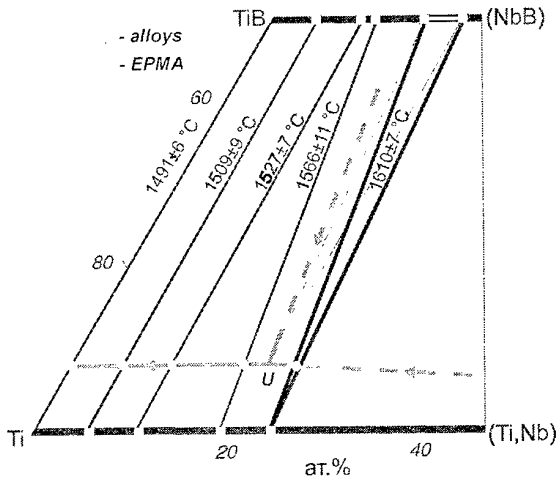


Fig. 1: The Ti-Nb-B melting diagram

The system in the range up to 25 at.% Nb and 50 at.% B is characterized by eutectic crystallisation of *bcc* metal and boride phases (Fig. 1). Niobium increases the melting temperature of the (Ti) + (TiB) eutectic alloys, up to the invariant four-phase equilibrium L + (NbB) = (Ti) + (TiB), taking place at 1610±7°C. With increasing the Nb content, microstructure of the alloys is not changed comparing with the binary eutectic alloy $Ti_{92.5}B_{7.5}$. EPMA data show that the Nb partitions between metal and boride phases in the ratio approximately 5:3. Based on the EPMA data, the conclusion may be made that the two-phase (TiB) + (NbB) and three-phase (Ti,Nb) + (TiB) + (NbB) fields are rather narrow in the ternary system.

DTA examination reveals the stabilizing role of niobium, the β transus temperature of (Ti,Nb) decreases by as much as ~620°C at 11 at.% Nb content in matrix (the alloy $Ti_{81.8}Nb_{10.7}B_{7.5}$). According to XRD data, the matrix of the latter alloy is of complex phase composition, containing metastable phases α" (based on α-Ti) and ω (in a little amount), together with the stabilized β-phase. The alloy $Ti_{87.1}Nb_{5.4}B_{7.5}$ is (α-Ti) + (TiB) and the $Ti_{75.1}Nb_{17.4}B_{7.5}$ is (β-Ti) + (TiB) and traces of (α-Ti) from XRD. The $Ti_{68.0}Nb_{24.5}B_{7.5}$ is three-phase (β-Ti) + (TiB) + (NbB), from XRD and EPMA data.

Investigation of the quaternary Ti-Al-Nb-B alloys containing 10 at. % Al brings to a conclusion that the Al content under studying does not change characteristics of phase relationship. The alloy constitution is the same, mainly.

The concentration dependence of Vickers microhardness $H_V$ shows clear maximum at the 11 at.% Nb content (7.5 at.% B), in the both ternary and quaternary systems. The hot hardness correlates with the microhardness at the temperatures up to 500°C. This strenghthening should be attributed at the expense of the multi-phase composition of matrix, together with contributions of alloying elements. The contributions of Nb, Al and B alloying additions to strengthening were analyzed basing on the hardness. The boride and Nb reinforcings are significant up to 500°C, and the Al alloying has effect in all the temperatures under investigation. Only the Al additions cause remarkable elevation of starting temperature of sharp softening by 100°C, and boron and Nb do not affect practically.

**Acknowledgement.** This research was suported by the Air Force Office of Scientific Research (USA) under the Project P-060.

**Reference.**

1. Yu.B. Kuz'ma, Poroshkovaya Metallurgiya (Kiev), (No.10), (1971) 298-300; English transl.: Sov. Powder Metall. Met. Ceram., **10** (10), (1971).

# PHASE EQUILIBRIA IN THE TERNARY SYSTEM Ti-Al-B AND HIGH-TEMPERATURE STRENGTH OF ALLOYS

**Artyukh L.V., Bilous O.O., Bondar A.A., Burka M.P., Martseniuk P.S., Tsyganenko N.I., Shapoval T.O.**

Frantsevich Institute for Problems of Materials Science Ukrainian National Academy of Science, Kyiv, Ukraine

The Ti-Al-B system is promising as a base for development of high-temperature strength titanium alloys using reinforcements of titanium matrix by aluminium and hard boride particles which are formed at eutectic crystallization. The Ti-Al-B phase diagram was not studied in the region rich in titanium (in the Ti corner). In the present work the ternary alloys of the Ti-TiB-$Ti_{62}Al_{38}$ region (Fig. 1) were studied by methods of metallography, XRD, DTA, EPMA, microhardness and hot hardness.

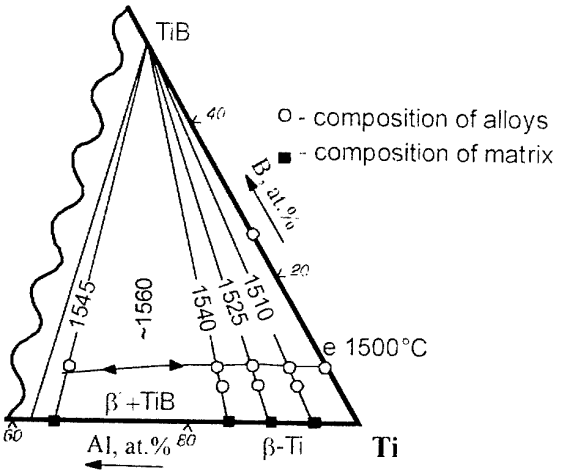


Fig. 1: The Ti-Al-B melting diagram.

The portion of Ti-Al-B melting diagram was constructed. It was found that in the region restricted by the tie-line $Ti_{62}Al_{38}$-TiB, the alloys crystallize to form the eutectic (Ti) + TiB. The solubility of aluminium in the boride phase is negligibly little. In the as-cast alloys metal matrix is $\beta \rightarrow \alpha$ or $\beta \rightarrow \alpha_2$ transformed.

With increasing Al content, the melting points of the (Ti) + TiB eutectic alloys elevate, passing trough the maximum ~1560°C at ~25 at.% Al. The boron content in the (Ti) + TiB eutectic composition is not practically affected by Al alloying. Therefore the volume content of reinforcing phase in the ternary eutectic alloys remains on the same level as in the binary eutectic, ~10 vol. %.

Mechanical properties of the alloys under investigation were estimated by measurements of hardness is the temperature interval from RT to 800°C and by compression tests at RT. The good correlation between data obtained by the both methods was noticed.

The investigation of boron influence (from 0.04 to 7.9 at. % B) on mechanical properties was carried out for the basic $Ti_{89.8}Al_{10.2}$ alloy. The microaddition of 0.04 at. B was shown to cause a diminution of hardness (strength) and a somewhat growth of plasticity. The negligible growth of hardness is detected at the boron content 0.2 at.% that seems to correspond to the limit of boron solubility, and the hardness of this alloy is the same as of the initial alloy. The hardness of alloys increases significantly at the appearance of boride phase, in accordance to growth of volume content of reinforcement. At 7.9 at. % B the hardness is maximal up to 500°C (~2.5 GPa at 500°C that is by 2.5 times higher than for the initial alloy). At 800°C the hardness of alloys is found to be 0.55 GPa.

The investigation of the influence of aluminium on the mechanical properties was carried out for two groups of alloys, eutectic and hypoeutectic containing 7.5 and 5 at.% B, respectively. The marked growth of hardness for the eutectic alloys as well as for the hypoeutectic ones was shown with the alloying. The difference in the hardness of the alloys with 12.8 at.% Al and the binary $Ti_{92.5}B_{7.5}$ eutectic is about 2 GPa in the temperature interval from RT to 600°C. At 800°C this difference is smaller (~0.5 GPa) but by four times higher in comparison with the base binary alloy. The difference between the eutectic and hypoeutectic alloys is little. The alloys, containing 30 and 40.5 at. % Al have the phase compositions $\alpha_2 + \alpha + TiB$ and $\alpha_2 + \gamma + TiB_2$, respectively, providing maximal values of hardness.

The contributions of Al and B alloying additions to alloys strengthening were analyzed basing on the hardness. The boride reinforcing was shown to be significant up to 500°C, while the alloying by aluminium causes the growth of hardness in all the temperatures under investigation and elevation of the starting temperature of sharp softening by 100°C.

**Acknowledgement.** This research was suported by the Air Force Office of Scientific Research (USA) under the Project P-060.

# SOLIDUS SURFACE PROGECTION OF THE Al-Rh-Ti SYSTEM IN THE RANGE OF COMPOSITIONS 0-50 AT. % Rh

**Korniyenko K.Ye., Khorujaya V.G., Martsenyuk P.S.**
Frantsevich Institute for Problems of Materials Science Ukrainian National Academy of Science, Kyiv, Ukraine

Development of new advanced materials for special purposes attracts researchers attention to objects capable of forming so-called quasicrystals. Unique structure of these compounds determines their special mechanical physical, and chemical properties. Quasicrystals are phases of variable composition which exist within a limited temperature range and may undergo various transformations. Search for quasicrystals is impossible without investigation of phase diagrams of systems in which their formation is expected. From literature data it is known that binary systems based on aluminium containing d-metals form quasicrystals. Thus, it is expedient to search for quasicrystals in three-component and more complex systems based on aluminium with d-metals.

The present work is concentrated on investigation of phase diagram of the Al-Rh-Ti system, in particular, its solidus surface in the range of compositions 0-50 at.% Rh.

The alloys of the system were prepared from the starting components in the arc furnace with a nonconsumable tungsten electrode on a water-cooled copper hearth in an atmosphere of purified argon. After measuring temperatures of start of malting by methods of differential thermal analysis and Pirani & Alterthum the alloys were annealed at a subsolidus temperature. Annealing was carried out either at the temperature of 20-30°C below solidus of the alloys in the "Solidus-1" setup or 50-70°C below their solidus in the SShVL furnace. The alloys annealed at subsolidus temperatures were investigated by methods of X-ray diffraction, metallography and electron probe microanalysis.

On the basis of obtained results solidus surface projection of the Al-Rh-Ti system in the range of compositions 0-50 at.% Rh was constructed.

It was shown that a continuous series of solid solutions exists between isostructural with CsCl phases AlRh and the high-temperature modification of the TiRh phase (δ-phase).The limits of the δ-phase homogeneity range connects the corresponding points in the binary systems.

A wide homogeneity range based on β-titanium is also observed.

Solubility of the third component in the binary compounds that are formed in the limiting binary systems is either absent or does not exceed 3 at.%. At subsolidus temperatures existence of two ternary compounds of stoichiometric compositions of $(Ti,Al)_6(Ti,Rh,Al)_{23+1}$ (G-phase) with the $Th_6Mn_{23+1}$ structure type and $(Ti,Al,Rh)(Ti,Rh,Al)_3$ (ι-phase) with the $Ti_2Ni$ structure type is established. The G-phase is found to have a wide homogeneity range (~10 at.% Al and Ti and ~5 at.% Rh width). It is in equilibrium with virtually all binary phases as well as with δ-, ι-phases and with <β-Ti>. Eight isothermal three-phase fields are observed on the solidus surface containing the G-phase. These fields are constituents of four-phase invariant equilibria containing liquid. Unlike the G-phase the ι-phase was not found to have a homogeneity range and its participation in four-phase equilibria is insignificant as compared with the G-phase.

# CONDUCTANCE OF DIRECTIONALLY CRYSTALLIZED EUTECTIC ALLOYS OF $B_4C$-$Me^{IV}B_2$ SYSTEMS

**Loboda P.I., Bogomol Yu.I.**
National Technical University of Ukraine "KPI", Kiev, Ukraine

Boron carbide has a good compatibility with boron cathodes and is a promising material for manufacturing of construction elements (heaters, cathode holders, etc.) cathode-heating units which are exploited under conditions of high temperature gradients (1000 degrees/cm.), high-rate heating and cooling and must provide a determined level of conductance. Boron carbide obtained through technologies of powder metallurgy is, as a rule, characterized by the low strength, high brittleness and its level of admixtures and conductance is difficult to control. Significant improvement of mechanical properties could be achieved through reinforcing by filaments of other refractory compounds. Since the interaction of boron carbide with transition metals borides is described by eutectic diagrams of state, so in this work the possibility to obtain composites on the base of boron carbides by a directional crystallization from melts was studied. Microstructure and conductance of directionally crystallized alloys of $B_4C$-$MeB_2$ systems (where Me-Ti, Zr, Hf) were investigated.

Crystals of eutectic alloys were grown in an atmosphere of helium following the crucible free zone melting of powder materials with a moving solvent of admixtures [1] in "Crystal-206" induced device equipped with a high pressure (10 MPa) chamber.

Powders of boron carbide, titanium diborides, zirconium and hafnium of 98.2-98.4 % purity were used as initial reagents. Amorphous boron (99.8 %) served as a solvent of admixtures, which was introduced into the powder by means of a mechanical mixing. Unsintered samples of 35-40% porosity pressed with adding of a bonding agent-2.5 % solution of polyvinyl alcohol in water were exposed to the zone melting.

Analysis of the microstructure and phase composition showed that crystals of directionally crystallized eutectic $B_4C$-$TiB_2$, $B_4C$-$ZrB_2$ and $B_4C$-$HfB_2$ are a matrix of transition metal rigid solution into boron carbide reinforced by rods and sheets of transition metal diborides.

Resistivity was measured by the potential method. It was found out that directionally crystallized eutectic alloys have 10 times higher resistance than that of similar in terms of composition hot-pressed composites and two orders lower (table) than calculated by the generalized conductance formula of composites with the matrix structure:

$$\lambda = \lambda_0 \frac{\lambda_1 \cdot (1+2\theta_1) + 2\lambda_0(1-\theta_1)}{\lambda_1 \cdot (1-\theta_1) + \lambda_0(2+\theta_1)} \qquad (1)$$

According to [3] for directionally crystallized eutectic alloys, when resistance measured along the direction of parallel crystallization, the current flowing through two phases is different (Kirhgoff's law) and resistance of material could be calculated taking into account the dependence:

$$\rho = \rho_1\rho_2/((1-\varphi_2)\rho_2 + \varphi_2\rho_1) \quad (2)$$

Results of calculations for systems studied correlate with experimental ones in order of value and not entirely take into account peculiarities of microstructures of directionally reinforced composites. Sharp drop of conductance of directionally crystallized alloys is related to an elongation of diboride impurities in the direction of the measurements. Accordingly to the generalized conductance theory a median element of the structure of directionally crystallized alloys could be two rods or sheets of boron carbide and diboride with the same dimensions and connected parallel. Since there are in three orders difference in conductance of diboride rods from boron carbide then, when they assembled parallel, conductance of a median element will be defined by the high conductance of the diboride phase. In case of hot-pressed composites the median element is a layer of $B_4C$ with homogenously distributed equally axed diboride grains which are separated in the direction of the current flow by the same thickness interlayer of a phase with the minimum conductance and are three resistors. Two of which are connected parallel and the third having the highest resistance-successively. Significant divergence of the calculated and

experimental values of hot-pressed composites evidently is due to their low purity.

In directionally crystallized alloys a role of the third successively assembled element is played by $B_4C$ thin interlayer between diboride impurities the presence of which was neglected by formula (2). Calculations by the median element with a thin and purified during the zone melting interlayer of the matrix phase allowed to obtain values of resistivity of composites closer to experimental ones.

Lower conductance of $B_4C$-$HfB_2$ composites in comparison with $B_4C$-$TiB_2$ and $B_4C$-$ZrB_2$ is in a good agreement with data of microscopic analysis and is due to the presence of single phase wide interlayers of $B_4C$ matrix phase.

Thus, it has been established that the resistivity of the directionally crystallized eutectic alloys rises in $B_4C$-$ZrB_2$ $\rightarrow$ $B_4C$-$TiB_2$ $\rightarrow$ $B_4C$-$HfB_2$ row and is defined by homogeneity of distribution and morphology of diboride impurities. Resistance of composites are commensurate with that of graphite (0,0014 Ohm*cm) that permits to use quasibinar eutectic alloys of $B_4C$-$Me^{IV}B_2$ systems for manufacturing of cathode units resistive elements of electron-ray assemblies of devices and facilities of technological purpose.

Table- The resistivity of the directionally crystallized eutectic alloys of $B_4C$-$Me^{IV}B_2$ systems.

| Eutectic alloys | Relative density, % | Diboride content, % | Resistivity, Ohm*cm. | | | |
|---|---|---|---|---|---|---|
| | | | Calculated by the median element | Calculated by formula (1) | Calculated by formula (2) | Experimental |
| $B_4C$-$TiB_2$ | 99.85 | 23 | 0.00112 | 0.053834 | 0.004774 | 0.00050 |
| $B_4C$-$ZrB_2$ | 99.04 | 23 | 0.000129 | 0.052866 | 0.000563 | 0.00019 |
| $B_4C$-$HfB_2$ | 94.86 | 23 | 0.00134 | 0.052871 | 0.000584 | 0.00117 |
| $B_4C$-$ZrB_2$ (hot-pressed) | 70 | 23 | - | - | | 0.0000125 |

## Literature

1. Лобода П.І. Зонная плавка порошковых, тугоплавких материалов // Проблемы специальной металлургии (Вакуумно-индукционная плавка). -1999. -№2.- с.59 - 67.

2. Скороход В.В. Порошковая металлургия тугоплавких металлов и соединений. – Киев: Техника. – 1982. – 147 с.

3. Курц В., Зам П.Р. Направленная кристаллизация эвтектических материалов. – М: «Металлургия». – 1980. – С.193-194.

# THERMODYNAMIC RESEARCHES FOR THE DECISION OF TECHNOLOGICAL PROBLEMS OF METALLURGY AND WELDING PRODUCTION

**Stukalo V.A., Sudavtsova V.S., Bieloborodova O.A.**
Department of Chemistry of Kyiv National Taras Shevchenko University, 64 Volodymyrska St., 01033 Kyiv, Ukraine

Development of new metallurgical processes, the choice of rational modes of synthesis of stuffs with beforehand specified by properties is impossible without knowledge of the fundamental thermodynamic characteristics. During many years on faculty of physical chemistry of the Kiev Taras Shevchenko University studied thermodynamic properties of alloys, the majority from which will utillize on different productions.

So, on faculty of electrometallurgy of the Dnepropetrovsk metallurgical academy the technology of ferroaluminum manufacturing was developed which will be utillized for deoxidation and doping high-quality of steel with the minimum contents of non-metallic incorporations. In this connection we investigated melts Ferri lactas with aluminium.

For definition of activity of aluminium in binary alloys with iron the method of allocation of components between two not blending phases of fluid is chosen. The affiliation of the obtained data with the thermodynamic characteristics of alloys of system Al-Fe, established with the help of a method EMF, has allowed to present to activity of aluminium in all range of compositions.

The development of effective flow diagrams of production low-phosphorous manganous alloys should be based on knowledge of physico-chemical laws underlying these processes. The efficacy of process of dephosphorization in manganous ferroalloy is determined from activity by thermodynamic properties and first of all by activity of phosphorus in those systems.

We carried out experimental research of activity of phosphorus in systems Mn-P, Mn-Si-P, Mn-Si-P-C at the contents of phosphorus close to its concentration in industrial manganous ferroalloys. In quality method of research the dynamic method of carrying gas allowing to determine steam tension of material, saturant was chosen at some temperature gas which is taking place above it. The results of our researches show on necessity of building at dephosphorization of manganese of conditions promoting weakening of forces of connections of phosphorus in liquid solutions. It can be achieved by introduction in a melt of elements promoting augmentation of quotients of activity of phosphorus. Those have appeared Carboneum and silicon. Thus, dephosphorization of alloys on the basis of manganese it is expedient to carry out at enough high concentrations in them of silicon and Carboneum, that corresponds on composition industrial silicomanganese.

For building materials with the special properties, which are characterized as thermally sound and undislocation stuffs with high mechanical hardness, stability to action of high temperatures, chemical mediums, will be utillized rare-earth metals and yttrium. The special place among alloying modifiers borrow alongside with metal yttrium.alloy on the basis of nickel.

For development of the production technology of alloys, which are alloying modifiers, deoxidizers became, the thermodynamic characteristics of melts of systems Ni-Y, Y-Si, Ni-Si and Y-Ni-Si are investigated. As a method of research the method of high-temperature calorimetry is chosen.

In binary systems (Y-Ni, and is especial Ni-Si and Y-Si) the essential negative deflections from theoretical behaviour are observed, that is explained by presence in them of the near order such as chemical combination. The essential negative deflections are peculiar also to all alloys of ternary system Y-Ni-Si.

For development of physico-chemical bases of an electrothermal method of reception of silumin from domestic raw material, the items of information on influence of admixtures of series of metals are necessary which contain in physical aluminium ores, on the thermodynamic characteristics of alumosilicic alloys. We investigated influence of the additives of titanium, Ferri lactas, nickel and copper on thermodynamic activity of aluminium in liquid silumin. The additives of metals result in depressing thermodynamic activity of aluminium in alumosilicic alloys. From the investigated additives (Fe, Ni, Cu) the greatest influence renders copper.

The quality of metal products, mould pieces, joint welds substantially depends on the contents in

them of gases, which harmful action is developed in formation of pores and fractures, sharp deterioration of plasticity, ductileness. In this connection the large value is got by operations of deoxidation, dephosphorization, desulphurations etc. For all these processes especially important the search of elements is, which introduction in a melt essentially would depress the contents and according to activity of gases, sulfur, phosphorus and other admixtures, not worsening thus is warm, electric conductivity, mechanical and other properties.

The results of our thermodynamic researches have allowed to prove an opportunity and to execute an evaluation of deoxidizing and desulphurating properties of elements of series of metals for multicomponent alloys on a basis Ferri lactas. The data on parameters of interaction $l_0^M, l_S^M, h_0^M, h_S^M$ utilised for a substantiation and perfection of the schemas of doping wires, used for welding steels, copper and nickeliferous alloys.

We have determined partial molar enthalpies and activities of silicon, aluminium, manganese, chromium and molybdenum in liquid multicomponent alloys on the basis of iron by a methods calorimerty and EFM. As an example in tab. 1. are given activity of manganese. For an estimation of a degree of influence of elements on activity of manganese the parameters of interaction are designed: $\varepsilon_i^M = (\partial \ln \gamma_i / \partial x_M)_{x_M \to 0}$. It is visible, that the introduction even of small amounts of silicon, nickel, molybdenum, titan, aluminium results in change of activities of manganese. Therefore dopant of an alloy it is possible to change of activity of the given components in the certain direction.

Partial molar enthallpies of components in investigated mullticomponent alloys also essentially change with introduction in their structure of small amounts such frequently used dopant elements as Si, Al, Mo, Ti etc.

The account of thermodynamic properties of liquid multicomponent alloys on the basis of iron has allowed from scientific positions to improve the circuits dopant welding wire of a type СВ-08Г2С.

We also have studied melts of systems Ni-O and Ni-O-M. Activity of oxygen in melts Ni-O, determined by a method EFM, will be satisfactorily coordinated to the literary data, and enthalpies of mixture of melts of this system investigated by a calorimetry, have appeared more negative, than results received by other methods ($\Delta\overline{H}_0^\infty$ = -200±15 kJ/mol) (tab. 2).

Testify to presence among them both weak, and very strong deoxidizers for nickel.

As the alloys containing 36 % of nickel and 64 % of iron (invars), are widely used in chemical mechanical engineering and the requirements to their quality are very high, it is necessary to study processes allowing to reduce the contents of oxygen, sulfur and other harmful impurity in them. We investigated influence chromium, tantalus and silicon on activity of oxygen in invar alloys by a method EFM, the received parameters deoxidation are given in tab. 3.

Table 3

| M | $-l_0^M$ | $K_P$ | [% M] opt. | [% O] min | Inclus. |
|---|---|---|---|---|---|
| Cr | 1 | | 1 | $1{,}7\cdot10^{-4}$ | $Cr_2O_3$ |
| Ta | 0,32 | $4{,}5\cdot10^{-31}$ | 0,5 | $1{,}6\cdot10^{-6}$ | $Ta_2O_5$ |
| Si | 9 | $5\cdot10^{-20}$ | 0,02 | $2{,}2\cdot10^{-7}$ | $SiO_2$ |

So, the thermodynamic properties of melts of various systems allow to prove conditions of carrying out of technological processes. Therefore development of express procedures allowing quickly now is observed to measure thermodynamical coordinates in a course interesting of process, for example, activity of components with the help of electrolytic gauges.

Table 1. Activity of manganese in liquid alloys on the basis of iron at 1870 K

| Alloy | $x_{Mn}$ | E·10³ V | $a_{Mn}$ | $\varepsilon_{Mn}^M$ |
|---|---|---|---|---|
| 98% Fe-2% Mn | 0,02 | 231 | 0,0563 | - |
| 97% Fe-2% Mn-1% Si | 0,0201 | 326 | 0,0176 | -18 |
| 96% Fe-2% Mn-1% Si-1% Ni | 0,0201 | 366 | 0,0107 | -22 |
| 96% Fe-2% Mn-1% Si-1% Ti | 0,0198 | 313 | 0,0184 | 4 |
| 96% Fe-2% Mn-1% Si-1% Al | 0,0199 | 335 | 0,0155 | -3 |
| 96% Fe-2% Mn-1% Si-1% Mo | 0,0199 | 308 | 0,0226 | 24 |

Table 2. The received parameters of interaction $l_0^M$ In liquid alloys of systems Ni-O-M

| M | Cr | Mo | V | Nb | Ta | Ti | Zr | Hf | Si | Al | La | Ge |
|---|---|---|---|---|---|---|---|---|---|---|---|---|
| $-l_0^M$ | 0,1 | 0,04 | 0,54 | 0,26 | 0,12 | 0,4 | 0,7 | 6 | 0,2 | 2,3 | 8,1 | 9,5 |

# THERMODYNAMICAL PROPERTIES OF Ni-Nb-Al SYSTEM

**Sudavtsova V.S., Vovkotrub N.E.**
Department of Chemistry of Kyiv National Taras Shevchenko University,
64 Volodymyrska St., 01033 Kyiv, Ukraine

Nickel-contaning alloys with refractory metals posses temperature resistant and corrosion-resistant properties. Therefore research of thermodynamic properties such and close to them by composition ternary systems will allow to improve methods of their reception and uses. By High temperature isoperibolic calorimetry [1] was studied binary boundary Al(Ni)-Nb system and four radial sections of ternary Ni-Nb-Al system at 1870-1900 K.

Some thermochemical properties of alloys, at which study in liquid bath entered niobium were specified by advanced in calorimetry experiment using method conserving in sample heating and fixation ΔT with thermobattery [2]. The accuracy of measurement $\Delta H$ and $\Delta\overline{H}_i$ in the advanced technique made ±1 and ±7%, accordingly. The defined values $\Delta H$ and $\Delta\overline{H}_i$ for the studied binary and ternary systems are given in table 1.

Table 1

Thermochemical properties of liquid binary Al(Ni)–Nb systems at 1900 K (in kJ/mol)

| Al-Nb | | | | | | | | | | |
|---|---|---|---|---|---|---|---|---|---|---|
| $x_2$ | 0 | 0.1 | 0.2 | 0.3 | 0.4 | 0.5 | 0.6 | 0.7 | 0.8 | 0.9 |
| $-\Delta H$ | 0 | 2.4 | 4.3 | 6.5 | 6.6 | 6.2 | 5.6 | 4.6 | 3 | 1.6 |
| $-\Delta\overline{H}_i$ | 16 | 29 | 20 | 13.5 | 7 | 4.5 | 2 | - | 1 | 0.5 |
| Ni-Nb | | | | | | | | | | |
| $x_2$ | 0 | 0.1 | 0.2 | 0.3 | 0.4 | 0.5 | 0.6 | 0.7 | 0.8 | 0.9 |
| $-\Delta H$ | 0 | 15 | 23 | 27 | 28 | 28 | 25 | 21 | 11 | 8 |
| $-\Delta\overline{H}_i$ | 183 | 126.5 | 70 | 50 | 30 | 22 | 13.3 | 9 | 6.6 | 3 |
| Ni-Nb-Al | | | | | | | | | | |
| $x_3$ | | 0.1 | 0.2 | 0.3 | $x_3$ | | 0.1 | 0.2 | 0.3 | |
| $-\Delta H(\frac{x_{Nb}}{x_{Al}}=\frac{0.1}{0.9})$ | | 22 | 35 | 44 | $-\Delta H(\frac{x_{Ni}}{x_{Ni}}=\frac{0.1}{0.9})$ | | 43 | 39 | 35 | |
| $-\Delta H(\frac{x_{Nb}}{x_{Ni}}=\frac{0.1}{0.9})$ | | 18 | 26 | 38 | $-\Delta H(\frac{x_{Ni}}{x_{Ni}}=\frac{0.1}{0.9})$ | | 44 | 43 | 41 | |

Using enthalpy of formation for $NbAl_3$ (29,7 kJ/mol) [3] and defined by us $\Delta H$, we have estimated $\Delta H$ of melts of Al-Nb system in all interval of compositions. In a similar way have simulated thermochemical properties of melts of liquid Ni-Nb systems. As can be seen from tab. 1 the niobium and nickel liquid alloys are characterised by strong interparticle interaction between different by sort atoms, that correlates with behaviour them in a solid state. Agrees with the state diagrams of a Ref. [4], Ni and Nb form a number of intermetallics. The studied ternary Ni-Nb-Al alloys also has been formed intermetallics with heat allocation. To obtained thermochemical property in all interval of compositions, we have calculated them by Toop equation from data known for binary boundary systems. It have been established, what exactly this equation allows to define $\Delta H$, close to experimentally. Enthalpy of mixing curve levels of Ni-Nb-Al system at 1900 K are given in figure.

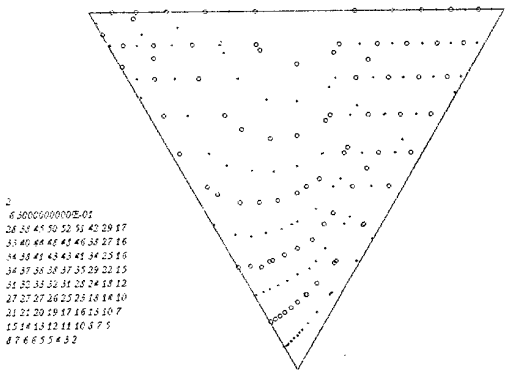

It is clear, that the minimum on a enthalpy of mixing surface is necessary on mono-aluminide of nickel, that it is no wonder, as the alloys Ni with Al are formed it with very large exothermal effects. In Ni-Nb-Al system it is more probable than all is not formed of ternary stable compounds. From $\Delta H$ in Ni-Nb-Al systems in section $x_{Ni} / x_{Al}$ = 1:1 have calculated thermochemical properties of liquid alloys of Ni-Al-Nb system. They have appeared positive, that testifies to stronger energy of connection in Ni-Al, than Ni-Nb and the more so Nb-Al. For reception by more complete TD information about liquid Ni-Nb system we have studied of activity Nb up to $x$Nb = 0,1 at 1900 K with using EMF of a concentration circuit:

$Nb\text{-}Nb_2O_5 \mid ZrO_2 - Y_2O_3 \mid (Ni_x\text{-}Nb_{1-x})\text{-}Nb_2O_5$

Activity Nb has appeared found smaller, than for ideal solutions (table 2).

Table 2

Activity Nb in liquid Ni-Nb system at 1900 K

| $X_{Nb}$ | 0.1 | 0.2 | 0.3 | 0.4 | 0.5 | 0.6 | 0.7 | 0.8 | 0.9 |
|---|---|---|---|---|---|---|---|---|---|
| $A_{Nb}$ | 0.01 | 0.018 | 0.035 | 0.076 | 0.21 | 0.37 | 0.56 | 0.71 | 0.87 |

In the field of balance a liquid solution $Nb_{solid}$ we have calculated $a_{Nb}$ from coordinates of a liquidus line by technique developed by us in Ref. [3], and in the field of existence intermetallics by advanced Hauffe-Wagner method. All results correlate among themselves and testify to negative deviations from the Raoults law. The introduction of small amounts of aluminium in investigated nickel-niobium liquid alloys results to small decreasing of activity of niobium, that confirms defined by calorimetry thermochemical properties.

Refetrences:


1. Sudavtsova V.S., Sharkina N.O. Interaction in Fe-Hf and Ni-Hf Melts // Unorganic Materials. – 1998. - V.34. – №12. – P.1231-1232.
2. Sudavtsova V.S., Kudin V. G. Thermodynamic Properties of Si-Ge and Si-Sn Melts // Unorganic Materials. – 2001. – V.37. - №4. – P. 319-320.
3. Sudavtsova V.S., Kudin V.G. Prediction of Same Thermodynamic Properties of Binary and Ternary Alloys from Phase Diagrams // Metalls. – 1999. - № 4. – P. 129-134.

# THERMODYNAMICAL PROPERTIES OF BINARY AL (IV-ELEMENT)-3D METAL

**Sudavtsova V.S., Podarevskaya O.V.[1], Zhuravlev V.S.[2]**
Department of Chemistry of Kyiv National Taras Shevchenko University, 64 Volodymyrska St., 01033 Kyiv, Ukraine
[1]Ukranian State University of Food Technology, 68 Volodymyrska St., 01033 Kyiv, Ukraine
[2]Frantsevitch Institute for Problem of material science NAS of Ukraine, 3 Krzhizhanovsky St., 03142 Kyiv, Ukraine

Silicon-, Germanium- and Aluminium-containing alloys are widely used as semiconductors, steel deoxidisers and modifiers. Tin is a basis of various solders. Therefore thermodynamic properties of silicon and tin alloys are of significant practical interest. However, as Si and Sn occupy IVb-subgroup of Periodic Table, they should find out close similarity and distinctions caused dimensionality factor. Thermochemical properties of alloys based on Si and Sn, stannides of Sc, Nb, Ti are determined by differ variants of calorimetry method. In a fig. 1 dependencies $\Delta \bar{H}_{d\,Me}$ in the liquid Si and Sn are represented

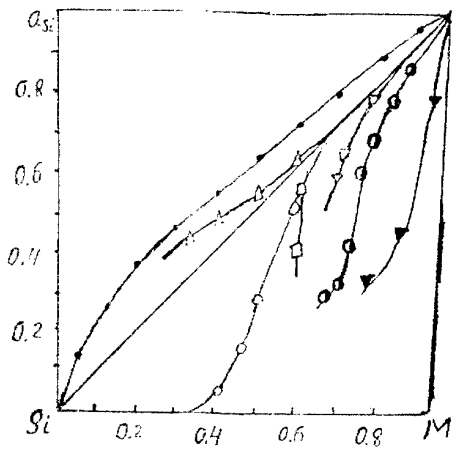


Fig. 1. First partial enthaphy of mixing of 3d-, 4d-, 5d-metals in Si (a) and Sn (b).

It can be easy observed, that the dependencies are close among themselves, but magnitude of thermal effects in Si-based liquid alloys are exothermal significantly, which is testifies about one stronger relation of Silicon to d-transition metals. For liquid alloys of noticed element with refractory metals it was possible to investigate only limited concentration area. So, we estimated thermochemical properties of the characteristic melts of Si(Sn), using standard enthalpy of formation for silicides and stannides. All data were defined by $\Delta_f H$ well correlate with experimentally one. In a fig. 2 are compared $\Delta \bar{H}_{3d\text{-}Me}^{\infty}$ of Si(Sn) with refractory metal in a wide range of compositions.

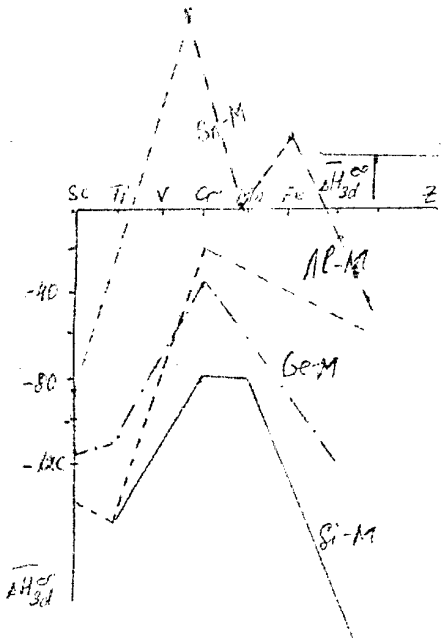


Fig. 2. $\Delta \bar{H}_{3d\text{-}Me}^{\infty}$ of Si(Sn) with refractory metal in a wide range of compositions.

It is stated, that all of them are high exothermal. Component Activity for considered alloys are determined by EMF with liquid or solid electrolyte. For refractory alloys are calculated activity and other thermodynamically properties using liquidus curves coordinates via us-developed technique. In the table are presented activity of components in most interesting labor-consuming for researches systems.

It has been established, that in Silicon and Tin melts with transition metals activity of component posses large negative deviations from ideal solutions. For alloys with intransitive metals was defined that activity of Si, Sn and other components characterised by positive deviations from the Raoults law.

Analysing dependencies $\Delta \bar{H}_{d\text{-}Me}^{\infty}$ and ΔH in binary Me-d-Me melts from serial numbers in Periodic Table of transitive metal, it is possible to show that they differ. And the thermodynamic properties of alloys containing 4d- and 5d-metal are more similar among themselves, than alloys of 3d-metals. As well known, the melts properties are now most completely investigated, especially for that one of which component is the 3d-metal, we in fig. compared dependencies for $\Delta \bar{H}_{d\text{-}Me}^{\infty}$ =f(z) for binary liquid alloys (Al, Si, Ge, Fe, Ni, Cu, and Sn)-3d-Me. As can be seen (see fig.) similar dependencies for binary liquid alloys of Fe and Ni, Al, Si, Ge, Sn, Cu. As to first two groups of alloys, similarity in their properties it is no wonder, as it is traced and on a number of other properties. Unexpected similarity in thermochemical properties of binary systems (Cu, Sn) -3d-metal was shown. We consider that it is a consequence for series of factors, by major of which is 3d-orbital filling. At formation of binary alloys with 3d-metals copper and tin plays role of electron donors also turn to ions close on the size ($Sn^{4+}$ - 0,074 nm; $Cu^{2+}$ - 0,07 nm).

Unexpected the distinction in thermochemical properties of binary alloys of systems of 3d-metals with silicon, germanium and tin is also. From a fig. it is clear, that liquid alloys Sn-3d-Me are characterised by smaller thermal effects of alloy formation, that it is more probable than all is caused large ionic radius of tin (0,074 nm) in comparison with those for silicon (0,039 nm). So, having established groups of alloys Me-3d-Me with similar properties, we can use it for forecasting properties of alloys containing 4d- and 5d-metal, on the basis of the limited quantity of experimental data.

It is known, that in liquid double alloys p-metals-(Fe, Co, Ni) the interparticle interaction amplifies in row: Fe→Co→Ni. This fact is explained by a structure 3d-orbital of metals of iron subgroup. Nickel on 3d-orbital has nine electrons; therefore at melt formation it will aspire to electron grasp and to pass in a stable state. As the thermodynamic properties of alloys Mn and Cu are now known, we have compared properties of double alloys of systems Al (Si, Ge, and Sn) - Mn (Fe, Co, Ni, and Cu). In tab. we result differences of radiuses, electron negativity of components of considered alloys, and also meaning for ΔH and $-\Delta G^{ex}$ in extreme points.

From the table it is visible, that the amplification of interparticle interaction is observed in the following lines:

1. Al-Cu ≈Al-Mn → Al-Fe → Al-Co → Al-Ni
2. Si-Cu → Si-Mn → Si-Fe → Si-Co → Si-Ni
3. GeCu → Ge-Fe → Ge-Mn → Ge-Co → Ge-Ni
4. Sn-Fe → Sn-Co → Sn-Cu → Sn-Ni → Sn-Mn

It is visible, that in series 1,2 interactions least in copper alloys, and at transition from Mn to Ni it grows. It is caused by a structure 3d-orbitals of considered transitive metals and dimension factors of related Al and Si. In the third series the dependence differs from those in 1,2 numbers (Mn and Fe change possition), and in alloys of tin it completely not such, as in 1, 2 slightly. Taking into account given in tab. data, it is possible to approve, that on interaction in alloys Fe-Sn and interatomic interaction renders influence of dimensions factor and electrochemical factor. Thermodynamical properties of Pb-3d metals alloys practically unknown, but taking into account phase equilibria we may stated that character of interaction in these alloys will be similar as tin-based one.

So, for the forecast of properties of binary alloys consisting of transitive and intransitive metal, it is necessary except for a structure 3d-orbital to take into account dimensional and electrochemical factors.

Table

The sizes both electrochemical factors and melts thermodynamic properties of systems intransitive metal - transitive metal

| System | Al-3d-Me | | | | Si-3d-Me | | | |
|---|---|---|---|---|---|---|---|---|
| d-Me | Δr | Δε | -ΔH | $-\Delta G^{ex}$ | Δr | Δε | -ΔH | $-\Delta G^{ex}$ |
| Mn | 0,12 | 0 | 18 | 12,2 | 0,07 | 0,4 | 33 | 21 |
| Fe | 0,16 | 0,22 | 20 | 12,6 | 0,07 | 0,1 | 40 | 19 |
| Co | 0,17 | 0,3 | 37 | 0,2 | 0,08 | 0,1 | 49 | 29 |
| Ni | 0,19 | 0,3 | 54 | 21,4 | 0,1 | 0 | 52 | 34 |
| Cu | 0,15 | 0,2 | 18 | 17 | 0,06 | 0,2 | 14 | 8 |
| System | Al-3d-Me | | | | Si-3d-Me | | | |
| Mn | 0,08 | 0,3 | 0,17 | | 0,20 | 0,3 | -6 | -1,2 |
| Fe | 0,12 | 0 | 10 | | 0,24 | 0 | 7,5 | 5,3 |
| Co | 0,13 | 0 | 22 | | 0,25 | 0 | -0,6 | -0,4 |
| Ni | 0,15 | 0,1 | 32 | | 0,27 | 0,1 | -4,6 | -4,1 |
| Cu | 0,11 | 0,3 | 8 | | 0,23 | 0,3 | -1,0 | -6,0 |

# A NEW APPROACH TO QUANTITATIVE EVALUATION OF DANGER OF SHALLOW CRACKS

**Kotrechko S.O., Meshkov Yu.Ya., Popovych V.O.**
Institute for metal physics, Kyiv, Ukraine

Shallow cracks are of interest to researches because the methods of classical fracture mechanics fail to give adequate estimates of their danger. At present, the analysis of the distributions of stresses and plastic strains at the tip of a shallow crack in the continual approximation seems to be a quite urgent problem [2]. The main difficulty encountered in its solution is connected with the fact that the continual approach is inapplicable to the description of plastic strains in the region whose characteristic size is comparable whith the grain size.

The aim of the present work is to establish a quantitative estimatte of the degree of danger caused by shallow cracks and formulae requirements on the properties of the metal guaranteeng that these defects are unable to initiate brittle (quasibrittle) fracture.

The proposed approach is based on the concepts described in [4]. According to these concepts, the expression for the generalized parameter $E_m$ characterizing the embritting action of an arbitary stress concentrator has the form

$$E_m = \frac{j(e_i^p / e_y)^n}{K_{ss}}, \qquad (1)$$

where $j$ is the stiffness of the stressed state created by the concentrator, $j = \sigma_1/\sigma_i$, $\sigma_1$ is the maximum level of tensile stresses at the tip of the concentrator, $\sigma_i$ is the intensity of stresses, $e_i^p$ is the intensity of plastic strains at the point of initiation of fracture, $e_y$ is the level of residual strains at the yield point, $n$ is the strain-hardening index of the metal, $K_{SS}$ and is the ratio of the local fracture stress $\sigma_C$ of the metal at the tip of the concentrator to the minimum fracture stress $R_{mc}$ under uniaxial tension.

In the case of quasibrittle fracture, we have

$$E_m = K_t, \qquad (2)$$

where $K_t$ is the coefficient of toughness of the metal,

$$K_t = R_{mc}/\sigma_Y, \qquad (3)$$

$R_{mc}$ is the minimum stress of brittle fracture of the metal under uniaxial tension. and $\sigma_Y$ is the yield limit of the metal.

As a specific feature of quasibrittle fracture initiated by shallow cracks and other small defects under the conditions of quasistatic loading. one can mention the fact that the temperature of cold brittleness $T_{cb}$ for specimens with defects of this sort is quite low, i.e., these defects cannot be responsible for the loss of the load-carrying ability of the specimen ($\sigma_N < \sigma_Y$) but may lead to a loss of plasticity of the metal . Therefore, for shallow cracks, one must know the value of $E_m$ at the temperature of zero plasticity $T_{zp}$.

The experimental values of $E_m$ for $T_{zp}$ were determined according to a procedure similar to that described in [4] for structural concentrators. For this purpose, we performed low temperature testingof smooth cylindrical specimens (without consentrators) for uniaxial tension.

We see that, despite a fairly broad range of values of strength of the investigated materials, the quantity $E_m^{\exp}(T_{zp})$ varies within a quite narrow range (from 1.62 to 1.88). The changes in this parameter are explaned by the different susceptibilities of 60 and 12KhN3MA steels to strain hardening. According to Eq. (1), this reflects the general law of fracture of metals under the conditions of stress concentration experimentally corroborated by testing speciments with structural concentrators and long cracks [4]. For steels, we get:

$$E_m(T_{HP}) = \frac{j}{K_{ss}}.10^n. \qquad (4)$$

We see that $j/K_{ss}$ is practically constant and equal to1.47. This fact enables us to deduce the following approximate formula for evaluation of the embrittling action of shallow cracks at the temperature of zero plasticity:

$$E_m(T_{HP}) \approx 1.47 \cdot 10^n . \qquad (5)$$

Computer modeling of samples fracture with shallow cracks for steel 60 was realized. Calculations were executed with the help of program complex for solution of boundary problems by finite element method. Criterion of yielding, which take into account features of low temperature slip in bcc lattice, was used [3]. Parameters of metal stress-strain state with shallow crack were determined. Value of ratio $j/K_{ss}$ equal 1.49, error less then 2%.

To evaluate the danger of shallow cracks quantitatively, it is convenient to use the toughness margin of a metal $K_{tm}$ [4]. This quantity is defined as the ratio of the toughness of the metal under uniaxial tension to the value of the parameter characterizing the embrittling action of the stress concentrator

$$K_{tm} = \frac{K_t}{E_m} . \qquad (6)$$

If $K_{tm} \leq 1$, then the toughness of the metal is insufficient for resisting the embrittling action of the stress concentrator. Otherwise, the metal has a toughness margin characterized by the absolute value of $K_{tm}$.

It is worth noting that products made of high-strength steels can be, as a rule, characterized as thin-walled structures. Therefore, structural concentrators and small surface technological defects play, in this case, the role of typical sources of dangerous local overstresses. In order to avoid the brittle fracture of broducts of this sort under overloads (in the case where tensile stresses can attain the value $\sigma_{0.2}$ in the entire section of the load-carrying element or in some parts of it), it is necessary that the toughness of these type of steels be not lower than $K_t \geq 1.65$. As an example of high-strength materials possessing the required proerties, one can take12KhN3MA alloyed steels with $K_t \approx$ 1.9-2.2 for $\sigma_{0.2} \approx$ 800-1000 MPa.

**Conclusions**

1.The embrittling action of shallow cracks is, to large extent, determined by the susceptibility of a metal to strain hardening and becomes more pronounced as the index of strain hardening increases.

2.Shallow cracks can be responsible for the brittle fracture of typical structural steels with a strength of 700-900 MPa and higher within the range of climatic temperatures (213-293 K).

3.To guarantee the safety of loading of load-carrying structural elements made of high-strength steels ($\sigma_{0.2} \geq 1000$ MPa), their toughness must be not lower than $K_t$=1.65.

**References**

1.M. Holzmann, I. Dlouhy and V. Kozak, "Current and perspective problems in fracture mechanics", in: Proc. Intern. Conf. FRACTOGRAPHY'97 (Kosice, Slovakia, October 1997), IMR SAS, Kosice (1997), pp. 189-199.

2. Kotrechko S.A., Meshkov Yu.Ya., Mettus G.S., Nikonenko D.I. Mechanics and physics of quasibrittle fracture of polycrystal metals at conditions of stress concentration// Probl. prochnosti 1999, №4, pp.5-16.

3. Kotrechko S.A., Meshkov Yu.Ya., Mettus G.S. Influense of triaxial stress state at yielding of iron and carbon steels// Probl. Prochnosti.-1994.-№11., pp.8-13.

# SPREADING OF CONDUCTIVE DROP OF METALLIC MELT IN MAGNETIC FIELD

**Kanchoukoev V.Z., Karamurzov B.S., Sozaev V.A.**
Kabardino – Balkarian State University, Nalchik, Russia, sozaevv@kbsu.ru

There is a lot of references dedicated wettability and adhesion interaction in solid – liquid systems. But inspite of extreme importance of investigation of wetting and spreading processes they are understood and known insufficiently yet [1] and some prominent problems of cappilarity are only in the beginning of solution. Processes of wetting and spreading of thin metallic melt over the solid surface are former and most fundamental stages of many physical and chemical phenomena accompanying modern technologies. The managing with these processes is actual task and aquires theoretical research of complicated physical – chemical phenomena and developing of novel cases of power influence on them through external fields such as thermal, electric, magnetic etc.

One should notice that even in absence of mentioned external fields the hydrodynamic conditions of liquid flux on solid surface with wetting are very complicated and determined by both properties of liquid and of solid and also by geometry of solid body and by the degree of surface roughness. Nowadays even for systems in which liquid has no chemical interaction with solid there is no approximate solution of Navier – Stokes equation which can satisfactorily describe all the steps of liquid spreading process over the surface of solid body.

The uniting of electromagnetic and surface phenomena with dynamics of liquid borns new physical phenomena giving opportunity of managing with the process of spread when exploring the flux of liquid conductive drop in electric and magnetic fields.

Let's consider the moving of metallic melt drop in the cylindrical frame of references in which $z$ axis is normal to non – deformable surface of the solid body. We suppose that drop with constant mass $m$ is moving as full phase layer in constant homogeneous magnetic field $\vec{H} = (0,0,H_z)$. The chemical interaction of contacting phases is negligible and all the natural characteristics of acting in spreading physical objects are constant. We put also following assumptions: (i) $t>>(\rho/\eta)\delta^2$ – the flux is quasistationar, (ii) $R_e=l/\delta$ - inertial effects are negligible, (iii) $V=\pi r^2\delta$ - the form of the drop is approximated as cylinder, where $\rho$, $\eta$ - density and viscosity of the drop, $l$ – the distance from the source (launch of references) to the front of liquid, $V$, $r$ – volume and radius of spreading drop, $\delta(t)$ – height of layer of coverage in time moment $t$.

Accounting made sentences and axial symmetry of flux the equation of quasistational flux of viscous conductive drop in magnetic field is apparent as

$$\frac{\eta}{\rho}\frac{d^2 v_r(z)}{dz^2} - \frac{1}{\rho}\frac{\partial P}{\partial r} + \frac{1}{\rho}\sum_i f_r^{(i)} = 0, \quad 0 < z < \delta(t), \quad (1)$$

where $\vec{U} = (v_r,0,0)$ – velocity, $P$ – pressure, $f_r$ – external force acting on unit of liquid volume in radial direction. The theoretical estimation of the influence of electric and magnetic fields on interface tensions shows that this contribution is small enough and less than $0.3\%$ for fields $\vec{E} \sim 10^5$ $V/m$ and $\vec{H} \sim 10^5$ $Oe$. That is why the influence of electric and magnetic fields on wet angle through change of surface tensions is negligible. But external magnetic field impacts on kinetics of wetting and spreading of conductive liquid on solid surface through the ponderomotive force $f_r^{(1)}$ which can be written as

$$f_r^{(1)} = \frac{1}{c}\left[\vec{j}\times\vec{H}\right]_r = -\gamma\left(\frac{H_z}{c}\right)^2 v_r(z), \quad (2)$$

where $\gamma$ - specific conductivity, $\vec{j}$ – current density, $c$ – rate of light distribution.

Acting on liquid layer through decreasing of free surface energy volume external force $f_r^{(2)}$ can be shown as

$$f_r^{(2)} = -\frac{\partial(\Delta W_s)}{(m/\rho)} = \frac{\pi r k(\sigma_{13}-\sigma_{12})}{(m/\rho)}, \quad (3)$$

where $\Delta W_s$ – change of free surface energy within wetting, $\sigma_{ij}$ – free specific surface energies on the boundary of solid ($i=1$) with environment ($j=3$) and ($j=2$), $k$ – coefficient of roughness.

Pressure gradient is determined through surface tension of liquid drop with environment $\sigma_{23}$,

which can be regarded as force acting on unit of length of contact line

$$\frac{\partial P}{\partial r} = \frac{2\pi r \sigma_{23}}{(m/\rho)}. \quad (4)$$

The solution of equation (1) accounting (2-4) with boundary conditions

$$\upsilon_r(z)_{z=0} = 0, \qquad (d\upsilon_r / dz)_{z=\delta} = 0 \quad (5)$$

is visible as

$$\upsilon_r(z) = \frac{\Delta\sigma}{\eta}\left(\frac{\delta_m}{H_a}\right)^2 \frac{\pi\rho}{m\delta}\left[1 + 0.5\rho g\delta^2\right] \times \quad (6)$$

$$\times\left\{1 - \left[\exp\left(-2H_a\frac{z}{\delta_m}\right) + \exp\left(-2H_a\frac{2\delta - z}{\delta_m}\right)\right]\left[1 + \exp\left(-2\cdot 2H_a\frac{\delta}{\delta_m}\right)\right]^{-1}\right\},$$

where $H_a = (\delta_m/c)H_z(\gamma/\eta)^{1/2}$ – Hartmann number serving as a criterion of magnetic field influence on moving of conductive drop comparing with influence of viscous, $\delta_m$ – characteristic size (height of layer of coverage).

In cause of moving front of conductive drop $z=\delta$ and $\upsilon_r(z) = dr/dt$ then we have from (6)

$$\frac{dr}{dt} = \frac{\pi\rho\Delta\sigma_{ef} r}{m\eta_{ef}} = \frac{m\Delta\sigma_{ef}}{\pi\rho\eta_{ef} r^3}, \quad (7)$$

where $\Delta\sigma_{ef} = \Delta\sigma\left(1 + \frac{gm^2}{2\Delta\sigma(\pi^2\rho r^4)}\right)$,

$$\Delta\sigma = k(\sigma_{13} - \sigma_{12}) - \sigma_{23},$$

$$\eta_{ef} = \eta\left(H_a^2\left(\frac{r_m}{r}\right)^4\left[\exp\left(2\cdot 2H_a\frac{r_m}{r}\right) + 1\right]\left[\exp\left(-2H_a\frac{r_m}{r}\right) - 1\right]^{-2}\right),$$

$r_m$ - final radius of circle wetted by liquid drop.

It follows from (7) that action of gravitational force animates the spreading process that can be interpreted as moving of conductive drop with effective coefficient of spread $\Delta\sigma_{ef}$, and that action of magneic field delaying the spreading process is treated as flux with effective viscous $\eta_{ef}$. We note that meanings of mentioned effective parameters are dependent from changeable geometric sizes of drop.

Keeping in mind received equation for the rate of conductive drop spreading (7) one may promote from equation

$$j_\varphi = -\frac{\gamma}{c} H_z \frac{dr}{dt} \quad (8)$$

the current density $j_\varphi$ and using then Maxwell's equation $(c/4\pi)(dh_z/dr) = j_\varphi(r)$ according the boundary condition get the equation for the magnitude of strength of induced by moving drop magnetic field.

Similarly to Hartmann number $H_a$ let's consider quantity $k_V = \rho g\delta_m^2/2\Delta\sigma$ serving as criterion of influence of gravitational force on process of spreading of drop comparing to influence of interface forces.

Then, particularly, when $k_V << 1$ $\Delta\sigma_{ef} \approx \Delta\sigma$ and when $H_a << 1$ $\eta_{ef} \approx \eta$ and when $r(0)=0$, we'll obtain from (7) the rule of viscous drop spreading with taking into the consideration the surface forces

$$r = \left(\frac{4m\Delta\sigma}{\pi\rho\eta}\right)^{1/4} t^{1/4}$$

which is the same result of [2].

References

1. P.J. de Jen, UFN, 151,4 (1987).
2. E.A. Raud, B.D. Summ, E.D. Schukin DAN USSR, 205, 5 (1972).

# CALORIMETRIC RESEARCH OF MIXING ENTHALPIES IN LIQUID ALLOYS OF Al-Ga-Y TERNARY SYSTEM

**Dubyna V.M., Zinevich T.M., Kotova N.V., Bieloborodova O.A.**
The Kiev National Taras Shevchenko University, Ukraine

The metallic yttrium is used as construction material in nuclear reactors [1]. That is why the investigation of yttrium alloys is actual.

In the present work using a method high-temperature calorimetry [2] at 1750 K for the first time are measured partial mixing enthalpies of yttrium in liquid alloys of ternary system Al-Ga-Y along intersections with a constant ratio of aluminium and gallium atomic percent 0,85/0,15; 0,7/03; 0,5/0,5; 0,3/0,7 and 0,15/0,85 for concentration area $x_Y < 0,6$. Experiments were carried out in an atmosphere of argon of high cleanliness. In work aluminium А995, gallium of mark Гл000, yttrium marks "Дистиллат иттрия ИтМд-2" (99,999%) were used. As reference substance tungsten of class А-2 (99,96) was used. Dependence of a constant of a calorimeter on weight of melt in crucible was approximated with linear function by least – square method. Partial enthalpies for overcooled liquid yttrium were calculated using the known equations of thermal balance. High-temperature enthalpy components necessary for calculation are taken from the directory [3]. It is shown, that all ternary alloys of the investigated sections of Al-Ga-Y system are characterized by significant exothermic yttrium partial mixing enthalpy values which decrease with increase of the yttrium contents. From the received data the integral mixing enthalpies on Darken method are calculated. Enthalpy values for initial double $Al_xGa_{1-x}$ alloys necessary for the integral mixing enthalpies calculation are taken from [4].

Integral mixing enthalpies in Al-Ga-Y system are characterized by large exothermic values which have maximum at yttrium concentration about 0,4 and gradually decreases from -69 kJ/mol for intersection 0,15/0,85 up to -47 kJ/mol for intersection 0,85/0,15. On the basis of the data received for five intersections integral mixing enthalpy isolines are constructed with step of 10 kJ/mol. At low yttrium content the isolines are parallel to Al-Ga side. The area of the maximal interaction of components in system Al-Ga-Y is located near Ga-Y boundary [5]. The thermodynamic

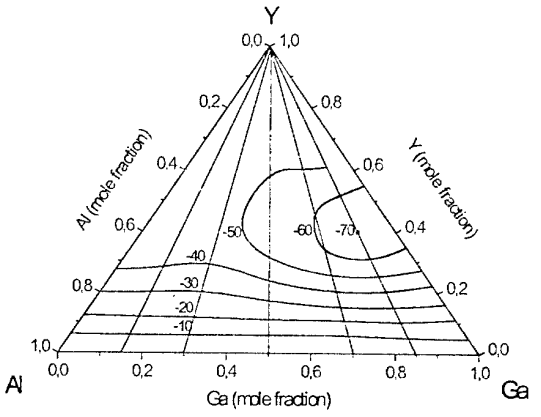


behaviour of I-Ga-Y system is determined by interaction of components in Ga-Y and Al-Y boundaries.

1. Terekhova V.F., Savitsky E.M. Yttrium. –M.: Nauka. – 1967. – P.28.
2. Nikolaenko I.V., Turchanin M.A., Batalin G.I., Bieloborodova E.A. A high-temperature calorimeter for metallic melt research // Ukr. chim. zhurn.-1987.-53.-№ 8.-p. 795-799.
3. Kireyev V.A. Methods of practical calculations in thermodynamics of chemical reactions. M.: Chimiya, 1975.-533p.
4. Batalin G.I., Bieloborodova E.A., Kazimirov V.P. Thermodynamics and structure of liquid alloys on a basis of aluminium.-M.: Metallurgy, 1983.-160p.
5. Dubyna V.M., Bieloborodova E.A., Zinevich T.M., Kotova N.V. The Mixing Enthalpies of Ga-Y Liquid Alloys at 1750 K // Abstracts of 6th International School-Conference " Phase Diagrams in Materials Science PDMS VI-2001 ". Keiv, 14-20. X.2001. - P. 89-90.

# INFLUENCE OF ULTRASONIC TREATMENT ON STRUCTURE OF ROLLED Mo SINGLE CRYSTALS

**Pronina L.N., Mazilkin A.A., Aristova I.M.**
Institute of Solid State physics Russian Academy of Sciences

The study of the deformation behaviour of b.c.c. refractory metals single crystals revealed that at a certain crystallography the initial orientation of the crystal is maintained up to very high degrees of total reduction. The structure of the so obtained monocrystalline strips and foils subjected to a high-temperature annealing was investigated in detail. It was shown, that initial crystal orientation is kept at the annealing of any duration.

There are some paper on evolution of dislocation structures in metal, ionic and semi-conductor crystals under the influence of ultrasound [1]. In the present work influence of ultrasound on structure of the deformed (001)[110] monocrystalline strips of molybdenum is investigated.

**Experimental**

Molybdenum single crystals with growth axis [110] received by an electron beam zone melting technique were used. Monocrystalline molybdenum strips were produced by rolling deformation along a (001) plane and [110] direction with the total degree of reduction of about 80%.

Samples for tests were cut out from the strips and had the sizes 20×30×0.2 mm accordingly in the directions [110], $[\bar{1}10]$ and [001]. Ultrasonic treatment was carried out using ultrasound generator of 1 kW power in frequency range 25 kHz. Standard Laue X-ray technique along with transmission electron and light microscopy was used for the control of the molybdenum single crystals structure at all stages of processing. Foils for electron microscopy investigations were prepared by jet electropolishing in 12% solution of the sulfuric acid in methanol. Study was carried out on JEM-100CX electron microscope.

**Results and discussion**

As it was shown in the previous works [2, 3] structure of the deformed molybdenum single crystals (Fig. 1) is characterized by the high dislocation dislocation density ($5 \cdot 10^{10}$ cm$^{-2}$), presence of dislocation tangles and individual

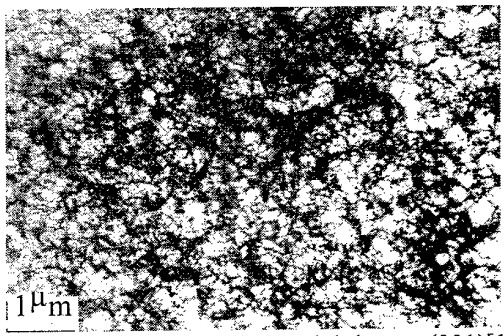


Fig. 1 Structure of the rolled molybdenum (001)[110] single crystal

mixed dislocations with Burgers vectors of **1/2*a*<111>** type distributed rather regular in crystal volume. From the results of chemical etching (Fig. 2a and 2b) it is visible, that the ultrasound initiates movement of dislocations, and that under the action of ultrasound subgrain boundaries are formed. X-ray Laue analysis approved that samples after ultrasonic processing has retained monocrystalline structure.

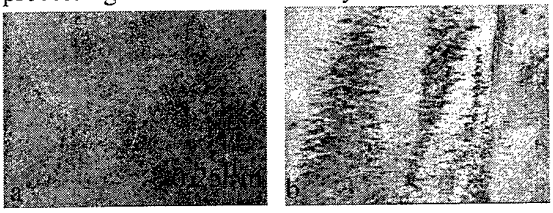


Fig 2. Micrographs of Mo single crystal surface (optical microscopy):
a. rolled single crystal
b. after ultrasonic impact

Electron microscopic studies show that ultrasonic treatment leads to significant changes in the dislocation structure of the crystal (Fig.3). Now it is characterised by areas, the density of dislocations in which has considerably decreased in comparison with initial state and makes about $3 \cdot 10^8$ cm$^{-2}$, and by extended, extensive subboundaries of a very high dislocation density, consisting from short dislocation segments. By estimations, the dislocation density in these subboundaries is not less than $10^{12}$ cm$^{-2}$. It is obvious, that exact determination of Burgers vectors at such dislocation density is impossible, however the analysis of diffraction contrast of electron-microscopic images allows to draw a conclusion, that

the majority of the dislocations in the subboundary has Burgers vector of ***a*<001>** type.

From the reported data it is obvious that at the ultrasonic impact on the deformed molybdenum samples starts the process of polygonization. A number of our works [2 – 4] is related to the processes occurring at annealing in the specified material in a wide temperature range.

Fig. 3. Structure of (001)[110] rolled Mo single crystal after ultrasonic impact

The dislocation structure is as well investigated in details. It has been shown that annealing of (001)[110] molybdenum monocrystalline strips at 2000°C resulted in polygonization while the processe of recrystallization is not observed. The structure is characterized by areas practically free of dislocations (with dislocation density $\sim 8 \cdot 10^7$ cm$^{-2}$) and of subboundaries network. Process of polygonization passes through several stages when the uniformly distributed dislocation tangles of deformed crystals are transformed to the subboondaries consisting from long, straight edge dislocations parallel to the rolling plane with Burgers vector ***a*/001/***. Molybdenum specimens remain monocrystalline with structure and orientation of an initial crystal.

Thus together with some qualitative similarity (presence in dislocation structure areas with various dislocation density after ultrasonic treatment that specifies the beginning of polygonization processes) we can approve that essential differences are observed in the character of dislocation structures. It is possible to explain the results received by an influence of a number of factors. In the crystals containing defects there are internal non-uniform fields of stress. When a harmoniously varied stress is applied to this crystal the dislocation segments should carry out the forced oscillations [5]. At combined action of ultrasound and a constant stress not only periodic but also the forward movement of dislocations can ake place resulting in their redistribution in specimen volume.

It is known also [6 – 7], that under the action of an ultrasonic wave, induced diffusion of vacancies takes place. As the dislocations serve as practically infinite sink of point defects it in turn can result in significant dislocation cross slip and climb. It is possible to assume that observed effect is connected with increasing of point defects concentration under the action of ultrasonic processing.

At achievement of the certain amplitudes of ultrasound the multiplication of dispositions can begin [1]. Each segment of dislocation net can work as a source if the stress exceeds critical value and the slip plane of a segment does not coincide with a subboundary plane. All observed subboundaries are extremely irregular. It can be a sequence of presence in a crystal of a set of dislocation sources with different length.

Thus it is possible to make the following conclusions:

1. Ultrasonic processing of rolled (001)[110] molybdenum strips, containing uniformly distributed dislocations with density of $5 \cdot 10^{10}$ cm$^{-2}$, results in essential change of the dislocation structures and to formation of polygonal subboundaries. The character of formed subboundaries considerably differs from that after annealing.
2. Physical processes of ultrasonic treatment can be connected with acoustic induced diffusion of vacancies that facilitates cross slip and climb of the dislocations.

**References**

[1]Tyapunina N.A. et al. Influence of ultrasound on crystals with defects (1999) Moscow (in Russian)
[2]Pronina L.N., Aristova I.M., Phys. Solid State, 35 (1993) 2701
[3]Pronina L.N., Aristova I.M., High Temperatures – High Pressures, 22 (1990), 9
[4]Aristova I.M., Pronina L.N., Phys. Solid State, 35 (1993), 2709
[5]Granato A., Luecke K., J. Applied Physics, 27 (1966) 789
[6]I.V. Ostrovskii, O.A. Korotchenkov, T. Goto, H.G. Grimmeiss. Phys. Reports 311, (1999) 1.
[7]Yermolovich I.B., Milenin V.V., Konakova R.V. et al. FTP 31, 4, 503 (1997) (in Russian)

# SINGULARITIES OF A INTERPLAY KINETICS FROM CO-GASES WITH IRON CATALYSTS

**Kirichenko A.G., Berenda V.V, Kolesnik N.F.**
The Zaporozhye state engineering academy, Zaporozhye, Ukraine

The originating of carbides in process of termocatalytic disintegrating of carbon gases, in particular, of white damp on catalysts from group of iron, is of interest for a number of engineering areas.

The review of the known literary data testifies to absence of the sufficient and reliable information about the gear and kinetics of passing of process of termocatalytic disintegrating of white damp on iron catalysts.

Research of a process kinetics of termocatalytic disintegrating of white damp, opening-up of reactionary gas mixtures and analysis of the obtained yields conducted on a technique described in activity [1].

As host materials the iron oxides are selected, as the preliminary researches have shown, that the overlapping of recovery process with a consequent carbonizing allows to receive a metallical phase possessing high catalytic properties [2]. In experience have utillized clean materials (iron oxide $Fe_2O_3$) and rich concentrates (Olenegorsk superconcentrate (OSK) with the contents Fe=71,39 %).

Weight of a sample in all experience made $3 \cdot 10^{-4}$ kg.

## 1. Influencing the components $H_2$ in CO-$H_2$-mix on kinetics of disintegration CO.

Process of termocatalytic disintegration CO is in stringent relation from contents of hydrogen in gas CO – $H_2$-mix.

Has appeared, that the components of hydrogen result in reactionary gas not only to essential increase of a mean velocity of a carbonizing is model, but also allow to lower temperature of process - with 560 $^0$C up to 500 $^0$C. It is necessary to mark, that the presence of hydrogen is a determinative acceleration of termocatalytic disintegration CO: this effect is exhibited at different temperatures, pressure and on different catalysts, i.e. has universal nature [3].

In figure 1 influencing the contents $H_2$ in CO-$H_2$-mix on a kinetics of recovery and carbonizing of catalyst is rotined. The nature of kinetic curves speaks about different influencing of hydrogen on stages of synthesizing - recovery and carbonizing. It is in case of the former increase of the hydrogen component with 0,9 up to 6,7 % results in ascending a velocity of recovery and reduction of an induction period, and the velocities of disintegration CO for both gas media appear practically identical. In second - the components of hydrogen (up to 18,25 %) not influencing noticeably on a velocity of recovery, slow down process of disintegration CO and deposition of carbon. The obtained experimental data can, apparently, find the explanation from a stand of the supposition of hydrocarbonyl complexes formation.

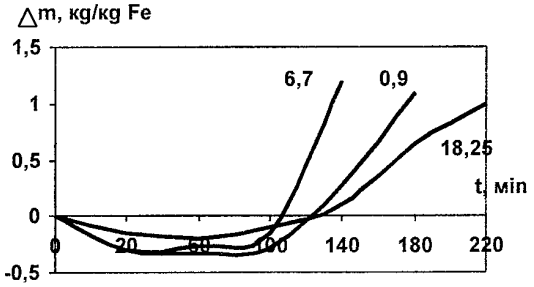


Fig. 1. Influencing of the hydrogen contents in CO-$H_2$-mix on a kinetics of recovery and carbonizing of iron catalyst (t=560 $^0$C). Digits at curves the contents of hydrogen in a mix, %.

From this point of view as a result of a hyperthermal chemosorption of CO molecules on a fissile surface of catalyst there is a formation and disintegration of composite reactive hydrocarbonyl complexes, and velocity CO disintegration is proportional to their concentration.

The interplay CO and $H_2$ during a joint adsorption with formation of hydrocarbonyl complexes is accompanied by a maintenance of electrons from a surface of catalyst on molecular orbitals of arising connection C-H. It results in essential easing of connection C-O and facilitation of its destruction with allocation of carbon atoms. The increase of hydrogen concentration in a CO-$H_2$-mix accelerates formation of fissile catalyst, that results in increase of a process velocity.

## 2. Temperature effect and structure of a catalysts material on a interplay kinetics of iron with CO - containing gas

Investigated an iron oxide $Fe_2O_3$ and OSK at temperatures 500 and 560 $^0$C, that corresponds to optimum temperatures of a carbonizing. The outcomes of experiments indicate composite intercoupling between a kinetics of process and all monitored factors, in particular, in temperature and contents of hydrogen in gas.

In figure 1 the reduction kinetics and carbonizings of

oxides are adduced in case of their processing by gas from 0,9 %, 6,7 % and 18,25 % $H_2$. The extreme nature of a velocity relation from temperature confirms a hypothesis about a development of two opposite tendencies [4] - increase of temperature conducts to increase of a velocity owing to increase of a fraction of the productive acts of CO molecules interplay with a surface of catalyst, though by virtue of thermodynamic strength increase of CO molecules quantity of these acts should decrease. At some temperature these tendencies are equilibrated - there is a maximum of a velocity.

As it is visible, $Fe_2O_3$ are restored at temperature 560 $^0$C approximately for 0,5 hours. Then the continuous enough induction period (1,5-2 hours) is observed, upon termination of which one the intensive increase of weight begins is model at the expense of CO disintegration and deposition of carbon. The induction period is characterized by appearance of carbide phases, which one at the given stage are dominating on a quantitative structure among yields of interplay. Only after disintegration of carbides the carbon-black deposition begins. The X-ray analysis of yields demonstrates, that termocatalytic disintegrating of CO begins, when the processes of recovery still completely were not completed - in yields of recovery $Fe_2O_3$ detected $Fe_3C$, $Fe_3O_4$, α - Fe.

For the step analysis of a disintegration velocity of CO decay on catalysts, the experience on a method "interrupted experiment" (fig. 2) with the consequent X-ray diffraction and microscopical analysis of the obtained yields were done.

In the table 1 the data of X-ray crystal analysis of recovery and carbonizing of a sample are shown.

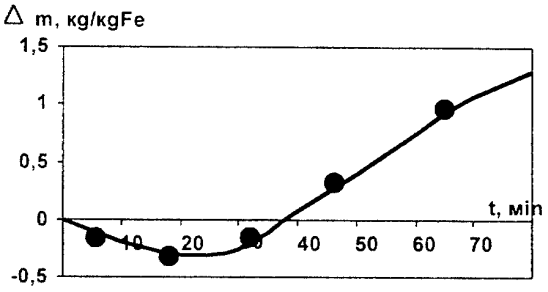


Fig. 2. A kinetics of interplay from gas ($H_2$=8,5 %) with $Fe_2O_3$ at t=500 $^0$C. Points on curves - moments of experiment discontinuing.

The table 1

Phase structure of yields of recovery and carbonizing

| Structure of a gas phase | stages | Value of an interference maximum, mm | | | | | | |
|---|---|---|---|---|---|---|---|---|
| | | $Fe_2O_3$ | $Fe_3O_4$ | α-Fe | FeO | $Fe_2C$ | C | |
| Ar | 20 мin | 25 | - | - | - | - | - | - |
| $H_2$-8,68 | 0 | 25 | - | - | - | - | - | - |
| CO-89,8 | 1 | - | 2 | - | - | - | - | - |
| $N_2$-1,41 | 2 | - | 35 | - | - | - | - | - |
| | 3 | - | 8 | - | - | - | - | - |
| | 4 | - | - | - | - | 15 | 20 | $Fe_{20}C_9$ |
| | 5 | - | - | - | - | 27 | 108 | $Fe_3C$ |

The tentative datas allow to suspect, that the essence of the gear of carbides formation is reduced to a generation of structural and electronic defects in crystal lattices, bound with dissolution of carbon in an iron matrix, change of a power condition of their surface, to creation of favourable requirements for development of adsorptive - desorptive processes and formation of carbides germs.

In general, influencing on a kinetics of CO disintegration temperature, kind of catalyst and the contents $H_2$ in CO-$H_2$ of a mix is in composite of relation: to each kind of catalyst there corresponds optimum temperature and particular structure CO-$H_2$-mix.

The combined effect of these factors has an effect that optimum requirements of carbides synthesizing are: temperature 500 $^0$C and 15-20 % $H_2$ in reactionary gas.

## List of utilised sources

1. Острик П.Н., Колесник Н.Ф. Экспериментальное исследование и методика расшифровки гетерогенного восстановления процесса в системе Fe-C-O-H / Новые методы исследования процессов восстановления черных металлов. - М.: Наука, 1974. - С. 20-23.

2. Bauklon W., Hieber G. Der Eiroflub verschiedener Metalle und Metalloxide auf die kohlenxydspaltung. // Zeit. Anorg. allgem. Chemie. - 1936. - B. 226. - h. 4. - S. 322-332.

3. Колесник Н.Ф. Термокаталитическое диспропорционирование монооксиси углерода 1. Экспериментальное исследование влияния $H_2$ $H_2O$ на скорость процесса и морфологию углеродного осадка. - Деп. в УкрНИИНТИ 1797-Ук. 87. Киев, 1987. - 29 с.

4. Колесник Н.Ф., Прилуцкий. О.В., Амосенок И.И., Кудиевский С.С. Влияние температуры на кинетику термокаталитического разложения монооксида углерода.//Изв. ВУЗов.Черная металлургия. - 1989. - №3. - С.1-3.

# AB-INITIO STUDY OF THE IMPURITY EFFECTS IN NIAL: FROM ELECTRONIC AND CRYSTAL STRUCTURE TO MECHANICAL PROPERTIES

**Medvedeva N.I.**
Institute of Solid State Chemistry, Ural Branch of RAS, Ekaterinburg, Russia

The simulation of the fracture and deformation behavior was carried out within full potential LMTO method for ternary NiAl alloys with substitutional impurities and compared with undoped NiAl. The description of brittle vs. ductile behavior was performed in terms of the Rice-Thomson approach based on a comparative analysis of two competing processes: (i) the opening of the crack and (ii) the emission of a dislocation near the crack tip. The resistance to dislocation emission at a crack tip may be measured by the maximum energy associated with the sliding of atomic planes This parameter, so called unstable stacking fault energy $\gamma_{us}$, is determined by extremal properties of the $\gamma$-surface, namely, the energy of the generalized stacking fault (GFS) associated with a rigid shift of one-half of the crystal along some direction in the slip plane.

Thus, both processes were analysed by the comparison two energy characteristics: the theoretical cleavage ($\gamma_s$) and the unstable stacking fault ($\gamma_{us}$) energies which were calculated in supercell approach as the energies required to cleave bulk crystal and to shift the part of crystal along some directions in the slip plane, correspondingly.

The calculated $\gamma_s/\gamma_{us}$ ratios are large (>10) and cleavage type of the crack propagation should be expected in NiAl, that means its intrinsic brittleness. Based on the $\gamma$-surface corresponding to the most important slip modes in NiAl, the structure of the dislocation core was constructed in the scope of the Peierls-Nabarro model with a generalized restoring force law. The <111>{110} dislocations in NiAl were shown to have compact core and are not splitted into two superpartials, in contrast with FeAl. Estimates of the Peierls stress yield the correct preferred slip systems for NiAl (<100> {110}) and for FeAl (<111> {110}).

The mechanical properties of NiAl strongly depend on the presence of the ternary additions which might be able to change such characteristics as ductility, fracture type, oxidation behavior. By now there are two ways for improving the mechanical properties of NiAl: intrinsic - when there is small percent of ternary additions -ternary alloys and extrinsic - eutectic composites where the microscopic fibers (rods) or lamellae (plates) of refractory element added to NiAl matrix. The mechanism of the impurity effects on the mechanical properties of intermetallics is rather complicated and includes direct and indirect reasons: the variation of phase equilibrium, vacancy concentration, the solubility of interstitial impurities, appearance of antisite defects, solid solution hardening and other effects. However, first of all, the alloying atom can alter the local electronic structure i.e. alter the energy characteristics which determine the dislocation mobility and bonding characteristics, which can change the fracture behavior and type of ordering and therefore grain boundary and ductile properties.

The electronic structure of NiAl doped with Ti, V, Cr, Mn, Fe, Co, Y, La and Zr additions in both sublattices was investigated with the local density FLMTO method. The peculiarities of chemical bonding for both undoped and with some ternary additions in NiAl alloy were analyzed using the LMTO-Green function method. The bonding characteristics for ternary alloys strongly depend on whether the impurity occupies Al or Ni sites. The density of states at Fermi level almost does not differ from the value for undoped NiAl for all impurities substituted at the Ni site. More striking differences in the electronic structure and bonding parameters were found for 3d-impurities substituting Al sites: they lead to a shift of Fermi level to the low energy region and to a substantial increase of $N(E_F)$. Our results indicate that Cr and Fe ternary additions might improve the mechanical properties of NiAl due to the reduction of the bond strength.

Based on the total energy calculations, we determined the preferable sublattices for a wide number of additives. We showed that the crystal relaxation around the impurity has an elastic nature and correlates with the difference between the ionic radii of substituting and host atoms. The sensitivity of preferable site energies to the crystal relaxation effects was investigated. The relaxation effect is large for Y, La and Zr additions and leads to a decrease of the preferred site energies for these

atoms. However, it does not change the sequence of additives calculated in the frozen lattice and of course the preferable sublattice. The relaxation energies for the 3d transition metals are small, but for Fe doped NiAl it might be important enough to alter the preferred site because the preference energy for Fe substitution in Fe-rich alloys is very small.

Within large supercells the calculations of cleavage ($\gamma_s$) and the unstable stacking fault ($\gamma_{us}$) were performed for Cr, Fe, Ti and Mo impurities and vacancies substituted in Al sublattice. The calculations of cleavage energies for ternary alloys showed that the appearance of Cr and Mo impurities on the fracture {110} plane of NiAl results in the increase of $\gamma_s$ and do not change the habit crack plane. The calculated cleavage energies for ternary alloys were found to correlate with surface energies of correspondent ternary metals and bond strength of NiM (M=Cr, Ti, Fe, Mo) alloys.

The unstable stacking fault energies $\gamma_{us}$ for <100> {110} slip with these impurities on sliding plane are higher than for undoped NiAl. There were a lot of experimental and theoretical efforts to use Cr for improving ductility and for modification of slip system. We found that the Cr substitutional impurity leads to lower value of $\gamma_{us}$ for a/2 <111> {100}(antiphase boundary energy-APB), but its value increase for the main deformation mode <100>{110}. The minimum of $\gamma_{us}$ was obtained for Fe alloying. The comparison of the $\gamma_s/\gamma_{us}$ ratios for ternary NiAl alloys allow to make the conclusion that according to the Rice-Thompson criteria only Fe impurity has the tendency to improve the ductility of NiAl. The vacancies result in a decrease both cleavage and shear energies, but their influence is less then the effect of impurities. One may conclude that large effects of ternary additions on mechanical properties are possibly due to the segregation of impurity atoms and indirect mechanisms.

Another perspective way for improving the mechanical properties of NiAl is the eutectic composites based on NiAl with the second phase containing refractory (Mo,Cr,V) fibers or plates. It was found that the room-temperature fracture toughness of these eutectics can achieve 2-3 times higher than for single NiAl crystals. First-principle FLMTO-calculations have been performed to study the electronic structure and fracture behavior of NiAl/Mo eutectic. The geometry of the NiAl/Mo interface was modelled with three-dimensional periodic boundary conditions containing a sequence of (5+3) layers of NiAl and Mo stacked in (001) direction. The calculations included all possible types of interface formation and the incoherency of interface was taken into account adding elastic deformations of both parts of interface.

Cleavage energies were obtained from the dependences of interfacial energy (adhesion) from the separation between NiAl and Mo parts and triclinic supercell with variable vector $c$ was considered for the calculation of shear process for a full fault vector <100>{100}. The calculations were performed for three cases: (i) only Mo part is strained, (ii) only NiAl part is strained and (iii) both Mo and NiAl parts are strained according to elastic theory. The calculated equilibrium constant of NiAl (or Mo) was used in the lateral plane for cases (i) and (ii) and the vertical positions of Mo (or NiAl) atoms were taken from the optimization of total energy for strained Mo (or NiAl) bulk. Crystal parameters of interface NiAl/Mo in case (iii) were obtained using elastic approach.

For all cases the cleavage energies (adhesion) are higher for Ni-terminated case. It is in an agreement with the results for NiAl:Mo ternary alloys, where we obtained that Mo addition substitutes for Al and therefore Mo-Ni interaction is more preferable than Mo-Al.

Taking into account the energy required for straining we obtained that the maximum of cleavage energy corresponds to the case (iii), where both parts of interface were strained. The cleavage energy for interface was obtained to be less than that for Mo and approximately equal one for NiAl. The calculated $\gamma_s/\gamma_{us}$ ratios show that the ductile properties at interface would not be worse than for NiAl. It means that ideal interface plane is not preferable place for crack propagation and the debonding is rather connected with defects and impurities. The efforts to enhance strength of interface and ductility of Mo phase by Re and Ti alloying are considered within 16-Mo-atoms supercell. For the better understanding of the mechanism of impurity influence the bulk and Young moduli were calculated for different Re (Ti) concentrations in Mo bulk.

Finally, this approach is not only able to give the information about both the electronic and crystal structures but also allows to make the prediction and explanation of mechanical properties based on the calculated cleavage and shear energies.

# COMPUTER SIMULATION OF THE CRACK NUCLEUS ORIENTATION EFFECT ON THE VALUE OF BRITTLE FRACTURE OF POLYCRYSTALLINE METALS

**Sergiy Kotrechko, Nataliya Stetsenko, Oleksandra Kucher**
G.V.Kurdyumov Institute for Metal Physics, National Academy of Sciences of the Ukraine
36 Vernadsky Blvd., Kyiv-142, 03680, UKRAINE

Conception on the crack nucleus (**submicrocracks**) as elementary defects of lattice underlies modern physical theory of brittle (quasi-brittle) fracture. Brittle fracture of solids arises from the crack nucleus unstable equilibrium and catastrophic propagation. These defects play an important role in the theory of fracture just as dislocations are the corner stone of the theory of plastic deformation. Now, regularities of crack length influence on fracture stress are studied most thoroughly. This is due to the fact that the crack nucleus length is determined by sizes of microstructural constituents in metals and alloys. The crack nucleus ensemble that forms in metal as a result of plastic deformation is characterises not only by crack lengths distribution but also by their orientation spatial distribution. Effect of distribution of the crack nucleus orientations on brittle fracture of polycrystalline metals is not yet investigated.

The aim of this paper is to show what macroscopic effects at brittle fracture may be attributed to the crack nucleus orientation distribution.

Computer simulation was carried out on the basis of model of quasi-brittle fracture of polycrystalline metals that enables to take into account peculiarities of structure and stress-strain state of polycrystalline aggregate as well as regularities of crack nucleation and catastrophic propagation in metal. The crack nucleus are sensitive, mainly, to the level of tensile stresses acting normally to crack plane. Dependence of critical tensile stress level on the value of angle between tensile stress and crack plane is the consequence of this property. The crack nucleus open in certain crystallographic planes. It means that the crack nucleus orientation distribution depends on kind and parameters of crystallographic texture. Therefore, two effect are analysed, namely:

- Increase in brittle strength of steel after tensile straining;
- Brittle strength anisotropy due to plastic deformation.

According to computer simulation findings and experimental data, brittle strength $R_{MC}$ of steel wire rises with raise in the value of its deformation. At true strains that don't exceed 0.9 decrease in the maximum value of angle between wire axis and the crack nucleus plane is the main reason for $R_{MC}$ growth. The value of this angle is predetermined by the value of texture scattering that fall with raising in plastic pre-strain. In the case of perfectly sharp texture this angle is equal to $30^0$.

At plastic deformation by upset inverse effect is observed namely brittle strength of deformed metal decreases. Physical interpretation of this effect is given in report. It is shown that texture that forms after upset gives rise to increase in the value of angle between the crack nucleus opening plane and normal stress direction [1]. Decrease in the value of critical stress of the crack nucleus unstable equilibrium is the result of above mentioned.

Anisotropy in the value of brittle strength of textured polycrystalline metal is one of the striking effects related to the non-uniform distribution of the crack nucleus orientations. It is demonstrated that texture mode of metal determines parameters and type of distribution function for the crack nucleus orientations. Findings of computer simulation of brittle fracture of iron with axial texture in longitudinal and transversal directions are represented. Calculated data were compared with experimental ones.

Effect of influence of dislocation microstresses on the crack nucleus unstable equilibrium is considered. It is shown that solely microstresses, which act within the region where the crack nucleus form and at the moment of nucleation, influence essentially the crack nucleus. It is ascertained that degree of such influence depends on the crack nucleus orientation.

**Reference**:

1. Kotrechko S. A., Dneprenko V. N. Physical nature of brittle strength anisotropy of polycrystalline metalls and alloys // Met. Phys. Adv. Tecn. 2002 To be published.

# CRITERION OF THE CRACK NUCLEUS UNSTABLE EQUILIBRIUM

**Kotrechko S., Meshkov Yu., Ovsyannikov O.**
G.V.Kurdyumov Institute for Metal Physics, National Academy of Sciences of the Ukraine, Kyiv

Crack nucleus are fundamental structural defects. They play the same role in fracture physics as dislocations in the theory of plastic deformation. Elaboration of criterion of the crack nucleus unstable equilibrium is main problem of modern fracture physics.

By conventional approach to this problem, macrocracks' properties transfer on the crack nucleus behaviour. According to such approach, force and energetic criterion of the crack nucleus unstable equilibrium are the same (equivalent) at brittle fracture [1]. It is shown in this report that for the crack nucleus oriented normally to tensile stress direction force and energetic criterion are the same accurate to the constant. It gives rise to many difficulties when selecting criterion for the crack nucleus catastrophic propagation. At the same time, dependences of the value of critical stress $\xi_c$ on the angle $\alpha$ (between the normal to crack nucleus plane and tensile stress direction) differ significantly for two these criteria (Figure 1).

It is follows from these dependences that at $\alpha > 0$ the necessary condition (gain in energy) of the crack nucleus growth occurs earlier (at less stresses) than sufficient one (break of atomic bonds at crack tip). This is because at $\alpha > 0$ shear stresses affect on crack lips. These stresses contribute to the value of elastic distortion energy accumulated at the crack nucleus tip, however, they doesn't influence the value of tensile stresses that are necessary for atomic bonds break at the crack tip.

Ratio of normal and shear stresses affected the crack nucleus changes at transition from uniaxial to bi- and triaxial tension. Use of force criterion of the crack nucleus unstable equilibrium enables to describe correctly effect of brittle strength fall observed in this case.

An attempt was made in this report to develop criterion of the crack nucleus unstable equilibrium based on conditions of atomic bonds break at the crack tip. To this end, concept of critical energy density in crystal offered earlier [2] was applied. According to this concept, fracture of crystal at the crack nucleus tip occurs when energy density reaches its critical value that is equal to sublimation energy for one (separate) gram-atom. This approach has allowed to estimate the value of specific energy of fracture of crystal at the crack nucleus tip. It is ascertained that without plastic relaxation of stresses at the crack nucleus tip the value of specific energy of fracture exceeds the value of specific surface energy of crystal.

Investigation findings show that unlike macroscopic cracks, force and energetic criteria of unstable equilibrium for the crack nucleus are not identical. Necessary condition (gain in energy) of the crack nucleus growth is fulfilled at stresses less than those for sufficient condition (atomic bonds break at the crack tip). Estimations carried out shows that ratio of these stresses might amount to twofold value.

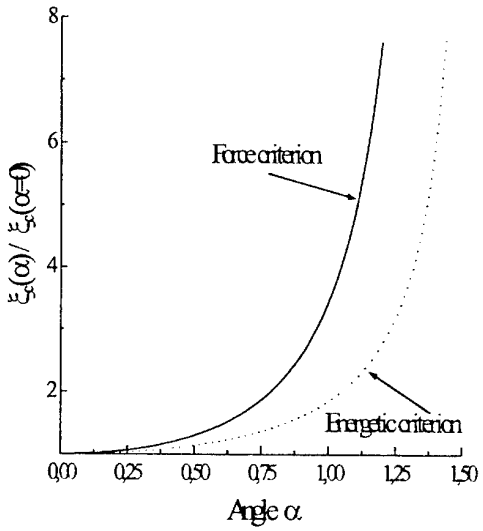


**Figure 1.** The crack nucleus orientation effect on the relative value of critical stress of the crack nucleus unstable equilibrium.

**References**:

1. Vladimirov V. I. Physical nature of fracture of metals - M.: Metallurgiya, 1984. - 280.

2. Meshkov Y. Y. Concept of critical energy density in solid fracture models // Uspehi fiziki metallov 2001 **т.2** с.7-50.

# ABOUT DENSIFICATION AND HARDENING OF POROUS BLANKS DURING AXIAL COMPRESSION

**Ryabicheva L.A., Kravtsova J.V.**
**East Ukrainian National University named after Vladimir Dahl, Lugansk, Ukraine**

The behaviors of porous materials hardening depend on evolution of porosity and hardening of solid phase of porous body during deformation. The strain rate and degrees of strain exert a substantial effect on these processes.

The influence of strain rate on densification and hardening of porous materials, expressing in structure change, is connected with properties change both during deformation and after it.

It is known, that deformation strength of compact metals increases with growing of strain rate. This is due to greater degree of metal hardening under alike value of plastic deformation. The studies of this question for powdered sintered materials are insufficient and carry the inconsistent nature.

The aim of our work is an experimental study of strain rate influence on densification and hardening of porous blanks under axial compression.

The experiments on axial compression were executed on cylindrical samples with a diameter of 7,8 mm and height of 15 mm. The samples with porosity within 6-20% produced from copper powder ПМС-1 by the method of cold bilateral compression on hydraulic press and the following sintering at 960$^0$C in vacuum for one hour are studied for peculiarities of their strain and rate hardening. The axial compression was executed on universal testing ZD-4 machine. The fluoroplastic film with thickness of 0,12 mm served as lubrificant. The samples were deformed before degrees of strain about 30%. The Strain rates were 0,002 $s^{-1}$; 0,01$s^{-1}$; 0,02 $s^{-1}$.

The studying of strain rate influence on evolution of porosity execute by the way of axial compression of samples with different initial porosity up to various degrees of strain. The current porosity is defined by hydrostatic weighting.

The values of porosity depending on strain under different strain rates are presented in a fig.1.

As it can be observed the different nature of samples' densification with various initial porosity is obviously during deformation. If a densification rate of samples with porosity less then 13% changes slightly, the densification of porous samples ($\theta_0$ >13%) is more intensity, but hinders under degree of strain about 18%. This fact is explained by formation of closed pores.

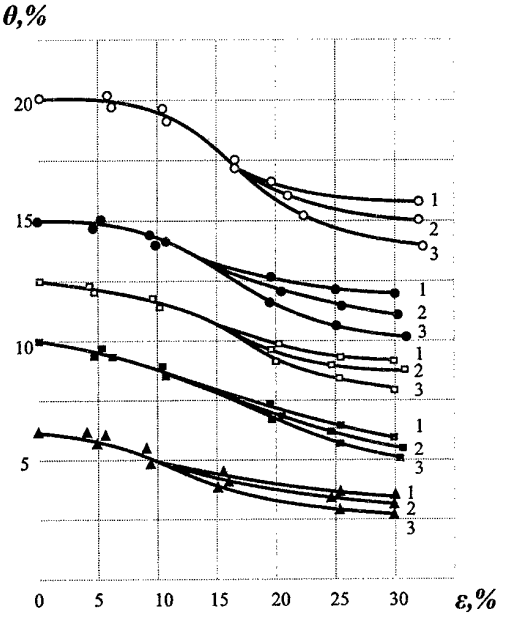


Fig.1. Porosity – strain depends during axial compression of porous copper:
1 - $\dot{\varepsilon}$ = 0,002$s^{-1}$; 2 - $\dot{\varepsilon}$ = 0,01$s^{-1}$; 3 - $\dot{\varepsilon}$ = 0,02$s^{-1}$;
▲ - $\theta$ = 6%; ■ - $\theta$ = 10%; □ - $\theta$ = 13%; ● - $\theta$ = 15%;
○ - $\theta$ = 20%;

As it is seen from fig.1 that under initial porosity of 6% and degrees of strain of 5 and 10% the changing of porosity of samples is small and practically constant. Under initial porosities 15 - 20% and strains 5-10% the reduction of porosity is also small. With strain increasing the changing of porosity is more intensively.

The strain rate influence is shown in activation of densification process. The increasing of strain rate results in reducing of porosity at constant value of strain. The lower position level of porosity–strain curves evidences about it.

With increasing of strain rate more intensive densification of samples (even for materials with porosity less then 13%) takes place in all investigated range of strains. Rate influence of strain rate to evolution of porosity the degree of strain about 15% is critical. It is possible to consider that under greater degrees of strain the reduction of porosity

and hardening of solid phase occurs. This is confirmed by fig.1 dependences, showing that reducing of porosity and growing of the solid phase hardening accompany increasing of strain rate and degree of strain.

The authors [2] propose to take into account sensitivity of material to strain rate by the way of consideration of rate-hardening factor $k$. According this hypothesis, the rate-hardening factor increases with growing its sensitivity to strain rate.

For the three values of strain rate the dependencies $\sigma = f(\dot{\varepsilon})$ are obtained (fig.2).

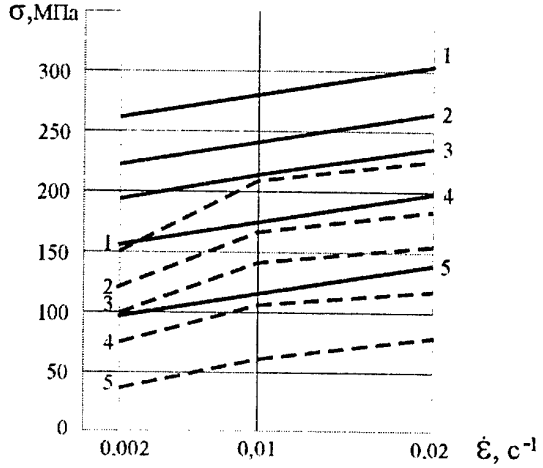


Fig.2. Stress-strain rate dependencies: 1-ε = 5%; 2-ε = 10%; 3-ε = 15%; 4-ε = 20%; 5-ε = 30%; —— $\theta_0$ = 6%; - - - - $\theta_0$ = 20%

Proceeding from obtained dependencies (fig.2), the hardening of material with initial porosity of 6% is characterized the united rate-hardening factor $k$=0,16. This factor will stay unchangeable with strain growing. The parallelism of corresponding lines of $\sigma = f(\dot{\varepsilon})$ dependencies evidence about it. These data evidence about that under initial porosity of 6% and further its reduction during deformation the growth of hardening takes place for account of solid phase deformation.

The increasing of initial porosity to 20% results in the broken nature of $\sigma = f(\dot{\varepsilon})$ dependencies. The bend occurs at strain rate of 0,01 $s^{-1}$. There are two stages in all dependencies. The first stage characterizes rate hardening of porous copper when strain rate increases from 0,002$s^{-1}$ to 0,01$s^{-1}$; the second stage – when strain rate increases from 0,01$s^{-1}$ to 0,02$s^{-1}$. The rate-hardening factor in the first stage is bigger than in the second stage. Its value for the first stage equals 0,21 at degree of strain about 5%, $k$=0,51 at degree of strain about 30%. For the second stage this factor changes within 0,088 - 0,11.

The obtained data are consistent with the porosity – strain dependencies, when at degrees of strain 20 and 30% and initial porosity of 20% the reducing of porosity is slightly too.

Under source porosity of 20% the rate-hardening factor turns out to be sensitive to changing of strain. The increasing of degree of strain results in growing of rate-hardening factor from 0,21 at degree of strain of 5% to 0,51 at strain of 30% at first stage and it remains practically constant under same degrees of strain.

Proceeded from obtained patterns, it can be supposed that one of the parameters defining sensitivity of porous copper to change strain rate is porosity. The growing of initial porosity of deformed body results in increasing its sensitivity to strain rate.

It can be also noted, that rate-hardening factor $k$ for initial porosity of 6% equals to 0,16. It turns out to be less this factor porosity about 20% on first stage and more on second stage under all degrees of strain. Thereby, for estimation of sensitivity of porous body to change of strain rate it can be possible to use the rate-hardening factor, either as for compact material.

The rate-hardening factor increases with growing of initial porosity of material. Under investigated loading scheme the porosity, reducing during deformation, acts as hardening factor, which influence became stronger, than strain rate higher.

Analyze of strain rate influence on densification and hardening processes is presented. It is shown that densification process depends on evolution of porosity during axial compression. The rate-hardening factor is used for characterizing of material's sensitivity to strain rate. The reduction of porosity with increasing of strain rate and compression strain is shown.

References

1. Ю.Н. Подрезов, Л.Г. Штыка, Д.Г. Вербило Деформационное упрочнение пористого железа при одноосном сжатии. – Порошковая металлургия, 2000, №1/2, с. 106-111.

2. Тарновский И.Я., Поздеев А.А., Ганаго О.А., Колмогоров В.Л., Трубин В.Н., Вайсбурд Р.А., Тарновский В.И. Теория обработки металлов давлением. М., «Металлургиздат», 1963. 672 с.

# InSe SOLAR CELLS

**Katerynchuk V.M., Kovalyuk Z.D., Zaslonkin A.V., Sidor O.M.**

Frantsevich Institute of the Materials Science Problems of the National Academy of Sciences of Ukraine, Chernivtsi Department, Chernivtsi, Ukraine

The searches of efficient photoconverters of solar energy are actual at present day. The choice of a type of photoconverter depends on many factors. The most important from them are: the connection of low cost and high efficiency of a photoconverter; the use of a crystal or thin film semiconductor substrate; techniques of a p-n junction formation.

The InSe compound is of great interest among many semiconductors, which are used in the solar power. Indium monoselenide belongs to materials with a layered crystal structure. This structure reflects a fact of the existence of two types of chemical bonds between atoms in it. A single layer is the sandwich of four monatomic planes in the succession chalcogen-metal-metal-chalcogen in which the strong covalent bonds between the atoms is realized. In such a layer all the chemical bonds are saturated, therefore the interaction between the layers is realized by weak Van der Waals forces. This means that InSe can be easily cleaved onto enough thin plates, which combine in themselves simultaneously the properties of the crystal structure and the possibilities of a preparation of thin InSe films of some microns in thick. The surface of the cleaved plates is mirror-like and inert to chemical adsorption in the environment. So, it does not need any mechanical or chemical treatment.

It is known that the InSe energy gap is 1.2 eV at room temperature [1] and from the point of view of the theoretical efficiency of photoconversion [2] this compound is optimum for using as a photoconverter. The previous investigations of the conversion efficiency were carried out for the materials of both n- and p-type conductivity of InSe [3, 4]. In both the above-mentioned articles gold was used as material for the preparation of the photoconverters that raises their cost. The maximum efficiency of the photoconversion is 2.5 % for the Au - n-InSe Schottky diodes [3] and 10% for ITO - p-InSe heterojunctions [4]. An obstacle for receiving higher values of the conversion coefficient is the overcoming of series resistance of the cells that is a consequence of the layered crystalline structure. Note, that the authors of [3] had used for the preparation of the solar cells the InSe substrates with a thickness 60 to 85 μm, and in [4] – less than 20 μm.

In this report the new approaches to the formation of potential barrier of InSe based photoconverters to lower their series resistance and to the preparation of ohmic contacts are proposed. These approaches are much simpler and cheaper than the methods known in the literature. During the diode structure preparation as a substrate we have used the InSe ingots grown by the Bridgman method and doped with cadmium for obtaining the hole conductivity. A substrate thickness was 0.3 to 0.5 mm. The substrates were placed into an electric furnace with controlled and stabilized temperature and thermally oxidized at a temperature between 450 and 500°C at an oxidation duration from several minutes to several hundreds of hours. The oxidation leads to the formation of oxide film on the InSe surface. The oxidized samples were divided onto two halves with a razor blade and cut off from all the sides with the object of the elimination of p-n junction closings. The heterojunctions thickness was done about 100 μm by of the consecutive cleaving the crystal layers. It is established that the oxide film on an InSe substrate has the properties, which are identical to the $In_2O_3$ film characteristics: it has metallic conductivity and high transparency. The film thickness can vary in wide limits. Its colour that varies depending on the oxidation time is evidence of it. For all the oxidation conditions the potential barrier formation was observed at the oxide-semiconductor interface. Under illumination of the created oxide-p-InSe structures the maximum value of open circuit voltage ($U_{oc}$) was registered on the level of 0.6 to 0.62 V. This value is although the biggest one known from the literature data. It is established that besides the formation of a surface oxide film, which plays a role of a heterojunctions active element, the oxygen diffusion into the depth of crystal also

takes place. This diffusion leads to a significant decreasing photoconverter series resistance. Besides, additional cleaving the substrate layers can decrease the series resistance. Pure indium has been used as a back ohmic contact deposited on the preliminary damaged substrate surface. The surface of the oxide was although covered by a grid indium electrode that promotes to a better photocarriers collection.

Under the conditions of a direct Sun illumination with a 75 mW/cm$^2$ incident power, for different photoconverters the short circuit current ($I_{sc}$) has attained a 20 to 30 mA/cm$^2$ value and the open circuit voltage is 0.58 to 0.62 V. The conver-sion efficiency was estimated on the basis of the measurements of the current-voltage characteristic of oxide-p-InSe solar cells and under the above-mentioned conditions of Sun illumination it was 5 to10 %.

References

[1]. Landolt-Börnstein. Numerical Data and Functional Relationships in Science and Technology. New Ser. Group III: Crystal and Solid State Physics. V. 17, sv.f / Ed. by O. Madelung. Berlin e.a.: Springer, 1983. 562 p.

[2]. Пикус Г.Е. Основы теории полупроводниковых приборов- М.:Наука, 1965.- 448 с.

[3]. Di Giulio M., Micocci G., Rizzo A, and Tepore A. Photovoltaic effect in gold-indium selenide Schottky barriers // J. Appl. Phys.- 1983.- Vol. 54., No.10.- P.5839-5843.

[4]. Martinez-Pastor J., Segura A., Valdes J.L., and Chevy A. Electrical and photovoltaic properties of indium-tin-oxide/p-InSe/Au solar cells // J. Appl. Phys.- 1987.- Vol.62, No. 4.- P.1477-1483.

# RADIATION STABLE PHOTODETECTORS BASED ON LAYERED III-VI COMPOUNDS

**Drapak S.I., Kovalyuk Z.D., Netyaga V.V., Orletskii V.B.**
Frantsevich Institute of Material Sciences Problems, National Academy of Sciences of the Ukraine, Chernivtsi Department, Chernivtsi, Ukraine

Photosensitive devices based on layered InSe and GaSe semiconductors have essential advantages over other analogues prepared from traditional semiconductors starting from the stability of their electrical and photoelectrical characteristics to the influence of ionizing radiation [1÷2].

We have developed the technology of preparation of some new photosensitive structures based on indium and gallium selenides for the spectral range 0.2 to 1 μm. Their properties are also investigated.

1. Semitransparent Sn film – p-InSe:Zn structures were prepared by thermal evaporation of tin onto fresh-cleaved (001) surfaces of InSe:Zn samples. Ohmic contacts to them were prepared according to the method proposed by us in [3]. For the prepared structures we carried out the measurements of helpfull signal $U_S$, noise $U_n$, and their ratio, which determine the limiting characteristics of photodetectors. These parameters were investigated depending on both technological conditions at preparing the structures and operating parameters of photodetectors (bias voltage, modulation frequency of light beam etc.)

It is established that a maximum value $U_S/U_n$ ≥300 is much higher than that in the case of photoresistive effect [3] but a bias voltage giving this value is the same for the both cases and lies between 0.5 and 1 V. The maximum value of the $U_S/U_n$ ratio was obtained at the modulation frequency of light beam f = 400 Hz when the Sn film was illuminated by a radiation with a color temperature equal to 2850 K.

The experimental dependences of spectral noise density on applied bias in the range 0 to 4 V can be described by the Hooge relation: $S(f)=const \cdot V^n/f^\gamma$. However as one can see from the S(V) dependence (Fig.1), the value of n is essentially less than 2 whereas for traditional semiconductors n≈2. In the range below 1 V we have n≈1 and with increasing a reverse bias to 4 V the value of n becomes 1.4 to 1.5 . Such regularity was typical in the case of photoresistive effect in n-InSe [4].

2. $In_2Se_3$ belongs to a wide group of layered semiconductors and differs from its other representatives by the availability of essential defects of the structure. Starting from this property and, therefore, radiation stability of the material the preparation of photosensitive devices on its base is very important.

$In_2Se_3$ films were prepared by the method of evaporation of n-$In_2Se_3$ single crystals with α-modification (Eg=1.4 eV) at a residual pressure not more than $2\cdot10^{-5}$ mm Hg. X-ray studies have shown that the obtained films have the well defined γ-modification (Eg=2.0 eV) independently of substrate temperature.

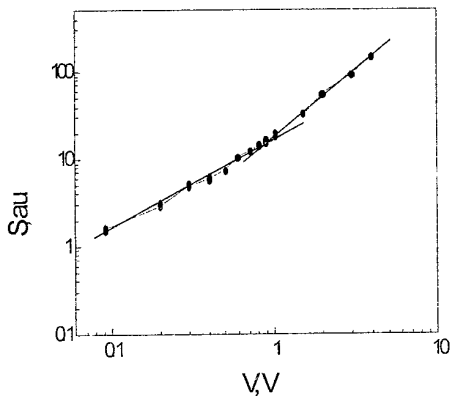


Fig.1.
Noise spectral density vs bias voltage for Sn- p-InSe:Zn structure.

The influence of technological conditions of n-$In_2Se_3$ films deposition on photoelectric parameters of radiation stable $In_2Se_3$ - GaSe structures has been investigated. It is established that the systems based on $In_2Se_3$ films, which were deposited at a substrate temperature between 100

and 150°C, have the most stable photosensitive parameters.

We have carried out a comparative analysis of the electrical and photoelectric properties of $In_2Se_3$ - GaSe structures prepared by the methods of vacuum evaporation and optical contact. The obtained values of the open circuit voltage at light illumination power of 100 mW/cm$^2$ are 0.7 - 0.8 V for the structures prepared by the vacuum evaporation method. They are twice higher than those for the structures prepared by the optical contact method. The difference, which was observed in current - voltage and capacitance - voltage characteristics for the structures prepared by both methods, could be well explained by the changes of the band parameters. Photovoltaic spectrums of n-$In_2Se_3$-p-GaSe heterostructures prepared by the methods of optical contact and vacuum evaporation are shown in Fig.2.

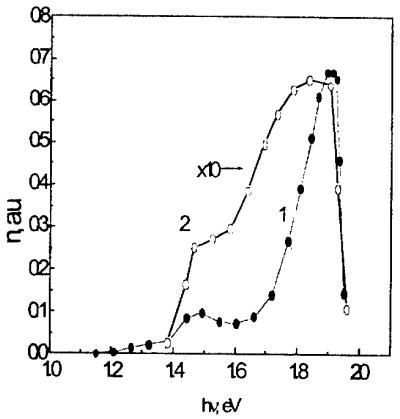


Fig.2. Spectral dependences of quantum efficiency for n-$In_2Se_3$-p-GaSe heterostructures prepared by the methods of optical contact (1) and vacuum evaporation (2).

3. Recently a great attention is directed to investigations of the structures based on III-VI layered semiconductors and prepared by their thermal oxidation. First of all it is caused by their sensitivity in ultraviolet spectral range [6÷7]. We propose a method for preparation of dielectric – semiconductor structures which give stable and reproduced photoelectric characteristics. It consists in the formation of thin $Ga_2O_3$ film onto substrates of other semiconductors. It eliminates a possibility of the formation of undesirable phases of GaO, $Ga_2O$, and $Ga_2Se_3$, which can appear under thermal oxidation of GaSe substrates and are less sensitive or non-sensitive in ultraviolet spectral range.

As follows from the electrical and photoelectric investigations, the above-mentioned structures can be used as radiation stable photodetectors in the spectral range 0.2 to 1 μm.

## References

1. E.G.Ashirov, V.L.Bakumenko, A.K.Bonakov, e.a. Abstracts of All-Union Seminar on Radiation Defects in Semiconductor Devices. 1980. Baku: Azernesher. P.91.
2. T.D.Ibragimov, E.A.Djafarova, E.B.Safarov. Fiz. Techn. Polupr., 2002, **36**, p.846-858.
3. Z.D.Kovalyuk, V.B.Orletskii, I.M.Budzulyak. Bulletin of Chernivtsi University, 2000, № 79, P.81-82.
4. Z.D.Kovalyuk, V.B.Orletskii, I.M.Budzulyak, V.V.Netyaga. J. of Physical Studies, 2001, **5**, p.43-45.
5. C. Tatscyama, S. Ichimura. Il Nuovo Cimento, **38B**, № 2, 1977, p. 352÷358.
6. V.P. Savchun, V.B. Kytsai. Thin Solid Films, **361÷362**, № 1÷2, 2000, p. 123÷125.
7. O.A. Balitskii, V.P. Savchun, V.O.Yukhymchuk. Semiconductor Science and Technology. **17**, 2002, p. L1÷L4.

# PHASE COMPOSITION & INTERFACE DESIGN OF HIGH COERCIVE SINTERED PERMANENT MAGNETS OF $SmCo_5$-TYPE

*** Andreeva A.V., Talijan N.M.,. Milutinovic-Nikolic A, Static-Trosic J., Jovanovic Z.D.**
* Institute of Microelectronics Technology RAS,142432, Chernogolovka, Moscow Region, Russia,
*Institute of Chemistry, Technology and Metallurgy, YU-11001, Belgrade, Yugoslavia*

The sintered permanent magnets (SPM) based on powders of rare earth metals are nonequilibrium multiphase ultradispersed systems (UDS). The processes of structure selforganization giving rise to special crystallographic and magnetic textures are characteristic of high tech. SPM. Crystalline interfaces are the main defects of UDS. The space symmetry of adjacent crystals and their mutual interconnection is a key to structure and properties of interfaces, topology of interfacial defects, phase transformations during grain growth and other contact phenomena in UDS. In many cases the processes in contact interface layer determine the final properties of UDS [1-4].

High performance SPM are based on outstanding intrinsic magnetic properties as well as optimized microstructures and chemical compositions. $SmCo_5$ is a widely used rare-earth magnet because of its high Curie temperature and high anisotropy field. The excellent magnetic properties of SPM, Hc~20-25kOe, high maximum energy products exceeds 20 MGOe have been achieved in anisotropy magnets by improving strong requirements on the grain and interface structure.

The influence of interface structure, boundary secondary phase distribution and chemical composition on the magnetic properties of SPM based on $SmCo_5$ high dispersion powder is investigated. The phenomenon of high coercivity of $SmCo_5$ magnets has been treated in the framework of the theory of interfaces (calculations of the crystallographic parameters and atomic models of special coherent grain and phase boundaries in the Sm-Co- system), which affords some new insight in its origin. The texture analysis and precipitation processes of secondary phases on grain boundaries are compared with interface crystallography. The model calculation based on bicomponent phase diagram and composition correction with oxygen content and magnet density is proposed.

Microstructure of Sm-Co magnets will be discussed in relation to the magnetic properties obtained in a series of 20 samples. The Sm content in the SPM ranged from 33 to 38 %. The SPM were prepared by standard powder metallurgy techniques, including milling to particles of 7,37 microns, compacting under pressure 638MPa and orientation in 60kOe field, optimize sintering and heat treatment [5] followed by quenching to room temperature. To obtain the high coercive SPM the optimization sintering regime [5] based on x-ray texture analysis with maximum intensity of {111}R $SmCo_5$ – phase was applied. . Micro X-ray diffraction spectral quantitative analysis was used for chemical analysis. Microstructure investigations of the SPM were carried out by optical, SEM and TEM microscopy. Magnetic properties were measured with hysteresisgraph.

A microstructure modelling based on the magnet density and secondary element contamination is applied.. Any changing of Sm content over the exact $SmCo_5$ phase composition (33,8%) plays an important role in magnetic properties of the SPM. To use phase diagram Sm-Co it is necessary to correct Sm content ($Sm_d$), because undesirable secondary elements (oxygen, carbon, nitrogen etc.) can extract Sm from matrix phase 1-5.

$$\%Sm_{(d)} = \{\%Sm_c - \Sigma[(\%Sm_i/\%I_i)\%I_c]\}/ [1- \Sigma(\%I_c/\%I_i)] \quad (1)$$

where $\%Sm_c$ – is the Sm content in SPM; $Sm_i$ is the Sm content in secondary phase Sm-I, $\%I_i$ is the secondary element (O, C,N etc.) content in the secondary phase Sm-I, $\%I_c$ – is the secondary element content in SPM.

The $Sm_d$ (diagram) concentration can be used to evaluate the volume fraction of 2-7 and 2-17 secondary phases and fraction of pores and oxides in the SPM of $SmCo_5$ - type, as in [ 6].

The samples with a higher oxygen content show a transition from the presence of super stoichiometric $Sm_2Co_7$ (2-7) phase, which is not (up to 10-14%) influence on decreasing of coercivity, to substoichiometric undesirable $Sm_2Co_{17}$ (2-17) phase, which considerably deteriorate magnetic properties of the SPM.

The secondary phases 2-17, oxides and pores are usually observed on interfaces of the SPM.

Interface microstructure for different compositions of the SPM is shown in Figs.1-3. When excess of Co is ~ 2% compared with exact $SmCo_5$ phase, then cell microstructure with amorphous 2-17 boundary phase is observed(Fig.1) This structure is characterized by low value of $H_c$. When excess of Co is <0,2%, then oriented crystalline precipitates of 2-17 boundary phase is formed (fig.2). The mutual phase orientation, determined by crystallographic calculations and computer modeling (fig.2) agrees with diffraction patern. Superstoichiometric compositions (with Sm excess) of the SPM with low oxygen content are characterized by high coercivity, reduced porosity, higher density and perfect interface structure (fig.3).

Fig.1

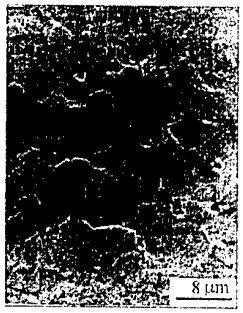


Fig3.

Fig.2

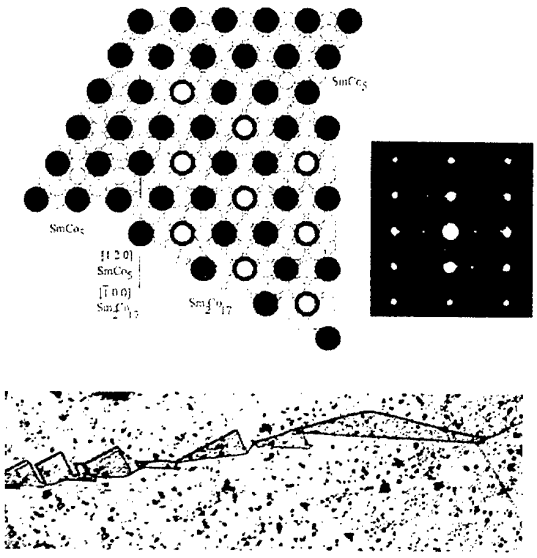

The experimental observations revealed

- the influence of external magnetic field during powder consolidation process on the shrinkage and interface pore distribution;
- the simultaneous increase in the rate of shrinkage and coercivity, as the Sm content in the alloy exceeds its stoichiometric amount in the $SmCo_5$ phase;
- the appearance of secondary $Sm_2Co_{17}$ phase, as interface phase leads to considerable decreasing of coercivity
- the definite crystallographic orientation of the secondary $Sm_2Co_7$ and $Sm_2Co_{17}$ phases, as interface precipitates and their influence on coercivity;
- the influence of nterface design on high coercivity of the SPM;
- the role of magnetocrystalline anisotropy and interface atomic structure in domain wall –grain boundary interactions, pinning and reverse domain nucleation mechanism in $SmCo_5$ magnets with one [0001] easy magnetisation direction

References

[1]Andreeva A.V. -Surface.Phys.,chem.,mech., 1990, N4, p.117-123 (in russian)

[2] Andreeva A.V,. Meiler B.L.- Cryst. Properties & Preparation, Trans.Tech.Publ.,1991, v.36-38, p.349-357

[3] .I. Il'in, A.V. Andreeva, and B.N. Tolkunov, *Mat.Sci.Forum*, **207-209**, 625 (1996)

[4] Andreeva A.V., Arsentieva I.P., Zakharov N.D Science of Sintering, 1999, v.31(3), 139- 150;

[5] Talijan N.M.,. Milutinovic-Nikolic A, Static-Trosic J., Jovanovic Z.D. – Science of Sintering, 1997, 29(2),69-75

[6] . Campos M.F., Landgraf F.J. –Proc.14 th Intern. Symp. «Magnetic Anizotropy and Coercivity in Rare Earth Transition Metals»- 1996, San Paolo, Brazil, p.321-338

# EFFECT OF GRAIN SIZE AND PLASTIC STRAIN ON WEIBULL PARAMETERS

**Zimina G., Kotrechko S.**
G.V. Kurdyumov Institute for Metal Physics of NAS of the Ukraine, Kyiv, Ukraine

At present, "Local Approach to Fracture" is conventional for description of fracture of metals and alloys under the condition of stress concentration [1]. Fracture criterion for reference pattern (representative volume) of polycrystal is key point in this approach. Weibull distribution is usually applied for estimation of probability of this volume:

$$F(\sigma) = 1 - \exp\left[-\left(\frac{\sigma - \sigma_{th}}{\sigma_u}\right)^m\right]$$

where $\sigma_{th}$ is threshold stress (low limit of strength), $m$ is parameter that determines the shape of probability function, $\sigma_u$ characterises sensitivity of fracture stress of metal to change in its volume (scale parameter).

In present day conception of local approach it is postulated that Weibull distribution parameters are material's constant and don't depend on stress-strain state of metal. Statistical model suggested in [2] enables to delimit effect of metal structure and influence of stress-strain state of metal near notch or sharp crack on both the value of fracture probability and the value of local fracture stress [3] by computer simulation.

Theoretical analysis of grain distribution parameters on Weibull distribution parameters has been carried out elsewhere [4]. Fracture probability function obtained by computer simulation of crack nucleation in polycrystal and its unstable equilibrium was approximated by tree-parameter Weibull distribution to this end. It permits to ascertain relations between Weibull distribution parameters and such microstructural parameters as the most probable grain size and grain size variance (Figure 1). It has been exhibited that at uniaxial tension and fixed value of plastic strain the value of shape parameter m is actually independent on the value of the most probable grain size. The value of shape parameter $m$ diminishes with rise in logarithmic grain size variance $D_{\ln d}$. Shape parameter $m$ is linear function of $\sqrt{D_{\ln d}}$ at that case. The threshold stress $\sigma_{th}$ is proportional to $d_{mpv}^{-1/2}$ ($d_{mpv}$ be a most probable value of grain size) and depends on grain size variance. This stress is approximately equal to $0.7R_{MC}$ ($R_{MC}$ be a minimum brittle fracture stress of unnotched specimens over ductile-brittle temperature region). The normalised scaling stress $\sigma_u/\sigma_{th}$ is a linear function of $D_{\ln d}$.

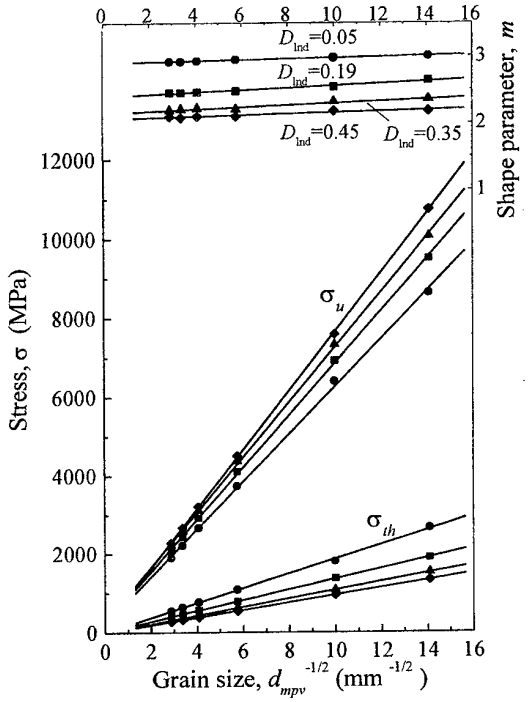


*Figure 1. Effect of the most probable grain size $d_{mpv}$ on Weibull distribution parameters; $D_{\ln d}$ is value of variance of grain size logarithm.*

Regularities of plastic strain effect on Weibull distribution parameters are presented in Figure 2. By applying this approach, only the shape parameter $m$ is nearly constant over the interval of small plastic strains (i.e. those which do not exceed critical one $e_c$ - Figure 2). As strain grows, threshold stress decreases approximately by 1.3 times. The value of $\sigma_u$ becomes 2.7 times greater.

Dependence of $\sigma_{th}$ on the strain value (Figure 2) may be approximated with sufficient accuracy by linear function: $\sigma_{th} = A_{th} - B_{th}\sqrt{e}$, where coefficients $A_{th}$ and $B_{th}$ depend on the values of both average grain size and their variance (Figure 3).

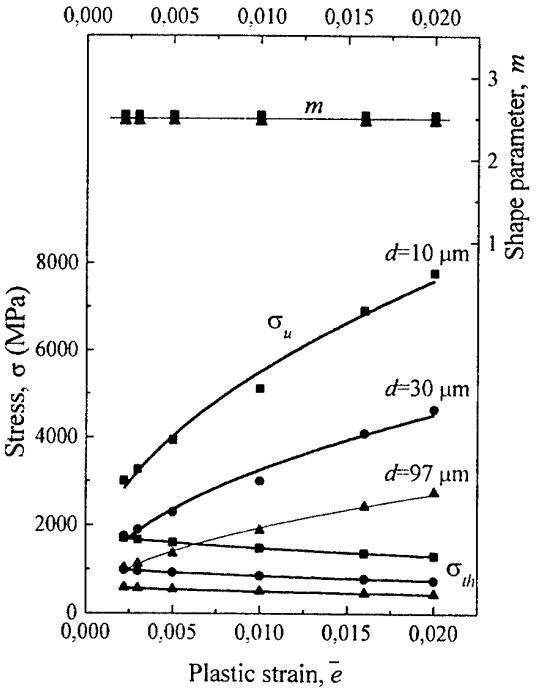


*Figure 2. Effect of the plastic strain on Weibull parameters for different grain sizes.*

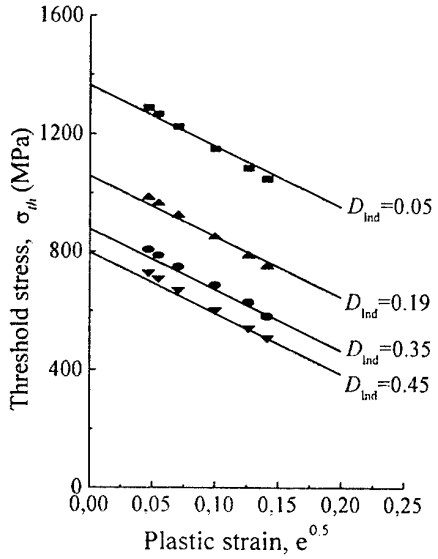


*Figure 3. Effect of the plastic strain on threshold stress $\sigma_{th}$ for $d_{mpv} = 30\ \mu m$*

Ratio $\sigma_u / \sigma_{th}$ is a linear function of the plastic strain value: $\sigma_u / \sigma_{th} = A_{th} + B_u e$. Coefficients $A_u$ and $B_u$ are metal structural constants depending on grain structure inhomogeneity.

Dependence of $\sigma_{th}$ and $\sigma_u$ on the plastic strain value is due to effect of dislocation stresses $\bar{\xi}$ on the crack nucleus unstable equilibrium:

$$\xi_c = \frac{k}{\sqrt{a}}\varphi(\theta,\eta) - \bar{\xi},$$

where $\xi_c$ is critical value of tensile stresses; $\eta$ is stress state mode parameter ($\eta = \xi_{22}/\xi_{11}, \xi_{11}$ and $\xi_{22}$ are the principal tensile microstresses); $\theta$ is angle between the crack plane and direction where principal tension microstress acts; K is the coefficient that characterises resistance of the crystal to the propagation; $\varphi(\theta,\eta)$ is the function that describes influence of microstress state $\eta$ and orientation of the crack $\theta$ on the critical stress.

As it is follows from this equation, rise in these stresses results in critical stress $\xi_c$ decrease and, respectively, to change in $\sigma_{th}$ and $\sigma_u$ values.

**Conclusions**

1. Parameters of Weibull distribution aren't the metal constants.
2. Shape parameter $m$ doesn't depend on the values of both grain size and plastic strain, but it is sensitive to the grain size variance.
3. Threshold stress $\sigma_{th}$ and scale parameter $\sigma_u$ depend not only on the value of grain size but also on the plastic strain value reached to fracture.

**References**:

1. Fant, M. Di, Cog, V. Le, Cleizergues, O., Carollo, G., Mudry, F., Bauvineau, L., Burlet, H., Pineau, A., Marini, B., Koundy, M., Sainte Catherine, C. and Eripret, C. (1996) Development of a simplified approach for using the local approach to fracture, *Journal de physique IV Coloque C6. - supplement au Journal de Physique III* **6**, 503-512.
2. Kotrechko, S. A. (1995) Statistic model of brittle fracture of polycrystalline metals, *Phys. Metals*, **14**, 1099-1120.
3. Kotrechko, S. A., Meshkov, Y. Y. (2000) On foundation of physical theory of quasi-brittle fracture of polycrystalline metals in the non-homogeneous fields created by stress concentrators, *Met. Phys. Adv. Tech.* **18**, 1393-1412.
4. Kotrechko, S. A., Zimina, G. P., Meshkov, Y. Y., Levin, G. I. (2001) Computer simulation of influence of grain size distribution parameters on statistic characteristics of strength of polycrystalline metal in brittle state, *Met. Phys. Adv. Tech.* **23**, №6, 821-831

# THE INFLUENCE OF DISPERCED NANOCARBON ON THE KINETICS OF MESOPHASE COAL TAR PITCH TRANSFORMATIONS

**Rimbu G. A., Banciu C., Bondar A. M., Stamatin I.**
Advanced Research Institute for Electrical Engineering (ICPE-CA),
313 Splaiul Unirii, 74204, Bucharest 3, ROMANIA
Tel/Fax: +40 1 346.72.83; e-mail: electmat@icpe.ro

The conversion process of a pitch material to the solid "green" coke, involves an intermediate phase, a liquid-crystal phase or mesophase. The formation of liquid-crystal from pyrolysing pitch materials is not a totally unique process to pitch. A considerable literature has existed for more than one hundred years, describing the formation, properties and application of liquid-crystal system. These materials are essentialy "*self organized sistems*", or "*self assembling systems*". In the earlier years, liquide-crystal were looked upon as curiosity materials, but about thirty years ago they found a major application in "high-tech" display components. Today, there is familiarity with the LCD (Liquid Crystal Display) system of electronic equipments. Brooks and Taylor, in 1968, reviewed the experience that petroleum pitch, coal tar pitch and some coals, on pyrolysis, generate molecular system wich form liquid-crystal. This discovery was a tremendous importance to the carbon and graphite industries, wich for the first time, now had a working theory of how graphitizable carbons could be formed.

Kinetic studies on mesophase transformation is important for practical applications because the mesophase transformation is a key process to control optimize and improve the utilization process of coal tar pitch (CTP). Many scholars have worked in this area. Singer and Lewis have determined that the activation energy of mesophase formation between 400°C and 430°C is 185 kj/mol with acenaphthylele pitch. Honda et all., have reported an activation energy of 164 kj/mol from the change of the quinoline insoluble (QI) fraction of CTP, assuming the reaction is first order. Yamada et all., have studied the influence of primary QI on the kinetic parameters of mesophase transformation of CTP. They have found that the rate constant increase with the amounts of QI at 400°C.

The objective of this work is to study the kinetic characteristics of the mesophase transformation of CTP in the presence on nanocarbon additives.

The aim of our researches is to obtain an optimum composite material used as annodes in Li-ion secondary battery.

# THE HEALING OF CRACK IN TRANSPARENT DIELECTRICS UNDER INFLUENCE OF ELECTROMAGNETIC RADIATION

**Feodorov V.A., Plushnikova T.N., Tjalin Yu. I., Chivanov A.V.**
Derzhavin Tambov State University, Tambov, Russia

It is known that in conditions of asymmetrical cleavage of a crystal (with pronounced plane of cleavage) the probability of lateral break off is high. The lateral break off takes place when the growing crack changes the plane of propagation. During the process, the tip of the crack may healed itself. We know a few methods of healing. On the base of the methods the regularities of the phenomena may be investigated at a microlevel.

The destruction of crystals is accompanied by plastic deformation, its intensity and degree of localization depends on a velocity of crack propagation. At stopping of a crack in alkali-halide crystals the plastic zones are formed, their structure is determined by a type of a destroying crack, geometry of a sample, properties of a material. It is known that in such crystals spontaneous and artificial healing of cracks possibly.

The purpose of this paper was to investigate experimentally the influence of electromagnetic radiation on processes of stress relaxation and healing of crack tip in alkali-halide.

The materials used in the present work were LiF, NaCl, KCl single crystals with impurity content $10^{-4}$ wt%, $10^{-3}$ wt% and $10^{-2}$ wt%. The size of the samples was 10x25x2 mm. The samples were cleft from big single crystals. The crack of asymmetrical cleavage was initiated on (100) plane by calibrated impact with energy $\approx$ 80 mJ. The point of crack initiation was situated at distance $S_1$ from axis of symmetry. The degree of asymmetry was determined as $S_1/0.5S_2$, where $S_2$ is width of sample. The sample was cleft in two equal parts on (010) plane for preparation of "control" and "testing" crystals [1].

At the first series of experiment crystals were heated in stove in the temperature range of 300 ÷ 773 K.

At the second series crystals were illuminated by tungsten lamps. The power of lamps was 20 and 100 W and the maximum energy in the spectrum was 1.06 and 1.24 eV correspondingly. The wavelengths were 350 ÷ 760 nm. The intensity of lighting was changed from 4 lx to 15 klx accordingly to power of lamp and lightfilter. The time of illumination was varied from 10 to 1500 hours.

In the third series the crystals subjected to action of ultraviolet and X-Ray radiation, with a wave length $\lambda$=250÷410 nm and $\lambda$=0,154 nm; $\lambda$=0,193 nm. An exposure of crystals by X-rays was made by X-ray diffractometer (DRON-2, DRON-0,5). The time of action varied from 3 minutes about 3 hours. Dose X-ray radiation 3R/min.

The behaviour of dislocations at tops of cracks is determined by the equation of equilibrium. At compiling of dislocations equilibrium (for dislocation emitted by a crack in a plane of a sliding) it is necessary to take into account stresses: operating on a dislocation from a leg of a crack $\tau^T(x_n)$, forces of an image $\tau_i$, interaction of dislocations $\tau^D(x_n, x_j)$ and resistance of crystal to a shift $\tau_S$. For the scheme of plastic current of a fig. 1 equations of equilibrium will look like the following:

$$\tau^T(x_n)+\sum\tau^D(x_n,x_j)-\tau_S-\tau_i=0,\ n=1,2,...,m.$$

The behaviour of dislocations at tips of cracks will depend from a relation of stresses.

The plastic flow in the tip of a stopped crack in LiF single crystal was investigated by numerical modelling [2]. Two stages of dislocation structure formation in the tip of crack were discussed. The first stage is the formation of gliding lines in the moment of crack stop. The second is their evolution and partial crack healing. It was shown, that in condition of unloading a few dislocations moved out of crystal on the crack plane under affect of mutual repel and forces of reflection. As a result of the process the dislocation density is maximal at some distance from the crack tip. There is a dislocation free area nearly the crack tip (fig. 2).

It was experimentally found, that electromagnetic radiation changed dislocation structure at tip of the crack (fig. 1). The summary density of dislocations was lowered. The healing at the crack tip was observed [1].

Electromagnetic radiation causes decreasing of mechanical stresses in tip of the crack of a reversible motion of dislocations and partial healing of the tip.

The exponential dependence of dislocation density both from temperature and from time of lighting was determined (fig. 3).

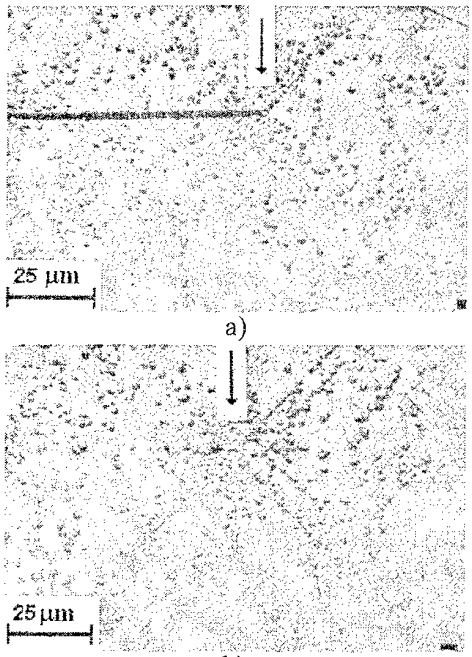


Fig. 1. Dislocation structure in neighbourhood of tip of cleavage crack in LiF single crystal to influence of X-Ray radiation E=6,25 keV: a) "Control" crystal, T=300 K. b) "Testing" crystal after t=5 min.

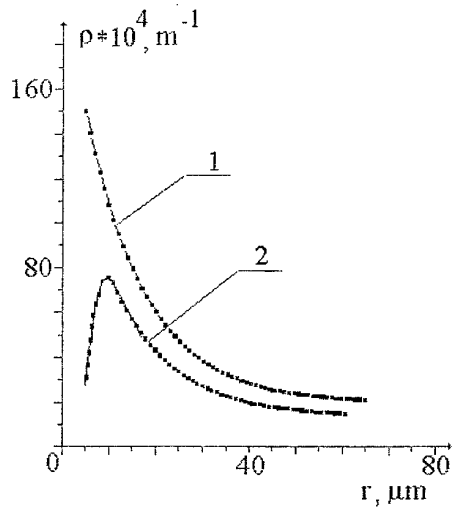


Fig. 2. The dependence of linear density of dislocation on ray rosette upon distance from tip of crack. 1 – before healing. 2 – after healing.

The intensity of healing and relaxation of stresses depends on material and spectrum of electromagnetic radiation. The processes of healing and stress relaxation depend on intensity of electromagnetic radiation. The greatest effect is observed at action of a X-rays.

The influence of small doses X-ray radiation on processes of healing microcrack was investigated.

The action X-ray radiation results in stress relaxation in tip of cracks for account a reversible motion of dislocations was established. The intensity of healing and stress relaxation depends from a wave of length of a X-rays.

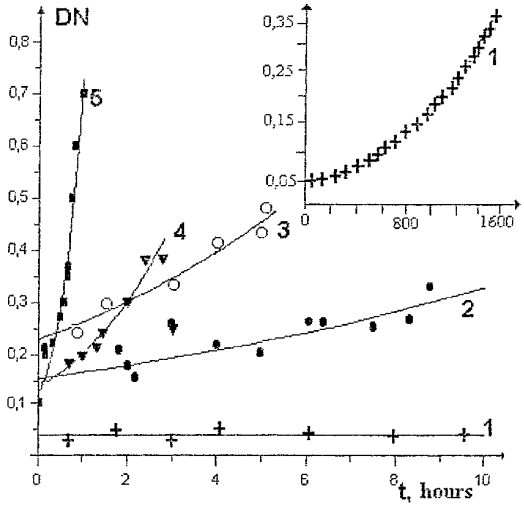


Fig. 3. The relationship between comparative changing of dislocations number at crack tip ($\Delta N/N$) and time (t) of treatment: 1. T=355 K, 2. $\lambda$=760 nm, 3. $\lambda$=350 nm, 4. $\lambda$=250÷410 nm,5. $\lambda$=0,154 nm.

The effect of healing microcrack was incremented at diminution a wave of length. The mechanisms of stress relaxation and healing resulted from X-Ray radiation were discussed.

**Conclusions**

1. Electromagnetic radiation causes decreasing of mechanical stresses in tip of the crack and partial healing of the tip.
2. The intensity of healing and relaxation of stresses depends on material and spectrum of electromagnetic radiation.
3. The processes of healing and stress relaxation depend on intensity of electromagnetic radiation.

This work was supported by a Grant of RFFR (project 02-01-01173).

References

[1] Feodorov V.A., Plushnikova T.N., Tjalin Yu.I. Healing of cracks, stopped in alkali-halide and calcite as a result of asymmetrical cleavage, *Solid State Physics*, **42**, 4 (2000), 685-687.

[2] G. Ortega and V. Reindbold. Iterative methods of a solution of systems of the non-linear equations with many unknown. Moscow, 1975, p.558.

# DENSIFICATION OF COMPACTS DURING LIQUID-PHASE SINTERING

**Romanov G.N., Tarasov P.P.[1], Tsypandin P.P.[1], Mestnikov N.S.[1], D'yachkovsky P.K.[1], Savitskii A.P.[2]**

Tomsk State the V.V. Kuibyshev University, Tomsk, Russia
[1]Yakutiya State the M.K. Ammosov University, Yakutsk, Russia
[2]Institute of Strength Physics and Materials Science, Tomsk, Russia

The rearrangement of solid-phase particles, solution-reprecipitation process and solid-state sintering of skeleton widely known from the literature are classical mechanisms of densification of powder bodies during liquid-phase sintering. As the theory of the three-stage sintering has arisen on the basis of studying systems with limited mutual solubility of solid and liquid phases, it considers the phenomenon of dissolution of solid-phase particles in liquid as an indirect factor which promotes densification only due to liberating particles from the mutual blocking interfering rearrangement. Therefore, the theory does not take into account the direct contribution of the dissolution phenomenon to densification of powder bodies caused by reduction of solid phase in volume during dissolution.

It is established as a result of dilatometric investigations that the process of liquid-phase sintering systems having appreciable mutual solubility of solid and liquid phases consists of two main stages. The first stage begins after formation and spreading of the melt throughout the volume of a powder body and finishes by growth of the compact in volume. The second stage is characterised by densification which occurs after termination of the growth.

However, the second stage takes place only in the case, if the composition of a mixture being sintered gets into region of the solid-liquid state on the phase diagram at the sintering temperature in the equilibrium condition. If a compact contains the forming liquid phase component in a quantity not sufficient that the mixture of the solid and liquid phases would be preserved for an infinite long time in the equilibrium condition at the sintering temperature, the process of liquid-phase sintering is finished only by growth of the powder body, i.e., at first stage. In the latter case we mean, so-called, transient liquid-phase sintering. In accordance with the theory of the three stages, the amount of the liquid phase ensuring densification of the powder body up to its full dense state is equal 35 vol. %. In reality, the quantity of the liquid phase formed can be rather significant, considerably exceeding the above critical content. For instance, no appreciable densification is observed in the Ti-Al system, if even 75 vol. % of the condense phase of a compact is the liquid phase.

The reason of such behaviour of powder bodies during liquid-phase sintering is a specific character of the diffusion interaction of two components, one of which is in the liquid state. Atoms belonging to the solid phase cannot pass into the liquid phase because of their strong ties with the crystal lattice. Therefore, atoms of the second component having the weaker ties with the melt diffuse into the solid phase during the all process of phases interaction, until the phase balance is established in the system. In this case, the concentration of the second component in the surface layer of the solid phase at some moment of time reaches a value enabling to this layer to pass into liquid state by melting. In such a way the dissolution process is carried out, or more accurate the transition of a solid phase into liquid one.

Such mechanism of the diffusion interaction of solid and liquid phases explains known laws of liquid-phase sintering and, in particular, why the growth of a powder body precedes its densification as well as why the absolute meanings of volume changes depend on mutual solubility limits of phases, the additive content, sintering temperature, particles sizes and etc. [1]. So, in the Al-Cu system having a small solubility of Cu in Al in solid state and a large solubility of Al in the eutectic melt, an absolute value of powder compacts densification appears to be much more than their growth, whereas in the Ti-Al system possessing a considerable solubility in solid phase and a small solubility in the melt, the growth of powder bodies essentially surpasses their shrinkage.

The densification of a powder body becomes more with increasing of the sintering temperature and/or the content of the additive forming the liquid phase due to an increase of the

melt quantity. The higher content of the liquid phase, the more amount of the solid phase is dissolved in it, the less the solid phase remains, the less sizes of the persisted particles become and the greater space is released for rearrangement of the particles.

The larger aluminium particles, the smaller the surface area of the solid phase particles over which the interaction with the melt takes place and the less densification value, including one at the expense of reduction of capillary forces caused by the presence of the larger interparticle pores.

Dilatometric researches of volume changes of powder bodies of the Al-Cu, Al-Si, and Al-Zn systems during sintering show that compacts on the base of the aluminium powder of technical purity have the more noticeable densification value in comparison with samples on the base of a high purity aluminium powder. This fact is connected with that the aluminium particles with impurities are inclined in the greater degree to disintegration during interaction with the melt. It is possible to suppose that disintegration of particles [2] promotes densification as a result of rearrangement of the fragments [3] owing to facilitation for sliding of the fragments along liquid phase layers with accommodation of the crystal shapes through the liquid phase [4].

Dark "stains" inside grains of sintered Al-Cu alloys found out with the help of metallography studies are of a scientific interest. An electron microprobe analysis has shown the presence of an increased content of copper in them. It is possible to assume that the stains form at the expense of precipitation of dispersed particles of the secondary $CuAl_2$ phase in aluminium lattice during cooling of solid solutions and subsequent coagulating of these inclusions.

As it turned out, the reduction of the aluminium lattice parameter up to a minimal meaning during liquid-phase sintering samples of the Al-Cu system is finished not by the end of the growth stage, but a bit late, until the beginning of the densification stage. This circumstance demonstrates that the growth of a powder body stops not because the diffusion of copper atoms in the aluminium lattice is finished by achievement of an equilibrium concentration in the solid phase, but because the growth stage is interrupted by occurrence of the densification process. As the system has not yet reached a chemical balance as relating to the content of copper in the solid phase as, probably, concerning composition of the liquid phase, densification in this moment to be carried out by means of the solid phase particles rearrangement due to their dissolving into the liquid phase. In subsequent period of time, when the lattice parameter becomes constant and it means that at least the solid phase already has reached a chemical balance, densification can proceed due to the rearrangement which is now connected to the classical solution-reprecipitation process.

An increase of the copper content in the Al-Cu mixture up to 30 wt. % permits completely to exclude the compact growth during sintering owing to formation of a large quantity of the liquid phase destroying its rigid skeleton before it begins to increase its volume as a result of diffusion from the melt. Densification at such amount of the liquid phase is caused only by a quick rearrangement of solid phase particles in the liquid.

**Conclusions:**

The main part of compacts densification during liquid-phase sintering systems with significant solubility of the solid phase in liquid proceeds by means of the rearrangement process of the solid phase particles caused by dissolution of them in the liquid phase. In subsequent period of time, when the solid phase reaches its chemical balance, some densification can be controlled by rearrangement which is connected now to process of solution-reprecipitation. At formation of a large quantity of the liquid phase densification proceeds as a result of the instantaneous rearrangement process.

**References**

1. Savitskii A.P. Liquid phase sintering of the systems with interacting components, 1993, Russian Academy of Sciences, Tomsk.
2. Magee B.E., Lund J. Mechanisms of liquid-phase sintering in iron-copper powder compacts, Z. Metallkunde, 1976, **67**, 9, S. 596-602.
3. Petzow G., Kaysser W.A. Liquid phase sintering, Sci. Ceram. Proc. 10th Int. Conf., Berchtesgaden, 1979, **10**, p. 269-278.
4. Panechkina V.V., Sirotyuk M.M., Skorokhod V.V. Liquid-phase sintering of highly fine tungsten-copper mixtures, Poroshkovaya metallurgiya (Kiev), 1982, 6, p. 27-31.

# EFFECT OF A SMALL AMOUNT OF BORON ON STRUCTURE AND PROPERTIES IN MOLYBDENUM ALLOYS

**Fumio MORITO*, Tetsuji NODA and Alexander V. KRAJNIKOV[(1)]**
National Institute for Materials Science, Tsukuba, Japan
[(1)]Institute for Problems of Materials Science, Kiev, Ukraine

Mechanical properties of molybdenum alloys have been improved by a small amount of boron addition [1-5]. We also studied boron distribution by particle-tracking autoradiography (PTA) [6-8].

Materials in this paper were prepared by plasma-beam, electron-beam and arc melting. Content of boron was between less than 0.02 ppm and 920 ppm.

Fig.1 shows the relation between bend angle and test temperature in PE alloys. DBTT was defined as the bend ductility of 30 degrees. Therefore DBTT of Mo-2.5 ppm B, Mo-1.3 ppm B and pure Mo was 170K, 210K and 275K, respectively. Yield stress of Mo-2.5 ppm was rather lower in the test temperature lower than 240K. However yield stress of Mo-1.3 ppm B was the highest in the temperature range of this experiment. It is clear that only a small amount of boron addition in molybdenum made a significant improvement of bend properties.

Solubility of boron to molybdenum was very small, less than 1 ppm at room temperature. With an increase of boron content, fine precipitates were uniformly observed in the matrix [1-5]. Such precipitates of molybdenum borides were considered to behave as a trapping site for hydrogen diffusion [2]. Above the content of 50 ppm B, we often recognized needle-like precipitates that grew to the <110> direction in the matrix and along grain boundaries [1-5]. In the case of Mo-920 ppm B, precipitates coalesced and fine needle-like ones were almost diminished in the matrix [2]. Strengthening effect of grain boundaries by boron addition and characteristics of boron precipitates will be discussed in detail.

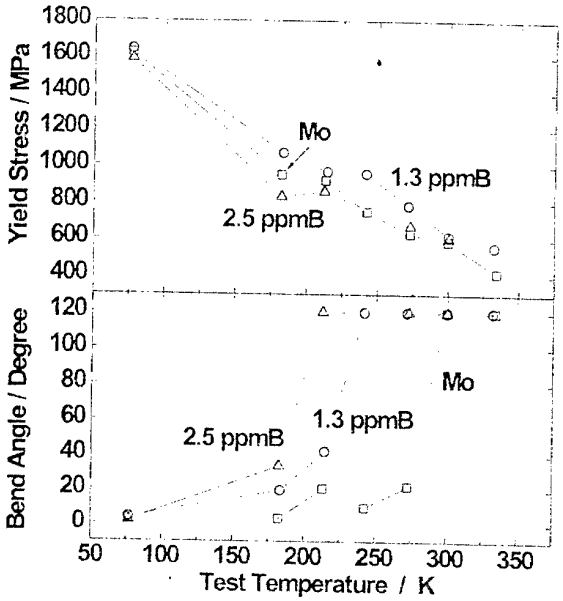


Fig.1 Bend properties of PE alloys.

References
1. T. Noda et al, Proc. 7th Inter. Conf. on Vacuum Metallurgy, The Iron and Steel Institute of Japan, (1982), 1290.
2. T. Noda and M. Okada, Trans. JIM., 28(1987), 517.
3. F. Morito, Colloque de Physique, C1-51(1990), 281.
4. F. Morito, Surface and Interface Analysis, 15(1990), 427.
5. F. Morito, Scripta Mat,. (2002), to be published.
6. F. Morito, A. V. Krajnikov and H. Saito, Proc. Int. Conf. Science for Materials 2002.
7. F. Morito and H. Saito, Scripta Mat,. (2002), to be published.
8. H.Saito and F.Morito, ISIJ Int., (2003), to be published.

*Corresponding author: morito.fumio@nims.go.jp

# LOCALIZED PLASTIC SHEAR PROPAGATION IN A METAL LAYER

**Stepanov G.V., Shirokov A.V.**
Institute for Problems of Strength, National Academy of Sciences, Kiev, Ukraine

Combined influence of the nonuniformity and adiabatic heating in material at dynamic loading reduce resistance to plastic deformation and results in localized shear or adiabatic shear bands formation.

The works [1–3] are devoted to numerical investigations of plastic deformation localization. The influence of applied velocity on the shear band propagation was analyzed in [4] and compared with the experimental results in [5]. The influence of specific effects at plastic shear (nonlinear viscosity, damage and temperature) on stress-strain distribution in one-dimensional problem was analyzed in [6]. But there are only scarce data on dynamic propagation (lengthening) of localization area.

The main aim of this work is numerical simulation of main features of propagation (lengthening) of the area of intense plastic shear in a thin metal layer.

Simple shear in the layer ($H$=6,0×10-3 m) of isotropic material was investigated. The initial conditions are zero. The velocities of shear $v_x$ at the boundaries (antisymmetric in relation to the center of the layer) along $x$ direction changing with time are used.

We assume the material to be elastic-viscoplastic. The modified Jonson-Cook's equation of state [7] in the form (1) that take into account viscosity effects was used in the simulation. It includes well established effects of strain hardening, thermal softening and linear viscosity (with viscosity factor $\mu$):

$$\sigma = \sigma_{st} + \mu \varepsilon_i^p; \quad (1)$$

$$\sigma_{st} = \sigma_y[1 + A \cdot (\varepsilon_i^p)^n][1 - (\frac{T}{T_c})^b],$$

where $\sigma_y$ is an yield stress of a metal under static loading; $\varepsilon_i^p$ is effective strain; $A$, $n$ are constants of strain hardening; $b$ is constants of thermal softening; $T$, $Tc$ are current and critical temperature of metal. A nonlinear temperature dependence of shear modulus was also included in the computation in the form (2):

$$G(T)=G_0(1-T/T_c), \quad (2)$$

where $G_0$ is shear modulus at 20°C.

Heat conduction was neglected because of short duration of high strain rate localization. The work of plastic deformation defines the law of temperature increase:

$$\frac{dT}{dt} = \frac{\dot{\varepsilon}_i^p \sigma_i}{c_v}, \quad (3)$$

where $c_v$ is thermal capacity of a material, $\sigma_i$ is intensity of instant stress.

A short linear defect of length $l$ ($l$=1,5.10-4 m) was included in the center of the layer. In such way was initiated shear localization. The boundaries velocities of the layer were increased in time till constant volume ($v_0$) for 2,5 $\mu s$ ($t_k$=50) at equation

$$v_x(t)=v_0(1-\exp(-t_k/3)), \quad (4)$$

where $t_k$ is a current step's number in time.

The layer was modeled as a two-dimensional array with 200×20 elements (nodes). $Nx$=200, $Ny$=20, where $Nx$, $Ny$ are number of nodes in $x$, $y$ direction. A step in time was chosen from stability condition by Kurant.

We assumed that elastic deformation $e_{ij}$ cannot be more than its theoretical value:

$$e_{ij} \le \frac{\sigma_y}{G_0}. \quad (5)$$

The linear defect was modeled as some nodes with decreased (on 20% ) yield stress.

The thermo-mechanical parameters of mild steel (Table 1) was taken in the account, where $\nu$ is module of Puanson.

The influence of the initial defect on distribution of plastic deformation in the metal layer before the localization is small. Increase of deformation in it is only 2% among neighbor nodes. After beginning of localization the plastic deformation propagation from initial defect had symmetric form. And farther the plastic deformation localization become a basic process in the layer.

The propagation rates of plastic strain of fixed levels along the layer (on nodes) from the initial defect graphed on fig. 1. Propagation rate $v_e$ of plastic strain level along the layer depends on

strain level and increases with distance from the initiate defect to the elastic shear wave velocity in metal.

Table1. The thermo-mechanical parameters of mild steel

| Material | Mild steel |
|---|---|
| $\sigma_y$, Pa×$10^6$ | 300 |
| E, Pa×$10^{11}$ | 2,1 |
| Tc, °C | 750 |
| n | 0,3 |
| A | 0,3 |
| b | 0.5 |
| ν | 0.27 |
| $v_0$, m/s | 45 |
| $\mu$, Pa×s [ 8] | 20000 |
| ρ, g/m3×$10^3$ | 7.8 |

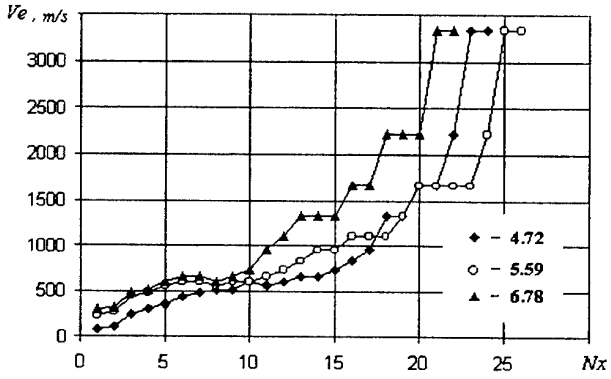


Fig.1. The propagation rates of plastic strain of fixed levels along the layer (on nodes) from the initial defect.

References

1. Stepanov G.V., Fedorchuk V.A. Localized shear in metals under impact loading. // Strength of materials.-2000.- V. 32, № 2, 125-135.
2. Batra R.C. Effect of material parameters on the initiation and growth of adiabatic shear bands. // Int. J. Solids and Struct. – 1987. V. 23, № 10.
3. Wright T.W., Walter J. W. On stress collapse in adiabatic shear bands. // J. Mech. Phys. Solids. – 1987. – V. 35, № 6.
4. A.-S. Lebouvier, P. Lipinski and A. Molinari. Numerical study of the propagation of an adiabatic shear band. // J. Phys. 4 France 10 (2000), 403–408.
5. Marchand A., and Duffy J., J. Mech. Phys. Solids 36 (1988), 251–283.
6. Stepanov G.V., Fedorchuk V.A. Localized shear in sheet material. // Strength of materials.- 1999.- V. 31, № 5, 467-474.
7. Jonson R.G., Cook W.H. Fracture characteristics of three metals subjected to various strains, stran rates, temperatures and pressures // Engng Fract. Mech. –1985.- 21, N 1. – P. 31 – 48.
8. Stepanov G.V. Elastic-plastic deformation and fracture of materials under impulse loading (In russian). – Kiev: Naukova Dumka, 1991. – 287c.

# THE DESCRIPTION OF THE SILICON MELT MOVEMENT AT THE FZ PROCESS

**Egorov S.G., Chervonyi I.F., Kolobov G.A., Nikonenko A.P.**
The Zaporozhye State Engineering Academy, Zaporozhye, Ukraine

Today FZ method is used for manufacturing of high resistance monocrystals of the silicon.

During the process of growth of the silicon monocrystals in a zone molten the convective, centrifugal, electrodynamic forces and forces of a surface tension work [1].

These forces call the melt movement, which plays a considerable role in the heat interchange and impurity distribution at the front of crystallization. The dimensionless parametric numbers because of difficulties of visual observation under operational conditions for describing of melt movement are used.

The Grashof ($Gr$), Prandtl ($Pr$) and Raleigh ($Ra$) numbers for describing of thermal streams in a melt are used. The Grashof number features operation of a free convection caused by presence of a temperature lapse rate. It represents the ratio of body forces in a nonisothermal homogeneous fluid as to friction forces:

$$Gr = \frac{g\beta\Delta T H^3}{\nu^2}, \qquad (1)$$

where $g$ - free fall acceleration, m/c$^2$; $\beta$ - coefficient of volume expansion, for silicon $\beta = 1.4\times10^{-4}$ K$^{-1}$; $\Delta T = T_1 - T_2$ – odds of the temperatures between heated and cooled areas, K; $H$ – the melt height, m; $\nu$ - kinematic viscosity, $\nu = 3.5\times10^{-7}$ м$^2$/с. While calculating the $Gr$ number it is necessary to take into account that for each diameter there is the odd of temperature [2].

The Prandtl number represents the ratio between coefficients of viscosity and thermal diffusivity $Pr = \nu/\chi$, where $\chi$ - thermal diffusivity, m$^2$/s. For silicon the Prandtl number is $Pr = 0.014$.

The Grashof and Prandtl numbers multiplication gives the Raleigh number

$$Ra = Gr \cdot Pr = \frac{g\beta\Delta T H^3}{\nu\chi}. \qquad (2)$$

The convection mode is determined depending on the quantity of Ra number's and quantity of the ratio $H/d$ (the ratio of zone molten height to its diameter).

If $Ra < Ra_{C1}$ then the convection in the melt is not present and the thermal conduction mode is carried out; if $Ra_{C1} \le Ra < Ra_{C2}$ then, a stationary convection develops; if $Ra_{C2} \le Ra < Ra_{C3}$ then the mode of convection development transfers from stationary to non-stationary one; if $Ra_{C3} \le Ra$, then the turbulent convection is observed, where $Ra_{C1}$, $Ra_{C2}$, $Ra_{C3}$ - are critical values for the relevant convection types [3]. The Ra number, similar to Gr number, will rise while increasing of the crystal radius.

It is necessary to note, that at the FZ-process the top heating ($T_1 > T_2$) is carried out (fig. 1). Hence, there are no the convection streams in the molten zone.

The diffusion mode of substance transport is carried out, and the heat is transmitted at the expense of the thermal conduction. In this case $Gr = 0$ and $Ra = 0$.

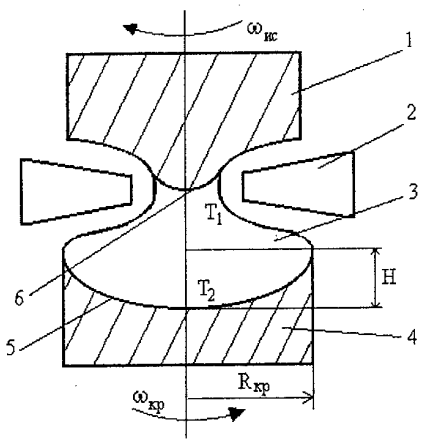


1 - seed; 2 - coil; 3 - melt; 4 - single crystal; 5 - solidified front; 6 - melting front.

Figure 1 - Scheme of the FZ-process.

The following type of the natural convection is the thermocapillary convection. It is due to the surface forces. The convection given is featured by the Marangoni number's ($Ma_T$), which is the ratio of the surface forces lapse rate caused by the temperature difference as to viscosity forces

$$Ma_T = \frac{-(\partial\sigma/\partial T)\Delta T R_{кр}}{\rho\chi\nu}, \qquad (3)$$

where $\sigma$ - surface force, N/m; $(\partial\sigma/\partial T)$ – lapse rate of the surface force, $(\partial\sigma/\partial T) = -0.13\times10^{-3}$ Н/(м·К).

The Marangoni streams work in the area near to the melt - atmosphere interfaces. With increasing crystal radius the $Ma_T$ number will rise and for crystals of radius 75 mm ($\Delta T = 72$°C [3]) is $Ma_T \approx 3\cdot10^4$.

Except for the natural convection, in the melt the forced convection caused by the presence of centrifugal and electrodynamic forces works.

The forced convection caused by rotation of the crystal is featured by a rotary Reynolds number

$$Re_{\omega} = \frac{\omega R_{kp}^2}{\nu}, \qquad (4)$$

where $\omega$ - speed of crystal rotation, $s^{-1}$.

With increasing of crystal dimensions the speed of its rotation reduces for a drop of inertial forces effective on the melt, which can give strait of a melt through the melt - atmosphere interface. For $R_{kp}$=75 mm and $\omega$=1.05 $c^{-1}$ the quantity Reynolds number is $Re_{\omega} \approx 1.7 \cdot 10^4$.

In paper [4] it is shown, that the electrodynamic forces work in surface area of the melt and make possible the melt movement, which is featured in the following parameter:

$$N_{md} = \frac{\mu H^2}{\rho \upsilon^2}, \qquad (5)$$

where $\mu$ - constant of a magnetic field, $\mu = 4\pi \times 10^{-7}$ H/m; $H$ – intensity of a magnetic field, A/m; $\upsilon$ - speed of melt fluxion , caused by electrodynamic forces, m/s.

For featuring the magnetic field influence, which is generated by the coil, the Hartman number, showing the ratio of magnetic forces as to viscosity forces, is used:

$$Ha = BR\sqrt{\frac{\sigma}{\eta}}, \qquad (6)$$

where $B$ – magnetic induction, T; $\sigma$ - electrical conductance of the silicon melt, $\sigma = 12.3 \times 10^5$ $(\Omega \cdot m)^{-1}$; $\eta$ - dynamic viscosity of the silicon melt, $\eta = 8.8 \times 10^{-4}$ Pa·s. At 75 mm single crystal growth the magnetic induction is equal 0.05 T [4]. In this case the Hartman number is $Ha$=143.

During single crystal growth all convection types work simultaneously, therefore, for the characterizing of the processes, taking place in the molten zone, we use the following ratios as to parametric numbers: $Gr/Re_{\omega}^2$, $Ma/N_{md}$, $Gr/N_{md}$, $Ha^2/Gr^{1/2}$, $Ha^2/Re_{\omega}$, etc.

In the absence of the thermal convection taking place in all the volume of the zone molten it is possible to include to the process rotation and electromagnetic forces having the similar order ($Ha^2/Re_{\omega}$=1.2÷2.4, depending on rotation single crystal speed). Driving the relation between these forces it is possible to influence on volumetric distribution of an impurity in the melt.

The electrodynamic forces and Marangoni streams work in a lamina of the melt near to a surface.

Here electrodynamic forces exceed all remaining ones by some orders [4]. However, with increasing of the zone molten height (increasing of the crystal radius) their influence on the impurity distribution near to the solidified front decreases.

Therefore, to run effectively the quality of the monocrystal is possible using its rotation and magnetic field.

**REFERENCES**

1. Технология полупроводникового кремния/ Фалькевич Э.С., Пульнер Э.О., Червоный И.Ф. и др. - М.: Металлургия. - 1992. - 408 с.
2. Muehlbauer A., Muiznicks A., Raming G. System of Mathematical Models for the Analysis of Industrial FZ-Si-Crystal Growth Processes//Cryst. Res. Technol. - 1999. - v.34. - №2. - P.217-226.
3. Мюллер Г. Выращивание кристаллов из расплава. Конвекция и неоднородности: Пер. с англ. - М.: Мир. - 1991. - 143 с.
4. Muhlbauer A., Erdmann W., Keller W. Electrodynamic convection in silicon floating zones// J. Cryst. Growth. - 1983. - v.64. - P.529 - 545.

# THE INFLUENCE OF INITIAL POWDERS DISPERSIVITY, ACTIVATING AGENTS AND HOT PRESSING TEMPERATURE ON $Si_3N4$-SiC CERAMICS DENSITY

**Goloubtsova E.S., Kaledin B.A, Malkevich N.G.**
Belarussian national technical university, Minsk, Republic of Belarus

The materials with heteroigeneous structure are perspective for the process design of wide class of resistors, conducting phase of with is evenly distributed in dielectric matrix. Silicon carbide and silicon nitride would be appropriate materials for use as base combinations for the production of thermal stable resistor's elements.

It was established, that the use of hot pressing (HP) makes possible to change the material composition over a wide range and to produce the materials with designated properties.

The purpose of the given work is to investigate the influence of initial powders dispersivity, activating agents (MgO and $Al_2O_3$) and hot pressing temperature (1920, 1970 and 2020 K) on density (porosity), and electrical-and physical properties of hot-pressed ceramic materials on the base of silicon carbide and silicon nitride.

The mixtures containing $Si_3N_4$powder with grain size 3—5 μm (20 vol.%) and SiC powder with grain size 1 and 10 μm were used for samples manufacture.

The methods of experimental design were also used for pursuance of the research and on this base was chosen the plan 2×2×3.

As optimization parameter was taken a porosity, % (y), and as the factors: $\widetilde{x}_1$—dispersivity of SiC powder, μm (1 and 10 μm),, $\widetilde{x}_2$— activating agents (MgO and $Al_2O_3$) and $\widetilde{x}_3$— hot pressing temperature (1920, 1970 and 2020 K). The tabulated factors for this plan were: $A_0$=0,25, $A_{01}$=$A_{02}$=0; $A_{03}$=0,25; $A_1$=$A_2$=0,08333; $A_3$=0,125; $A_{11}$=$A_{22}$=0; $A_{33}$=0,375; $A_{12}$=0.08333; $A_{13}$=$A_{23}$=0,125; t=2,179. A replication error ($S_y$) was 0,4. Plan matrix and porosity values are listed in the following table:

| № | $x_1$ | $x_2$ | $x_3$ | $x_1x_2$ | $x_1x_3$ | $x_2$ $x_3$ | $x_3^2$ | $y_э$ | $\hat{y}$ |
|---|---|---|---|---|---|---|---|---|---|
| 1 | - | - | - | + | + | + | + | 2,5 | 2,9 |
| 2 | - | - | 0 | + | 0 | 0 | 0 | 1,0 | 0,94 |
| 3 | - | - | + | + | - | - | + | 0,5 | 0,14 |
| 4 | - | + | - | - | + | - | + | 8,1 | 7,68 |
| 5 | - | + | 0 | - | 0 | 0 | 0 | 3,9 | 4,02 |
| 6 | - | + | + | - | - | + | - | 1,2 | 1,52 |
| 7 | + | - | - | - | - | + | + | 9,2 | 8,88 |
| 8 | + | - | 0 | - | 0 | 0 | 0 | 8,1 | 8,02 |
| 9 | + | - | + | - | + | - | + | 7,9 | 8,32 |
| 10 | + | + | - | + | - | - | + | 20 | 20,4 |
| 11 | + | + | 0 | + | 0 | 0 | 0 | 17,8 | 17,8 |
| 12 | + | + | + | + | + | + | + | 16,8 | 16,4 |
| $\sum$ | 62.6 | 38.6 | -13.4 | 20.2 | 4.4 | -6.8 | 66.2 | 97 | |

Activating agents content comprises 5 vol.%.

The adequate regression equation establishing the link between porosity ($y_э$) and above mentioned factors was received after processing of experimental results ($y_э$) and validation of the factors significance:

$$y = 7,7 + 5,22x_1 + 3,22x_2 - 1,68x_3 + 1,68x_1x_2 + 0,55x_1x_3 - 0,25x_2x_3 + 0,58x_3^2$$

The analysis of this equation shows, that the greatest influence on porosity renders a dispersivity of SiC powders ($x_1$), then comes activating agent ($x_2$) and temperature of hot pressing ($x_3$).

It should be used SiC powder with grain size ~1 μm ($x_1$=-1); MgO as activating agent ($x_2$= - 1) and hot pressing temperature equal 2020 K ($x_3$=+1) for reduction of porosity.

In this case the calculated value is $\hat{y}_3 = 0,14$ (experimental value is ~0,5%).

Dense hot pressed samples $Si_3N_4$—SiC produced with use of activating agent MgO or $Al_2O_3$ represent heterophase compositions, , wherein SiC particles are evenly distributed in silicon nitride matrix.

The pores having mainly isometric form and, as a rule, small size (about 1 μm) are arranged at the interfaces between some grains.

X-ray phase analysis has shown, that independently of activating agent SiC conserves thermodynamic stability in $Si_3N_4$—SiC composition, does not form new compounds and solid solutions.

Therefore the formations in silicon nitride matrix is governed by identical regularities as occur in dielectric materials $Si_3N_4$—MgO and $Si_3N_4$—$Al_2O_3$.

Thus, the use of MgO as activating agent under hot pressing makes possible $Si_3N_4$—SiC compositions without essential change of phase composition and with high values of density.

# INVESTIGATION OF THE INTERACTION IN THE Cu-Mg-C SYSTEM UNDER HIGH PRESSURE AND TEMPERATURE

**Turkevich V.Z., Kulik O.G., Osipov A.S., Garan A.G.**
Bakul Institute for Superhard Materials of the National Academy of Sciences of Ukraine, Kiev, Ukraine

Phase diagrams of the Cu-Mg-C ternary system and involved binary systems under atmospheric and high pressure are unknown. Experiments on spontaneous diamond crystallization have not been carried out yet, while the peculiarities of diamond growth on seed crystals in the Cu-Mg-C system have been already studied [1]. It has been found that at 6GPa and 1550 °C, diamond crystals grow intensively on seeds. The most perfect crystals were obtained when Cu-Mg alloys contained 40-50 at.% Mg.

In this paper we present the results of our studies on the phase composition and structure of the samples produced at 7.7 GPa between 1220 and 1850°C, the holding time being 100 s. The sample compositions are 30 Cu, 15 Mg, 55 $C_{gr}$ and 15 Cu, 30 Mg, 55 $C_{gr}$. (all at.%).

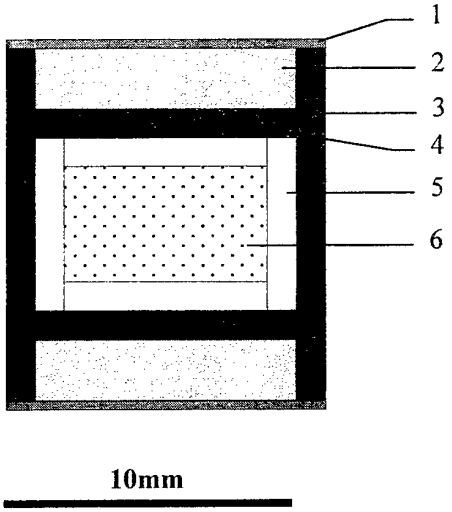


Fig. 1. Thoroid-type HPA cell: 1-molibdenum plate, 2-pyrophilite disc, 3-graphite heater, 4-graphite disc, 5-$Al_2O_3$ shield, 6-experimental Cu-Mg-C mixture.

The samples were made using a toroid-type high-pressure apparatus (HPA) with a 20-mm-in-diameter recess. The experimental assembly is shown in Fig. 1. Temperatures were estimated using a Pt/Pt-10%Rh thermocouple without regard for the pressure effect on the thermoelectromotive force. The HPA was pressure graduated from polymorphic transformations of bismuth Bi I-II (2.54 GPa), Bi VI-VII (7.71 GPa) and lead selenide PbSe I-II (4.23 GPa) at 20 °C.

Alloys containing 66.7 at.% Cu, 33.4 at.% Mg and 33.4 at.% Cu, 66.7 at.% Mg were preliminary produced at 4 GPa and 1600 °C. Then alloys were crushed into powder, mixed with 55 at.% graphite and the mixture was placed into the HP cell (Fig. 1).

The phase composition and structure of samples were studied by scanning electron microscopy, X-ray diffraction and microstructure analyses.

The structure of alloys containing 30 at.% Cu, 15 at.% Mg produced at 7.7 GPa and 1220-1610 °C are shown in Figs. 2, 3. It is seen that coarse grains of the $Cu_2Mg$ intermetallide prevail in these alloys. There are inclusions of graphite and carbide phases of small sizes. With increasing temperature the differentiation between individual phase constituents is clearer.

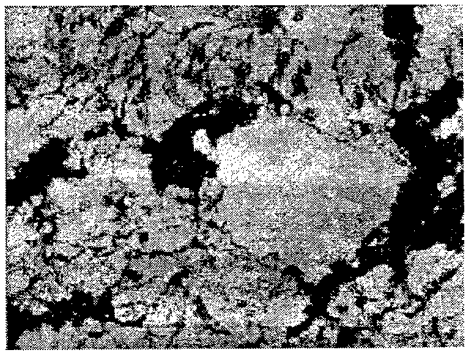

Fig. 2. SEM-micrograph of alloy obtained at 1220°C and 7.7 GPa, (360×).

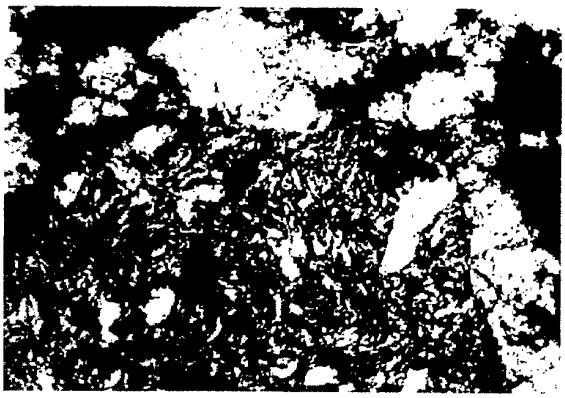

Fig. 3. Microstructure of alloy obtained at 1610°C and 7.7 GPa, metallography (500×).

$CuMg_2$ phase and carbide MgC form in the samples containing 15 at.% Cu, 30 at.% Mg and prepared at 7.7 GPa and 1220-1610°C (Figs. 4-6). The formation of MgC carbide agrees with the data reported in [2]. Also, more eutectic is observed as compared with that in samples containing 30 at.% Cu, 15 at.% Mg.

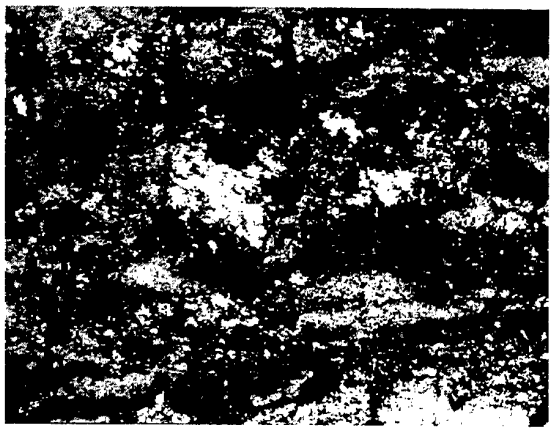

Fig. 4. Microstructure of alloy obtained at 1220°C and 7.7 GPa, (200×).

The region of diamond-liquid stable equilibria under the p,T conditions being studied was not reached.

Our findings have allowed us to predict the melting diagram of the Cu-Mg-C system under atmospheric and high pressures, which should be characterized by the nonvariant four-phase eutectic equilibrium with participation of carbon.

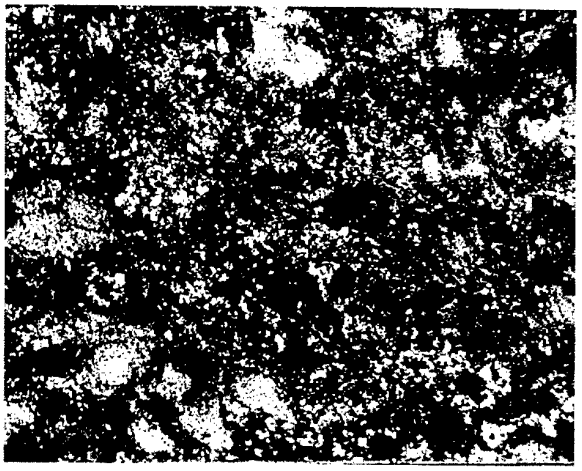

Fig. 5. Microstructure of alloy obtained at 1430°C and 7.7 GPa, (200×).

Fig. 6. Microstructure of alloy obtained at 1850°C and 7.7 GPa, (200×).

**References**

1. *A.V. Andreyev, H. Kanda* Diamond formation and wettability in a Mg-Cu-C system under high pressure and high temperature // Diamond and related materials. –1997. –№6. –P. 28-32.
2. *A.A Shul'zhenko, I. Yu. Ignat'eva, N.N. Blyavina, and I.S. Belousov* Phase diagram of magnesium-carbon system at a pressure of 7.7 GPa // Soviet Journal of Superhard Materials.–1988. №6.– C. 3-5.

# SHORT-SAMPLE MODELING OF STRESS EFFECTS IN SUPERCONDUCTING COMPOSITES

KISLYAK I., DOTSENKO V.[(1)], TIKHONOVSKY M.[(2)], SHKILKO A.[(3)], ZAGORUIKO L.[(3)]
Verkin Institute for Low Temperature Physics & Engineering of NAS of Ukraine, Kharkov, Ukraine
[(1)]Ukrainian Medical Stomatological Academy, Poltava, Ukraine
[(2)]National Scientific Centre "Kharkov Institute of Physics & Technology", Kharkov, Ukraine
[(3)]Ukrainian Academy of Engineering & Pedagogics, Kharkov, Ukraine

***Introduction:*** Design and functioning of contemporary powerful superconducting systems involve tremendous mechanical stresses. So, changes of the composites characteristics under the conditions (or mechanical stresses effects on critical parameters of superconductors) still remain an urgent scientific and technological problem because they can be significant and are to be taken into account.

The major part of relevant research deals with tension and bending effects on the critical current density $j_c$ and the upper critical field $H_{c2}$. Studies of the critical temperature $T_c$ changes under mechanical loads are less numerous, and only in some instances loads other than listed, e.g. transverse compression, were used. Therefore, we carried out investigations of the effects of both uniaxial tensile and transverse compressive stresses on critical parameters of a number of superconducting composites.

***Materials:*** 1) Cu-Nb *in situ* composite wires that are of growing interest in virtue of unique combination of their high strength and high normal electrical conductivity combined with their superconductivity [1,2]; 2)Cu-NbTi and bronze-$Nb_3Sn$ commercial composites. Two sets of multifilamentary composites Cu-Nb prepared *in situ* from the initial alloy Cu-40 wt% Nb were investigated [3]. They differed in their final diameters $d_2$ and true strain $\delta=\ln(d_1^2/d_2^2)$, used as the measure of deformation at the final stage of wire production.

***Experimental technique:*** two sets of experiments were carried out: a) uniaxial tension ($\sigma,\varepsilon$) vs. resistive critical field ($H_r$ ) study of Cu-Nb *in situ* composites (*a-studies*); b) uniaxial tension and uniaxial transverse compression ($\sigma,\varepsilon$) vs. critical temperature ($T_c$ ) studies of all the three types of composites (*b-studies*). Resistive measurements in the both sets of studies were carried out using 4-probe scheme. Voltage drop $U$ across the potential leads on a sample test section was applied to the Y-input of a plotter. Then, for *a-studies,* composite samples were mounted at the axis of a superconducting solenoid and subjected to tensile load. Signal proportional to the solenoid current and, hence, to generated magnetic field, was applied to the X-input of the plotter. Gradual or step-like feeding of the solenoid caused transition of a sample from superconducting to normal state (and back), and the transition curve was registered by the plotter. Value of resistive critical field $H_r$ was determined at the middle point of the transition curve. These measurements were carried out in liquid helium at 4.2 K for both the initial and loaded states of a sample.

For *b-studies,* under uniaxial tension, samples were placed inside an electrical heater wound on copper tube, the whole assembly being installed then into two-wall dewar that separated the assembly from liquid helium environment. Temperature sensor was mounted in the middle of a sample test section in good thermal contact with it, and signal from the sensor was applied to the X-input of the plotter. The middle point of a superconducting transition curve was adopted as a sample critical temperature $T_{cm}$ . For uniaxial transverse compression studies, a section of a composite under investigation with soldered potential leads was placed between compressing surfaces. Space between potential leads was less than the compressed section to eliminate edge effects. Additional precautions to make experimental environment more isothermal were undertaken. Other details of the experimental procedure were similar to those for uniaxial tension studies.

***Results and discussion:*** *a-studies* produced the following results for Cu-Nb *in situ* composites:

1. $H_r$ increases gradually from $H_{r0} \approx 12.3$ kOe to $H_{r\,max} \approx 16.8$ kOe as the composite uniform deformation proceeds, that is for stress $\sigma$ increasing from 0 to 1.6 GPa. So, the initial $H_r$ value absolute increase is $\Delta H_{r\,max} \approx 4.5$ kOe and the relative one ($h_r = H_r / H_{r0}$ ) is $\delta h_{r\,max} \approx 37\%$, the average derivative $dH_r/d\sigma \approx 2.8$ Oe/MPa (280 Oe/kbar);

2. Superconducting-to-normal state transition width $\Delta H$ increases also from the initial value $\Delta H_0 \approx$ 3 kOe to $\Delta H_{max} \approx 4.8$ kOe at $\sigma$=1.6 Gpa.

3. $h_r$ irreversible increase due to plastic strain of the sample, after the initial loading to $\sigma$ =1.6 Gpa followed by unloading, is $\delta h_{r\,irr} \approx 12\%$.

4. Dependence for the relative critical field vs. stress $\delta h_r$ ($\sigma$) under cyclic loading is similar to that for the stress-strain curve $\sigma(\varepsilon)$, which, as shown by our earlier studies [4], is of hysteretic character. Dependence for the relative critical field vs. total strain $\delta h_r$ ($\varepsilon_t$ ) is single-valued under these conditions for the region of the composite uniform loading.

To account for $H_r$ changes under mechanical loads, consider relation between the upper critical field $H_{c2}$ and the thermodynamic critical field $H_c$,

$$H_{c2} = \sqrt{2}\,\kappa H_c, \quad (1)$$

where $\kappa$ is Ginzburg-Landau parameter. It follows from Equation (1) that, in principle, either $\kappa$ or $H_c$ (or both) increase can account for $H_{c2}$ increase. As concerns $H_{r0}$ ($\delta$) dependence, here, no doubt, an important role is played by $\kappa$. According to Gor'kov-Goodman formula,

$$\kappa = \kappa_0 + 7.5\bullet 10^3\,\gamma^{1/2}\,\rho_n, \quad (2)$$

where $\kappa_0$ is the parameter of an initial material, $\gamma$ is Sommerfeld constant, $\rho_n$ is a material specific electrical resistivity in the normal state. An *in situ* composite preparation process involves very high plastic deformations resulting in formation and storage of dramatic number of strain defects. These factors reduce significantly the electron mean free path and, therefore, increase $\rho_n$ As our results evidence, niobium filaments real defect structure is characterized by the "knife-like" boundaries between relatively dislocation-free regions of the material [5]. This brings to very high dislocation densities and internal stress levels in the boundaries and, therefore, to substantial increase of local $\kappa$ and $H_c$ values and, finally, to $H_{c2}$ increase.

Our experimental results demonstrate that technologically formed dislocation structures of *in situ* composites favour significant rise of the resistive critical field $H_r$ and its mechanical load sensitivity. Analysis of our data shows that Ginzburg-Landau parameter $\kappa$ and the thermodynamic critical field $H_c$ of niobium filaments are the most probable causes of both $H_r$ (and $H_{c2}$) value increase and its load sensitivity $dH_r/d\sigma$ (or $dH_r/d\varepsilon_t$ ) rise. Ginzburg-Landau parameter $\kappa$ changes, resulting from Cu-Nb *in situ* composites preparation technology, bring to $H_{r0}$ increase and $H_{r0}(\delta)$ dependence, and relationship between $H_c$ and $\sigma$ results in the observed $H_r$ ($\sigma$) dependence.

*b-studies* resulted in the following findings:

*In situ* Cu-Nb composites: $T_{cm}$ under uniaxial tensile stress behaves itself qualitatively similar to the composite resistive critical field $H_r$ : the dependence on stress, $T_{cm}$ ($\sigma$ ), is of hysteretic character, while that on total strain, $T_{cm}$ ($\varepsilon_t$), is uniquely determined. The latter result indicates a universal dependence of $T_{cm}$ on stress $\sigma$ applied to niobium filaments. The average derivative $dT_{cm}/d\sigma = 4\bullet 10^{-4}$ K/MPa for the Cu-Nb composite (as well as its $dH_r/d\sigma$ ) exceeds respective value for pure Nb about an order of magnitude.Again, the real dislocation structure of the composite (particularly, very high dislocation density at the "knife-like" boundaries) may be responsible for so high $dT_{cm}/d\sigma$ values.

Uniaxial compression of the composite, similarly to tension, results in $T_{cm}$ increase, the effect being of a threshold character.

Composite Cu-NbTi: Its $T_{cm}$ ($\sigma$ ) and $T_{cm}$ ($\varepsilon_t$ ) dependences under uniaxial tensile stress are similar to those of Cu-Nb, but have the contrary sign. The most probable physical mechanism of $T_c$ decrease in this composite under a load is strain induced martensitic transformation in NbTi.

Uniaxial compression produces no measurable effect on the composite $T_c$ .

Composite bronze-Nb 3 Sn: both uniaxial tension and compression of the composite result in its $T_c$ decrease. As well as in the case of Cu-Nb composite, the observed effect under uniaxial compression is of a threshold character.

These results, along with our and reference evidence on excellent combination of high mechanical and electrical properties of Cu-Nb *in situ* composites, prove them to be promising for use in specific superconducting devices and circuits.

**References**

1. K.Watanabe, S.Avaji, K.Takahashi, and M.Motokawa, *Physica B* **294-295**; 541; (2001)

2. L.Tilly, F.Lecouturier, G.Coffe, J.P.Peyrade, *Physica B* **294-295,** 648 (2001)

3. V.I. Dotsenko, I.F. Kislyak, F.F. Lavrentiev, V.T. Petrenko, Yu.A. Pokhil, and M.A. Tikhonovsky, *Mekhanika Kompozitnykh Materialov* N 1, 50 (1988) (in Russian)

4. E.M. Bronina, V.I. Dotsenko, I.F. Kislyak, and N.M. Chaykovskaya, *Cryogenics* **30**, 889 (1990)

5. V.K. Aksenov, N.F. Andrievskaya, O.I. Volchok, M.M. Oleksienko, Ya.D. Starodubov, and M.A. Tikhonovsky, *Metallofizika* **13**, 24 (1991) (in Russian)

# BEHAVIOUR FEATURES OF QUARTZ CERAMICS WHEN CONTACTING WITH ALKANOTROPHIC RHODOCOCCI

**Antsiferov V.N., Ivshina I.B.[(1)], Porozova S.E., Ritchkova M.I.[(1)]**
Research Powder Material Center, Perm, Russia
[(1)]Institute Ecology and Genetics of Microorganisms, Ural Branch, Russian Academy of Sciences, Perm, Russia

Alkanotrophic rhodococci is one of the most biotechnologically prospective bacteria groups being developed in microbiology. This increased interest is caused by their functional variety and intrinsic complex of metabolic properties to survive in extreme living circumstances. Exclusive plasticity and high adaptability of rhodococci, non-specific action of ferments synthesized by them, ability to attack the diversified components of environment provide a high survival rate of rhodococci and, as a rule, their leading position under extreme conditions of external environment [1].

Data concerning influence of microorganisms on composite ceramic materials are practically not present. Nevertheless, it is known that more than 50 % of all corrosion damages of inorganic materials is connected with activity of various groups of microorganisms. In most cases they promote creation of aggressive environments due to accumulation of metabolism products, in which the corrosion processes are accelerated.

When solving the problem of ceramics reliability, that is ability to operate in adverse conditions for many years, many factors are required to be considered in detail, and among them not the least important is the microbial cells interaction with ceramic materials. The issue of microorganisms influence only on natural minerals, used as raw material for manufacture of ceramics, has been most fully investigated [2].

Ceramic materials with a high porosity are of interest as biocatalyst carriers in organic synthesis or bioagents for cleaning an environment [3, 4]. Efficiency of their operation in this case is directly connected with the problem of microorganisms and ceramics interaction. In earlier studies of bacteriological resistance of high-porosity aluminosilicate materials [5, 6] it was experimentally shown that rhodococci intensify not only destruction processes of ceramic material, but also epitaxial processes accompanied with samples mass and strength increase. The determination of phase composition of products precipitation is a quite difficult task, as it concerns the surface phenomena in thin ceramic films of irregular shape.

As objects for investigation of influence of rhodococci alkanotrophic cells and /or their life products on destruction processes and phases formation in aluminosilicate ceramic materials, a line of various composition materials, including quartz ceramics, were considered. The quartz ceramics, produced by sintering the amorphous silica or quartz glass breakage at temperatures lower than melting temperature, differs from the overwhelming majority of ceramic materials by the absence of crystal phase [7]. The dual nature of a quartz glass surface containing silanol and siloxane groups, i.e. simultaneously hydrophilic and hydrophobic microsites [8], relates to prospective features of quartz ceramics.

In this work a pure culture of *R. ruber* IEGM 231 rhodococci received from Regional profiled collection of Alkanotrophic microorganisms of Institute Ecology and Genetics of Microorganisms Ural Branch of Russian Academy of Sciences was applied [9]. Bacteriological resistance of high porosity quartz ceramics was tested by feeding the test samples into mineral environment containing 0.003 % acrylamide as a carbon source and $4.0^{x}10^{9}$ rhodococci cells / ml concentration. Into a reference sample, the bacterial suspension was not entered. X-ray structure phase analysis was performed with DRON-3M diffractometer in a cobalt radiation with application of β-filter. Infrared spectra were recorded with IFS-66 Fourier spectrometer (Bruker, Germany). The received spectra were transformed to a zero base line.

The quartz ceramics produced by sintering of a quartz glass is considered as an amorphous material crystallized at temperatures more than 1000 °C with formation of crystallite. Nevertheless, infrared spectra of an initial material have alongside with halo a doublet typical for α - quartz in the 780 $cm^{-1}$ region. When surveying by points, the quartz relicts can also be selected on diffractogram (fig. 1).

After holding for 1 week in control conditions, quartz relicts disappeared and

amorphization of the material occured. The holding in culture environment promoted a crystallization of quartz ceramics marked on infrared spectra by increase of absorption intensity in the region of 1000-1200 $cm^{-1}$ being a typical area of absorption for the condensed groups [-$SiO_4$], and, also, on diffractograms.

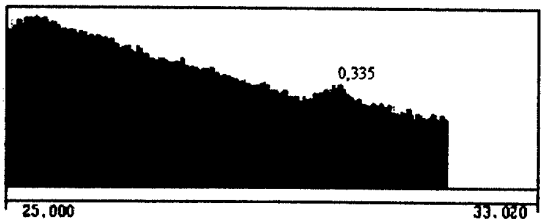


Fig. 1. A diffractogram fragment of an initial sample of quartz ceramics.

To perform an exact identification of crystallized compounds for such short holding periods is difficult. Longer exposures will allow to determine which silica crystal shapes are newly formed and whether the quartz remains as relict in an initial material.

The mass losses of quartz ceramics in the reference and test specimens are practically identical (0.37±0,04 % and 0.40±0,06 % correspondingly). Strength of high-porosity materials in general, and, in particular, quartz ceramics, strongly depends on material density. When density is reduced there is an essential decrease of strength characteristics, less appreciable for crystal materials such as corundum or cordierite, and very sharp for amorphous materials. In this connection, it is most correct to appreciate the change of strength at compression not by average values, but by the strength curve at compression vs. apparent density of material. Such plots are given in a fig. 2.

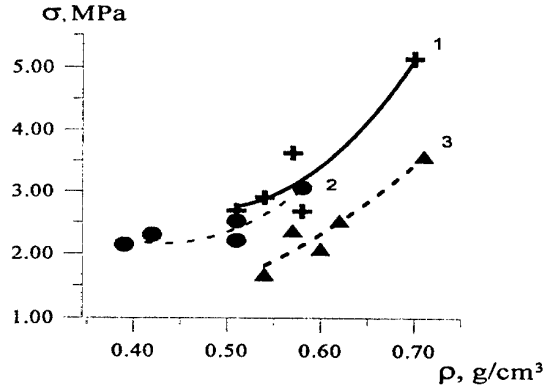


Fig. 2. Dependence of strength on density: 1 - initial material; 2 - reference;3 – test.

Amorphization of material marked in reference conditions is not accompanied with change of its strength. The plots 1 and 2 practically coincide. When holding in culture environment there is a strength decrease of quartz ceramics (plot 3). It is necessary to note that the crystallization of quartz ceramics at high temperatures is also accompanied with reduction of material strength down to destruction. So, even at the treatment for 1 week the difference of material behaviour under reference and test conditions can be recorded.

References

1. Ivshina I.B., Pshenichnov R.A., Oborin A.A. Propane oxidizing rhodococci. Sverdlovsk: Ural Research Center, USSR, 1987, 125 p.

2. Influence of microorganisms on properties of porcelain masses at holding / G.N.Maslennikova, Y.T.Platov, R.A.Hallilullova et all. // Glass and ceramics. 1999. № 10. P.15-23.

3. Conversion of special technical chemistry. Blasting powders, fuels, explosive charges / V.N. Alikin, G.E. Kuzmitsky, L.V. Zabelin, et all. Perm: Perm Research Center of Ural Department of Russian Science Academy, 1999. 176 p.

4. Carbon materials as adsorbents for biologically active substances and bacterial cells / G.A. Kovalenko, V.A. Semikolenov, E.V. Kuznetsova, et all. // Colloid magazine. 1999. Vol.61, № 6. P.787-795.

5. Study of feasibility of a bacterial destruction of high porosity ceramic materials / S.E. Porozova, A.M. Makarov, I.B. Ivshina, M.I. Ritchkova // JPC. 1997. Vol.70, № 12. P. 2076-2079.

6. Porozova S.E., Ivshina I.B., Ritchkova M.I.. Intensification of destruction-epitaxial processes in ceramic materials by bacteria of *Rhodococcus sensu stricto* // Materials and coatings in extreme conditions: researches, application, ecologically pure technologies and recycling: the theses of reports of International conference. September 18-22, 2000, Katsively, Crimea, Ukraine. Katsively, 2000. P.76.

7. Pivinsky Y.E., Romanishin A.G. Quartz ceramics. M.: Metallurgy, 1974. 264 p.

8. Iler P. Chemistry of silica /USA, 1979: Translated from English. M.: Mir, 1982. Part 4. 721 p.

9. Strains Catalogue of Regional Profiled Collection of Alkanotrophic microorganisms / Editor: I.B.Ivshina. Institute of Ecology and Genetics of Microorganisms, Ural Branch of Russian Science Academy. M.: Science, 1994.

# EFFECT OF HARDENING ON INTERNAL FRICTION IN Ti-ALLOY

**Konstantinova T.E., Ryumshina T.A.[1], Nosolev I.K., Pilipenko N.P.**

Donetsk Physicist-Technical Institute NAS of Ukraine, Donetsk, Ukraine
[1]Donetsk National Technical University, Donetsk, Ukraine

Internal friction is one of methods for investigation of structure and properties in materials. Importance of this method consists in its non-distractive action. The effect of mechanical and heat treatment on the properties of titanic allow VT22 was investigated by studying of temperature dependence of internal friction.

The Ti-allow VT22 used in this study contained the followed impurities (%): 5 Al, 5 Mo, 5V, 1Cr, 1Fe. The alloy had two-phase and temperature of phase transition $\alpha + \beta \rightarrow \beta$ in interval was 840-870°C. The cylindrical-shaped samples 3.2 mm in diameter and 24-35 mm in length, depended on the temperature of hardening, were annealed at 600-1200°C for 1 h and water cooled to 20°C. Part of samples was hardened in vacuum quartz ampoules. After hardening samples were hydroextruded and uniaxial strain deformed before 10%. Ultrasound absorption within temperature interval 80-300 K was measured by method of component piezoelectric vibrator, agitating in sample longitudinal oscillations on frequency 73 kHz.

The maximum of internal friction is discovered at 145-160K as a result of measurements. The location of maximum depends on hardening temperature. Increase the hardening temperature from 600 before 900°C cause a change of temperature of maximum from 145 to 160K, at that the value of logarithmic decrement $\delta(T_{max})$ changes almost by order of magnitude greater (fig.1). Further mechanical deforming practically does not influent on location of maximum. There is small increase of the damping at 200 – 300 K only.

It is known that the ultrasound absorption in material is connected with energy dissipation as consequence of viscosity and thermal conductivity. Since study of internal friction was conducted under comparatively low temperature, we suppose that warm-up contribution is small and the main contribution to damping was due to the absorption of impulse on the defect structure of material. The value of energy of activation, calculated on Marx-Verts equation, points to grain boundary nature. In all probability the formation of damping maximum is connected with a growth and relaxation of the boundary micro stresses when temperature decreased. Really, the temperature decrease causes a misfit deformation on the phase boundary which is conditioned by difference of elastics modulus and thermal expansion factor, as well as their different anisotropy.

Hardened from the temperature 600-900°C from $\alpha + \beta$ - state alloy VT22 consists β-phase (BCS-lattice) and a certain amounts α-phases (HCP-lattice). Lattice parameters of phases and their elastic modules essentially differ from each other, and the factor of anisotropy for α-phase is A = 1.33, for and for β-phase 0.96. When the hardening temperature increases from 600°C to 900°C, the amount of β–phase increases from 20 to 90%. The growth of β-phase separations is accompanied by increasing of phase boundaries amount, theirs total extent and volume share, residing under influence this boundaries too. This growth of boundary is revealed as increasing of the damping on the function $\delta(T)$, (fig.1).

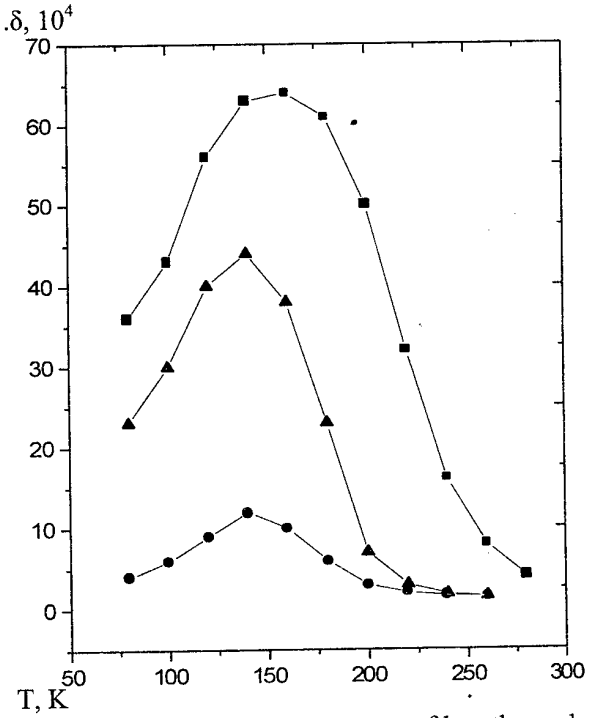


Fig.1. Relaxation spectrum of low thermal internal friction after different temperature of hardening ■ - 800°C, ▲ - 700°C, ● - 600°C

The additional boundary stresses induced by misfit deformation on the phase boundary at temperature decrease have been valued on equation in the limit of elastic theory:

$$d\sigma_i = \frac{d\alpha_k / dn}{s_{ik}^{(1)} + s_{ik}^{(2)}} T \qquad (1)$$

where $d\sigma_i$ is additional thermal misfit stresses, $T$ is temperature, $s_{ik}^{(1)}$ и $s_{ik}^{(2)}$ -are modules of flexibility for α– and β-phase, which are inverse to modules of elasticity, $d\alpha_k / dn$ is a change of thermal expansion coefficient on the phase boundary.

Estimations ed on formula (1) show that value of thermal misfit stresses is approximate 0.2 MPa/K. These stresses reach 20-40 MPa when the temperature decreases on 100 – 200°K. They can relax by means forming the new defects. In our allows the relaxation is realized on martensite. Formed in samples the new structure changes the material characteristics

The Value of Young's modulus was calculated on experimental results by means of equation:

$$C = \sqrt{\frac{E}{\rho}\left(1 - \frac{\pi^2 v^2 r^2}{4l^2}\right)} \qquad (2)$$

where $C$ is velocity of sound in material, $\rho$ is the material density, $v$ is Poisson's coefficient, $r$, $l$ are the radius and length of sample. Magnitudes of Young's module as function of hardening temperature and under different conditions shown on the fig.2.

The decrease of Young's module was observed in interval of hardening temperature 600-900 °C, but module much increased from the temperature above 900 °C in water-hardening samples in contrast with samples, which were hardened in vacuum ampoules. The decrease of Young's module at hardened from 900°C was obtained earlier and one was explained by increase of the volume share of less packed metastable BCS-phase.

However, observed in given work the increase of module beside 35% is an enough big to its possible was explain change of phase from HCP- to BCS-structure, which gives the contribution to module not more than 10%.

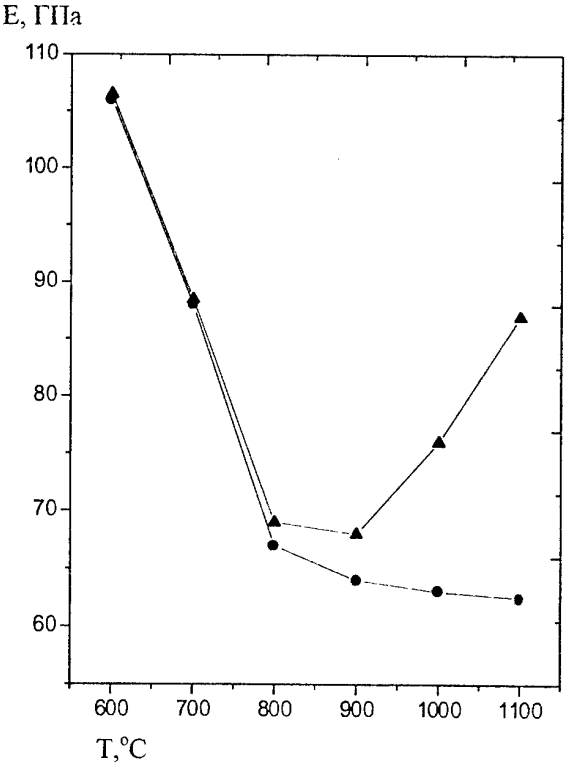


Fig.2 . Hardening temperature dependence Young's module in vacuum (●) and in water(▲).

In our opinion, stabilizing elements, in particular hydrogen, enrich β–phase and cause the observed increase of Young's module. It is known that hydrogen solubility in β - phase greatly above, than in α- phase, but essential absorption hydrogen occurs under the temperature above 850 – 960°C under gas heating. Consequently, titanium alloy in β-state absorbs hydrogen intensive and the hydrogen concentration is increases with the growth of hardening temperature in this conditions.

Data of mechanical test on strain are evidence of essential decrease of plasticity within the temperature interval that points to increase hydrogen concentration in β – phase too. Elastic module almost didn't change in exposed to hardening in vacuum quartz ampoules samples. Thus obtained results allow to expect that hydrogen influences upon elastic modules and properties of titanium alloy VT22.

# ABOUT NANOSIZABLE STRUCTURES UNDER THE ELECTROPLASTIC DEFORMATION

**Petrunin V.A., Tzellermaer V.Ya., Gromov V.E.**
Siberian state university of industry, Novokuznetsk, Russia

The synergetic ideology of the laving of the plastic deformation by large scale displacements of the medium for the calculation of theoretical and experimental micro- and macroparameters of the medium. Microparameters are connected with physical phenomena on atomic and defect (dislocated) levels, and macroparameters -- with grain and pore (sometimes cracks as for the fatigue) ones.

Physical phenomena, realized under the electrostimulated drawing and the fatigue are similiar, especially on the meselevel (slaving of fixed dislocation by mobily ones, the critical degree of the plastic deformation). It is expressed in the transformation of large scale displacements from the grains level to the microcracks level on the language of physical quantities, used in [1]. This transformation from the one scale to another one (grain to crack) can be connected with the realization of the phase transition with the physical quantity (the order parameter [1] ) – nonequilibrium displacements. But such growthing of the space scale is nonadequate to the kinetic phase transition and have the character of the scaling, that is typical for usual (equilibrium) phase transitions. So the transition from the one level to another one possible can be explained by not details of the dislocation ansamble reconstruction and its selforganization with the growth of the plastic deformation degree [1] (because of the pure experimental information), but space peculiarities of the plastic deformation evolution. Thesepeculiarities of the plastic deformation can be result of the another scheme of the cooperative evolution of meso- (defects, fragments [1] ) and macrodeformation (grains, macrocracks, pores, etc [1] ).

The result of the universality and the scaling [1,2] is, for exemple, the formation of the nanosizable structure of second phase particles ($Fe_3C$) on the fragments boundaries [2]. This formation is connected with mobili dislocations. Dislocations of the grain boundary (dislocations walls -- small angle biundaries) possibly are characterized by the universality and the scaling too. The experimental visialization of the scaling under conditions of the nonequlibirium transition is discussed in [2]. Calculations of related mesoscopic characteristics of the dislocation ansamble and the deformed medium ($\xi$ - the correlation length etc) are realized in [2].

Many experimental results about the electroplastic deformation are very good correlated with expression for electron wind stresses $\sigma = (m\upsilon_F/e)j$, used by us in [1], where m – the electron mass, $\upsilon_F$ – the electron velocity on the Fermi surface, e – the electron charge, j – the electrical current density.

So, the growth of own stresses of mobile dislocations (determined by the electron wind) is the source of nanosizable structures in the material.

1. V.A.Petrunin, V.V.Kovalenko, S.V.Konovalov, V.E.Gromov, O.V.Sosnin // Izv.vuzov. Tcheurnaya metallurgia.- 2000.- № 12.- p.46-50.
2. V.A.Petrunin, V.Ya.Tsellermaer, V.E.Gromov // IY international school-seminar "Evolution of the defects structures in condenced media" (Brief reports, 2-7 september, 1998), AltGTU, Barnaul, Russia, ed.M.D.Staros-tenkov,- p.50.

# ALUMINUM ALLOYS HARDENING BASED ON PHASE TRANSFORMATIONS OF PERITECTIC TYPE

**Zinkovsky G., Spiridonova I., Litvin B.**
Dnipropetrovs'k National University

It was shown in [1] that while annealing below the temperatures of a solidus in binary Al-Mn, Al-Cr, Al-V, Al-Mo systems during the completion of unfinished peritectic transformations a microhardness of a solid solution of aluminum increases and its lattice parameter changes. Subsequently, the effect of supersaturation of an aluminum-based solid solution with transition elements was observed in the same conditions and for ternary Al-Cu- (Mn, Cr, V, W, Mo) alloys[2]. Besides, in this work, the increase of microstresses in the solid solution was fixed as a result of peritectic transformation due to a difference in specific volumes of the phases.

In this abstract, the attempt is taken to utilize the found phenomena of the improvement of a strength of high- alloyed aluminum alloys using an example of ternary Al-Cu- (Mn, Cr, V, W, Mo) systems.

The alloys were melted using pure aluminum of AB000 grade, double rich alloys, and electrolytic copper in graphite crucibles. Melt was poured at temperatures from 1073 to-1173 K.

Strength tests were carried out using specimens obtained as follows. .The casting 30 by 30 mm in cross section and from 240 to-250 mm in length was cut in 4 pieces along longitudinal- direction. The bars had been subject to the heat treatment, then three test samples t were fabricated. Heat treatment was carried out in a retort furnace in a massive metal box. with temperature accuracy of 5 K. An artificial aging of alloys was carried out at a temperature of 453 K. The mechanical tests were implemented on small five-multiple samples made to ГОСТ 1497 ($d_0$=5mm, $l_0$ =25 mm), using "ЦДМ-2.5t"machine.

Five alloys (their percentage compositions by weight are specified in Table) were prepared for exploration of influence of heat treatment on mechanical characteristics. A first stage of heat treatment should be a homogenizing annealing (Hom)at temperatures below the melting point of an eutectic. A consequent high-temperature annealing (HTA) and age-hardening (AH) should increase alloy properties. For comparison, one more group of samples - homogenized and aged was produced. The AH, in this case, was preceded by hardening heat up to temperature of the HTA.

The microstructure analysis has shown that in the initial condition (IC) the cast alloys consist of a supersaturated solid solution, an Al-$Al_2Cu$ eutectic, being situated along the boundaries of grains, and dispersible aluminides, namely: $Al_4Mn$, $Al_5Mo$, $Al_3V$, $Al_4W$, $Al_7Cr$ - depending on alloying elements. The first stage of heat treatment - homogenizing annealing- leads to the dissolution of the $Al_2Cu$phase, and on the microsection only the traces of the varnished eutectic are visible. In Al-Mn-Cu, Al-V-Cu systems after homogenizing annealing substantially phase transformations $Al_4Mn \rightarrow Al_6Mn+Cu_2Mn_3Al20$ and $Al_3V \rightarrow Al_{11}V$ proceeds. In Al-W-Cu system the beginning of transformation $Al_4W \rightarrow Al_{12}W$ is observed. To determine the highest possible temperature of the HTA, the differential thermal analysis was carried out for homogenized samples. The results are presented in the Table

Table

Results of differential thermal analysis

| | | Temperature, K | | | |
|---|---|---|---|---|---|
| | | Eutectic | a solid solution | | $Al_xMe$–$Al_yMe$ |
| N | Composition % by weight | cooling | heating | cooling | heating |
| 1 | Al+4%Mn-2,5%Cu | 821-819 | 918-993 | - | 985 |
| 2 | Al+5%Mo-2.5%Cu | 821 | 888-938 | - | 985 |
| 3 | Al+2.5%V-2.5%Cu | - | 893-933 | 945-933 | 998-1005 |
| 4 | Al+3%W-3%Cu | 823 | 887-927 | 923-928 | - |
| 5 | Al+3%Cr-2.5%Cu | 821 | 878-933 | 933-923 | 1008 |

Temperature from 873 to 878 K was selected for HTA. The time of the HTA calculated using kinetic curves of transformations, was determined as follows: Al-Mn-Cu system - 10 hours; Al-W-Cu, Al-Mo-Cu, Al-Cr-Cu, Al-V-Cu systems - 20 hours. The microstructure investigations after the HTA have shown that in alloys containing W, Mo, Mn the phase transformations have completed in

full: $Al_4W$ transformed into $Al_{12}W$; $Al_4Mo$, $Al_5Mo$ - in $Al_{12}Mo$ and $Al_4$ Mn - in $Al_6Mn$, and the ternary phase; $Al_3V$ in $Al_6V$. In Al-Cu-Cr alloys any traces of transformations were not detected. It is explained that the system contains only phase $Al_7Cr$ out of aluminides of chrome that appears not due to peritectic transformation, and is stable in the pointed out temperature range.

Results of mechanical tests are presented by an average value of a ultimate strength, yield stress, as well as an average of two highest values, to eliminate the influence of numerous defects, such as: nonmetallic, pockholes, etc. (Fig. 1). In Al-Mn-Cu system the mechanical characteristics of an alloy after the HTA, were improved by 18 %, in comparison with an alloy after homogenizing annealing. The same results are obtained for Al-5%Mo-2,5%Cu alloy. The strength of the alloy after the HTA and AH, is by 40 % higher than that of the initial alloy, and by 30 % higher than the strength of the alloy after homogenizing annealing with the following artificial aging. Alloy containing vanadium after the HTA and AH, has the higher strength than the initial alloy by 67 %, and alloy after the HTA is harder- than homogenized one by 80 %. The alloy containing tungsten after the HTA and artificial aging is characterized by the higher strength than the initial one by 34 % and by 22 % than homogenized and aged alloy The less improvement of mechanical characteristics, by 28 %, is observed for Al-3%Cr-2,5%Cu alloy. The specific elongation measured on samples after destruction for alloys after the HTA and AH, increases by up to 6 or 7 % against approximately 3 % for the initial alloys. As to a yield stress, it increases, in the same degree as strength. (Fig. 1) It means that with strength improving the plasticity of alloys also increases.

Thus, the HTA improves mechanical characteristics of investigated alloys. The effect of supersaturation of a solid solution on a base of aluminum as a result of peritectic transformations allows to offer a perspective mode of heat treatment described above. The annealing at high temperatures allows to achieve the transformation of the intermetallic compounds with the high content of alloying elements into less brittle phases containing more aluminum with the less specific surface of the interfaces. The diffusion processes eliminate the majority of defects, and supersaturation of solid solution of aluminum and increase of microstresses created in this phase promote hardening of the alloy. It is possible to conclude that the more evident effect will be found if the content of transition elements in aluminum alloys increases while the

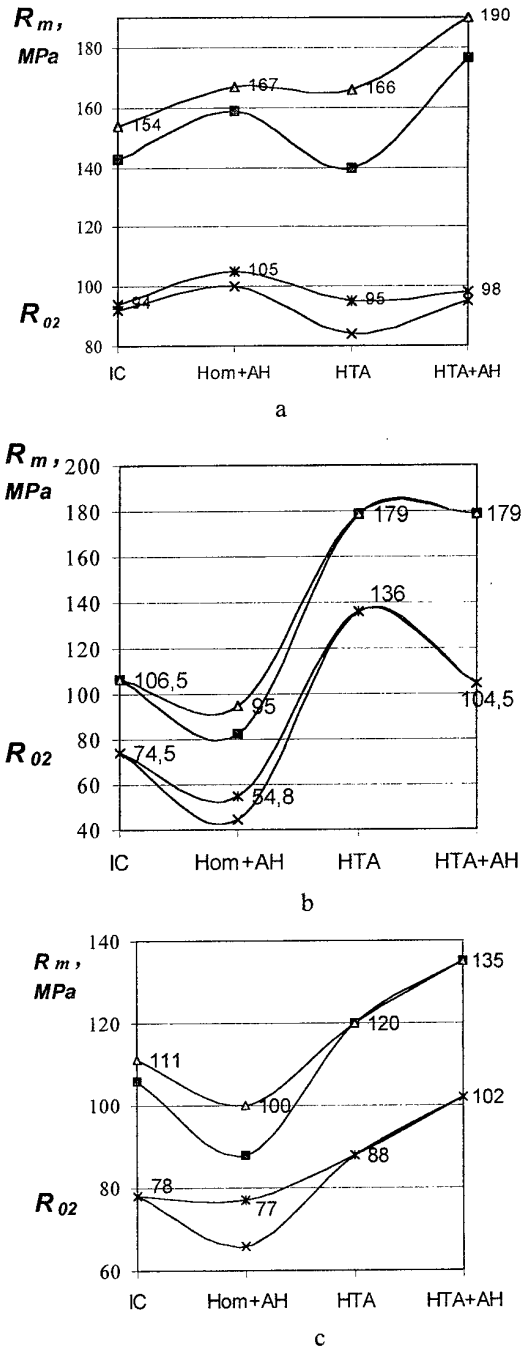


Fig.1 Strength of alloys at different stages of heat treatment: a–Al-Mn-Cu; b–Al-V-Cu; c–Al-W-Cu.

complex of alloying elements is added to the above alloys and special technologies are used that ensure high cooling rates of melts.

1. Венгринович Р.Д., Псарев В.И. О фазовых превращениях в неравновесно закристаллизованных сплавах//ФММ.-1969.-Т.29.-N3.-С.540-546

2. Зинковский Г.В., Литвин Б.Н., Спиридонова И.М. Свойства и тонкая структура твёрдого раствора алюминия в сплавах алюминия с медью и переходными металлами. Вісник Дніпропетровського університету. Фізика. 1999.- Вип. 5.-С.39-45.

# EFFECT OF LOW-ENERGY ELECTRON AND ION IRRADIATION ON THE COMPOSITION OF THE ZnS SINGLE CRYSTAL SURFACE

**Ivanyshyn I.M., Mishchuk O.A.[(1)], Telemko O.V.[(1)]**
Vasyl Stefanyk Precarpathian University, Ivano-Frankivsk, Ukraine
[(1)]UkrNDINP "MASMA", Kyiv, Ukraine

The mechanisms of effect of electron and ion beams on a solid can be different. A bombardment energy influences essentially. In case of low-energy beam of ions of noble gases (with the energy of some kiloelectronvolts), it is known that the elastic interplay of beam ions and atoms of a solid surface is prevailing. At these energies the ions do not penetrate into solid deeply (1-3 constants of crystal lattice). As the result, quasi-equilibrium and statistically monotonous sputtering of a surface takes place.

On the other hand, the electronic irradiation of $A_2B_6$ surface induces desorption of the lattice elements. But preferentially, as known, it is the electron stimulated desorption of chalcogen atoms. It leads to distortion of stoichiometric surface composition and to generating of different non-equilibrium defects, which change properties of the semiconductor.

As a whole, the processes, induced by low-energy electron bombardment are investigated unsufficiently. Specially it relates to semiconductors. The primary electrons penetrate into their surface layers much more deeply than ions. They fall to a space-charge region and change it. There is a gradient of non-equilibrium electric charge in surface layers. Its influence on diffusion processes is more essential in high bandgap semiconductors.

In this paper the effect of electron- and ion-beam exposure on the transformation of the ZnS single crystal surface are studied. The surface of ZnS single crystal was previously passivated and thus specially protected by a chemisorption layer, for shadowing from oxidation and electron-stimulated desorption of lattice elements.

The (110) surface of ZnS fcc single crystal had been passivated during heat treatment in medium of surfactant. Crystalline surface has been irradiated by means of low-energy electron- and ion-beam (no more than 5 and 3кеВ respectively) in the ultra-high vacuum chamber and *in situ* studied by the methods of Auger electron spectroscopy and scanning electron microscopy. At such energies, the electrons are injecting in a space-charge region of the semiconductor. The ionization losses prevail. Electron beam density, dia 1 micron, was varied in range up to 100 mA/mm$^2$.

Accordingly, the $Ar^+$ ion beam density, dia 2 mm, was varied in range up to 1 μA/mm$^2$. At these parameters, ion sputtering of ZnS surface takes place.

The relative atomic concentrations of elements estimated from Auger spectra of a surface according to the well-known equation:

$$C_i = (I_i / g_i) / \sum_k^n I_k / g_k \,, (1)$$

where $C_i$ – relative atomic concentrations of $i$-th element; $I_i$ – intensity of main spectral line of $i$-th element; $g_i$ – factor of relative sensitivity of $i$-th element; $n$ – full number of elements.

Intensities of spectrum lines of elements were also normalized to values of beam density. It has allowed to analyze not only relative atomic concentrations of elements in thin surface layer of ZnS (equation (1)), but also to evaluate, in relative units, change of spatial concentrations of these elements

$$n_i \propto N_i = I_i / (J \cdot g_i) \quad (2)$$

and conforming concentrations of non-equilibrium vacancies, which were derived as a result of electron irradiation:

$$n_{\upsilon,\mathrm{Me}} \propto N_{\upsilon,\mathrm{Me}} = N_{\mathrm{Zn},0} - N_{\mathrm{Zn}} \,, (3)$$

$$n_{\upsilon,\mathrm{Ch}} \propto N_{\upsilon,\mathrm{Ch}} = N_{\mathrm{S},0} - N_{\mathrm{S}} \,, (4)$$

where $n_i$, $n_{\upsilon,\mathrm{Me}}$ and $n_{\upsilon,\mathrm{Ch}}$ – spatial concentrations of $i$-th element, vacancies of metal and chalcogen atoms in cationic and anionic sublattices of ZnS crystal accordingly; $N_i$ – intensity of spectrum line of $i$-th element normalized to values of beam density $J$ and the factors of relative sensitivity $g_i$; $N_{\mathrm{Zn}}$ and $N_{\mathrm{S}}$ – normalized intensities of Zn and S spectrum lines pursuant to an equation (2); $N_{\mathrm{Zn},0}$

and $N_{S,0}$ – normalized intensities $N_{Zn}$ and $N_S$ for stoichiometric ZnS crystal.

The Auger-analysis of the crystal surface has revealed a chemisorption layer of Carbon and full absence of oxygen. The relation of initial concentrations of basic elements was in good conformity with a stoichiometry of ZnS.

Experimentally is affirmed, that the surface concentration of Carbon practically does depend neither on a dose, nor from radiation intensity. Therefore, the chemisorption layer precludes from processes of desorption. In this case, changes of surface concentrations of Zn and S ions are predominantly a result of diffusive exchange between the volume and the surface.

Increase of density of electron probe leads to decrease of concentrations of sulfur, first of all, and zinc. A ratio of atomic concentrations (equation (1)) of sulfur and zinc for surface layer of the single crystal had been reduced essentially (Fig.1).

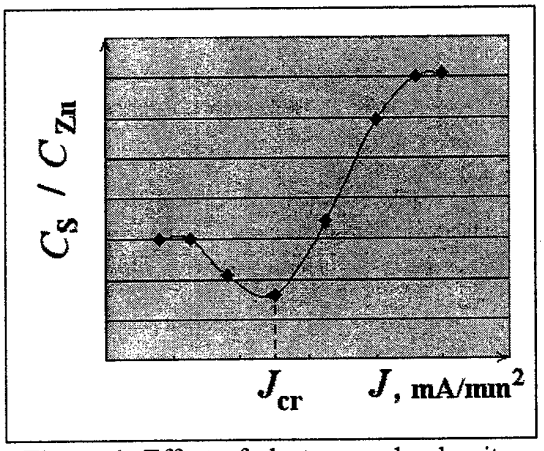


**Figure 1**. Effect of electron probe density on the ratio of atomic concentrations of sulfur $C_S$ and zinc $C_{Zn}$.

Fig.1 displays: there is a critical value $J_{cr}$ of the current density. After this value, the further increase of electron radiation intensity results in rapid restoring of initial concentration of S and to the same quick decreasing of concentration of Zn. As a result, a ratio of atomic concentrations of sulfur and zinc had been increased rapidly.

At critical value of electron probe density $J_{cr}$, in accordingly with equations (2)-(4) the surface layer gains a structure: $(Zn_{0,92}V_{Me\ 0,08})(S_{0,79}V_{Ch\ 0,21})$, where $V_{Me}$ and $V_{Ch}$ – vacancies of metal and chalcogen atoms accordingly. This structure of ZnS surface layer are characterized by a maximum concentration of vacancies in anionic sublattice (Fig.2).

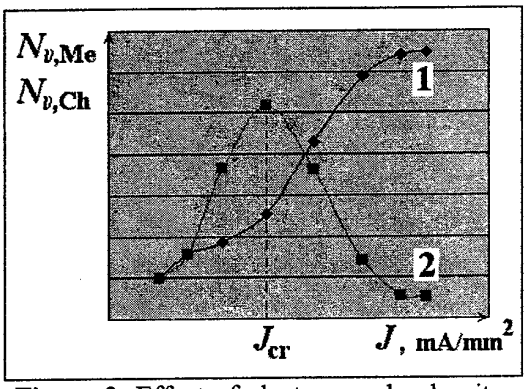


**Figure 2**. Effect of electron probe density on the concentrations of non-equilibrium vacancies: 1 – $V_{Me}$ (value of $N_{v,Me}$; equation (3)); 2 – $V_{Ch}$ (value of $N_{v,Ch}$; equation (4)).

Perhaps, the 21 % are the critical value of anionic vacancies which promotes the counter diffusions of zinc and sulfur atoms and the structural transformation of crystal surface layer. As a result of similar transformation, the surface layer gains a structure: $(Zn_{0,77}V_{Me\ 0,21}S_{0,02})S$. This structure of ZnS surface layer has a new characteristics – a maximum concentration of vacancies (also 21 %) in cationic sublattice (Fig.2).

Same transformation of structure of ZnS surface layer takes place for crystals without protecting chemisorption layer at simultaneous irradiation by $Ar^+$ ions and electron beam with density exceeding critical (Fig.3).

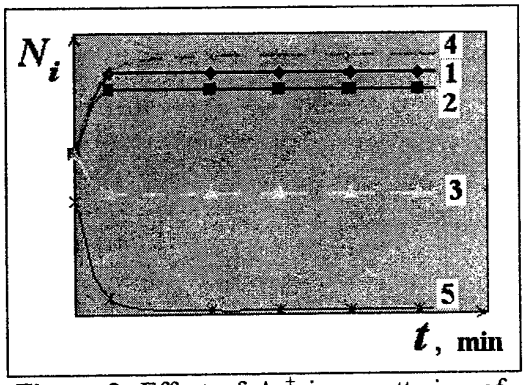


**Figure 3**. Effect of $Ar^+$ ion sputtering of (110) ZnS surface at various values of electron probe density (1 and 2 for $J<J_{cr}$; 3 and 4 for $J>J_{cr}$; 5 for various $J$) on spatial concentrations of zinc (1, 3), sulfur (2, 4) and Carbon (5).

The reviewed outcomes are discussed in the frames of the models of non-equilibrium space charge and crystal chemistry of atomic defects in $A_2B_6$.

# POSSIBILITIES OF INDEPENDENT GASEOUS ATMOSPHERE IN STRUCTURAL ENGINEERING OF FUNCTIONAL MATERIALS

**I.G.Slys**
Frantsevich Institute for Problems of Materials Science,
National Academy of Sciences of Ukraine, Kyiv, Ukraine

Sintering is the final thermal operation in the technological cycle of powder metallurgy. It is usually carried out in the protective gas flow or vacuum.

Authors [1] were the first to use containers with a fusible seal (CFS) to sinter stainless steel powders in the independent gaseous atmosphere.

The independent gaseous atmosphere produced in CFS allows us to realize the growth of area for interparticle contacts according to evaporation and condensation mechanisms under (ideal) closed space conditions. As B.Y.Pines has shown [2], in this (ideal) closed space the growth of a neck diameter follows the dependence $x^7=t$, and in the flowing medium (when the part of atoms is not condensed in the neck) author has obtained the dependence $x^3=t$. Thus, sintering in the independent gaseous atmosphere of CFS providing transfer processes through the gas phase leads to the increase in the rate of interparticle contact growth $10^4$ times as much.

Relying on the fundamentally new technological possibilities that provide sintering chromium based powder materials in the independent (isolated) gaseous atmosphere in CFS, we have formulated the principles for structural engineering to produce functional materials with the necessary level of physical and chemical properties.

At the microlevel we have raised a problem of deep refining bcc-metal by interstitial impurities (oxygen, nitrogen, carbon) to provide the possibility for plastic flow of material.

At the mesolevel (the mesolevel means only intergrain boundaries and the grain size) we have formulated a problem of refining intergrain boundaries to prevent intercrystallite destruction and blocking the process of crystallization.

At the macrolevel (it means interparticle boundaries, particles, pores) we have put a problem of providing the high level of consolidation of interparticle contacts and controlling the porous structure due to interaction between components of the active gaseous atmosphere.

Relying on the formulated scientific principles of structural engineering, we have developed fundamentally new technologies that integrate activated sintering with refining the chromium matrix, grain boundaries, surfaces of particles and pores from interstitial impurities [3,4,5].

The developed technology has provided the possibility of producing the impact strong (impact strength 1 kgm/cm$^2$) articles (16000 pieces) from powder chromium of the given nuclide purity. Those articles have been used to conduct the unique research to refine the nuclear constants of chromium [6] (Institute for nuclear energy in Obninsk).

The developed technology of the activated consolidation has been found especially resultative to produce functional materials showing the maximum high porosity (90-95%). These materials are based on foam metals and knitted semifinished items. In this case intensification of material mass transfer through the gas phase provides not only the quality of interfiber contacts in such systems but also leads to the increase in material precipitation due to the chemical and thermal process. Joint proceeding above processes provides activated consolidation of high porous material structures and production of materials showing the high level of rigidity [7].

***References***

1. И.М.Федорченко, И.Г.Слысь, Л.А.Сосновский.–Киев: Порошковая металлургия, 1972, 5.
2. Б.Я.Пинес. УФЖ, 52, 501, 1954.
3. И.Г.Слысь, В.И.Трефилов, И.М.Федорченко. Способ получения дисперсно-упрочненных спеченных сплавов. А.С. СССР N633436, 1979.
4. И.Г.Слысь, Л.А.Сосновский. Смесь для получения пластичного хрома. А.С. СССР N930964.1980.
5. И.Г.Слысь, В.И.Трефилов, И.М.Федорченко и др. А.С. СССР N1478503. 1989.
6. V.I.Trefilov, V.I.Golubev, I.G.Slys et al. About nuclear constants of chromium. Theses of Int. Conf. on radiation material science. Alushta. V.4, p.23-24, 1990.
7. В.В Скороход, А.Н.Леонов, С.М.Солонин и др. Особенности деформации высокопористых металлических материалов.-Киев: Порошковая металлургия, (в печати).

# MACROSCOPIC TURN OF SOLID CYLINDRICAL PARTICLE UNDER ELECTRIC CURRENT ACTION

**Derev'yanko O.V., Popov V.P., Raychenko O.I., Pavlenko T.P.**
**I.M. Frantsevych Institute for Problems of Materials Science,**
**National Ukrainian Academy of Sciences, Kyiv, Ukraine**

## Introduction

Some composition materials (CM) in its contain foreign inclusion variable forms. This is inclusions cylindrical, oval and other forms, rods, oblong grains, etc, which may be specially input into body of melting matrix. Usually electroconductive and physics properties for its inclusions are difference from electroconductive and physics properties of surrounding melting matrix. Usually inclusions are having more high temperature of melt.

At making, thermo-treatment or exploitation CM for some case is need for understanding of picture and character of interaction between foreign inclusions and surrounding current-carrying medium, when under condition of direct current passing arising processes head- and mass-transfer. Investigation its processes to represent some practical interest, because of arising some effects: temperature gradients, thermo-clacking, electro-hydrodynamic flows, convective diffusion mass-transfer (dissolve of inclusion) for boundary solid – liquid media (melt matrix) [1, 2].

## Investigations

A macroscopic motion – turn of cylindrical particles around axis up to $90^0$ under passing direct electric current through heterogeneous composition system bronze Br10 (inclusions of cylindrical form) – tin (melting matrix) was observed. Scheme of experiment is shown in figure.

The whole time of experiment was 120 s, current density through graphite matrix was about 80-120 A/cm$^2$.

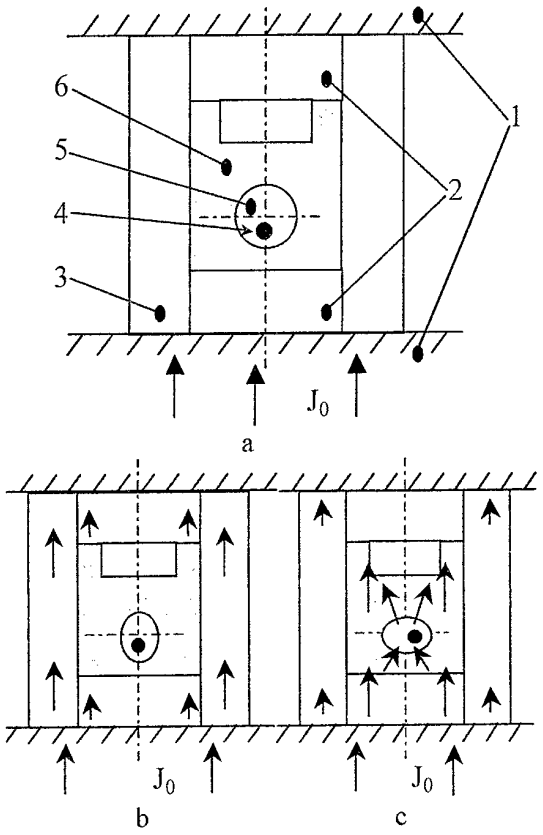


**Figure.** Scheme of experiments:
a) beginning experiment stage;
b) intermediate state and placement of cylindrical inclusion;
c) final state and placement of inclusion after whole turn but before moment of whole dissolution;
1- top and bottom current lead plates of press; 2- punches; 3- electroconductive matrix; 4- mark point; 5- inclusion (Br10); 6- surrounding current-carrying melting matrix (tin).

The cylindrical inclusion at first dissolving on side surfaces at beginning of experiment (see Fig. b). After a while inclusion did a turn around axis up to

$90^0$, how showed mark point on butt-end surface of inclusion (Fig. c). After time of 120 s and with increased of temperature in volume of composition cell to 550 $^0$C bronze inclusion whole dissolved in surrounding liquid medium.

## Discussion

The electrical contact between non-melting tin powder and bottom graphite punch is non-enough for good passing of electric current through powder at first of experiment. Because at first electrical current is passing in generally through body of graphite matrix. Powder of tin must to heat on out sides of surface pressing for this case. This leaded at arising of temperature gradient for direction from outside to center axis of backfilling. When tin is melted the cylindrical inclusion must to do dissolve process on its outside surfaces under thermo convection process action (Fig. b) [3]. Later electrical contact is enough for passing of electrical current through melted tin. The increasing of passing electrical current through heterogeneous system must to lead at turn of inclusion around axis. Electroconvection flows "at left" and "at right" from outside surface of cylindrical inclusion really is unequal, because its torques is unbalanced. This is an explanation of turn by this time oval inclusion around axis.

The inclusion is oriented in liquid medium (melting tin) thus what bigger diameter of cross-section (for present time inclusion in cross-section is oval form) to have placement perpendicularly at direction of passing electrical current through composition cell.

Because which bronze is more electroconductive, electrical current must to "collected" into inclusion body (Fig. b). Consequence of its increasing of value dissolution inclusion body on bottom and top zones of surface (in points of concentration electrical current) [3-5]. Latter process of dissolving must to do by thermo- and electroconvection mechanism.

## Conclusion

The present observation to can possibility sharply to explain details of behaviour dissolves foreign inclusions, what surrounding melted matrix under electric current action. Inclusions can to be reinforcing fibrous for matrix, rods, and oblong grains.

## References


1. A.G. Lanin, V.V. Borunov, V.S. Yegorov and V.P. Popov. Fracture of cylindrical bodies of brittle materials at thermal loadings. // Problems of Strength. – 1973. – N 3. – P. 56-60. (In Russ.).
2. V.V. Tul'sky. A problem on the fusion of steel waveguide inside the melt.// Metal Physics and Advanced Technologies. – 1996. – N 3. – P. 8-14. (In Russ.).
3. O.I. Raychenko, V. P. Popov, O.V. Derev'yanko. Calculation of the stationary two-dimensional temperature field, which arising by electroheating tree-layered cylindrical medium. // Metal Physics and Advanced Technologies. – 1999. – Vol. 21. – N 10. – P. 80-86. (In Russ.).
4. O.I. Raychenko, O.V. Derev'yanko, V. P. Popov. Computer calculations of diffusion from a solid inclusion in the surrounding liquid current-carrying metal under electric current action // Second International Conference on CFD in the Minerals and Process Industries, Melbourne, Australia, 1999. (on Compact Disk).
5. O.I. Raychenko, O.V. Derev'yanko, V. P Popov. Calculation of the stationary two-dimensional temperature field in a cylindrical three-layered conductive medium with an electric cross-current. // Heat and MassTransfer. (to be published

# THE INVESTIGATION OF STABILITY OF COMPOSITE SCREENS ON THE BASIS OF ALUMINIUM TO EFFECT BY A LASER IMPULSE

**Maiboroda V.P., Revo S.L.,(1), Ivanenko K.O.(1), Molchanovskaya G.M., Shkolniy V.K.**
I.Franzevich Institute of Materials Sciense Problems of National Academy of Scienses of Ukraine, Kiev, Ukraine
(1) T.Shevchenko Kiev National University of Ukraine, Kiev, Ukraine

In the given activity the effect of a laser impulse of energy 20 J/cm$^2$ was studied at duration 4 m·s and wavelength 1,06μ on screens made of composite materials. The laser beam in a point of an occurring with a screen had an angle diameter of 0,5-0,6 mm (on an isoenergetic contour limiting 70-80 % of a beam energy).

The screens represented sheets by depth of 1 mm of the square form with the party of a square of 30 mm. In a radiation time they placed perpendicularly to beam. The cooling implemented at the expense of a natural air convection. The properties of screens from laminated composite materials (CM) Al-Sn and Al-C, from a solid aluminium, from a CM in a tinned layers of which one were contained quartz fibers (Al-Sn+$SiO_2$) and CM consisting of a laminated part Al-Sn+$SiO_2$, coated by pressed by quartz cotton (Al-Sn+$SiO_2$-$SiO_2$) are studied.

Samples CM of Al-Sn were produced a compacting method of the package which has been compounded of foils of aluminium, interleaving with tin foils. The cold welding of layers implements at the compression of a package on an altitude h equal to $\Delta h/h > 30$ % at speed $\Delta h/\Delta t > 10$ mm/s. The edges of a package on perimeter usually contain lack of penetrations on spacing interval of 3-4 mm. They are shear. Then a package roll at a room temperature, the foil of desirable depth will not receive yet.

A CM Al-Sn+$SiO_2$ was produced as follows. Layers of tin keeping the fibers of quartz, executed from two tin foils, between which one made of felt from quartz fibers. Then a package extruded with compression $\Delta h/h=10\div15\%$, hearted up to 200$^0$C under pressure, maintained 5÷7 min, chilled and again extruded at room temperature with compression $\Delta h/h=25\div30\%$. The fiber of a diameter 1-3μ were blasted on pieces of length 4-8 mm at cold pressing and rolling.

The composite screens Al-Sn+$SiO_2$-$SiO_2$ consist of a layer Al-Sn+$SiO_2$ and felted layer from quartz fibers applied on an aluminium layer without coupling. The depth of a felted layer was selected so that weight of 1 cm$^2$ of felt equalled to weight of a quartz plate by the area of 1 cm$^2$ and depth of 0,5 mm. Therefore it is possible to consider, as in this case we deal with a pore-free screen with general depth of 1 mm.

The screens Al-C are made by a packing of foils of Al, on which one the hydrocarbon black from a flame of a paraffinic suppository was previously marked. The coupling between in layers was gentle, therefore between them there were planar pores. The depth of a screen was selected so that its weight at the area of 1 cm$^2$ equalled to weight of a pore-free screen from aluminium and graphite of the same structure. Usually depth of a screen oscillated within the limits of 1,2-1,3 mm, therefore porosity made 20÷30% volumetric.

The stability of a screen was determined by quantity of impulses indispensable for its breakdown. Between impulses the pause of 1 min for cooling of a screen by air was made. The results of tests are submitted in the table 1.

The table 1.

| Screen | A mean bed depth, μ | Quantity of punching impulses |
|---|---|---|
| Al | 1000 | 2 – 3 |
| Al-Sn | 15 | 1 |
| Al-Sn | 0,15 | 2 – 3 |
| Al-Sn | 0,05 | 3 – 4 |
| Al-C | 15 | 2 – 3 |
| Al-C | 0,15 | 3 – 4 |
| Al-Sn+$SiO_2$ | 15 | 4 – 5 |
| Al-Sn+$SiO_2$-$SiO_2$ | 15 | 5 – 6 |

At planing of experiments on shields it was supposed, that steady should be screens from the composite materials which have been compounded from interleaving fusible and high-melting (rather) layers. It was supposed, that the fusible layer (Sn, for

example) at effect of a laser beam will be fused and will exhale at the expense of that the energy will be occluded.

So, in a fig.1 rags of craters (finger A) are viewed clearly. They could be derivated at the expense of pressure of metallical vapors. There are interquartile vapours of aluminium and tin in identical concentration, wherefore both metals are to the same extent inclined to vapourization. So, the vapour pressure Al makes 10 mm Hg at 1148$^0$C, and tin - at 1189$^0$C. It is comparable digits.

Fig.1

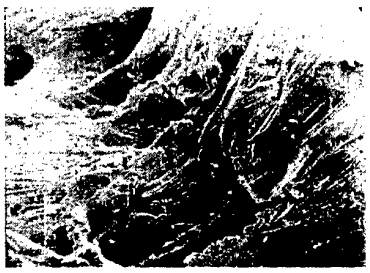

a

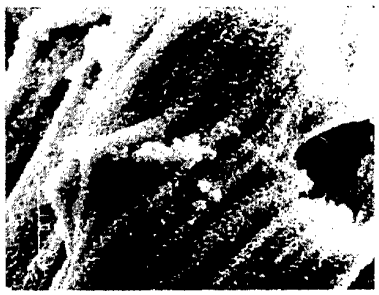

b

Fig.2

In a fig.2,a,b, the destruction of a package from thin (0,009 mm) foils of Al is shown. We see, that edges of craters lacerated, that testifies to explosive nature of destruction without a melting. As the energy occluded at a sublimation of a stuff, the is more, than more bond energy of a grating, and the destruction of screens from composite materials goes on the gear of explosion at the expense of formation a vapour without a melting of metal in bulk of layer to plot screens it is necessary from stuffs with large coghesion. The melting heat, apparently, should be allowed not first of all. This conclusion is confirmed also by the table 1. So, in a CM Al-C at h=0,15μ steadier, than CM Al-Sn at same h.

In areas with smaller density of a beam energy, more remote from center, there is a melting.

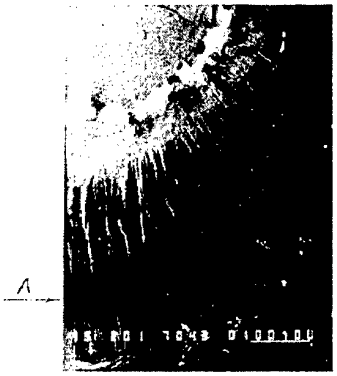


Fig.3

So, in a fig.3 the molten zones of thick layers (0,1 mm) Al with radial arrangement of crystals which are generatrix after a crystallization of a molten layer are visible. Characteristicly, that the ring-type zones look like ring-type surges, disjointed metal with a nonperturbed surface (finger A).

On the basis of the conducted experiments it is possible to make following conclusions:

1. With thinning-down of a layer the protective potency of screens from laser effect increases.
2. Actuations, disseminating light, (quartz fibers in tinned layers the CM Al-Sn+$SiO_2$) is significant (in 2-3 times) augment stability of screens.
3. With increase of refractoriness of layers (the replacement Sn on C in compositions on the aluminium basis) increases protective potency of screens.
4. The arrangement of a quartz fiber before a metallical screen is the most perspective method of protection from a laser radiation.
5. The investigated screens can be arranged in a number on increase of stability: Al, Al - C, Al - Sn, Al-Sn-$SiO_2$, Al-Sn+$SiO_2$-$SiO_2$.

# STRUCTURAL CHANGES IN a CRYSTALLINE FILM OF Co AT HEATING

**Maiboroda V.P., Maksimova G.M., Molchanovskaya G.M.**
I.Franzevich Institute of Materials Sciense Problems of National Academy of Scienses of Ukraine, Kiev, Ukraine

As is known, the cobalt at the temperature of 422$^0$C undergoes phase polymorphic transformation (HCP-FCC), and consequently introduces successful object for researches of the structural processes which are flowing past in metal at heating. The film was made from wrougth bar of a electrolyticaly refined cobalt of cleanliness 99,76 mas%, the main admixtures are Ni , Fe.

The researches conducted in a electron microscope ЭМВ-100Л in vacuum ~$2\cdot10^{-3}$ Pa.

As an initial structural condition for binding the place with reference frame, fig.1, a, was selected. The striate fragmentation is a consequent the casting blocks and conditions of preliminary machine work of a film before electrolytic thining are ductile. The electron diffraction pattern of metal, fig.1,b, contains jerks of highly-packed α-phases.

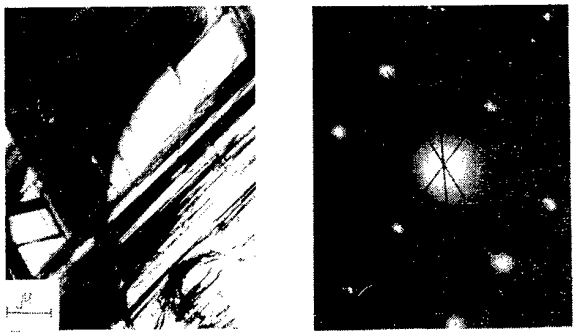

a b

Fig.1

The instrument constant in the data conditions of filming makes 94 A•mm. Diameters of families of 3 maxima make 43, 63 and 87/90 mm. These parameters correspond to interplanar spacing intervals - 2,18; 1,49; and 1,06/1,04 Å, fig.1, b, also coincide the tabular data for lines (100), (102) and (201)/(004). There are jerks also from other planes. The temperature in a zone of a sample was determined on a current pursuant to a calibration curve. The exposure before filming at the install temperature implemented within 5 minutes. At a sample temperature rise up to 400-410$^0$C the visible changes in frame do not descend, however, on an electron diffraction pattern in the field of jerks (100) and (201) are watched pools, fig.2, which one testify to originating a flap-type fragmentation as a minimum in two directions.

Fig.2

Effect of a thing-plate fragmentation [1,2] as a rule, will precede to phase structural transformation and its availability demonstrates, that the cobalt is not exception of this rule.

The rising up of a sample temperature up to 600$^0$C results in regulation of substructure, fig.3, a. However the recrystallization effects are exhibited is gentle. On an electron diffraction pattern, fig.3, b, the appeared new jerks of a FCC-lattice of β-phases of cobalt are watched, according to diameter of rings 45, 75 and 89 mm. These parameters correspond to interplanar spacing intervals 2,04; 1,25 and 1,06 Å of lines (111), (220) and (311). Inside the maiden ring of the β-phase are available jerks and of α-phase (100), and also jerk of a line (102) (at the left, at the top of an electron diffraction pattern). These data confirm that fact [3], that the polymorphic turning in a cobalt flows past in a temperature band, since

422$^0$C. In case of a thin film this process does not finish and at 600$^0$C, fig.3, b.

The electron diffraction pattern from a sample at 755$^0$C completely consists of lines of β-phase, fig.4, accordingly (111), (220) and (311). The broadened ring of a line (111) and pools between dot jerks testify about finely divided, including striate, the fragmentation of frame of a crystalline film in the result of α→β transformation.

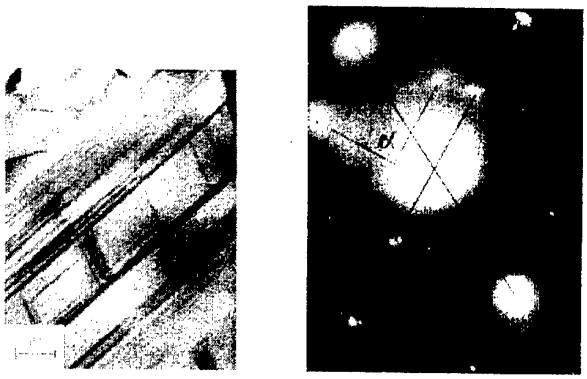

a b

Fig.3

Fig.4

The essential changes are watched also in frame of a film. On a surface of a sample there are oval, drifting zones, spearhead of a film as though melting. At cooling of a sample the processes cease, in a fig.5, a, is shown the modified as a result of heating, map of an investigated film.

a

b

Fig.5

The electron diffraction pattern of a sample, fig.5, b, contains gentle jerks α-phases (on a snapshot a line 2), β-phases (bright jerks in a direction of a line 1) and two gentle jerks apparently of oxide CoO (line 1) with interplanar distance 2,52 Å (tabulared - 2,45 Å). As follows from last data, fig.5, a, b, as a result of cooling of a thin film from area of β-phases (755$^0$C) at room temperature coexisting both modifications of a cobalt is watched. Also follows that direct and partial converse α↔β transformation for such scale of a sample is not accompanied by formation of the doubles and, apparently, flows past not on martensitic transformation to the gear, but on mechanism of arising of the defects of packaging. About it testify pools on electron diffraction patterns, fig.2,4.

Literature

1. Pushin V..G., Yurchenko L.I., Pavlova S.P., Turhan U.E.//FMM, -1988.- V66, №4.-P.777-787.
2. Maiboroda V.P.//Physics and chemistry of processing of materials.-1996.- № 3, -P.30-35.
3. F.M.Perelman, A.Ya.Zvorikin and N.V.Gudima. A cobalt. Moscow, AS USSR, 1949, 175 P.

# STRUCTURAL CHANGES IN ALLOY OF A CHROMIUM AT LOW TEMPERATURE PHASE TRANSFORMATION

**Maiboroda V.P., Adeev V.M., Maksimova G.M., Molchanovskaya G.M.**
I.Franzevich Institute of Materials Sciense Problems of National Academy of Scienses of Ukraine, Kiev, Ukraine

It is known, that the low temperature (-150$^0$C) magnetic transformation of a chromium and alloys on its basis is accompanied by isomorphous phase by transition [1]. The transformation descends on martensitic mechanism, accompanied by originating of stresses and fragmentation of a crystal.

The crystallographic feature of this transition consists in appearance of tetragonal in a BCC-symmetry of a crystal.

The indicated processes [1] were investigated only with the help of a low-temperature X-ray method [2] at the temperature up to -180$^0$C. Therefore in activity [1] there are absence the comparative data about nature of changes of dislocation frame and morphology of a surface of a microsection. The purpose of the given report is the attempt to fill this gap.

The activity was conducted on alloy BX2K with the contents Ta-0,5 mas %, V-0,5 mas % and La-0,2 mas %. The ingot is obtained of an inductive fusible electrolytic chromium in argon medium and did not subject of padding cleaning by a method of zone melting. Samples for researches were carved from hot-rolled recrystallization of a band.

The direct visions of structural changes of a surface of a microsection conducted with the help of an Auger spectrometer working also in a mode of a raster microscope. The vacuum in the chamber made ~10$^{-6}$Pa, the cleaning of a surface of a microsection implemented during 2 minutes with the help of ions Ar. A jack of a sample was incorporated by cold conductor with a vessel keeping fluid azote. As a result of losses in cold conductor temperature of a sample made - (155÷160) $^0$C.

In a fig.1, a, b, the original image of a surface of a microsection of a polycrystallic sample with a well bitten-into crystal boundary is submitted. The pits available on a surface of a microsection are oriented, fig.1, b, and testify, that their formation is connected to manufacturing of a microsection. The image is obtained after 2 multiple ion-beam cleanings. At sample temperature fall up to -(155÷160)$^0$C and exposure not less than 20 minutes, on a surface of a microsection there is a corrugated ramp relief, fig. 2, a, b. In separate places far from boundaries at an ion-beam cleaning there are pits, which during exposure 5-10 minutes are displaced to the boundary of a grain, fig.2, a, b.

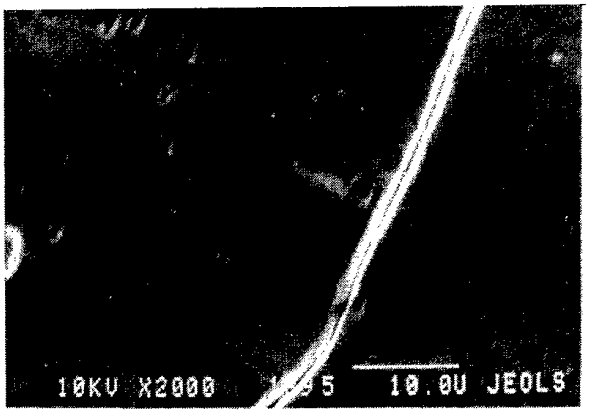


a

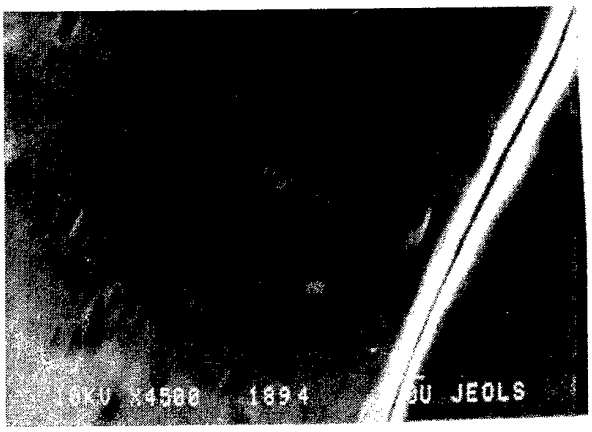


b

Fig.1

The originating of motility of dislocations testify the availability of stresses in a chromium at decreasing of the temperature up to –180$^0$C [1]. Width of crystal boundaries, fig.2, b is augmented

too. On an internal surface of a grain, the fig.2, b,I, occurs a relief of the prolated honeycombs, reference for a surface of metal, particulate or completely undergo the martensite transformation.

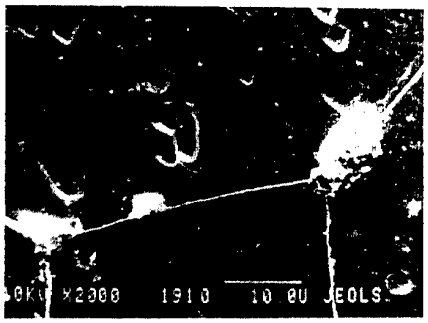


a

b
Fig.2

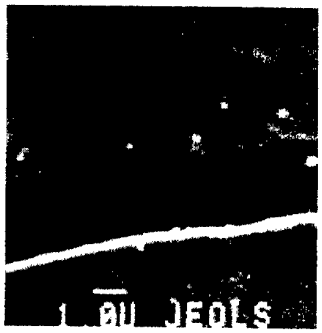


Fig.2,b,I

The electron microscopy researches were conducted on a film obtained on technique of mechanical thining up to 0,1-0,15 nm. Further thining until obtaining transparent edges executed electrolytical method. In a fig.3, a the joint of 3 grains is submitted. The small dislocation density in a reset state testifies to qualitative manufacturing of a foil. For analysis of influencing of low temperature the samples before electrolytical thining were immersed in fluid nitrogen, were maintained 40 minutes with subsequent heating up to room temperature. The map of theirs substructure is shown in a fig.3, b, which one differs by availability of a large dislocation density, glomal congestions and by broadened crystal boundaries. The absence in substructures, fig.3, b, doubles, apparently, is connected to a scaling factor of a cooling foil. At all events, this problem demands padding researches. As a whole, the obtained data will be agreed and supplement outcomes of activity [1].

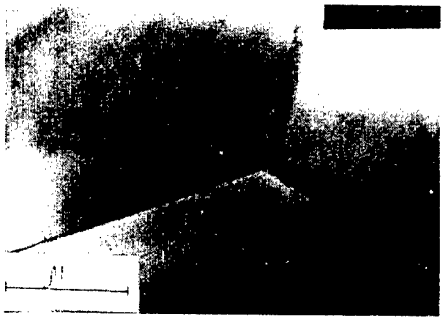

a

b
Fig.3

Literature

1. Larikov L.N., Baklanova L.M., Drachinskaya A.G., Uctinov A.N.//Metally, -1978.- № 5.-P.182-183.

2. Lysak L.I., Vovk Ya.N., Polischyc Yu.M.// Zavodskaya laboratoriya.-1968.- № 8.-P.1021-1023.

# INFLUENCE OF ROLLING ON THE STRUCTURAL STATE OF 2HBN PARTICLES

**Volkogon V.M., Oleynik G.S., and Avramchuk S.K.**
Frantsevich Institute for Problems of Materials Science, National Academy of Sciences of Ukraine, Kiev, Ukraine

Wurtzite boron nitride (2H BN) prepared from graphite-like boron nitride by static or dynamic compression under high pressures is the base of producing hexanite-R type superhard materials [1]. These materials are sintered under high pressures at high temperatures. The treatment of 2H BN powders by rolling favors the improvement of their compactibility characteristics and a decrease in the initial temperature of the transformation of the wurtzite modification in the sphalerite (3C) modification during sintering of these materials [2]. According to [2, 3], this is mainly due to the mechanical grinding and fragmentation of particles during rolling.

In the work, we present results of transmission electron microscopy (TEM) studies of the structural state of 2HBN particles after single and double rolling. This corresponds to a pressure in the rolling zone of 0.2 and 0.7 GPa, respectively. The rolling procedure has been described in [2, 3]. The starting powder with a particle size ranging from 3 to 5 μm in the plane (0001) and from 0.1 to 0.01 in the orthogonal direction was used. For the most part of particles, the azimuthal disorientation in the basal plane was not more than 3–5°.

On the base of our investigations, several elementary processes that cause structural transformations in particles during rolling were identified. Let us describe their mechanisms.

1. Mechanical disintegration proceeds by spalling. Brittle spalling proceeds along the prismatic planes $\{11\bar{2}0\}$ and $\{1\bar{1}00\}$, and so-called "plastic" spalling develops along the plane (0001), which is a plane of easy slip in the lattice of 2H wurtzite. As a result of this disintegration, the particle size decreases on the developed surface in the former case and in the direction perpendicular to it in the latter case.

2. Turns of packages of the basal layers within the limits of whole particle about the axis [0001] through angles up to 30° and over. In an individual particle, a single turn occurs rarely, in most cases, a turn is a combination of turns through different angles. Turns accompanied by shifts in the basal plane also take place.

3. Turns of local microregions in particles about the axis [0001], that favor their fragmentation, i.e., their splitting into disoriented regions.

4. Smooth bends of local zones of particles about arbitrary axes located in the plane (0001).

5. Changes in the shape of the basal plane of particles with the formation of a microrelief in the form of strips whose longer sides are parallel to the directions $[11\bar{2}0]$ and $[1\bar{1}00]$. The presence of the microrelief is also substantiated by observations of the developed surfaces of particles by TEM with using carbon replicas. In an individual particle, strips can intersect at angles of 30 and 60°. The displacement of microvolumes of particles along the conjugation boundary of strips, which cases the formation of steps on lateral surfaces of the cuts of particles, often occurs. Disintegration of particles by spalling of individual strips from the surface, leading to the formation of elongated small fragments, also takes place.

6. The reorientation of the developed basal plane of particles proceeds both locally and completely in the case of small particles. In electron diffraction patterns (EDP) from the developed surfaces of large particles, against the background of reflections of the basal plane, systems of reflections from pyramidal planes (one or two) most often appear. In this case, all orientations share the direction of the type $[1\bar{1}00]$ with the initial basal direction. As a result of the complete reorientation, pyramidal orientations, that most often correspond to the planes (031), (011), (021), (012) and (121), also appear. This indicates that the reorientation of the developed plane of particles occurs as a result of turns about axes located in the basal plane, i.e., axes perpendicular to the prismatic planes $(1\bar{1}00)$, $(11\bar{2}0)$, and $(12\bar{3}0)$.

7. The reorientation of the developed plane of particles caused by twinning. As a result of an analysis of EDP, twins characteristic of graphite [4] and graphite-like boron nitride [5] were identified. They arise due to turns of basal

layers about axes of the type $[1\bar{1}00]$. In isolated particles, twins differing in the rotation angle about this axis were detected. Twins formed as a result of turns about the axes $[11\bar{2}0]$ are identified more rarely. Such twins are known for graphite [4]. If the indicated twins are present, in electron micrographs of particles, the regular stranded contrast is observed. In small particles with the complete reorientation of the basal plane, along the planes $(10\bar{1}1)$, twins characteristic of graphite and metals with hexagonal close-packed lattices were also detected [6]. In isolated particles, 90°-twins were detected.

8. The local twisting of the layers (0001) of thin particles with the formation of fragments of tubular structure with an axis of the type $[1\bar{1}00]$. The conclusion that this structural reconstruction proceeds was made on the base of an analysis of the geometry of EDP from microregions of particles.

9. The formation of basal and prismatic stacking faults. Their presence manifests itself as broadening of node reflexes of *hol* rows in directions parallel to the axes *c* and *a* in EDPs from the prismatic spalling surfaces $(11\bar{2}0)$ of crystals. In EDPs from the planes (0001), basal stacking faults are also identified from the presence of continuous streaks between point reflections of hol rows in EDPs from the sections $(11\bar{2}0)$.

10. Local disordering in the direction of the axis [0001], which manifests itself as the presence of continuous streaks between nodel reflections of *hol* rows on EDPs from sections.

11. The phase transformation of the wurtzite BN modification into the graphite-like modification. This takes place in individual regions of particles.

Thus, during rolling, the structural transformations in 2H BN particles proceed as a result of mechanical disintegration and plastic deformation. Deformation proceeds by two mechanisms. These are: a) translational (lattice) slip, favoring the formation of stacking faults in the basal and prismatic $(11\bar{2}0)$ planes and structural disordering of BN on the direction of the axis [0001]; b) material (rotational) turns of regions of particles about the axis [0001] and axes perpendicular to prismatic planes. In the latter case, both twinning (on turning about the axes $[1\bar{1}00]$ and $[11\bar{2}0]$ and deformation by the way of kinking, i.e., by turning about the indicated axes through arbitrary angles, proceeds. These processes cause the orientation instability of particles, i.e., the reorientation of their developed surface.

The mechanisms of deformation through kinking on 2H BN particles under conditions of sintering of heganite-R type materials under high pressures at high temperatures have been considered in [7]. Deformation mainly occurs as a result of group turns of basal layers of crystals about axes perpendicular to prismatic planes as well as the combination of these turns with turns about the axis [0001] and displacements with respect to it. These data enable us to draw the following conclusions: a) structural transformations in 2H BN particles during rolling are mainly caused by the action of shear stresses; b) the structural state of 2H BN particles forming during rolling is one of the major factors that favor a decrease in the temperature of the 2H→3C phase transition during sintering.

**References**


1. Superhard Materials (edited by Frantsevitch I.N.), – Kiev: Naukova Dumka, 1980.– 286 p.
2. Volkogon V.M., // Sverkhtverd. Materialy, – 1993. – No. 3. – P. 19–22.
3. Volkogon V.M. and Ostrovskaya N.F., // Sverkhtverd. Materialy, – 1993.– No. 2. – P. 38–41.
4. Electron Microscopy, 1966 (the 6th Intern. Congress for E.M. Kyoto, 1966), P.365.
5. Kurdyumov A.V., Ostrovskaya N.F., and Pilyankevich A.N., // Kristallographiya. – 1976. –No. 2. – P. 418–419.
6. Fainbron A.S., Notkin A.B., and Utevskii L.M. // Zavodsk. Laborator. –1977. – No. 6. – P. 694–700.
7. Oleynik G.S.// Works of IPM NANU. Electron Microscopy and Strength of Materials. – Kiev, 2001. – Issue No. 11. – P. 146–157.

# THE INVESTIGATION OF ELECTRONIC FRAME In AND Sn I N SOLID AND LIQUID CONDITION BY A METHOD OF X-RAY-PHOTOELECTRON SPECTROSCOPY

**Maiboroda V.P., Sinelnichenko A.K.**
I.Franzevich Institute of Materials Sciense Problems of National Academy of Scienses of Ukraine, Kiev, Ukraine

The absence of abnormal mean square displacement of atoms Sn at transition from solid in a liquid state at researches by a EXAFS method, which one is responsive to short-range nuclear environment [1], is interpreted in this and other activities [2], as availability of tetragonal-like ordering of atoms in a microgroupings of a melt. However, the areas of short-range ordering are not an alone piece of the composite motive of a constitution of liquids. As shown in activities [3-5], the composite motive of melts consists of a system of Brown drifting polypieces, hierarchically bound among themselves.

In activity [3] is shown, that only drips of a melt by the size of 100 nm and above has the oval or spherical forms. More small-sized zones $\leq$ 50 nm has plate-similar, rectangular geometry. The area comparable to the size of a microgrouping (2-5 nm), is hardly prolated and with the darkfield diffraction methods is watched as crystal-like area of coherent dissipation [4].

The purpose of the given activity is the realization of comparative researches of X-ray photo-elecnron spectra of 3d levels and constitution of valence bands of Sn and In in solid and liquid condition. The spectra are obtained on the device ЭС-2401 in vacuum $10^{-6}$ Pa, in X-ray Kα radiation Mg. The step of scanning made 0,05 eV, and set of number of pulses in a maximum not less than 25000. The received discrete form of curves allows to conduct mathematical processing of the obtained spectra - smoothing of curves, calculus of a maximum of a pica, its half-width etc. We had designed the software package ensuring these functions. The smoothing was conducted by method of least squares by interpolation of polynomials of 3-rd degree. The same method determined also reference points of an experimental curve - position of a maximum, point of bends, width of a chord on half of peak height and its center etc. Error in definition of a maximum did not exceed $2\sigma \approx 0{,}012$ eV ($\sigma$ – average-square deviation). It is so-called «statistical» error, which one is determined by the extremely discrete form of submission of a curve.

The special researches on given ЭС 2401 have shown, what despite of high stabilization of supply voltages, the absolute values of measured energies "sail" in due course and can reach 0,3÷0,5 eV for one day. However, these changes have monotonic, smoothly varying nature, that allows them to take into account (from the point of view of relative researches) with the help of a procedure repeated and continuous process of repetition of measurements: I condition - II condition - I condition - II condition. As a result of such experiment we receive interconnected time sweeps of some parameter E (we allow, value of energy of a maximum of a pica): $E_I(t_1)$, $E_{II}(t_2)$, $E_I(t_3)$, $E_{II}(t_4)$ etc., where the index at E means a condition of object of filming. If now to approximate temporary drift of the device by a polynomial (it is customary 3-rd or 4-th degrees): L (t) on points of a I-st condition $L(t) \sim E_I(t)$, after the logician of reasoning a polynomial $(L(t) + \Delta E)$ must to describe points of a II-nd condition, and minimum of a functional $\Sigma((L(t) + \Delta E) - E_{II}(t))$ characterizes error of measurements ΔE. For more full count of errors the procedure repeated inverntory - the polynomial on $E_{II}(t)$ and functional for $E_I(t)$ was calculated. For outcome received average value of these two values (fig. 1).

Table 1.

Parameters of 3d-spectra of Sn and In in liquid and solid condition (eV)

| Line | $E_{max}$ | $E^{liq}_m - E^{sol}_m$ (±0,03) | $\Delta E^{liq}$ *) (±0,015) | $\Delta E^{sol}$ *) (±0,015) |
|---|---|---|---|---|
| Sn3d5/2 | 484,6 | 0,05 | 1,29 | 1,27 |
| Sn3d3/2 | 493,0 | 0,05 | 1,43 | 1,46 |
| In3d5/2 | 443,1 | 0,04 | 1,22 | 1,23 |
| In3d3/2 | 450,7 | 0,04 | 1,25 | 1,26 |

*) ΔE - width of a pica on half of altitude

By described above techniques were investigated Sn 3d- and In 3d-levels in a solid

state at temperature (T) 20$^0$C and in a liquid state (T=260±20$^0$C for Sn and T=200±20$^0$C for In), and also valence bands. The experimental data on In3d- and Sn3d- to spectra are adduced in tab. 1, curves of valence bands - in a fig. 1.

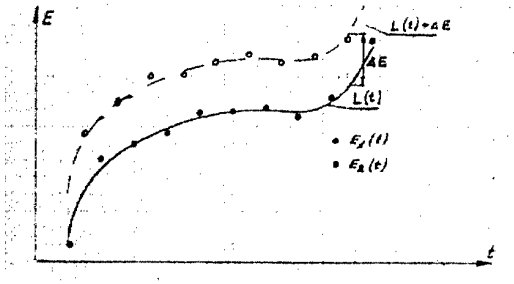


Fig.1

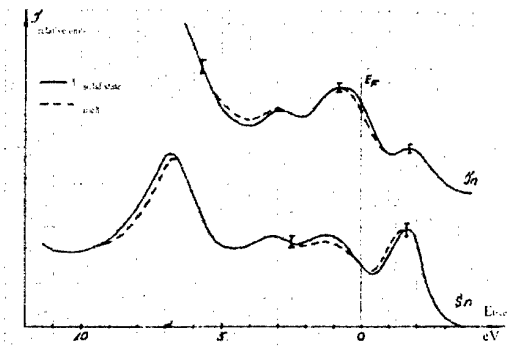


Fig.2

It is necessary to mark, what the valence bands of the indicated metals formed by s- and p-electrons have the lowest intensity, the process of filming lasted 5÷6 hours, the statistical dispersion therefore took place, which one was allowed by a special technique. The marked changes in valence bands, at transition from a solid state in liquid it is possible to regard only as the tendency. In this direction it is expedient to prolong researches. The interpretation of features of a valence band both In and Sn is complicated by that on this area the 4d-pikes In and Sn from satellites MgKα superimposed of X-ray radiations, which even exceed on the intensity the structure of the most valence band. The special problem arises with interpretation of maxima arranged on 1,6 eV above the Fermi level. If for In with some strained interpretation. it is possible to explain by monochromium of a X-ray radiation, so for Sn the explanations to this maximum no also problem demands careful experimental study.

As a whole experiment has shown, that the changes in X-ray photo-electron spectra at transition from a solid state in the fluid of indicated metals are insignificant and can be interpreted, as preservation of chemical coupling and nature of packaging of atoms in clusters, fragmentation derivated during melting.

Literature

1. Orton B.R., Marba G.R., Steel A.T.//J.Phys. F.-1987, V.17. P.45.
2.V.G.Bar'yachtar, L.E.Michailov, A.G.Ilyinskiyi, A.V.Romanova, T.M.Christenko//JETPh -1989, - V.95, №4, P. 1404-1411.
3. Maiboroda V.P., Maksimova G.A., Sinelnichenko A.P.//The Ukrainian Physical Journal -1991, - №11, P. 1752-1758.
4. Maiboroda V.P.//Thin Solid Films. 195, N1-2 (1991), P.357.
5. Maiboroda V.P.//Rasplavy.-1996, - №2, P. 82-89.

# PHASE EQUILIBRIA IN THE TERNARY SYSTEMS $Al_2O_3$ – $ZrO_2$ – RARE EARTH ELEMENTS OXIDES

**Lakiza S.M., Red'ko V.P., Lopato L.M.**

Frantsevich Institute for Problems of Materials Science NAS of Ukrajina, Kyiv, Ukrajina

Systems $Al_2O_3$ – $ZrO_2$ – REE oxides (REEO) attract much attention as a source for design of refractory oxide materials with complex composition. The initial oxides are very hard, stiff, have low thermoconductivity and high chemical stability. REEO are the best $ZrO_2$ stabilizers, alumina improves thermomechanical properties as well as inhances the stability of ceramics at hydrothermal conditions.

Phase diagrams are the best technologist assistant for constructing advanced materials. So the aim of the present investigation was to study $Al_2O_3$ – $ZrO_2$ – REEO phase diagrams, where REEO – La, Nd and Y. These REEO are the representatives from Ce and Y lanthanoid subgroups, so we expected distinctions in structure of these ternary systems.

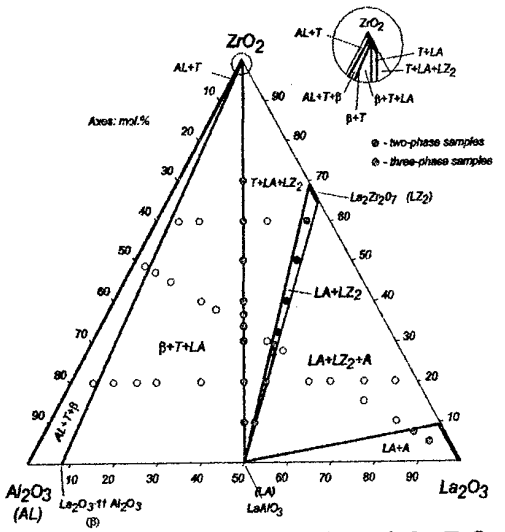


Fig. 1. Isothermal section of the $Al_2O_3$-$ZrO_2$-$La_2O_3$ phase diagram at 1250 °C.

Samples for the investigation were prepared of 99,9 pure oxides, melted in high-temperature DTA set and analysed by DTA, X-ray, petrodraphic and microstructural methods. The results of investigation are presented in Fig. 1, 2 and 3 as isothermal $Al_2O_3$ – $ZrO_2$ – REEO phase diagram sections at 1250 °C.

The izothermal section of $Al_2O_3$-$ZrO_2$-$La_2O_3$ phase diagram at 1250 °C (fig. 1) consists of four three-phase fields and four two-phase fields. Solid solutions single-phase fields as well as ternary compounds were not found in the system. Two-phase field $LaAlO_3$ + $La_2Zr_2O_7$ corresponds to the same denoted quasibinary section as far as samples of this section contain only $LaAlO_3$ and $La_2Zr_2O_7$. Two-phase field $LaAlO_3$ – T-$ZrO_2$ corresponds to the same denoted partially quasibinary section since $LaAlO_3$ phase was found in equilibria with solid solution $ZrO_2$ + 1,5 % mol. $La_2O_3$ and therefore the composition of the equilibrium phases were not found in the section plane in all temperature interval. Two-phase field $La_2O_3 \cdot 11Al_2O_3$ – T-$ZrO_2$ outlines the partially quasibinary section of the same name since alumina-rich phase decomposes at 1848 °C. Zirconia is the phase that defines interaction the ternary system.

The isothermal section of the $Al_2O_3$-$ZrO_2$-$Nd_2O_3$ phase diagram at 1250 °C (fig. 2) consists

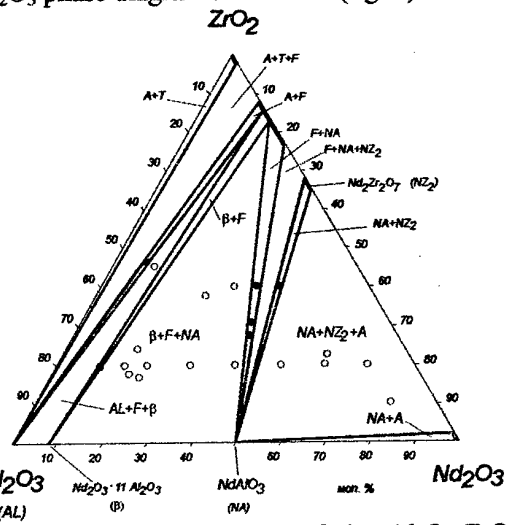


Fig. 2. Isothermal section of the $Al_2O_3$-$ZrO_2$-$Nd_2O_3$ phase diagram at 1250 °C.

of five three-phase and six two-phase fields. Solid solutions single-phase fields as well as ternary compounds were not found in the system too.

Two-phase fields $NdAlO_3$ + F-$ZrO_2$, $Nd_2O_3 \cdot 11Al_2O_3$ + F-$ZrO_2$ and $NdAlO_3$ + $Nd_2Zr_2O_7$ correspond to the equilibria of compounds, that are formed in binary bounding

system $Al_2O_3$ – $Nd_2O_3$, with $ZrO_2$ – $Nd_2O_3$ solid solutions of different compositions and ordered phase $Nd_2Zr_2O_7$ with homogeneity region. Therefore they outline the partially quasibinary sections that triangulate the ternary system.

Unlike the system with $La_2O_3$, where the compound $La_2Zr_2O_7$ with pyrochlore-type structure congruently melts at 2340 °C, the compound $Nd_2Zr_2O_7$ with the same type of structure is actually the ordered phase and exists in solid state only at the temperatures below 2220 °C.

The isothermal section of the phase diagram $Al_2O_3$-$ZrO_2$-$Y_2O_3$ (fig. 3) consists of six three-phase fields and seven two-phase fields [1]. Solid

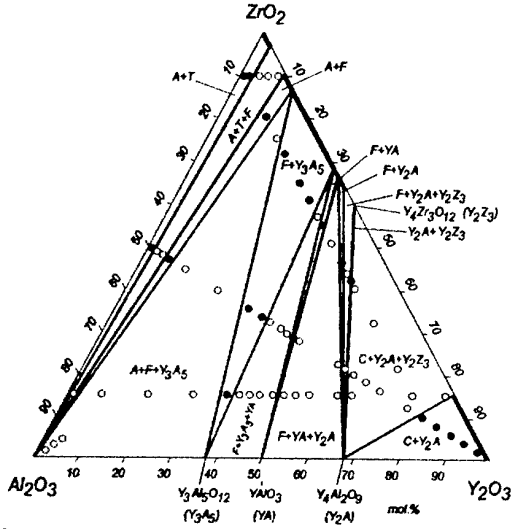


Fig. 3. Isothermal section of the $Al_2O_3$-$ZrO_2$-$Y_2O_3$ phase diagram at 1250 °C [1].

solutions single-phase fields as well as ternary compounds were not found in the system too. Two-phase fields $Al_2O_3$ + F-$ZrO_2$, $Y_3Al_5O_{12}$ + F-$ZrO_2$, $YAlO_3$ + F-$ZrO_2$, $Y_4Al_2O_9$ + F-$ZrO_2$ and $Y_4Al_2O_9$ + $Y_4Zr_3O_{12}$ correspond to the equilibria of compounds, that are formed in binary bounding system $Al_2O_3$ – $Y_2O_3$, with $ZrO_2$ – $Y_2O_3$ solid solutions of different compositions and ordered phase $Y_4Zr_3O_{12}$, that is stable below 1382 °C. Therefore they outline the partially quasibinary sections that triangulate the ternary system.

The izothermal sections analysis of $Al_2O_3$-$ZrO_2$-(La, Nd, $Y)_2O_3$ systems allow to draw some conclusions. Interaction in these systems has some common and some different features.

Differences in the ternary systems studied are the result of interaction changes in binary bounding systems. The last arise from the ionic radii value difference of La (0,114), Nd (0,104) and Y (0,092). It is necessary to note, that the ionic radii value difference of La and Nd is not still sufficient to change interaction in the system $Al_2O_3$ – $Nd_2O_3$, but is already evident in the system $ZrO_2$ – $Nd_2O_3$. Thus the phase with pyrochlore-type structure $La_2Zr_2O_7$ melts congruently at 2340 °C, while the analogous compound $Nd_2Zr_2O_7$ is stable in the solid state below 2220 °C only. Besides this ion $La^{3+}$ at 1250 °C stabilizes only tetragonal form of $ZrO_2$, while $Nd^{3+}$ ion – fluorite-like cubic form.

The comparison of two mentioned above ternary systems with the system $Al_2O_3$-$ZrO_2$-$Y_2O_3$ reveals even greater differences. In the binary bounding system $ZrO_2$ – $Y_2O_3$ the phase with pyrochlore-type structure is replaced by rombohedral ordered phase $Y_4Zr_3O_{12}$, that is stable below 1382 °C. The F-$ZrO_2$ and C-$Y_2O_3$ solid solutions areas increase a lot. In addition to the compound $YAlO_3$ the compounds $Y_3Al_5O_{12}$ and $Y_4Al_2O_9$ appear in the system $Al_2O_3$ – $Y_2O_3$, while the compound of the $Ln_2O_3 \cdot 11Al_2O_3$ type disappear.

The common feature of these ternary systems is the absence of solid solutions single-phase fields as well as ternary compounds. It is very important that $ZrO_2$ defines the interaction in the systems and exists in equilibria with almost every other phases. It forms two-phase regions which triangulate ternary systems. This fact allows to make a conclusion that in these ternary systems it is possible to construct composite materials in which phase components, i.e. matrix and reinforcement phases, do not react in the course of high-temperature runing. One should also note that $ZrO_2$ is in equilibria as solid solutions with tetragonal ($Al_2O_3$-$ZrO_2$-$La_2O_3$) or cubic fluorite-like ($Al_2O_3$-$ZrO_2$-(Nd,$Y)_2O_3$) structures.

## Literature

1. Лопато Л.М., Назаренко Л.В., Герасимюк Г.И., Шевченко А.В. Изотермическое сечение диаграммы состояния системы $ZrO_2$-$Y_2O_3$-$Al_2O_3$ при 1250 °C // Неорганические материалы.– 1992.– **28**, № 4.– С. 835 – 839.

# COMPLEX MODELLING OF THE PHASE EQUILIBRIA IN Al – Ti SYSTEM AND SEGREGATION IN THE GRAIN BOUNDARY PHASE OF ITS POLYCRYSTAL ALLOYS

**Danylenko V.M. , Yagodkin V.V.**
J.N. Frantsevich Institute for Problem of Material Science NAS of Ukraine, Kyiv, Ukraine

The Al-Ti based alloys are perspective heat-resistant construction materials. Solid phases on the basis of starting components: HCP <α-Ti> (α), BCC <β-Ti> (β) and FCC <Al>, as well as titanium aluminides $AlTi_3$ ($\alpha_2$), AlTi (γ), $Al_2Ti$ (η), $Al_{11}Ti_5$ (ξ), $Al_3Ti$ (ε) have been formed in the Al -Ti system. The consistent system of model constant sets of all condensed phases in Al-Ti was constructed as a result of analysis of experimental information and optimisation of phase equilibria and thermodynamic properties data. This gives possibility to calculate the phase diagram of this system. The coordinates concentration Z and temperature T of the character points of the Al-Ti phase diagram are presented in the table1.

The table 1.

| Nonvariant equilibrium. Reaction | Calculated | |
|---|---|---|
| | Z,at.%Al | T,K |
| Melting L ↔ <Al> | 100 | 933.47 |
| Peritectic L + ε ↔ <Al> | 99.9999 | 938 |
| | 75 | |
| | 0.3686 | |
| Eutectic α ↔ $\alpha_2$ + γ | 40 | 1388 |
| | 39 | |
| | 50 | |
| Ordering α ↔ $\alpha_2$ | 33 | 1472 |
| Peritectoid ξ + γ ↔ η | 68.75 | 1483 |
| | 66.6667 | |
| | 65.01 | |
| Peritectic L + ξ ↔ ε | 80.12 | 1698 |
| | 75 | |
| | 68.75 | |
| Peritectic L + γ ↔ ξ | 69.8 | 1723 |
| | 59.6 | |
| | 69.78 | |
| Peritectic L + α ↔ γ | 59.9 | 1758 |
| | 50.1 | |
| | 52 | |
| Peritectic L + β ↔ α | 52 | 1793 |
| | 42.7 | |
| | 44.1 | |
| Congruent melting L ↔ β | 7.75 | 1975- |
| Melting L ↔ <β-Ti> | 0 | 1941 |

We took the modern thermodynamic properties of the phases of elements from SGTE [1].Constants of interaction depending on the temperature by four-term formula $G_q = A_q + B_qT + C_qlnT + D_qT^2$ [2].

Very valuable construction materials on the basis of Al-Ti alloys are intercrystallite fragile mainly due to the grain boundary impurity segregation. In our the grain boundary equilibrium segregation substitution atoms model [3] polycrystal assumed to be two-phase system of solid solution ( s ) and grain boundary ( b ) phase which have small volume fraction a«1. Introducing internal deviation parameter X from mean impurity concentration Z, we may determine the middle-phase concentrations as follows $Z^s = Z + X$ for solid solution and $Z^b = Z - (1-a)X/a$ on the grain boundaries. Assume that molar Gibbs potential of policrystal is: $G = (1-a)G^s + aG^b$, where $G^s$ and $G^b$ are molar potentials of solid solution and boundary phases, respectively. Substracting the non-segregation $G^s_0$ and $G^b_0$ potentials we obtaine the energy dependences of the segregation relaxation potential $-G_R$ and the grain forming one $-G_F$, respectively: $G = (1-a)G^s_0 + aG^b_0 + G_R = G^s_0 + G_F$ . If the volume of grain boundary phase is constant (a = const), this two-phase system is in equilibrium state when the condition $dG/dX = 0$ is fulfilled. Using for potentials of both phases the model of subregular solutions where all $G_q$ are thermodynamic potentials components phases, constants of interaction in solid phase and in grain boundary phases depending on the temperature by four-term formula we obtaine the transcendental equation for segregation, which we must resolve by numerical methods.

We investigated at the grain boundary segregation in the liquid-like grain boundary model [3] with a = 0.01 for systems with the broad homogeneity regions: α( HCP-Al,Ti ), β( BCC-Al,Ti ), $\alpha_2$( $AlTi_3$ ), γ( AlTi ) .

We have obtained by computer modelling the temperature dependences of the grain boundary concentration $Z^b$ and the temperature dependences of the energy characteristics $G_R$, $G_F$.

We have obtained also the regions of phase existence (consistent with corresponding phase diagram) and zero- segregation lines $L_0$ . There are general tendency of increasing the isoconcentration sections $Z^b$ for Al – Ti with temperature growth.

In the α - Al ,Ti phase we obtained zero-segregation line $L_0$ from ( Z = 31 at.%Al , T =1530K ) to ( Z =33 at.%Al, T=1470K. In the β - Ti,Al phase we obtained line $L_0$ from ( Z = 6 at.%Al, T =1970K ) to ( Z = 31 at.%Al ,T =1620K ). In the $\alpha_2$ - Al,Ti phase we obtained line $L_0$ is external for the region of phase diagram existence. Impoverishment of aluminium atoms on the boundary under cooling was found for whole region of $\alpha_2$ phase: $Z^b$ = 27.5 at.%Al at the top of this region (1472 K, 33 at.% Al ) and at 1000 K we have $Z^b$ from 37 at.%Al ( Z = 45 at.%Al ) to $Z^b$ = 0.85 at.%Al ( Z = 20 at.%Al ). In the γ - Al,Ti phase we obtained line $L_0$ from ( Z = 47.5 at.%Al, T =1650K ) to ( Z =61at.%Al, T =1350K), with tendency of increasing $Z^b$ changes to saturation at Z = 65.5 at.% Al with instability at T ≤ 1200K. Regions of phase domaines intersections reveale decreasing of grain boundary equilibrium segregation with cooling: $Z^b/Z$ changes from 1.2 (Z=52 at%Al, T=1793K) and later to 0.42 at 1000 K.

We have obtained also general tendency of correlation between the temperature dependences of the energy characteristics $G_R$ , $G_F$ and the temperature dependences of the concentration $Z^b$ on grain boundaries under the equilibrium segregation substitution atoms.

We have obtained the segregation maximums of temperature $T_m$ and concentration $Z^b_m$ are presented in the table 2.

The table 2.

| Phase | Z,at.%Al | $T_m$,K | $Z^b_m$,at.%Al |
|---|---|---|---|
| α(Al,Ti ) | 50.1 | 1793 | 86 |
| β(Al,Ti ) | 42.7 | 1793 | 55 |
| $\alpha_2$( $AlTi_3$ ) | 39 | 1388 | 34 |
| γ( AlTi ) | 65 | 1483 | 77 |

## Conclusions

The complex adequate to the modern investigation level description of the Al-Ti system was done.

The Al-Ti alloys with aluminium content of about and higher then 50 at.% revealed the segregation of aluminium atoms on the grain boundaries. We have obtained also general tendency of correlation between the segregation maximums of temperature $T_m$ and concentration $Z^b_m$ and concentration Z and temperature T of the character points of the Al-Ti phase diagram.

Analysis of the grain boundary segregation tendencies for the γ phases in the Al –Ti system also permit other intermediate micro-phases nucleation prognozis on boundary regions. These effects may explain the high-temperature intercrystalline fragility of these alloys.

## References

[ 1 ]. Dinsdale A.T. SGTE data for pure elements, CALPHAD, 1991, 15(4) , P.317 .

[ 2 ]. Danylenko V.M. Real crystals models , Kyiv: Naukova dumka, 1983, P.224.(in Russian).

[ 3 ]. Danylenko V.M., Yagodkin V.V. Modelling of the temperature dependence of the equilibrium substitution atoms segregation on grain boundaries of binary alloys , Kyiv, Preprint of Institute for problems of material science NASU; 1993, N2 , P.22 . (in Russian).

# HIGH-PERFORMANCE MATERIALS BASED ON $ZrO_2$

**Shevchenko A.V., Ruban A.K., Dudnik E.V., Lopato L.M.**
I.N.Frantsevich Institute for Problems of Materials Science, Kiev, Ukraine

Ceramic materials, including oxides, are classified in application on conventional and advanced. The conventional materials market grows slowly as opposed to the advanced ceramics market, which is reasonably large now and continues to develop intensively. Advanced materials are used principally for both structural and functional materials. Under manufacturing of structural materials the attention is focused on strength behaviours, whereas under producing of functional materials emphasis is placed on the electrical and magnetic properties.

High-performance materials based on $ZrO_2$ are characterized with the unique combination of high strength and fracture toughness, stability to influence of corrosive medium, low thermal conductivity and especial electrophysical properties, which are perspectived for creation of both structural and functional ceramics.

The aim of this paper is to present the Department's research results on creation of ceramics based on ZrO2 for various applications.

Our combined approach to improvement of the $ZrO_2$ - ceramic materials consists in establishment of the relationship between producing of starting powders, forming of green bodies and sintering together with both strength behaviour and electric properties of ceramics. This non-separable process line-up allows to design ceramic materials in the various systems based on ZrO2 at a microstructural level. The behaviors of designed ceramics have progressed to the stage where they were promising for creating of a variety of materials: from refractory products up to converters of energy and bioimplants.

The most attention has been concentrated on producing of materials with fragmentary, coarse-grained macrostructure under creating of refractory products. The active bonding materials from the nanocrystalline powders based on $ZrO_2$ were among the materials component. That had allowed to produce the high-strength sintered materials with increased durability to thermal-fatigue loads. Using of this process had created crucibles and shell forms with the covering layer for melting of refractory, chemical active metals and alloys (up to $2000^0$C); high-temperature heaters for exploitation in an oxidising medium at the temperature up to 2000 $^0$C in the conditions of repeated switching on / switching off; cermet crucibles for multifold vacuum distillation and evaporation of metals with in the temperatures range from 1200 up to 2200 $^0$C.

The development of new structural ceramics presumes the creation of the certain microstructure both in volume and surface of the materials. This is due to the fact that the various destroying factors should be relaxed. These factors are : creation of the local stress zones; origin, accumulation and confluence of microcracks, their rising and development to the arterial crack. Appropriate microstructures are arisen by the purposeful variation of the matrix chemical and phase composition as well as the concentration and morphology of disperse phases. Variation of the starting powder synthesis conditions along with the methods of their forming, pre-heated treatment and sintering affect as well.

Chemical pure, homogeneous ultra-fine isomeric powders with a narrow particles size distribution are necessary to producing of fine-grained ceramics with both high density and strength. Our main attention under producing of the starting nanocrystalline powders of complex composition (from binary up to four-components) was given to the combined method of hydrothermal synthesis and sol – gel technology. The powder activity, which provides the high strength behaviour of ceramics, was occurred on this step. Slip casting followed by cold isostatic pressing provides the creation of the "regular" microstructure of monolithic and layered green bodies. Slip casting of aqueous slips was used for the powders forming. Slips were stable and did not require of additional stabilisation. The solid concentration varied from 50 to 70 % depending on chemical composition. Castings of "regular" microstructure as well as relative densities from 0,35 to 0,4 were produced. Hydrostatic pressing was used for increasing of the slips relative densities up to 0,45. The sintering conditions variation had allowed receiving the structural materials based on ZrO2 with fine-grained, two-scale "self-reinforced" and layered microstructures.

The structural materials with bending strength of 1000 – 1200 MPa and $K_{1c}$ - up to 15 - 20 MPa.m $^{0,5}$ were produced as a result of this complex approach.

The following technology were developed: targets for electron-beam plotting of heat-protective coatings; cutting ceramics for various purpose; dies for spraying of abrasive, loose and liquid materials; drags for drawing of an aluminium and copper wire; bioceramics.

The further improving of the properties of the structural ceramics based on $ZrO_2$ will be centred around increasing of both strength behaviour and fracture toughness as well as searching of physical-chemical regularities for formation of the "self-reinforced" structures of composite ceramic materials. Non-isometric "self-reinforced" phases are in a thermodynamic equilibrium with a matrix and are formed as the result of chemical reactions, ordering or eutectoid disintegration of solid solutions. The certain perspectives are connected with the development of the multilayer and gradient materials producing. In these materials the thin discrete layers (up to 20 - 100 microns) represent the "self-reinforced" ceramic composites, which were treated with non-traditional thermal treatment, for example, plastic forming with a large cubical strain of all package.

The ceramic fuel cell has attracted considerable interest of scientists owing to high efficiency under transformation of the fuel chemical energy immediately to electrical. Designing of the solid electrolytes with ionic conductivity in the multicomponent systems based on both ZrO2 and oxides of elements of II and III groups of Periodic system with the crystalline structures such as fluorite, pyrochlore and perofskite is carried out now in the Department. Long-term phase stability of the SOFC' solid electrolyte, contacting with 2 chemical dissimilar electrodes over prolonged period at the temperature 1000 $^0$C, is one of the problems under investigation. It demands the careful researches of technological steps both for forming of electrodes (cathode, anode) during the solid oxide fuel cell manufacturing and under collecting of separate cells to the commutator of necessary capacity. It, in turn, presents increased requirements to both strength behaviours and electrical properties of the oxide interconnection.

Reducing of the solid electrolyte thickness is of importance to designing of planar fuel cells. It should result in increasing of the efficiency of the fuel using, decreasing of the operation temperatures and raising of the cell efficiency as a whole. Therefore, producing of the $ZrO_2$ layers from 8 to 30 μm thickness is an issue of the day. We used the electrophoretic deposition for solution of this problem.

Designing of the supporting construction for planar fuel elements is topical problem. We designed the technology for producing of the gasproof tubular ceramic elements based on stabilised zirconia for solid electrolytes of fuel cells (oxygen pumps).

# THE PHYSICO-CHEMICAL BASES of MELTING the HIGH PURE ALLOYS of Ti, Zr, Cr And DEVELOPMENT of PERSPECTIVE TECHNOLOGIES FOR ITS PURPOSE

**Uljanov V.L., Rakitskij A.N., Kyznetsova T.L., Jakimenko I.L.**
Institute for problems of materials science NAS of Ukraine, Kiev, Ukraine

The development of perspective technologies of melt of high pure alloys of highly reaction refractory metals is based on thermodynamic accounts of refining processes and also on research of structure change kinetics of liquid melt during various kinds of melting with the purpose of an establishment of optimum parameters of melting and deep refining.

The researches of refining have been carried out depending on specific capacity $\Delta W$ (kW / kg), time of exposure for metal at the maximal capacity t (minutes) and degree of pollution of the melting atmosphere ($\Sigma$ % impurities).

The influence of various technology factors on gas saturation - degassing of metal and removal of non-metal inclusions of deoxidation products have been investigated by various ways of the melting.

Proceeding from physic-chemical properties of high pure refractory metals (Ti, Zr, Cr) the optimum parameters their melting and refining have been substantiated, and the perspective technologies of reception high pure alloys on their basis have been investigated and tested.

It has been established, that for melting and refining of zirconium alloys, which have low vapour pressure at the melting temperature (P = $10^{-3}$ Pa), and easily deoxidate in vacuum at the expense of evaporation of monoxide ZrO, electronic beam sculled smelting (EBSS) with electromagnetic mixing of melting are the most perspective technology .

Taking into account rather high vapour pressure of titanium at the melting temperature (P = $5.10^{-1}$ Pa) the melting technology of titanium alloys in vacuum-induction sculled furnace with "cold" crucible in high pure argon is optimum. However, taking into account, that the shock viscosity of titanium alloys is basically determined by the contents of hydrogen, for melt of plastic titanium alloys it is represented perspective electronic beam sculled smelting with electromagnetic mixing of melting. At this technology the decrease of hydrogen in titanium up to 0,001% is possible.

As chromium vapour pressure at the melting temperature is about $10^{-1}$ Pa, the smelting of high pure of chromium alloys is necessary to carry out only in inert medium in an induction furnace with "cold" crucible.

The experimental researches of melting both refining of titanium and zirconium alloys in electron beam skilled furnace, and chromium alloys in vacuum-induction furnace with ceramic or "cold" crucible have been carried out.

The developed technological parameters the electronic beam sculled smelting (vacuum . $10^{-1}$-$10^{-2}$ Pa, overheat the melt before 0,1 $T_l$, electromagnetic mixing a fluid metal, use special deoxidisers) have allowed to ensure thermodynamic parameters of deeper refining the titanium alloys from gas impurities, than under vacuum-arc melting (VDS) [1,2]. In alloys VT-5L EBSS the hydrogen contents is within 1-3.$10^{-3}$ %, that in 10-100 once below in contrast with the metal, received by method VAS. Thus it was possible to reduce the contents of impurities O and N to a level 0,03-0,05 and 0,01 % accordingly. The mechanical properties of a cast alloys, received by the method EBSS vastly exceeded the properties of same alloys VDS, thus the striking viscosity formed 0,5-1,0 MN·m$^{-1}$ under tolerance for this alloys - 0,3 MN·m$^{-1}$. The reason of them is more full refining this alloys from gas impurities and, in the first of all, from hydrogen. Carried out TEM has not shown hydrides layers over the grain borders casting alloys VT-5L, received on the developed technology.

The conditions of melt high pure zirconium alloys without oxidation and gas saturation by a method electronic beam sculled smelting are established, the sources of contamination of the metal and role the factors influencing to getting of alloys with the contents of impurity inculcation at a level less than 0,1 % are investigated [3]. The influence of the different factors on degassing of metal at melting is investigated. In the results melting refining of the scraps of a zirconium alloy Zz-1%Nb in vacuum $10^{-2}$ Pa, at power 20кW/кg, time refining 60-90 s and intensive electromagnetic intermixing of a

melt the contents of oxygen in ingots has decreased from 0,15-0,2 % up to 0,07-0,09%.

The complex of the carried out technological researches has allowed making a conclusion, that the basic sources gas saturation the chromium alloys at melting (at exception of influence the ceramic crucible) are the melting gas atmosphere and chemically active gases, adsorbed on a surface of the furnace, foundry equipment and stock [4].

Therefore the reception of ingots with the low contents of the impurities inculcation is possible only under condition of providing preliminary deep ($10^{-3}$-$10^{-4}$ Pa) oil less pumping out of melting space, degassing of an internal surface of the furnace and the stock in conjunction to filling of the furnace high pure argon and application of highly effective methods of circulating purification of inert gas at melting process with multiplicity of an exchange not less than 25-30 and - or using the vapours of the high-active low-boiling elements (Mg, Ca, Ba, Sm), ensuring decrease of oxygen, moisture and nitrogen in a gas melting atmosphere less $(1\text{-}3).10^{-4}$ %.

The important role in providing of high purity alloys is the technology of preparing the burden materials (chromium and alloys components). The developed technology of preparation chromium burden includes high-vacuum (below $10^{-4}$ Pa) degassing the burden at 1200-1250° C, vacuum pressing of briquettes or consumable electrodes and superficial electron beam smelting of consumable electrodes. The preparation alloys components includes operations the cutting alloys components, splitting its with ultrasonic washing.

The refining (deoxidation and decarbonisation) of the metal in the melting process is reached by alloying the high-active elements. As a result of analytical and experimental researches the optimum parameters of deoxidation chromium melt by rare-earth metals (Sc, Y, La) at arc sculled and induction sculled smelting in "cold" crucible are established. Is shown, that deep deoxidation ([O] Cr < $10^{-5}$ %) is reached at introduction REM in quantity 0,2-0,5 % into melt for 40-60s before input chemically active alloys components (V, Ta, Al, Ti, Zr). For reduction impute into melt chemo adsorbed gases from the surface REM, REM should be entered into metal only as specially prepared alloys. The complex of the described measures has made possible to reduce the contents of impurity of introduction in alloys to a level - 0,0005-0,003, 0,001, 0,003-0,002 % of oxygen, nitrogen and carbon accordingly.

Thus as a result of the carried out researches and scientific development the optimum perspective technologies and melting-foundry equipment are offered which make possible to receive high-pure alloys on a basis highly - reaction refractory metals (titanium, zirconium and chromium), that opens new opportunities for their application.

References

1. Ульянов В.Л., Кузнецова Т.Л. Яковлев В.Т. А condition and prospects of development of shaped moulding of alloys titanium. Препринт. Kiev: ИПЛ АН УРСР.- 1982.- 35с.

2. Kuznetsova T.L. Hydrogen embrittlement of casting titanium alloy VT-5C and methods of its removal. // 6th International conference" Hydrogen Materials Sci. And Chemistry of Metal Hydrides", ICHMS'99, Ukraine, 1999, P.213.

3. Kuznetsova T.L. Investigation of peculiarities melting refining and crystallization of cast remake storage from high purity zirconium alloys // International conference "Advance materials", NAS of Ukraine, Kiev, 1999, P.204.

4. Ракицкий А.Н., Кузнецова Т.Л., Якименко И.Л. Исследование физико-химических особенностей выплавки высокочистых хромовых сплавов // Процесы литья.- 2000, N3.-С.16-21.

# RESEARCH OF STRUCTURE AND MECHANICAL PROPERTIES OF CHROMIUM FILM CONDENSATES IN AN INTERVAL AT TEMPERATURES 20-1100° C.

**Pisarenko V.A., Rakitsky A.N., Rogul T.G., Sameluk A.V., Pavlov V.S.**[(1)]
I.N.Frantsevich Institute for Problems of Materials Science NAS of Ukraine, Kiev, Ukraine
[(1)] NSC Kharkov of Physic-Technical Institute NAS of Ukraine, Kharkov, Ukraine

The structure and mechanical properties of an Cr-0,35La-0,2Ta alloy film condensates 0,25mm in thickness, received by a method of vacuum arc dispersion on a copper substrate were investigated at temperature of condensation 650° C. The copper substrate in accuracy corresponded to the sizes of a sample the for mechanical stretching tests, which was etched in a solution of a nitric acid. The received samples were tested as in an initial state, and after the annealing at 900-1300° C in vacuum during the various times' exposure endurance in a wide interval of the temperatures.

In an initial state of delute alloying chromium condensates have the fine crystalline structure. The average a grain size is changed from 0,6 up to 2,7 microns depending on the temperature condensation. High density of prismatic dislocation loops of subtraction is observed inside grains. Its average of grain size is changed from 0,05 up to 0,2 microns at the increasing of the condensation temperature from 200 up to 900° C. The loops are formed by the complete dislocations, have a Burgers vector b = <100> and deposited on {100} planes of crystal BCC a chromium lattice. The maximum quantity of prismatic loops is observed in chromium condensates, received at 300° C and reaches value $5 \cdot 10^{13}$ $cm^{-3}$.

The carried out researches were been established, that in an initial state samples of condensates are fragile and have the low mechanical characteristics at the room temperature (50-60 MPa), due to huge internal presses because of the high density vacancies defects. The destruction thus occurs by intergranular type. The stability of defects is very high. Their absolute annihilation, and also removal of internal stress take at the annealing temperatures 1100° C and above. At these temperatures it are begin the processes caused by collective recrystallization that results to disappearance of columnar structure, increase of the size of a grain and decrease of a limit of fluidity and destroying press at some increasing of plasticity and also decrease of temperature brittleness up to the room temperature and lower. The assumption is stated that the increase of a limit of fluidity in the field of test temperatures 700-800° C is caused probably by ageing vacancies type. That the condensates have rather high purity on impurity of introduction, effect Porteven-la-Shatelie, which display on characteristic of dynamic deformation ageing, was not observed during stretching test at the temperatures, at which was fixed increase of a limit of fluidity and decrease of the plastic characteristics. For the first time it was observed stratification in neck of chromium samples tested at 400° C, that also testifies to high purity of the researched condensates to impurity of introduction. The problems intergranular destruction and stratification in neck of chromium alloys samples at stretching tests are discussed.

Summary.

1. The forming defects by vacancies origin at condensation of chromium alloys are capable to cause huge internal presses, which can raise the brittleness temperature up to 700° C and above, causing destruction along the boundary of columnar structure (intergranular destruction).

2. The annealing at 1000-1300° C result to gradual annihilation of the vacancies defects, removal of internal presse, and at 1150° C and higher to recrystallization processes, that has an salutary effect for mechanical properties and plastic characteristics of condensates.

3. The increase of the mechanical characteristics (at simultaneous decrease of plastic) at the test of temperatures 600-800° C is connected the most probable with usual ageing of vacancies character, instead of with processes accompanying dynamic deformation ageing.

4. The processes of mixed trans- and intercrystalline destruction's, and also stratification in neck of the tested samples testify about the same nature of destruction inherent to metals of У1А group, and at that the anomalies connected to difficulties of display of intercrystalline destruction for chromium alloys, most likely are conditioned by metal purity or character of the intense condition realised during test.

# THERMOELASTIC MARTENSITIC TRANSFORMATION IN Fe-Co-Ni-Ti ALLOYS AND STRUCTURE OF MARTENSITE

**Shevchenko O.M., Kozlova L.E.**[(1)]
Institute of Materials Science Problems named by I.N.Frantsevich NAS of Ukraine, Kiev, Ukraine
(1) Institute of Magnetism NAS of Ukraine, Kiev, Ukraine

Long lasting study of the $\gamma \leftrightarrow \alpha$ transformation in Fe-Ni-Co-Ti alloys has given the opportunity to find the conditions of its reverseability. In aging the austenite of Fe-Ni-Co-Ti alloys the formation of homogeneously distributed coherent with the surrounding matrix spherical particles of $\gamma'$- phase ($Ni_3Ti$) occurs. The particles including in austenite retain coherency with the crystal lattice of martensite, thus leading to its tetragonality. It makes easier the coherent connection of the austenite and martensite lattices and decreases the level of strains between them that determines the proceeding of thermoelastic martensite transformation. By means of the proper selection of the alloys composition (taking advantage of the invar anomaly) and their aging it has been managed to obtain in the above alloys the thermoelastic transformation with hysteresis from 250 to 20K [1-3]. The aim of this research was the investigation of the thermoelastic martensite structure in Fe-Ni-Co-Ti alloys and its mutual connection with the transformation hysteresis.

The alloys 1 – Fe-30,3%Co-20,1%Ni-7,7%Ti; 2 – Fe-37,1%Co-18,5%Ni-8,2%Ti and 3 – Fe-44,4%Co-12,2%Ni-8,0%Ti were melted in an induction furnace in argon atmosphere, hot rolled, homogenized, then water quenched from 1423K and aged in a salt bath at T=923K. The characteristic temperatures of martensitic transformation and its hysteresis were determined by the low field magnetic permeability. The metallographic and X-ray studies of the martensite structure at low temperatures were carried out too. The degree of tetragonality c/a of the crystal lattice of martensite and the volume effect of transformation $\Delta V/V$ were calculated using parameters of the $\gamma$- and $\alpha$- phases lattices defined from the positions of corresponding diffraction lines. The martensite quality was also determined by X-ray method.

When aging time increases, the particles of $\gamma'$- phase grow. Thus, owing to lower content of Ni and Ti in austenite the characteristic temperatures of martensite transformation increase and Curie temperatures decreasing is observed. Also the quality of appeared martensite grows and hysteresis of $\gamma \leftrightarrow \alpha$ transformation becomes smaller. The further growth of $\gamma'$- phase particles leads to the break of coherency with the matrix and the enlarging of hysteresis accordingly. It is clear from the results obtained, some correlation between such characteristic of transformation reverseability as its thermal hysteresis and the structure of the thermoelastic martensite in Fe-Ni-Co-Ti alloys exists, figure 1.

During thermoelastic $\gamma \leftrightarrow \alpha$ transformation the formation of martensite in cooling and its disappearance on followed heating occurs as a result of the reversible moving of martensite crystals borders. It can be noted, that the martensite crystals are thin plated with straight boundaries and forms well-defined relief on the surface of the preliminary polished specimens. The length of martensite plates, as a rule, is comparable with the austenite grain size. The disappearance of thermoelastic martensite plates comes about in reverse order of their formation, that is, the earlier forming plates disappear later.

The morphology features of thin plated martensite evidence of high moveability of the plates borders and that there is no relaxation of the strains which are brought about by the plates growth owing to coherent connection of the austenite and martensite lattices. In an austenite grain the relaxation takes place because of the energy advantageous directions of martensite plates growth and the formation of the parallel plates.

When considering the martensite structure in alloys with different hysteresis of $\gamma \leftrightarrow \alpha$ transformation, it can be noticed, that the smaller hysteresis is, the thinner plates of martensite become, figure 1. Besides, in the alloys with narrow thermal hysteresis the relief height lowers that evidences of the smaller form deformation on the transformation while the volume changes are equal. It was shown, the martensite transformation hysteresis essentially depends on the aging time and is evidently influenced by the volume part of $\gamma'$- phase particles, which retained coherent with austenite.

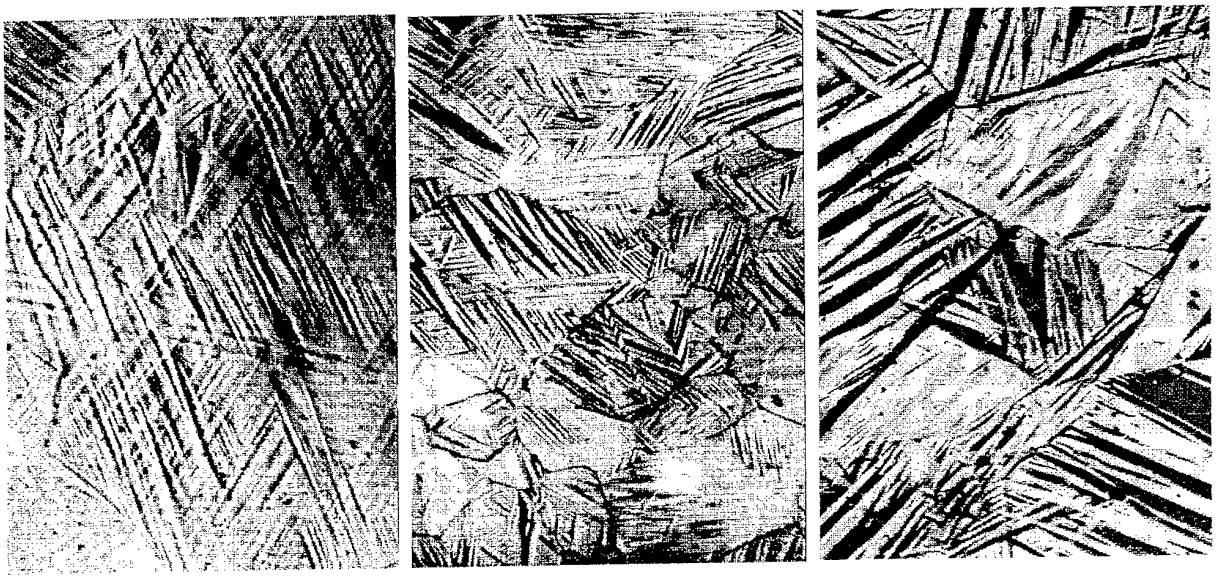

a) b) c)

Figure 1. Martensite in Fe-Ni-Co-Ti alloys with different hysteresis of $\gamma \leftrightarrow \alpha$ transformation (x100):
а) alloy 1, aging time – 13 min, H=85K;
б) alloy 2, aging time – 1 min, H=120K;
в) alloy 3, aging time – 5 min, H=200K.

But there are reasons to suppose the morphology and crystal structure of martensite be determined by the volume part of coherent γ'-phase particles too. Disperse coherent γ'- phase particles become the centers of a shift in martensite and cause large tetragonality of its crystal lattice. The increase of c/a leads to the lower of martensite crystal elastic energy in austenite and, thus, to decreasing coherent strains on the interphase of austenite and martensite, that determines the reverseability of martensite transformation in the alloys investigated. It should be noted, that the correlation exists between the transformation hysteresis and the degree of martensite crystal lattice tetragonality: the maximum of c/a corresponds to the minimum of thermal hysteresis.

As it is known, at early time of aging the volume part and size of γ'- phase particles grows, that resulted in increasing the shift centers in martensite and, as a consequence, in rising c/a. While aging time increased, the values of tetragonality reach maximum and, then, start decreasing. We can suggest the γ'- phase particles when grew to some critical dimension lose their coherency with the matrix, that causes the diminishing of martensite crystal lattice tetragonal distortion.

Thus, the alloy 3 with small content of Ni (that also influences the volume part of $Ni_3Ti$ precipitations) has considerable hysteresis: the minimal feasible one, obtained by aging in this alloy, consists 185K and corresponds to c/a=1,105; the increase of Ni content in the alloy 2 leads to the narrowing of hysteresis – $H_{min}$=100K, c/a=1,13; and, then, the alloy 1, having the largest Ni content, reveals the follow parameters: $H_{imn}$=65K, c/a=1,15.

Thus, increasing the degree of tetragonality c/a of the crystal lattice of martensite resulted in narrowing hysteresis of $\gamma \leftrightarrow \alpha$ transformation in Fe-Ni-Co-Ti alloys. It has been shown that hysteresis of $\gamma \leftrightarrow \alpha$ transformation in the investigated alloys is quite strong controlled by the time of aging. The martensite in these alloys is thin plated with straight borders (that is, with the character configurations of its crystals decreasing the elastic energy) that evidenced of their high moveability. The thickness of plates reduces and martensite relief becomes lower when the transformation hysteresis diminished.

[1] Кокорин В.В., Гунько Л.П., Козлова Л.Е., ДАН СССР **286**, №4 (1986) 883-886.
[2] Kokorin V.V., Shevchenko O.M., Materials Science Forum **79-82** (1991) 545-550.
[3] Kokorin V.V., Gunko L.P., Shevchenko O.M., Scr. Metal. **28** (1993) 35-40.

# PHYSICAL ASPECTS OF ACTIVATED SINTERING OF METAL POWDERS BY HIGH-RATE ELECTRIC CONTACT HEATING

**L.O.Andrushchik, S.P.Oschkaderov**
Institute for Metal Physics G.V.Kurdymov
National Academy of Sciences of Ukraine
Kiyyv, Ukraine

Sintering is one of the most important and continuous operations in powder metallurgy. Intensification of this process, especially by using new technologies, is am important problem of science, technology, and economics.

This paper is devoted to the theoretical and experimental consideration of the influence of defects on the conventional and bulk heating sintering. The vacancy path in a crystal, containing grain boundaries, pores and dislocations is discussed. The diffusional process rates have a maximum at the dislocation density about $10^{11}$ $cm^{-2}$ Influence of the pore surface quality on the diffusional process rates is considered.

The experimental results in the study of the physical processes during electric contact sintering as compared with other methods of sintering indicate. The theoretical concepts of an activating effect of electric current during sintering are real and is accelerated. Healing of the large pores is accelerated and their total number is reduced during the electric contact sintering, unlike during radiation and induction heating, during which a coaqulation and qrowth of the large pores, accompanied with an increase in their total number, takes place. The pores are spheroidized and distributed uniformly over the whole bulk of the sintered material during electric contact sintering. The method of direct electric contact sintering has advantagies in comparison with the others from the point of view of efficiency of the process (the duration of the sintering is reduced, the eguipment is cheaper, power consumption is lower, producton area is smaller).

As has been shown the sintering process of metallic powders can be intensified considerably by using the high-rate electric contact heating technigue of compacted samples and subseguent isothermal holding for not very long time at the sintering temperature. For industrial use of this method the physical processes taking place during electric contact sintering are to be studied comprehensively. One or another structure is formed depending on these processes to determine, in turn, the properties of sintered materials. It should be noted that properties of sintered materials are largely determined by a formation process of interparticle juctions, arrising between sintered powders at high temperatures. Whereas these processes during conventional furnace sintering, which is used widely in powder metallurgy, are more or less studied, in the case of electric contact sintering they are not practically investigated. So the theoretical and experimental invetigations of a possible local increase of temperature near the interparticle contacts during electric contact sintering and an influence of this possible effect on the properties of sintered materials and, in particular, on sintered powder steels were the aims of this work. It is noteworthy that during usual furnace sintering an effect of the local increase of the temperature near the interparticle contacts is not arising. During electric contact sintering a local increase of the temperature near a contact arises due to the condensation of the current lines near the contact resulting in Joule heat increase. As will be shown below an inccrease in electric resistance of the contact due to the present oxides and/or the fine qeometrical structure of the contact is the main cause of the local temperature increase.

Theoretical results on calculating a temperature difference in a particle-contact region and in a bulk of a grain are considered. In the regi-on an electric resistance is often increased due to changes in chemical composition (as a result of oxidation, seqreqation, etc.) as well as fine structu-re of electric contact. As a result at passing an electric current through compressed powder mate-rial the temperature increases in the contact region resulting in a local formation of a liquid phase there at a final stage of high-rate electric heating. The theoretical results on a possibility of the local formation of the liquid phase in the interparticle contact regions are experimentally confirmed on powder steels alloyed with Cr, Mn, Mo and Ni.

Fractographic and metallographic investigations as well as measurements of the changes in the mechanical properties were performed to support conclusion of local melting.

Thus the results of the experimental investigations (properties, structure, quality of the interparticle junctions) confirm the theoretical calculations as to local increase of temperature in the region of the interparticle contacts during electric contact sintering resulting in the formation of the liquid phase in contact sites. This, in turn, results in a formation of more large-sized interparticle junctions having more perfect structure and geometry. As a result of that the ductile pit-shaped interparticle failure occurs during fracture. Therefore the mechanical properties of the samples sintered by the electric contact method are considerably higher than those of ones obtained by the usual furnace sintering.

# SOME ASPECTS OF PLASTICITY OF FINE-GRAINED TITANIUM

**A.V.Kotko, I.S.Malashenko [(1)], V.F.Moiseev, S.V.Ulshin [(2)]**
I.N.Frantsevich Institute of problems of material science NAS of Ukraine, Kyiv, Ukraine
[(1)]Paton Welding institute NAS of Ukraine, Kyiv, Ukraine
[(2)]G.V.Kurdyumov Institute for metal physics NAS of Ukraine, Kyiv, Ukraine

Conventionally Ti and its alloys are used where the high unit strength and good corrosion resistance play a main role. Among the properties interesting to a physical metallurgy and physics of metals, we can select the followings: small number of slide systems, mechanical twinning in addition to already operating slide during plastic deformation, phase transformation and bound with it behavior of deformation structure and others. In case of fine-grained Ti (d<10 μm) peculiarities of strain at low temperatures conditioned by presence of material texture or super-plasticity occur.

The aim of present work was the analysis of peculiarities of structure formation at deriving of titanium condensates and examination of parameters of grain boundaries hardening in commercially pure titanium at room temperature in wide interval of grain size. Different grain sizes were obtained both by deformation with thermal treatment and by evaporation and condensation of titanium in vacuum (physical sedimentation - PS) [1].

As a host material we use Ti-alloy VT1-0 (commercially pure titanium). After rolling and recrystallization thermal treatments samples for tensile tests with different (15...100 μm) grain sizes were prepared. The same alloy was applied in a molten state to consequent pulverization and sedimentation to obtaine by PS method fine-grained titanium condensate (2...3 μm in diameter and 20...30 μm in length at condensing temperature 600...60 °C). The regime of PS was following: temperature in an interval 0,3...0,5 Tm, velocity of condensation of steam of titanium on steel substrate ~14 μm/min. All key parameters of process were expressly selected for titanium.

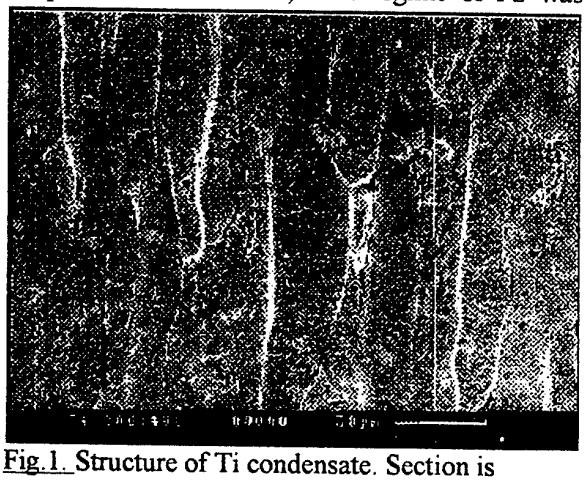

Fig.1. Structure of Ti condensate. Section is perpendicular to sedimentation surface. SEM, x500

For stabilization of a composition and deriving of grains in interval of sizes from 3 up to 50 microns the heat treatment under lower than phase transformation temperature (400...700 °C) were used. The typical structure of condensate obtained by scanning electron microscopy (SEM) is shown on fig.1.

As an initial curve for grain size dependence of Hall - Petch (fig.2) the already known literary data on titanium [2] which were confirmed in present work was utilized. Tensile tests of all specimens were carried out at 20 °C with strain rate $1,5*10^{-3}$ $s^{-1}$. SEM and optical microscopy were used for monitoring of grain size. The texture of samples was studied by X-ray method , and transmission electron microscopy (TEM) to analysis of plastic deformation in fine-grained Ti condensate was used.

The first obtained result was a little bit unexpected. Data of tensile tests of all specimens obtained by PS method appeared in 1,5...2 times above expected grain size dependence (fig.2).

In one of last models [3] (deformation one), the following equation for coefficient of grain size hardening $K_y$ in the Petch-Hall expression was proposed: $K_y = 3\,\tau_c M \Delta m \sqrt{r}$ ,

where $\tau_c$ is critical shear stress, M is Teylor's

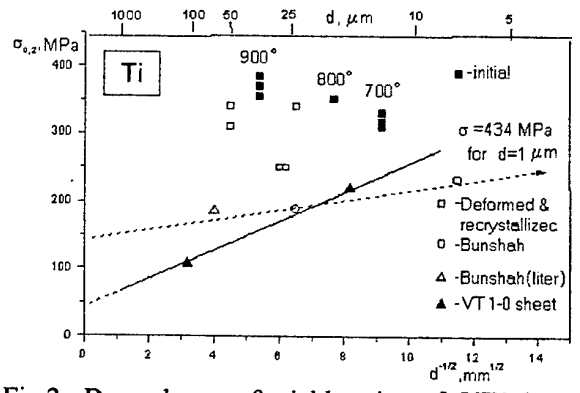


Fig.2. Dependence of yield point of VT1-0 on grain size at different modes of deriving and treatment.

orientation factor, Δm is Shmidt's orientation factor and r is constant with dimensionality of length.

The factor M defines a level of yield stress of material for given polycrystal. Magnitude Δm, on definition [3], reacts only on disorientation of optimum oriented slide systems of two neighbour grains due to necessity of fulfillness during plastic deformation of polycrystal.

The experimental research of textures was carried out on Schulz procedure (on reflecting). Polar figures (fig.3) are obtained with declination up to $70^0$ (a dotted line). For comparison the textures were studied in two cases: (a) in a sheet after strain and recrystallization annealing and (b) in material made by PS method. For first case the polar figure (0002) indicating the strong anisotropy is obtained (fig.3, a), its arises during rolling of given alloy up to big enough level of strain ($\varepsilon >$ 0,5). It is rolling texture of $(0001)[10\bar{1}0]$ type, and rolling direction coincides with axis of sample (or with tension direction ) at consequent tensile tests.

For sample made by PS method, polar figures (0002), $(10\bar{1}0)$ and $(10\bar{1}1)$ were studied. On polar figures (0002) and $(10\bar{1}1)$ we can't saw the presence of any preferential orientations, This fact testifies to random allocation of normal lines of the relevant planes. As against, the polar figure $(10\bar{1}0)$ represents (fig.3, b) an axial grown texture of $(10\bar{1}0)$ type, that uniquely speaks about preferential grown in crystal along direction of normals to planes of a prism $\{1010\}$ [4].

The results obtained in work permit to derive the following conclusions:

1. The grown texture which is formed in sedimented from vapour phase condensate leads to substantial growth (1.5...2 times) of yield stresses of fine-grained titanium and, most likely, due to the influence on the Teylor's orientation factor of given material. However such texture considerably differs from texture of conventional sheet after thermomechanical treatment, and it does not allow to use the obtained results for build-up of dependence of grain size hardening on fine-grain sizes.

2. In titanium, deposited from a vapour phase, numerous micro-pores by a size from 0,05 up to 0,1 microns are observed in grain bodies (but not just on boundaries).

3. Under plastic deformation of fine-grained titanium the formation of dislocation cellular structure that functionally necessary for assimilation of shift and rotary modes of strain is delaying. In this connection there is a supposition was made that in a fine-grained material the role of boundaries of grains and a role of a cellular structure in part may be superimposed, that promoted by a state of a material. This one is close to a state having a super-plasticity behavior.

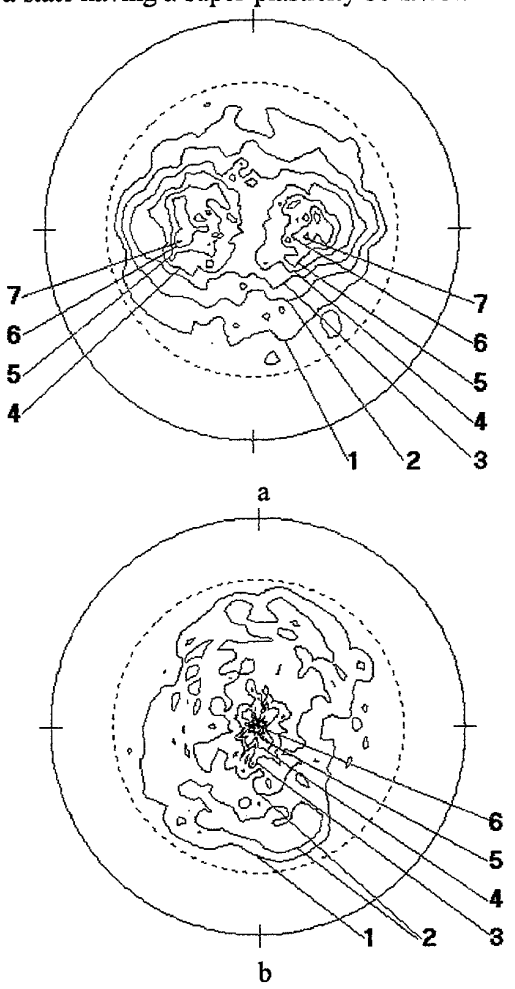


Fig.3. Textures of Ti samples in initial state
a) strain and recrystallization, a polar figure (0002)
b) sedimentation from a vapour phase, a polar figure $(10\bar{1}0)$.

References

1. Movchan B.A., Malashenko I.S. /High-temperature coverages, deposited in vacuum. Kiev: Nauk.Dumka,-1983.-232 p.

2. Strain hardening and fracture of polycrystalline metals/ V.I..Trefilov, V.F.Moiseev, E.P.Pechkovsky et al. Kiev: Nauk.Dumka, 1989, 258 p.

3. Moiseev V.F., Gornaya I.D., Problems of strength, 1989, v.3, p. 50-56. – in Russian.

4. Vasserman G., Greven I. Textures of metal materials. M.: Metallurgy, 1969,564 p.- in Russian.

# INVESTIGATION OF PHASE TRANSFORMATIONS IN THE $Al_3(Ti_{1-x}Zr_x)$ INTERMETALLIC BY IN SITU X-RAY DIFFRACTION METHOD

**Karpets M.V., Milman Y.V., Miracle D.B.[(2)], Barabash O.M. [(1)], Korzhova N.P., Legkaya T.N. [(1)], Voskoboinik I.V., Senkov O.N.[(2)]**

I.N. Frantsevich Institute for Problems of Materials Science of NAS of Ukraine, Kiev, Ukraine
[1]G.V. Kurdyumov Institute of Metal Physics of NAS of Ukraine, Kiev, Ukraine
[2]Air Force Research Laboratory, 2230 Tenth Street, Wright-Patterson AFB, OH 45433

The intermetallics $Al_3Ti$ and $Al_3Zr$ possess many attractive characteristics, such as a relatively low density (3.388 and 4.140 g/cm$^3$, respectively), increased oxidation resistance and high melting temperatures. These properties make these materials to be very attractive for use in high temperature applications.

Both compounds have similar atomic structures (i.e. $D0_{22}$ in $Al_3Ti$, $D0_{23}$ in $Al_3Zr$) with the same tetragonal space group of I4/mmm. Relative structural stability of these phases is determined by (i) mean value of valence electrons per atom, (ii) atomic radius ratios of the components, (iii) existence of internal stresses in specimen [1]. At certain combinations of these factors, the $D0_{22}$ и $D0_{23}$ structures can be present simultaneously or partitioned with other phases. For example, transformation of the tetragonal $D0_{22}$ into a cubic $L1_2$ phase (space group Pm3m) in the $Al_3Ti$ intermetallic alloyed with Cr, Mn, Fe, Co, Ni, Cu, Zn, Ag and Pd was reported [2]. According to [1, 3], the cubic symmetry of the $L1_2$ structure makes it more ductile, as compared to $D0_{22}$. In addition to the above mentioned structures, a polymorphous modification of the $D0_{22}$ structure with the quadruplicate lattice spacing *c* was reported for the $Al_3Ti$ intermetallic [4, 5]. This phase was designated as $Al_{24}Ti_8$ [4]. The temperature range of existence of this phase was 585-638°C in the alloy of the stoichiometric composition, and it extended up to 950°C in the alloys with higher concentration of Ti [5].

In the present work, an in-situ XRD method was used to study phases in the $Al_3(Ti_{1-x}Zr_x)$ alloy system in temperature range of 20-1100$^0$C and the composition range, x, of 0-1. Hardness and plastic properties of these alloys were also determined.

The alloys were produced by arc melting in a purified argon atmosphere. X-ray analysis of specimens, in as cast and grinded in an agate grinder conditions, was conducted using a DRON-UM1 diffractometer with monochromatic Cu $K_\alpha$ radiation . A graphite single crystal was used as monochromator.

High temperature X-ray investigations were performed in helium atmosphere, using a UVD-2000 add-on device. Scanning step was $2\theta=0.05^0$. A DBWS-9411 software was used to conduct full-profile analysis of the diffraction patterns and determine lattice parameters of the phases.

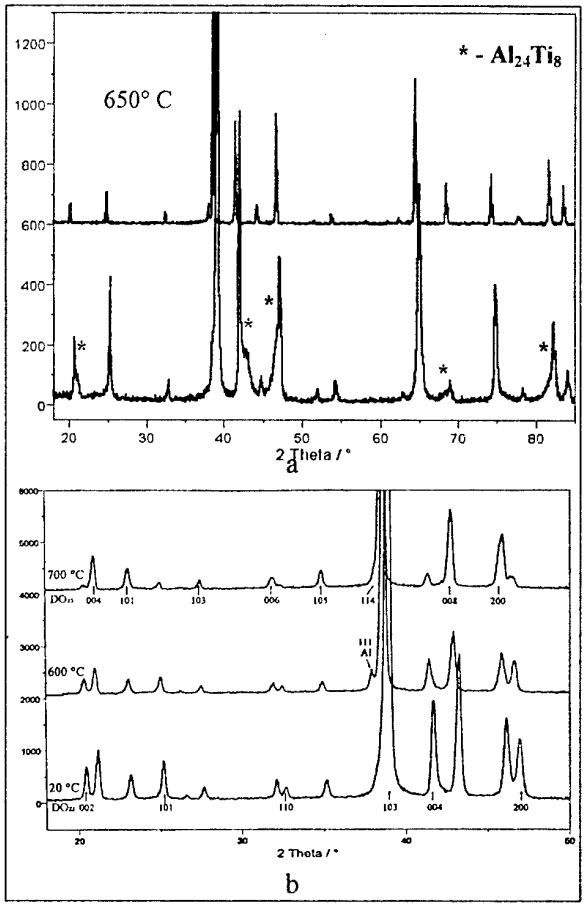


Fig. 1. XRD – Pattern (a) of the sample $Al_3Ti$ at temperatures 20 and 650°C; (b) of the sample $Al_3(Ti_{0.84}Zr_{0.16})$ at temperatures 20, 600 and 700°C.

In addition to main diffraction peaks from the $D0_{22}$ structure and weak peaks from the FCC aluminum lattice, series of additional peaks were registered on the diffraction pattern of the $Al_3Ti$ cast alloy, as it is shown in Figure 1a. The additional lines which do not belong to the $DO_{22}$

and FCC structures, were identified satisfactorily as pertaining to a low temperature polymorphous modification $Al_{24}Ti_8$ [4], with the parameters of the tetragonal lattice $a = 0.3875$ and $c = 3.384$ nm.

The $Al_{24}Ti_8$ phase was detected only at temperatures below 650 °C, and above this temperature the XRD peaks from this phase were not revealed (Fig. 1a). This phase also was not observed after heating the specimen to a temperature above 650°C and following cooling to room temperature. However, the $Al_{24}Ti_8$ phase was detected again after grinding of these annealed specimen. It was therefore suggested that formation of the $Al_{24}Ti_8$ phase is initiated by internal stresses formed in the surface layer during grinding. To prove this suggestion, the grinded material was treated with a hydrochloric acid to remove the deformed surface layer. After this treatment the XRD lines from the $Al_{24}Ti_8$ phase indeed disappeared.

Mechanism of $D0_{22} \rightarrow Al_{24}Ti_8$ phase transformation, is related probably with shear processes. In order to obtain the $Al_{24}Ti_8$ structure from $Al_3Ti$, necessary each second unit cell should be shifted in $Al_3Ti$ on vector $1/2(\mathbf{a}+\mathbf{b})$ in (001) plane. Positional parameters in these structure $Al_{24}Ti_8$ are given in table.

Table

| Compound | Atom | Position | x/a | y/b | z/c |
|---|---|---|---|---|---|
| $Al_{24}Ti_8$ | Al(1) | 4c | 0 | 1/2 | 0 |
| | Al(2) | 4d | 0 | 1/2 | 1/4 |
| | Al(3) | 4e | 0 | 0 | 0.1875 |
| | Al(4) | 4e | 0 | 0 | 0.4375 |
| | Al(5) | 8j | 0 | 1/2 | 0.375 |
| | Ti(1) | 4e | 0 | 0 | 0.0625 |
| | Ti(2) | 4e | 0 | 0 | 0.3125 |

The $D0_{22}$ and $D0_{23}$ structural types are the main structural constituents of $Al_3(Ti_{1-X},Zr_X)$ cast alloys. At 0% Zr, the $Al_3Ti$ compound has the distinct $DO_{22}$ crystal structure. The $D0_{23}$ phase ($Al_3Zr$ type) is detected when some titanium in the $Al_3Ti$ compound is substituted with zirconium atoms. The volume fraction of the $D0_{23}$ phase increases rapidly from 0 to 90% when the atomic fraction of zirconium, X, increases from X = 0 to 0.24. At $X \approx 0.5$ or higher, the $D0_{23}$ is the only phase detected by XRD.

Presence of zirconium in alloys causes also a peculiar passing of the phase transformations at high temperatures. These peculiarities were studied in the present work for alloy ($Al_3Ti_{0.84}Zr_{0.16}$), containing equal quantities of phases with $D0_{22}$ and $D0_{23}$ structures in initial as-cast state, formed at arc melting in conditions of fast cooling.

X-ray "in situ" investigation of this specimen at heating to 1000°C followed by cooling has permitted a consecution of phase transformations of $D0_{22}$ and $D0_{23}$ structures to be determined (Fig. 1b). It was shown that heating to 600°C followed by holding for 1 hour at this temperature causes increasing of $D0_{23}$ phase quantity to 70%, and in temperature range 650-700°C this increasing is up to 95 % (Fig. 1b). At heating to higher temperatures (1050-1100°C) structure transition $D0_{23} \rightarrow D0_{22}$ is registered. Content of these phases becomes at that to be equal approximately to that of the phases in cast alloys, cooled in arc furnace on copper bottom. Following cooling and holding of the alloy at 650°C gives rise to $D0_{22} \rightarrow D0_{23}$ transition again.

Hardness of $Al_3(Ti_{1-x}Zr_x)$ alloys appeared to be significantly lower, than hardness of $Al_3Ti$ and $Al_3Zr$ alloys. At the same time plasticity characteristic $\delta_H$ [3] is lower for $Al_3Ti$ and $Al_3Zr$ that for $Al_3(Ti_{1-x}Zr_x)$ alloys.

## Conclusion

A low temperature phase modification $Al_{24}Ti_8$ was also detected in the surface layer in the temperature range below 650 °C and it was found to be a result of the surface grinding. The phase transformation of a tetragonal structure $D0_{22}$ into another tetragonal phase $D0_{23}$ was observed at the zirconium content of 1 at.% and above. On cooling, this transformation occurred in the temperature range 600-650°C. The inverse $D0_{23} \rightarrow D0_{22}$ transformation was found to occur on heating at temperatures 1100 °C and above. The addition of both Zr in $Al_3Ti$ intermetallic and Ti in $Al_3Zr$ causes hardness decreasing and increasing of the plasticity characteristic.

## References


1. Kumar, K.S. In *Structural Intermetallics*, ed. R. Dragolia et al. Proceedings of the First International Symposium on Structural Intermetallics,The Minerals, Metals and Materials Society, Warrendale, PA (1993) 87.
2. Durlu, N., Inal, O.T., *J. Mat. Sci.*, 27 (1992) 3225.
3. Milman, Yu.V., Miracle, D.B., Chugunova, S.I. et al., *Intermetallics*, 9 (2001) 839.
4. Van Loo, F.J.J. & Rieck, G.D., *Acta Metall.*, 21 (1973) 61.
5. Braun, J. & Ellner, M., *Met. and Mater. Trans.*, 32A (2001)1037.

# PHASE EQUILIBRIA AND SOME PROPERTIES OF PHASES IN TI-CORNERS OF THE TI-ZR-SI AND TI-ZR-SI-AL SYSTEMS

**Marina Bulanova, Ludmila Tretyachenko, Konstantin Meleshevich, Anatoly Samelyuk and Vyacheslav Saltykov**

I.N.Frantsevich Institute for Problems of Materials Science NAN Ukraine, Kiev, Ukraine

Zr is usually added to Ti-alloys to increase their workability and corrosion resistance. Two isothermal sections, at 1200 and at 1050°C were published for the Ti-Zr-Si system. Equilibria at crystallization are unknown. Very scarce information is available on phase relationships in the Ti-Zr-Si-Al system. Thus, the goal of this report is to present results of our examination of Zr influence on the structure and properties of as-cast Ti-Si alloys and of Ti-Si-Al alloys, both as-cast and annealed.

The most prominent feature of the Ti-corner of the Ti-Zr-Si system is appearance of the ternary eutectic L ↔ <β-(Ti,Zr)> (β) + $(Ti,Zr)_5Si_3$ (Z) + $(Ti,Zr)_2Si$ (S2) at the composition ~80Ti-10Zr-10Si The eutectic temperature was determined to be ~1330°C. Three in-coming reactions are the following: L ↔ β + Z; L ↔ β + S2; L + Z ↔ S2. Location of the corners of appropriate three-phase field were established. β+S2 eutectic was found to be finer than β+Z, that might promote higher plasticity of the samples.

Silicon content in the solid solution was found to drastically decrease versus zirconium growth. At Zr concentration about 15 at.% Si content in the solid solution is close to zero.

Wide two-phase fields β + S2 and α + S2 occur in the system, β↔α-transformation temperature decreases when zirconium content increases. At Zr concentration more than 30 at.% the three-phase field α + β + S2 should have the temperature minimum.

Al additions increase this temperature significantly. However, in the quaternary system additional low-temperature equilibria (700-800°C) take place.

In the whole, the character of phase equilibria in the Ti-corner of the quaternary Ti-Zr-Si-Al system is similar to that in the ternary Ti-Zr-Si.

Microhardness of the primary phases and of eutectic mixtures was measured.

# PHASE EQUILIBRIA AND THERMODYNAMICS OF THE PHASES IN THE R-PB BINARY SYSTEMS

**Marina Bulanova, Yuri Buyanov and Vladislav Sidorko**
I.N.Frantsevich Institute for Problems of Materials Science NAN Ukraine, Kiev, Ukraine

Available information on the crystal structures, phase diagrams and thermodynamics of alloys (both solid and liquid) in the R-Pb (R = rare earth metal) binaries is considered. Revealed regularities of physico-chemical interaction in the R-Pb systems are being compared with those previously discussed for the systems R-Si [1], R-Ge [2], R-Sn [3].

At present 9 experimentally constructed phase diagrams are known (Sc, Y, La, Pr, Eu, Gd, Dy, Yb, Lu). Information on thermodynamic properties of solid and liquid R-Pb alloys is scarce, as well. Analysis of the available information on R-Pb systems together with that for R-Si, R-Ge, R-Sn systems [4] allowed us to find out the following peculiarities of R-Pb systems:

1. Mutual solid solubility of the components is no more than 1 % (at.) at subsolidus temperatures.
2. All the systems are characterized by formation of several compounds: 2 for the Sc-Pb, 7 for the Pr-Pb. All these are the line phases, except $Y_5Pb_3$, $Gd_5Pb_3$ and $Dy_5Pb_3$. The last have narrow (no more than ~2 % (at.)) homogeneity regions at near melting temperatures.
3. The following stoicheometries are more typical for R-Pb systems: $R_5Pb_3$ (17 compounds), $R_5Pb_4$ (14), $RPb_3$ (16). In contrast to R-Si [1] and R-Ge [2] intermetallics, the crystal structure of isostoicheometric compounds does not change along the row of rare earths.
4. $R_5Pb_3$ are the most refractory compounds in all the systems. For the systems of heavy rare-earths {Sc,Y,Gd,Dy,Lu} - Pb these are the only congruently melting compounds, as well. In the systems of light rare-earths (La, Pr) $RPb_3$ compounds melt congruently in addition to $R_5Pb_3$.
5. Equilibrium with Pb is degenerative and takes place at 320-329°C.
6. The temperatures of uni-type equilibria gradually change along the lanthanide row and correlate with the melting points of pure rare earths.

It is known that these are congruently melting compounds defining both shape of the phase diagram and concentration dependence of thermodynamic functions. On the basis of this fact and of above regularities we have made the prognosis of 8 unknown R-Pb phase diagrams and of unmeasured values of thermodynamic functions of plumbides formation.

Peculiarities considered are typical for the R systems with normal valency (+3). Bivalent Eu and Yb interact with Pb in a different way, more similar to Ca and Ba. This is reflected in the character of phase diagrams and in the values of thermodynamic functions.

## References

[1] Yu.I.Buyanov, T.Ya.Velikanova, S.P.Luzan et al. Peculiarities of interaction of rare earth metals with silicon. - Kiev, 1997, Preprint FIPM; № 5. (In Russian). – 94 p.

[2] Yu.I.Buyanov, T.Ya.Velikanova, P.S.Martsenyuk et al. Phase equilibria and thermodynamics of the phases formation in the binary systems of rare earth metals with germanium. - Kiev, 1998, Preprint FIPM; № 2. (In Russian). – 98 p.

[3] M.V.Bulanova and V.R.Sidorko. Interaction of rare earth metals with tin. - Kiev, 1994, Preprint FIPM; № 6. (In Russian). – 73 p.

[4] M.Bulanova, V.Sidorko, Yu.Buyanov, K.Meleshevich and T.Velikanova. Influence of metallo-chemical factors on physico-chemical interaction of the components in the systems REM – {Si, Ge, Sn, Pb}. – Abstr. VI Internat. Conf. "Phase Diagrams in Materials Science" – October 14-20, 2001, Kiev, Ukraine. – P.7-8.

# THERMODYNAMIC PROPERTIES OF BISMUTH SELENIDES AND TELLURIDES AND QUASIBINARY SYSTEM $Bi_2Se_3$-$Bi_2Te_3$.

**Mykola Gorbachuk, Vladislav Sidorko, Oleksandr Bolgar, Larisa Goncharuk.**

Institute for Problems of Materials Science, NAS of Ukraine, Kyiv, Ukraine.

Materials based on halcogenides of metals are promising for the needs of optoelectronics and microsensor apparatus. Semiconducting compounds of $A_2B_3$ type where A and B are the elements of group V and VI, respectively are of the same class of materials. These compounds are being used successfully in thermoelectric apparatus during few last decades. Recently, the compounds possessing the structure of chalcopyrite or purite was shown to be used in photoelectric apparatus.

Practically, the more complicated compounds formed from semiconducting binary compounds are more promissing. This fact is due to that the properties of multi-compounds system change in wide ranges and one can obtain the material with needed characteristics by composition changing.

In the present paper the thermodynamic properties of bismuth selenides $Bi_2Se_3$ and bismuth tellurides $Bi_2Te_3$ and their mutual solid solutions have been studied. The Gibbs energies, enthalpies and entropies of formation of the alloys was determined using the measurements of EMF concentration galvanic cells within the temperature range 300-540K. The low temperature heat capacity were measured by using adiabatic method with current heat input in vacuum with the temperatures 60-300K and the standard values of thermodynamic functions nave been calculated.

The enthalpies of individual compounds and their solid solution were measured by mixing method of high temperature differential calorimeter from room temperature up to the melting temperature.

The obtained experimental data for the individual compounds are listed in the tables. They are in agreement with published literature values.

Table 1. Gibbs energy, enthalpy (kJ·mol $at^{-1}$) and entropy (J·mol $at.^{-1}$ $K^{-1}$) of formation of $Bi_2Se_3$ and $Bi_2Te_3$ at 359K.

| Compound | $-\Delta_fG$ | $-\Delta_fH$ | $-\Delta_fS$ |
|---|---|---|---|
| $Bi_2Se_3$ | 28,65 (±142) | 29,0 (±0,8) | 0,93 (±2,09) |
| $Bi_2Te_3$ | 22,28 (±0,18) | 19,9 (±1,9) | 6,6 (±5,3) |

Table 2. Enthalpy ($J·mol^{-1}$), heat capacity, entropy and reduced Gibbs energy ($J·mol^{-1}$ $K^{-1}$) of $Bi_2Se_3$ and $Bi_2Te_3$ at 298,15 K.

| Compo-und | $H^0(T)-H^0(298,15)$ | $Cp^0(T)$ | $S^0(T)$ | $\Phi^0(T)$ |
|---|---|---|---|---|
| $Bi_2Se_3$ | 28278 (±142) | 124,53 (±0,50) | 215,1 (±1,8) | 120,3 (±1,8) |
| $Bi_2Te_3$ | 31048 (±156) | 126,19 (±0,50) | 256,6 (±2,1) | 153,6 (±2,3) |

# THERMOCHEMISTRY OF LIQUID Co-Ce AND Co-Sm alloys.

**Michael Ivanov, Vadim Berezutski and Natalia Usenko.**

Institute for Problems of Materials Science, NAS of Ukraine, Kiev, Ukraine.

The enthalpies of mixing of binary liquid alloys of Co-Ce and Co-Sm alloys were measured by isoperibolic calorimetry. The experimental data show exothermic effects of alloy formation, in agreement with previously measured enthalpies of mixing of cobalt with the lanthanides (Ln). The values of the limiting partial enthalpies in the Co-Ce system are (kJ/mol) at 1850K: $\Delta\overline{H}_{Ce} = -87{,}6 \pm 5{,}8$ and $\Delta\overline{H}^{0}_{Co} = -34{,}0 \pm 2{,}9$. In the Co-Sm system $\overline{H}^{0}_{Co} = -50{,}5 \pm 3{,}9$ at 1400K. The tendency of increasing absolute values of $\Delta\overline{H}$i for Co-Ln melts traversing the row of rare earths metals has been established. Cerium was shown to display non-integer valence in alloys with cobalt (between 3 and 4) due to s-f hybridization near the Fermi level.

The cerium mixed valence model has been used to explain the results of thermochemical measurements in Co-Ce liquid alloys.

The significant negative enthalpies of mixing of lanthanides with cobalt can be explained by a transfer of 5d electrons from the lanthanide to the depleted cobalt d shell.

In the case of Co-Ce systm there is a significant difference beyween the Fermi energies of the compo-nents: about –3,3 eV for Ce and –4,4 eV for Co. Therefore, the alloys of cobalt with lanthanides should be formed with large exothermic effect.

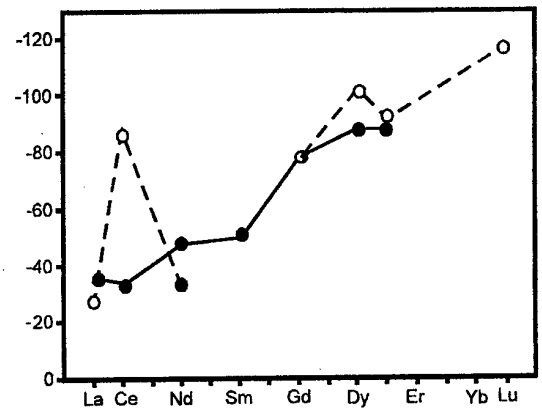


Variation in the $\Delta\overline{H}^{0}_{i}$ data through the lanthanides row for Co-Ln alloys (kJ/mol).

● $-\Delta\overline{H}^{0}_{Co}$ ○ $-\Delta\overline{H}^{0}_{Ln}$

# INFLUENCE OF IRON FAMILY ADDITIONS FOR ADHESIVE CHARACTERISTICS AND FORMATION INTERPHASE BOUNDARIES IN THE SYSTEM CR-CU

**Lesnik N.D., Minakova R.V., Homenko E.V.,**
I.N. Frantsevich Institute for Problems of Materials Science, NASU, Kyiv, Ukraine

New demands on composite materials in the systems Mo(W)-Cu require their characteristics to further improve. Effective method of improving the characteristics of these materials is strengthening of structure components and their boundaries by alloying. The alternative way is to find out new materials on the base of systems with different physical-chemical characteristics, for instance Cr-Cu. Powder composite materials in these systems may be interesting for welding, energetic, electrical engineering applications.

The paper seeks to study adhesive interaction in system Cr-Cu and effect of additions Fe, Co, Ni, and Si (up to 10 %mass.) on spreading of copper over Cr surface adhesive characteristics and formation of interphase boundaries. The choice of alloying elements was limited by both increasing adhesion characteristics in the contact pair refractory component-melting metal and strengthening low melting composite components (at insignificant changing copper electroconductivity). In addition, the composite materials structure with alloying additives made by liquid phase sintering or impregnating Cr porous samples with pure copper or its alloys (Cu + additions), were investigated.

The structure and phase composition of interphase volume (formed in the spreading drop process and when contact pair was cooled) were studied by the up-to-date analytical methods: local X-ray spectral analysis (EMPA) and metallography (scanning electron and optical microscopy).

The experiment included the following stages: the refinement of wetting technique in system in question; the investigation of Cr wetting by Cu and Cu-Cr alloys (up to 6 % mass Cr) and Cu-addition alloys and forming of interphase boundaries in vacuum $(2 - 4) \cdot 10^{-3}$ Pa at the temperature region 1373-1573 K; optimization of the condition for preparation Cr - Cu composites at the liquid phase sintering and investigation of impregnating samples structure.

The wetting of Cr by pure Cu and Cu-Cr alloys was studied by variation of rested drop method, with separated heating of the samples and activation their contact at temperature of experiment. The contact angles were determined by measuring of shadow view of cooled drop.

Good wetting, high value of adhesion work and weak temperature dependence of contact wetting angles (2340-2300 mJ/m2 in the temperature rage 1373-1573 K) characterize the system in question. Complete wetting of Cr by Cu was not observed: the contact angle in all cases had a finite value ($\theta < 90$ degrees) [1].

The component of contact pare volatilizes at a high rate under the experiment condition. The temperature (where vapor pressure reaches $10^{-3}$ Pa) is equal for Cu and Cr 1180 and 1219 K correspondingly. In this connection the contribution of the phase spreading in the process of substance propagation over surface is comparable with contribution of evaporation-condensation. Preliminary saturation of Cu by Cr do not caused of the wetting change, what it is evidence of high-speed solution of substratum substance in melt and spreading of saturating melt.

Composite materials on the base of Cr-Cu (50:50 by mass.) was prepared by mechanical mixing of Cr and Cu powders, pressing and impregnating of porous specimen by Cu. Content of refractory component in the composite corresponded to the development of the biggest capillary forces, that affected particles with liquid phase between them in the disperse system refractory component-low melting metal. Impregnation was carried out at the surplus pressure of technical hydrogen and hydrogen received by decomposition $TiH_2$ in vacuum. In this work the powders of electrolytic chromium and chromium received by reducing of chromium oxide by $CaH_2$ was used. Microstructure of Cr-Cu composite was studied by modern analytical method. It was established, that if specimens were prepared by Cu impregnation in the technical hydrogen large area without wetting of refractory particles surface was observed in the fracture surface. Impurities: S, O, C, N, Ca, Na, Cl were present on the non-wetting surfaces. The area without wetting by the melt metal were absented in the specimens prepared from electrolytic refined Cr-powder, high quality Cu in the vacuum-hydrogen ($TiH_2$) medium.

By spreading and wetting experiments it was established that addition in question are interphase active and they improve adhesive characteristics in Cr-Cu systems, for example, 2600 mJ/ $m^2$ in the system Cr – (Cu+7 %mass. Si.) The concentrate enrichment of interphase boundary volume by alloying elements in contact pair $Cr_s$ - $(Cu+Fe)_l$, $Cr_s$ - $(Cu+Co)_l$, $Cr_s$ - $(Cu+Si)_l$ was detected (Fig 1). The structure and composition of the interphase layers are varied with additions and reflected the character of the phase equilibrium in the corresponded metallic systems.

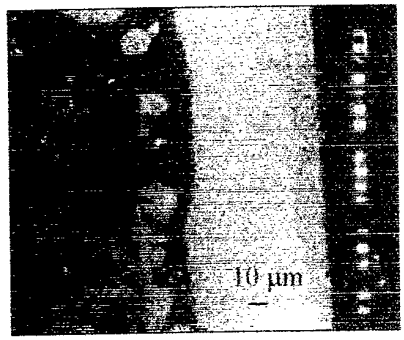


a

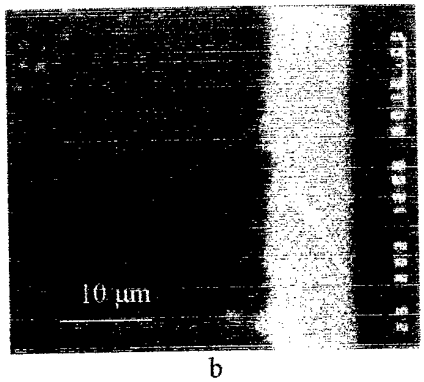


b

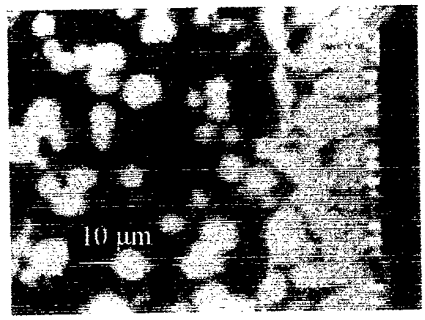


c

Fig.1 The R-x microscopic images of interphase boundaries after wetting experiments (at 1200°C, 2 min), in contact pairs $Cr_s$-$(Cu+Si)_l$, Kα Si (a); $Cr_s$-$(Cu+Fe)_l$, Kα Fe (b); $Cr_s$-$(Cu+Co)_l$, Kα Co (c).

The most extended interpfase layer (intermetallic nature) was found in the contact pair is fixed in contact pair $Cr_s$ - $(Cu+Si)_l$ at 1150°C with around 70 μm. It was possible to observe two layers with different properties (hardness) and chemical composition. The intermetallic layer at the interphase near $Cr_s$ can be formed in solid state by mechanism of reactive diffusion in distinction from layer at the interphase near the low temperature component of the contact pair crystallization. It was noticed that structure of the transition layer in contact pair $Cr_s$ - $(Cu+Fe)_l$ and $Cr_s$ - $(Cu+Si)_l$ are sufficiently similar. But in this case thickness of the layer sixtimes smaller (10-15 μm) then thickness $Cr_s$ - $(Cu+Si)_l$ contact pair layer. A well defined and rish Co layer was formed at the liquid solid interphase in contact pair $Cr_s$ - $(Cu+Co)_l$
(with around of 40 μm). No reactivity is observed at the $Cr_s$ - $(Cu+Ni)_l$ contact pair interphase layer.

It was found out the phenomenon Cr-particle dispergation in the microstructure of the $Cr_s$ - (Cu + additions)$_l$ composition compacted in the presence of liquid phase ( for electrolytic powder) [2].

SUMMARY

The results of investigation of addition effect on adhesive characteristics and interphase boundaries formation in Cr-Cu systems were summarized. Peculiarities of interphase structure formation and microstructure of powder composition compacted in the presence of liquid phase were studied. Cr-particle dispergation in the microstructure of investigated Cr-Cu composition was detected.

REFERENCES

1. Lesnik N.D., Minakova R.V., Kresanova A.P., Homenko E.V. // Reviewed Proceed. of the 2-nd Inter. Conf. "HTC-97", Cracow, Poland. - 1998. P. 227-282.

2. Лесник Н.Д., Минакова Р.В., Хоменко Е.В.. Система хром-медь: адгезионные характеристики, легирование, структура переходной зоны и композиционных материалов // Порошковая металлургия, 2001. - № 7/8 - С.137-147.

# SYNTHESIS OF POROUS MATERIALS, BASED ON SILICON CARBIDE IN ULTRA-DISPERSED REACTIVE SYSTEM

**Antsiferov V.N., Gilev V.G., Sung J.S.**[(1)]
Research center of powder materials science, Perm, Russia
[(1)]Korea Institute of Energy Research, 71-2 Jang-dong, Yoosong, Daejeon, Korea

Silicon carbide is considered for sorption and membrane separation thanks to the inertness to chemicals, stability at high temperature and abrasion durability. Carbon promotes the sorption of organic impurities in fluid as a filter [1, 2].

The microporous silicon carbide is expected to have high temperature stability because of high melting point of SiC, $T_{melt}$=2,540°C. And the SiC sintering temperature is as high as 0,8 $T_{melt}$ [3], while those of the ultra-dispersed powders of TiN and AlN is about 0.45 $T_{melt}$ [4]. The reactive SiC synthesis is promising to obtain microporous materials [5].

The synthesis of porous SiC in reactive system $Si_S + C_S = SiC$ was studied. The influences of specific surface of reactive mixture, pressing and thermal conditions were studied with characteristics of permeability, durability of samples.

The mixtures with surface 40-120 $m^2/g$ were obtained through the grinding in high energy ball mill. As shown in the Fig. 1 dependence of the specific surface of reactive mixtures had sharp maximum.

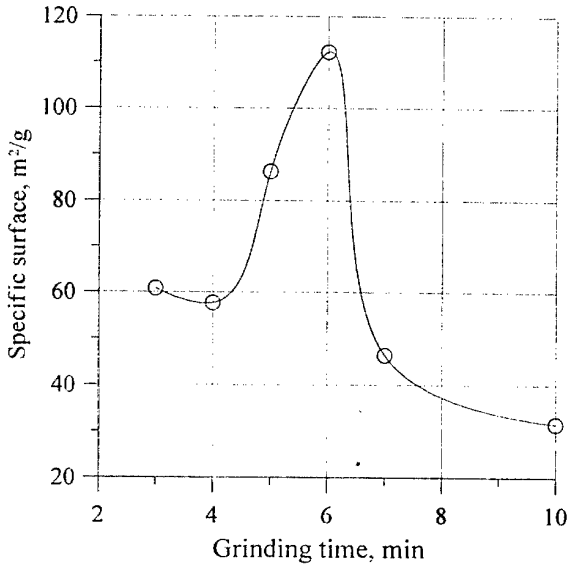


Fig 1. Dependence of the specific surface of reactive mix on grinding time in high energy ball mill

As shown in Table.1 we obtained the samples with porosity of 45-60%, pore size up to 0,3 μm measured by the bubbling method and specific surface of 40 $m^2/g$.

With the increase up to 40 $m^2/g$ of specific surface of sintering mixture the sintering time and temperature and isotherm reaction time were increased comparing to initial mixtures of high $S_{sp}$.

Mechanical strength and shrinkage absence during synthesis needs the frame of more hard melted, graphite-added mixtures and then the quick SiC reaction is realized in high-dispersed mixtures.

Table 1. SiC specific surface synthesized in argon with reaction mixtures and types

| $S_{sp}$ of mix, $m^2/g$ | Pressure of pressing, MP | Sintering T, °C, t, h | Poro-sity, % | $D_{por}$, μm | $S_{sp}$, $m^2/g$ |
|---|---|---|---|---|---|
| 85 | 50 | 1600-1 | 61 | 0,5 | 5,9 |
| 85 | 100 | 1600-1 | 58 | 0,47 | 6,5 |
| 85 | 150 | 1600-1 | 54 | 0,41 | 11,0 |
| 32 | 50 | 1300-2 | 57 | 0,5 | 24,2 |
| 85 | 50 | 1600-0,5 | 57 | 0,36 | 8,2 |
| 32 | 50 | 1600-0,5 | 56 | 1,0 | 2,3 |
| 85 | - | 1600-2 | 58 | 0,56 | 3,6 |
| 61 | 50 | 1150-0,33 | 47 | - | 28,7 |
| 115 | 50 | 1150-0,33 | 54 | - | 37,9 |
| 115 | 50 | 1650-0,17 | 59 | - | 2,6 |
| 46 | 50 | 1650-0,17 | 50 | - | 3,7 |

X-Ray analysis data (fig.2) showed that the change of mixture into high dispersed state ($S_{sp}$ = 115 $m^2/g$) by grinding provide synthesis of SiC during 0.33 hours at 1150°C in argon. If $S_{sp}$ = 61 $m^2/g$ there is essential quantity of non-reacted silicon.

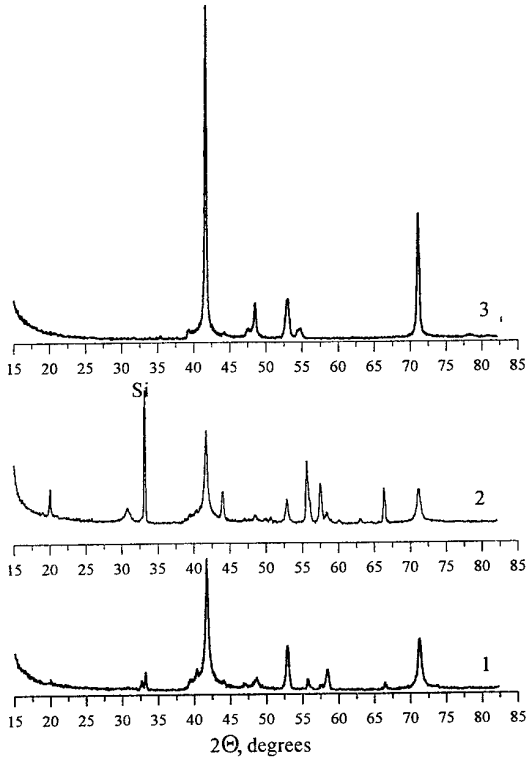


Fig 2. X-Ray diffraction ($\lambda$, $K_\alpha Cu$) of SiC samples, synthesized in argon medium as per modes: 1 - 1650°C – 0.17 h; 2 - 1150°C – 0.33 h; 3 - 1150°C – 0.33 h. $S_{sp}$ of reactive mix, $m^2/g$ 2 - 61, 1, 3 - 115.

Table 2 shows the nitrogen isotherm sorption of samples.

Table.2. Pore structure of SiC by $N_2$ adsorption isotherm

| $S_{sp}$ of mix, $m^2/g$ | 85 | 85 | 32 | 115 | 46 |
|---|---|---|---|---|---|
| Sintering T, °C | 1600 | 1600 | 1600 | 1150 | 1350 |
| Sintering τ, h | 1 | 2 | 0,5 | 0,33 | 0,5 |
| Sintering medium | Ar | Ar | Ar | Ar | $CO_2$ |
| Porosity, % | 61 | - | 57 | 54 | 47 |
| $S_{BET}$, $m^2/g$ | 6,1 | 8,6 | 18,5 | 37,9 | 20,7 |
| $S_{Mi}$, $m^2/g$ | 3,8 | 6,8 | 16,2 | 30,0 | 17,3 |
| $V_{Mi}$, $cm^3/g$ | 0,003 | 0,004 | 0,007 | 0,015 | 0,009 |
| $V_{Me}$, $cm^3/g$ | 0,008 | 0,012 | 0,019 | 0,045 | 0,029 |
| $W_S$, $cm^3/r$ | 0,011 | 0,016 | 0,026 | 0,060 | 0,038 |
| $r_п$, nm | 3,6 | 3,7 | 2,8 | 3,2 | 3,7 |

As the dimension of micropore (radius) is about 2,8-3,7 nm, this may be used as for a filtering of water solutions from the organic molecules such as methylene blue and phenol.

With porosity 50% (at $S_{sp}$ = 30 $m^2/g$; $S_{sp}^v$ = 50 $m^2/cm^3$) the effective pore radius estimated to be 20 nm by formula $r_p = 2P/S_{уд}$,, which is comparable to hydrogen –selective nanoporous membranes.

Therefore, there is possibility of low-temperature synthesis of porous silicon carbide with high specific surface (up to 40 $m^2/g$) with micropores.

REFERENCES

1. Tomilina E.M, Lukin E.S., Kagramanov G.G. Durable porous ceramics based on silicon carbide with low sintering temperature, *Refractory and Ceramics,* 2000. №4. pp.12-14.

2. Mathere J., Mirzhanov A.G., Borovinskaya I.P. and others Ceramic filters for drinking water filtering, *Refractory and Ceramics*, 1999. №1-2. pp.43-47.

3. Andrievski R.A. Nanocrystalline High melting point compound based materials, *Journal of Materials Science*. 1994. V.29. P.614-631.

4. V.V. Dalidovitch, N.V. Fedorov, O.Ed. Babkin, Deriving and properties of sorption-active ceramic materials based on ultra-fine TiN and AlN powders, *Journal Appl. Chem.*, 1994. V.67, №6. P.942-945 (in Russian)

5. Gilev V.G., Silicon carbide membrane materials, Advanced materials and technologies problems, *Perm,* Issue.5, 2000, pp.45-52.

# NEW TRENDS IN SUPERHARD MATERIALS SCIENCE

**Ilyasov V.**
Don State Technical University, Rostov-on-Don, Russia

The problem of creation of superhard materials on a basis cubic boron nitride remains urgent at the moment. The successful search of new materials requires the understanding of the laws of formation of the chemical bonding, determining their high mechanical properties. The analysis of the tendencies of reception both formation of properties of composites and opportunities of designing of superhard materials with of new by properties on the basis of parameters of the electronic structure of a material is carried out. The scientific concept of designing of new materials with and by properties is developed which includes physical principles of modeling of electronic structure of composites of complex structure and structures, theoretical method of account of density of electronic condition of a material, technique of account of energy of chemical bonding, physical and mechanical properties, technique of computer modeling of structure of superhard material. By result of scientific development formation of physical bases of creation new superhard material, determining a new perspectiv direction in structure of metallurgy was. Practical use of the given approach has allowed to define the peculiarities of chemical bonding in composites of difficult structure and to open an electronic nature of mechanical properties in them.

The study of electronic structure of complex substances usually represents a difficult problem, including both experimental, and theoretical researches of electronic structure and physical properties of the given connections. Composites, received usually by the methods powder metallurgy, have high dispersion. The part of metal atoms (and their connections) will form a matrix, but some of them penetrate into grains of a refractory phase. On borders grains, for example c-BN, there are the exotic phases, for example as $AlB_{12}$ or crystals of complex structure. Along with with many factors, determining individual properties of composites on a basis with c-BN is impossible to exclude probability of partial replacement by atoms - components of the positions N or B in the lattice c-BN; i.e. formation on the basis of cubic boron nitride of limited firm solutions, keeping structure of an initial of a matrix c-BN. However, there is no theory clearly explaining mechanisms of interaction at an electronic level of various components as in connections of complex structure, and in composites on a basis boron nitride.

At development of physical principles of modeling of superhard materials were based on the following rules[1]:

1. The change of zoned structure in new materials, in the first approach, is possible to consider as caused imposing of zones, connected to zones an initial component, and density of condition is defined by the contributions of the appropriate zones of components in the same parity, as concentration appropriate a component of a superhard material:

$$N(E) = C_1 \cdot N_1(E) + (1-C_1) \cdot N_2(E),$$

Where $C_1$ - concentration of the first system, making a basic matrix, Ni - complete DOS of i-that system;

2. Establishment of laws of formation of electronic structure and chemical bonding in base refractory materials allows to simulate on their basis new tool materials.

3. In systems as BN-Me there is the high robability of replacement of vacancies boron and nitrogen by atoms of 3d-metal, as the electronic configuration last corresponds to positive ions, covalent the radiuses of which are commensurable with radiuses of atoms boron and nitrogen. Thus, at introduction of transitive 3d-metal in c-BN are kept structure and parameters of an elementary cell c-BN.

4. Increase of density of electronic condition (DOS) at a level Fermi in superhard materials as BN-Me/TiC can specify occurrence in them of metal making chemical bonding and indirectly to characterize increase of resistance of superhard materials.

5. In tool materials with dot and volume defects arises some DOS at a level Fermi, and in solutions of replacement is observed some nonlocalization of electronic condition of top valence band.

In the present work is used model of a «solid state», which is defined following:

- the structure and parameters of a cell c-BN are kept at introduction in him of transitive 3d-metal;
- at replacement of atoms boron and the nitrogen by metals of formation of other phases does not occur.

Using advanced physical bases and accepting the advanced concept of change of structure of system by means of partial replacement the atoms of metal of positions of nitrogen and boron in an elementary cell c-BN develop the block diagram of the basic stages of designing by it of difficult structure.

Results of the complete characteristic of new superfirm materials and the development of bases of designing of superhard materials include a database about electronic structure, communication between peculiarities of electronic condition and parameters of durability of superhard materials. Some fragments of these data are resulted below.

Effects of introduction allow flexibly to adjust physical properties of an initial matrix cubic BN and allows to enter metal making bonding, that can ensure increase of resistance of a material. Is investigated character of influence, carried out s, p - elements on, on electronic structure cubic . afraid in system BN1-xMex (Me = Mg, Al, Si) [2]. Is shown, that in threefold systems BN- (Mg, Al, Si) increase of condition in to a strip is observed. The reduction of chemical communication in them (rather binary c-BN) can be connected to partial breakage of chemical bonding in threefold system. The elastic properties of system BN-(Mg, Al, Si) raise, that will be coordinated with experiment. It correlates with downturn of statistical weight of an electronic $sp^3$-configuration for atoms boron and nitrogen. Number and the intensity of maxima DOS for BN-(Mg, Al, Si) decreases, that can specify increase of statistical weight nonlocalisation electron in system. Is shown, that the character of influence of introduction s, p-elements on electronic structure is largely defined by peculiarities of a power rule of maxima LDOS of an introduced element. Character curve complete DOS of top valence band in considered systems speaks about presence of influence s, p-impurity on width of a forbidden band. In the field of forbidden energy growth DOS takes place, that can result in increase a heat-conducting. The reduction of chemical bonding in comparison with binary c-BN can be connected to partial breakage of chemical bonding in threefold system, caused by reduction by quantity valence electrons, owing to introduction.

In systems BN- (Mg, Al, Si) area forbidden energy narrower than in c-BN and density of filled condition electrons at a level Fermi appear significant, that conducts to essential change of major physical properties. Study of electronic structure cubic boron nitride at it doped by transitive 3d-metals, i.e. material on a basis BN-Me (Me = Ti, Cr, Mn, Fe, Ni, Cu), allows to make the preliminary conclusion about distinction of mechanisms of formation electronic structure of considered systems. In the given systems width valence band grows. Is shown [3], that in systems BN-Me transitive 3d-metals represent itself as positive ions, the covalent radiuses of which are commensurable with radiuses boron and nitrogen.

Being based on physical principles of computer modeling and developed block diagram of the basic development cycles of structure superhard materials on data of account of their electronic structure and established communication between peculiarities of an electronic structure, the structure and properties of substance, and also, using a database about electronic structure of threefold materials, carries out modeling new perspectiv superhard materials: as (BN-Ti) / (TiC - V) and as (BN - Ni) / (TiC - V). The analysis them electronic structure shows, that varying concentration of systems, included in a composite, it is possible to predict occurrence of located electronic condition in a new material. Accounts of physical properties of considered above composites testifies to a real opportunity to supervise physical properties of simulated cutting tool materials.

The spent computer modeling electronic structure of new materials on a basis (BN - Me) / (TiC-Me) opens ample opportunities in a theoretical prediction of physical properties of similar composites and development of his optimum structure for synthesis of new superhard materials with predicted properties. A basic opportunity and expediency of computer modeling of new tool materials, with theoretically predicted physical properties, and development of optimum structure of a powder for synthesis of new materials is shown.

**Reference**

[1] V.V Ilyasov. Physico-Chemical Fundamentals of Formation of Boron Nitride for Tool of Cemented Carbides: Proceeding of Inter. Conf. «Deformation and Fracture in Structural PM Materials», Piestany, Slovac Republic, 1999, 219.

[2] V.V. Ilyasov, I.Ya. Nikiforov: Physics of Metals and new technology, 1997, 19, 69.

[3] V.V. Ilyasov, I.Ya. Nikiforov, Yu.V. Ilyasov: Physics of Solid State, 1997, 39, 1338.

# STRUCTURAL TRANSFORMATIONS IN SURFACE LAYERS OF GRANITES IN DYNAMIC CONTACT ZONE

**Paschenko E., Shilo A., Lazhevska O.**
V.N.Bakul Institute for Superhard Materials of the National Academy of Sciences of Ukraine, Kiev, Ukraine

The granites widely used in facing and building usually are exposed to finishing machining: to fine grinding and polishing. The surface layer formed in an outcome of such machining, also is the basic carrier of their aesthetic and, at a microlevel, physico-mechanical properties. At the same time a few who was set by the purpose to study a structure of this surface layer, as for facing works is usual visual evaluation of quality of a surface. Except for superficial properties, the structure of a treated stratum can much tell about processes happening in contact zone at grinding and polishing of granites, that represents practical interest for development of new finishing tools. These processes are substantially investigated for machining a glass and metals, and practically are not investigated for a stone.

The granites of various deposits on 85-95 % by volume consist of three basic groups of minerals: quartzes, calcium feldspars (such as anorthite) and alkaline feldspars (for example, microcline). The content of a microcline and its nearest analogs for all deposits is rather considerable and vary from 20 up to 60 % by volume. In whole by the phase structure the granites represent completely crystalline rocks, in which amorphous phase are absent in full.

The method of X-ray phase analysis was used for the research of structural modifications in surface layer of granites of various deposits caused by their contact interaction with abrasive composites at polymeric binding during finishing machining. For all investigated samples the appearance of intensive amorphysation of a microcline and its analogs is fixed. Since defined critical magnitude of contact pressure, various for different structures of polymer-abrasive composites, on the rentgenograms vanishing of lines of alkaline feldspars (fig.1) is observed. Thus, according to datum of X-ray spectral microanalysis, the chemical composition of surface layer of granites during finishing machining does not vary.

Hence, as a result of shift strains in contact zone, explicatings on a phone of physico-chemical interaction with components of polymer-abrasive composites, in a surface layers of granites are formed new, amorphous phases. The IR-spectra of these phases in surface layers of a treated granite differ from spectra of crystalline alkaline feldspars by smaller intensity of bands of an absorption, that confirms the supposition about their amorphous structure.

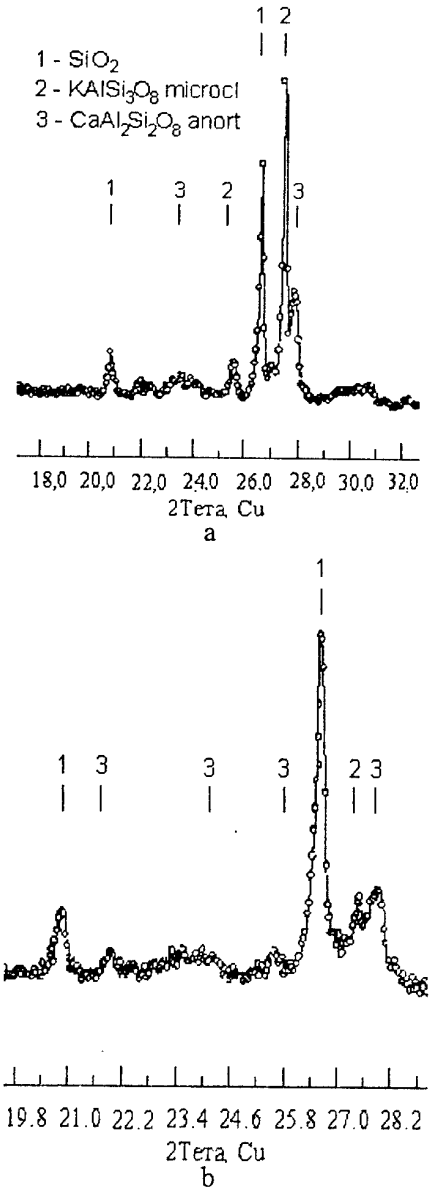


*Fig. 1 Rentgenograme of granite of Kapustynske deposit (a) and its surface layer, obtained after finishing machining (b)*

They practically are similar to IR-spectra of an absorption of glasses of the appropriate structure. Nevertheless, the found out new phases differ on a structure from glasses having the relevant composition. The essential difference of their luminescent spectra confirms it. Besides the features of small-angle X-ray dispersion for detected amorphous phases allow to assume presence in their structure of a great many of vacuities by the size about tens nanometres, absolutely not characteristic for customary glasses.

Thus, the new amorphous phases incipient in surface layers of granites during a finish machining are detected. On composition they are similar to initial crystalline minerals - feldspars, but on structure essentially differ both from them, and from glasses obtained by fusion of the relevant oxides.

The major interest represents the mechanism of an appearance, detected by us, amorphysation of surface layers of a natural stone during dynamic contact with abrasive composites. At present time we spend intensive researches in this field. Nevertheless, already now it is possible to state, that the formation of amorphous layers of silicate and silica-alumina minerals during their finishing grinding is stipulated by intensive plastic deforming of their structure as a result of contact interaction with polymeric composites. The spectrums of relaxation times describing molecular mobility in surface layers of used polymeric composites, on the one hand, and in surface layers of explored granites, to another were compared. Thus was clarified, that an obligatory requirement of intensive distorting action of a polymeric composite on a surface of granite is the presence at its structure of some share of kinetic devices possessing smaller molecular mobility, than silicon-oxygen tetrahedrons of surface layers of silica-alumina rock.

The obtained results allow to state, that the registration of a relation of their hardnesses in traditional understanding of this property is unsufficient for exposition of contact interaction of materials of a different physicochemical nature. For exposition of contact interactions it would be interesting to enter and to justify concept of dynamic hardness or relative dynamic hardness of materials, founded on the registration of molecular mobility of kinetic unites of their surface layers.

Under our judgement, the account of spectra of times of a relaxation of a contact pair of materials opens prospect of more deep understanding of the mechanism of plastic deforming of a treated surface in process of polishing and, accordingly, creates a possibility of a significant raise of effectiveness of finishing machining of a natural stone.

# CALCULATION OF INTERNAL STRESSES IN THE COATINGS COHERENT WITH A SUBSTRATE

**Kosenko N.S.[(1)], Ustinov A.I.[(1,2)], Kosenko, P.N.[(3)]**
[(1)]G.V.Kurdumov Institute for Metal Physics, Kyiv, Ukraine
[(2)]International Center of Electron Beam Technologies of E.O.Paton Electric Welding Institute, Kyiv, Ukraine
[(3)]National Technical University of Ukraine "KPI" , Kyiv, Ukraine

The life time and performance attributes of functional coatings are largely determined not only by their composition, structure, adhesion and cohesion strength, but also by internal stresses. In addition, information on the magnitude and nature of the latter is important both in terms of forecasting the coating properties and for optimising the conditions of their formation.

The main reason for development of internal stresses is mismatch of the crystal lattices of the phases of substrate and coating in the plane of their coherent conjugation. Energy of the strsses is also depending on the coating shape and volume [1,2]. Therefore, the problem of elasticity of internal stresses of the substrate-coating system is rather complex. If, however, the interface is regarded to be plane, and the interface length is much greater, than the coating thickness, the problem is significantly simplified as it becomes one-dimensional. The problem becomes solvable if we further neglect the difference in the moduli of elasticity of the substrate and the coating. It results from that the stresses will only depend on the interface orientation, as well as on the so-called self-strain $\varepsilon^0_{ik}$ This strain is determined both by the difference of the crystal lattice parameters of the undistorted phases of the substrate and the coating, and by the ratio of the crystallographic orientations of the planes, conjugated over the interface.

In this study, proceeding from the conditions of [3]: (i) mechanical equilibrium on a plane interface, (ii) resultant force of internal stresses in the coating and the substrate being equal to zero, as well as (iii) equality of their moduli of elasticity $\lambda_{iklm}$, the internal stresses tensor in an anisotropic single-crystal coating, coherent with the substrate, has been derived in the form:

$$\sigma^c_{ik} = L_{ikmn}(\mathbf{n})\varepsilon^0_{mn}, \qquad (1)$$

where

$$L_{ikmn}(\mathbf{n}) = \lambda_{ikmn} - \lambda_{ikl\rho}n_l\left(n_\alpha\lambda_{\alpha\rho l\beta}n_\beta\right)^{-1}n_r\lambda_{lrmn} \qquad (2)$$

is a certain effective tensor of the moduli of elasticity, dependent on the orientation of the interface **n**. Expression (1) is valid for the case, when the coating thickness is much smaller, that that of the substrate, and it can be used to calculate the stressed states of the coating for any orientation of the interface, as well as any crystal lattices of the substrate and coating.

Calculation of the normal ($i = k$) and tangential ($i \neq k$) components of the tensor (1) was made for the case of an elastically isotropic medium. As an example, the cubic phase with lattice parameter $a_0$ for the substrate and the tetragonal phase with lattice parameters $a$ and $c$ for the coating was considered. In the case of coincidence of the principal axes of self-strain with the axes of the substrate cubic lattice, tensor $\varepsilon^0_{ik}$ had the following form:

$$\varepsilon^0_{ik} = \begin{bmatrix} \varepsilon & 0 & 0 \\ 0 & \varepsilon & 0 \\ 0 & 0 & -\varepsilon_3 \end{bmatrix}, \qquad (3)$$

where $\varepsilon = (a - a_0)/a_0$, $\varepsilon_3 = (c - a_0)/a_0$. For this case dependencies of the components of tensor (1) on the degree of tetragonality of self-strain $\tau = -\varepsilon_3/\varepsilon$ were derived for the main crystallographic orientations of the interface. Their analysis showed that in a single-crystal coating a uniaxial stressed state is achievable for orientations **n**=[100] and [010] (Fig.1a) at $\tau = \nu$ , and for orientations **n**=[101] and [011] (Fig.1b) at $\tau = 1 + 2\nu$. (Here, $\nu$ is the Poisson's ratio taken to be 0.3 in calculations). This state is the tensile stress (at $\varepsilon > 0$ ) of magnitude $2G(1 + \nu)\varepsilon$ that is equal to 4.6 GPa in the case of values of shear modulus $G = 30$ GPa and $\varepsilon = 0.05$, typical for metals. All the orientations, corresponding to this state, at the indicated above values of $\tau$ are equilibrium ones,

as the minimal elastic energy $E = G(1 + \nu)\varepsilon^2$ corresponds to these orientations.

With greater thickness of the coating, the elastic energy of internal stresses increases, and this may lead to formation of a domain structure, as this is a powerful mechanism for relaxation of the elastic stresses field [2]. Domains may be the twins, regions of different concentration of the alloying element (decomposition products) or various polymorphous modifications of the crystal phase of the coating. Coating fragmentation into domains with different self-strain may lead to lowering of internal stresses not only due to the change of orientation of the interface **n**, but also due to the change of the ratio of volume fractions of domains $\alpha$. Parameter $\alpha$ can vary from 0 to 1; single-crystal states with different self-strains correspond to extreme values of $\alpha$.

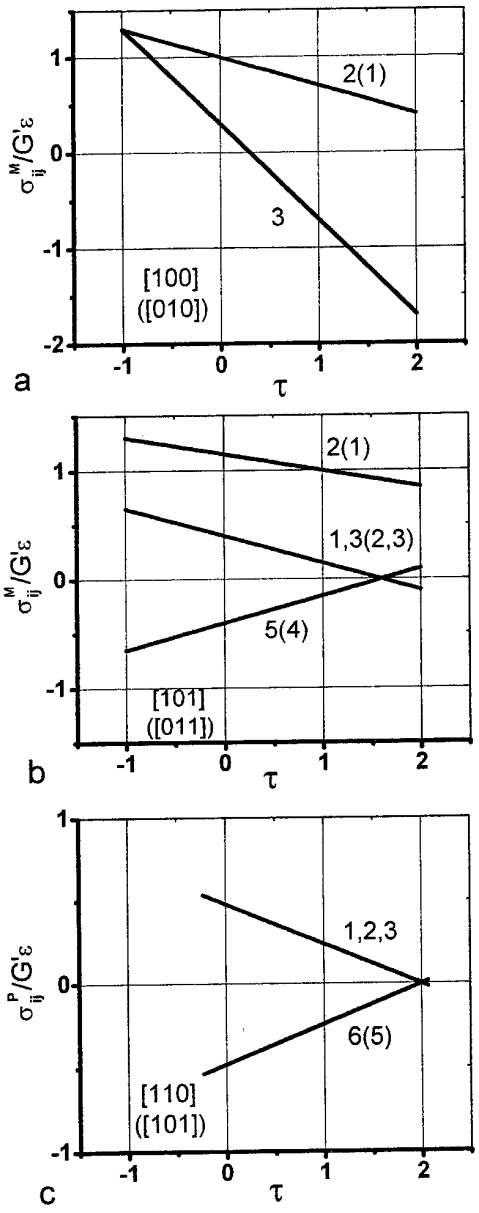


Fig. 1. Dependencies of normal $\sigma_{11}$ (1), $\sigma_{22}$ (2), $\sigma_{33}$ (3) and tangential $\sigma_{23}$ (4), $\sigma_{13}$ (5), $\sigma_{12}$ (6) components of the internal stresses tensor (normalized by $G'\varepsilon$, where $G' = 2G/(1 - \nu)$) for a single-crystal (a, b) and polydomain (c ) coatings on the degree of tetragonality of self-strain for different orientations of the interface.

For polydomain state the self-strain should be regarded as the average strain. For instance, for a coating, consisting of two domains with tetragonal self-strains $\varepsilon_{ik}^{01}$ and $\varepsilon_{ik}^{02}$, it will be equal to:

$$\overline{\varepsilon_{ik}^{12}(\alpha)} = (1-\alpha)\varepsilon_{ik}^{01} + \alpha\varepsilon_{ik}^{02}. \qquad (4)$$

Substitution of (4) into (1) yielded the components of the tensor of internal stresses $\sigma_{ij}^{p}$ for a polydomain coating. Analysis of their dependencies on $\tau$ showed that the coating fragmentation into domains may lead to a complete disappearance of the macroscopic stresses field for orientations **n**=[110] and [101] (Fig. 1c) at $\tau = 2$, as well as for **n**=[100] at $\tau = 1$. The cause for disappearance of internal stresses is not the avearsge self-strain tending to zero, but the fact, thet it is a strain with invariant plane at the above $\tau$ values. The interface is, at that, an invariant plane. Growth of such coatings is equilibrium.

In conclusion it should stated that the results, obtained in this study can be also used for analysis of the stressed state of platelike precipitations of phases and martensite crystals, in which the orientation of the habit plane and domain composition deviate from the equilibrium values, for instance, at martensite phase growth in the external stress field [4].

## REFERENCES

1. Roitburd, A. L. and Kosenko, N. S., *Phys. Stat. Sol. (a).*,1976, **35**, 735.
2. Roitburd, A. L., *Phys. Stat. Sol. (a)* , 976, **37** ,329.
3. Orlov, S.S., Indenbom, V.L., *Kristallography* 1969, **14**, 780.
4. Kosenko, N.S., Roitburd, A.L., Khandros, L.G., *FMM* ,1977, **44**, 956.

# THERMOMAGNETIC ANALYSIS OF TRANSFORMATIONS DURING THE HEATING OF AMORPHOUS FOILS OF THE ALLOY $Fe_{80}Si_6B_{14}$

**Gryhoryeva O.V.**
National Technical University of Ukraine "Kyiv Polytechnic Institute", Kyiv, Ukraine

The research of phase transformations during the heating of amorphous alloys is one of the most actual problems of the today's physics of the solid state. This problem is actual as from the point of view of physical representation and also in the plane of possible practical applications.

We investigated the changes of magnetization during the heating of amorphous alloys $Fe_{80}Si_6B_{14}$, expecting to receive information about formation of phases in process of crystallization of this alloy, and also about it magnetic properties. However deriving of reliable results in this area is connected to significant difficulties because of very small of registered magnetic effects. We have made an attempt to study these effects during phase transformation in amorphous alloys using the differential analysis. This method was found to be effective in studying the small magnetic effects of phase transformations in bulk alloys of iron [1].

The method of the differential thermomagnetic analysis with use of two etalon of armko-iron was applied. The method of so-called internal etalon was applied also, in which a graduation of registered changes of magnetization was carried out using the well-known magnetic effect in the Curie point of carbide of iron θ-Fe3C [2]. The X-ray researches were carried out using standard diffractometry (Fe-anode).

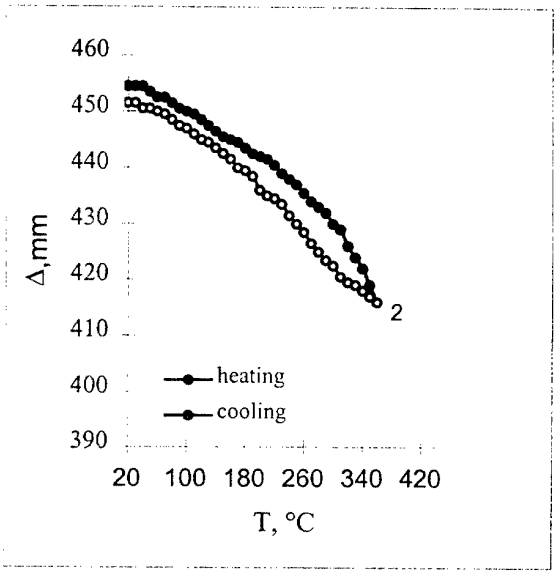


Fig. 1. The reversible part of the thermomagnetic curve of $Fe_{80}Si_6B_{14}$.

The thermomagnetic curve of cyclic heating of the alloy $Fe_{80}Si_6B_{14}$ is shown in fig. 1 and fig. 2. In the initial state the alloy was in amorphous state. The method of getting the data of magnetic parameters of amorphous foils is described by us in [3].

The state 1-2-3 on fig. 1 corresponds to the alloy that has the amorphous structure. The changes of magnetization are reversible (the part 1–2 on fig. 2) if the temperature of heating is no more than 470°C. This leads to conclusion that Curie temperature of the amorphous alloy is close to 410–420°C.

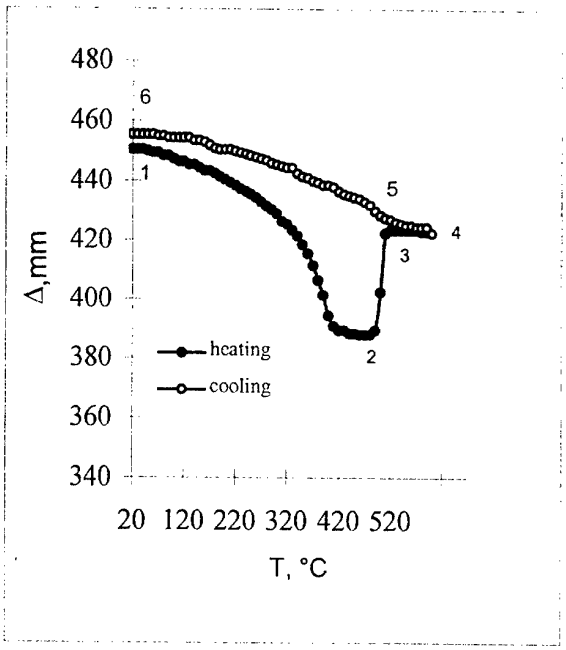


Fig. 2. The full curve of the heating and cooling of $Fe_{80}Si_6B_{14}$.

Beginning from the temperature of 480°C the sharp irreversible increasing of the magnetization of the alloy is registered (the part 2–3) of the thermomagnetic curve, fig. 2. The heating to 600°C and the consequent cooling up to room temperature has shown, that the irreversible increase of a magnetization registered in an interval of the temperatures 480–500°C, is not exhibited at the temperatures close to room temperature. The difference of the evidence of the

magnetometer in the states 1 and 6 is within the limits of a measurement error.

The well-known relations of the thermodynamical theory of the temperature dependence of the spontaneous magnetization of a ferromagnetic near Curie point permit to estimate approximately the value of Curie temperature of amorphous alloy $Fe_{80}Si_6B_{14}$. In this case we to use the corresponding thermodynamic coefficient. This value is unknown for the amorphous alloy. We calculated the principal thermodynamic coefficient for pure ferromagnetic Fe, Ni, Co and for phases θ-$Fe_3C$, $Fe_4N$, $Fe_3B$, FeB, $Fe_2B$. The middle value this coefficient was used for estimating Curie temperature of amorphous alloy $Fe_{80}Si_6B_{14}$. The value we got (405°C) is according to data published very reasonable [4].

The increase of the magnetization of the alloy in the temperature interval 480–500°C is the result of the crystallization of amorphous alloy $Fe_{80}Si_6B_{14}$.

The X-ray analysis carried out by us showed that after the heating to 500°C the alloy contains α-Fe (strong interferentional lines) and borides FeB and $Fe_2B$ (fig. 3).

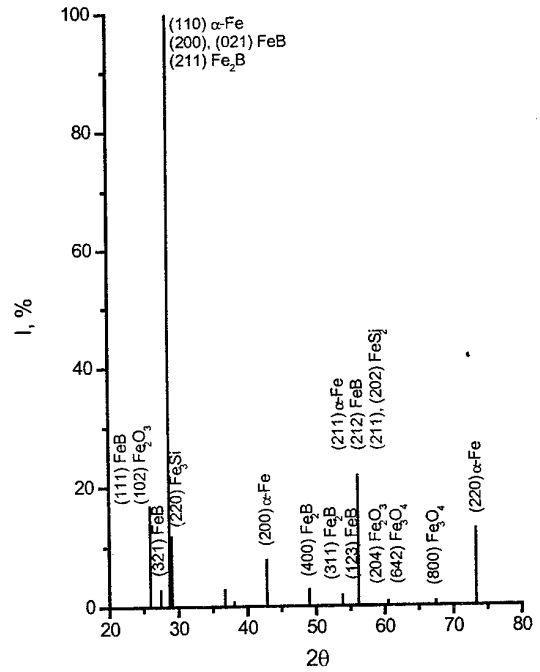


Fig. 3. The diffraction X-ray patterns $Fe_{80}Si_6B_{14}$.

To establish the nature of experimentally registered irreversible changes of magnetization consider the magnetic moments of the specimen in the states 2 and 5 (fig. 2).

$$(I_0V_0)_2 = \sigma^{(480°C)}_{Fe_{80}Si_6B_{14}} M_{Fe_{80}Si_6B_{14}} \quad (1)$$

In (1) $\sigma^{(480°C)}_{Fe_{80}Si_6B_{14}}$ is the specific magnetization of the amorphous alloy, $M_{Fe_{80}Si_6B_{14}}$ is the mass of this phase.

In the same way:

$$\Delta(I_0V_0)_5 = \sigma^{(480°C)}_{\alpha} M_{\alpha} + \sigma_{Fe-B} M_{Fe-B} \quad (2)$$

In (2) $\sigma^{(480°C)}_{\alpha}$ is the specific magnetization of $Fe_\alpha$ at the temperature 480°C, $M_\alpha$ is the mass of $Fe_\alpha$ in the state 5. The value $\sigma_{Fe-B}$ and $M_{Fe-B}$ have the same sense for the boride phases.

Forming the difference $\Delta(I_0V_0)_5 - \Delta(I_0V_0)_2$ it's possible to receive the expression that describes the magnetic effect of the crystallization of the amorphous alloy:

$$\frac{\Delta_{25}}{\Delta_{\theta-Fe_3C}} = \frac{\sigma^{(480°C)}_{\alpha} M_{\alpha} + \sigma_{Fe-B} M_{Fe-B}}{15C \cdot 10^{-2} M^e_0 \sigma_\theta} \quad (3)$$

In (3) $C$ is the carbon content in Fe-C alloy that is used as the etalon in the differential method of thermomagnetic analysis, $M^e_0$ is it's mass, $\sigma_\theta$ is it's specific magnetization.

The calculations carried out by using (3) showed that the specific magnetization of Fe-B phase in the amorphous alloy $Fe_{80}Si_6B_{14}$ is about 208 units (in CGSE) and the Curie point is near to 410°C.

The method of analysis of magnetic properties that is described above could be used in the investigation of thin diffusional layers,coatings of different nature, zones are obtained by laser treatment, thick films etc.

**References**

[1] Belous M.V., Shatalova L.A., Sheiko Yu.P., "The states of carbon in annealed and coldforming steel. First transformation during anneal", Physyka metallov metallovedenie, Vol. 78 (2), (1994) p. 99-106.

[2] Belous M.V., Hryhoryeva O.V., Lakhnik A.M., Moskalenko Yu.N., Novogilov V.B., Sidorenko S.I., "The phase formation during the heating of the steel containing the great quantities of the retained austenite", Met. Phys. Adv. Tech., Vol. 23(10), (2001) p. 1393-1401.

[3] Belous M.V., Hryhoryeva O.V., Lakhnik A.M., Moskalenko Yu.N., Sidorenko S.I., "Thermomagnetic analysis of amorphous alloys Fe-B", Met. Phys. Adv. Tech., Vol. 23(12), (2001) p.1639-1650.

[4] Vonsovsky S.V., "Magnetism", Science, Moscow (1971) p. 1032.

# EFFECT OF POWDER PARTICLES' SIZE DISPERSION ON SYNTERING KYNETICS AND STRUCTURAL GENESIS OF A SINTERED POWDER BODY

**Nurkanov E.Y., Kadushnikov R.M., Alievsky V.M.**
Ural State Technical University, Ekaterinburg, Russia

Dispersion characteristics of powders are the key link of structure-geometric sintering predefiniteness. They do define the inclination of the sintered powder systems towards zonal segregation or coherent sintering, high or low speed of densification. It seems important to evaluate the effect of particles' sizes dispersion on powder system sintering quality using numeric methods. For computational experiments it is offered to use the three-dimensional structural-imitating model (TSI) model of sintering a powder body [1]. Physico-mathematical interpretation of TSI model looks like a system of Newton's motion equations for spherical particles:

$$\begin{cases} \dot{\mathbf{r}}_i = \mathbf{v}_i - \alpha \sum_{j \to i} \left( \mathbf{v}_{ij} - f(|\mathbf{r}_{ij}|)\mathbf{r}_{ij} \right) g(|\mathbf{r}_{ij}|) \\ \dot{\mathbf{v}}_i = \dfrac{\mathbf{F}_i}{m_i} - 3\dfrac{\mathbf{v}_i |\dot{\mathbf{r}}_i|}{R_i |S_i|} \cdot \Xi_i - \alpha \sum_{j \to i} \left( \mathbf{v}_{ij} - f(|\mathbf{r}_{ij}|)\mathbf{r}_{ij} \right) \\ \dot{R}_i = \dfrac{|\dot{\mathbf{r}}_i| \cdot \Xi_i}{|S_i|} \end{cases}$$

here

$$m_i = \frac{4}{3}\pi R_i^3 \rho, \quad \mathbf{r}_{ij} = \mathbf{r}_i - \mathbf{r}_j, \quad \mathbf{v}_{ij} = \mathbf{v}_i - \mathbf{v}_j,$$

$$g(x) = f(x) + xf'(x),$$

$$\Xi_i = \iint_{\Psi_i} \frac{\dot{\mathbf{r}}_i}{|\dot{\mathbf{r}}_i|} \mathbf{n} ds, \quad |S_i| = \iint_{\Phi_i} ds = \frac{\partial V}{\partial R_i}$$

where $\mathbf{r}_i$ – coordinates of the particles' centers, $\mathbf{v}_i$ – velocities of particles' movement, $\mathbf{r}_{ij}$ – distance between the centers of incident particles, $\mathbf{v}_{ij}$ – velocities of incident particles approach (withdrawal) to (from) each other, $R_i$ – particles' radii, $\rho$ - theoretical density of a material, $\alpha$ - weight multiplier, responsible for the effect of sintering on the movement of particles system, $\Xi_i$ – area of projection of the $i$-th particle occupied surface $\Psi_i$ on a plane, normal to $\dot{\mathbf{r}}_i$ ($\mathbf{n}$ – unary vector normal to the surface), $S_i$ – free surface area of the $i$-th particle, $f(|r_{ij}|)$ – function, responsible for mass transfer mechanism during the pair interaction of the particles.

The sintering quality evaluation was performed for powder systems with various dispersion characteristics using TSI model. Three types of spherical particles dense packages were selected as model powder systems: monodisperse $N(R=1,0;\sigma=0,0) = 10^4$, with normal distribution of particles according to size $N(1,0;0,2) = 10^4$, and with lognormal distribution of particles according to size $N(1,0; \ln\sigma=0,3) = 10^4$, where N is the number of particles, R – average radius of the particles, $\sigma$ – standard deviation. Diffusion-viscous flow mechanism was selected as a sintering mechanism, respectively $f(|r_{ij}|)=(1/|r_{ij}|)3\gamma/4\eta$. Values of viscosity $\eta$ and surface tension $\gamma$ coefficients were assumed equal.

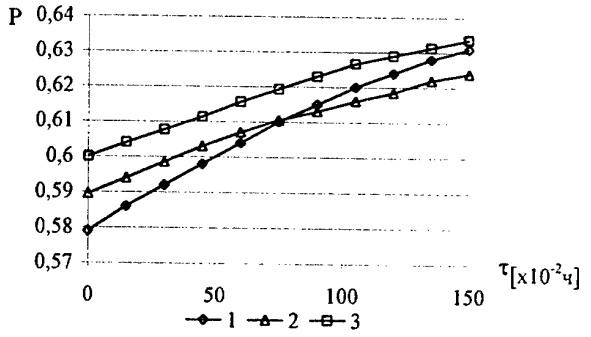


Fig. 1. Time dependency of relative density P of spherical particles model consolidating systems; (1) $N(1,0;0,0) = 10^4$, (2)$N(1,0;0,2) = 10^4$, (3) $N(1,0; \ln\sigma=0,3) = 10^4$; sintering time in computational experiment $\tau=100[x10^{-2}ч]$ is adequate to 1 hour duration of natural sintering

It is possible to judge about sintering quality using two main factors: densification speed and density characteristics of a sintered compact. Computational experiment did demonstrate that the package of monodisperse particles $N(1,0;0,0) = 10^4$ possesses the largest densification speed. Less values of densification speed are possessed by packages with normal $N(1,0;0,2) = 10^4$ and lognormal $N(1,0; \ln\sigma=0,3) = 10^4$ particles distribution according to size. Thus, kinetic curves (see

Fig. 1.) do indicate the fact that particles' size dispersion lowers densification speed.

Geometrical density and porosity factors are called density characteristics. Lognormal particles distribution by size $N(1,0; \ln\sigma=0,3) = 10^4$ did provide the largest value of geometrical density for sintering time equal to $\tau=150$ [$x10^{-2}$hrs] among three examined powder systems morphology types.

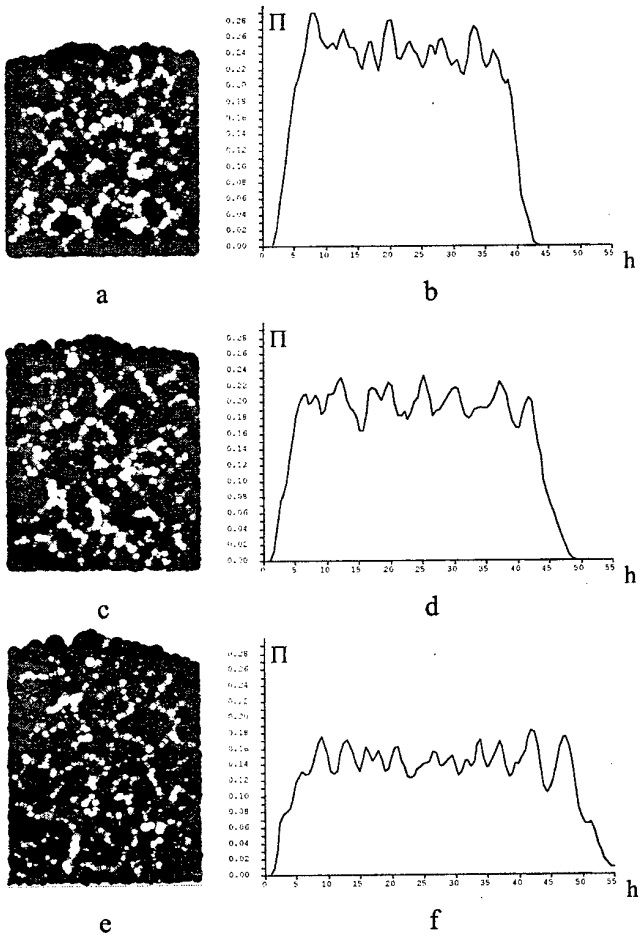


Fig. 2. Sections of sintered compacts composed of spherical particles:
(a) $N(1,0;0,0) = 10^4$, (c) $N(1,0;0,2) = 10^4$, (e) $N(1,0; \ln\sigma=0,3) = 10^4$; pores on sections are white-colored. Distribution of porosity П along the height h of the package:
(b) $N(1,0;0,0) = 10^4$, (d) $N(1,0;0,2) = 10^4$, (f) $N(1,0; \ln\sigma=0,3) = 10^4$

Sintering did take place under conditions of zonal segregation, that is why porosity formation should have become intergroup. Indeed, large intergroup pores did really form in a monodisperse package $N(1,0;0,0) = 10^4$ and in a package with normal particles distribution by size $N(1,0;0,2) = 10^4$ (Fig. 2.). At the same time in a $N(1,0; \ln\sigma=0,3) = 10^4$ sintered package intergroup pores are compatible with pores inside the groups and are uniformly distributed across the complete volume, i.e. intergroup porosity growth was suppressed (Fig. 2.). Therefore, consolidated model package of spherical particles with lognormal particles distribution by size $N(1,0; \ln\sigma=0,3) = 10^4$ does possess the best porosity characteristics among the packages with considered dispersion characteristics types.

The results obtained demonstrate fair congruence with experimental data and serve as a proof of model adequacy [1] for sintering processes in real powder systems.

**References**

1. Kadushnikov R.M., Skorohod V.V., Nurkanov E.Yu., Kamenin I.G., Alievsky V.M., Alievsky D.M. Computer modelling of of sintering of spherical particles. Powder metallurgy. - № 3/4. 2001. pp. 71-82.

# PHASE TRANSFORMATIONS IN ELASTICS-CRYSTALS OF THE STRUCTURE $G5_1$

**Matysina Z.A., Zaginaichenko S.Yu.[(1)], Eremenko A.M.**
Dniepropetrovsk National University, Dniepropetrovsk, Ukraine
[(1)]Institute for Problem of Materials Science, Kiev, Ukraine

The concept of ferroelasticity in a general massive of phase transformations was formulated in the work [1]. Broad theoretical and experimental analyses of such materials followed. Now ferroactive materials are used more widely.

In the present paper a statistics theory of deformation ordering crystals-elastics with the structure $G5_1$ of boric acid $H_3BO_3$ type has been worked out on the basis of molecular-kinetic concept. Such a theory for crystals with the structure H4 of a scheelite $CaWO_4$ type is worked out [2]. The inside configuration energy $u$, thermodynamical probability $G$, free energy $f$ and thermodynamical potential $\psi$ of the system in the dependence of the temperature $T$, the degree of the deformation order $\eta$ , energy constants $w$, $\alpha$, the amount of outer mechanical oriented stress $\sigma$ have been calculated. Equations of equilibrium state have been obtained. The temperature dependence on the deformation order parameter, the way mechanical stress $\eta(T, \sigma)$ influences the dependence mentioned have been determined. The conditions of realizing in the system of first- and second- kind phase transformation from para- into ferro-elastic state, determining energy parameter $\alpha$, have been stated. The possibility of appearance due to the outer stress of non-disappearing order and the possibility of order-order phase transition, i.e. spasmodic decreasing or increasing the order parameter with or without changing its sign, has been made clear. The deformation hysteresis and the dependence of the order parameter on the outer stress $\eta(\sigma)$ pointing of the first-kind phase transition from para- to ferrophase has been studied. The possibility of appearing one or two hysteresis loops, which can exist in a definite small temperature interval near the temperature of phase transition, has been shown. Configuration heat capacity $C(T, \alpha)$ in the vicinity of Curie point has been calculated; its peek type temperature dependence and the growth of the heat capacity jump at the transition order-disorder due to the great values of constant $\alpha$ has been stipulated. The later determines quadratic dependence of the ordering energy $w$ on the deformation order parameter. Functions determining temperature dependences of elastic compliance $S(T, \eta)$ and the longitudinal elasticity modulus $E(T, \eta)$ in ordered and disordered states of elastics have been calculated. It is grounded that dependences $E(T)$ at $\eta = 0$ are linear but at $\eta \neq 0$ are fractional rational functions of the temperature. As to the vicinity of the Curie point, the validity of the Curie-Weiss Law and the rule of the negative deuce is stipulated. It has been also grounded that elastic compliance $S(T)$ grows unlimitedly at the Curie point.

The type of the discovered regularities should arrear qualitatively for elastics of both viewed and other structures. Here only the concrete cases of realizing phase transitions of the first-kind and the second-kind phase transition, values of residual deformation and coercive form in the deformation hysteresis, the height of the peak and the jump of the heat capacity at the Curie point, the steepness of the curves of temperature dependence of elastic compliance and the elastic modulus, etc. may vary in the dependence on the value of the structure-energy constant.

All the functional dependences $\eta(T, \alpha)$, $\eta(\sigma)$, $C(T, \alpha)$, $S(T, \eta)$, $E(T, \eta)$ have been revealed experimentally for many ferroelastics and ferroelectrics of various structures, and they correspond to the results of other theories [2-5]. That is why we can hope that the obtained theoretical calculations are realistic.

As an example, Figures 1-3 show the dependence of the order parameters $\eta_1$ and $\eta_2$ in sublattices of the crystals, configuration heat capacity C, elastic compliance S, the longitudinal elastic modulus E on the temperature T, energy constant $\alpha$ and the amount of outer of mechanical oriented stress $\sigma$.

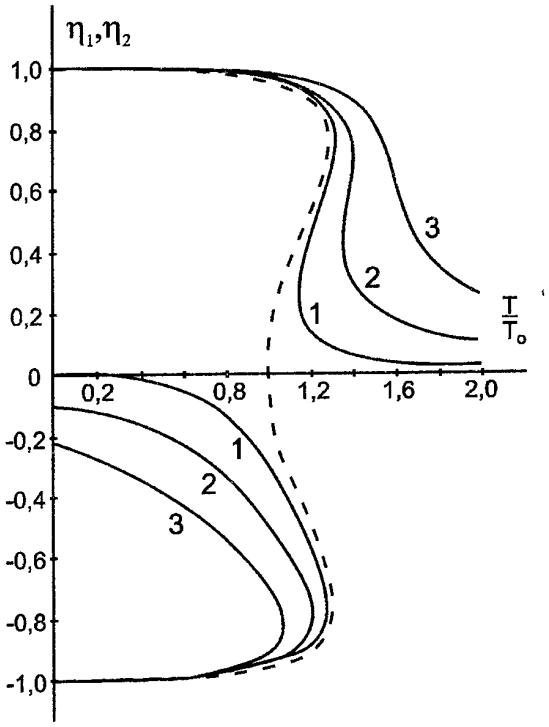


Fig. 1. The influence of the outer mechanical oriented stress on the temperature dependence of the deformation order parameter. The diagrams above the abscissa axis determine $\eta_1$; and those below determine $\eta_2$. The dependence $\eta_1(T)$, $\eta_2(T,)$ at $\sigma=0$ is marked by the dotted line.

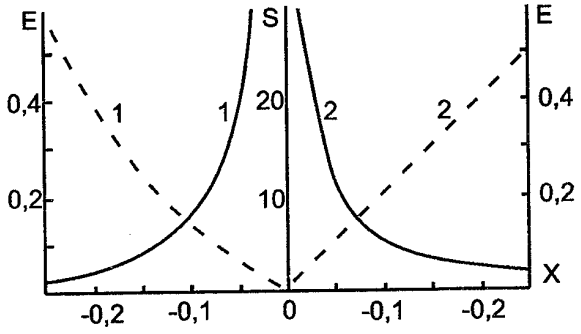


Fig. 3. The diagrams of the elastic compliance S (solid curve) and elastic modulus E (dotted curve) on the temperature. Curves 1 correspond to of the deformation ordering state ($\eta \neq 0$), curves 2 — to disordered state ($\eta=0$).

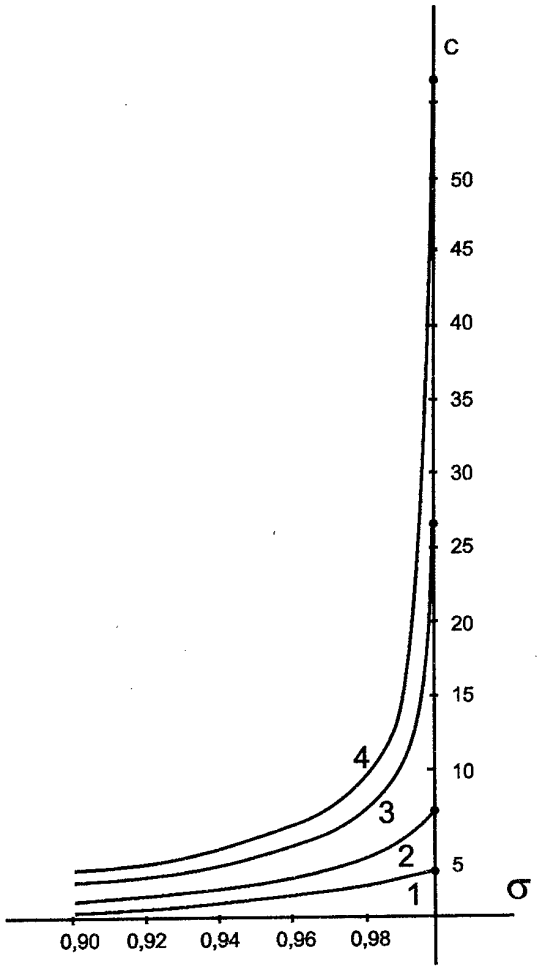


Fig. 2. The diagrams of temperature dependence of the configuration heat capacity for $\sigma=0$ and different values of the energy parameter $\alpha$.


1. Aizu K.-J. Phys. Soc. Japan. 1969. v.27. p. 387.
2. Matysina Z.A., Chumak V.A., Ukr. fiz. zhurn. 2001. V.46. № 9. p. 957.
3. Tsedrik M.S. Fizicheskie svoistva kristallov semeistva triglitsinsulfata. Minsk: Nauka I tekhnika. 1986. p. 216.
4. Yurkevich V.D. Fizika fazovykh perekhodov v segnetoaktivnykh tverdykh rastvorakh. Rostov-na-Donu: RGU. 1988. p. 320.
5. Rudyak V.M. Fizicheskie svoistva segnetoelektricheskikh kristallov. Kalinin: KGU. 1989. p. 84.

# DIFFUSION WAY OF STRUCTURE AND PROPERTIES FORMATION IN Fe-BASED ALLOYS UNDER DEFORMATION EFFECT AND DOPING WITH N AND C

**Demchenko L.D.**
National Technical University of Ukraine "KPI", Kiev, Ukraine

The improvement of mechanical properties of mechanisms parts and instruments is an important scientific and technical problem of many researches. One strengthening way of construction and instrumental steels products is a surface/selective processing using chemical heat treatment, in particular, *nitriding* and *carburization*. Advantages of such treatment are providing high hardness and strength of surface/local parts under conservation of product core viscosity that promotes exploitation term increase. The rise of surface layer mechanical and anticorrosive properties during diffusion saturation with N/C occurs at the expense of nitride/carbide phases formation and N/C solution in basic metal lattice.

The urgent task of this investigation is to study the deformation and doping effect on Fe nitriding process, diffusion layers structure, phase composition, atom distribution and properties.

In previous investigations [1-3] it was established that Fe-based alloys preliminary plastic deformation (PPD) being used before diffusion doping with N/C under certain conditions (the best results were achieved after 15-30 % deformation) accelerated nitriding/carburization processes and surface diffusion layers formation, and increased these layers mechanical properties. Also PPD affects chemical and phase composition, final structure and properties of surface diffusion layer, and phases' formation kinetics.

The work aimed to investigate the influence of PPD within the range of compression degree 0-70% on chemical and phase composition, structure and mechanical properties (microhardness and wear resistance) of surface diffusion layers formed in Fe-Cr-Ti alloys containing as doping elements 0.5-2.2 wt. % Cr and Ti under saturation with N/C from gaseous atmosphere dissociated ammonia ($NH_3$)/propane-butane ($C_3H_8$-$C_4H_{10}$) at T = 853 K.

Iron doping with titanium well known as nitride/carbide-forming element increases N/C solubility in α-phase, nitride/carbide phases, can bring to titanium special nitrides/carbides form and dissolve in iron nitrides/carbides that results in considerable increase of diffusion layers mechanical properties. Moreover, iron doping with chromium increases bond energy of interstitial atoms with dislocations that can increase the mass transfer of N/C with mobile dislocations by dislocation-dynamic mechanism.

As a result of microstructure and microhardness investigations it was established that deformation degree rise up to 30 % led to the total diffusion layer and surface carbonitride phase layer thickness increase, as well as to surface layers microhardness rise when different ammonia/ propane-butane ratios (from 100 % $NH_3$ to 100 % $C_3H_8$-$C_4H_{10}$ in step 10 %) were used. The maximum layer thickness rise under deformation effect was achieved after saturation in 80-90% ammonia and 10-20% propane-butane environment: the total layer thickness increased 1.4 times, i.e. from 140 μm (in undeformed specimens) to 200 μm (in 30 % deformed specimens). Microhardness increased from 14 GPa (in undeformed specimens) to 16 GPa (in deformed with 30 % specimens) as well.

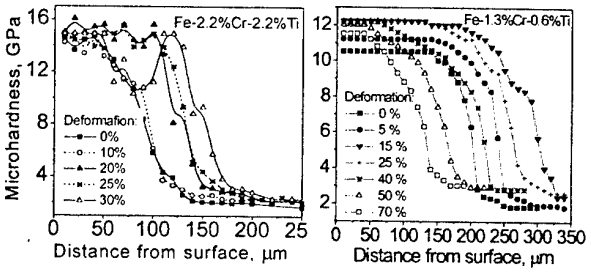


The results of wear resistance tests obtained by friction method showed that nitrogen and carbon ratio in saturating environment as well as cold deformation degree affected wear resistance of surface diffusion layers. Diffusion layers wear resistance increased with the raise of propane-butane content in saturating environment. The best characteristics of wear resistance were acquired after 20-30 % deformation and further saturation in 80-90% ammonia and 10-20% propane-butane.

Thus, the optimal combination of surface diffusion layers performance attributes was achieved after doping of 20-30 % deformed Fe-Cr-Ti alloys with N and C in 80-90% ammonia and 10-20% propane-butane environment.

The (N+C) concentration distribution in diffusion layer depends on specimens' deformation degree. With deformation degree increase up to 30 % the (N+C) penetration depth increased 1.5 – 1.6 times as compared with recrystallized specimens.

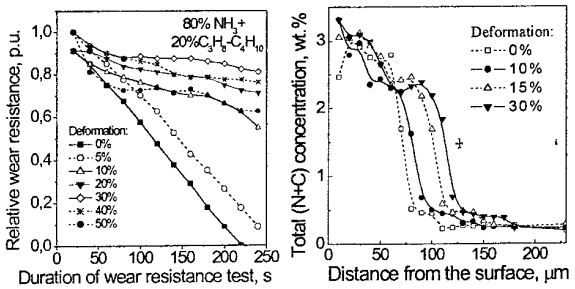


X-ray investigations of surface diffusion layers phase composition showed that cold deformation affected phase formation in surface layers during Fe-Cr-Ti alloys doping with N/C. According to microstructure and XRDA data the surface diffusion layer depending on ammonia and propane–butane quantitative ratio in saturating environment consisted of:

- a thin surface layer of $\varepsilon$ - phase with hcp lattice of $Fe_{2-3}N$ type (under saturation in 100 % ammonia) or $\theta$ - phase with orthorhombic lattice isostructural to cementite ($Fe_3C$) crystal lattice (under saturation in ammonia with the addition of 10 or more vol. % of propane-butane) and
- a layer of nitrogen and carbon solid solution in α-phase alloyed by Cr and Ti with bcc lattice.

The $\theta$-phase formation occurred both in deformed and undeformed Fe-2.2%Cr-2.2%Ti specimens under saturation with N and C in presence of 10 or more vol. % of propane-butane in mixture with ammonia.

Deformation affected the phase composition of diffusion layers formed under saturation of Fe-1.3%Cr-0.6%Ti specimens by N and C in ammonia environment with addition of 10 vol.% of propane-butane. It led to the $\theta$-phase formation in surface layers after deformation within the range of 25-30 % degrees. The $\varepsilon$-phase was formed in this environment after deformation out of 25–30%. The diffusion layers containing $\theta$-phase showed maximum microhardness, wear resistance and layer thickness.

Furthermore, deformation accelerates diffusion layer formation and changes its growth kinetics. Analysis of layer growth kinetics showed that the diffusion layer and ε- and θ-phases layer formation in deformed alloys (as compared with undeformed ones) proceeds in two stages. On the first stage (up to 2 hours) the rate of these layers growth is 1.5–2.5 times greater than on the second one. The maximum these layers growth rate in deformed alloys on the first saturation stage is observed after 20–25% deformation, and on the second stage – after 10-15% one.

The reasons of surface layer mechanical properties rise, phase formation change and interstitial atoms mass transfer increase in deformed Fe-Cr-Ti alloys as compared with undeformed lie in structures distinctions of deformed and recrystallized metal.

As a consequence of deformation increase the dislocations density rises. When certain (15-30%) deformation conditions occur the most mobile dislocations number is generated. So, in deformed material there arise conditions under which accelerated N/C transport is possible by diffusion mechanisms different from interstitial ones. The interstitial atoms (N and C) are known to dissolve on dislocation with Cottrell atmospheres formation increasing N and C solubility in α-phase. Formed in such a way dislocations complexes with the interstitials atoms can be thermally activated, can move under the internal stress influence caused by N and C diffusion in surface layers and transport the interstitials atoms on dislocation-dynamic mechanism [4, 5].

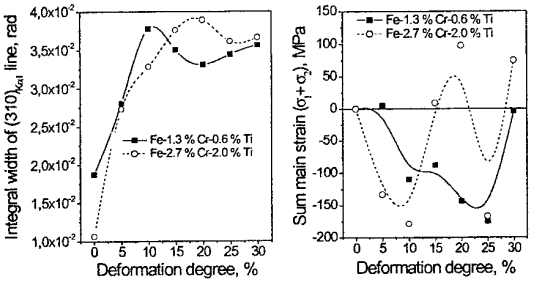


X-ray investigations of surface layers' structure after different deformation showed that integral width of $(310)_{K\alpha 1}$ diffraction line increased with deformation degree rise up to 10-20% that could be caused by increase of dislocations density and mobile dislocations number. Macro-strain investigations on specimens surface testified to compression stress rise in surface layers of deformed alloys that could cause ascending diffusion of interstitial atoms (N/C) at the beginning of diffusion process as well.

[1] Tinyaev V.G., Nazarenko V.F., Lakhnik A.M.: Met. Phys. Adv. Tech. Vol. 16 (1996) p. 189

[2] Sidorenko S.I., Tinyaev V.G., Demchenko L.D. et al.: Met. Phys. Adv. Tech. Vol.18 (2000) p. 753

[3] Sidorenko S.I.,Tinyayev V.G.,Demchenko L.D. et al.: Met. Phys. Adv. Tech. Vol.18 (2000) p.1383

[4] Klyavin O.V., Chernov Yu.M., Pravdina N.N. et al.: Fizika Tverdogo Tela Vol. 20 (1978) p.3100

[5] Orlov A.N.: Fizika Tverdogo Tela Vol. 22 (1980) p. 3580

# AB INITIO INVESTIGATIONS OF THE EFFECT OF CHEMICAL BONDING ON THE SPIN STATE OF HYDROGEN ATOM IN $ZrH_2$

**Yuryeva E.I., Pletnev R.N.**
Institute of Solid State Chemistry, Ural Branch of the Russian Academy of Sciences, Yekaterinburg, Russia

The interest in transition metal hydrides is due not only to their extensive use in engineering and energetic, but also to the possibility of application of this class of compounds in solving some fundamental physical problems. In the latter case two aspects can be distinguished. On the one hand, hydrogen may serve as a doping element allowing smooth (sometimes reversible) changes in the properties of the metallic matrix. On the other hand, hydrogen atoms forming an intrinsic subsystem interact strongly with each other and this may give rise to various phase transitions. In addition, hydrogen atoms in metals have a very high diffusion mobility. Sometimes the hydrogen sublattice may exhibit distinctive quantum properties even at room temperature. At the same time many (including electronic) characteristics of hydrides have been poorly studied hitherto.

It was suggested earlier that three phase transitions may take place in the hydrogen sublattice of the cubic $\delta$-$ZrH_x$ ($x<2$). Not long ago stoichiometric cubic zirconium dihydride has been synthesized. NMR 1H spectra were obtained and the time of proton spin-lattice relaxations was measured for this compound. Thermally activated hydrogen diffusion was observed at temperatures above 290 K. In the region of 230 K there occurs a reversible phase transition caused by a variation in the state of hydrogen. This transition is detected by a temperature-dependent behavior of the Knight shift and the relaxation characteristics. The Knight shift in electronic conductors is proportional to the spin density on resonating nuclei. In view thereof, the variation in the spin density on hydrogen nuclei in zirconium hydride may be brought about both by the redistribution of electronic density due to chemical bonding effects and the polarization of electronic density on hydrogen atoms by conduction electrons from zirconium atoms.

The polarization of closed shells by intrinsic (localized) unpaired electrons can be calculated by quantum chemical methods. However the calculation of polarization by conduction electrons calls for new computational techniques. In this work, the non-empirical discrete variation $X_\alpha$ method was used to calculate superfine magnetic fields $B_{Fc}$ generated on hydrogen atoms by a zirconium atom in the model cluster $[ZrH_8]$ for the cubic phase of $ZrH_2$. A specific feature of the calculation is the application of the neutral cluster approximation, which implies that atoms constituting a cluster are considered primarily in the neutral state. Subsequently, chemical interatomic coupling results in the redistribution of electronic density. This leads to a variation in orbital and spin populations of atomic orbitals. The self-consistent spin-polarized calculation yields the following populations of atomic orbitals of hydrogen atoms:

| AO | N (spin up), e | N (spin down), e |
|---|---|---|
| 1s | 0,7053 | 0,4001 |
| 2s | 0,0115 | 0,0085 |

The Fermi-contacting contribution to the superfine magnetic field on hydrogen atom nucleus performed after the technique developed by the authors gives the following contributions from H1s- and H2s-AO:

$B_{Fc}$ (1s) 5,17 T
$B_{Fc}$ (2s) 0,01 T

To perfect the computational technique of the Knight shift in zirconium hydrides in terms of the employed method, it is necessary to assume the possibility of freezing Zr(1s-4p)-AOs. The effect of cluster dimensions on the calculated values should be also considered.

This work was supported by the Russian Foundation for Basic Research (project № 02-03-32979).

# TECHNIQUE OF PARAMETR'S DEFINITION OF DYNAMIC PHASE TRANSITIONS IN METALS

**Usherenko S.M., Ovchinnikov V.I., Koval O.I.**
Research Institute of Impulse Processes, Minsk, Belarus

**Introduction** Spreading of shock waves on a firm metal body is accompanied by the polymorphic transitions changing its structure. Till present time polymorphic transitions under influence of pressure are found in many metals (iron, thallium, tin, the titan, bismuth etc.), semiconductors, oxides and practically in all minerals and rocks. Cottrel assumed that besides intervention of the liquid phase (i.e. fusion), polymorphism should be a rule for all metals because the phase which is stable at 0 °Kwill become less stable at higher temperatures. Certainly, there are some exceptions this rule, however, for the majority of experimentally investigated metals this idea is correct.

Proceeding of the phase transition in conditions of dynamic loading and unloadings facilitates the occurrence of the new condition of the substance [1] representing metastable phase in which transformation develops, inhibited at a stage of loss of connections between atoms.

Authors of the given work did the analysis oftheoretical and experimental data on dynamic phase transitions in the metals. This analysis allows to draw a conclusion about proceeding of dynamic phase transition during loading time in copper and other metals in whichphase transformations were not observed in firm condition at pressure 1 athm.

**The purpose of the work** is a technique developmentof parameter's definitionof the dynamic phase transitions, based on the connection betweenthe structure of the material formed in loading processbystream of high-speed particlesand pressure of thephase transition initiation.

**Statement of theexperiment**. Objects of theresearch were cylindrical samples from steel 45, copper, titan, subjected triple processing by powder SiC of fraction 63-70 microns, weight 80g, with speed 700 м/sec under the standard circuit [2]. Microstructure of thesamples was investigated with the help of an electronic microscope " Scan - Met " and metallographicoptical microscope " Metam PB-21".

**Results of the experiment anddiscussion of them.**

Discussion of the results of the research on forming the material structure in conditions of dynamic loading is in the work of S. I. Usherenko, V. I. Zeldovich, I. V. Homskaya, V. I. Ovchinnikov, O. I. Koval "Forming of composite metal materials in conditions of shock-wave loading'.

In the examined loading conditions the stream of the powder particles accelerated by explosion will penetrate into metal barrier on depth of 60-200 mm and at the same time in the volume of steel there are some zones which come out due to a difference in structure of zones and the basic material of the barrier. The data on change of the microstructure of the work materials in depth is received during the research. The density of the registered defects after processing and their diameter: steel 45 – d=5,44mkm, $\rho=299mm^{-2}$, copper d=0,74 mkm, $\rho=9048mm^{-2}$, titan d=1,90mkm, $\rho=1217mm^{-2}$,is taken as an estimated parameter of efficiency of superdeep penetration process(SPP).

Influence of shock waves on copper does not result fixing "break" on shock adiabatic curve , however, in structure there are some defects connected to reverse transformation, on structure similar to defects from наклепа. Such a kind of phase transition should be accompanied by volume increase of a new phase. The theoretical calculations that are based on experimental data in residual change of copper microstructure of sample after dynamic loading, allow to claim, that at the moment of dynamic loading ($400*10^{-3}$sec) material in narrow local zones of defects - channels where shock energy localization is observed, exists in condition of plasma. The analysis of the received results allows to draw a conclusion, that dynamic phase transition in copper is convertible and a phase of high pressure after removal of loading are not remained.

At calculation of pressure of phase transition initiationin copper, authors of the given work as basic modelling representations about causality SPP accepted:

1. Parameters of dynamic phase transitions may be defined on material ofbarrier changes.
2. Processof superdeep loading of particles inbarrier occurs in zones where due tosuperexposition of fields of pressure conditions sufficient for course of phase transition are created.
3. Change of the material microstructure formed at dynamic loading occurs at the pressure that isnecessary for the beginning of phase transition.
4. Formation of a new superplastic condition of material as a result of dynamic loading is made only due to energy of a stream of particles.

Shock adiabatic curve for iron, determining dependence of specific volume on shock pressure, tests a break in an interval of pressure 12 - 20 GPa and 298 °K. This break arises due to a sharp change of compressibility or specific volume and because of transition from lattice of □ - phase tolattice of □ - phase. It is shown in [3], that appreciable change of microstructure in iron occurs if shock pressure exceeds pressure of transition.

Calculation of pressure of phase transition initiation in copper in the given work is based on the assumption, that the ration of volume size ofchanged microstructure ( defective zone) zone to volume of a zone претерпевшей phase transformation is a constant for all the metals under identical conditions of processing (*VdFe/VzFe = VdCu / VdCu = Const*)

$$Vd = \pi\, d2/4\, \rho\, Vo. \qquad (1)$$

On the basis of the considered features of channel –crater formation in [2] it is established that the specificity of crater creation consists in the character of energy redistribution of shock stream with a barrier in channels zones . Total value of the energy that is generated at impact of a clot of microparticles with barrier at triple processing makes:

$$E = 3\, mv\, 2/2 \qquad (2)$$

Pressure of initiation of phase transition is defined by:

$$P = Å/Vz \qquad (3)$$

As for iron it is established, that pressure of phase transition makes 12 GPa, it is possible to calculate volume of transformation zone . Calculation of pressure of the phase transition initiation in copper gives value 18,9 GPa. For reliability check of the offered technique calculation of pressure of phase transition initiation in titan was made.

It is experimentally established, that pressure of phase transition in titan makes 17,5 GPa [2], and the value that was received in the given work is 19,6 GPa, and error makes 12 %. The given interest of the error is taken into account at updating calculations of pressure of dynamic phase transition in copper on experimentally-analytical technique.

**Conclusions** 1) In the given work the hypothesis about existence of dynamic phase transition in copper in an interval of pressure 17,0 - 18,9GPa [2] was put forward and theoretically proved. 2)The experimentally-analytical technique of pressure definitionof dynamic phase transition in metals was offered.

**The list of designations:** *Vd* - volume of defective zone; *d* - diameter of defect; □ - density of defects; *Vo*- volume of sample; *E* - the energy generated at impact of microparticles clot withbarrier; *m* - weight of particles' clot; *v* - speed of particles' clot; *P* - pressure of phase transition initiation ; *Vz*- volume of phase transformation zone.

**The literature**

1.Presnjakov A.A. Superplasticity of metals and alloys. Alma-Ata, the Science, Kazakh SSR, 1969. 197p.
2.Dynamic reorganization of structure of materials// S. M. Usherenko /Minsk, 2000, 188p.
3.Dynamic researches of firm bodies at high pressures//A. I. Zharkov./M., Mir, 1965, 235p.

# CALCULATION OF FORCE OF INTERPLANE INTERACTIONS AND STRENGTH CHARACTERISTICS OF TITANIUM AND CERAMIC MATERIALS AT HIGH RATE LOADING

**Zakarjan D.A., Kartuzov V.V.**
Frantsevich Institute of Problems of Materials Science, NAS of Ukraine, Kyiv

Forces of interaction among atomic planes (at shear or tension) play the important role for accurate solution to a problem of materials deformation and fracture.

The primary goal of this investigation, considering hexagonal highly densed structure of titanium and cubic modifications of ceramic materials, is to simulate these forces and to calculate materials mechanical characteristics at high rate loading.

Materials strength characteristics and (at high rate shock deformations, high temperatures, etc.) resistance of those materials against extreme conditions are usually estimated on the basis of calculation of ideal strength of materials with defect free and ideal structure.

To describe interatomic interactions the method of none local pseudo-potential was employed.

At deformation, because of anisotropy, a crystal is more easily deformed on some crystallographic directions. To shear are much easy exposed highly densed atomic planes. To tensile a crystal is easier on a direction perpendicularly to highly densed planes. Therefore we carried out calculations for titanium who is one of the important constructional materials to protect against high rate loadings. Titanium is a laminated material, which layers (basic planes) are densely packed. Thus, characteristic types of deformations appearing in these materials at loading are shear of densely packed planes or tension (compression) on a direction perpendicular to basic planes.

Used interatomic potentials are built under the following scheme: characteristic function of zoned structure is introduced, this function together with a potential of direct interaction describes total effective interaction among ions, when summarizing which on two parallel densely packed layers we obtain energy of interaction between two layers.

Table below presents the obtained results.

Table Stress $\sigma$ at low deformations $g_{33}$, respective values of Young's modulus $E$; theoretical strength $\sigma_{max}$ (at tension and compression).

| Tensor of deformation $g_{33}$ ($g_{11}=0$); ($g_{22}=0$) | Stresses $\sigma$ (GPa) | Young's modulus $E$ (GPa) |
|---|---|---|
| 0,0151006 | 4,916 | 323 |
| 0,0201342 | 6,52 | 323 |
| 0,0251677 | 8,1437 | 322 |
| 0,0302013 | 9,742 | 323 |
| 0,14 | $\sigma_{max}$ = 39,6 (tension) | $E_{cp}$ = 323 |
| -0,109 | $\sigma_{max}$ =34,5 (compression) | |

Distinction between theoretically calculated and experimentally obtained values of materials resistance against fracture appears because of the presence of microcracks and crack-like defects. For example, if introduce a microcrack with a length $2\ell = 0.2$ mkm it would be enough to reduce $\sigma$ to 1GPa.

At transition from FCC lattice to hexagonal one, the structure of ceramic materials is described with three-layer alternation of planes (001) like $aa'bb'cc'$ where $a,b,c$ consists of atoms of one grade (B or Si), and planes $a',b',c'$ – from atoms of other grade (N or C), and a packing is dense.

For hexagonal modification coordinates of atoms and distances among highly densed atomic planes are calculated. Calculations have shown, that distances between two planes making a layer, are $d = 1/4\,c$, where $c$ - length of a spatial diagonal of a cube (for cubic modification). Inside a layer on atomic planes atoms are in identical positions, and layers are displaced from each other on a vector

$$\vec{\rho} = \frac{2}{3}\vec{\tau}_a + \frac{1}{3}\vec{\tau}_b,$$

where $\vec{\tau}_a$ and $\vec{\tau}_b$ - vectors of hexagonal lattice on basic plane. The distance between layers makes $1/12\,c$.

To build matrix elements of pseudo-potential we offer the following technique.

At the beginning the pseudo-potential of separate layer consisting of two atomic planes where the first plane goes through the beginning of coordinates and the second – is displaced on $1/4\,c$ has to be built.

Results summary of calculation of force of interaction of atomic planes and strength for diamond is illustrated in Fig. 1 and 2.

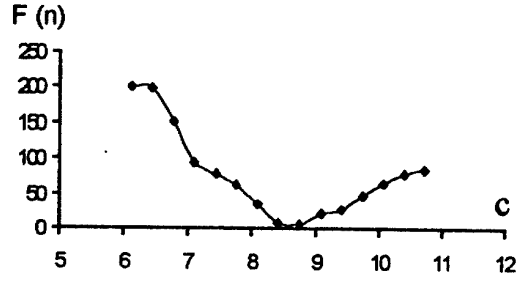


Fig. 1 Dependence of force of interaction among basic planes versus lattice parameter at compression and tension.

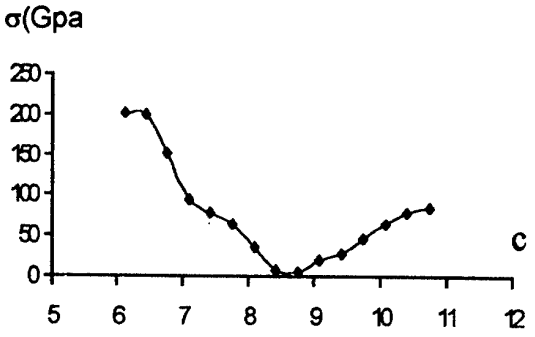


Fig. 2 Dependence of strength versus lattice parameter on a direction [111] at compression and tension.

When $c_1$ = 7.98 (compression) and $c_2$=8.95 (tension) it is obvious, that function (dependence force – deformation or strength – deformation) has points of inflection where derivatives of these functions change a sign. Modules of elasticity are defined by the same derivatives. Hence, it is quite possible to say, that at these values of argument - the system is not that stable. Thus, these values of strength ($\sigma$ =93GPa, and $\sigma$=28 GPa) will correspond to ideal strength of diamond at deformations along [111].

RESUME

The technique developed on the base of none local pseudo-potential enables to calculate at hyper velocity impacts the forces of interaction among the deformed atomic planes.

At transition of cubic structures into hexagonal one the layers that consist of two atomic planes on which atoms are in identical position are formed, and layers are displaced relative each other.

At tension and compression separate layers are deformed much easy. Graphic illustration of dependence of force of interaction from lattice parameter evidently shows at what values of deformation system is unstable.

# A NOVEL BORON-BASED SUPERHARD MATERIAL PRODUCED AT HIGH PRESSURES AND TEMPERATURES

**Shulzhenko A.A., Sokolov A.N., Belyavina N.N.[(1)], Markiv V.Ya.[(1)]**
V.N. Bakul Institute for Superhard Materials of the National Academy of Sciences of Ukraine, Kiev, Ukraine;
[(1)]Taras Shevchenko Kiev National University, Kiev, Ukraine

In the last few years the interest of researchers in searching for novel superhard phases has quickened. This is attributable, firstly, to the theoretical generalization of the accumulated experimental data on the relationship between the formation of structure and properties of materials produced under different conditions, including high pressures and temperatures, and the prediction on this basis of novel phases with a unique combination of physico-mechanical properties. Secondly, this is a result of the development of novel structural materials that require specific machining processes, which can be implemented only by the use of new superhard materials.

The possibility of obtaining a novel ceramic superhard material by hot pressing has been shown by the AMES Laboratory (USA). The chemical composition of this material corresponds approximately to the $AlMgB_{14}$ + X formula, where X is BN, AlN, Si and some other additives, which greatly increase the material hardness [1]. The production technology imposes specific requirements upon the particle size and quality of the initial materials as well as upon protective medium. Sintering time is 60 min. Depending on the production conditions and additives, the resultant material hardness ranges from 35 to 42 GPa.

The Institute for Superhard Materials of the National Academy of Sciences of Ukraine has also obtained an $AlMgB_{14}$-based superhard material under high pressures and temperatures. The material is characterized by an orthorhombic structure and the following crystal lattice parameters: $a$ = 0.58368 nm, $b$ = 0.81176 nm and $c$ = 1.03073 nm [2].

The use of high-pressure technique has made it possible to essentially simplify the technologies of preparation of the initial mixture and making the material as well as to intensify the synthesis process (a complete cycle of synthesis decreases several times). The optimization of the chemical composition and the conditions of preparation has allowed stable-in-quality samples of the new superhard material to be obtained.

The results of our investigations into peculiarities of the phase formation in the Al-B-C system over wide ranges of pressures and temperatures have allowed us to define the conditions of production of the $AlB_{40}C_4$-based superhard material. An X-ray spectrum of the material is given in Fig. 1 and the data on hardness and fracture toughness are given in Fig. 2 and Table 1, respectively, in comparison with those of some other superhard materials.

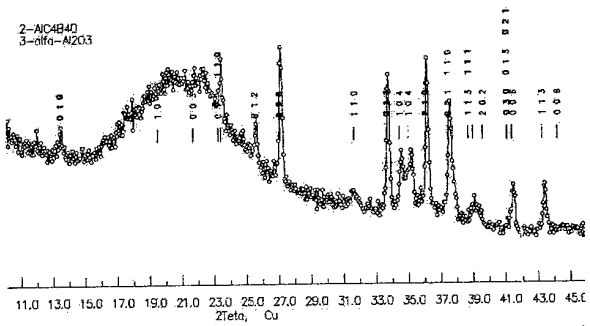


Fig. 1. X-ray spectrum of the $AlB_{40}C_4$-based superhard material.

Table 1. Fracture toughness of the $AlB_{40}C_4$-based material as compared with that of other superhard materials

| Material | Fracture toughness, $K_{1C}$, MPa·м$^{1/2}$ | References |
|---|---|---|
| Synthetic diamond crystals | 5,3 ÷ 6,2 | [3] |
| *CBN crystals* | 3,5 | [4] |
| $AlB_{40}C_4$-based material | 8,5 | - |
| Amborite AMB90 | 6,4 | [5] |
| Meganite *MN*-100 | 7,2 | [6] |
| Kiborit II | 10,5 | [7] |

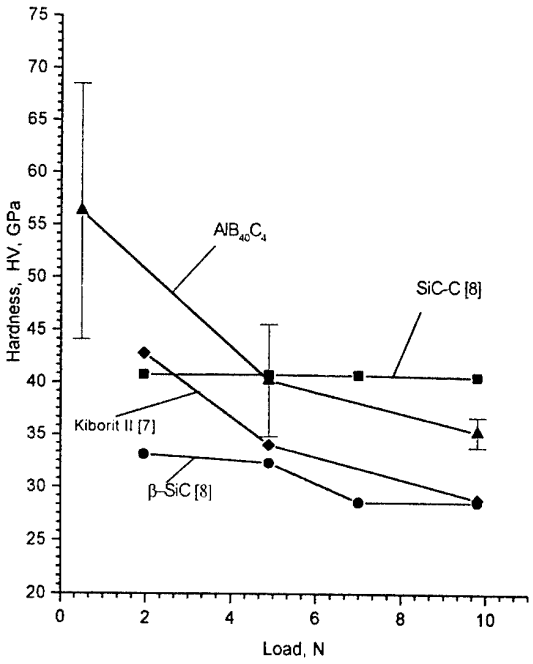


Fig. 2. Hardness of the new material as compared with that of other superhard materials.

It is our opinion that due to sufficiently high physico-mechanical characteristics, tools of the new material can be competitive in performance with cBN tools.

References:

[1]. US Patent No. 6,099,605. Superabrasive boride and a method of preparing the same by mechanical alloying and hot pressing /Cook Bruce A., Harringa Joel L., Russell; Alan M. – Publ. 08.08.2000.

[2]. A. A. Shulzhenko and A. N. Sokolov. A Novel Boron-Based Superhard Material Produced at High Pressures and Temperatures //Superhard Mareials. - 2001. - № 4. - P. 74-75.

[3]. Synthetic Superhard Materials, in 3 volumes. Synthesis of Superhard Materials / N.V. Novikov (Ed.). - Kiev: Naukova Dumka, 1986. – vol..1. - 280 p.

[4]. Synthesis, Sintering and Properties of Cubic Boron Nitride/A.A. Shulzhenko, S.A. Bozhko, A.N. Sokolov, et al. – Kiev: Naukova Dumka, 1993. – 255 p.

[5]. Introduction to De Beers PCD and PCBN Cutting Tool Materials: 1.2.3. – The Publication of De Beers Industrial Diamond Division. – 13 p.

[6]. Megadiamond PCBN Products for Industrial Tooling. – USA: The Publication of Megadiamond. – 11 p.

[7]. N. V. Novikov, A. A. Shulzhenko, N. P. Bezhenar, et al. Kiborit: Production, Structure, Properties, Application // Superhard Materials. – 2001. - № 2. – P. 40-51.

[8]. Gadzyra M., Gnesin G., Mikhailyk O, Shulzhenko O., Bochechka O. SHS of new superhard material based on nonstoichiometric β-SiC //International Journal of Self-Propagaing High-Temperature Synthesis. - 2000.- **9**, N 1. - P. 85-96.

# THE ROLE OF IMPURITY STATE IN SILICON CRYSTALS AND THEIR ELECTRONIC EXCITATION IN THE FORMATION OF MECHANIC-AND-PLASTIC PROPERTIES

**Makara V.A., Steblenko L.P., Rudenko O.V., Naumenko S.M., Kravchenko V.M.**
Taras Shevchenko Kyiv National University, Kyiv, Ukraine

The pace of progress in science and engineering is to a great extent determined by a successive development of semiconductor materials science a principal problem of which is the study of semiconductor material strength and plasticity and thus the study of the crystalline structure imperfections.

One of the basic crystals used in semiconductor engineering is still single-crystal silicon. In fabricating semiconductor structures, silicon crystals are subject to various types of treatment: mechanical, chemical, thermal, etc. Certain stages of fabrication and operation of silicon structures are accompanied by the action of electronic excitation caused by electric current flow and the action of various physical fields. The action of the mentioned external factors may result in the alteration of the characteristics of inelastic deformation and in the evolution of both dislocation structure and numerous microdefects.

The problem of interaction between point defects (impurity atoms and their complexes) and spatial defects (dislocations) is of increasing interest in doing research in semiconductor physics and engineering. This is due to the fact that a great number of the possible processes of interaction between these two groups of defects in a crystal determines the technological properties of semiconductors.

The urgency of the outlined scientific problem prompted us to carry out the present work. The aim of our studies was to determine the role of an impurity state in silicon crystals and their electronic excitation in the formation of microplastic properties (caused by dislocation mobility characteristics) and mechanical properties (dependent on microhardness).

In this work it is shown both experimentally and theoretically that one can control the dislocation behavior both when a dislocation is in an atmosphere and when it leaves the atmosphere by means of various types of treatment of silicon crystals: high temperature treatment, metalization, treatment by electric current, magnetic field or laser radiation.

According to our model, the velocities of short near-surface dislocations in an atmosphere ($V_a$) and beyond it ($V_{b.a.}$) are related by the formula

$$V_{b.a.} = \frac{V_a}{NP},$$

where $N$ is the maximum number of interatomic distances which a dislocation overcomes while moving in the atmosphere and $P$ is the probability that the energy of a double kink after its formation does not exceed its initial value on moving from an initial to adjacent valley of the Peierls potential landscape.

The obtained formula indicates that the dislocation motion velocity after leaving the atmosphere depends on the velocity in the atmosphere as well as on parameter $P$. The latter is determined by a difference of defect concentrations in an initial and adjacent Peierls valleys and by alteration of the energy of interaction between a dislocation and point defects. As is followed from the above formula and the results of our experiments, the dislocation motion velocity beyond the atmosphere correlates with the velocity acquired by dislocations in the atmosphere.

It is found that the state of atmosphere around a short dislocation which is in a start position determines the dislocation dynamics after leaving the atmosphere. The dislocation "remembers" how it moved in the atmosphere, and if the atmosphere slowed it down (the latter corresponds to a great delay time "at the start"), the dislocation will move slowly even after leaving the atmosphere.

In an actual semiconducting silicon which contains dislocations there occur a variety of processes that to some extent or another affect all its basic properties, mechanical ones in particular.

In this work it is established that a dislocation cannot be isolated from not only a variety of structural defects caused by thermal fluctuations, various kinds of treatment, but also elementary excitations of electronic subsystem. It is shown that the processes of dislocation mobility in silicon crystals can be controlled with help of electric current of different densities and physical fields.

The secondary ion mass-spectrometry has shown that the electronic excitation of silicon crystals with dislocations induces low-temperature recombination-stimulated diffusion of impurities, stimulates their recharging and intensifies the gettering ability of the surface, slip planes and dislocations.

As a result of the studies, it was found that a change of impurity composition of the atmosphere as well as electronic excitation of silicon crystals lead not only to alteration of dislocation dynamic behavior, but also to alteration of microhardness and to appearance of electromechanical effect, which turned out to be a near-surface one.

For the first time in this work carried out was a comparative analysis of microplastic and micromechanical properties of silicon crystals as well as an analysis of how these properties change under different kinds of treatment of Si crystals.

It is shown that on correct interpretation the indentor tests provide an express information on a change of microhardness and its relation to dislocation mobility in samples with different prehistory. For the first time established is a correlation between the microplastic and micromechanical parameters of silicon. This correlation makes it possible to develop new methods of controlling mechanical-and-plastic properties of silicon and eventually to fabricate new constructional materials with improved characteristics and parameters, which remains to be an undoubtedly urgent problem.

# INVESTIGATION OF HOT STRETCHING PROCESS OF THIN-WALLED TUBES ON CONIC MANDRELS

**Petrosyan G.L., Petrosyan V.G., Hambardzumyan A.F.**
State Engineering University of Armenia, Yerevan, Armenia

The problem solved on the basis of unmoment theory of rotation shells with accounting of the following dependencies of short-term creep theory of porous materials [1]:

$$\sigma_{eq} = \beta^{-0.5}\left(\frac{1}{2}\left[(\sigma_1-\sigma_2)^2+(\sigma_2-\sigma_3)^2+(\sigma_3-\sigma_1)^2\right]+ \right.$$
$$\left. +\alpha(\sigma_1+\sigma_2+\sigma_3)^2\right)^{0.5}, \quad (1)$$

$$\xi_{eq} = \beta^{-0.5}\left(\frac{2}{9}\left[(\xi_1-\xi_2)^2+(\xi_2-\xi_3)^2+(\xi_3-\xi_1)^2\right]+ \right.$$
$$\left. +\frac{(\xi_1+\xi_2+\xi_3)^2}{9\alpha}\right)^{0.5}, \quad (2)$$

$$\left.\begin{aligned}
\xi_1 &= \frac{\xi_{eq}}{2\sigma_{eq}}\left[2\sigma_1-\sigma_2-\sigma_3+2\alpha(\sigma_1+\sigma_2+\sigma_3)\right]\\
\xi_2 &= \frac{\xi_{eq}}{2\sigma_{eq}}\left[2\sigma_2-\sigma_3-\sigma_1+2\alpha(\sigma_1+\sigma_2+\sigma_3)\right]\\
\xi_3 &= \frac{\xi_{eq}}{2\sigma_{eq}}\left[2\sigma_3-\sigma_1-\sigma_2+2\alpha(\sigma_1+\sigma_2+\sigma_3)\right]
\end{aligned}\right\} \quad (3)$$

$$\theta = \frac{3\alpha(1-w)(\sigma_1+\sigma_2+\sigma_3)\xi_{eq}}{\sigma_{eq}}, \quad (4)$$

where $\sigma_{eq}$ – equivalent stress, $\sigma_1$, $\sigma_2$, $\sigma_3$ – principal stresses, $\xi_{eq}$ – equivalent velocity of deformation of creep, $\xi_1$, $\xi_2$, $\xi_3$ – velocities of principal deformations of creep, w – porosity of material, $\theta = dw/dt$ -speed of material's porosity alteration, t–time, $\alpha$ & $\beta$-porosity functions of material. Analysis of porosity functions shows, that using of well-founded and comparatively simple porosity functions (5) suggested by V.V. Skorokhod is more convenient. This functions have the following shape [2]

$$\alpha = \frac{\theta}{2(1-\theta)}, \quad \beta = (1-\theta)^3. \quad (5)$$

By the reason of complexity of hot stretchnig problem solution as an equation of state comparatively simple model of nonlinear-viscous body [3] chosen

$$\sigma_{eq} = a\cdot\xi_{eq}^{m}, \quad (6)$$

where a and m – coefficients depending on type of material and temperature of its treatment.

On the Fig. 1 the scheme of tube stretching and element of tube at the stretching process shown.

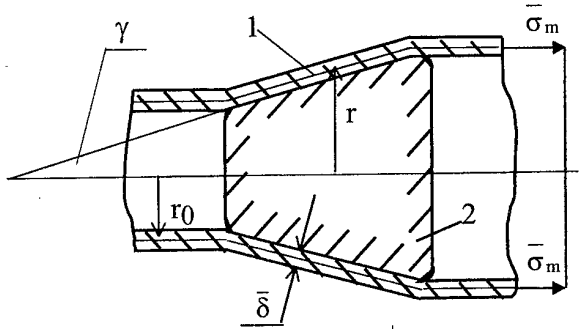


a) Scheme of stretching process
1-tube, 2-mandrel

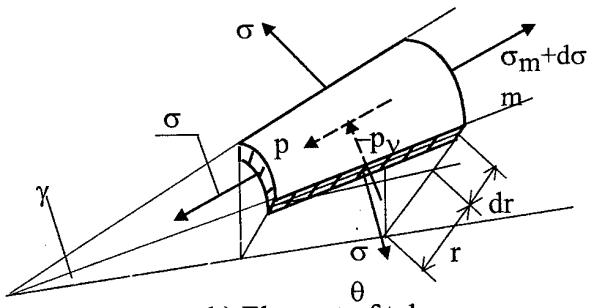


b) Element of tube

Fig. 1.

On Fig. 1 following denotations done: $r_0$ and r – initial and current radius of tube correspondingly, δ–tube's wall thickness, γ - angle between meridional tangent and axis of tube, $p_m$ and $p_\nu$ - intensities of distributed loads on meridional and normal directions of element correspondingly, $\sigma_m$ and $\sigma_\theta$-meridional and circumferential principal stresses.

As a result the system of equations, where are three differential equations obtained for determination of tube's meridional stress $\sigma_m$, tube's wall thickness δ and material's porosity w on all the length of sample's deformation zone

$$\frac{d\bar{\sigma}_m}{d\bar{r}} = \frac{1}{\bar{r}}\left[\frac{\bar{\sigma}_m(1-2\alpha)\left[3\bar{\sigma}_m+\bar{Q}(1+k)\right]+k\bar{Q}^2}{2\bar{Q}(1+\alpha)}-\bar{\sigma}_m\right] \quad (7)$$

$$\frac{d\bar{\delta}}{d\bar{r}} = \frac{\bar{\delta}}{\bar{r}}\cdot\frac{(2\alpha-1)(3\sigma_m+\bar{Q})}{2\bar{Q}(1+\alpha)}, \quad (8)$$

$$\frac{dw}{d\bar{r}} = \frac{1}{\bar{r}} \cdot \frac{3\alpha(1-w)(3\bar{\sigma}_m + \bar{Q})}{\bar{Q}(1+\alpha)}, \qquad (9)$$

where k=1+f·ctgφ and f – coefficient of contact friction between tube and mandrel,

$$\bar{Q} = \sqrt{4(1+\alpha)\bar{\sigma}_{eq}^2\beta - 3\bar{\sigma}_m^2(1+4\alpha)}, \qquad (10)$$

$$\bar{\sigma}_\theta = \frac{(1-2\alpha)\bar{\sigma}_m + \bar{Q}}{2(1+\alpha)}, \qquad (11)$$

$$\bar{\sigma}_{eq} = \left[4(1+\alpha)\beta - 3(1+4\alpha)\left(\frac{\bar{\sigma}_m}{\bar{\sigma}_{eq}}\right)^2\right]^{-\frac{m}{2}} (\bar{r})^{-2m} \times$$

$$\times (\bar{\delta})^{-m}\left(\frac{1-w}{1-w_0}\right)^{-m}, \qquad (12)$$

$\bar{r} = r/r_0$, $d\bar{r} = d(r/r_0)$, $\bar{\delta} = \delta/\delta_0$, $d\bar{\delta} = d(\delta/\delta_0)$, $\bar{\sigma}_{eq} = \sigma_{eq}/\sigma_*$, $\bar{\sigma}_m = \sigma_m/\sigma_*$, $\bar{\sigma}_\theta = \sigma_\theta/\sigma_*$ $\delta_0$– initial value of tube's wall thickness, $w_0$ – initial porosity of material, $\rho_0$=1-$w_0$ & ρ=1-w -initial & current density of material, $\sigma_* = a\xi_*^m$, $\xi_* = \upsilon_0 \sin\varphi/r_0$.

Comparison of obtained final theoretical formulas of hot stretching process with corresponding dependencies of cold stretching [4] shows, that the main difference between them consists in specific peculiarities of using different equations of state. For solution of the problem of cold stretching it is necessary to have the diagram of material deformation & know level of its deformation on the length of tube's conic part. Revealing of these successfully done in [4]. At the tube's stretching in hot condition main role plays complex enough defined the equivalent velocity of deformation of creep, which depends on all the initial and current parameters of technological process: radius r, tube's wall thickness δ and density of material ρ, speed of its motion on the entrance of mandrel $\upsilon_0$ and etc. Despite on this differences, numerical solution of tube's hot stretching process brought to the method [4].

For obtaining particular data of the hot stretching process the method of numerical integration algorithmized in [4] used, on the basis of which in the media of programming package "MATLAB" an universal computer program for investigation of tubes' hot stretching processes composed.

All the main components of stress-strain state of hot deformed tubes for different values of material initial porosity defined.

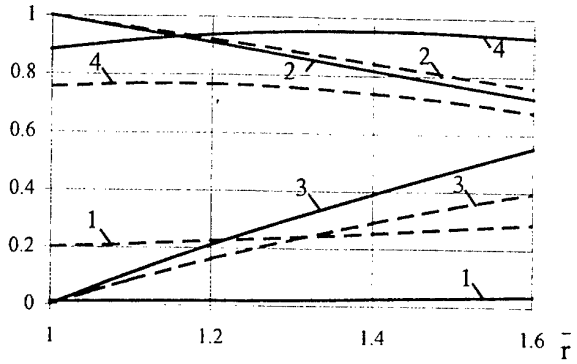


Fig. 2.

On the Fig.2 diagrams of porosity w (1), dimensionless values of tubes' wall thickness $\bar{\delta}$ (2), meridional $\bar{\sigma}_m$ (3) and circumferential $\bar{\sigma}_\theta$ (4) stresses alteration depending on dimensionless radius $\bar{r}$, are brought. Continuous lines corresponds to the deformation of tubes with intial porosity $w_0$=0.01, dashed – $w_0$=0.2 for $\gamma=14^0$, f = 0.1, m=0.143.

As we can see from the Fig. 2, porosity of material grows and wall becomes thinner. Meridional stresses during hot stretching process grow, and increasing of initial porosity value brings to lower forces of deformation and significantly reduces circumferential stresses.

**References**

[1] Petrosyan G.L. Theory of Short-Term Creep of Porous Materials. Yerevan. YSU, 1991. PP.150-153.

[2] Skorokhod V.V, Tuchinsky L.I. Plasticity Condition of Porous Bodies. Powder Metallurgy, 1978, N№11. PP. 83 – 87.

[3] Malinin N. N. Creep in Metals Treatment. Moscow. Mashinostroenie, 1986. 221 P.

[4] Petrosyan G. L., Hambardzumyan A. F. Stress – Strain Analysis of Powder Tubes at the Stretch Process. Proceedings of 6–th European Powder Diffraction Conference. Trans-Tech Publications (Switzerland–Germany–UK–USA), 2000. PP.754-759.

# THE EFFECT OF TEMPERATURE, PRESSURE, AND ADDITIONS OF ALUMINUM IN SINTERING OF cBN POWDERS ON THE cBN→hBN PHASE TRANSFORMATION

**Shulzhenko A.A., Bezhenar M.P., Bozhko S.A., Belyavina N.M.[(1)], Markiv V.Ya.[(1)]**
V.N. Bakul Institute for Superhard Materials of the National Academy of Sciences of Ukraine, Kiev, Ukraine
[(1)]Taras Shevchenko Kiev National University, Kiev, Ukraine

In a complete multifactorial experiment, we have systematically studied the cBN-hBN phase transformation in sintering of cBN submicron (KM 1/0) and close to them in dispersity (KM 2/1 and KM 3/2) powders in wide ranges of $p,T$-parameters of sintering with and without addition of aluminum to the mixture. Four factors were varied: pressure and temperature in the cBN thermodynamic stability region ($p$ = 7.7 GPa, $T$ = 300, 1300, 1750, 2100, 2300 and 2700 K; $p$ = 4.2 GPa, $T$ = 300, 1300 and 1750 K; $p$ = 2.5 GPa, $T$ = 300 and 1300 K); dispersity of the initial cBN micron powders (Table 1); additions of aluminum (0, 2 and 10 mass%). The impurity composition being (mass%): C 0.3, O 0.2, Si < 0.01, Mg < 0.03, Fe < 0.01. The hBN phase was not been revealed in KM 2/1 and KM 3/2, while in KM 1/0 it made up about 1 mass%.

Table 1
Particle Sizes and the Specific Surfaces of the Initial Powders

| Powder | $D_{max}$ μm | $D_{med}$ μm | $D_{min}$ μm | σ $m^2/cm^3$ |
|---|---|---|---|---|
| KM1/0 | 2,5 | 0,6 | 0,1 | 12,2 |
| KM2/1 | 3,0 | 1,4 | 0,8 | 4,54 |
| KM3/2 | 5,0 | 2,3 | 1,0 | 2,75 |
| Al | 65,0 | 25,0 | 6,0 | 0,285 |

The following equipment has been used for sintering: a 10-MN press, a toroid-type (recessed anvil) high-pressure apparatus, a graphite heater. The phase composition of the initial powders and as-sintered polycrystals has been studied by X-ray diffraction analysis using the computerized instrument for studying polycrystalline substances from their X-ray diffraction spectra, which incorporates a DRON-3 diffractometer (Cu-$K_\alpha$ radiation) and a software. The procedure of phase analysis has included the calculation of the intensity of reflections of XRD spectra of cBN and hBN as well as the use of the reference samples. The hBN percentage has been found corrected for the total phase composition of the sample [1]. The method sensitivity limit is 0.5 mass%. The experimental results have been processed using methods of the mathematical statistics. Depending on the number of varied factors, the number of samples for calculations of the average values ranged from 3 to 27. The confidence interval was determined with the confidence probability of 0.68.

The hBN percentage depending on the sintering temperature is a curve with a maximum. At a pressure of 7.7 GPa the maximum shifts to the high temperature region. (Fig. 1).

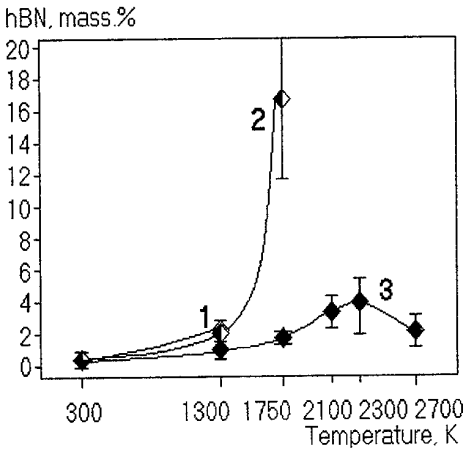


Fig.1. cBN-to-hBN transformation vs. $p$, $T$ parameters of sintering at 2.5 (1), 4.2 (2) and 7.7 (3) GPa.

In sintering of submicron powders, the phase transition is more intensive at the initial stage (up to 1750 K) and terminates earlier, i.e. at a lower temperature in a subsequent stage ($p$ = 7.7 GPa, $T$ = 2100-2700 K) (Fig. 2). Addition of Al to the initial mixture hinders the cBN-hBN transformation below 1750 K and intensifies it at temperatures from 2100 to 2700 K (Fig. 3).

Our experimental data on the effect of the basic factors (temperature and pressure) on the cBN→hBN phase transition (see Fig. 1) do not

contradict the known ideas of the equilibrium line between boron nitride polymorphous modifications and the region of the thermal activation of cBN→hBN and hBN→cBN transformations according to the Corrigan-Bundy phase diagram [2].

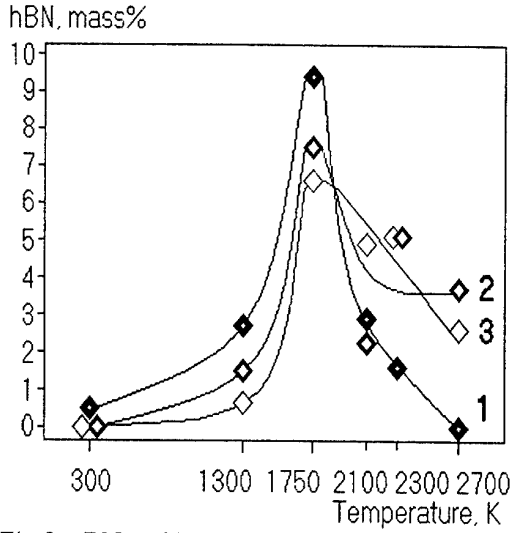


Fig.2. cBN-to-hBN transformation vs. dispersity of the initial cBN powders: 1 – KM 1/0, 2 – KM 2/1, 3 – KM 3/2.

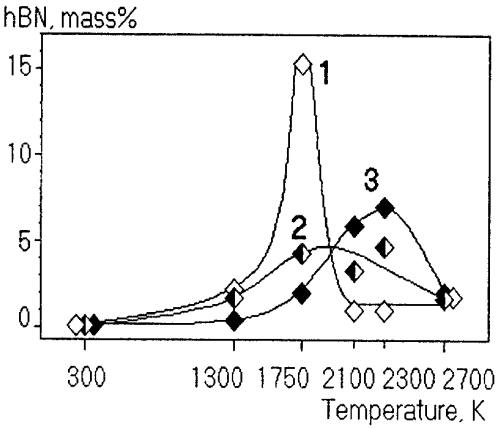


Fig.3. Effect of the amount of the Al addition to the mixture on the cBN-to-hBN transformation: 1 – with no Al addition, 2 – 2% Al and 3 – 10% Al.

The nature of the joint influence of the initial cBN dispersion (see Fig. 2) and aluminum additives to the mixture (see Fig. 3) on the cBN→hBN phase transformation at the early stages of sintering (1300-1750 K) indicates that the transformation is intensified by impurities, which are adsorbed by the cBN powder surface, and that during the reaction sintering aluminum interacts with the impurities. A high reactivity of the aluminum melt with respect to impurities of light elements (O, C) has been the first factor to stabilize the cBN phase in our experiments [3]. The second factor to hinder the cBN-hBN transformation lies in the fact that the presence of the liquid phase levels the gradients of pressures in local volumes making them closer to the average values. Both the factors are better realized with an increase of the contact area between the cBN powder and Al melt. The cBN + Al → AlN + $AlB_2$ reaction is accompanied by the volume and thermal effects $\Delta V$ + -0.047 $cm^3/g$ and $\Delta Q$ = + 2.48 kJ/g, respectively. In a similar manner (with volume and thermal effects to –0.02 $cm^3/g$ and to +3 kJ/g, respectively), reactions proceed to form $AlB_{10}$, $AlB_{12}$ higher borides and $Al_3B_2C_{48}$, $Al_3C_2B_{44}$ and $AlC_4B_{24}$ ternary phases. As the reactions in the liquid phase end and go to the stage of the solid-phase reaction (2100-2700 K), the aluminum nitride content increases and p, T-conditions in the local volumes become corresponding to the thermodynamic stability of the hBN phase (pressure decreases and temperature increases). In the initial stage of sintering, oxygen and carbon play the role of initiators of the cBN-to-hBN transformation, while at the final stage this role is evidently played by AlN, which is a known initiator of cBN synthesis.

References:

[1]. N. P. Bezhenar, S. A. Bozhko, N. N. Belyavina, V. Ya. Markiv, and P. A. Nagorny. Pase composition of polycrystals produced by the reaction sintering of cubic boron nitride with aluminum // J. Superhard Materials – 2002. –No.1, P.37-48.

[2] Corrigan F. R., Bundy F. P. Direct transitions among the allotropic forms of boron nitride at high pressure and temperatures // J. Chem. Phys. – 1975. - **63,** No.9. - P.3812-3820.

[3] Bezhenar N.P. Physicochemical interaction between cubic boron nitride and aluminum in high-pressure sintering // J. Superhard Materials – 1999. – 21, No.2, P.4-11.

# THE INFLUENCE OF BEND – TENSILE STRAINING PARAMETERS ON THE SUBSTRUCTURE OF COLD ROLLED SHEET STEELS

**Vakulenko I.A., Levchenko G.V.**
Iron and steel institute National Akademy of Sience, Dniepropetrovsk, Ukraine

The investigation were carried out on the st 08пс and st 20сп low carbon steels with the thickness of 0,4-0,2 mm after cold rolling by 20 – 60 %. The bend-tensile straining (BTS) was carried out on the hydraulic operated plant with reciprocate movement of the deforming stand [1].

The increase in amount of alternating bending cycles is followed by the progressing loss of strength and metal plasticity growth. Unlike the evolution of Bauschinger effect (when alternate the unaxial loading sign) and in addition to the change in small plastic deformations resistance, it is shown the decrease in ultimate strength. The amount of maximum decrease in yield strength of BTS of st 08пс steel prerolled by 20 –60 % is 12 – 18 % respectively and for st 20сп analogical decrease was 12 –14 %.

The substructure of cold rolled steel investigation shows decreasing the wide of x-ray interference (β) after two alternating bending cycles. .Decrease of β by BTS is a result of dislocations density (ρ) decrease by its introduction into the metal by cold rolling. The estimate of ρ according to the relation [2]:

$$\rho = m\left(\frac{\beta \cdot ctg\,\theta}{b}\right)^2$$

where m – orientation factor, equals to 0,8; θ - angle of x-ray interference; b – Burgers vector.

Shows, that in the examinated steel after any cold rolling deformation decrease ρ about 1,3-1,5 times.

So, after 20 % deformation $\rho_1 = 2{,}8 * 10^8$ $mm^{-2}$, after two cycles BTS $\rho_2 = 1{,}8 * 10^8$ $mm^{-2}$. Relation of $\rho_1/\rho_2$ for $\varepsilon = 20$ % equals to 1,55, and for $\varepsilon = 60$ % this parameter decreases up to 1,35. When the estimation of ρ is the according to strain hardening [3]:

$$\sigma = \sigma_1 + \alpha\mu b\sqrt{\rho}$$

here: σ and $\sigma_1$ – stresses of metal flow before and after BTS respectivety, α - coefficient, μ - displacement module.

Thus, we can suppose that the decrease of common density of dislocations is one of the reasons of decreasing the tensile characteristics of cold steel after BTS. The other cause – experimentally observable easing of the cold deformation texture and growth of the polar density orientations, nonconventional for the given kind of deformation – such as rolling.

As a result of electron microscopy investigation is stated that after 20 % deformation the significant volumes ferrite of metal contain the periodical dislocational structures similar to cellular (fig.1).

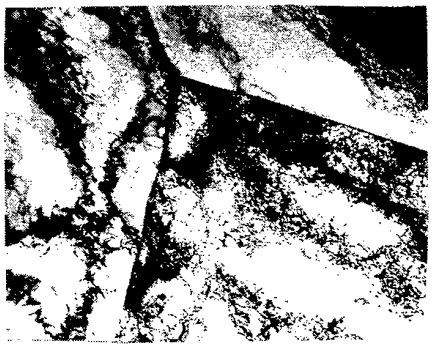

Fig.1. Electron microscope image the dislocation structure of cold rolled steel after 20% deformation (x 19500)

The existence of certain quantity of cells with increased density of dislocations into them shows about noncompleted process of cellular substructure forming. As early as after 2 –4 cycles of BTS the chaotic distribution into separate cells after rolling is changed with appearance the unmonotonity in distribution of dislocation. The cause of that is appearance of stresses from an asymmetric the energy field of dislocations by it moving in straight and back directions. As a result the observe annihilation of dislocations is an effect of turning on a small angles the particular microvolumes causing of shift or forming the new subgrain boundaries. The example of such of subgrain boundary after BTS is a plot A in fig.2.

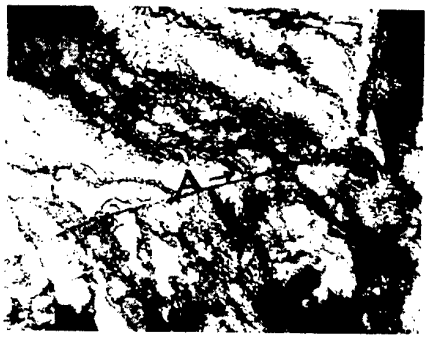


Fig.2. Electron microscope image the dislocation structure after BTS cold rolled steel (x 19500)

Thus, the base of softening process after BTS of cold rolled steel are a rotational effects of substructure elements caused by noncompensated moments of stresses.

References

1. Вакуленко И.А., Богачев Ю.А., Пирогов В.А. Деформирование по схеме изгиб – растяжение холоднокатаных низкоуглеродистых листовых сталей. – Изв. АН СССР. Металлы., 1991, №5, с.155 –159.
2. Миркин Л.И. Справочник по рентгеноструктурному анализу поликристаллов. – М.: ГИФМЛ, 1961,- 863 с.
3. Conrad H. On the mechanism of yeilding and flow in iron. – J. Iron steel Inst., 1961,v 198, part 4, p. 364 - 375.

# ROLE OF THE CRYSTALLINE ELECTRIC FIELD ON THE PHYSICAL PROPERTIES OF $REB_{12}$ COMPOUNDS

**Czopnik A., Shitsevalova N.[(1)], Paderno Yu.[(1)], Krivchikov A.[(2)], Pluzhnikov V.[(2)], Bat'ko I.[(3)], Flachbart K.[(3)]**

W.Trzebiatowski Institute of Low Temperature and Structure Research of PAS, Wroclaw, Poland
[(1)]I.Frantsevich Institute for Problems of Materials Science of NASU, Kiev, Ukraine
[(2)]B.Verkin Institute for Low Temperature Physics and Engineering of NASU, Kharkov, Ukraine
[(3)]Institute of Experimental Physics, SAS, Košice, Slovakia

Rare earth dodecaborides - $REB_{12}$ (RE: Tb÷Lu) crystallize in a cubic *fcc* lattice of $UB_{12}$-type (sp.gr. $Fm3m$-$O_h^5$) which may be considered as a simple cubic closest-packed lattice formed by two framework units: $B_{12}$-cubooctahedrons and metal atoms [1].

$REB_{12}$ compounds exhibit a variety of magnetic properties, which predominantly result from the well-localized 4f-shelll of RE-ions. Diamagnetic $LuB_{12}$ becomes a superconductor below 0.4 K [2], $YbB_{12}$ is a Kondo semiconductor [3], whereas $TbB_{12}$, $DyB_{12}$, $HoB_{12}$, $ErB_{12}$, and $TmB_{12}$ reveal antiferromagnetic (AF) ordering at low temperatures [4, 5]. The indirect exchange interaction of RKKY type was proposed as the dominating mechanism leading to AF [5, 6]. However, Gubbens et al. [7] have pointed to the important role of the crystalline electric field (CEF) for the understanding of magnetic properties of $TmB_{12}$.

CEF represents one of the single-ion interactions that plays a major role in formation of the physical properties associated with 4f-magnetism [8]. In order to determine the role of CEF in magnetic dodecaborides, we have undertaken the study of these compounds, above all of phenomena which are sensitive to the CEF - heat capacity, thermal expansion and electrical resistivity. Here, we will present mainly their analysis in the paramagnetic range, i.e. beyond AF transition. The Neél temperatures of $TbB_{12}$, $DyB_{12}$, $HoB_{12}$, $ErB_{12}$ and $TmB_{12}$ are equal to 22.05 K, 16.35 K, 7.38 K, 6.65 K and 3.28 K, respectively.

As the above mentioned properties are additive functions of several contributions (electron, lattice, magnetic) we have separated the components associated with the CEF - Schottky heat capacity ($C_{Sch}$), magnetic thermal expansion coefficient ($\alpha_m$) and magnetic resistivity ($\rho_m$) - using, respectively, heat capacity, thermal expansion and resistivity data of the diamagnetic reference material $LuB_{12}$, in which the magnetic component is absent.

For measurements we used high-pure sintered $TbB_{12}$ samples and single crystals of $REB_{12}$ (RE = Dy, Ho, Er, Tm, Lu) grown by the crucibleless inductive zone melting in an envelope atmosphere of argon gas. For more details see Ref. [9].

The specific heat between 2.6 and 70 K was measured by a pulse quasi-adiabatic method; details are described in [10]. The temperature dependence of the relative length change ($\Delta l/l$) was measured in the range (5÷200) K by a three-terminal capacitive method. The thermal expansion coefficient is then a result of differentiation of the $\Delta l/l$ *vs* $T$ dependence on $T$. Details are given in [11]. The temperature dependence of resistivity was measured in a $^4$He cryostat in the range (1.6÷300) K using a standard dc four-probe method.

In the Fig. 1 the magnetic components of the $REB_{12}$ heat capacity are presented. Besides peculiarities connected with AF ordering one can see there the falling branches of $C_{Sch}$ for $TbB_{12}$ and $DyB_{12}$, and the increasing ones for $HoB_{12}$, $ErB_{12}$ and $TmB_{12}$ in the paramagnetic range.

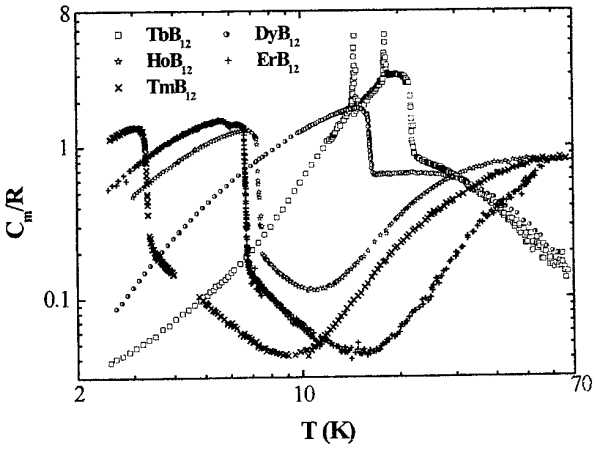


Fig. 1. $C_m$/R *vs* $T$ for $REB_{12}$ (RE: Tb ÷ Tm)

The analysis of $C_{Sch}$ allowed to estimate the CEF parameters and the ground states of RE-ions in $REB_{12}$ crystal field (Table 1). The parameters obtained for $TbB_{12}$, however, are doubted, as under consent between fitting and experimental $C_{Sch}$ curves the experimentally received and estimated ent-

ropies differ considerably. For other dodecaborides the ground states are magnetic, and determine thus their magnetic ordering. For $TmB_{12}$ the neutron study provided similar results [12, 13].

Table 1

The CEF characteristics of $REB_{12}$

| $REB_{12}$ | W (K) | $x$ | The ground state |
|---|---|---|---|
| $TbB_{12}$ | -0.29 | -0.017 | $\Gamma_2$ |
| $DyB_{12}$ | -2.00 | -0.40 | $\Gamma_8^{(3)}$ |
| $HoB_{12}$ | 0.73 | 0.42 | $\Gamma_5^{(1)}$ |
| $ErB_{12}$ | -0.85 | 0.38 | $\Gamma_8^{(3)}$ |
| $TmB_{12}$ | 1.25 | -0.12 | $\Gamma_5^{(1)}$ |

In the Fig. 2 the magnetic thermal expansion coefficients $\alpha_m$ for $HoB_{12}$, $ErB_{12}$ and $TmB_{12}$ are presented. In the paramagnetic region the $\alpha_m$ behavior is complex due to CEF. For $ErB_{12}$ two regions of negative thermal expansion are observed.

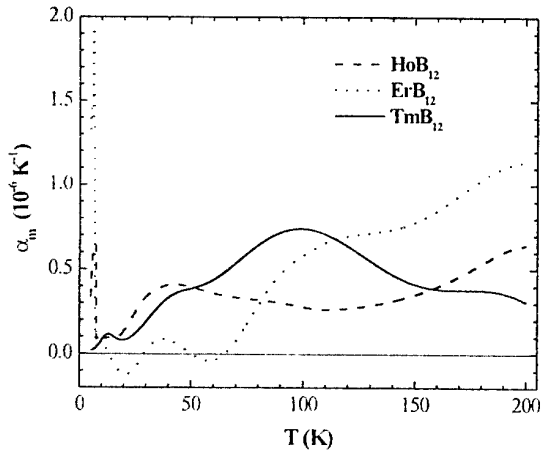


Fig. 2. $\alpha_m$ *vs* $T$ for magnetic $REB_{12}$ (RE: Ho÷Tm)

In case of two-level or quasi two-level systems a direct proportionality between $C_{Sch}$ and $\alpha_m$ exists, and so one can estimate the Grüneisen parameter $\gamma_{CEF}$ for each CEF level [14]. For given magnetic $REB_{12}$, however, such proportionality prevails only in a narrow temperature range (see e.g. Fig. 3). The evaluation of temperatures, at which the contribution from individual CEF levels to $\alpha_m$ or $C_{Sch}$ begins to prove, has shown, that these systems have to be considered as multilevel ones even from (15÷20) K.

The $\alpha_{CEF}$ sign for a corresponding level is defined by the sign of its partial $\gamma_{CEF}$, and the sign of the total $\alpha_m$ is determined by the combination of contributions from all levels. So, an existence of negative regions for $ErB_{12}$ $\alpha_m$ is connected with the predomination of contributions from CEF levels with negative $\gamma_{CEF}$.

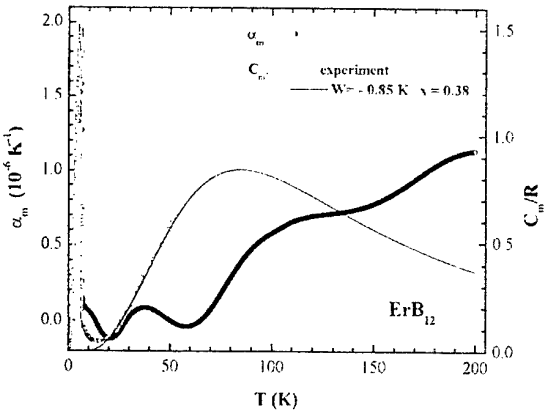


Fig. 3. Temperature dependencies of $\alpha_m$ and $C_m$ for $ErB_{12}$.

The magnetic resistivity $\rho_m$ of $REB_{12}$ (RE: Dy ÷ Tm) is shown in the Fig. 4. In the paramagnetic region $\rho_m$ behaves unusually: for $HoB_{12}$, $ErB_{12}$ and $TmB_{12}$ a Schottky-like maximum is observed, for $DyB_{12}$ a maximum is only slightly indicated.

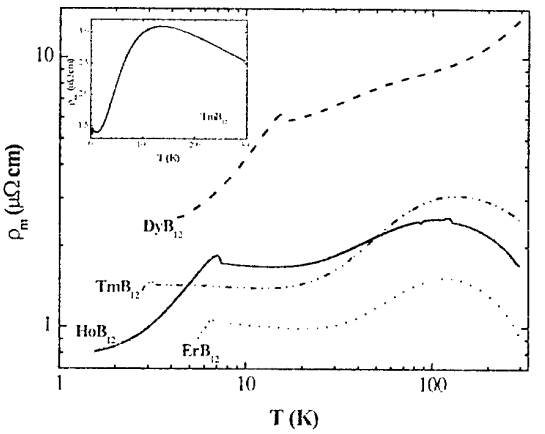


Fig. 4. $\rho_m$ *vs* ln$T$ for magnetic $REB_{12}$. Insert: the magnetic resistivity of $TmB_{12}$ in $\rho_m$ *vs* $T$ axis.

It is known that the interaction of conduction electrons with localized 4f-electrons results into two types of scattering mechanisms, and respectively, into two types of resistivity contributions [15-18]. One of them is connected with the exchange interaction, the second with Coulomb scattering of conduction electrons on the aspherical distribution of the 4f-shell charge. Both contributions – ex-

change and quadrupolar - are positively monotonous functions of temperature, and thus they can't account for the experimental results. A similar $\rho_m(T)$ dependence is usually observed in dense Kondo-systems. But, the energy of the 4f-shell in magnetic dodecaborides is essentially smaller than their Fermi energy $E_F$ (~5 eV [19]), which permits to neglect in this case the effect of the 4f- and conduction electron hybridization. Similar results as in $REB_{12}$ were detected in $TmGa_3$ [20] and $TmIn_3$ [21], both showing a similar 4f-level to $E_F$ relation.

We don't know the mechanism, which would enable to describe the observed $\rho_m$ dependencies. Nevertheless, the difference in the $\rho_m(T)$ behavior for various dodecaborides may be qualitatively explained using the above information about CEF levels. As the ground state of $HoB_{12}$ and $TmB_{12}$ is the same - $\Gamma_5^{(1)}$, a qualitative comparison of their $\rho_m(T)$ maxima positions (108 K and 133 K) and energies of the first excited levels (63.3 K and 78.5 K) may be reasonable. And indeed, the larger splitting $\Delta E$ (78.5 K) for $TmB_{12}$ is related to the higher temperature of the $\rho_m$ maximum (133 K).

The total splitting for $HoB_{12}$ is equal to 416 K, for $TmB_{12}$ - 337 K. The possible scheme of CEF level splitting for $DyB_{12}$ can be displayed as $\Gamma_8^{(3)}(0) \rightarrow \Gamma_8^{(2)}(53.9\ K) \rightarrow \Gamma_8^{(1)}(594\ K) \rightarrow \Gamma_6(605\ K) \rightarrow \Gamma_7(676\ K)$, i.e. the energy of the first excited level for $DyB_{12}$ is lower than the same energy of other magnetic dodecaborides, but the total splitting for it is more essential. These results agree with the slightly indicated $\rho_m$ maximum at ~50 K and with the continuing monotonous rise of $\rho_m$ for $DyB_{12}$ at higher temperatures.

Thus, we have shown the importance of the CEF on formation of the physical properties of $REB_{12}$ compounds. We have estimated the CEF parameters, determined the ground state of RE-ions, and proposed the corresponding splitting schemes. Furthermore, we qualitatively explained the temperature dependence of their magnetic resistivity in the paramagnetic range. The obtained CEF parameters are needed to be confirmed by direct methods as it has been done for $TmB_{12}$. The results of the magnetic electrical resistivity demand the development of a corresponding model.

This work was supported by National Academy of Sciences of Ukraine under contract 1.6.2.7-98, and by the Slovak Agency VEGA under contracts 2-1168-01 and 2-3195-23.

REFERENCES

1. Gmellin Handbook of Inorganic Chemistry. Compounds with Boron. Vol. C11a, System 39. Ed. H.Bergman. Springer-Verlag: Berlin-Heidelberg-N.-Y.-London-Paris-Tokyo. 1990, pp.275.

2. I.Bat'ko, M.Bat'kova, K.Flachbart, V.Filippov, Yu.B.Paderno, N.Yu.Shicevalova, Tm. Wagner, J. Alloys & Compounds **217**, L1 (1995).

3. M.Kasaya, F.Iga, M.Takigawa and T.Kasuya, J. Magn. Magn. Mater. **47&48**, 429 (1985).

4. L.L.Moiseenko, Ukr. Phys. J. **30**, 1181 (1985).

5. S.Gabani, I.Bat'ko, K.Flachbart, T.Herrmannsdörfer, R.König, Y.Paderno, and N.Shitsevalova, J. Magn. Magn. Mater.**207**, 131 (1999).

6. L.L.Moiseenko, V.V.Odintsov, J. Less-Common Met. **67**, 237 (1979).

7. P.C.M.Gubbens, A.M.van der Kraan, K.H.J.Bushow, Physica B **130**, 412 (1985).

8. D.Gignoux, D.Schmitt, in: K.A.Gschneidner Jr., L.Eyring (Eds.), Handbook on the Physics and Chemistry of Rare Earths, Vol. 20, Elsevier, Amsterdam, 1995, p. 239, Chapter 138.

9. Yu.Paderno, V.Filippov, and N.Shitsevalova, in: Eds. D.Emin, T.L.Aselage et al. (Eds.), Boron-Rich Solids, AIP Conference Proc., Vol. 230, Albuquerque, 1991, p. 460.

10. A.I.Krivchikov, B.Ya.Gorodilov, A.Czopnik. Proc. of Conf. Low Temperature Thermometry and Dynamic Temperature Measurement. p. V7. Wroclaw, 1997.

11. A.Czopnik, N.Shitsevalova, A.Pietraszko, V.Pluzhnikov, Yu.Paderno, A.Krivchikov, be publ.

12 A.Murasik, A.Czopnik, N.Shitsevalova, Y.Paderno and L.Keller, IAE Annual Report 1999, IAE, Warsaw, 69 (1999).

13. A.Murasik, A.Czopnik, L.Keller, N.Shitsevalova, and Y.Paderno, Phys. Stat. Sol. (b) **221,** R7 (2000).

14. T.H.K.Barron, J.G.Collins, G.K.White, Advances in Physics **29**, 609 (1980).

15. N.H.Andersen, P.E.Gregers-Hansen, E Holm. and H.Smith, Phys. Rev. Lett. **32**, 1321 (1974).

16. Z.Fisk, Solid State Commun.18, 221 (1976).

17. Z.Fisk and D.C.Johnston, Solid State Commun. **22**, 359 (1977).

18. N.H.Andersen, J. de Physique. **40**, Coll. C5, suppl. au №5, C5-118 (1979).

19. F.Iga, Y.Takakuwa, T.Takahashi, M.Kasaya, T.Kasuya, T.Sugawa, Solid State Commun. **50**, 903(1984).

20. Z.Kletowski, P.J.Markowski and A.Czopnik, Solid State Commun.65, 593 (1988).

21. A.Czopnik, private communication.

# MATERIALS AT THE FRONTIER OF CENTURIES

**Levina D., Chernyshev L.**
Frantsevich Institute for Problems of Materials Science of NASU, Kyiv, Ukraine

XX century can be called as a golden one for the materials science. Rapid development of technology and industry has demanded new structural and functional materials having high level of service properties and their unique combination, which are able to operate in aggressive media, vacuum, under increased load, at high and low temperatures, and other extremal conditions.

Every scientist can have his own viewpoint with respect to the most important event in the history of materials science in XX century, so we state here our version. It is impossible to consider all achievements of last century within one brief report. We will concentrate only at principal and revolutionary from our viewpoint.

Great hopes of the mankind are connected with possible use in practice the phenomenon of superconductive state of materials, which was discovered by Camerling-Onnes in 1911. The wide use of this phenomenon was hindered by the necessity of application very low temperatures close to that of liquid helium (4.2K). Last decades of XX century were marked with the discovery of so called high-temperature superconductors, in which series the first was ceramics based on Cu-La-Ba system with the transition temperature to superconductive state 30...35K. The scientists from many countries have strongly investigated the possibility to design superconductors having higher transition temperatures to the superconducting state. The results obtained now allow for hope that high-temperature superconductors for practical applications will be designed.

As a prerequisite for development of electronics and computational technology - the field which determined to a considerable extent the progress achieved by mankind in XX century - was the production of superpure semiconductive single and polycrystalline materials in which the concentration of harmful impurities was one atom per billion. The reliability, diminutiveness, fast-action, good economical and service characteristics of most (unless of all) devices of micro-, opto-, bio- and quantum electronics are assured by the use of contemporary materials with unique properties.

Mechanical processing of new (and also well known old) materials requires making use of tool materials with high hardness and strength. The development in Germany in twenties the material consisting of cobalt binder and tungsten carbide particles initiated the use of materials of new kind, so called "hardalloys". Such alloys made a revolution in the cutting technology enabling to considerably (by several times) increase the cutting speed and giving the possibility to process hard metal and non-metal (glass, porcelain etc.) materials with machines.

In 1953 Liander and Loodblud have manufactured for the first time an artificial diamond, based on fundamental researches of P.Y.Bridgeman, and this made it possible to design unique the hardest tools for processing hard and superhard materials. At present, not only fine polycrystalline and rather large single crystals of artificial diamond are produced. However, it should be pointed out that diamond cutting tools are little suitable for processing such materials as cast irons and steels, since high temperatures develop at the tool surface resulting in degradation of diamond.

The fundamental researches of the mechanisms for transformation graphite-like phases in diamond-like ones have resulted in discovery of a number of high-pressure phases. Among them only wurtzite boron nitride (known as hexanite, elbor, cubanite) has found its application in the second half of century in making superhard tools operating in hazard conditions of processing hardened and high-speed cutting steels, high-strength cast iron, hardalloys, wear-resistant fused-over materials.

To meet the requirements of aviation, cosmonautics, nuclear energy making, transport-machine building, and other branches of new techniques, the works aimed to development materials with special properties have been initiated in XX century. Among those are so called "smart" materials, which respond to change in outside influence. To such "smart" materials are first of all

related the discovered in 1949 in Ukraine by G.V.Kurdyumov and L.G.Handros materials having the effect of shape memory, i.e., the ability to restore upon heating the original shape which was changed by deformation. As an example of using these materials could be the unfolding of large (up to 15 m) space constructions after delivering them at orbit in folded, compact state.

A promising discovery was the superplasticity of materials revealed upon studying the mechanisms of plastic deformation. The yield strength of very fine-grained material deformed at very high rate at the temperatures close to 0,3-0,4 $T_{melt}$ was shown to drastically decrease. This finding gives hope for solving very complicated problem, namely the mechanical processing of hard and superhard materials. It is necessary to design new technologies for high-speed deformation and appropriate equipment.

For last 10-15 years the term "nanostructural system" has been widely used in materials science. To those are related the systems in which the specific dimensions of structure elements are in the range from 1 to 100 nm. It was asserted that nanostructural state can ensure the principally new level of properties of both structural and functional materials.

Recently the so-called quasicrystals have been discovered. It is impossible to describe their structure with lattice consisting of periodic cells because it is characterized by rotational 5- or 7-fold symmetry, which is forbidden by classical crystallography. Due to their low friction coefficient and high wear resistance, high hardness and compression strength, the quasicrystalline alloys have found wide application for manufacturing parts of friction assemblies and as structural materials. Low specific thermal and electrical conductance of quasicrystals open the possibility to prepare thin films from them (with the thickness from several thousand nanometers to a few hundred micrometers) for the purposes of modern electronics.

To the materials, which were unknown few decades ago, the fullerites should be related. These are the molecular crystals with high strength and low specific density, which are promising as reinforcing materials for high-strength composites and also as molecular dielectrics for micro-electronics.This substance is the new third form of pure carbon. At present, a number of fullerites are known consisting of molecules-fullerenes of different sizes: $C_{28}$, $C_{32}$, $C_{60}$, $C_{240}$, $C_{540}$, $C_{960}$.

In the second half of the last century the attention of scientists has been attracted by so-called "progressive" ceramics. Along with low specific weight, high hardness and chemical inertness it retains its high strength at temperatures up to 1500 °C. In order to widely use those ceramics, especially as structural material the scientists worldwide work for increase its reliability and stability of properties.

The materials science of composite materials has been developed strongly in XX century. As a strengthening phase, the metal and ceramic powders, metal, mineral and carbon fibers and wires are introduced in metal, polymeric, ceramic or carbon matrix. Just with composites the amazing combination of properties are possible, which can not be achieved in other materials. Such composites as hardalloys, pseudoalloys, dispersion - strengthened metals are widely used now.

An intense interest has arose last years from so-called "in-situ" composites which are prepared by natural way upon crystallizing eutectics. For instance, the alloys of eutectic type based on Ti-Si system have structure of plastic titanium matrix strengthened with eutectic formations based on silicides and other intermediate phases of ceramic type, they are able to perform under dynamic loads, have high heat resistance and fracture toughness at 700-850 °C.

Certainly, the materials science will as usual be actively response for challenges of time in XXI century. Well known materials will be improved and new materials will be designed, that will support the creation of new techniques.

# NEW DEVELOPMENTS IN MATERIALS ENGINEERING: FROM COORDINATION POLYOXOMETALATE COMPOUNDS TO SEMICONDUCTING THIN FILMS AND COVERINGS

**Lisnyak V.V., Stus N.V., Sudavtzova V.S., Popovich P.[1], Slobodyanik N.S.**

Chemical Department of Kyiv National Taras Shevchenko University,
64 Volodymyrska Str., 01033 Kyiv, Ukraine
[1] Carls Eberhard Tuebingen universität, Universitätstraße 10, Tuebingen, Deutschland

Design and manufacturing of industrial semiconducting materials for novel devices of various application such as: photovoltaic convertors, sensors, sensitive pH electrodes, semiconductor thin films and covering are off special interest.

Synthesis of complex oxide materials was carried out using polytungstenoxometalates of monovalent metal (Li, Na, K, Ag), and $NH_4^+$ or organic ammines with Keggine structure as precursores. First soluble in the nonaqeuse solutant complexes were painted on the various substrates and dried in vacuum. Then thin films solids or in some cases a covering formed by complex oxide of tungsten were obtained. Several techniques were applied: reductive heating in a ultra-thin hydrogen beam; sample treatment using microwave or gamma irradiation. The special attention was given to synthesis of thin films and novel semiconductive coverings based on tungsten-phosphate bronzes [1-3].

Elemental content was determined by the electron probe microanalysis (Jeol Microprobe-1500). The covers and thin films were studied by XRD (full profile analysis of diffraction pattern). Surface study were performed by XPS. NMR 31P spectra were recorded on Bruker instrument in University of Paris. Magnetic susceptibility measurement provided on SQUID apparatures at 50 – 100 K. DSC, DTA and thermal gravimetrical analysis of initial complexes decomposition was carried out using Calvet type caloremeter and Paulik-Erdei derivatograph. The electrical resistance *vs.* temperature was measured by standard two-probe technique using General Electric applience.

Series of self-obtained monophosphate tungsten bronzes with hexagonal tunnels ($MTB_H$) $M_x(WO_3)_{2m}(PO_2)_4$, (M=Li, Na, K, Ag, m is integer) have been synthesised, the series representatives differ by W-O layer thickness, which is equal to m.

The lithium members of $MPTB_H$ have not been reported till present time. The $MPTB_H$ [2,3] usually posses 2D metallic conductivity due to presence of $ReO_3$-type isolated layers formed by corner sharing $WO_6$ octahedra. The semimetallic properties are attributed to delocalized electrons in partially filled $\pi^*$ conduction band formed by the overlap of tungsten $t_{2g}$-5d and oxygen $\pi$-2p orbitals. The conductivity as well as resistivity anomalies, electronic instabilities and charge-density-wave properties of $MPTB_H$ phases are connected with peculiarities of their framework construction according to Whangbo-Canadell theory [4].

The $ReO_3$-type connected ribbons can be distinguished in the $MTB_H$ frameworks. For m=6 and m=4 representatives of the $MTB_H$ series the ribbon composition is defined as $W_6O_{26}$ and $W_4O_{18}$, respectively (see Fig.1).

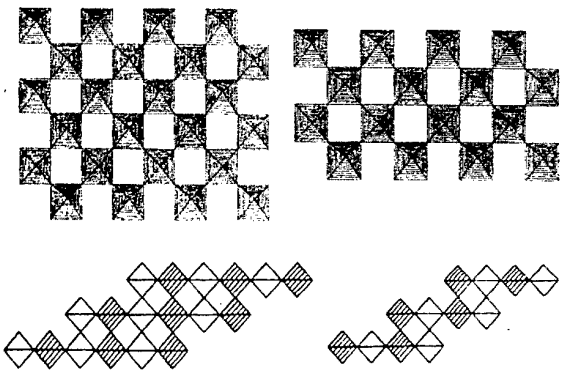

Fig.1. $ReO_3$-type connected ribbons and staircase-like layer for $M_x(WO_3)_{2m}(PO_2)_4$ m=6, 4; view on [101] and [010].

The first tungsten octahedron of every ribbon shares its axial oxygen atom with the third tungsten octahedron of the adjacent ribbon. The

staircase-like layer with each $W_6O_{26}$ or $W_4O_{18}$ ribbon as a step is formed. Ribbons $W_6O_{26}$ and $W_4O_{18}$ and related staircase-like layers are represented in fig 1 (left and right pannel).

The preferable orientation of $MTB_H$ detected by XRD is [010] direction normal to the substrate surface (see Fig. 2). Thus high-conductive perovskite-like layers are perpendicular to substrate surface, obtained thin films are one-dimensional conductors.

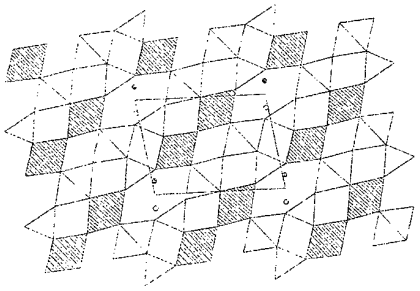

Fig.2. Projection of $M_x(WO_3)_{2m}(PO_2)_4$ m= 4; crystal structure on [010]

For measured $MPTB_H$ MAS $^{31}P$ NMR spectra only one type of a signal is observed, which is characteristic for isolated ortho-phosphate groups. The signal displacement in area of low fields testifies the assumption about phosphorus atom participation in electronic density exchange with $\{W_{2m}O_{6m+8}\}$ layers at charge super-exchange interaction.

On the base of surface study by XPS and spectra simulation, valent state of tungsten atoms was suggested.

The wide interval of conductivity values $10^{-5}$-$10^{4}$ Ohm×cm$^{-1}$ and high anisotropy (2-3 orders of magnitude) are characteristic for obtained thin films series. The considerable influence of substrate type on covering electrical characteristics has been observed.

Typically the representatives of series with m < 6 are quasi-metals. $MPTB_H$ with m > 8 are classic semiconductors. It has been determined, that conductivity of lithium containing $MPTB_H$ is higher, than conductivity of other representatives, caused by the influence of monovalent atom dimensions. For members with m=6-10 the conductivity is on the order below than for $MPTB_H$ with m=4-5. It is connected with decrease of current carriers quantity and by layer thickness enlargement constructed of $WO_6$ groups, which led to charge density redistribution.

The conductivity value for obtaned thin film increases by two or three orders of magnitude at wide temperature interval. The part of lgσ vs T dependence contradict with Arrhenius eqn. and deals with alkali metal fast ionic-transport contribution realized by cross-jumping mechanism between alkaline metal ions position. The low temperature part of dependence is typical for metallic and semimetallic systems.

Using complex polyoxometalates synthetic rout and controlled reductive decomposition the thin films and novel covering of tungsten phosphate bronzes were obtained. Synthesised thin films posses quasi one–dimensional properties, which never been obtained by routine solid-state synthesis. Materials can be used for novel semiconductor design, besides as sensors for portative chromatograph [5] and model objects for surface phenomena study.

[1] B. Domenges, M. Hervieu M, B., Raveau. *Acta crystallogr.* **1990**, *B46*, 610.
[2] B. Domenges, M. Hervieu, and B. Raveau. *J. Solid State Chem.* **1988**, *72*, 155.
[3] J.P. Giroult, M. Goreaud, Ph. Labbe, B. Raveau. *Acta crystallogr.* **1981**, *B37*, 1163.
[4] E. Canadell, M-H. Whangbo, and I. El-I. Rachidi. *Inorg. Chem.* **1990**, *29*, 3871.
[5] V.V. Lisnyak, N.S. Slobodyanik, V.K.Yatsimirsky *at el.* in A. Corma, F.V. Melo (Eds.), *Studies in Surface Science and Catalysis*, Elsevier Science, B.V. **2000**, *130*, 3870.

# СИНТЕЗ СУБМИКРОННЫХ ПЛЕНОЧНЫХ СТРУКТУР ПОД ВОЗДЕЙСТВИЕМ ФРАКТАЛЬНО-МАТРИЧНЫХ ТРАНСПАРАНТОВ

**Серов И.Н., Алексейцев А.В., Бельская Г.Н., Бонштедт Б.Э.[(1)], Егорова Н.Б., Марголин В.И.[(2)], Потсар Н.А.[(2)]**

Исследовательский центр Фонда развития новых медицинских технологий "Айрэс", Санкт-Петербург, Россия

[(1)]ВНЦ ГОИ им. С.И. Вавилова, Санкт-Петербург, Россия

[(2)]Санкт-Петербургский государственный электротехнический университет "ЛЭТИ", Санкт-Петербург, Россия

Развитие субмикронной технологии и нанотехнологии приводят к необходимости разработки новых методик получения тонкопленочных покрытий, что связано с жесткими требованиями к чистоте и структурному совершенству материалов. Те недостатки, с которыми можно мириться в объемных образцах, совершенно нетерпимы в наноразмерной пленке толщиной в несколько атомных слоев, поскольку примеси, инородные включения или структурные несовершенства совершенно изменяют ее физические и эксплуатационные свойства.

Однако для получения наноразмерных и наноструктурных пленок особую важность имеет даже не столько решение проблем чистоты материалов, сколько возможность создания наноразмерного изображения на поверхности наноразмерной пленки. Для микроэлектроники структурирование состояло в создании изображения на поверхности пленки и последующем переносе рисунка на структуру пленки (удаление материала). Для нанотехнологии единственным путем структурирования является создание пленок, состоящих из прецизионно локализованных групп атомов и в идеале, из отдельных строго и упорядоченно локализованных атомов. Этого можно в принципе добиться применением прецизионных методов субмикронной и нанотехнологии (электронная литография сканирующим пучком, туннельно-зондовые технологии).

К сожалению, они являются практически недостижимыми, т.к. являются методами индивидуальной обработки, что приводит к практически нереализуемым затратам времени на процесс создания пленки. Поэтому представляется целесообразным обратиться к применению групповых методов обработки, позволяющих за один цикл обрабатывать значительные площади подложки и создавать регулярную упорядоченную структуру одновременно на всей площади обрабатываемого образца.

Наиболее привлекательным с практической и технологической точек зрения является создание в соответствии с процессами самоорганизации и самокоррекции вновь получаемых наноразмерных структур на поверхности подложки максимально свободного от примесей и структурных несовершенств переходного тонкопленочного или толстопленочного слоя и реализация на его поверхности наноразмерной и наноструктурированной пленки.

Анализ имеющихся работ по созданию структурированных объектов, в том числе и тонких пленок показывает, что крайне важным является тот факт, что все приведенные эксперименты посвящены взаимодействию с веществом физических явлений или агентов, не находящихся в состоянии резонансного взаимодействия с исследуемой или обрабатываемой структурой, а ограничивающихся простыми энергетическими воздействиями. Переход к резонансным явлениям открывает, по нашему мнению совершенно новые перспективы в области материаловедения.

Особенно привлекательным для экспериментов является метод магнетронного ионного распыления, позволяющий получать однородные тонкие пленки с локализацией атомов в точке их осаждения. При этом получаемая пленка практически повторяет структуру подложки.

Поскольку пространственную структуру любого объекта на атомарном или молекулярном уровне можно представить как систему волновых пакетов или как некую волновую структуру, обладающую строгой периодичностью, то эта периодичность будет

однозначно связана со структурными характеристиками решетки материала.

Поскольку структурный каркас кристаллической решетки можно представить как некий полевой каркас, статическое поле которого может быть топологически выражено, а топология поля агента и структуры кристаллической матрицы должны быть подобны, причем в соответствии с неким масштабным коэффициентом, то таковым достаточно универсальным агентом представляется соответствующим образом структурированное электромагнитное поле.

Предлагаемый подход заключается в создании условий для резонансного воздействия электромагнитного поля на материал таким образом, чтобы в результате генерации пространственных структур воздействующего агента активировать в структуре обрабатываемого объекта внутриструктурный резонанс его бездефектных базовых единиц и, следовательно, - процесс самокоррекции.

Результат подобного взаимодействия будет зависеть от точности топологического соответствия структуры поля и структуры объекта в случае масштабированного соответствия.

Однако обычное облучение ЭМ полем с резонансной частотой не приведет к самосогласованию и самокоррекции структуры, т.к. поле необходимо информационно структурировать. Чисто резонансное взаимодействие приведет только к неупорядоченному поглощению энергии и возможному хаотическому структурированию. Частотное и временное структурирование ЭМ поля не позволяет добиться нужного результата, поэтому остается только возможность пространственного структурирования ЭМ поля.

Целесообразно для информационного структурирования резонансного электромагнитного поля воспользоваться разработанными и изготовляемыми фондом Айрэс фрактально-матричными транспарантами, представляющими собой фотошаблон с нанесенной фрактально-матричной топологией и являющимися геометрически синтезированными голограммами с размерами штриха к настоящему времени 1мкм. Основной задачей является получение так называемого графического поля, имеющего внутриструктурную динамику, но при этом сама его структура остается статической и имеет конструкцию, которая может быть выражена графически.

Проведенные эксперименты по получению субмикронных тонких пленок на поверхности оптически полированных пластин кремния показали, что имеется однозначно выраженное влияние использованных для целей структурирования получаемых пленок фрактально матричных транспарантов «Айрэс».

Поэтому можно заключить, что единственным реальным путем создания наноразмерной и наноструктурированной пленки является использование процессов самоорганизации и самокоррекции образуемых структур под воздействием информационно-структурированного электромагнитного поля либо в процессе её модификации и структурной перестройки.

# О ПРОГНОЗИРОВАНИИ ПРОЧНОСТИ ЧАСТИЦ ЖЕЛЕЗНЫХ ПОРОШКОВ И СПЕЧЕННЫХ МАТЕРИЛОВ

**В. Я. Буланов**

Государственное учреждение Институт металлургии УрО РАН, Екатеринбург, Россия.

При разработке технологических процессов изготовления спеченных деталей с требуемыми физико-механическими свойствами необходимо знать физические характеристики как частиц исходного материала, так и спеченного ансамбля из них и их возможные предельные значения.

Автором сделана попытка определения пределов прочности и текучести различных зон частиц железных порошков и спеченных материалов на их основе, используя метод микротвердости [1].

На первом этапе работы ограничились определением микротвердости отдельных частиц порошков, считая их свободными от каких-либо примесей (искусственных или природных), для чего использовали функциональную зависимость [1-3]:

$$H_\mu = 2{,}92\left(\alpha k \frac{\omega_a \omega_k}{d^2}\beta\gamma\right)^3, \qquad (1)$$

где α - коэффициент пропорциональности, учитывающий силы отталкивания между атомами и зависящий от валентного типа соединения (соотношения валентности аниона и катиона); k – коэффициент относительной прочности химической связи, непосредственно зависящий от степени ковалентности; $\omega_k$, $\omega_a$ – валентности катиона и аниона; d – межатомное расстояние, Å; β - коэффициент ослабления прочности связи между атомами, обусловленный не принимающими участие в химической связи валентными s или d электронами; γ - коэффициент упаковки атомов, определяемый их координационным числом. Данная формула справедлива для бездефектных частиц.

Микротвердость многокомпонентного материала может быть рассчитана по фазовому составу на основании закона аддитивности по микротвердости отдельных составляющих:

$$H_{\mu_{\text{сплав}}} = \sum_{i=1}^{n} H_{\mu_i} a_i, \qquad (2)$$

где $H_{\mu_i}$ - микротвердость фазовой составляющей (феррита, цементита, гематита, магнетита), рассчитанная по формуле (1); $a_i$ – относительное содержание тех фазовых составляющих в объеме материала порошка.

Известно, что прочность материала зависит от его твердости. Для определения характеристик прочности частиц порошка в зависимости от их твердости воспользуемся уравнениями, полученными в работах [5,6].

Известно, что метод микротвердости отличается от испытания на твердость по методу Виккерса только меньшими нагрузками [5], и поэтому твердость и Виккерсу и микротвердость без учета упругого восстановления диагонали выражаются теми же числами. Кроме того, в определенном интервале HV ≤ 400 твердость по Виккерсу равна твердости по Бринелю [5], поэтому, очевидно, можно записать :

$$HV = H_\mu = HB. \qquad (5)$$

С учетом выражения (5) возможно использование зависимости между твердостью по Бринелю и другими механическими характеристиками

$$\sigma_T = 0{,}333HB = 0{,}333H_\mu, \qquad (6)$$

$$\sigma_b = 0{,}36HB = 0{,}36H_\mu \qquad (7)$$

Отсюда, учитывая выражения (1) и (2), получим

$$\sigma_{b_i} = 1{,}05\left(\alpha_1 k_1 \frac{\omega_k \omega_a}{2}\beta\gamma\right)^3, \qquad (8)$$

$$\sigma_{T_i} = 0{,}972\left(\alpha_1 k_1 \frac{\omega_k \omega_a}{2}\beta\gamma\right)^3, \qquad (9)$$

$$\sigma_{b_\Sigma} = 0{.}36\sum_{i=1}^{n} H_{\mu_i} a_i, \qquad (10)$$

$$\sigma_{T_\Sigma} = 0{,}333\sum_{i=1}^{n} H_{\mu_i} a_i. \qquad (11)$$

Сравнение полученных результатов показывает удовлетворительное согласие предела прочности, полученное по различным зависимостям (3) - (10).

Характеристики прочности, полученные для железных порошков по выражениям (8) - (10), очевидно, справедливы для бездефектного материала и значительно превышают прочность реальных частиц.

Механические характеристики материалов значительно ниже прочности отдельных исходных частиц, что говорит о наличии резерва прочности, заложенного в исходных частицах ("эффект микропрочности"), при реализации которого возможно значительное увеличение прочности материалов.

С увеличением прочности частиц путем их легирования возрастает и прочность спеченных материалов на их основе.

На основании вышеизложенного можно высказать следующее:

1. Полученные выражения (2), (6)-(11) позволяют с достаточной точностью оценить твердость и прочность материала частиц железного порошка.

2. Материал частиц железного порошка имеет прочность выше прочности материала, спеченного из ансамбля этих же частиц.

3. Частицы легированного железного порошка и материалы на их основе имеют большую прочность по сравнению с нелегированными.

4. Целесообразна разработка методов получения материалов повышенной прочности с использованием выявленного "эффекта микропрочности" частиц порошков.

Литература


1. *Хрущев М.М.* Докл. АН СССР. 1950. Т. 72. № 4. С. 40-55.
2. *Поваренных А.С.* Кристаллохимическая теория твердости. В кн.: Методы испытаний и микротвердость. Приборы. М.: Наука, 1965. С. 50-55.
3. *Буланов В.Я., Рабинович И.Б.* К расчету режимов прессования металлокерамических материалов. В кн.: Материалы семинара Секции порошковой металлургии. Челябинск, Южно-Уральское из-во, 1970. С. 41-45.
4. *Хрущев М.М.* Проблемы унификации оценки твердости. Тр. Метрологических институтов комитета стандартов. М., Л.: Изд-во стандартов, 1967, вып. 91(151). С. 21-27.
5. *Шахтер В.Я.* Завод.лаборатория. 1953. № 4. С. 462-464.
6. *Варнелло В.В., Пастухов А.А.* Микротвердость как метод определения констант пластичности структурных составляющих сплавов. В кн.: Методы испытаний на микротвердость. Приборы. М.: Наука, 1965. С. 165-170.
7. *Hutting G.F.* – Arch. Metalk. 1948. V. 2. P. 93-99.
8. *Hutting G.F.* – Jn: Schwab G.M. Handbuch der Katalise. Wen. Springer. 1943. V. 6. P. 318-577.
9. *Friche R.*- Haturwiss. Rdsch. 1948. V. 1. P. 9.

# SECTION III. SPECIFIC TECHNOLOGIES

# A WAYS FOR IMPROVING QUALITY OF POWDER TOOL STEELS

**Poznyak L.A., Ulshin V.I., Tychomyrov S.V., Sorokin U.V.**
Institute for Problems of Materials Science
National Academy of Sciences of the Ukraine, Kiev, Ukraine

The possibilities of improving of operational properties of a carbide hardened tool due to alloying are now practically depleted. The further increase of tool service life can be done only by application in manufacture of high-alloyed tool steels: modifying and microalloying, special ways of smelting, treatment outside of the furnace and also application of new powder metallurgical practices including Osprey, that provides improvement of microstructure and properties.

Distinctive feature of powder steels obtained by dispersion of liquid metal is high speed of a crystallization of a powder ($10^3 - 10^5$ °C/sec.). Due to this it is possible to obtain structure completely distinct from structures formed at low solidification rates of liquid metal in ingots.

Proceeding from this, in manufacturing of powders of a high-speed steel of the grade M3 the decision was made to combine overheating technology of a melt and technology of gas dispersion. The choice of temperature of a melt overheating is proved by presence of a hysteresis of properties (density, viscosity etc.) in overheating it up to certain temperature higher than a liquidus temperature ($T_l$) for the given steel grade. The melt thus becomes more homogeneous. Temperature of a melt has been lowered up to 1580-1600°C before dispersion. Dispersion of a melt of steel M3 was carried out by nitrogen at pressure 0.8 MPa. The shape of a powder is mainly spherical in a particle-size distribution -630 +50 μm. The particles of more then 630 μm size had less than 3 % of blanket mass, fractions with the size less 100 μm were about 52 %, and fractions by the size -630+500μm were about 6 % (Table 1).

Table 1. Technological characteristics of powders and powder compacts from steel M3.

| № | The technology of powders preparation | Fraction % | |
|---|---|---|---|
| | | <100μm | >500μm |
| 1 | Usual | 45,0 | 7,0 |
| 2 | With overheating of a melt | 52,0 | 6,0 |

Continuation of Table 1

| Density, g/cm³ (%) | | | | |
|---|---|---|---|---|
| Bulk | Pressing | Compression, (%) | Sintering | Shrinkage, (%) |
| 4,6 (57) | 6,3 (78) | 23 | 6,4 (79) | 1,0 |
| 5,0 (62) | 6,4 (79) | 17 | 6,9 (85) | 6,0 |

The powders of steel M3 obtain by usual technology of dispersion at 1580-1600°C contained 45 % of particles with the size <100μm and 7 % with the size –630+500 μm. It follows from above, that the homogenization and thermodynamic stabilization of a melt displaces a particle-size distribution -630+100 μm towards finer fractions in comparison with usual dispersion.

The photos of microstructures of a powder of high-speed steel M3 without overheating and with overheating of a melt are shown in Fig. 1.

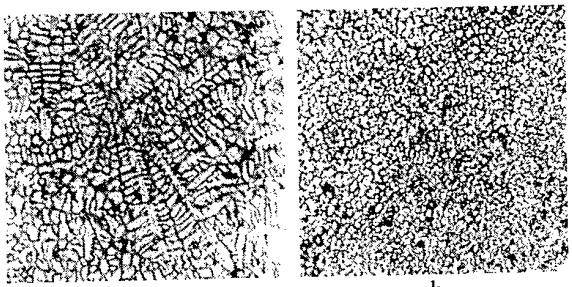

a b

Fig. 1. Structure of a powder of steel M3 (x1000):
a - usual dispersion;
b - with overheating of a melt before dispersion.

The dendrite-cellular structure is characteristic for usual dispersion, while for dispersion with overheating - cellular structure with a high degree of uniformity and finely - dispersed equiaxial grains representing a strongly supersaturated (metastable) solid solution with practically complete degeneration of eutectic

carbides on boundaries of granular structure, as we see from Fig. 1.

The technological characteristics of powders and powder compacts from a high-speed steel M3 after sowing, pressing and sintering are given in the Table 1.

Compacts from powders were obtained by static pressing in a floating lower die at loading 800-900MPa. The sintering was carried out in a vacuum furnace at 1180°C for 1 hour.

The solidification shrinkage at sintering of tests pieces fabricated from powders with overheating is equal to 6 %. It is determined by difficult kinetics and sequence of transformation of a supersaturated solid solution (metastable structures): a structural relaxation, lamination, dissolution, crystallization and growth of a grains. Thus driving forces of these processes are: a fluctuation of chemical composition arising in decomposition of strongly supersaturated metastable solid solutions and excess of grain-boundary energy.

The testing results on resistance of end milling cutters by a diameter 10mm from steel M3 at milling of mortises in blanks from a stainless steel such as S 32100 have shown, that the resistance of steel fabricated from powders with application overheating of a melt is 2,5 times higher than that of standards powder steel M3-PM.

The development of technology for making blanks with the given shape by a method of dispersion by gas of liquid metal and deposition of a jet of liquid and solid - liquid drops (particles) on a substrate (OSPREY-process) was caused by problems of pollution of alloys by oxides of powders and also with the purpose to speed up the whole process of manufacturing alloys, as it excludes a lot of power-intensive operations, such as: dispersal of a powder, annealing, degasification of capsules, cold hydrostatic pressing and hot gas-static pressing.

The blanks of tool steels have been produced on laboratory unit for gas dispersion of liquid metal by OSPREY technology. The rate of dispersion is about 30 kg/min. Density of blanks is 96-98 %.

Figure 2 shows the micrographs of steel M3 structure of blanks after annealing, which were produced by usual dispersion technology (a) and with meet overheating (b), respectively. The size of a carbide is less than 1,5 μm.

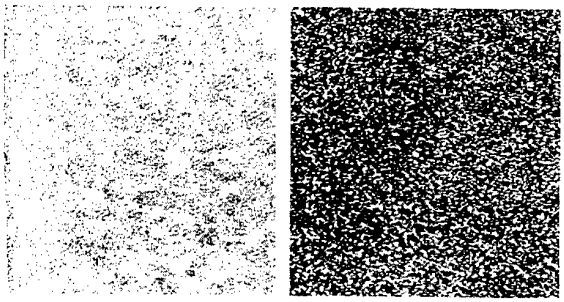

a b

Fig. 2. Microstructures of steel M3 after an annealing of blanks (x600)

a – by usual dispersion technology;

b - with overheating of a melt.

Mechanical testing showed that steel M3 obtained by OSPREY-process with melt overheating and by traditional PM have practically identical mechanical properties.

Thus powder high-speed steels made from a powder produced with application of overheating of a melt, are perspective for manufacture of the cutting tool not only because of fabricability of processes at stages of pressing and sintering, but also on their high serviceability. Thus, received results specify the large availability of new economic technology OSPREY-process for making blanks of fine steels and expediency of holding further explorations on development and realization of this technology in an industry.

# EVOLUTION OF PRIMARY IRONMAKING TO THE UNTRADITIONAL COKE-LESS TECHNOLOGY WITH POWER GENERATION

**Tovarovskiy I.G.**
Iron and Steel Institute NAS of Ukraine by name of Z.I. Nekrasov, Dnepropetrovsk, Ukraine

The traditional metallurgical technology, basically of which is the blast furnace technology, was born from primitive method of reception of metal in bloomery hearthes more than six centuries ago. It was developed under influence of growth of the requirement in metal by reduction of the resources base of the production. During the XIV÷XIX-th centuries the blast furnace technology developed by increasing rates, which have not decreased also in XX century. The growth of specific productivity of the best blast furnaces in the end of each century was exponential and the decrease of a specific coke rate - close to linear, that testifies the large internal reserves of blast furnace technology . Decrease of the heat consumption and the replacement of coke by less deficit fuels have resulted in decrease of coke consumption on separate furnaces to the end of XX-s century up to 270-280 kg/thm. By injection of coal gasification products the coke rate may by decreased to the level of 180-200 kg/thm [ 1].

The development of coke-less metallurgy as alternatives to classical sinter-coke-blast-furnace scheme has gone by the way of division of the solid- and liquid-phases processes with realization them in different units. It caused new problems, that results in increasing of the energy consumption and returning to the integrated technologies, one of which - COREX has received industrial realization.

The most effective direction of the further development is the coke-less blast furnace technology with injection of coal gasification products. The bases of this technology were developed at the Iron and Steel Institute of National Academy of science of Ukraine. The main goal researches consists in development pulverized coal gasifying reactor for generating hot reduction gas injected into the blast furnaces and units of coke-less metal production [2].

It is supposed to replace in the blast furnace more then a half quantity of coke by noncoking coal (in limit – coke rate up to 180-200 kg/thm) at the first stage, and on second – creation of new coke-less technology for primary metal production.

- The tuyere reactor-gasifier is developed and partially tested. It construction futures allow to put it into existing tuyere device of the blast furnace (Figure 1).

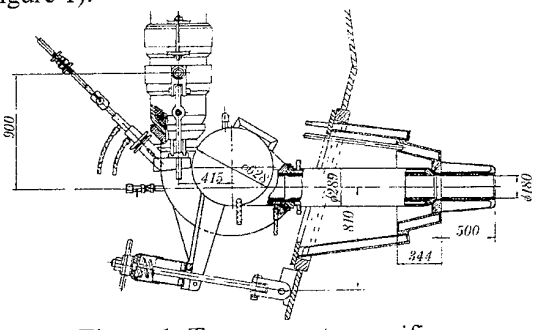


Figure 1. Tuyere reactor-gasifier

The second development part supposes reorganization of blast furnace on coke-less technology. It means reconstruction of the traditional blast furnaces to the furnaces (Figure 2) with hot reduction gases injection through established around hearth pulverized coal reactors-gasifiers (10) and dividing of furnace space into a zone solid phase reduction (1-shaft) and smelting-reduction hearth (3) with arch (4) – bottom for shaft. Charge of materials from shaft into hearth is carried out by transporting screws (5) through gutters (6), and the gas from hearth in shaft acts through gas branch pipes (7) after cooling up to 900°C.

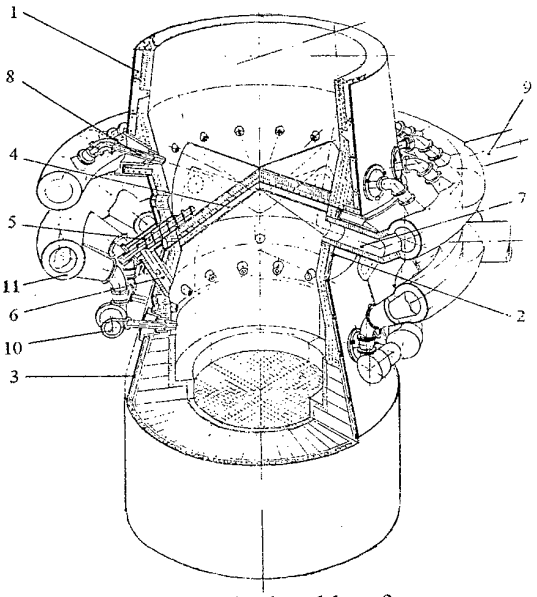


Fig.2. Coke-less blast furnace

The realization of new technology will allow to reduce the price of metal by 20 % and gives repaying of capital expenses less then 1 year. Side benefits of technology are an opportunity of reception of metal with the adjustable contents of carbon (down to steel) and preservation of an existing infrastructure of metallurgy.

The blast furnace technology as a uniform technical organism that was build up during the evolution has its system properties, which excludes the attempts of its "division". Therefore it remains the determining technological module of ferrous metallurgy, the development of which will form shape of whole metallurgical complex. The further evolution with its reorganization to coke-less ironmaking completely determines its dominant items in metallurgy [2,3].

Besides of metallurgical functions (melting of pig-iron, ferroalloys and special slags) the blast furnace will execute power functions (reception of gaseous fuel) and sanitary-ecological functions (waste products processing).

The power functions can be and must be extended. In usual on balance of metal conditions some blast furnaces are liberated and are suitable for performance of function of coal gasification. The received reducing gas can be used as for injecting in others blast furnaces for replacement of natural gas and coke [4-6], and for use in other technological and power units including coke ovens as a high-heating fuel. So the structure of fuel balance of the work can be rationalized . This task can be decided by replacement natural gas by coke gas on the blast furnace technology, earlier developed by Iron and Steel Institute [7].

The main feature of use of the blast furnace as a gas producer is that temperature of gases, departing from a stock column, should exceed a level, at which there is an intensive stressing of pitches adversely influencing a condition of gas pipelines and complicating technology. Most intensively pitches are allocated in an interval 300 – 500 °C, and at temperatures is higher 840°C there is their breaking-up. As the maintenance of temperature of a top gas at a level, demanded on the specified conditions, (> 500°C) is inadmissible on conditions of a service of the equipment of charging, it is necessary to apply untraditional reception - sharp refrigeration of gas at a run-out from a melting stock column.

Essence of reception that above a stock level of materials, which have at the bottom edge of a shaft top, on a circle establish tuyeres for injecting cooled top gas (50-80°C), that allows after melting it with mine gas to receive temperature of a 300-500°C top gas, departing from the furnace. The heat-eliminating gas recirculate in the system. Off-site gas can be added to it. The quantity of recirculating gas can be determined from simple balance ratio of gas components. At a choice coals it is necessary to prefer hard (non-bitumnious) coals, which allocate at heating insignificant quantity of pitches and are accessible enough.

While run on the specified technology a blast furnace of volume 2000 $м^3$ the quantity of gasification coal will make at least 1500 t/day, manufacture of gas 208000 $м^3$/h, and metal 570 t /day. At the expense of the made gas can be released 33000 $м^3$/h of natural gas, that will match to annual economic benefit 23 million Dollars USA at capital expenses, commensurable with expenses on dismantling of the blast furnace.

BIBLIOGRAPHY

1. Tovarovskiy I.G. 'A minimum of coke rate in blast furnace technology' Moskov: Stal, 2002. # 3, p. 5 – 7 (Ru).

2. Tovarovskiy I.G., Lyalyuk V.P, 'The evolution of the blast furnace technology'. Dnepropetrovsk: "Porogi", 2001, 424 p. (Ru).

3. Tovarovskiy I.G., Severnyuk V.V., Lyalyuk V.P, 'The analysis of parameters and processes of the blast furnace technology'. Dnepropetrovsk: "Porogi", 2000, 420 p. (Ru).

4. 'Exploration of high-temperature properties of non coking coal in conditions of blast-furnace smelting'. I.G. Tovarovskiy, N.A. Gladkov, A.S.Nesterov etc. Stal. Moskow, 1996. # 11, p.14-16 (Ru).

5. Patent of Russian Federation # 1770362. C 21 B. 7 / 00. Shaft Furnace . I.G. Tovarovskiy, S/I/ Suchkov, V.I. Babiy etc. Bulletin of inventtions.1992. # 39, p.78.

6. 'Production and application of coal gasification products in blast-furnace smelting'. I.G. Tovarovskiy, I.I. Solodkiy, I.Ya. Tolmachev etc. Moskov: Chermetinformatsiya.1992, 101 p.(Ru).

7. 'Blast furnace smelting with blowing of coke gas' V.F.Pashinskiy, I.G. Tovarovskiy, P.E. Kovalenko, N.G. Boykov. Kiev: "Technika", 1991, 104 p.

# INFLUENCE OF MELTING CONDITIONS AND OF ALLOYING WITH TRANSITION AND RARE-EARTH METALS ON STRUCTURE AND PROPERTIES OF HIGH-STRENGTH ALUMINUM ALLOYS

**Patsyna R.V., Voropaev V.S., Goncharuk V.A., Danylenko M.I., Zakharova N.P., Lotsko D.V., Milman Yu.V., Samelyuk A.V., Sirko O.I.**
I.M.Frantsevych Institute for Problems of Material Science of NAS of Ukraine, Kyyiv, Ukraine

Alloys of the Al-Zn-Mg-Cu system belong to the most high-strength aluminum alloys[1-3]. The content of the main alloying components in these alloys is: Zn - (5-8.5) wt. %, Mg – (2.0-3.0) wt. %, Cu – (1.0-2.3) wt. %.

The most studied alloys of this system are the alloy 7075 that contains about 0.2 % Cr (USA) as well as the alloys V95 and V96Ts (Russia) alloyed with (Cr + Mn) and (Zr + Mn), respectively. After the T1 (T6 in USA) thermal treatment that consists in alloy solid solution treatment with subsequent aging at an optimum temperature the highest tensile test properties $\sigma_{0.2}$ = 608 MPa, $\sigma_U$ = 650 MPa, $\delta$ = 5% were observed in extruded rods of the alloy V96Ts1.

A further growth of strength can be achieved on the account of increasing the content of the main alloying elements Zn and Mg, i.e. of increasing the amount of the $\eta'$ hardening phase. This way leads to a significant lowering of alloy ductility, in a large part due to the precipitation in grain and subgrain boundaries of rather coarse $MgZn_2$ and $Al_3Mg_3Zn_2$ intermetallics.

Improving the melting conditions in combination with an additional alloying that influences the size of grains, subgrains and intermetallic precipitates may allow to achieve a combination of high strength properties with good ductility in high-strength wrought alloys of Al-Zn-Mg-Cu system.

It is known that strength and ductility of wrought alloy samples that after the thermomechanical and thermal treatments preserved a non-recrystallized fiberlike structure are as a rule higher than in samples with a recrystallized structure. The most effective way for increasing the recrystallization temperature in aluminum alloys is introducing small additions of scandium or scandium together with zirconium [4]. It is also shown a favorable influence of these additions on the formation in wrought semi-products of a uniform substructure with fine equiaxial cells [4, 5]. The additional optimum alloying by transition metals (TM) and rare-earth metals (REM) may also influence the formation of the cellular structure as well as the formation of precipitates while aging, and consequently the level of mechanical properties.

In this work the results of investigating the influence of various melting techniques as well as TM and REM additions (Zr, Sc, Mn, Ti, Ni, Nb, Ce, Cr, Hf) on the structure and mechanical properties of the alloy Al-9Zn-3Mg-2.3Cu are presented.

Melting was carried out in an induction furnace in graphite and ceramic crucibles in the air or with the use of blowing the melt by argon. The melt was poured through a hole in the bottom part of the crucible with using a ceramic filter or without it into a water-cooled copper mold.

Ingots of 55 mm in diameter and of 130 mm in height were extruded to rods 6 mm in diameter (extrusion ratio $\lambda$ = 81) at a temperature of 400 °C.

Structure of ingots and rods was studied by light as well as transmission and scanning electron microscopy. The distribution of chemical elements in the structure of as-cast and wrought metal was investigated in a Superprobe-737 device. To follow the strength in various stages of alloy treatment the Vickers hardness was measured. Tensile tests were carried out for samples of rods in T1 condition with the gauge diameter of 3 mm and the gauge length of 15 mm.

It is shown that after melting in the graphite crucible ingots contained graphite inclusions that led to lowering the ductility of wrought alloys. The substitution of graphite crucibles for ceramic ones with using filters facilitated the removal of inclusions that deteriorated the ingot quality. A more complete purification of the melt from oxides was provided by the use of blowing the melt by argon. Monitoring the ingot quality was carried out by the "Dobatkin test" [6] technique (Fig. 1 a, b).

A rod sample from the alloy Al-9Zn-3Mg-2.3Cu manufactured in the graphite crucible in the air was completely recrystallized and failed during tensile test without signs of macroplastic deformation, the fracture being mainly intercrystalline. A rod sample of the same alloy produced in the ceramic crucible with blowing the melt by argon and pouring through a ceramic filter was also completely recrystallized, but showed a high ductility $\delta$ = 20 %.

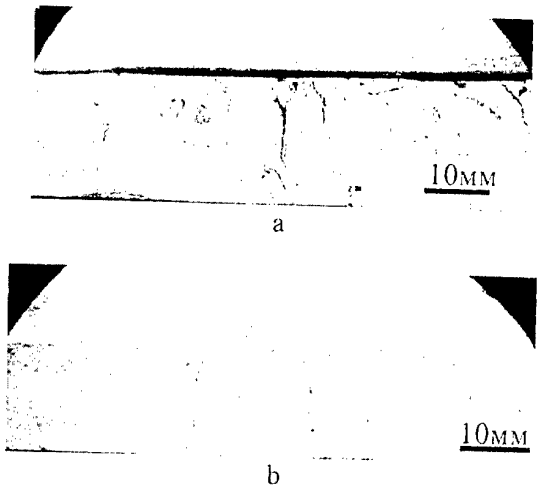


Figure 1. Detection of the content of oxide films in ingots by Dobatkin test:
a – melting without blowing by argon;
b – melting with blowing by argon.

The structure of the as-cast alloy Al-9Zn-3Mg-2.3Cu additionally alloyed with (Mn+Zr) was of a dendritic character. In the case of using the blowing by argon the dendrite structure was more clearly delineated, because the content of oxides that could be crystallization centers was in this case strongly reduced.

In the extruded rod of this alloy melted with the use of blowing the structure in T1 condition consisted of coarse recrystallized grains (Fig. 2a). Fine oxides in the alloy produced without blowing obviously retarded the growth of recrystallized grains themselves and/or facilitated the formation of retarding $Al_3Zr$ particles, and the rod after T1 treatment remained non-recrystallized (Fig. 2b).

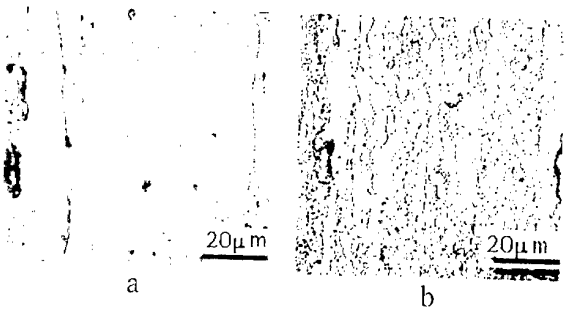


Figure 2. Structure of T1 treated extruded rod of the alloy Al-9Zn-3Mg-2.3Cu-0.3Mn-0.15Zr:
a) with the use of blowing the melt by argon;
b) without blowing the melt by argon.

It is established that introducing Mn or Mn+Zr into the alloy Al-9Zn-3Mg-2.3Cu has led to the growth of the strength of rod samples together with some lowering of the plasticity. Evidently, the influence of Mn to a large extent is caused by solid solution hardening [1].

Alloying the alloy Al-9Zn-3Mg-2.3Cu-0.3Mn-0.15Zr by Sc has led to the formation of a fine-grained structure in ingots produced by both techniques, and in extruded and T1 treated rod the structure was of a fiberlike and non-recrystallized character.

The Table shows that the additional alloying by TM or REM of the alloy containing Zr, Sc and Mn with using for melting a ceramic crucible and blowing the melt by argon permitted to increase the strength characteristics with the preservation of a good ductility.

Table. Tensile properties of T1 rods from ingots melted in ceramic crucible with blowing the melt by argon

| # | Chemical composition, wt. % | $\sigma_{0.2}$, MPa | $\sigma_{U}$, MPa | $\delta$, % |
|---|---|---|---|---|
| 1 | Al-9Zn-3Mg-2.3Cu | 530 | 619 | 20.4 |
| 2 | Al-9Zn-3Mg-2.3Cu-0.3Mn-0.15Zr (baseline) | 545 | 621 | 13.8 |
| 3 | baseline + 0.3Sc | 696 | 789 | 12.3 |
| 4 | baseline + 0.3Sc + 0.25Hf | 700 | 810 | 14.1 |
| 5 | baseline + 0.3Sc + 0.2Ni | 735 | 807 | 10.2 |
| 6 | baseline + 0.3Sc + 0.15Nb | 722 | 824 | 11.4 |
| 7 | baseline + 0.3Sc + 0.2Ce | 744 | 809 | 9.56 |
| 8 | baseline + 0.3Sc + 0.2 Cr | 725 | 804 | 10.2 |
| 9 | baseline + 0.3Sc + 0.2 Ti | 718 | 779 | 10.3 |

The content of elements is given by charge.

This work was partially supported by STCU, project P061.

1. Fridlyander I.N. Structural Wrought Aluminum Alloys. – Moscow: Metallurgia, 1979.
2. Mondolfo L.F. Aluminum Alloys: Structure and Properties. – London: Butterworth and Co., 1976.
3. Aluminum and Aluminum Alloys. ASM Specialty Handbook // Ed. J.R. Davis. - ASM Internat. – 1993.
4. Milman Yu.V., Lotsko D.V., Sirko O.I. // Mater. Sci. Forum. – 2000. – **331-337**. – P. 1107.
5. Lotsko D.V., Milman Yu.V., Yefimov N.A. et al. // Metallofiz. Noveishie Tekhnol. – 1999. – **21**, No. 6. – P. 9.
6. Dobatkin V.I. Ingots of Aluminum Alloys. – Moscow: Metallurgizdat. – 1960.

# PRESSURE WELDING OF DISSIMILAR METALS

**Zamkov V.N., Kireev L.S., Sabokar V.K.**
E.O.Paton Electric Welding Institute of the NAS of Ukraine,Kyiv, Ukraine

Progress in engineering stipulated the need to use different materials in one structure and, therefore, weld metals possessing different physical-chemical properties. The overwhelming majority of pairs of structural materials have a limited mutual solubility and form brittle intermelattic phases during welding. Thus, in welding dissimilar metals the proper choice of a method and technology for welding is of a decisive importance. Solid-state welding holds the highest promise for joining dissimilar metals.

Main parameters of the process are temperature, pressure and time. As proved by investigations, the welding temperature and deformation conditions should cause relaxation processes, and primarily dynamic recovery and recrystallization, to occur in the near-contact layers. In welding dissimilar metals it is sufficient that the above near-contact processes occur in one, as a rule more ductile, of the metals welded.

In welding dissimilar metals with a limited mutual solubility the quality of a welded joint is determined by the processes of mutual diffusion of materials in contact. Therefore, the temperature and time of welding should be selected so that they allow avoidance of formation of intermetallic phases in the joining zone. If there is no way for achieving it, then intermediate layers are used in such cases.

The E.O.Paton Electric Welding Institute developed a process for welding titanium to other metals without the use of intermediate barrier layers and without formation of intermetallic phases in the contact zone. Welding is performed at relatively low heating temperatures to retard diffusion processes, as well as under high pressures.

Welding is carried out in collapsible mandrels to preserve shape and sizes of the parts welded.

It was experimentally found that for a pair of titanium-aluminium the welding temperature is 500-520 °C, for titanium-copper it is 500-550 °C and for titanium-steel – it is 650-690 °C. Welded joints made at such temperatures and under appropriate pressures fracture in tensile tests in a less strong metal (Table).

Table. Tensile strength of welded joints

| Materials joined | Tensile strength, MPa | Fracture location |
|---|---|---|
| VT1-0 + AD1 | 84-93 | Aluminium |
| 12Kh18N10T + ADO | 77.9-82.2 | Aluminium |
| VT1-0 + M1 | 228-236 | Copper |
| VT1-0 + 2Kh13 | 486-494 | Titanium |
| VT1-0 + 12Kh18N10T | 463-478 | Titanium |

The technology for welding bimetal transition pieces was developed. The above pieces are used then for arc welding of the corresponding metals. For example, such transition pieces were employed for making of an original structure of the all-welded titanium-copper cathode for electrolytic deposition of copper. Such a cathode has a continuous service life 3-5 times as long as a riveted cathode, and allows an increase in yield of deposited copper per time unit owing to a substantial decrease in electrolytic losses at the mating surfaces.

Titanium-steel transition pieces were employed for manufacture of thermoelectric heaters with a titanium shell used to heat sea water in water-desalinating plants. Replacement of a steel shell of the thermoelectric heater by a titanium one allowed a fundamental extension of its service life.

As shown by the tests conducted, the described welding method makes it possible to join dissimilar metals with a limited mutual solubility, avoiding the use of intermediate layers, and provides mechanical properties of welded joints at a level of a less strong of the metals joined.

# ELABORATING OF THE MULTILAYER BRAZED JOINT OF NONMETALLIC CERAMIC PLATE TO METALLIC ROD

**Zhuravlev V.S., Naidich Y.V., Grigoriev O.N., Prokopenko A.A., Mosina T.V., Koval A.Y.**
Institute for Problems of Materials Science, National Ukrainian Academy of Sciences, Kiev, Ukraine

The procedures of nonmetallic ceramic plate to metallic rod nonseparated joint obtaining by brazing are perspective in order to solution of a number of technical problems. There are joints of the automobile ceramic turbine to metallic shaft, metallic electric current input to ceramic heater, ceramic cutter to metallic base etc.

The difficulties of ceramic to metal brazed joints obtaining are caused by the specific of ceramic material properties:

1) the thermal expansion mismatch (t.e.m.) is low in comparison to one of metal;
2) the brittleness is high;
3) the traditional metallic fillers do not wet the ceramic.

The complex solution of $Si_3N_4$ or AlN ceramic rod to steel shaft of 12 mm diameter brazed joint producing is presented in the study. The next works have been carried out in this aim.

1. It is proposed and realized the brazed joint multilayer structure, which consists of several brazed plates with set of difference for t.e.m. The differences of t.e.m. have been set by changing of the adjoining plates composition. The plates had been prepared by hot-pressing of $Si_3N_4$-TiN or AlN-TiN powder mixture (t.e.m. of $Si_3N_4$, AlN and TiN is respectively $3{,}5\times10^{-6}$ $K^{-1}$, $5{,}0\times10^{-6}$ $K^{-1}$ и $7{,}5\times10^{-6}$ $K^{-1}$).
2. The appropriate compositions of the fillers based on Cu-Ga-Ti and Cu-Sn-Ti and the conditions of the multilayer structure brazing process are determined.
3. The foil composite fillers of different thickness up to 70 μm are prepared.
4. The influence of the filler layer thickness on the brazed joints strength is established. It is indicate that the brazed joints strength is much greater than the filler alloy strength when the filler layer thickness is less than 30 μm. The explanation of the results is based on Hall-Petch effect.
5. A few methods of brazing process of the ceramic disk to the steel shaft, e.g. by means of the preliminary brazed multilayer insertions (the diameter is 12 mm, the thickness is 8 ÷ 12 mm), are elaborated. It is discovered that the adjoining plates composition may be changed no more than of 10 vol.% at the edges of insertions prepared with $Si_3N_4$-TiN mixture. It is shown the perspective of hard alloys using, e.g. BK-8, as the insertions.

Torsion strength of the joints of hot-pressed ceramic (both based on $Si_3N_4$ and based on AlN) to steel is 70 ÷ 110 MPa.

# THE DEVELOPMENT OF THE TECHNOLOGY OF THE PRODUCTING OF THE CHEMICALLY STABLE POROUS POLYMERIC MEMBRANES FOR THE BAROMEMBRANE MIXTURE SEPARATION

**Goncharenko V.V., Gvozd G.V., Churpita Ya.V., Gleevoi Yu.V., Ponirko E.F.**
National Thechnical University "Kyiv Polytechnical Institute", Ukraine, Kyiv

The membrane processes permits to pass by the energy unbenefitial phase phenomena,so that why this type of treatment seems to be attractive. Therefore, the membrane technologies are widely used in the various branches of technology, for example to remove disperse colloides, ionic admixtures (micro-, ultra-, nanofiltration, reverse osmosis) from aqueous solutions, to separate water-organic and gas mixtures (cleaning of spent oil and gases and so forth). It is the modern approach to solve such problems. In Ukraine the membrane methods employ to treat the drinking and technical water,to separate the gases. Domestic membranes do not produce, however there are own Ucrainian resourses for arrangement of the domestic membrane production. There are developed polimer industry in Kalush, Gorlovka, Severodonetsk (producting of polyethylen, polypropylen, polyvinilchloride, stirol and divinilbenzene etc.).

The process of porous chemically stable membranes based on polyurethan formation by termoformation was developed in this work. The membranes may be used for micro-, ultra-, nanofiltration, membrane electrolysis.

Main core of the membrane producting technology: 1 stage-preparation of homogenized polymer composition at determined quantity of the porogenerating fillers; 2 stage-the formation of the porous membranes of equal maintained thickness, high mechanic strengthening from the granulated polymer. To gomogenize the polymer composition the original disk mixer, there mixing, melting and disrergation make in the thin surface lauer, has been suggested.

The membrane formation realises by the transformation method.

In the dependence on quantity of porous agent, temperature of formation, the the membrane samples have the characteristics as follows: the complete porousity of 100-150%, average pore dimensin of 0,1-0,5 μm, the water capasity under tangencial regime from 0,3 to 25 $м^3/м^2 \cdot h$. It has been stated, that the samples obtained have rather fit water permeability, and retention ability for high disperse mechanic and colloid particles

Main efforts will be directed to determine the optimum composition, to reach desirable physic-chemical and expluatation characteristics, to optimize the technology process and arrangement, the trial performing as well.

**Main advantages of the suggested membrane obtaining method**

- The obtaining of the aim product with the minimization of wastes;
- The possibility of technology updating without resourse spending.

# LOW TEMPERATURE SYNTHESIS OF MICROPOROUS SILICON CARBIDE MEMBRANES

**Antsiferov V.N., Gilyov V.G., Sung J. S.[(1)], Kim T.W.[(1)], Choo K.Y.[(1)]**
Research Center of Powder Materials Science, Perm, Russia
[(1)]Korea Institute of Energy Research, 71-2 Jang-dong, Yoosong, Daejeon, Korea

Silicon carbide can be used for high temperature membrane separation because of the inertness to the corrosive atmosphere. Carbon is able to adsorb organic impurities from fluid like as a filter [1, 2].

As because SiC melting point is $T_{melt}$=2,540°C and the sintering temperature is 0,8 $T_{melt}$ [3], the microporous silicon carbide is stable at high temperature. On the other hand the sintering temperature of the ultra-dispersed powders of TiN and AlN is about 0.45 $T_{melt}$ [4]. Therefore low temperature SiC synthesis is promising to get microporous materials [5,6].

The reaction of $Si_S + C_S = SiC$ is studied. The influences of specific surface on the reactive mixture, pressing and temperature are studied with the permeability, durability of samples.

The surface 40-120 $m^2/g$ of mixtures were obtained through the grinding with ball mill. As shown at Table.1 we obtained the samples with porosity of 45-60%, pore size up to 0.3 μm measured by the bubbling method and specific surface area of 48 $m^2/g$.

Table 1. Characteristics of SiC synthesized in argon

| $S_{sp.}$ mix. $m^2/g$ | Pressing pressure, MP | Sinterin T, °C, time, h | Porosity % | $D_{por}$, μm | $S_{sp}$, $m^2/g$ |
|---|---|---|---|---|---|
| 85 | 50 | 1600-1 | 61 | 0,5 | 5,9 |
| 85 | 100 | 1600-1 | 58 | 0,47 | 6,5 |
| 85 | 150 | 1600-1 | 54 | 0,41 | 11,0 |
| 32 | 50 | 1300-2 | 57 | 0,5 | 24,2 |
| 85 | 50 | 1600-0,5 | 57 | 0,36 | 8,2 |
| 32 | 50 | 1600-0,5 | 56 | 1,0 | 2,3 |
| 85 | - | 1600-2 | 58 | 0,56 | 3,6 |
| 61 | 50 | 150-0,3 | 47 | - | 28,7 |
| 115 | 50 | 150-0,3 | 54 | - | 37,9 |
| 115 | 50 | 650-0,1 | 59 | - | 2,6 |
| 46 | 50 | 650-0,1 | 50 | - | 3,7 |
| 115[1] | 50 | 1100-0.5 | 54 | - | 48.7 |

As shown at the X-Ray analysis (Fig.1) the high-dispersed mixture ($S_{sp}$ = 115 $m^2/g$) is completely synthesized to SiC for 0.33 hours at 1150°C in argon atmosphere. With the high-dispersed mixture of $S_{sp}$ = 61 $m^2/g$ there are not-reacted silicon quantities.

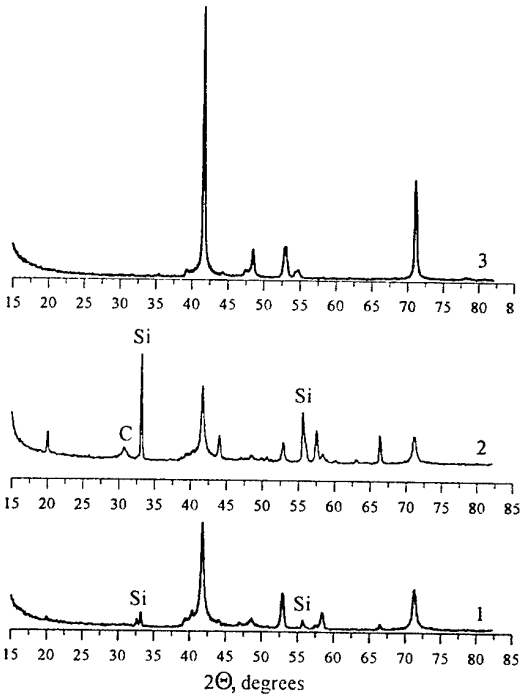


Fig 1. X-Ray diffraction (λ, $K_\alpha$Co) of SiC samples synthesized at argon atmosphere at various synthesis modes: 1 -1650°C, 0.17 h, 115 $m^2/g$ ($S_{sp,\ mix}$); 2 - 1150°C, 0.33 h, 61 $m^2/g$; 3 - 1150°C, 0.33 h, 115 $m^2/g$

Table 2 shows the nitrogen isotherm of samples. As the micro pore (radius) size is about 2,8-3,7 nm, SiC membrane may be used as a filter to separate water from the organic molecules such as methylene blue and phenol.

With the porosity 50% (at $S_{sp}$ = 30 $m^2/g$; $S_{sp}^{v}$ = 50 $m^2/cm^3$) the effective pore radius estimated to be 20 nm by the equation of $r_p = 2P/S_{уд,,}$ which is comparable to hydrogen selective nanoporous membranes.

[1] Synthesis at $CO_2$ atmosphere

Table.2. SiC pore structure ($N_2$ adsorption isotherm)

| | | | | | |
|---|---|---|---|---|---|
| $S_{sp}$ of mix, $m^2/g$ | 85 | 85 | 32 | 115 | 115 |
| Sintering T, °C | 1600 | 1600 | 1600 | 1150 | 1100 |
| Sintering hours, h | 1 | 2 | 0,5 | 0,33 | 0,5 |
| Sintering medium | Ar | Ar | Ar | Ar | $CO_2$ |
| Porosity, % | 61 | - | 57 | 54 | |
| $S_{BET}$, $m^2/g$ | 6,1 | 8,6 | 18,5 | 37,9 | 48,3 |
| $S_{Me}$, $m^2/g$ | 3,8 | 6,8 | 16,2 | 30,0 | 44,7 |
| $V_{Mi}$, $cm^3/g$ | 0,003 | 0,004 | 0,007 | 0,015 | 0,020 |
| $V_{Me}$, $cm^3/g$ | 0,008 | 0,012 | 0,019 | 0,045 | 0,058 |
| $W_S$, $cm^3/r$ | 0,011 | 0,016 | 0,026 | 0,060 | 0,078 |
| $r_{p.}$, nm | 3,6 | 3,7 | 2,8 | 3,2 | 3,2 |

Therefore, the low-temperature synthesis method is useful to make the porous silicon carbide with high specific surface (up to 48 $m^2/g$) with micro pores volume $V_{Mi} = 0{,}020$ $cm^3/g$.

Usually the tensile strength of the SiC obtained by normal sintering of powders is improved as the synthesis temperature increase. In the case of the reactive sintering such as the SiC obtained by $Si_т + C_т = SiC$, the tensile strength increase along with temperature decrease. Obviously, it is correlated to the pore size of synthesizing materials. Macro-pores formed at high temperature of synthesis and longer isotherm expositions decrease the tensile strength of material.

These low temperature reactive sintering method could be used to make the two layers membrane selective coating where two layer membranes are coated by nanoporous SiC on the substrates made of SiC and alumina oxide.

To obtain two-layer coated membrane the high-dispersed mixture of Si-30%C was used, of which specific surface was 115 $m^2/g$. The mixture was coated on the substrate by layer and pressed by pressure 25 MPa. Sintering of reactive layers was done in argon atmosphere at 1100°C within 30 minutes. The thickness of membrane layer, estimated by the mass of coating is about 200 μm. The obtained layer strength withstands the test of reverse gas blowing at 5 Bars.

Permeability of two-layered membrane for the hydrogen is 3.3 times higher than that for nitrogen.

Proportion is closed to 3,7, as per Knudsen equation for diffusion coefficient [7]:

$$D_i^K = \frac{l}{3}\sqrt{\frac{8RT}{\pi M_i}}, \qquad (1)$$

where Mi – mass of molecules, $R$ – gas constant, $T$ – temperature °K.

Dependence of gas flow rate on pressure drop is linear. While for viscous flow usually gas flow rate deviate from the linear. Besides the viscosity of nitrogen and hydrogen differs in less than 2 times. Accounted abovementioned we can say that in selective layer Knudsen flow is prevailed, what can be reached at normal pressure in nanoporous materials only.

Two-layered membrane with substrate made of SiC was tested within water filtration with Mn concentration, 1,2 mg/*l*. After filtration this concentration decreased up to 0.1 mg/*l* (measured by atomic-sorption analysis, made by "Proton" measuring device.

REFERENCES

1. Tomilina E.M, Lukin E.S., Kagramanov G.G. Durable porous ceramics based on silicon carbide with low sintering temperature, *Refractory and Ceramics,* 2000. №4. pp.12-14.

2. Mathere J., Mirzhanov A.G., Borovinskaya I.P. and others Ceramic filters for drinking water filtering, *Refractory and Ceramics*, 1999. №1-2. pp.43-47.

3. Andrievski R.A. Nanocrystalline High melting point compound based materials, *Journal of Materials Science*. 1994. V.29. P.614-631.

4. V.V. Dalidovitch, N.V. Fedorov, O.Ed. Babkin, Deriving and properties of sorption-active ceramic materials based on ultra-fine TiN and AlN powders, *Journal Appl. Chem.*, 1994. V.67, №6. P.942-945 (in Russian)

5. Gilyov V.G., Silicon carbide membrane materials, advanced materials and technologies problems, *Perm,* Issue.5, 2000, pp.45-52.

6. Gilyov V.G., Reaction sintering with negative bulk effects // Inorganic materials. 2002. №3. P.371-377.

7. Dytnersky Yu.I, Brykov V.P., Kagramanov G.G.. Membrane gas separation Chemistry 1991. 341 p. 3,3

# MMT-PROCESS INCREASES THE LIFE OF CEMENTED CARBIDE ARTICLES

**Lisovsky A.**
Institute for Superhard Materials, Kiev, Ukraine

The experimental results have shown that a sintered pore-free composite imbibes metal melt [1]. In the process of metal melt imbibition there occurs a liquid flow in the sintered article volume, deconsolidation of high-melting skeleton and changes in the composite material structure. The metal melts imbibition we called MMI-phenomenon [1]. The MMI-phenomenon occurs in the following composite materials: WC-Co, WC-Ni, WC-Fe, WC-TiC-Co, TiC-Co, TiC-Ni, $Cr_3C_2$-Ni, Fe-Cu, etc.

Based on MMI-phenomenon as well as on theoretical and experimental studies of liquid phase migration in the sintered article volume [2,3] the new process of metal melts treatment of a sintered article has been devised (MMT-process). The MMT-process allows the formation of new structures in a cemented carbide article after its final sintering and develops high physico-mechanical properties (Table 1). In the Table1 the WC-10Co specimens prepared by a traditional procedure and the WC-10Co-MMT specimens produced from WC-6Co cemented carbide by the MMT-process were the same in composition, the Co-phase and WC contents, the size of WC particles, and differed in values of specific interface $S_V^{WC/Co}$. The WC-10Co-MMT specimen featured a more developed WC/Co interface which was responsible for higher values of bending strength ($\sigma_{bm}$), work of deformation ($A_{tot}$), plastic ($\varepsilon$) and fatigue characteristics (Fig.1) as compared with the WC-10Co specimen [4]. The develop WC/Co surface of the WC-10Co-MMT specimen formed during the imbibition of the cobalt melt. This process was accompanied by a partial fracture of the carbide skeleton [1]. Addition of Ni caused a market improvement in plastical and fatigue characteristics of the specimens (Table 1, Fig.1), in this case, a slight decrease in $\sigma_{bm}$ and $\sigma_{comp}$ was observed as compared with the reference WC-10Co-MMT specimen. It should be noted that nickel stabilized the cubic modification of cobalt in the specimens. Cubic modification of Co ($Co_{fcc}$) is more plastic phase as compared to hexagona modification of Co ($Co_{hcp}$). This means that in cemented carbides in which the Co-phase has a cubical crystal lattice, stress relaxation proceeds easily by the Co-phase deformation. Thus, using the MMT-process, one can produce cemented carbides with higher mechanical properties.

The treatment of cemented carbide articles with metal melts allows us to form gradient structures. The MMT-process comprises the analysis of stresses, which appear in a cemented carbide article when operates, computer modeling of a gradient-structured article, solution of differential equations for the liquid phase migration and diffusion, optimization of technological conditions for an article treatment with metal melts and production of cemented carbide article with gradient structures [5]. The melt being imbibed can introduce into a cemented carbide article various components, e.g. Ti, Zr, Hf, V, Ta, Nb, Cr, B, Si, Ni, Al, Ru, Re, Cu, etc., thus alloying the article locally. By using different-in-composition metal melts, multilayered composites can be produced. Additionally, this process enables one to control the polymorphic transformation of the cobalt phase and thus to develop or to suppress the formation of nanostructures in the cemented carbide at the submicrolevel [6]. The process of the cobalt polymorphic transformation and, hence, the process of the gradient substructures formation can be controlled through the use of alloy additives. Alloying elements, which have a great affinity for carbon, form substructures at interfaces due to the precipitation of dispersed carbide particles from the liquid melt of the Co-phase. Alloying elements, which have a low affinity for carbon, form gradient substructures in the Co-phase due to polymorphic transformation of Co. Alloying elements, which increase the stacking fault energy, stabilize the Co(fcc) phase, while those, which decrease the stacking fault energy, stabilize the Co(hcp) phase [7].

Cemented carbide articles produced by the MMT-process acquire new features (high reliability and wear resistance as against the carbide articles with homogeneous properties). In-process tests suggest that the MMT-process allows wear reduction on milling cutters when mashining steel and iron by a

factor of 2 – 3, on cutters when turning high-temperature alloys by a factor of 2, on drilling bits by a factor of 2 – 3 and dies for production intricately profiled steel parts by a factor of 2.5. The MMT-process is a novelty in world practice of cemented carbides production.

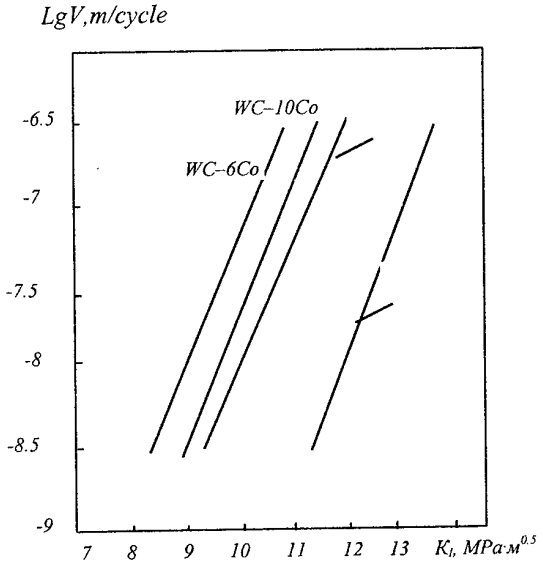


Fig. 1. Kinetic diagrams of the fatigue fracture toughness of the WC-Co spesimens, 1- WC-10Co-MMT, 2- WC-10Co,Ni-MMT

**References**


1. A.F. Lisovsky. Powder Metallurgy Intern. 1987, vol. 19, N5, pp. 18-21.
2. A.F. Lisovsky. Powder Metallurgy Intern. 1989, vol. 21, N6, pp. 7-10.
3. A.F. Lisovsky. Intern. Journal of Heat and Mass Transfer, 1990, vol. 33, N8, pp. 1599-1603.
4. A.F. Lisovsky. Proc. 15-th Int. Plansee Seminar, Eds G. Kneringer, P.Rodhammer and H. Wildner. Plansee Holding AG, Reutte (2001), P/M Hard Materials, vol. 2, pp. 168-179.
5. A.F. Lisovsky. Proc. European Conference on Advances in Hard Material Production, Turin, EPMA(ed.), 1999, pp. 301 – 306.
6. A.F. Lisovsky. Physico-chemical bases of forming nanostructures in the binding phase of cemented carbides. "Sci. Powder Metal 1998. World Congress and Exhibition. 18-22 October 1998, Granada, Spain, Hard Mater. Vol.4." EPMA (ed), London, 1998, pp.115-118.
7. A.F. Lisovsky, N.V. Tkachenko. On the Use of the MMI-phenomenon for the Formation of Nanostructures in WC-Co Cemented Carbides. Int. J. of Refractory Metals and Hard Materials, 1997, vol.15, N4, pp. 227-235.


Table 1. Physico-Mechanical Properties of WC–Co specimens

| Specimen designation | *HV*, GPa | $K_{Ic}$, MPa·m$^{0.5}$ | $\sigma_{bm}$, MPa | $\sigma_{comp}$, MPa | $\sigma^{c}_{0.1}$, MPa | $A^{tot}_{def}$, MJ/m$^3$ | $A_{pl}$, MJ/m$^3$ | $\varepsilon_{tot}$, % | $\varepsilon_{pl}$, % |
|---|---|---|---|---|---|---|---|---|---|
| WC–6Co | 15.00 | 12.3 | 2000 | 5000 | 4620 | 65 | 33 | 1.1 | 0.5 |
| WC–10Co | 13.20 | 14.6 | 2310 | 4550 | 4010 | 78 | 46 | 1.4 | 0.8 |
| WC-10Co-MMT | 13.10 | 14.9 | 2530 | 4460 | 3890 | 84 | 53 | 1.8 | 1.1 |
| WC-10Co,Ni-MMT | 13.00 | 15.3 | 2460 | 4340 | 3780 | 101 | 71 | 2.4 | 1.7 |

# USE OF PROCESSES OF BURNING FOR RECEPTION OF MATERIALS ON A BASIS TUNGSTEN AND ZIRCONIUM BORIDES

**Verchoturov A.D., Nikolenko S.V., Lebuchova N.V., Gostishev V.V.**[(1)]
Institute of Material Science KSC FEB RAS Russia, Khabarovsk, Russia
[(1)]Institutes of mountain business of FEB RAS Russia, Khabarovsk, Russia

The processes of burning are poorly investigated and are accordingly poorly in chemical technology of synthesis of refractory not metal connections: carbides, nitrides, borides, effective as a basis of materials showing high stability to influence of deterioration, friction, chemically aggressive environments. The certain interest represents reception dispersion metalloceramice materials on the basis of refractory borides with use of the so-called combined way [1], combining metallothermal reaction of connections MeYm (Y - O, S, Cl, F etc.) and restoring metal Me/ (Al, Mg, Ca), previous of high-temperature reaction of metal with contentsed boron component. Thus the synthesis of powders passes in one technological stage, in a material all spectrum of formed connections is used, and there are no difficulties with branch of collateral products, the high degree homogeneous and monodispersion of particles is provided, and in case of reception of powders refractory borides and materials on their basis is excluded negative influences of carbon on process of formation borides of phases.

The purpose of the present work is the search of systems initial reagents, capable in a mode of burning to form target and collateral products appropriate to structure of composite ceramic materials on a basis tungsten boride $W_2B_5$ and zirconium boride $ZrB_2$.

The experiments were carried out on mixes including chemically pure reagents: connections zirconium - $ZrO_2$, $ZrF_4$, Zr $(SO4)_2$ and - tungsten - $WO_3$, and also enriched a mineral concentrate containing $WO_3$ till 95-90 of mas. %, $CaWO_4$ up to 3-7 mas. %, $SiO_2$ up to 2-3 mas. %; boron components - $B_2O_3$, $B_4C$; a metal aluminium powder of the mark A7, in ratio appropriate stehiometric of reactions of formation $W_2B_5$ and. $ZrB_2$. Metallothermal process carried out on air. A thermodynamic estimation of the maximal temperatures developing at burning of mixes for a case of complete passage of reaction [2], is carried out in the assumption of adeabatical of process. All allocated heat goes on heating of products of reactions up to Tad - adeabatical of temperature of burning, that is entalpy of initial substances at reference temperature and final at temperature of burning are equal:

$$\sum_{i=1}^{n}[H(T_{ad}) - H(T_0)] = Q$$

Where $T_0$ - reference temperature of products of reaction; $T_{ad}$ - temperature, up to which the products of reaction, Q - thermal effect of reaction are warmed up. Are used help thermodynamic given [3], including tabulated dependences of a difference entalpy $H(T_{ad}) - H(T_{298})$ from temperature. In a number of cases of meaning are received extrapolation of settlement results. A choice of processes, in which the designed temperatures are sufficient for realization of burning, carried out on the basis of experience of experimental data processes of burning given in work [2], which shows, that at $T_{ad} < 15000K$ the burning does not occur, at $T_{ad} > 25000K$ of system always burn, at $15000\ K < T_{ad} < 25000\ K$ there is no clearness and the additional researches are necessary.

As the combined way of reception borides assumes consecutive passage aluminiumthermal reaction of restoration of chemical connection up to pure metal, which then cooperates with boron component, the thermodynamic estimation adeabatical temperatures is carried out by us for separate reactions in system.

The absence of burning in mixes including connection zirconium, is caused as show thermodynamic accounts unsufficient adeabatical in temperatures at a stage of development 1-st metallothermal reaction - of restoration up to metal zirconium. Introduction of superfluous quantity of aluminium will allow to carry out local warming up reagentes for the account high exothermal reaction of burning of aluminium ($T_{ad} \sim 4000$ K). In mixes with zirconium fluorid the process of evaporation

$ZrF_4$ is higher 1179 K. Passes of aluminiumthermal restoration of gaseous zirconium fluorid results in growth Tad in a mix up to 1700 K. Similarly in mixes including zirconium sulphate, the development aluminiumthermal of reaction thermodynamical is feasible at warming-up of a sample up to temperature above 673 K, when there is a decomposition $Zr(SO_4)_2$ up to $ZrO_2$ and gaseous $SO_3$.

The superfluous quantity of aluminium paid off on thermal balance of system reagentes in adeabatical conditions and in view of heat of phase and chemical transformations. In experiments with mixture including $ZrF_4$ or $Zr(SO_4)_2$, $B_2O_3$ and superfluous quantity of aluminium from 25 up to 35 mas. %, the intensive burning of mixes was observed, whereas in mixes stehiometric composition under the same conditions the wave of burning does not occur. The greatest exit $ZrB_2$ is fixed at restoration zirconium sulphate (62-66 mas % from theoretical), the products of synthesis represent porous glass mass with inclusions of particles $ZrB_2$ by the size 1-6 microns. In products of restoration zirconium fluorid were discovered $ZrB_2$ reach 50 microns.

In case of restoration tungsten oxide at both stages adeabatical temperatures are sufficient for distribution of a wave of burning, that will well be coordinated to experimental results. Use $B_2O_3$, in quality boron reagent in processes boron reagent with tungsten oxide results in primary formation metal tungsten and lowest tungsten borides It is probable, that the development of high temperatures at the first stage of process results in essential changes in parities reagentes at the expense of evaporation $B_2O_3$ and even at his(its) surplus up to 50 % of weights. It fails to receive a good output $W_2B_5$. Satisfactory results on reception of a phase $W_2B_5$ (increase of an output $W_2B_5$ till 65-79 of % from theoretical) gives introduction additional refractory boron reagent – boron carbide.

In view of the revealed features aluminiumthermal of restoration tungsten oxide the mode of synthesis of a composite material on a basis $W_2B_5$, with use was developed as initial reagent enriched mineral concentrate. The received powder material includes from 42 up to 55 weights. %, particles tungsten boride $W_2B_5$, size from 1 up to 3 microns, rest - particle glass phase by the size from 5 up to 45 microns. The hardness of particles borides reaches 32 GPa, glass phase 12-19 GPa.

The literature:

1. Мержанов А.Г. Проблемы технологического горения // Процессы горения в химической технологии и металлургии. Черноголовка: Редакционно-издательский отдел ОИХФ АН СССР, 1975. С. 5-28.

2. Новиков Н.П., Боровинская И.П., Мержанов А.Г. Термодинамический анализ реакций самораспространяющегося высокотемпературного синтеза //Там же. С. 174-188.

3. Киреев В.А. Методы практических расчетов в термодинамике химических реакций. Москва: Химия, 1970. 519 с.

# A NEW MODEL OF PHASE AND STRUCTURE FORMATION IN SELF-PROPAGATING HIGH-TEMPERATURE SYNTHESIS

**Khina B.B., Rabinovich O.S.[1], Formanek B.[2]**
Physico-Technical Institute, National Academy of Sciences, Minsk, Belarus
[1]A.V.Luikov Heat & Mass Transfer Institute, National Academy of Sciences, Minsk, Belarus
[2]Silesian University of Technology, Katowice, Poland

Self-propagating high-temperature synthesis (SHS) is as a cost and energy effective method for producing refractory compounds and composite materials. Along with high purity due to volatilization of impurities, SHS-materials possess superior properties in comparison with similar compounds obtained by conventional means. This is due to non-traditional interaction mechanisms associated with extreme conditions in SHS waves (temperature up to 3500 °C, heating rate ~$10^6$ K/s, temperature gradient ~$10^5$ K/cm, rapid cooling after SHS and fast accomplishment of conversion, ~1 to 10 s). Hence experimental researches are combined with modeling, which plays a significant role in studying phase formation and developing SHS-technologies [1].

In modeling SHS, most used is a formal model "imported" from the combustion theory where the reaction rate is described as $\partial\eta/\partial t=(1-\eta)^n\cdot\exp(-m\eta)\cdot k\cdot\exp[-E/(RT)]$, where $\eta$ is the conversion degree, n, m, k are formal parameters and E is the activation energy. Such approach permits studying oscillating and spinning regimes of SHS but it is not linked to the phase formation mechanisms. Since in many SHS-systems apparent E values are close to the activation energy for solid-state diffusion, a "diffusion-controlled growth" concept has gained acceptance for modeling SHS [2 *et al*]. However, in such works modeling is performed either with dimensionless parameters varied in a certain range, or with apparent activation energy estimated from experimental data.

Numerous experiments have shown that, along with solid-state diffusion, melting and spreading of the reactants followed by crystallization play an important part in the product formation during SHS [3 *et al*].

Thus, the objectives of this research are: (i) to analyze the applicability of the "quasi-equilibrium diffusion-controlled growth" concept to SHS on the example of the most studied Ti-C system using available data on the diffusion coefficients and taking into account a change of the geometry of reacting particles due to melting, and (ii) to develop a new model of phase and structure formation in SHS waves.

A diffusion-controlled growth of a thin TiC film on the surface of Ti particles is considered within the frame of diffusion-type Stefan problem in non-isothermal conditions. Experimental data on diffusion coefficients in TiC [4,5] were used for estimations. Since the diffusion coefficient in β-Ti is much higher than in TiC, it is implied that β-Ti is saturated with C at the temperature below the Ti melting point, $T_m(Ti)$=1940 K. Similar assumption is made for the molten Ti at $T_m(Ti)<T<T_{SHS}\approx$2600 K [6]. Then, an asymptotic solution for the diffusion-controlled TiC layer growth can be used [7]. Calculations for non-isothemal conditions in an SHS wave have shown that with the real values of diffusion coefficients, the thickness of the product is small (max. 0.2 μm), and the adiabatic heat release associated with the TiC formation is insufficient for sustaining the SHS wave.

At the attainment of $T_m(Ti)$, titanium can break the TiC case and spread because the density of solid Ti at $T=T_m(Ti)$ is $\rho_{Ti(s)}$=4.26 g/cm$^3$ while for molten Ti at the same temperature $\rho_{Ti(m)}$=4.12 g/cm$^3$. Thus, at $T=T_m(Ti)$ a problem for the rupture of the outer TiC case is considered within the frame of the theory of elasticity taking into account the non-compressibility of liquids. Using available data on the mechanical properties of TiC at elevated temperatures [5], we receive an upper level estimate: the molten Ti can be kept inside the primary TiC case only if its thickness exceeds $\approx 0.7R_0$ where $R_0$ is the particle radius. This is possible only for slow heating rates typical for traditional synthesis methods and sintering, and is not possible in SHS waves. Hence, at $T>T_m(Ti)$ molten Ti spreads and the geometry of the reacting system changes.

Then, another situation is considered implying

fast spreading: solid carbon particles are surrounded with liquid titanium retaining the stoichiometric Ti-to-C mass ratio. In this case, a thin equilibrium spherical film of TiC forms at the Ti/C interface (it should be noted that within the quasi-equilibrium diffusion theory a direct contact of solid carbon and liquid Ti below the TiC melting point is impossible). Asymptotic solution found on the basis of Ref.[7] demonstrates that for small-sized C particles (e.g., carbon black with a typical size ~0.1 μm) TiC layer growth can provide fast heat release necessary for sustaining the SHS wave. But for graphite particles with the radius $R_0 \geq 2$ μm, adiabatic heat release due to the TiC formation is lower, and complete conversion of the reactants into the product requires a "long" (~1 s) isothermal exposure to the SHS temperature. Since the diffusion coefficient of Ti in TiC is by orders of magnitude lower than that of carbon, which is typical for interstitial compounds, the TiC layer growth occurs mainly at the TiC/Ti interface, and the final TiC particles will be hollow. At the stoichiometric Ti-to-C mass ratio and the ultimate formation of $TiC_{1.0}$, the final density of the product particles will be $\rho_{pr} = [(\rho_{TiC1.0})^{-1} + (5\rho_C)^{-1})]^{-1} \approx 3.3$ g/cm$^3$ $= (2/3)\cdot \rho_{TiC1.0}$. This disagrees with numerous experimental data [3 and other works].

Therefore, numerical estimates performed on example of a classical Ti-C system reveal that the concept of diffusion-controlled product formation is not applicable to SHS. Hence, only a non-equilibrium phase-forming mechanism, which involves a direct contact of solid carbon with molten Ti without a continuous TiC interlayer, can operate in the SHS wave. Product formation will occur through dissolution of C in the melt and crystallization of TiC particles.

For the latter situation, a new model of phase and structure formation during SHS is proposed. In the preheat zone, solid-state diffusion-limited interaction of the reactants results in the growth of a thin layer of a refractory product on the surface of metal particles. In the zone of thermal reaction, melting of the metal particles occurs. Because of the volume change, the molten metal disrupts the core of the primary product and comes into direct contact with a non-metallic reactant which dissolves in the melt. The grains of the final product crystallize from the melt, which brings about the major heat release responsible for the SHS wave propagation. The crystallization process accomplishes in the after-burn zone. The model includes heat transfer equation, the equation for the diffusion-limited growth of the primary product and the crystallization kinetics of the final product based on the Kolmogorov-Avrami approach.

Partial support from the Belarussian Fundamental Research Foundation (grant X02P-037) is acknowledged.

References

1. Merzhanov A.G. *Russian Chemical Bulletin*, 1997, v.46, No.1, p.1-27.
2. Nekrasov E.A., Smolyakov V.K., Maksimov Yu.M. *Fiz. Goren. Vzryva*, 1981, v.17, No.2, p.77-83.
3. Merzhanov A.G., Rogachev A.S., Mukasyan A.S., Khusid B.M. *Fiz. Goren. Vzryva*, 1990, v.26, No.1, p. 104-114.
4. Andrievskii R.A., Spivak I.I. Prochnost Tugoplavkih Soedinenii i Materialov na Ih Osnove. Spravochnik. Chelyabinsk, Metallurgiya, 1989 (in Russian).
5. Samsonov G.V., Upadhaya G.S., Neshpor V.S. Fizicheskoe Materialovedenie Karbidov. Kiev, Naukova dumka, 1974 (in Russian).
6. Kirdyashkin A.I., Maksimov Yu.M., Nekrasov E.A. *Fiz. Goren. Vzryva*, 1981, v.17, No.4, p.33-36.
7. Lyubov B.Ya. Teoriya Kristallizatsii v Bolshih Ob'yomah. Moscow, Nauka, 1975 (in Russian).

# MECHANOCHEMICAL SYNTHESIS OF NANOCOMPOSITES IN METAL-OXIDE SYSTEM

**Grigorieva T.F., Ivanov E.Yu.[1], Barinova A.P., Boldyrev V.V.**
Institute of Solid State Chemistry and Mechanochemistry SB RAS, Novosibirsk, Russia
[1]Tosoh SMD Inc., Grove City, Ohio, USA

Metal-oxide nanocomposites can be used to obtain ultrafine metal catalysts on an oxide substrate, current-conducting ceramics, magnetic materials, etc.

Mechanochemical approach allows obtaining such nanocomposites by the joint treatment of a metal – oxide mixture. However, this requires substantial consumption of power and time, and is accompanied by the contamination of the product with the material of milling bodies. Higher dispersity and uniformity are achieved in the systems in which one can perform mechanochemical reduction of the oxide with a metal.

The processes involving mechanochemical reduction of copper, bismuth, tin, indium by various metals were investigated; the list of thus obtained nano-dispersed composites include bismuth on aluminium and zirconium oxides; copper on nickel, magnesium and iron oxides; tin on aluminium and tantalum oxides.

It is demonstrated that this mechanochemical process occurs for pairs with negative reaction enthalpies; the process dynamics is determined by the mechanical properties of the components.

# MODELLING HOT-WIRE CHEMICAL VAPOUR DEPOSITION OF NANOCRYSTALLINE SILICON THIN FILMS

**Bruehne K., Rakhlin M., Schubert M.**
Institute of Physical Electronics, University of Stuttgart, Stuttgart, Germany

The need for large-area and flexible microelectronic devices has stimulated significant interest in thin film silicon deposition technologies. Hot-Wire Chemical Vapour Deposition (HWCVD) presents the advantages of high depositi on rate for amorphous silicon (a-Si) solar cells, and low-temperature processing of dielectrics like $SiN_x$.

Since little is known about the decomposition and gas phase processes which eventually lead to film growth, we test a simple two-phase model against a wide range of experimental data on deposition kinetics [1, 2].

For this study, amorphous silicon (a-Si) and nanocrystalline silicon (nc-Si) films are deposited in a multi-chamber cluster tool (MV Systems Inc., Golden, CO, USA) by HWCVD. The volume of the multi-wire HWCVD chamber amounts to $0{,}15m^3$, and the distance between substrate and wire to 5 cm. The Si films are deposited onto 5x5 $cm^2$ 7059 Corning glass. The deposition pressure varies within the limits of 3 ÷ 800 mTorr (0,27 ÷ 53 Pa); the flow rate of $H_2$-diluted $SiH_4$ within 1 ÷ 100 sccm; the substrate temperature between 300 ÷ 500°C; and the filament temperature within 1500 ÷ 1900°C. The filament materials under investigation are pure tungsten, tantalum, and graphite.

In order to refine our modelling, we check the dependency of the growth rate on substrate temperature, deposition pressure, temperature and material of the filaments [1]. We analyse the type of gas flow in the reaction zone, and calculate the effect of thermal diffusion on single components of the flowing process gas at the substrate site. Moreover, Structural characteristics of deposited films [1].

As a result of these investigations, we can deduce: i) The molecular gas flow in the reaction zone is laminar; ii) Two well separated areas control the film growth, one area of catalytic reactions close to the filaments, where activated complexes [$Si_2H_n$*, n = 2,4,6] are formed, and a thermal diffusion area, where these complexes diffuse and decompose to form thin silicon films at the substrate. iii) The rate-limiting step is thermal diffusion of the activated complexes [$Si_2H_n$*, n = 2,4,6] towards the substrate.

This finding is consistent with a low activation energy of the deposition process ($E_{act} \approx 1{,}8$ kJ/mol), and with the growth-rate dependency on deposition pressure, gas flow rate and filament temperature. By identifying the rate-limiting step, we are able to present a diffusion-controlled description equation for the film growth, which well reproduces the experimental data.

The proposed two-zone model not only accounts for the kinetic parameters of the HWCVD process, but also explains the influence of other deposition parameters, like substrate as well as filament temperatures, or filament material.

*1. K. Bruehne, et.al.* Thin Solid Films **395**, 163-168 (2001).
*2. E.C. Molenbrock et.al.* J.Appl.Phys.., **82**(4), 15.08.97, pp.7278-7292

# Structure and properties of coatings from the chromium-based alloys.obtained at supersonic plasma speed

**V. Gorban[1], S. Petrov[2], E. Grechishkin[1]**

[1] Institute for Problems of Material Science, National Academy of Sciences of Ukraine, Kiev,
[ě] Scientufic production assosiation "TOPAC", Kiev, Ukraine

Parameters of mechanical and service properties, and profitability of the process of gas-thermal coatings appreciably depends on the speed of plasma flow. Now processes with the use of supersonic plasma are most perspective for industrial application [1,2].

The work purpose is research of influence of supersonic air–gas plasma and detonation coatings on the structure and service characteristics of coatings from chromium-based alloys as alternatives of galvanic chromium plating.

The influence of frictional structure of granulated powder on properties of coatings has been determined. Such characteristics, as hardness, porositu, adhesion and roughness of the surface of coatings are in direct dependence on the size of the used powder fraction. So the hardness and porositu of coatings change from 10 GPa and 1 % at the size of a powder 20-30 microns to 7 GPa and 3 % at increase of a fraction up to 50-100 microns accordingly.

The comparison of properties of coatings from chromium-based alloys obtained with the help of supersonic air-gas plasma and detonation coatings on a fraction of powder 20-40 microns is carried out. The differences in properties are submitted in Table. 1

Table 1. Some properties of coatings from the chromium-based alloys depending on technology

| Method of coatings | Spraying distance, mm | Hard-ness, GPa | Porosi-tu, % | Adhesi-on, MPa |
|---|---|---|---|---|
| Supersonic plasma | 200-250 | 9 | 2 | 50 |
| Detonation | 15--200 | 10 | 1 | 60 |

The structure of the coatings from chromium-based alloys is investigated. The characteristic feature of their structure is poorly expressed layering. The electron-microscopic structure of supersonic coatings showde thet their matrix is a Cr–base fcc solid solution with grain size raning from 0..5–3.0 microns. The grain boundaries were smooth as in the crystallized material. The defects were indentified as the dislocation loops with an average densitz $10^{12}$ см $^{-2}$.

The phase structure of coatings is determined, presence of oxides $Cr_2O_3$, $Cr_3O_4$ is characteristic of them, in connection with high affinity of chromium to oxygen. High-temperature instable oxide CrO characteristic only of coatings from the chromium-based alloys received in flows of supersonic plasma is found out for the first time. Tetragonal $Cr_3O_4$ is present in all gas thermal coatings from the chromium-based alloys and is caused by high speeds of cooling. It is established, that for formation of CrO except for high speed of cooling it is necessary that temperature of heating of particles did not exceed 1600 K. This is promoted by small time of powder stay in a flow of supersonic plasma and formation of a steam jacket of sublimation products around them.

High-temperature characteristics of the given coatings (hardness, strength, bend angle) are determined in the work. So the ultimate strength of coatings produced using supersonic air-gas plasma reaches a level of 200 MPa, that is a little bit lower than a level of ultimate strength of compact chromium (210 MPa).

The researches of the characteristics wear resistance of coatings in conditions of dry friction and borderline lubrication (Table 2) are carried out.

Friction-induced deformation is localized as structural inhomogeneities indicate. Study of surface microhardness of the friction has revealed three typical structural components with different values of hardness.

Electron microscopical stude of the coatings surface after frictional indicated same regions coatong grains of initial size with clear 0,2-0,3 microns fragments and regions with numerous microcracks.

Direct dependence of the weaf level on the coating microhadness is the basic found regularity, which is characteristic of the friction points in conditions when the mechanism of elastic rejesction provails.

Table 2. The characteristics of deterioration (micron) of coatings from the chromium-base

alloys depending on technology of reception and test specifications

| Conditions testin | | Supersonic plasma | Deto-nation |
|---|---|---|---|
| Dru frictin, v=0,15m/s, P=30H | Stutic Weaf, μm f | 0,33 0,041 | 0,21 0,036 |
| | dinamics wear, μm f | 3,4 0,22 | 2,7 0,26 |
| Boundaru grising, T=473 K v=14m/s, P=1H | wear coating | 32 | 64 |
| | wear rider | 21 | 70 |

The influence of technology напыления on the characteristics of corrosion stability(resistance) of coatings from the chromium-base alloys is established. Is shown, that with increase of speed of a flow of plasma the protective characteristics of coverings (Table. 3) raise.

From the table follows, that at supersonic flows of plasma a current dissolution of system the coatings - Ст 3 decreases, i.e. comes in conformity with corrosion resistance materials of itself coatins. It speaks about high density of a coatings and its good adhesions to a basis materials.

Table 3. The characteristics of corrosion resistance of coatings from the chromium-base alloys in 0,5 $H^2SO^4$

| The characteristics of coatings | Superso-nic plasma | Detona-tion | Cr compact |
|---|---|---|---|
| Porosity common transparent | 2 0,025 | 1 0,05 | 0 0 |
| Speed of dis-solution, $A/m^{2*}$ | 1,0 | 0,25 | 0,20 |
| Heat resistance at 1273 K, $mg/sm^2$ | 0,0101 | 0,0101 | 0,0092 |

* - at potential 0,70 B.

Thus detonation coatings have higher hardness increased characteristics adgesion and wear- and corrosion resistens, however considerably lose in productivity and demand narrower fraction of powders for reception optimum behaviour of coatings.

Literature

1. Boricov J.S., Petrov C.V. Ispolsovanie cverxzvycovoy strui v texnologii gas-termicheckogo napylenij // Avtomaticheskaj svarka - 1995. - N 1. - P. 41-44.

2. Petrov C.V., Saakov A.G. Plasms produktov sgoranij v ingenerii poverxnosti. - Kiev: TOPAC. - 220 p.

# INVESTIGATION OF CONDITIONS FOR FORMATION OF INTERMETALLIC PHASES DURING DETONATION SPRAYING OF CLAD NI-AL POWDERS

**Astakhov E.A., Mitz I.V., Kildiy A.I., Kokorina N.N., Kaplina G.S.**
E.O. Paton Electric Welding Institute of the NAS of Ukraine, Kyiv, Ukraine

The processes of plasma spraying of nickel clad aluminium powder are studied in [1]. Coatings of the above powders posses high properties, such as resistance to fretting corrosion at low and high temperatures, resistance to wear under the effect of a flow of abrasive particles at high temperatures, corrosion resistance, etc. These properties allow the Ni-Al coatings to be applied for protection of surfaces of different-purpose parts: thread feeders in textile industry, gas turbine engine components, heat exchangers, boiler and petrochemical facilities, crucibles for metal melting, crankshafts, cylinders, pistons and valves in internal combustion engines, etc. Thermal spray coatings of Ni-Al are widely applied as a sublayer for $ZrO_2$ heat-protection layers, and for repair of parts made from different grades of steels.

High properties of the Ni-Al coatings are provided by intermetallics NiAl and $Ni_3Al$.

As detonation coatings are superior to the flame and plasma ones in porosity (porosity is less than 1 %) and adhesion strength, it is of interest to study the possibility of producing coatings as a result of the exothermical reactions by the detonation spraying process.

We investigated the effect of detonation spraying parameters on the process of phase formation, morphology, phase composition and some properties of coatings resulting from spraying the nickel clad aluminium powder.

Powder PALN-80 (according to TU 48-3-92-84) with a particle size of 40-60 μm, produced from the carbonyl gas phase in a vibro-fluidized bed, was used as a spray powder. The ratio of Ni:Al was 80:20.

Spraying was performed using the "Perun-S" detonation gun.

In detonation spraying the time of the dynamic and thermal effect by detonation products (temperature 3000-3250 °C) on the powder is approximately $\sim 3 \times 10^{-3}$ s, and the time of impact deformation of the spray material particles moving at a velocity of 500 m/s to 1000 m/c is approximately $\sim 10^{-7}$ s. This time is enough to heat the nickel powder particles 40 μm in size to a melting point. Therefore, spraying of the clad Ni-Al particles, where the initial stage of formation of intermetallics begins as early as at a temperature of 600 °C, provides all necessary conditions for occurrence of reactions. In addition, it was confirm the possibility of formation of inetrmetallic $NiAl_3$ with microhardness of about 4500 MPa even at the boundary of interaction of the nickel coatings with an aluminium foil.

Spraying process conditions are given in Table and structure coating on the figure.

Table. Detonation spraying parameters

| № | Working gas flow rate, $m^3/h$ | | | | Fuel to oxidizing and neutral gas ratio | Channel length, mm | Shooting rate, Hz | Spraying distance |
|---|---|---|---|---|---|---|---|---|
| | Fuel | | Oxidizer | Neutral gas | | | | |
| | Propane-butane | Acety-lene | Oxygen | Nitrogen in compressed air | | | | |
| 1 | 0.45 | | 1.55 | 0.68 | 1.0:3.5:1.5 | 550 | 6.6 | 100 |
| 2 | 0.45 | | 1.55 | 0.68 | 1.0:3.5:1.5 | 550 | 6.6 | 200 |
| 3 | | 0.60 | 0.80 | 0.68 | 1.0:1.3:1.1 | 550 | 6.6 | 100 |
| 4 | | 0.60 | 0.80 | 0.68 | 1.0:1.3:1.1 | 550 | 6.6 | 200 |
| 5 | | 0.60 | 0.80 | 0.68 | 1.1:1.3:1.1 | 1100 | 3.3 | 100 |
| 6 | 0.45 | | 1.55 | 0.68 | 1.0:3.5:1.5 | 1100 | 3.3 | 100 |

The coatings sprayed were studied by metallography using the "Neofot-32" microscope and by X-ray diffraction phase analysis (XDPA) using the "Dron-3" diffractometer in $K_\alpha Co$ radiation.

XDPA identified the presence of almost the same phase in the coatings produced under all process conditions: γ - Ni (solid solution), $Ni_3Al$, NiAl, γ-$Al_2O_3$, α-$Al_2O_3$, NiO and $Ni_2O_3$. The coatings sprayed using a long channel and both acetylene

and propane-butane employed as fuel gases contained no free aluminium. That could be caused by several factors: increase in the degree of occurrence of the reaction to form intermetallic compounds, higher oxidation degree or both, which most probable. Metallography of microstructure of the coatings (modes 5 and 6) confirms the presence of about 25 % of the oxide phase in the case of using acetylene and about 40 % in the case of using propane-butane as the working gases. It should be noted at this point that XDPA does not allow evaluation of the quantitative relationship of phases present in the coatings because of often coincidence of values of their interplanar spacing. Metallography identification of phase components of the coatings was based on earlier investigations of plasma spraying of composite powder Ni-Al [1], which had proved the presence of the following phase components in coatings:

1. Gray-blue phases with microhardness of 5300-6200 MPa – NiAl
2. Light-yellow phases with microhardness of 4500-5000 MPa – $Ni_3Al$
3. Phases of variable colours, from dark-yellow to blue, with microhardness of 7500-9000 MPa – solid solution of Ni in NiAl of a variable composition (from NiAl to $Ni_3Al$)

Comparison of the spray coatings with acetylene used as a working gas shows that all the modes share the yellowish colour dominating in structures of the coatings, which is indicative of the presence of a large amount of the γ-Ni solid solution and $Ni_3Al$ phase. Also they share the absence of initial non-reacted composite particles and a lamellar structure, the degree of elongation of lamellae being different for different variants of spraying. The most favourable structure characterized by a high density and high adhesion of a coating to the substrate, low porosity and uniform distribution of phase components is that of a coating spraying using mode 3, 4 (Fig.c, d).

Structure of this coating is characterized also by a low content of oxide inclusions, which is proved by a minimum value of hardness, $HV_{300}$ = 2830 MPa.. A coating sprayed by mode 5 has the highest hardness $HV_{300}$ = 4810 MPa, which resulted from an increase in the degree of completion of the reaction and insignificant oxidation: up to 25 % of finely dispersed oxides were revealed in structure of the coatings. In addition, the coatings contained cracks located normal to the substrate (Fig. e). The cracks were caused most probably by an increase in the amount of the powder fed to the detonation unit channel per cycle.

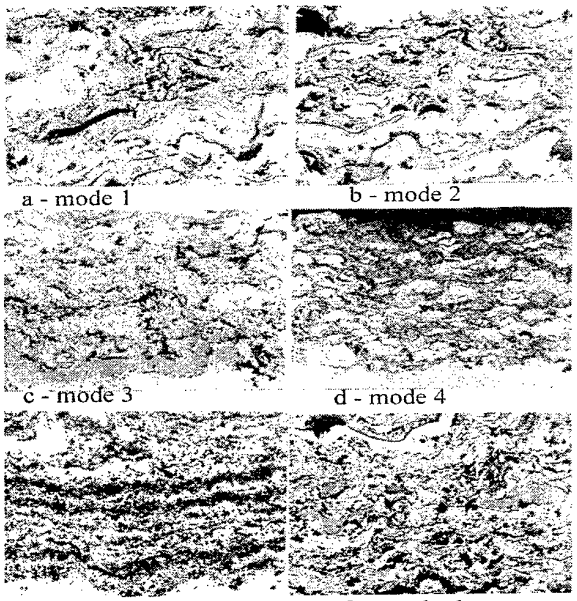


Fig. Structure of detonation coatings from Ni-Al, x400.

The main distinctive feature of the spray coatings produced with propane-butane used as the fuel gas is an increased amount of non-reacted composite particles (Fig. a, b) and an increase of up to 40 % in the content of oxides, especially in the case of a long channel of the detonation unit. In this case a coating has a clearly defined laminated structure with smeared boundaries between phase components (Fig. f). The high content of oxides results in high hardness of the coatings, i.e. $HV_{300}$ = 5140 MPa. The metal component of structure of all the coatings sprayed with the propane-butane fuel gas, which is yellowish in colour, is most probably γ-Ni. In addition, in the case of propane-butane used as the fuel gas the degree of homogeneity of structure the coatings is lower and hardness is higher, varying from 3210 to 5140 MPa, in comparison with hardness of the coatings sprayed with the acetylene fuel gas, which varies from 2830 to 4010 MPa.

Therefore, it was established that the exothermic reactions did take place during spraying, resulting in formation of intermetallic phases.

**Reference**

1. Borisov Yu.S. et al. Plasma heat-resistant coatings of composite powders // Heat-resistant and high-temperature coatings. – L.: Nauka. – 1969. – P. 273-286.

# EVALUATION OF SERVICEABILITY OF PLASMA COATINGS ON BODIES OF ROTATION

**Shevchenko V., Belchikov E.**
Zaporizhzhe National Technical University, Zaporizhzhe, Ukraine

The development of mechanical engineering is defined by an opportunity of creation of new constructional materials and technologies, which correspond to a complex requirements of modern industry and new technologies. The application of plasma has given an opportunity to create new compositions, which combine high durability with reliability.

With the help of plasma coatings they receive special properties of working surfaces (high-temperature strength, heat conduction etc.); and also economy of expensive metals. It is necessary to note a role of coatings for increasing of constructional durability as conditions, which provide formation of a composite product with different properties of a surface and volume.

The increasing of durability, hardness and wear resistance of metal is accompanied by increasing of probability of fragile destruction. The plasma coatings technologies allow to create composite materials (detail), which unite wear resistance surface with plastic and crack resistance basis.

Developing of new materials for protective plasma coatings it is necessary to predict and evaluate the mechanical characteristics of deposited layers, which define their serviceability. The inadequate values of adhesion, characteristics of elasticity and plasticity, thermal expansion of a coating etc., in aggregate, can cause crack creation during the initial stages of coating formation. Work ability of a coating is function of significant quantity of deposition parameters, which amount more than 60 [1]. These factors and also influence of probability processes define difficulty of forecasting of serviceability of coatings and optimization of technological processes. For example, the adhesion nature is investigated and is classified in works [1,2]:

1. Force of mechanical connection;
2. Force Van-der-Vaalse;
3. Force of chemical connection.

The forces of chemical connection are most important. That is explained by a low level of forces of previous types (10,0-20,0 MPa). I.e. forecasting and management of adhesion can be carried out at the expense of definition of set of chemical and power conditions of "basis-coating" interaction. In work [1] is proved, that consideration of process of interaction "coating - basis " only from a position of the theory of welding processes gives results, which not exact and do not give a complete picture. Besides they characterize only qualitative part.

The complex researches of the mechanic characteristics and properties of coatings, analysis of dependence " parameters of technological process - structure of a coating - property " are a perspective direction in the field of new materials development.

The plasma coating, is a body, which limited by two surfaces, distance between these surfaces is small in comparison with other sizes of a body. Prevailing amount of details, which is suitable for restoration and hardening by deposition - body of rotation. Thus, the coating for this type of details can be considered as thin-walled shell. That affords a capability for research of stress - strained state of plasma coatings) with the help of a differential equation of a radial trough of a shell, which one is under operating of axially symmetric mechanical and temperature loads [3]:

$$D\frac{d^4\omega}{dx^4}+\frac{Eh}{a^2}\omega = P+\frac{Eh}{a}\alpha T_0 - D(1+\mu)\frac{d^2}{dx^2}(\alpha\frac{\Delta T}{h}), \quad (1)$$

where: $D=\frac{Eh^3}{12(1-\mu^2)}$ - flexural rigidity, Nm;

$E$ - modulus of elasticity of the maiden kind, Pa;

h - depth of a shell, m;

$a$ - radius of a median surface of a shell, m;

$p$ - the spread load (pressure), which one is applied on a median surface of a shell, $N/m^2$;

$a$ - coefficient of linear expansion, $°C^{-1}$;

$T_0$ - temperature of a median surface of a shell

$\Delta T$ - temperature difference external and internal surfaces of a shell, , °C;

$\mu$ - Poisson's constant.

If the basis for coating to produce in the shape of a lengthy cylindrical shell, radial movements of points of a median surface of a basis (radial trough) under condition of absence of temperature stresses *($T_0$=0, $\Delta T$=0)*:

$$\omega = (p-p')\frac{a^2}{Eh}. \quad (2)$$

And $p'$ - radial effort, which one arises between the basis and coating under operating of internal pressure p and residual stresses in coating $\sigma_r$*:

$$p' = \sigma_p^r + \sigma_r^*, \quad (3)$$

Where: s pr - pressure, which one arise in coating only under operating of pressure $p$.

The equation (2) allows to construct empirical-formula dependencies of a trough of a shell from internal pressure $w = f(p)$ under conditions:

a) The shell is under operating only internal pressures ($p' = 0$);

б) The shell is under operating of internal pressure and pressure on the part of coating ($p' \neq 0$). It allows to receive a function of relation of pressure on the part of coating on the basis $p'$ from internal pressure $p$ on a shell:

$$p' = f_1(p). \quad (4)$$

The computational scheme of coating can be presented as a shell, which one is under operating of internal pressure.

Then a radial trough of coating:

$$\omega_n = \frac{p' a_n^2}{E_n h_n}. \quad (5)$$

Thus, the modulus of elasticity of the maiden kind of coating is determined under the formula:

$$E_n = \left| \frac{\Delta p'(\Delta p)}{\Delta \omega_n} \right| \cdot \frac{a_n^2}{h_n}. \quad (6)$$

For research of a state of stress of coating is applicable equations of the Laplace [4]. Then for coating, which one represents a lengthy cylindrical shell:

$$\frac{\sigma_t}{a_n} + \frac{\sigma_m}{\infty} = \frac{\sigma_r}{h_n}, \quad (7)$$

where: $\sigma_t$, $\sigma_m$, $\sigma_r$ tangential, meridional and radial stresses in coating.

It is ground equations (7) we shall receive:

$$\sigma_t = \sigma_r \frac{a_n}{h_n}. \quad (8)$$

It is known, that for a cylindrical shell [4]:

$$\sigma_m = \sigma_r \frac{a_n}{2h_n}. \quad (9)$$

Thus, stress in coating (is apparent, that $\sigma_r = p$):

$$\sigma_r = f_1(p),$$
$$\sigma_t = f_1(p)\frac{a_n}{h_n}, \quad (10)$$
$$\sigma_m = f_1(p)\frac{a_n}{2 \cdot h_n};$$

If $p=0$, the values of radial, meridional and tangential stresses correspond to residual stresses in coating:

$$\sigma_r^* = f_1(0),$$
$$\sigma_t^* = f_1(0)\frac{a_n}{h_n}, \quad (11)$$
$$\sigma_m^* = f_1(0)\frac{a_n}{2 \cdot h_n};$$

But, as to stresses $\sigma_r$* or $\sigma_r$, direction which one normally to a surface of coating, - on an external surface of coating $\sigma_r = 0$. And, the value $\sigma_r$ is much less $\sigma_t$ and $\sigma_m$, $a_n >> h_n$. Therefore value $\sigma_r$ can be neglected ($\sigma_r \to 0$).

The following research stage is the solution of a problem of a failure theory - estimation of strength coating by a known stress-strained state. For example, for IVth of a failure theory the expression takes place:

$$\sigma_{екв}^{IV} = \sqrt{\sigma_m^2 + \sigma_t^2 - \sigma_m \sigma_t} \leq [\sigma], \quad (12)$$

Where $[\sigma]$ - is determined experimentally at construction and research of the chart

$$\sigma_t = f_2(\varepsilon_n), \quad (13)$$

$\varepsilon_n$- relative radial deformation of coating.

The solution of a differential equation of a radial trough of a shell (1) under condition of $T_0 \neq 0$ and $\Delta T_0 \neq 0$ affords a capability to allow at designing of coatings) static and dynamic thermal loads. The estimation work ability of coatings implements with the help of a reserve factor on residual and operational stresses and count of probability of destruction.

**The literature**

1. Кудинов В.В. Плазменные покрытия. – М., «Наука», 1977, 184 с.

2. Тушинский Л.И., Плохов А.В. Исследования структуры и физико-механических свойств покрытий. – Новосибирск, «Наука», 1986, 197 с.

3. Биргер И.А., Шорр Б.Ф., Иосилевич Г.Б. Расчет на прочность деталей машин: Справочник. – М. «Машиностроение», 1979, 702 с.

4. Писаренко Г.С., Яковлев А.П., Матвеев В.В. Справочник по сопротивлению материалов. – Киев: Наукова думка, 1988, 736 с.

# GRANULAR SILICON TECHNOLOGY OF MONOSILLANE IN A FLUIDIZED BED REACTOR

**Borodulia V.A., Vasilevich V.P.[1], Vinogradov L.M., Rabinovitch O.S., Stepanenko V.N.[2], Akulitch A.V.**

A.V. Luikov Heat and mass transfer Institute, Minsk, Belarus

[1] "Plastma" Ltd., Minsk, Belarus

[2]State-run Cmpny "Minsk Inst-t of Radio Materials", Minsk, Belarus

Silicon has a growing demand at the global market of solar cells manufacturing and microelectronics. Conventional raw materials sources (high-purity quartz sand) and silicon technology – carbothermic reduction of silicon dioxide in arc furnaces under 1800°C, subsequent chlorination of crude silicon, rectification of the nascent chlorosillanes and their further reduction under 1200-1300°C with hydrogen ("Siemens-process") are underproductive, energy-consuming and are not capable to satisfy market needs.

A conceptually new manufacturing technology for highly pure polycrystal silicon is based on utilization of a secondary product apatite concentrate recycling into phosphoric fertilizers. The processing flowchart implies that sodium silicofluoride is generated out of silicofluoride acid (a by-product that results from refining extraction phosphoric acid to eliminate fluoride compounds). Further, at stage I, gaseous silicon tetrafluoride is extracted as a result of thermal decomposition of sodium silicofluoride. At stage II silicon tetrafluoride is being reprocessed into monosilane. Stage III is pyrolytic decomposition under 1000°C of monosilane with silicon and hydrogen generated.

The conducted laboratory experiments proved feasibility of the suggested polycrystal silicon technology. However, depositing polycrystal silicon on a heated silicon base rod results in bulky sample with restricted surface leading to reduction in efficiency of this technique.

Pyrolytic decomposition of monosilane in a fluidized bed reactor with silicon precipitated on minute silicon particles is deemed a possible solution to enhance efficiency of the process.

Seed particles of silicon appearing as granular material, so-called nuclei, are injected into the reactor; then a gaseous mixture of monosilane with either hydrogen or inert gas (argon, nitrogen) is fed in. Monosilane decomposition takes place when the temperature exceeds 600°C with silicon generated and further precipitated on silicon particles fluidized with gas flow. Pending silicon precipitating the sizes of particles grow from several hundreds of microns to 0.6 mm and greater. Dense granular polycrystal silicon generated has monodisperse composition, that facilitates its subsequent loading into containers, transportation, and recycling; as well as enables the process automation.

Application of the boiling bed reactor to generate polycrystal silicon is associated with a number of advantages over conventional rod-type reactors, among which a possibility of continuous process and high yield of the reactor are worth emphasizing. Isothermal nature of fluidized bed provides improved thermal productivity of the reactor and growth in the silicon yield; and fine mixing of silicon particles ensures their uniform surface. All these factors contribute to considerable reduction in the prime cost of the marketable product.

Thermal decomposition of monosilane is a complex process containing various stages.

1. Processes related to heterogeneous deposition of silicon on inoculating particles.
2. Formation of fine particle aerosol hampering the product yield.
3. Agglomeration of primary particles that is turning of several particle compounds into a single primary particle.

When generating granular silicon as a result of chemical precipitating of silicon from monosilane in a fluidized bed reactor it should be borne in mind that formation of fine fractions - aerosol and agglomerating effect of silicon particles deteriorate the quality of the derivable product and its yield. All mentioned stages of monosilane pyrolysis are closely interrelated and have mutual influence on each other.

An experimental set up has been developed and built up to prove the technology of generating granular silicon of monosilane exploiting a fluidized bed reactor. The fluidized bed reactor is the key process apparatus to accommodate the process of pyrolytic decomposition of monosilane resulting in silicon and hydrogen, and subsequent precipitating of silicon on heated silicon particles. It appears as a vertical tube of stainless steel having the internal diameter of the working zone as large as 50 mm and consists of a housing with a cover, expanding in the top part, water-cooled gas distributing device, a cyclone separator and resistive electric heat unit case, placed outside. The complete set-up is maintained in a heat-insulating jacket. The gas-distributing grate comes as a perforated plate of stainless steel, placed into a water-cooled device. The temperature regulation is performed with the aid of four different-level thermocouples, fixed in the reactor cover.

The fluidized bed of inoculating silicon particles is heated in a stream of inert gas (argon). Monosilane is fed into the reactor upon temperature's reaching the required level, the consumption of which is kept so that it allows maintaining its content in the blowing gas mixture from 10 to 40%.

Comprehensive experimental investigation of the process in the fluidized bed reactor employing state-of-the-art chemico-physical approaches and theoretical modeling enable to generate its full picture and to select optimized operating conditions for a highly productive energy-effective technology.

# FLUORIDE HYBRIDE TECHNOLOGY OF POLYCRYSTALLINE SOLAR SILICON PRODUCTION FROM THE RECYCLE PRODUCT OF APATITE RECYCLING

**Khitko V.I., Stepanenko N.V.[1], Vasilevich V.P.[1]**
The Minsk Research Institute of Radiomaterials
[1]The Belarusian State University of Informatics and Radioelectronics

The work on the production of semiconductor silicon using as a raw material the recycle product of apatite concentrate recycling into phosphorus fertilizers is carried out in the Republic of Belarus. Hydrofluorosilisic acid $H_2[SiF_6]$ is taken as a recycle product. It is produced in the process of making phosphoric fertilizers when purifying extraction phosphoric acid of fluorine compounds. Hydrofluorosilisic acid is then transformed into sodium silicofluoride by interacting with sodium carbonate:

$$H_2SiF_6 + Na_2CO_3 \rightarrow Na_2SiF_6 + H_2O + CO_2$$

The Homel chemical plant delivers hydrofluorosilisic acid $H_2[SiF_6]$ to the Polotsk plant "Izmeritel" on the grounds of which stage by stage recycling of hydrofluorosilisic acid into monosilanes and silicon is done on special laboratory installations.

Silicon production technology envisages three stages.

Stage I – Thermal decomposition of sodium silicofluoride with the discharge of gaseous sodium tetrafluoride and the production of a solid compound of sodium fluoride and the remains of the undecomposed sodium silicofluoride.

$$Na_2SiF_6 \xrightarrow{t\sim780^0C} SiF_4\uparrow + 2NaF$$

Sodium tetrafluoride is put into containers.

Stage II – Chemical transformation of the sodium tetrafluoride into monosilane. The transformation is done by the equation

$$SiF_4 + 2CaH_2 \rightarrow SiH_4\uparrow + 2CaF_2\downarrow$$

Lithium and potassium chloride (LiCl:KCl = 1:1,18) are mixed, poured into monosilane synthesis reactor, melted at 360 – 390°C. 3 – 5% calcium hydrate is solved in the smelt.

Sodium tetrafluoride gets into the reactor and barbotates through the smelt. The produced monosilane is purified and goes into a collector.

Stage III – Thermal decomposition of monosilane by the equation:

$$SiH_4 \xrightarrow{t\sim850^0C} Si + 2H_2\uparrow$$

The stage is carried out in the reactor on the heated silicon base where silicon is deposited and the uncombined hydrogen goes to the annealing unit.

It is supposed that Stage III may be carried out more effectively if the decomposition of silane is done in the reactor with the boiling layer of the heated silicon particles.

As a result of stages I – III technological process samples of polycrystalline semiconductor silicon have been obtained. Silicon quality analysis was done in the laboratory of mass spectrometry and chromatography of the State Institute of Rare Metals, Russian Federation, Moscow and by the specialists of the Minsk Scientific Research Institute of Radiomaterials.

Using a spark mass spectrometry method complete impurity composition of a silicon sample has been defined. [Table I]

The average specific resistance of a silicon sample with n-type electrical conductances is 160 ohm / cm, and those of p-type – 1270 ohm / cm.

The conducted laboratory experiments have above all proved the efficiency of the suggested by the authors technology of obtaining polycrystalline silicon from the recycle product (practically from the waste material) for the production of fertilizers from the Kolsky apatite concentrate.
The quality estimation results of the obtained silicon sample have shown the actuality of the

problem. Profound scientific research of the basic and auxiliary processes has been found to be expedient for working out the optimal suggestions for the design and production of the industrial equipment.

Table I
Silicon Sample Chemical Composition

| Element | ppm mass | Element | ppm mass |
|---|---|---|---|
| H | ND | Rh | <0,01 |
| Li | <0,003 | Pd | <0,1 |
| Be | <0,002 | Ag | <0,05 |
| B | <0,003 | Cd | <0,2 |
| C | 4 | In | <0,05 |
| N | ND | Sn | <0,1 |
| O | 500 | Sb | <0,1 |
| F | 0,02 | Te | <0,2 |
| Na | 0,09 | I | <0,03 |
| Mg | 0,06 | Cs | <0,1 |
| Al | 0,08 | Ba | <0,1 |
| Si | base | La | <0,2 |
| P | 0,5 | Ce | <0,02 |
| S | 0,2 | Pr | <0,02 |
| Cl | 0,4 | Nd | <0,05 |
| K | 0,2 | Sm | <0,06 |
| Ca | 0,7 | Eu | <0,07 |
| Sc | <0,05 | Gd | <0,09 |
| Ti | <0,05 | Tb | <0,03 |
| V | <0,01 | Dy | <0,08 |
| Cr | <0,02 | Ho | <0,02 |
| Mn | <0,03 | Er | <0,08 |
| Fe | <0,01 | Tm | <0,02 |
| Co | <0,02 | Yb | <0,09 |
| Ni | <0,02 | Lu | <0,02 |
| Cu | <0,02 | Hf | <0,03 |
| Zn | <0,02 | *Ta | <0,02 |
| Ga | <0,01 | W | <0,03 |
| Ge | <0,01 | Re | <0,02 |
| As | <0,02 | Os | <0,02 |
| Se | <0,05 | Ir | <0,03 |
| Br | <0,03 | Pt | <0,1 |
| Rb | <0,01 | Au | <0,05 |
| Sr | <0,1 | Hg | <0,2 |
| Y | <0,1 | Tl | <0,03 |
| Zr | <0,2 | Pb | <0,2 |
| Nb | <0,05 | Bi | <0,03 |
| Mo | <0,1 | Th | <0,03 |
| Ru | <0,06 | U | <0,03 |

* Ta is a structural material of the iron source

# EFFECT OF DOPING ON THE RESISTIVITY AND MICROSTRUCTURE OF CARBON FILMS

**Onoprienko A., Artamonov V.[1], Yanchuk I.[1]**
Institute for Problems of Materials Science, Ukraine National Academy of Sciences, Kiev
[1]Institute of Semiconductor Physics, Ukraine National Academy of Sciences, Kiev

Doped diamond and diamond-like carbon (DLC) films are now considered as promising materials for application in microelectronics. Doping with electrically active elements results in a shift of Fermi level, optical and electrical properties of films [1-3]. In present work the effect of substrate temperature on the resistivity of boron-doped C-films is studied and compared with that of non-doped C-films. Structural aspects of this effect are discussed.

The carbon films were deposited by a planar dc magnetron unit. Both non-doped and boron-doped films were prepared for study. In the first case as a target was the disk (60 mm in diameter and 3 mm thick) made from pure graphite (99,97 % purity). In the second case the target of the same dimensions was composed from graphite and a compound $B_4C$. The amount of $B_4C$ in the composed target was adjusted so that the concentration of boron in deposited films was close to 2 at. % as determined by the electron-probe microanalysis (EPMA) method with Camebax SX-50 instrument. A sputtering gas, argon of 99,97 % purity at constant pressure 1 Pa, was used in all experiments. As substrates, the polished platelets of Si-Ti-Al-O ceramics were used.

The resistance of films was measured in two directions: parallel and perpendicular to the substrate surface. For this purpose the specially configured nickel film contacts were magnetron sputtered onto substrates before carbon film deposition, and on the top of as-deposited carbon films. Such configuration of nickel electrodes made it possible to measure the resistances $R_\perp$ and $R_\parallel$ of carbon films. Carbon film resistivities $\rho_\perp$ and $\rho_\parallel$ were calculated from the measurements of $R_\perp$ and $R_\parallel$, the geometry and thickness of carbon film between metal contacts. The resistivity anisotropy coefficient was determined as $K=(\rho_\perp/\rho_\parallel)$.

Film thickness was measured with an optical interferometer, and it was 400-600 nm. Film structure was examined by high-energy electron diffraction in reflection mode (RHEED) and Raman spectroscopy.

As was revealed, $\rho_\perp$ has a tendency to decrease with an increase in $T_s$ for films of both types, but to a small degree. Quite different behavior was observed for $\rho_\parallel$ which decreased appreciably with an increase in $T_s$ in the temperature range 20-400 °C, and with further increase in temperature remained almost constant for the films of both types. However, the transition to the sharp decrease in $\rho_\parallel$ occured at higher temperature for boron-doped C-films.

The dependence of resistivity anisotropy coefficient K on $T_s$ for non-doped and boron-doped C-films is shown in Fig. 1. An increase in $T_s$ to ~400 °C resulted in abrupt increase in resistivity anisotropy for the films of both types. Further increase in $T_s$ did not change the value of K. Note, that in contrast to dependence of K on $T_s$ for non-doped C-films, for boron-doped C-films an increase in the degree of resistivity anisotropy was more slow in the temperature range 20-200 °C, and then the value of K also increased sharply with increase in $T_s$ to ~400 °C. At the same time the electron diffraction study revealed that the films of both types are amorphous in the temperature range 20-400 °C, i. e., the electron diffraction patterns from films have the view of several halos peculiar to amorphous structure. Only at $T_s$>400 °C the halos transformed in broadened lines characteristic of fine-grained defected polycrystalline structure of graphite.

The phenomenon of resistivity anisotropy in amorphous carbon films was discovered for the first time by he authors of [4] and studied in more details in [5]. The results of study in [5] made it possible to propose the mechanism of microstructure formation of non-doped a-C films, which governs the observed changes in a-C film resistivity. According to that mechanism, the evolution of structure of non-doped a-C film in the temperature range 20-400°C proceeds via nucleation of graphite-like G-phase in amorphous D-phase. An increase in $T_s$ above 400 °C results in

direct formation of graphite-like clusters onto the substrate instead of nucleation of G-phase nuclei in amorphous D-phase. With increase in $T_s$ these clusters become of more ordered internal structure and exhibit mutual ordering .

As was mentioned above, the behavior of resistivity in non-doped and boron-doped a-C films is quite close. The observed difference for $\rho_{\parallel}$ and K in boron-doped films allows to suppose that boron atoms hinder the nucleation of graphite G-phase in amorphous D-phase in the temperature range 20-200 °C, and then their influence on the velocity of nucleation of G-phase becomes insignificant. To this indicate also the dependencies of integral intensity ratio of D and G peaks on $T_s$ in Raman spectra from non-doped and boron-doped a-C films.

According the ideas formulated in [6, 7] the appearance of D-peak in Raman spectra for amorphous phase indicates the ordering of the structure in aromatic rings and graphite-like clusters, and its intensity is proportional to the cluster size or, in other words, to the degree of structure ordering. At the same time, the presence in C-film structure the rings with symmetry other than hexagonal decreases the height of D-peak. Based on these results one can suppose that the atoms of boron incorporate into aromatic rings, which nucleate in disordered D-phase. Since the size of boron atoms differs from that of carbon, then such rings are distorted. At low substrate temperature (20-200 °C) the portion of distorted aromatic rings is rather large and therefore the disordered phase prevail in the structure of growing film. With increase in $T_s$ above 200 °C the rate of formation for aromatic rings increases and they become more ordered in graphite-like clusters, oriented parallel to the substrate [5]. Since the concentration of boron in a-C film is constant and quite low (2 at. %), then more non-distorted aromatic rings form which do not contain boron atoms and join into graphite-like clusters. As a consequence of formation of such a graphite-like structure the resistivity $\rho_{\parallel}$ decreases. At $T_s$>400-450 °C, according to [5], the mechanism of C-film changes and the C-film grows by direct formation of fine-grained graphite phase. In this temperature range the boron atoms being electrically active impurity seem to serve as the sites for nucleation of G-phase. Since the resource of boron atoms is limited by their low concentration in C-film, then their influence quickly comes to naught with increase in $T_s$ because of high rate of formation of clusters with graphite structure.

As to the character of changing $\rho_{\perp}$, it was shown in [5] that the transformation of structure in non-doped a-C films with change in $T_s$ occurs mainly in direction parallel to the substrate surface. The change of the structure in boron-doped a-C films seems to be of the same nature and for this reason $\rho_{\perp}$ depends little on the condensation temperature and follows the dependence peculiar to non-doped a-C films.

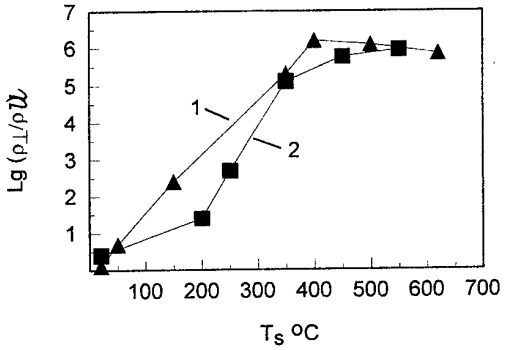


Fig. 1. Dependence of resistivity anisotropy coefficient $K=(\rho^{\perp}/\rho_{\parallel})$ on substrate temperature $T_s$ for non-doped (1) and boron-doped (2) C-films.

References

1. C. Ronning, U. Griesmeier, M. Gross, et al., Diamond Relat. Mater., 4, 666(1995).
2. B. R. Stoner, C. T. Kao, D. M. Malta, and R. C. Glass, Appl. Phys. Lett., 62, 2347 (1993).
3. G. A. J. Amaratunga, V. S. Veerasamy, C. A. Davis, et al., J. Non-Cryst. Solids, 164-166, 1119
4. A. A. Onoprienko and L. R. Shaginyan, Diamond Relat. Mater., 3, 1132 (1994).
5. L. R. Shaginyan, A. A. Onoprienko, V. F. Britun and V. P. Smirnov, Thin Sol. Films, 397 (1-2), 288 (2001).
6. M. Chhowalla, A. C. Ferrari. J. Robertson. and A. J. Amaratunga, Appl. Phys. Lett., 76 (11), 1419(2000).
7. A. C. Ferrari and J. Robertson, Phys. Rev. B, 61(20), 14095 (2000).

# OUTLOOKS OF MANUFACTURING OF COMPOSITE MATERIALS USING ULTRASONIC TECHNOLOGIES

**Kozlov A.V., Mordyuk B.N., Prokopenko G.I.**
Kurdyumov Institute for Metal Physics, Kiev, Ukraine

The conventional approach to control of properties of materials is based on using of alloying by some impurities. However in a number of cases this approach comes across principled limitations conditioned by absence in the naturc of impurities indispensable for obtaining of materials with given properties. Therefore large attention of the explorers is attracted with composite materials hardened by dispersed particles, discrete or continuous fibers of phase that higher melting, strong and rigid than matrix.

The different combinations of hardening phases and matrixes, methods of obtaining from them of composites allow to receive a broad spectrum of materials with a complex of desirable properties.

The application of power ultrasonic vibrations in a number of composite materials manufacturing technologies can essentially improve their physical-mechanical and functional properties.

In the present work three directions of application of power ultrasound for production of composites are reviewed. The physical backgrounds of joint deformation in a ultrasonic field (drawing, flattering, pressing), application of ultrasound together with powder metallurgy techniques at miscellaneous stages of composites production and at last crystallization of composites with dispersed solid particles in a ultrasonic field is discussed.

Superposing of ultrasonic vibration during joint deformation of bars for composites allows improving the quality of a received material.

Firstly, due to the acousto-plastic effect the yield strength of matrix is degreased, and consequently the hollow's filling is improved, that in turn results in a decrease of a porosity of a final aggregate. Secondly, at ultrasonic processing the processes of diffusion and mass-transfer (see fig.1,2) are intensified [2,3] that allow receiving composites with high strength of interphase border (matrix - reinforcing phase). It should be noticed that regimes of ultrasonic processing must be strictly definite to avoid the intensive interaction of composite consistents between one another, invoking a degradation of structure and properties, both reinforcing phase and matrix [4].

The application of ultrasonic vibrations during composites manufacturing by powder metallurgy techniques is also effective at different stages of process. The optimum regimes of ultrasonic mixing and stirring of powders and also mechanical alloying of different systems using ultrasonic mill designed in Institute for Metal Physics (IMP) are studied [5]. In ultrasonic grinding mill three mechanisms of effects on powders are realizing:

- effect of ultrasonic vibrations;
- mechanism of shock ultrasonic treatment (with free working elements);
- effect of an ultrasonic cavitation and acoustic flows.

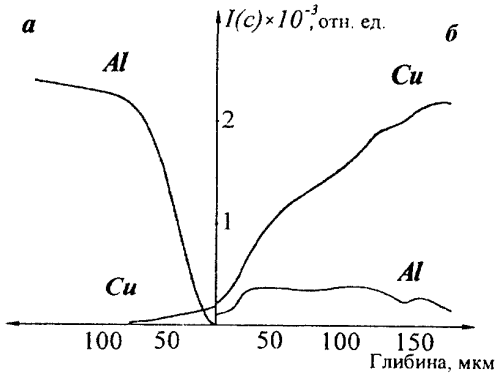


Fig.1. Arengement of copper in aluminium (a and aluminium in copper (б) after ultrasonic treatment of pair Cu-Al [2].

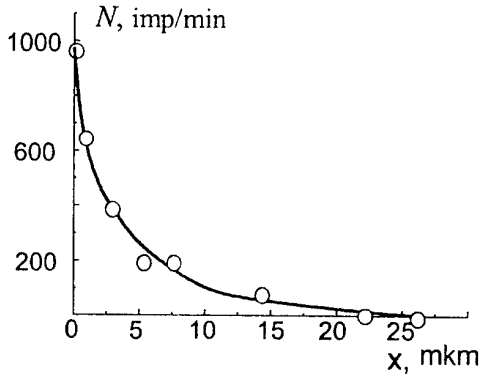


Fig.2. Distribution of radioactive Ni in Al after pressing in ultrasonic field [3].

Optimum regime of ultrasonic treatment of powders depends on power and duration of

processing, different liquids (ethyl spirit, glycerin, acetone or water), spacing coefficient of the chamber for processing by balls, energy tensity and temperature in the chamber, influencing of hydrostatic pressure increasing.

The possibility of modifying of powder materials surface for improvement of their wettings by metals melts or for improvement sintering in ultrasonic field is investigated.

The peculiarities of mechanical alloying or, in other words, intensification of solid phase reactions is shown on a number of systems (Fe-Cu after joint deformation in ultrasonic field, Cu-Ni after cavitation treatment, Cu-Ni-Fe after ultrasonis ball milling).

Compacting of powder materials with superposition of ultrasonic vibrations using special equipment designed in IMP [6] allows to considerably increase the density of obtained samples, and in case of powder mixtures (matrix - reinforcing phase) – to increase the strength of interphase border in composite. The features of selection of regimes of ultrasonic processing are subject to the rules set up above for a case of joint deformation. The physical reasons of increase of functional properties of the obtained composites remain valid also (fig.3.).

The third direction, in which the investigations of influencing of ultrasound on process of composite materials production are conducting, is crystallization in an ultrasonic field of melt with disperse solid particles of a reinforcing phase.

In this case ultrasonic action can be characterized by following consequent processes in indurating melt, having different structural components [7]:

1) Equalization of a solidified front;
2) Dispersion and metalization of solid phase particles due to ultrasonic cavitation and distri-bution in volume of centers of crystalline phase;
3) Initialization of acoustic flows in a melt that lead to intensive stirring and;
4) Removal of capillary limitations at a stage of growth of crystallization centers and improvement of wettability by stayed liquid.

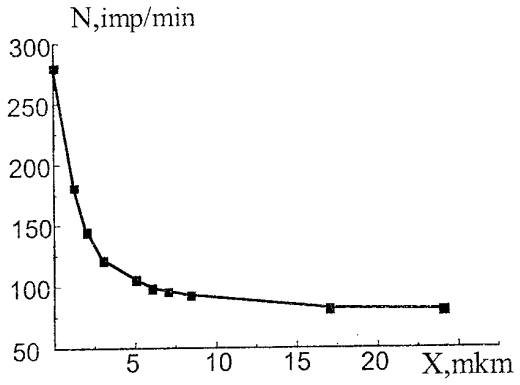


Fig.3. Distribution of radioactive Ni in Al after ultrasonic cavitation treatment [3].

The situation becomes more complicated in case of a directional crystallization. There are some problems become essential. Namely pushing/ engulfment of solid phase particles by a solidified front, rate of solidification, gradient of temperatures and width of a boundary layer. The connective processes in a melt leave on the foreground.

From the point of view of heat effects on the one hand convection in liquid renders stabilize influencing on a solidified front. With other hand - amplification of conventional flows leads to decreasing of boundary layer width and increasing of concentration deviation of ingot from initial concentration of a melt. Generally for acquisition smaller on the size of disperse solid particles is indispensable more high speed of crystallization.

The introducing in a melt of ultrasonic vibrations of sufficient power essentially changes a situation. The conventional flows undergo operating acoustic flows. Under operating of ultrasonic cavitation the wettability of solid particles is increased, besides solid particles pushing to solidification front by acoustic pressure. The complex of physical phenomena arising in melt under ultrasonic action allows uniformly arranging the reinforcing phase in composite ingot volume.

The support of the projects # NN32 and # 2354 is gratefully acknowledged.

References

1. A.I.Kolpashnikov, B.A. Arefiev, V.F. Manuilov / Deformation of composite materials. M.: Metallurgy.- 1982.- 248 p. - in Russian.
2. M.Vasiliev, G.Prokopenko, B.Mordyuk, A.Kozlov // Metal Phys. Adv. Tech., 1995, v.15, p.1251-1255.
3. A.Kozlov, G.Prokopenko et al. // Metal Phys. Adv. Tech., 2001, v.23, spec. ed., p.232-235.
4. Povarova K.B., Bannukh D.A. // Mater. Sci. Trans.- 2001, v.56, N 11.- p. 24-32.
5. A.Kozlov, A.Perekos et al.// Metal Phys. and Adv. Tech., 2001, v.23, spec. ed., p.220-223.
6. A.Kozlov, V.Kolomytsev et al. // Metal Phys. New Tech., 2001, v.23, spec. ed., p.228-231.
7. Aramov O.V. Crystallization of metals in a ultrasonic field.M.:Metallurgy,1972,256 p.

# EFFECTIVE METHODS OF SYNTHESES OF PRODUCTS FROM COMPOSITE MATERIALS WITH USE OF FOUNDRY TECHNOLOGIES

**Zatulovsky A.S., Lakeev V.A.**
Physico-technological Institute of Metals and Alloys of the NAS of Ukraine, Kiev, Ukraine

The modern methods of syntheses of products with use of granules, powders, particles allows to get the broad gamma of new materials, which have unique characteristics or their combination: from macro heterogeneous cast composite materials (CCM) to powdered materials. The choice of optimum method of reception of products from composite material (CM) is defined by complex technical, economic, conjuncture and others factors. The traditional method of technology of solid-phase consolidation of products from CM on metallic base is the powdered metallurgy, which use for production of functional CM as an iron-graphite, and others types. Liquid-phase methods, which founded on melted matrixes (copper alloys) using in technological process, which consolidate the hard reinforcing elements (for instance, steel granules), have number of important advantages:

-more short and more inexpensive production cycle;

-smaller force influence on the brittle reinforcing elements (carbon, glass-ceramic and others fibres);

-expansion of nomenclature of initial row materials: possibility of secondary colour alloys using, metal scrap, shavings;

-more simple apparatus registration, possibility of existing melting, termal and others equipment using.

However in connection with high reactionary ability of the high temperature matrix melt the more strict record of physico-chemical characteristics of CM components, their changing and interactions at process of solid-fluid technology needs. How the studies have shown, process of CCM forming may be divided into the following stages: 1) matrix melts moistening and spreading on reinforcing elements surface; 2) termal , diffusion or chemical interaction between phases; 3) crystallisation of the fluid phase (the matrix melt); 4) dissolved-diffusion interaction between components (phases) in process of cooling, heat treatment, other finish processing. The technology optimisation depends on time of contact of solid and fluid phases: interaction of phases must not have negative influence upon characteristics of CM.

For event of the solid-fluid holding the time of phases contact must be a smaller then period of an retardation of diffusion processes that provides the reception of CCM by method of solid-fluid consolidation without connecting layers on separating border of phases:

$$t_{cn} < t_{ct} < t_r < t_{gd} < t_{in}, \text{ where}$$

$t_{cn}$- the necessary time of arising of strong connections between CCM elements, $t_{ct}$- the optimum time of the fluid and solid phases contact, $t_r$- the incubation time of heterodiffusion or retardation of diffusion, $t_{gd}$- the duration of geterodiffusion, which necessary to forming of the layer of brittle phases, $t_{in}$ - the duration of formation of a intermetallids layer on borders of phases.

Optimum time of contact ($t_{ct}$), as the main parameter of solid-fluidphases technology of CM production, is a polyfactor function which dependent on reinforcement parameters, construction and measured-geometric factors. $t_{ct}$-is yielded to exact calculation and is defined experimentally for concrete CCM and half-finished products. The diagram is built in the temperature-time coordinates, which allow to forecast the optimum parameters of definite CCM structure from the system of bronze - steel shot.

Requirements to row materials, which take into account the specific requirements of solid-fluid consolidation of the composite half-finished products with use the foundry technologies are formulated.

The composite production perspective technology are considered and recommended as gravity casting (soaks) and special types of casting with use the external influences. Each method has their own specific particularities, are optimum for production of products with concrete types of sizes, CCM composition and others features. They are tested and mastered technologies of composition casting, which allow to cast from CCM the bushes with diameter: 30-500 mm, height before 200 mm, thickness of wall 5-40 mm. In mode of dry friction at slide velocities 1-10 m/c; they are allowed the loads 5-15 MPa, in the field of the temperature before 600-850 $^0$C.

The experience of industrial operation of tribo-detail from CCM has shown that using of the new high wear-resistant tribo-material and the composition casting technologies gives the significant technical-economic effect in such priority areas of technology, as energy, metallurgy, car-, tractor-machine building, agricultural engineering, processing and food industry, special engineering and others.

# EVOLUTION OF STRUCTURE OF COPPER AFTER TORSION EXTRUSION

**Varyukhin V.N., Pashinskaya E.G, Domareva A.S., Tkachenko V.M., Pashinskaya O.V.**
Donetsk Physical-Technical Institute, NASU, Donetsk, Ukraine

Processes of ultrafine-dyspersated formation in copper, which was produced by new method of intensive plastic deformation by torsion hydroextrusion (TH), was investigated with help of methods of optical microscopy, diffractometer analysis and measuring of microhardness. It was demonstrated, that process of structure formation in process of deformation is developed not linearly, but in a few stages. It was fixed, that in every phase of deformation structure is formed, which in general case is a superposition of microcrystalline grains and nanoregion. Nanoregions are anisotropic and have a size of 80-200 nanometres. Degree of stability of structures in process of deformation, which are originated after initiation of rotation mode in it, was evaluated with help of computer experiment by method of molecular dynamics.

Last time more attention is called to receiving and investigating of materials with particular submicrocrystalline structure, or nanostructure. In Donetsk Phisical-Technical Institute method of TH for producing of nanocristalic structure is proposed. Method permits to achieve large plastic deformation on the massive test specimens (deformation during the production cycle reach e=2).

For investigation of transformation of structures in copper in deformation processes, test specimens were researched in initial condition (e=0), after the first (e=2.7) and following deformation cycles (e=4,7; 6,7; 8,7; 12,7). The changes was controlled by methods of durometry, optical metallography, X-ray structural analysis, optical microscopy. It was realized a computer experiment for probably description (by method of molecular dynamics) of initiation of rotation modes after large shear deformation.

All groups of the specimens are characterized by the equal structure of section, which isn't differs in the centre and on the rim. After deformation e=2.7 the grains are disintelattice and vortical structure is formed, which makes 100% of specimens' area. After deformation, which cumulatives, is increased to e=12.7, in the centre single large equiaxial grains appear (140-180 mkm). It was shown by methods of X-ray and electron microscopy, that with help of this type of deformation it is possible to make a fragmentation nanostructure alike quasy-two-dimensional klasters with interplanar intervals, which were change.

It is impotent to pay attention, that nanoregion are anisotropic in volume of crystallites, and when e=4,7, the destruction of the received structure takes place. We can see it from changes of the axes of a crystalline lattice and microdistortions, extension of sizes of the nanoregions, etc.

The investigation has shown that after the annealing ( 500$^0$C for a one hour) specimens had grains the size of 2000 nanometres – 100 mkm ( the Table 1).

The boundaries of the grains are straights, it was marked the twins of growth. The deformed specimens with degree of deformation e=2.7 were characterized by maximum refinement of grains (figure 1). On the specimens with deformation degree e=4.7 the beginning of recrystalization with growth of the grains was marked. .There are the regions, which contain the very little fragments and the tracks of the sliding in the grains and the slipping between ones. When degree of deformation is e=6.7, the processes of recrystalization and the formation of the submicrocrystalline regions are go on, that is why boundaries of the grains become rough, they are consist of the kinks.

With this degree of deformation the porouness of specimens is developed. Size of the pores is from 20 nm to 150 nm. Next deformation to degree e=8.7 is accompanied by further recrystalisation.. In contrast to the specimens after the annealing, specimens, which were deformated with that degree of intensive plastic deformation, have indirect wide boundaries, twins of growth are absent, and there are stripes of the sliding in the grains and the slipping between ones.

The peculiarities of nanofragments, which were described, permit to surmise, that one of the variants of mechanisms of the forming of that regions probably may be the continuous nucleation of rotation mode in the plane of deformation.

It was shown, that at fixed parameters of model and speeds of deformation primarily an ideal

structure is transformed, and a new region of ideal crystal is formed, in which the axes of symmetry are turned relatively the initial plane at some angle.

The regions are parted by the boundary of thinning. This boundary is continuously change its position in space (figure 2). If we change direction of deformation to the opposite in this situation, old region in the centre of the crystall will part from the other part of crystall as a localized region.

Figure 1.The surface of deformated copper with help of high-resolution carbonic replicas e=2.7 (a-x6600 и b-x27200)

The diminution of free space between the envelope and the initial crystallite is a cause of suspension of the forming of rotation mode.

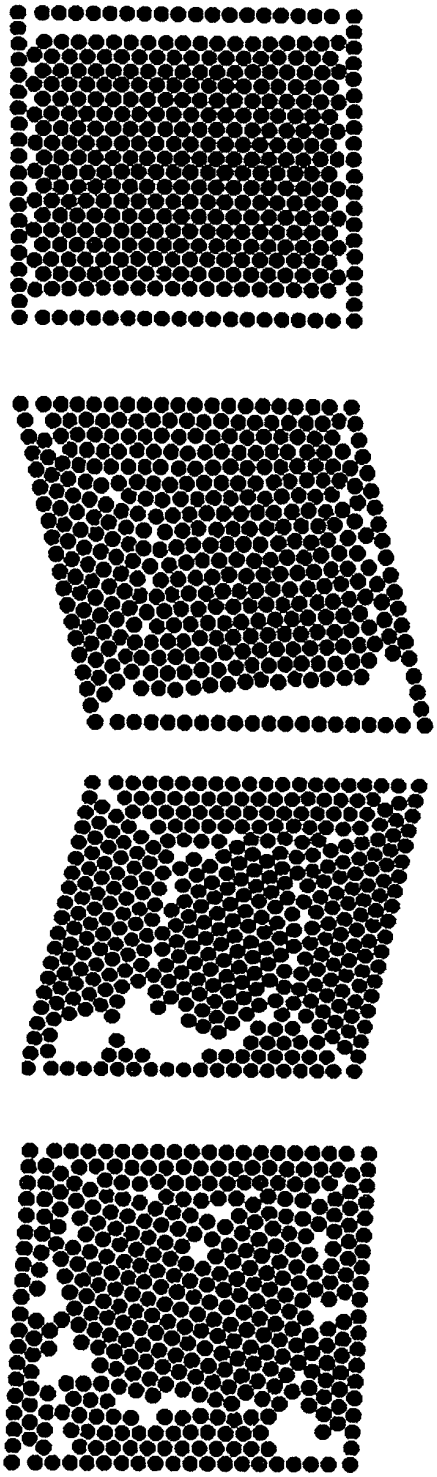

Figure 2. The calculated significances of position of the atoms in the lattice of copper at intensive deformation: a – initial condition, b – resilient deformation, c – the rotation nanoregion, d – nanoregion at next stages of deformation.

# SYNTHESIS OF SILICON CARBIDE POROUS MATERIALS BASED ON ULTRA-DISPERSED REACTIVE SYSTEM

**Antsiferov V.N., Gilyov V.G., Sung J.S.[(1)], Kim T.W.[(1)]**
Research Center of Powder Materials Science, Perm, Russia
[(1)]Korea Institute of Energy Research, 71-2 Jang-dong, Yoosong, Daejeon, Korea

Silicon carbide could be used for sorption and membrane separation due to the inertness to chemicals, high temperature stability and abrasion durability. Carbon promotes the sorption of organic impurities of fluid like a filter [1, 2].

The microporous silicon carbide is expected to have high temperature stability because of high melting point of SiC, $T_{melt}$=2,540°C and high sintering temperature, 0,8 $T_{melt}$ [3], while sintering temperature of the ultra-dispersed powders of TiN and AlN is about 0.45 $T_{melt}$ [4]. The reactive SiC synthesis is promising to obtain microporous materials [5,6].

The synthesis of porous SiC in reactive system, $Si_S + C_S = SiC$ is studied. The influences of specific surface of reactive mixture, pressing and thermal conditions are studied with the characteristics of permeability, durability of samples.

The mixtures with surface of 40-120 $m^2/g$ were obtained through the grinding with ball mill. As shown at the Fig. 1 the sharp maximum specific surface area is shown at a certain grinding time.

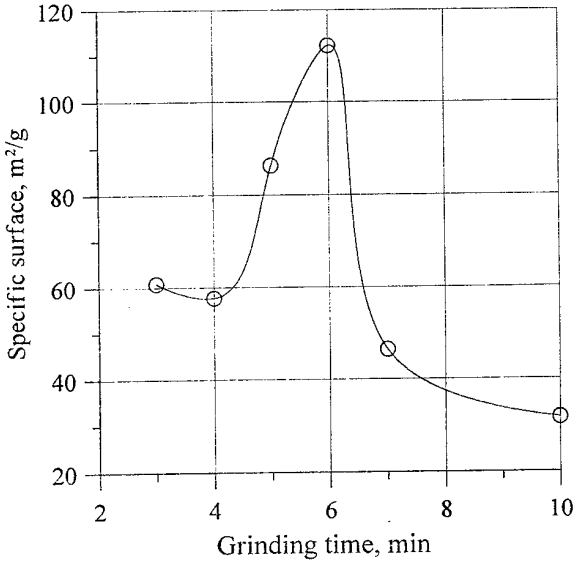


Fig 1. Dependence of the specific surface area of reactive mixture on grinding time with ball mill

As shown at Table.1 we obtained the samples with porosity of 45-60%, pore size up to 0.3 μm measured by the bubbling method and specific surface area of 40 $m^2/g$.

As the specific surface area of sintering mixture was increased up to 40 $m^2/g$, the sintering time and temperature and the isotherm reaction time were increased comparing to the initial mixtures of high $S_{sp.}$

For high mechanical strength and absence of shrinkage during synthesis the harder melted frame and graphite-added mixtures were needed and then the quick SiC reaction is realized in high-dispersed mixtures.

Table 1. Specific surface area, porosity and pore size synthesized in argon with reaction mixtures

| $S_{sp,}$ mix. $m^2/g$ | Pressing pressure, MP | Sintering T, °C, time, h | Poro-sity, % | $D_{por,}$ μm | $S_{sp,}$ $m^2/g$ |
|---|---|---|---|---|---|
| 85 | 50 | 1600-1 | 61 | 0,5 | 5,9 |
| 85 | 100 | 1600-1 | 58 | 0,47 | 6,5 |
| 85 | 150 | 1600-1 | 54 | 0,41 | 11,0 |
| 32 | 50 | 1300-2 | 57 | 0,5 | 24,2 |
| 85 | 50 | 1600-0,5 | 57 | 0,36 | 8,2 |
| 32 | 50 | 1600-0,5 | 56 | 1,0 | 2,3 |
| 85 | - | 1600-2 | 58 | 0,56 | 3,6 |
| 61 | 50 | 1150-0,33 | 47 | - | 28,7 |
| 115 | 50 | 1150-0,33 | 54 | - | 37,9 |
| 115 | 50 | 1650-0,17 | 59 | - | 2,6 |
| 46 | 50 | 1650-0,17 | 50 | - | 3,7 |

As shown at X-Ray analysis (Fig.2) the high-dispersed mixture ($S_{sp}$ = 115 $m^2/g$) provides complete synthesis of SiC during 0.33 hours at 1150°C in argon. With not so high-dispersed mixture ($S_{sp}$ = 61 $m^2/g$) there are essential quantities of not-reacted silicon.

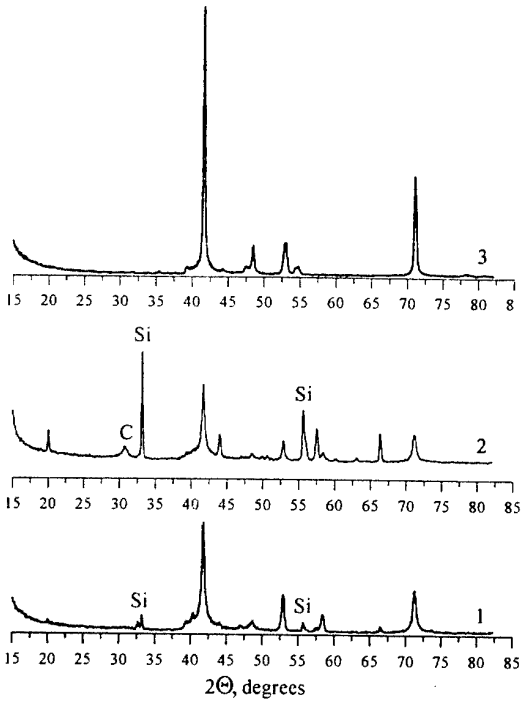


Fig 2. X-Ray diffraction (λ, $K_\alpha Co$) of SiC samples synthesized in argon at different modes: 1 - 1650°C, 0.17 h, 115 $m^2/g$ ($S_{sp, mix}$); 2 - 1150°C, 0.33 h, 61 $m^2/g$; 3 - 1150°C, 0.33 h, 115 $m^2/g$

Table 2 shows the nitrogen isotherm of samples. As the micro pore (radius) size is about 2,8-3,7 nm, this may be used as a filtering of water from the organic molecules such as methylene blue and phenol.

Table.2. SiC pore structure ($N_2$ adsorption isotherm)

| $S_{sp}$ of mix, $m^2/g$ | 85 | 85 | 32 | 115 | 46 |
|---|---|---|---|---|---|
| Sintering T, °C | 1600 | 1600 | 1600 | 1150 | 1350 |
| Sintering τ, h | 1 | 2 | 0,5 | 0,33 | 0,5 |
| Sintering medium | Ar | Ar | Ar | Ar | $CO_2$ |
| Porosity, % | 61 | - | 57 | 54 | 47 |
| $S_{BET}$, $m^2/g$ | 6,1 | 8,6 | 18,5 | 37,9 | 20,7 |
| $S_{Mi}$, $m^2/g$ | 3,8 | 6,8 | 16,2 | 30,0 | 17,3 |
| $V_{Mi}$, $cm^3/g$ | 0,003 | 0,004 | 0,007 | 0,015 | 0,009 |
| $V_{Me}$, $cm^3/g$ | 0,008 | 0,012 | 0,019 | 0,045 | 0,029 |
| $W_S$, $cm^3/r$ | 0,011 | 0,016 | 0,026 | 0,060 | 0,038 |
| $r_p$, nm | 3,6 | 3,7 | 2,8 | 3,2 | 3,7 |

With the porosity 50% (at $S_{sp}$ = 30 $m^2/g$; $S_{sp}^v$ = 50 $m^2/cm^3$) the effective pore radius estimated to be 20 nm by the equation of $r_p = 2P/S_{уд}$,, which is comparable to hydrogen selective nano porous membranes.

Therefore, there is possibility of low-temperature synthesis of porous silicon carbide with high specific surface (up to 40 $m^2/g$) with micropores.

REFERENCES

1. Tomilina E.M, Lukin E.S., Kagramanov G.G. Durable porous ceramics based on silicon carbide with low sintering temperature, *Refractory and Ceramics,* 2000. №4. pp.12-14.

2. Mathere J., Mirzhanov A.G., Borovinskaya I.P. and others Ceramic filters for drinking water filtering, *Refractory and Ceramics*, 1999. №1-2. pp.43-47.

3. Andrievski R.A. Nanocrystalline High melting point compound based materials, *Journal of Materials Science*. 1994. V.29. P.614-631.

4. V.V. Dalidovitch, N.V. Fedorov, O.Ed. Babkin, Deriving and properties of sorption-active ceramic materials based on ultra-fine TiN and AlN powders, *Journal Appl. Chem.*, 1994. V.67, №6. P.942-945 (in Russian)

5. Gilyov V.G., Silicon carbide membrane materials, Advanced materials and technologies problems, *Perm,* Issue.5, 2000, pp.45-52.

6. Gilyov V.G., Reaction sintering with negative bulk effects // Inorganic materials. 2002. №3. P.371-377.

# TWO-STAGES SCHEME OF CARBONLESS IRON POWDER PRODUCTION

**Khovavko O.I., Svyatenko O.M., Semenyuk N.I., Bondarenko B.I.**
The Gas Institute of National Academy of Sciences of Ukraine

Last tenth years a demand on iron powders with unusual properties as in traditional productions has been increased in particular on carbonless one, which is base of soft-magnetic materials [1].

Extant methods of direct iron production do not allow an obtaining of carbonless powder because of carbon-containing components presence in the used reducing gases, which inevitably get to finished product. For the purpose of carbonless powders production the authors have developed two-stages reducing process under atmosphere of hydrogen, cleaned from carbon impurities.

It is shown that electrolytic hydrogen gives the best results. An use of technical hydrogen does not allow to obtain carbonless iron powder. So the presence even tenth part of % of carbon-containing components in the form of $CO_2$ imports carbon to powder not less than 0,05% (because of $CO_2$ secondary conversion to CO by hydrogen).

The gas-tight conveyor electrical furnace was selected as a base of reducing reactor. It has shown excellent results in processes of hydrogen reducing and annealing of iron powders [2].

During reducing in one device it can portioned 2 different stages on kinetics, namely [3]:
- basic reducing process, which passes with high speed and big consumption of reagents to reducing rate of 90-96%;
- process of final reducing (finishing), which runs extraordinarily slowly and with small reagents intake.

As process comes into braking part (final reducing) effectiveness of intensive process falls. It's occurred due to lowering of gas-using coefficient along of that a cost increases. Besides, when full oxides reducing is hold in one stage, non-uniformity reducing on height of layer is observed because top-crust on the surface of charge is created. The crust prevents material from hydrogen penetration into, and also from rejection of connected oxygen outside. This fact limits the height of initial super-concentrate charging on a belt of conveyor electric furnace.

It is necessary to decrease a strength against hydrogen supply into the middle of reducing material. An intermediate grinding of cake allows liquidating sintered "crust", fulfilling a magnetic separation, averaging powder heterogeneity on reducing degree. A bulk density while single-stage process does not exceed 1,4-1,6 g/cm$^3$. But according to the acting GOSTs a bulk density of iron powder should be within 2,3-3,0g/cm$^3$. An interruption of reducing process enables to make pre-compacting of pre-reduced iron powder to increase a bulk density. The interruption allows decreasing the height of charging layer, and thus multiplies productivity on ready product. One of such method, which has been approved, is rolling of powder and next grinding of obtained sheets.

The offered at the Gas Institute of NASU conception of reduced iron powders production on two-stage scheme consists following.

At first stage spongy iron with reducing degree of 90-96% is obtained by dint of processing of carbonless iron super-concentrate in atmosphere of electrolytic hydrogen (reduction furnace). Temperature of the process is 800-900□C. Second stage is deep iron reducing in atmosphere of dried hydrogen under 800-900□C (annealing furnace). Such process of obtaining reduced iron powder does not request operation of carbon elimination, and also enables to get final product with good technological properties.

Although the use of electrolytic hydrogen enables to get splendid carbonless powder but given technology is rather energy intensive. It explains by expends on production of electrolytic hydrogen (app. 5kW per 1 m$^3$ of $H_2$). Therefore authors carried out an attempt to improve the two-stages scheme of reduced iron powder production in gas atmosphere with injection into system the re-circulation hydrogen contour.

The offered scheme of a gas-supplying system provides with feeding into annealing furnace only electrolytic hydrogen, but into reducing furnace a dust-free, chilled, worked-out hydrogen after annealing furnace and re-circulation gases are supplied.

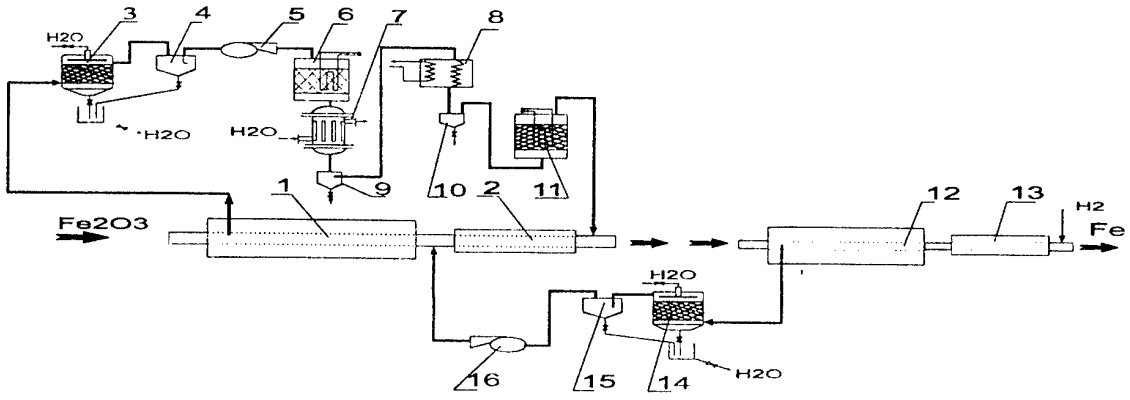


Fig. 1. Two-stages scheme of carbonless iron powder production.1-reducing furnace; 2,13-fridges; 3,14-scrubbers; 4,9,10,15-drop catchers; 5,16-blowers; 6-reactor of catalytic conversion; 7-heat changer; 8-crio-fridge; 9-adsorber; 12-annealing furnace.

Such scheme is created taking into account that oxygen is removed from charge reducing furnace in quantity 88-95% and 5-12% from charge annealing furnace. If we use martite super-concentrates, quantity of removed oxygen is 26,5-28% in reducing furnace and only 3-4% in annealing furnace.

Herewith it's necessary to note that hard reduced low-porosity particles and off-the-shelf in a charge the double and triple oxides such as hertsenite, phayalite and etc. can be additionally reduced in annealing furnace. A pure hydrogen feeding for one passageway into annealing furnace allows using its high reducing ability.

But considerable part of hydrogen oxidizes to $H_2O$ in reducing furnace. We need to support sufficient reducing potential of worked-out gas and removed it from the furnace as quick as possible and dehydrate it. The computations show that optimum rate of fresh (from annealing furnace) and re-circulating flows is 1:3; 1:4.

Among the used reducing gases as endogas, technical hydrogen, cracked ammonia, electrolytic hydrogen we have fixed on the last one for feeding into annealing furnace. This has been done taking into account that carbon-containing components, which are in the first two reductants, get inevitably into a final product during raw powder annealing. It is inexpedient to re-circulate cracked ammonia, which contains 25% of nitrogen, because during gas re-circulation a residual nitrogen will be accumulated in system. Therefore a quantity of nitrogen will reach ~52% after second circulation and 70 % after third one accordingly hydrogen content will be app. 25 and 15 % (when $Fe_2O_3$ loading is 75 kg/h, quantity of circulated gas Q=100 $m^3/h$). So after several circulations gas-reducing potential becomes lowers and process economy drastically falls down. An application of a clean dried electrolytic hydrogen allows obtaining of a clean on carbon iron powder. Low moisture content in reducing gas enables to get final iron powder with high degree reduction.

Only gases, outgoing from reducing furnace are well handled to regenerate and re-circulate. Such gas-supplying system decreases the requirements on cleanness of gases-reductants concerning admixtures rate at reducing stage, and guarantees high quality of iron powder after annealing, if a fresh clean electrolytic hydrogen is only used. This allows simplifying and making cheaper the gases regeneration and re-circulation system for reducing furnace.

Process partition on 2 stage with application of re-circulation contour on reducing gas gives possibility improve not only powder quality, its chemical composition and technological properties and to save energy with point of view of used $H_2$ generation.

**References**

1. Bondarenko B.I., Fedorov D.N., Khovavko A.I., Sundaresan C.R., Shivakumar AND., Karanjai M., "Study of Soft Magnetic Iron Powder Production", Workshop on "Production and Applications of Soft Magnetic Materials for Electric Motors", Munich, 2000.

2. Бондаренко Б.И., Курганский Н.П., Пекач В.Ф. Восстановительно-обезуглероживающий отжиг металлических порошков. Киев: Наук. Думка, 1991. – 328 с.

3. Бондаренко Б.И. Восстановление окислов металлов в сложных газовых атмосферах. – Киев: Наук. Думка, 1980, 368 с.

# SYNTHESIS OF THE MODIFIED BIOACTIVE CALCIUM HYDROXYAPATITE

**Zaslavskaya L.V., Belousova E.E, Rosantsev G.M.**
Donetsk National University, Donetsk, Ukraine

Calcium hydroxyapatite (HA) is a perspective biologically active material used in medicine as a substitute of a bone substance [1]. Synthetic HA has no the sufficient physics--mechanical characteristics in comparison with a human bone. With the purpose of increase of durability hydroxyapatite ceramics enter various modifiers [2]. It is known, that in quality of implants can be used the bioactive glasses and sitalls, which synthesis is carried out on a basis of calcic and phosphoric systems [3]. The majority of the researchers connect bioactivity of these materials to formation of the apatite layer in a transitive zone implantant-bone .

The purpose of the given work is the research of an opportunity of formation the calcium hydroxyapatite , modified by lanthanum ions, silicon and tantalum with the subsequent study of durability of ceramic samples. In the work it was given the conditions of synthesis of calcium hydroxiapatit modified by the lanthanum and silicon ions using the method of precipitating from the water solutions. It was determined that pH of initial solutions and precipitation, concentration and temperature processing influence on the composition of the modified product. It was shown that the introducing of the oxygen compounds of tantalum improve the physical and mechanical properties of ceramics.

Synthesis calcium hydroxyapatite, containing ions lanthanum and silicon (HALS) of structure $Ca_9 La (PO_4)_3 (SiO_4)(OH)_2$, carried out under the circuit:

$$9Ca^{2+} + La^{3+} + 5PO_4^{3-} + SiO_3^{2-} + 4OH^- \rightarrow Ca_9La(PO_4)_5(SiO_4)(OH)_2$$

In this reaction $OH^-$ groups carry out two functions :transfer metasilicate-ion to the ortoforme and enter in the structure of a HALS

The choice of area pH precipitated of the specified connection was carried out on the basis of modeling processes in initial solutions. Is established, that the first function of OH- group is carried out in area pH 12,5. The metasilicate-ion practically passes in ortoforme, calcium is as $CaOH^+$, phosphorus - as $PO_4^{3-}$. There fore, synthesis HAJIS carried out at pH from 12,5 up to 13,5. The workers meanings were been chosen pH:12,5; 12,75; 13,0; 13,25; 13,5, and for comparison one synthesis was been carried out at natural meaning pH of initial solutions ($pH_{An}$=11,2).

Synthesis carried out in reactor at t=1000C within two hours. The received deposits were been filtered, washed out and dried up. The synthesized samples were been tempered at t=800 0C within 2,5 hours, pressed in hydrostatic conditions and annealed at 1200 $^0$C. The received ceramics was been subjected to methods of the chemical, X-ray phase and IR-spectrum analysis.

On the data XRA powders synthesized at natural meanings $pH_{An}$11,2 with subsequent annealing at 800 $^0$C, represent a mix of average calcium phosphate (TCP), lanthanum and silicate calcium $CaSiO_3$. Is shown, that the introduction of OH - groups during synthesis for increase pH up to 12,5 is accompanied by formation alongside with lanthanum phosphate TCP and calcium hydroxyapatite. At increase pH up to 13,25-13,50 there is a formation of a product to structure calcium HA, which reflexes are displaced in the party of smaller corners, the IR-spectra of these samples are typical for calcium HA except for three strips: 515, 890-925 $sm^{-1}$, which can be referred to fluctuations of anion $SiO_4^{4-}$, included in structure HALC.

The measurements of destroying pressure on a ceramic sample and account of border of durability on a bend have shown, that the durability modified hydroxyapatite HALC twice is more, than at pure HA. However, the maximal durability has ceramic samples representing a mix $Ca_3 (PO_4)_2$ and HALC. The satisfactory results are received also with the additive representing a firm solution of the calcium hydroxyapatite on a basis calcium tantalate , received by the above-stated way.

As a result of work the circuit of synthesis HALsilicium is offered and the ceramics with improved strong by the characteristics is received.

With the purpose of preparation of the second kind modified hydroxyapatite was investigated chemical precipitated in systems from ammonium hydrophosphate, tantalum acid, calcium nitrate and ammonia depending on mole correlation of initial solutions.

The data of residual concentration testify that tantalum and phosphorus is completely connected with calcium as difficult dissoluble connections. Obtained the samples are represented by heterogeneous mixes consisting from of the calcium hydroxyapatite,of the tantalum acid and of the insignificant quantities Ca $(OH)_2$ , that is confirmed by the data of the X-ray analysis.

Is established, that at $1000^0$C in structure of heterogeneous products the phases $Ta_2O_5$, $Ca_4Ta_2O_9$ and not identified phase are found out. At increase of temperature up to $1200^0$C as a result of chemical interaction the reflexes of the not identified phase disappear, and the final product consists of various quantity $Ca_4Ta_2O_9$,, $Ca_2Ta_2O_7$ with an impurity hydroxyapatite. At $1200^0$C the formation of compound $CaTa_2O_6$ with orto-rhombic structure is observed. The displaced reflexes on X-ray diagram assume formation of a firm solution calcium hydroxyapatite on a basis $CaTa_2O_6$ of the following composition: $0{,}7Ca_{10}(PO_4)_6(OH)_2+3CaTa_2O_6$. In conditions of experiment for tantalum the formation calcium tantalate with pirochlorine structure of composition $Ca_2Ta_2O_7$ is characteristic. The displaced reflexes calcium hydroxyapatite and $Ca_2Ta_2O_7$ on X-ray diagram assume their mutual solubility.

The results of researches of series with tantalium were used for preparation of ceramics on a basis calcium hydroxyapatite , received by precipitation from water solutions. Carring out. of research have allowed to choose optimum quantity of the modifier, and also to fulfil conditions of heat treatment, including temperature and duration of the kilning of a product. The quantity of the modifier (the samples with tantalium and other), added in calcium hydroxyapatite in all cases made 2,5 mole of %.

From the received results follows, that the satisfactoriest results have turned out with the additive representing a prospective firm solution calcium hydroxyapatite on a basis $Ca_2Ta_2O_6$. Received parameter practically coincides with parameter organic bone and in this case -90 MPa(tensile strength).

The introduction tantalium oxyde has given unsatisfactory results, since the ceramics turned out friable. The same result has turned out on the additive representing of a firm solution of the calcium hydroxyapatite on a basis calcium niobiumate. The ceramics with the additive niobium oxyde (v), yttrium oxyde (III) and lanthanum oxyde (III) has practically identical meanings. This parameter (tensile strength) on pure calcium hydroxyapatite makes 48,73 MPà. But it is lower than result with the additive representing a mix of the calcium hydroxyapatite and $Ca_2Ta_2O_7$, and also mix of the calcium hydroxyapatite and his firm solution on a basis of the calcium tantalate.

The data X-ray of the analysis of ceramics have shown, that its structure does not vary after heat treatment.

Thus, it is possible to consider, that most perspective in creation hydroxyapatite of ceramics are the combinations on a basis of calcium hydroxyapatite, modified by oxyde compounds of the tantalium.

The literature

1. Арсеньев П.А. Саратовская Н.В Синтез и исследование материалов на основе гидроксиапатити кальция. Стоматология, 1996, №5, с.74.
2. Родичева Г.В., Ежова Ж.А., Орловский В.П и др. Изучение условий совместного осаждения гидроксиапатита кальция и гидроксидов циркония и алюминия аммиаком из водных растворов. Журн.неорган.химии, 1998, т.43, №6, с.914.
3. Шумкова В.В., Погребенков В.М., Карлов А.В. и др. Гидроксиапатит-волласитонитовая биокерамика. Стекло и керамика, 2000, 310, с.18.

# THE ANODE DISSOLUTION OF LA (III) IN WATERLESS SOLVENT

**Kostyuk N.N., Dick T.A., Tereshko N.V.**
Institute of Applied Physical Problems of Belarus State University, Kurchatov str. 7, 220064 Minsk Belarus

In the last years the chelate complexes of rare earth elements which capable to sublimate at moderate temperatures are of considerable chemical and industrial interest.β-Diketonates have the special place among them. Thank to it property this compounds are widely used in an application to the deposition of metal films, coatings [1], in the optics and electrotechnical industry and in analytic chemistry [2].

At perspective, the development of chemistry of β-diketonates leads to it heavy industrial aplication, so a very actual problem is a search for the new methods of synthesis the given class of compounds and investigations of it physical and chemical properties.

At present, many methods of obtain of given compositions are existing. The most perspective of them are the next: a direct interaction of zero-valent metal with a ligand, reactions of ligand exchange and electrochemical method. The last one is more universal unlike others. It has many advantages, such as the one-step process, the absence of by-products and others.

The anode dissolution of La with acetylacetone (2,4-pentanedion, $C_5H_8O_2$, HAA) has been done in this work. The electrolysis was carried out in the glass cell without diaphragm, described early [3]. The test for the presence of the metal has been pursued by burn of the charge of the substance at temperature of 900°C. The IR-spectrum of the allocated substances was registered by spectrophotometer "Specord 75 IR" in the regions of frequency from 4000 to 400 $sm^{-1}$ from the films of acetone and from the suspension of vaseline oil. The weight loss in the termogravimetrical studies was registered on the apparatus, has been specially developed, in an inert atmosphere and in an air.

At the present work the metalic La was used as anode, the nickel foil as cathode, for a supporting electrolyte lithium chloride (LiCl) for the ethanol and tetraethylammonia bromide ($N(Et)_4Br$) for acetonitrille. The basic data of the electrolysis are represented in the table I.

Table I.

The basic data of the electrolysis

| № | metal | Ligand | T,K | electrolyt | Current density $mA/sm^2$ | Reaction time | Quantity of electricity Q, Kl | Current efficiency of the metal % | Isolate complex, % | Calculate formula |
|---|---|---|---|---|---|---|---|---|---|---|
| 1 | La | HAA | 293 | EtOH+LiCl | 28-8 | 2h.40min | 905,3 | 148 | 85 | $La(AA)_3 \bullet 0{,}5C_2H_5OH$ |
| 2 | La | HAA | 293 | $CH_3CN$+TEAB | 21-6 | 3h.10min | 529,48 | 117 | 72 | $La(AA)_3$ |

The element metal analysis of the allocated substance (tab. II) has allowed to assume, that as a result of synthesis are compounds of composition $La(AA)_3 \bullet 0{,}5C_2H_5OH$ (substance I) in ethanol solvent and $La(AA)_3$ (substance II).

Table II

The data of The element analysis on metal

| № | The formula of the substances | Find, La% | | $La_{midle, \%}$ | Calculate , La% |
|---|---|---|---|---|---|
| | | 1 | 2 | | |
| 1 | $La(AA)_3 \bullet 0{,}5C_2H_5OH$ | 30,20 | 30,22 | 30.21 | 30,25 |
| 2 | $La(AA)_3$ | 32,12 | 32,08 | 32,10 | 32,06 |

The assumed data about the structure of chelate complexis was supported by IR-spectroscopy method. The frequencies of the absorption bands of the allocated substances are tabulated in Table III.

Table III

The vibration frequencies of chelate complexes.

| The vibration frequencies of $La(AA)_3 \bullet 0,5C_2H_5OH$ | The vibration frequencies of $La(AA)_3$ | The characteristic of frequencies |
|---|---|---|
| $3600\text{-}3000_{st.}$ | | υ(OH) |
| $1585_{v.st.}$ | $1580_{v.st.}$ | υ(CO), υ(C÷C), δ($CH_3$) |
| $1555_{sh.}$ | | δ($CH_3$) |
| $1490_{st.}$ | $1480_{st.}$ | υ(CO), υ(C÷C) |
| $1460_{sh.}$ | $1455_{sh.}$ | δ($CH_3$) |

*v.st. – the very strong bands; *st. – the strong bands; *sh. – the shoulder.

The absorption bands in the spectrum of the substances in the region 1600-1480 $cm^{-1}$ shows the coordinative connection between central atom and the organic ligand ($1585_{v.st.}$, $1550_{sh.}$,$1490_{s.}$ for the substance I and $1580_{v.st.}$, $1480_{st.}$ for the substance II).In the $La(AA)_3 \bullet 0,5C_2H_5OH$ spectrum is the wide absorption band in the region 3500 – 3000 $cm^{-1}$, related to the valence vibration of the OH-groups, suggesting that ethanol is present in the composition of the complex.

Our assumption about the complex composition were confirmed with the help of thermogravimetry (TG) method. Based on the data about the weight loss of the charges, the TG-curves have been build. It follows from these that the maximum weight loss in the region 250-320°C for the substance I and 190-260°C for the substance II are 74,3% and 73,1% respectively. On TG-curves $La(AA)_3 \bullet 0,5C_2H_5OH$ forms the plateau in the region of temperatures 120-147°C, where weight change is 5,75%. So as calculated loss is 5,3%, it is felt that the molecules of ethanol is out from the complex.

On the basis from the data of TG-analysis isothermal warming up of the $La(AA)_3 \bullet 0,5C_2H_5OH$ sample to constant weight in an inert atmosphere at 120°C has been done. The weight loss is proves to be 5,8%. It is in complete agreement with the calculated data, when 0,5 moles of ethanol are out from the complex. There is no the absorption bands in the region 3500-3000 $sm^{-1}$ in the IR-spectrum of the warming substance. It proves an absence of ethanol in the complex.

Thus, it was shown, that anode dissolution of La (III) in waterless solvent at presence acetylacetone leads to formation an adducting complex $La(AA)_3 \bullet 0,5C_2H_5OH$ in ethanol and $La(AA)_3$ in acetonitrile.

*REFERENCE*


1. Syrkin V.G. "CVD Method. Chemical Vapor-Phase Metallization". Moscow, 2000, 496 p.
2. Suglobov D.N., Sidorenko G.V., Legin E.K. 'Flying organic and complex substances of the f-elements'. Moscow, 'Energoatomisdat', 1987, 209 p.
3. V.I. Shirokii, N.N. Kostyuk, T.A. Dick, A.G. Trebnikov, I.I. Vinokurov "Possibillity of electrochemical synthesis of Sm(II) and Sm(III) acetylacetone complexes" International conference "Metaloorganic compounds are materials of the future millenium.", 2000, p. 135

# THE THERMAL PROPERTIES OF THE TRIS-PIVALOYLTRIFLUOROACETONATE RARE EARTH METAL COMPLEXES

**Kostyuk N.N., Dick T.A., Trebnikov A.G.**
Institute of Applied Physical Problems of Belarus State University, Kurchatov str. 7, 220064 Minsk Belarus

It is known, that for reception films of the high-temperature superconductors, alongside with physical, various chemical methods are widely used. From the last the method of chemical deposition from a vapor phase is most perspective. When development of the technology CVD by the first and basic question is the choice of the flying substances satisfing as minimum two requirements: they should have a technologically acceptable pair pressure and pass in a vapor phase (to evaporate and to sublimate) without decomposition [1, 2]. β-Diketones of metals satisfy these conditions. They have high volatibility at rather low (100–300°C) temperatures. Based on a literary data [1], the replacement of atom of hydrogen by fluorine in α-position of the β-diketone results in increase volatibility of the β-diketonates, however thus there is a reduction thermostability of the chelate complexes. In this connection it is very important to know thermal property of the CVD technology substances.

In the present work the purpose concerning research of thermal behaviour tris-pivaloyltrifluoroacetonate rare earth metal complexes (1,1,1-trifluoro-5,5-dimethyl-2,4-hexandione) has been done. It was put for their thermal stability and volatibility on the basis of the data thermogravimetry. There are the data concerning the beginning of sublimation researched chelate complexes, the interval of temperatures which characterize directly processes of sublimation and thermal decomposition, and also the maximal losses of weight in the table.

**The given thermal research date of the tris-pivaloyltrifluoroacetonate rare earth metal complexes**

| Tris-chelate complexes | Max. losses of weight at thermogravimetry., % | $T_{beg.}$ °C | $T_1$-$T_2$°C |
|---|---|---|---|
| $PrL_3$ | 77,8 | 60 | 208-290 |
| $PrL_3$•0,75Phen | 96,5 | 150 | 250-334 |
| $SmL_3$ | 77,3 | 60 | 232-286 |
| $EuL_3$ | 86,6 | 89 | 198-284 |
| $EuL_3$•Dip | 92,9 | 150 | 240-323 |
| $EuL_3$•0,5Dip | 92,9 | 140 | 252-320 |
| $EuL_3$•0,25Phen | 92,0 | 90 | 256-347 |
| $YL_3$ | 94,7 | 70 | 198-282 |
| $GdL_3$ | 86,0 | 60 | 222-254 |
| $TbL_3$ | 88,7 | 80 | 248-280 |
| $DyL_3$ | 87,8 | 60 | 212-300 |
| $DyL_3$•0,5Phen | 96,7 | 100 | 244-324 |
| $HoL_3$ | 86,4 | 110 | 220-300 |
| $TmL_3$ | 87,8 | 100 | 178-290 |
| $YbL_3$ | 97,7 | 90 | 182-268 |
| $LuL_3$ | 90,6 | 120 | 204-284 |

Where $T_{beg.}$ - temperature at which changes of weight begin; $T_1$-$T_2$ - an interval of temperatures of the maximal loss of weight; L - pivaloyltrifluoroacetonate; Dip - α, α′-dipyridile; Phen - 1,10-phenantroline.

It is possible to notice, that for many tris-pivaloyltrifluoroacetonate rare earth metal complexes rather small temperatures of the beginning of it sublimation are characteristic: less 100°C for $YL_3$, $GdL_3$, $TbL_3$, $DyL_3$, $PrL_3$, $SmL_3$, $EuL_3$•0,25Phen and $YbL_3$.

The data given in the table testify that for tris-chelate complexes of the easy trivalent metals have the lower values of the maximal losses of weight (less than 78 % for tris-chelate complexes Sm and Pr), than for the tris-complexes of heavy metals ittrium subgroups (from 86 % at $GdL_3$, up to 97,7 % at $YbL_3$). It is obviously connected with different stability of the substances: tris-chelate complexes of the heavy rare earth metals because of lantanium compression are steadier [3]. It is shown, that adductoformation results in increase volatibility of the tris-pivaloyltrifluoroacetonate rare earth metal complexes that well is coordinated to the literary data [3]. For example, the maximal losses of weight for $EuL_3$ is 86,6 % while for $EuL_3$•Dip, $EuL_3$·0,5Dip and $EuL_3$•0,25Phen one grow up to 92,9; 92,9 and 92,0 % accordingly. It speaks that the adductformation due to a saturation of the coordination sphere of the metal - complexoformate, resulting at suppression of processes of polymerization the tris-pivaloyltrifluoroacetonate rare earth metal complexes.

Thus, the received results of the thermogravimetry researches testify that the tris-pivaloyltrifluoroacetonate rare earth metal complexes have high an ability to sublimation. They may be used for substances, which may be apply in CVD processes. It is shown, that adductformation with neutral ligands results in increase volatibility tris-pivaloyltrifluoroacetonate rare earth metal complexes.

REFERENCE

1. G.V. Bazuev, L.D. Kurbatova "The chemistry of volatile β-diketonates and theirapplication in synthesis of high-temperature superconducting thin films". Successes of chemistry, 1993, T. 62, V. 10, P. 1037-1046.
2. Syrkin V.G. "CVD Method. Chemical Vapor-Phase Metallization". Moscow, 2000, 496 p.
3. Suglobov D.N., Sidorenko G.V., Legin E.K. 'Flying organic and complex substances of the f-elements'. Moscow, 'Energoatomisdat', 1987, 209 p.

# THE ION IMPLANTATION FOR IMPROVEMENT OF THE PROTECTIVE NITRIDE LAYERS PROPERTIES FOR APPLICATION IN BIOCOMPATIBLE ENVIRONMENT

**Fedirko Victor, Pohreliuk Iryna, Yaskiv Oleh, Mynyk Switlana**
G. V. Karpenko' Physico-Mechanical Institute of NASU, L'viv, Ukraine

The complex of the high service properties such as corrosive resistance, ductility, specific strength and hardness causes the wide using of titanium and its alloys as biocompatible implantator in medicine [1]. Lately in the case of foreign body embedding into living tissue of human organism the titanium alloys samples with surface layers modified by interstitial elements (nitrogen, boron, carbon) were started to use [2]. The aim of this report was to determine the using effectiveness of additional surface treatment of titanium (boronizing, nitriding) in the term of its biocompatibility in human organism circulatory system.

The titanium saturating of interstitial element was carried out by chemical and thermal treatment and ion implantation and also consecutive treatment of these both methods. The latter let combine the advantages of both treatment such as the possibility of treatment the complex form samples, obtain the depth modified layers at thermodiffusive saturation and make the controlled alloying during ion implantation.

The VT1-0 titanium alloy samples (15×10×1μm) typical purity were investigated. Prior to saturating the samples surface were polished (Ra=0,4 μm). The chemical and thermal treatment was carried out in nitrogen atmosphere at the temperature range of 750...950 °C for 5 hours. The nitrogen of typical purity has been cleared from oxygen and humidity (≤0,05%) by passing trough the chamber with silicagel and titanium shaving. The samples had been ion implanted with voltage E = 40 keV and current I = 20 μmA/sm$^2$ and boron ion flux D = $10^{16}$ ion/sm$^2$. The electrochemical tests were performed with potentiostat PI-50-1.1. The potentials are reported with the respect to a chlorine -silver electrode. The polarization curves were obtained with a scan rate of 0,2 V/s.

The corrosive behaviour tests were carried out in 0,9% aqueous solution of sodium chloride possesses the most like human blood chemical biological properties.

The boron ion implantation of nontreated (without nitriding) VT1-0 titanium alloy samples results in not only boron dissolution but also start the boride formation. The low intensity of lower borides ($Ti_2B$ and $Ti_2B_5$) indicates the presence of these phases in small amount at surface. It already results in the surface hardness increasing by 0,3 GPa.

It is known that borides possess the highest hardness among wide using interstitial phase (oxides, nitrides, carbides, and borides) [3]. But the large size of boron atoms is the obstacles the depth strengthened layers forming. In this paper the boron ion implantation influence on the strengthening of nitrided samples obtained by thermodiffusive saturation was determined.

The weigh growth tests revealed the influence of nitride layer structure on boron saturation process. That is the largest weigh growth in respect to area unit is observed for nitride layer with considerable imperfection due to thermocycling after boron implantation. The reduction of nitride layer structural heterogeneity complicates the diffusion boron penetration. It was established that the boron modification the pretreated samples promotes the surface increasing by 3,4...4,2 GPa for nitrided samples at low temperature (750 °C) and cycling (750↔850 °C) and by 2,3...5,0 GPa for nitrided samples at high temperature. It can be attributed to the fact of the different state of the surface nitride film preceded ion implantation process. The oxygen impurities in nitrides in the case of nitrided samples cooling in air flow and also structural microstresses provoked thermocycling or high temperature (950 °C) result in the active saturation of boron atoms and than significant strengthening of surface layer.

This surface strengthening is accountable for by the forming of lower boride phase $Ti_2B_5$ (the main observed boride phase) and $Ti_2B$ (solitary observed reflexes) and also due to the boron dissolution in the mononitride lattice with the possible boronitrde formatting. The evidence of the former is appearance of the boride phases reflexes. The latter is confirmed by the increasing of TiN lattice parameter. The considerable strengthening while the low intensity of boride phases reflexes

signifies the efficiency of additional boron saturation the nitride layers.

The nitrogen and boron saturation make change the open corrosion potential of the samples and in most cases to negative values (Table). Only after high temperature nitriding the ennobled potential is observed. It indicates that the predominant inhibitting of the anodic reaction takes place. Whereas in the rest cases it indicates about slowing down the cathodic reaction rate. It is significant that polarization curve trend of high temperature nitrided sample conforms to surface passivation stage in the range of corrosion potential.

The additional boron saturation of nitrided surface changes the sample electrochemical properties. The potential ennobling concerning to the nontreated sample and the most considerable current decline are observed for the samples treated at the high temperature (950 °C). However at the anodic polarization (under identical potentials) the dissolution currents with respect to boron unimplanted nitrided samples are higher. It indicates that the boron presence in nitrided layer reduces the surface resistance to anodic polarization.

At the same time the corrosion currents of the samples with nitride layers and additional boron saturation layers concerning to untreated sample is reduced. It indicates the beneficial protective effect of such treatments of titanium alloy.

References

1. J. Probst, U. Grubeck, R. Thull. Binary nitride and oxynitride PVD coating on titanium for biomedical applications // Surface and coating Technology. - 148 (2001). - P. 226-233.

2. J.F.Pierson, F. Bertran, J. P. Bauer, J. Jolly. Structural and electrical properties of sputtered titanium boronitride films // Surface and coating Technology.- 142-144 (2001) .- P.906-910.

3. C. Pfohl, A. Bulak, K.-T. Rie. Development of titanium diboride coating deposited by PACVD // Surfae and coating Technology. - 131 (2000). - P. 141-146.

Table. Electrochemical properties of VT1-0 titanium alloy exposured to 0,9% aqueous solution of NaCl after nitriding and boron implantation

| Conditions | After nitriding | | | | | After nitriding and boron implantation | | | | | Nontreated |
|---|---|---|---|---|---|---|---|---|---|---|---|
| | 750 °C | 850 °C | 750↔850 °C | 900 °C | 950 °C | 750 °C | 850 °C | 750↔850 °C | 900 °C | 950 °C | |
| $E_{cor}$, mV | -420 | -395 | -294 | -243 | -238 | -404 | -475 | -448 | -298 | -245 | -290 |
| $I_{cor}$, $A/m^2$ | 0,047 | 0,05 | 0,056 | 0,042 | 0,01 | 0,05 | 0,04 | 0,1 | 0,03 | 0,04 | 0,058 |
| $I_D$, $A/m^2$ | 2,0 | 0,63 | 0,8 | 0,25 | 1,5 | 1,5 | 1,3 | 1,0 | 0,4 | 1,0 | 2,5 |

# TECHNOLOGY OF PRODUCING THE SMOOTH POWDER BUSHES WITH HIGH DENSITY

**Ryabicheva L.A., Tsirkin A.T., Khichenko V.F.**
East Ukrainian National University named after Vladimir Dahl, Lugansk, Ukraine

The smooth bushes are widely used in engineering. The significant amount of such parts works in condition of high pressure and at presence of impact loads. The high requirements are shown on strength and toughness of materials, from which one this parts are made. Such bushes are produced from carbon and alloyed steels by machining of castings, forging,, thick-walled tubes and less often rods. The labor input of bushes manufacturing is high and metal utilization coefficient makes of 0,34-0,7 [1].

Allowing advantages of a powder metallurgy (wasteless and high productivity), the bushes from metallical powder is found the increasing applying. However, such parts produced on conventional technology – pressing and sintering – have a high porosity that reduces mechanical properties of material and limits a feasibility of powder bushes in loading units. Especially it concerns bushes with wall thickness less than 5 mm and height – wall thickness ratio more than 10 mm. Such thin-wall and high bushes have much higher porosity in center then in end faces area. The increasing of density by double pressing and sintering isn't obviously possible, because the punches have low stability and can't bear high pressure which is necessary for attainment of demanded density. The ways of long-sized articles producing by densification of porous blanks in radial direction by a central punch with a conical effective part are known [2]. After such technology the tubes with density up to 0,70-0,85 and high equidensity used as filters are produced.

The development of such technology is interest for smooth thin-wall bushes producing, which one will supply attainment of high-density and equidensity at smaller energy consumption.

The researches are executed on samples dimensioned 50,5×41,5×50 mm. The blanks pressed from iron powder and sintered at 950$^0$C for one hour are pressed in a die by a central punch with a conical effective part.

It is determined that at penetration of a punch into the blank there is a flow of metal in radial and axial directions. The density of the bush increases by displacement of part of metal in radial direction. The displacement of metal in axial direction results in increase of the height and in the burr formation at the lower end face. The produced parts on height didn't comply with requirements of the drawing and relative density didn't exceed 0,90.

The removal of these lacks gives rise to design the new pressing scheme at which one the flow of metal in an axial direction was limited by upper fixed punch. The height of produced blank is less than height of part and it has a bevel at the lower face end. During deformation the volumes were formed and executed the role of compensators. The axial displacement of material during deformation was limited by fixed punches.

We investigated the influence of blanks' density, its height, bevel's size on density and equidensity of bushes. The blanks were made with relative density of 0,70, 0,75, 0,80, and 0,85. The height was changed from 46 mm up to 50 mm with a step of 1 mm. The outside diameter was took on a value of diameter of the part, and inside diameter was defined from weights of blank and part constancy principal. At the lower face and a bevel was made with height 2,5, 5, 10, 15 mm. Its maximum diameter equalled to inside diameter of a part and minimum diameter to outside diameter of blank. The angle of shaping punch made of 3$^0$.

The density was determined by calculation method on weight and volume solved on the sizes of bushes and by hydrostatic weighting. For determine of equidence the bushes were cut up on five rungs and determined their density on the same technique. The equidence was valued on a factor $S_i = \gamma_i \gamma_m^{-1}$, where $\gamma_i, \gamma_m^{-1}$ - density of investigated segment and mean density of all sample.

It is established, that the mean relative density of samples makes 0,95 – 0,98, except those samples, which was pressed from blanks with relative density 0,70 and height of 46 mm. In this case mean relative density of samples didn't exceed 0,95. The high allowance on diameters (2,8 mm on side) increases a volume of metal, displaced in axial direction. The extrusion of metal into a clearance between central and lower punches and formation of a burr are watched. There are concentric cracks on an internal surface of parts.

The density of blanks and their height exerts an influence to equidence. The increase of density results in reduction of blanks' volume. The volume of displaced metal decreases. The value of this volume was calculated from a ratio [3]:

$$V_{CM} = \frac{M_д}{\gamma_k} \frac{\theta_д - \theta_з}{\theta_д \theta_з},$$

where $M_д$ - weight of a part;

$\gamma_k$ - density of compact metal.

So, at $H_з$=49 mm and $\theta_з$= 0,85 the volume of displaced metal make of 4,97 cm$^3$, at the same height, but at $\theta_з$= 0,80 this value was $V_{CM}$=7,31 cm$^3$, and at $\theta_з$= 0,70 this value was $V_{CM}$=13 cm$^3$. The samples produced from blanks with relative density 0,85 have most uniformly distributed density and least - from blanks with $\theta_з$= 0,70.

The change of height of blank at constantly values of weight and volume results in change of inside diameter. The reducing of height results in increasing of diameter and decreasing of allowance. At equalling of height of blank and part the high layer of the bush appears denser.

The reducing of height results in increasing of inside diameter of blank and allowance. In this case the underlayers are denser. The optimal residual between heights of blank and part makes up to 1 mm at value of relative density of 0,85; 2 mm at value of relative density of 0.80 (fig.1).

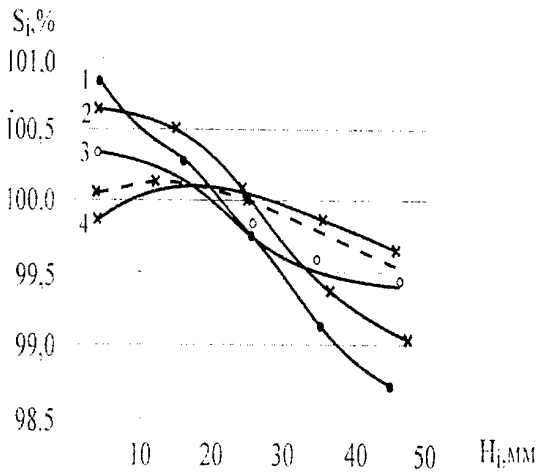


Fig.1. Distribution of density on height of a part at an height of blank $H_з$=49 mm and relative densities $\theta_з$: 1 – 0,70; 2 – 0,75; 3 – 0,80; 4 – 0,85; 5 - $H_з$=48 mm; $\theta_з$= 0,80

One more factor exerting influence on distribution of density on height of a part is the sizes of chamfer in bottom of blank. The burr is formed on samples produced from blanks with height of 49 mm and relative density 0,85 and when the height of chamfer equals to 2,5 mm. When the height of chamfer equals to 15 mm the shape formation doesn't take place, resulting in to its filling. The samples are manufactured from blanks with the height of chamfer equals to 5 mm. At pressing of blanks with relative density of 0,8 the best distribution of density is obtained when the height of chamfer equals to 10 mm. It is explained that the allowance (from 0,90 up to 1,3 mm), and, therefore, the volume of metal displaced in axial direction was increased.

The executed researches have shown that at radial deformation of porous blanks (RDPB) the high level of density and equidensity is reached. It is established, that the quality of articles manufactured on such technology increases with growing of blanks' density and depends on its geometrical parameters – height and chamfer's sizes on inside diameter in bottom of blank.

The results of investigations are utilized at development of technology of bushes producing by the sizes of 84×74 mm and with height of 80 and 106 mm. The technological process of their producing incorporates next operations: preparing of charge, consisting from iron powder ПЖ2.200 – 97% and pencil graphite – 0,3%; pressing of blanks with chamfer in bottom of blank; sintering in endothermic gas environment at 950$^0$C for one hour; radial deforming of porous blank; repeated sintering at 1120 - 1150$^0$C in same environment for one hour. The produced bushes had density of 7,60 – 7,66 g/cm$^3$, Brinell hardness 95 – 125 HB, compression strength of ring-type - 450-540 MPa. The parts correspond to a drawings use conditions.

References

1. Изготовление втулок в крупносерийном и массовом производстве / Под ред. М.О. Якобсона.- М.: Изд-во ЭНИМС, 1983. – 81 с.

2. Багинский Л.С., Петюшок Б.Е., Штерн М.Б. Установка для радиально-изостатического прессования пористых длинномерных изделий из порошков // Порошковая металлургия. – 1990. - №8. – С. 10-14.

3. Ковальченко М.С. Теоретические основы горячей обработки поистых материалов давлением. – К.: Наук. думка, 1980. – 145 с.

# DIE FORGING OF COPPER FIBRES

**Ryabicheva L.A., Tsyrkyn A.T., Losiev U.A.**
East Ukrainian National University named after V. Dahl, Lugansk, Ukraine

The researches of pressing of metallic copper fibres having diameter about ten micrometers is carried out by many writers. It is known, that thus there is a plastic deformation of contact surfaces and plastic deformation of fibres bending. These data are obtained during pressing fibres of small diameters at producing of high porosity materials and with relative density up to 90 %.

We conducted researches of a capability of parts obtaining from copper fibres with diameter from 0,6 up to 1,3 mm having property of a compact material.

Initial M1 copper fibers previously is annealed m hydrogen containing environment of synthesizing - gas for obtaining of high brittleness. The copper fibers of length 15-20 mm and diameters 1,0-1,3 mm is produced by grinding. The billets had density from 7,8 up to 8,2 g/cm$^3$ after cold pressing of fibres. Their strength was near 140-170 MPa. However, the analysis of a microstructure has shown, that in produced billets there is no general consolidation of fibres (fig. 1).

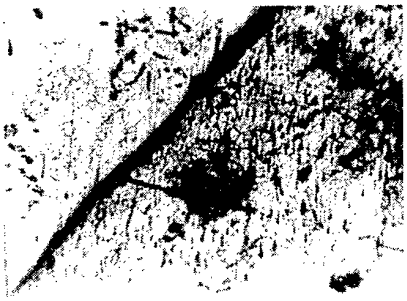

Fig. 1. The microstructure of fibrous copper with density up to 8,2 g/cm$^3$ (x 500)

On the basis of analysis of stress - strain state at cold pressing of fibres is obtained, that the increase of consolidation level, and, therefore, mechanical properties is possible to achieve at forging with high strains.

In papers [1, 2] is shown, that at forging of porous powder blanks by upsetting in closed die the residual porosity makes not less than 2 % for account of radial deformation.

The initial blanks with different density are subjected to die forging. Thus diameter of blank was less then inside diameter of die. The densification of material was accompanied by a radial flow with formation of definite structure and properties of a forging.

The blanks is heated in environment of synthesizing - gas to temperature 800-850°C and pressing on a hydraulic press by a capacity 1000 kN and pneumatic hammer with weight of falling parts 160 kg. The change of samples density during pressing on hydraulic press and pneumatic hammer is shown in a fig. 2.

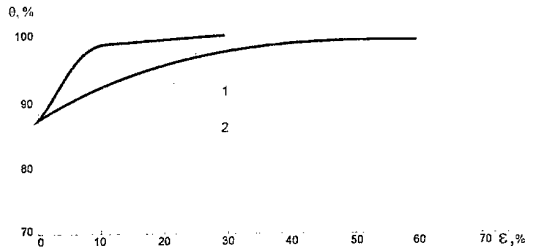


Fig. 2. Variation of density of samples depends on strain: 1-press; 2-hammer.

At pressing on a hydraulic press the increase of density of samples is watched up to 8,8-8,9 g/cm$^3$ at a redial strain 7,3-10,2 %. The analysis of microsections is shown, that grain size has compounded 2-15 microns; mechanical properties - hardness 85 HB; compression strength 400 MPa. The pressing on a hydraulic press hasn't resulted in disappearance of fibers boundary and formation of a defectless compact material (fig. 3).

Fig. 3. Microstructure of fibrous blank after die forging on press (x 500)

At pressing of samples on a hammer their density was increased, that is a consequent of in-

fluencing of high strain rate. When initial density of samples is equal to 7,8 g/cm$^3$ the pore-free material with density 8,9 g/cm$^3$ is obtained when a radial strain volume is equal to 54 %. At hot forging of blanks with density 8,2 g/cm$^3$ same density is reached at strain 33 %. It testifies that for obtaining of pore-free a material it is necessary to have initial blank with maximum obtained density (fig. 4.). The density of blanks exerts influence on this process. The forgings, density 8,9 g/cm$^3$ are produced from blanks of a different porosity at the same blow energy of falling parts of a hammer at a miscellaneous strain.

Fig. 4. Microstructure of fibrous blank after die forging on hammer (x 500)

For more dense blanks a smaller degree of structural deformation, and, accordingly, smaller degree of deformation of metal. In an outcome at equal density hotwork hardening of samples, produced from more dense blanks is less.

For definition of a stress level arising at die forging, the method of microhardness is utilized, which one measured on ПМТ-3 devise. The sensings conducted on cross-section of a sample with a step of 0,2 mm. As it is on fig. 5, average value of microhardness of samples with density 8,9 g/cm$^3$ is growth with increase of a degree of structural strain that is a consequent of growth of stresses. With increase of structural strain the nonuniformity of a stress distribution is augmented, that indicates about spread in values of microhardness.

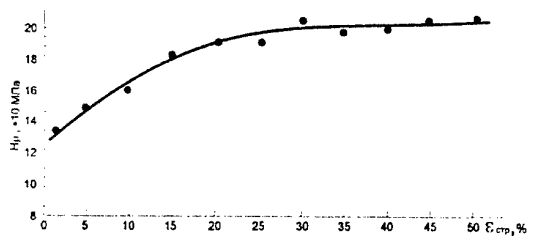


Fig. 5. The influence of structural strain to microhardness of parts

The variation factor has compounded 0,98. So, at density of blank 7,8 g/cm$^3$ the average value of microhardness has compounded 134 MPa at a difference between maximum and minimum value 66 MPa, and at the higher values microhardness testify density 8,2 g/cm$^3$ the average value of microhardness equalled 101 Mpa at a difference its value 31 MPa. It is obtained that at an identical strain the stress in samples produced by forging more dense blanks is higher, about what the higher values of microhardness testify.

The process of a die forging on a hammer goes with high speed, therefore at a contact of blank with walls of die there is joint deformation of contact surfaces and formation of new bounding between fibers. It is known, that for welding of copper the strain of contact surfaces should be not less than 10 %. The increasing of a degree of structural strain conducts to growth of deforming of fibres and stress level about what the increase of hardness and microhardness testifies. The produced parts after a final annealing in vacuum at temperature 500-600$^0$C have hardness 39-42 HB, compression strength 225 MPa, specific elongation 40 %, and density makes 8,9 g/cm$^3$. The structure of metal is isotropic, grain size is 5-7 microns. There was a full fibres consolidation.

Thus, the applying of die forging of initial fibrous blanks of high strain rates results in producing articles free of defects in structure.

References

1. Рябичева Л.А., Цыркин А.Т., Лосьев Ю.А. Экспериментальное исследование уплотнения волокон меди// Физика и техника высоких давлений. Донецк, 2000, №4 - С.42-46.

2. Рябичева Л.А., Цыркин А.Т., Лосьев Ю.А. Механизм деформации и упрочнения твердой фазы при прессовании волокон меди// Удосконалення процесів та обладнання обробки тиском в металургії і машинобудуванні/ Краматорск, 2001. - С.395-397.

3. Хун Шенгохан Исследование зависимости между деформирующим усилием и плотностью при горячей штамповке пористых заготовок// КШП. - 1991. - №7. - С.4-5.

4. Дорофеев Ю.Г. Динамическое горячее прессование в металлокерамике. - М.: Металлургия, 1972. - 176 с.

# DESIGNING AN AUTOMATIC MACHINE FOR ELECTROSPARK ALLOYING OF STEEL

**Nikolenko S.V., Verchoturov A.D., Kovalenko S.V.**
Institute of Material Science KSC FEB RAS Russia, Khabarovsk

## 1. Introduction

Development of new effective methods of hardening and restoring surfaces of machinery parts, with predefined and controlled physico-mechanical properties, is a demanding task of contemporary material science. Electro-physic methods of hardening and deposition of protective coatings are standing out among other modern techniques. Electrospark alloying (ESA) is one such method. This technology is based upon the transfer of anode's (electrode) material to a cathode (treated part) during the spark discharge flowing in a gaseous environment. This phenomenon together with the influence of impulse heat and mechanical stresses results in the forming on the surface of a treated part of a layer with modified structure and composition. Recently, most of the ESA technology has concentrated on the complication of equipment, namely modification of the impulse generator's parameters, for the purpose of advancing the exploitation characteristics of machine parts. However, in order to develop a systematic approach to ESA, which would allow for the flexible definition of characteristics and parameters of technological processes, and testing different modes of coating deposition, it is necessary to create a mechanical (technological) system.

The purpose of this work is to describe the development of mechanical, automatic devices with a rotating electrode and controlled, stable interelectode space (IES), which assures the continuity of treatment, i.e. constant electrode-instrument's pressure at the alloyed surface of the part.

## 2. Results and discussion

The staff of the "Powder metallurgy and protective coatings" (PM&PC) group have designed a mechanical ESA machine based on a turner rig TV-16 (Pic. 1). The machine consits of:

- Modernized turner rig TV-16;
- Impulse generator;
- Mechanical electrode head with a IES tracking system;
- Detachable device for the vertical transportation of the treated part;
- Detachable polishing device;

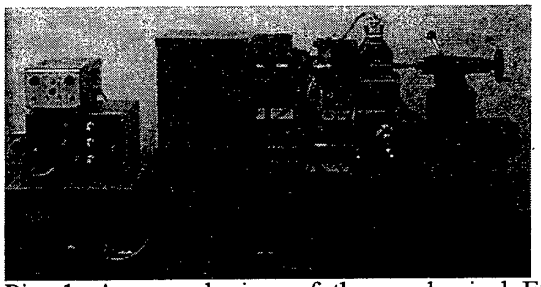

Pic. 1. A general view of the mechanical ESA machine.

The mechanic complex allows to test ESA technological processes on rotating bodies, while the detachable transporting device makes it possible to treat flat surfaces. During ESA, anode erodes in liquid and vapor phases and the erosion products are transferred to the cathode as a result of the thermomechanical influence of the spark discharge. As a result of a micrometallurgical process, a specific composite material, which includes the material of both electrodes and products of their interaction with each other and the environment, is formed on cathode's surface.

It is known that the ESA process's efficiency and physico-chemical properties of the alloyed layer decrease as the internal stresses and secondary structures accumulate in the electrode's material, facilitating the need for correction measures. This purpose is served by the polishing device, which can be attached to the support of the turner rig. The device allows polishing the surface layer between the two ESA cycles, therefore assuring higher continuity and lower porosity after the alloying. The designed system for the positioning of the alloying electrode in the interelectrode space controls the electrode's wear and significantly stabilizes the ESA process, which in its' turn positively affects the forming of a high-quality alloyed layer. The machine stands out from the rest of its' counterparts due to its' ability

to treat interrupted surfaces with grooves acceding in size the diameter of the alloying electrode.
Modification of the turner rig is accomplished by the mounting of an isolated jaw chuck and its' connection to the impulse generator with a negative polarity wire. Furthermore, parameters of horizontal transportation (from 1 to 25 cm/min) and vertical rotation (from 0,5 to 7 RPM) of the part were changed. The machine is fitted with an "IMES"-type impulse generator (Pic. 2), which was also designed in our laboratory. The generator is meant to be used together with a mechanical rotating electrode head, as well as with a manual vibrator.

Pic. 2. Impulse generator

The built-in tachometer allows choosing and controlling the rotation speed of the electrode in the limits of 10-3500 RPM. The new mechanical electrode head with a positioning mechanism improves physico-chemical properties of the alloyed layer. Electric drives of the machine are equipped with optical electronic motion sensors. The output signal of these sensors is represented by a sequence of voltage impulses. The machine has a convenient interface and can be connected to a computer, which can be used to monitor and control the ESA process. All of the abovementioned features allow to systematically solve the problems of creation of surface layers with predefined and controlled properties.

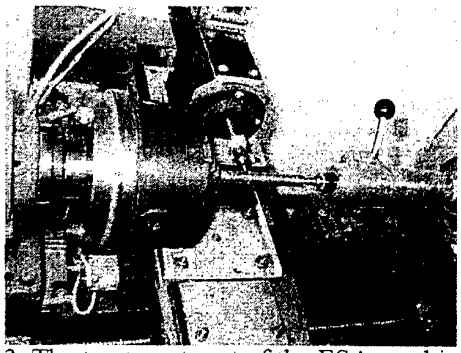

Pic. 3. The treatment part of the ESA machine.

The part shown on Pic. 3 consits of:
- mechanical device, including fastening, positioning and transporting parts, as well as detachable devices for the polishing and vertical transportation of the treated part;
- tracking system responsible for maintaining the given IES.

*Technical parameters of the machine*

| | |
|---|---|
| Voltage (50±1Hz), V | 220±22 |
| Power consumed on nominal voltage, kV·A | <1,0 |
| Layer thickness, micron | 2-500 |
| Productivity, $cm^2$/min | 0,1-3 |
| Roughness, micron | <10 |
| Impulse time, microsceonds | 2-200 |
| Amplitude value of the current, A | 1-100 |
| Mass of the impulse generator, kg | 18 |
| Mass of the machine, kg | 50 |
| Part's rotation speed, RPM | 0,5-7 |
| Part's horizontal speed, mm/min | 0,5-25 |

Working mode – manual or automatic.

## 3. Conclusions

1. An automatic machine for electrospark alloying, allowing to test technological processes on flat and rotation bodies, was produced.
2. Mechanical electrode head equipped with the positioning system, which assures the deposition of alloyed layers with increased physico-mechanical and exploitation properties and generally stabilizes the ESA process, was designed.
3. Complex has a convenient interface, which can be linked to a computer, allowing computer-aided monitoring and control of the ESA process.

## 4. Bibliography:

1. Verkhoturov A.D., Physico-chemical foundations of the process of electrosprk alloying of metallic surfaces. Vladivostok. Dal'nauka, 1992. pp. 180.
2. Verkhoturov A.D., Forming of surface layers of metals during electrospark alloying. Vladivostok. Dal'nauka. 1995. pp.321.
3. Nikolenko S.V., Kovalenko S.V et al., Designing an automatic machine for electrospark alloying. Proceedings of an international conference: Automotive vehicles of the Far East 2000. Khabarovsk 2000. pp.229-231.

# THE METHODS OF COMBUSTION CHAMBER WALL PROTECTION FROM INFLUENCE OF HIGH-INTENSIVE HEAT FLOW

**Arinkin S.M.**
Lykov Heat and Mass Transfer Institute, Nat.Acad.Sci.Belarus, Minsk, Belarus

It's considered the walls heat protection problem of the devices witch have temperature of active volume ~ $(10^3 - 10^4)^0$C [1,2]. This is plasma reactors, gaseous phase nuclear engines [], the aviation and rocket engines combustion cameras constructed from porous refractory materials [5]. In [] one has proposed to use the ligth – fused refractory materials witch have the evaporation temperature within the range (15-350)$^0$C. After passing of porous wall they are cooling a wall and at the exit of chamber (temperature (1200-1700)$^0$C) the boilable combinations are restored to ligth – fused metals. At the chamber wall the gas – powder layer is created. This layer absorbs and reflects microwave within wide range of a waves lengths. In [7] one has obtained that gas – powder medium flow is accompanied by the magnification of powder size. The medium reflection property change continuously. In [8] one has obtained that within the waves lengths range (0,005-1) mkm an extremal reflaction is achieved at the particles sizes within the range (0,03-0,1)mkm.

At a partical size decrease the exremum of screening effect replace to ultraviolet.

At the active volume temperature $10000<T<100000^0$C the main emmition take place within the waves lengths range (0,005-0,04)mkm. This is X-rays – vacuum ultraviolet range. For reflection and emission effect one required to use the particles with the sizes ~10 angstremm. The particles with such sizes are appeared at restoration of $WCl_6$, $WF_6$ at the exit of combustion chamber.

REFERANCES.

1. S.M.Arinkin The methods of the combustion camera protection.//Physical Engineering Journal, vol.74, N6, 2001.
2. V.Cheberlain, E.Pfender The combustion camera porous cooling.//Heatconduction, N2, 1971.
3. S.V.Dresvin and all. Low- temperature plasma physics and technics. M.:Atomizdat, 1975.
4. G.K.Tom, F.K.Shvenk The systems on the gaseous nuclear fuel. RTK, vol,16, N1, 1978.
5. High temperature reactors gaseous cooling.M. Atomizdat, 1975.
6. S.M.Arinkin, M.S.Tret'yak. High energy deces walls protection approach, a.s.N130724, 1992.
7. The microwaves energy relaxation by the gase – powder fluxes."Heat – Mass Tranfer –78," Minsk, ITMO, 1978.
8. G.Chust. The light reflaction by small particules.1961.
9. The relaxation coefficient in the gase – powder systems investigation. Report N1298, HMTI – New – York University. 1976.

# SYNTHESIS OF TERNARY GRAPHITE-LIKE PHASES IN THE B-C-N SYSTEM

**Lyashenko V.I., Tomila T.V., Zelyavskii V.B., Krushinskaya L.A., and Kurdyumov A.V.,**
Institute For Problems of Materials Science, National Academy of Sciences of Ukraine, Kiev, Ukraine

Synthesis of ternary phases in the B-C-N system is of interest in view of the possibility of producing new promising materials both in the graphite-like an diamond-like form. Ternary compounds with a graphite-like structure can be used as semiconductors operating at high temperatures [1].

There exists a great number of developed methods for preparing materials with a graphite-like structure in the B-C-N system, however, synthesized products are not always single-phase.

In the present work, the possibility of synthesizing graphite-like boron carbonitride with a nanocrystalline structure by the solution method was investigated. This method has found application in the production of highly disperse and monodisperse powders. The procedure for preparing mixtures provides their high dispersivity and homogeneity, as well as a good contact between components.

As starting materials for the synthesis, boron acid, carbamide, and saccharose were used. The saccharose content was varied from 40 to 80 mass %. The components dissolve well in water, which guarantees their ideal mixing.

The mixtures of the following compositions were investigated:
mixture I: $H_3BO_3$ + carbamide + 40 mass % saccharose;
mixture II: $H_3BO_3$ + carbamide + 60 mass % saccharose;
mixture III: $H_3BO_3$ + carbamide + 80 mass % saccharose;
mixture IV: $H_3BO_3$ + carbamide + 60 mass % saccharose + 10 mass % $NH_4Cl$.

The pyrolysis was carried out in a nitrogen flow, whose rate guaranteed the removal of gases and water vapor formed during thermal treatment. It was established that the largest loss in mass occured at a temperature of 200°C and that the process was completed at 400°C. The conditions of pyrolysis made it possible to prepare a mixture of boron oxide and carbon in which a homogeneous distribution of components and a good contact between them were retained. Carbon is in the amorphous state and retains its active reduction power. The mixtures prepared do not require additional grinding, and the particle size did not exceed 0.001 μm.

The mixtures were nitrided in a purified nitrogen atmosphere in the temperature range 1200-1450°C with an exposure time of 1-3 h.

According to the chemical analysis data, in samples, oxygen was present, the boron content exceeded its calculated content, and the maximum nitrogen content was 28%.

According to the X-ray analysis and IR spectroscopy data, in heat treated samples, boron oxide was detected. Moreover, the presence of absorption bands at $\nu \sim 1380$ and 815 cm-1 indicates the presence of B-N bonds, and the region at $\nu \sim 1250$ $cm^{-1}$ characterizes C-N bonds [2-4]. This gives grounds to think that, during heat treatment at a temperature ≥1300°C, the process of formation of a B-C-N structure occurs. A decrease in the intensity of the absorption band at $\nu \sim 815$ $cm^{-1}$, which characterizes interlayer vibrating mode in graphite-like BN substantiates the made suggestion [5]. The IR spectroscopy data show the presence of C-O and N-O bonds in the frequency ranges $\nu \sim 1400\text{-}1600$ $cm^{-1}$ and 1000-1100 $cm^{-1}$, which characterizes the incompleteness of the process of formation of boron carbonitride [6].

The maximum carbon content was detected in samples prepared by nitriding mixtures containing 80% saccharose and those containing $NH_4Cl$.

In X-ray diffraction patterns of the powders prepared, only smeared lines 002 and 10 from graphite-like phases are present. The line 002 is asymmetric. The lines hkl where $l \neq 0$ (101, 102, 112, etc.) are absent due to the two-dimensional character of diffraction caused by the turbostraticity of graphite-like structures.

According to data of work [5], in X-ray diffraction patterns, for single-phase graphite-like boron carbonitride, the practically symmetric line 002 is typical. In X-ray diffraction lines of the samples obtained, the line 002 is asymmetric (Fig. 1).

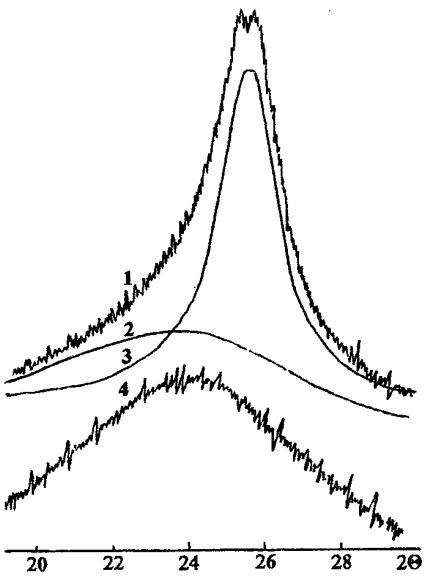


Fig. 1. Profiles of diffraction lines 002 from graphite-like structures: 1 – experimental curve; 2 – after separation; 3 – C and BN; 4 – $BC_{1.28}N$ [5].

This enables one to suggest that the obtained samples are mixtures of graphite-like phases consisting of $BN_g$, carbon, and $(BN)_xC_{1-x}$. The IR spectroscopy data confirm this suggestion by the presence of absorption bands characteristic for both BN and disordered carbon at $\nu \sim 950$ $cm^{-1}$ [7] and by the presence of bands corresponding to C-N bonds.

It was established that the boron carbonitride contents in the powders synthesized from mixtures containing 60 mass % saccharose and mixtures containing NH4Cl were above 60 mass %.

The results of investigations show that the solution method of synthesis of boron carbonitride is promising. It makes it possible to prepare powders containing up to 60 mass % graphite-like boron carbonitride at relatively low temperatures. Powders synthesized by this method have turbostratic structure characteristic for ternary graphite-like phases in the B-C-N system.

References

1. Kurdyumov A.V. and Solozhenko V.L. Synthesis and structure of ternary phases in the B-C-N system.//Sverkhtv. Mater. - 1999. – No. 6. – P. 3-17.
2. Bartnitskaya T.S., Vlasova M.V., Lyashenko V.I., et al. Formation of high-dispersion boron nitride during carbothermal reduction in the presence of lithium compounds. //Poroshk. Metallurg. – 1993. – No. 1. – P. 64-73
3. Sanchez N.A., Rincon C., Zambrano G., and Prieto P. Characterization of the Plasma during the Growth of $CN_x$ Films by RF Magnetron Sputtering.//Phys. Stat. Sol. – 2000. – V.220, N.1. – P. 697-701.
4. Wixom M.R. Chemical Preparation and Shock Wave Compression of Carbon Nitride Precursors. //J. Amer. Ceram. Soc. – 1990. – V. 73, N.7. – P. 1973-1978.
5. Hubacek M. and Sato T. Preparation and Properties of Compound in the B-C-N System. //J. Sol. Stat. Chem. – 1995. – V.114. – P. 258-264.
6. Nakamoto. K. Infrared Spectra of Inorganic and Coordination Compounds. – J. Willey & Sons, INC., New York, London, 1966. – 411 p.
7. Stein H., Aselage T., Emin D. Infrared Absorption in Boron Carbides: Depedense on Isotopes and Carbon Concentration. /AIP Confererence Proceedings 231. Boron - Rich Solids albuguergue, 1990. - N. 14 - P. 322-359

# DEVELOPMENT OF METHODS OF DEPOSITION OF DISCONTINUOUS NICKEL COATINGS ON POWDERS OF $AB_5$ TYPE ALLOYS

**I. Slys', L. Shcherbakova, A. Rogozinskaya, D. Shchur, and A. Rogozinskii**
Institute for Problems of Materials Science of the NAS of Ukraine,

## INTRODUCTION

From the viewpoint of hydrogen storage, lanthanum nickelide $LaNi_5$ and its alloys are considered to be most promising. To improve service properties of $LaNi_5$-based electrode materials, microencapsulating of particles of $LaNi_5$-based alloys by different metals, which enables one to decrease significantly the oxidation and disintegration of electrodes during hydrogen adsorption/desorption, is used. Deposition of coatings on alloy powders is traditionally performed by chemical methods in aqueous solutions with using reducers.

In the present work, we present results of a study of the possibility of using two alternative methods of deposition of a nickel coating on the surface of powders that are hydrogen sorbents as a result of decomposition of nickel oxalate either during reducing heating in hydrogen or during intensive grinding in a planetary ball mill by the reaction

$$NiC_2O_4 = Ni + CO_2$$

## EXPERIMENTAL DETAILS

The intermetallic compound $MmNi_5$ (Mn = $La_{0.84}Ce_{0.16}$) was obtained by induction melting in argon followed by grinding of the ingot and cycling in a hydrogen atmosphere with the aim of its further comminution. The reducing heating of an alloy-nickel oxalatate mixture was carried out in a hydrogen flow at temperatures of 250-450°C for 2.5 h. The mechanochemical modification of the surface was performed in a planetary mill in different gas atmospheres (air, argon, hydrogen, and vacuum) for 6 h under conditions of intensive grinding of the alloy-nickel acetate mixture. Electrochemical measurements (plotting of voltammograms and charging curves) were carried out in a three-electrode cell, with an anodic and a cathodic space being separated , with using a P-5848 potentiostat. The investigated electrode made in the form of a pellet 1 cm in diameter was pressed into a nickel holder-current tap. As a reference electrode, a Hg/HgO electrode was used, and a platinum plate served as a counter electrode.

Changes in the morphology of the surface and phase composition, as well as transformation of the crystal lattice of the investigated objects depending on the conditions of deposition of coatings were controlled by methods of X-ray diffractometry, local X-ray local microanalysis and scanning Auger spectrometry.

## RESULTS AND DISCUSSION

Thermal decomposition of nickel oxalate. It was established that the amount of nickel oxalate introduced into the alloy powder influences essentially the structure, phase composition, and electrochemical characteristics of the heat treated powder. On addition of about 10 mass % (in terms of Ni) of oxalate, in X-ray diffraction patterns of the heat treated powder, significant decreases in the intensities of lines characteristic for the $MmNi_5$ alloy are observed, and the intensive lines of the free nickel phase are detected. Alloy particles are covered with a nickel layer 5 μm in thickness, the coating is dense, which leads to an abrupt decrease in the surface area accessible for proceeding volume (for hydrogen) reactions. The electrochemical discharge capacity decreases from 190 mA·h/g for the initial alloy to zero, and the hydrogen capacity in the gas atmosphere decreases from 165 ml/g to 70 ml/g. In Auger spectra obtained for mixtures of alloy powder with less than 1 mass % of nickel oxalate (in terms of nickel) after heat treatment at 400°C for 2.5 h, lines of the Ni phase are present. On local scanning of the surface, the intensities of the lines of this phase change by several orders of magnitude, which indicates the nonuniform distribution of conglomerates and individual Ni nanoparticles on the surface of alloy particles. The hydrogen capacity of the powders modified by nickel is equal to that of the initial alloy. It is likely that the electrochemical capacity on discharge falls by 40-50% as a result of the partial contamination of the surface of the $MmNi_5$ alloy by products of

thermal decomposition of nickel oxalate (CO, $CO_2$, and $H_2O$).

A method of mechanical treatment in the presence of nickel oxalate. The high-energy mechanical grinding of the $MmNi_5$ alloy powder with small amounts of nickel oxalate (1.5 mass % and 3 mass % in terms of nickel) was carried out in air, an argon and hydrogen atmosphere, and vacuum. During grinding in the planetary mill for 6 h, amorphization of the alloy does not occur. The initial alloy powder is uniphase, while, in X-ray diffraction patterns of the products of grinding of the alloy-nickel oxalate mixtures, the weak line (110) of nickel is present. The presence of individual nickel nanoparticles and nickel microclusters, that are rather uniformly distributed over the surface of alloy particles, was detected with using scanning electron microscopy and Auger spectroscopy. The volume of the crystal lattice remains practically unchanged after grinding of the mixtures in vacuum and in air, and increases slightly after grinding in argon (by 1%) and hydrogen (by 5.8%). A noticeable increase in the lattice size along the axis *c* after grinding in hydrogen gives ground to suggest its active penetration into the cell and the preferential location of its atoms between hexagonal planes along the axis. The discharge capacity of the alloy after mechanical grinding rises by 30-35%, which is connected with the formation of a highly developed surface which is active it terms of hydrogen-exchange reactions.

The combination of by nickel grinding with the simultaneous modification of the surface particles and the increase in the nickel oxalate concentration in the alloy powder from 1.5 to 3 mass % (in terms of nickel) exert practically no effect on the electrochemical characteristics of the alloy. The grinding of the powder mixtures in air results only in the partial oxidation of the surface and in a fall of the discharge capacity almost by 20% in comparison with that of powders ground in vacuum. The powders modified by nickel during grinding retain their electrochemical characteristics on long standing in air.

## CONCLUSIONS

1. On thermal decomposition of nickel oxalate in hydrogen at 350°C, either continuous or patch-like nickel coatings form. During deposition of coatings, the discharge capacity of the alloy powders decreases due to the contamination of the surface by the decomposition products of the salt.
2. During mechanical treatment of the alloy in the presence on nickel oxalate, isolated nickel particles and their conglomerates that are uniformly distributed over the surface form. As compared to other methods of grinding of the alloy, the discharge capacity increases almost by 30% and varies within 20% depending on atmosphere used in grinding.

# DIFFUSION BONDING APPLICATION FOR MANUFACTURING OF OXIDE CERAMICS JOINTS IN AIR ATMOSPHERE WITH THE USE OF PLATINUM OR PALLADIUM GASKETS

**Naidich Yu.V., Gab I.I., Stetsyuk T.V., Kurkova D.I**
Frantsevich Institute of Materials Science Problems, NAS of Ukraine, Kiev, Ukraine

The permanent joints of oxide ceramics units among themselves, and with metal ones obtained by metal solders brazing [1], or by diffusion bonding using metal gaskets [2] are applied successfully for a long time in various areas of engineering and are maintained in a broad range of temperatures from cryogenic [3] up to 800 $^0$C [4, 5]. However, during development of new advanced and more reliable instrumentation which can be operated frequently in extreme conditions there is more often necessity in obtaining of high-temperature ceramics strong joints, capable to work at temperatures up to 1200 - 1400 $^0$C in various conditions including air atmosphere. At the moment there are the high-temperature ceramic materials based on alumina and zirconium oxide suitable for long operation in air atmosphere at high temperatures up to 1800 $^0$C. But manufacturing of these materials permanent joints able to work at the above mentioned temperatures in air atmosphere is complicated problem a rather, which the given paper is devoted to the solution of. It is quite obviously that solders able to work in such conditions can be platinum group materials resistant to oxygen action at high temperature only. We selected palladium and platinum as solders and the samples for joining were made from alumina and zirconium oxide. Besides great technological difficulties (very high temperature of solders melting in vacuo, especially in case of platinum, evaporation of these metals in vacuo, etc.), active brazing selected ceramics by melted platinum and palladium solders method is also not acceptable because of bad wetting chosen ceramics by these melts [6]. Therefore our selection of a joining method of alumina and zirconium oxide was based on these materials diffusion bonding carried out in air atmosphere. For this purpose the high-temperature furnace SVK 5163 with chromite-lanthanum heaters was used, which was equipped by specially developed appliance for pressure transmission on samples being joined. It consisted from lever system in which pressure was transmitted from separable metal loads suspended on the end of the long metal lever to a refractory ceramic rod entering inward furnace chamber and contacting directly with samples being joined. These are ceramic bars 10x4x2 mm by size, collected pairwise with the appropriate metal gasket (palladium, platinum) between them in a special equipment made from an alumina or zirconium oxide for samples centre-of-gravity position and fixation. Ceramic samples ends to be joined were polished up to a roughness Ra = 0,25 micrometers. The initial platinum or palladium gaskets thickness was 0,1 - 0,2 mm. Samples joining was carried out in air atmosphere at temperatures 1300 - 1400 $^0$C for palladium gasket and at 1400 - 1500 $^0$C for platinum one. The welding pressure in both cases was 10 - 15 MPa, soaking period under pressure was 20 - 30 min. Obtained samples subjected to mechanical bending tests at three-point loading and to thermocycling in the air. Samples strength was about 500 MPa in the case platinum gasket and 400 - 450 MPa in the case of palladium one. The destruction of joints in all cases occures on ceramics near to the joint zone. Samples thermal resistance was also high since they have withstanded without destruction during 100 cycles at heating them in air up to 1100 $^0$C and then them down cooling to room temperature.

Thus, the tests results enable us to recommend manufactured joints of alumina and zirconium oxide for use them in units of devices and instrumentation working during long time in conditions of heating them up to 1300 - 1400 $^0$C in air, for example, in fuel cells, oxygen transducers, etc.

References

1. Heat-resistant dielectrics and their junctions with metals in new engineering / M.A.Rubashev, G.I.Berdov, V.N.Gavrilov, et al. – M.: Atomizdat, 1980. – 246 p. (in Russian).
2. Kazakov N.F. Diffusion bonding of materials. - M.: Engineering, 1976. – 312 p. (in Russian).
3. Development of obtaining methods and properties study of brazed metal/quartz portholes for cryogenic engineering / Naidich Yu.V., Kondratskii V.A., Zhuravlev V.S., et al.

// Adhesiya rasplavov i paika materialov. – 1976. – No. 1. – P. 74-78 (in Russian).

4. Metal/sapphire output windows for gyrotrones manufactured by diffusion bonding using the aluminium gasket / Naidich Yu.V., Gab I.I., Zhuravlev V.S., et al. // Automaticheskaya svarka. – 1996. – № 11. – P. 33-36 (in Russian).
5. Investigation of adhesion properties of copper-silver-titanum solders melts in sapphire/titanum brazing process / Naidich Yu.V., Zhuravlev V.S., Frumina N.I. // Adhesiya rasplavov i paika materialov. – 1978. – No. 3. – P. 99-101 (in Russian).
6. Wetting studies of oxide ceramics by platinum group metals using light-radiation heating technique / N.F.Grigorenko, A.I.Stegny, I.E.Kasich-Pilipenko, et al. // Reviewed Proceeding of the first international conference "High Temperature Capillarity '94", Smolenice Castle, Bratislava, Slovakia, May 9-11, 1994, Edited by Nicolas Eustathopoulos, P. 123-127.

# ANTIFRICTION COMPOSITION MATERIALS WITH ULTRADISPERSE DIAMOND POWDERS OBTAINED BY CONVENTION AND ELECTRODISCHARGE SINTERING

**Istomina T. I., Dubrova O. E.1[(1)], Volkogon V.M., Raychenko O.I., Pavlitchuk T.V., Kostenko A.D**
Frantsevych Institute for Problems of Materials Science,
Ukrainian National Academy of Sciences, Kyiv, Ukraine,
[1]Bakul' Institute for Superhard Materials,
Ukrainian National Academy of Sciences Kyiv, Ukraine,

The antifriction composition materials are applicable in industry [1]. It is desirable that antifriction materials for bearings have of a high resistance to vibrations. It is important for bearings having small dimensions. The "soft" work of such bearings is characteristic The main destination for them is ensuring low coefficient of friction, small dissipation in friction at low value of wear. Criterions for antifriction materials are coefficient of friction, loading and velocity characteristics.

The general requirements to antifriction materials, which are used in assemblies of friction as construction details (bearings, supports) are high physico-mechanical characteristics, support property, low coefficient of friction, high resistance to wear, good ability to run-in. The main materials for plain bearings are alloys on copper base. The copper has high heat conductivity, flexibility and corrosion resistance. The state and quantities of addition must change properties of bearings. The additional elements Al, Zn, Sn, Fe, Ni might increase strength and hardness of copper alloy. Zinc adding can to influence on wear resistant of alloy. Including graphite, sulfides sulfur, tin, lead, selenides etc allows to withstand adhesion in friction surface and to create materials with high antifriction characteristics.

For improvement of mentioned characteristics (i.e. for safe of friction surface from high wear and adhesion may be used others materials also, including diamond. It has high heat conductivity, strength and low coefficient of friction. The very fine disperse diamond powders (40-500 nm), which are made by means of ware used of dynamic synthesis. These dimensions are smaller than surface roughness on contact pairs of friction. Thus application of such fine powders excludes opportunity of scratching [2].

The metallic binder on copper base, which contains counter 80 Cu, 8 Sn, 12 Zn (mass.%), was used.

Ultra disperse powders of two types: were used clean diamond powders (see figure) and "semi-product" (50% diamond powder and 50% non diamond graphite component).

Properties of ultra disperse diamond powders are the following [3]:

- density – (2,97-3,00) g/cm$^2$;
- crystalline structure – cubical and hexagonal;
- bulk density – 0,4 g/cm$^3$;
- specific surface – (250-350) m$^2$/g.

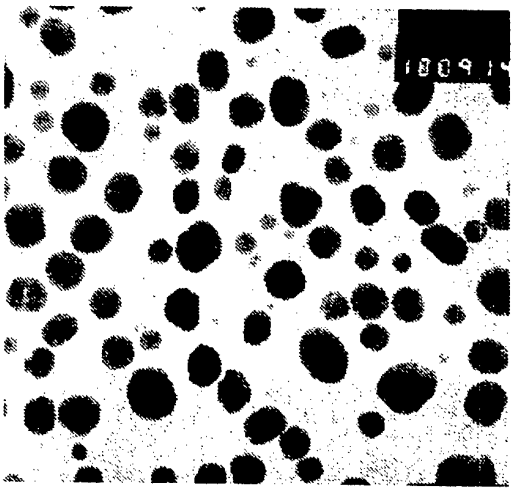

**Figure.** Diamond powder of dynamic synthesis, scale: 1 cm – 1 mkm, ×10000.

The ultradisperse powders were added in to binder: 3, 5, 6, 7 and 9 vd. %. The (24x7x7 mm) were made at two technologies:

1) conventional technology of powder metallurgy: compacting at pressing 30-60 MPa (up to porosity 15-17 %), sintering at temperature 840-950 $^0$C

during 1220 min, (under gaseous sate medium and covering) ;
2) electrodischarge sintering 51 s, current density 500 A/cm$^2$, end pressing 60 MPa.
The hardness of samples obtained was 50-70 HRB. The testing during 2 hours in oil medium, with counter body – steel 65G; at velocity 110 m/s and loading 50 N was made. At manufacture of samples by electrodischarge sintering technology for compositions with clean ultradisperse diamond powders increasing their concentration from 4 up to 9 % of coefficient of friction was accompanied by decreasing from 0,14 up to 0,12, but increased their wearing simultaneously from 0,55 up to 10,38 mg/km.
After addition of 3 % "semi product" and using electrodischarge technology wearing was 0,42 mg/km, and coefficient of friction 0,13.
From results presented can a give at a conclusion that the addition of ultradisperse diamond powders or "semi product" (~3 %) instead of $MoS_2$ can decrease of wearing antifriction materials very essentially.

## References

1. Abstracts of International conference "Advanced materials'99". - Kiyv. - 1999. - 366 p.
2. Volkogon V.M. The perspectives of create and application antifriction composition materials on bronze base, which reinforced detonation diamond // Superhard materials. - N 4. - 1998. - P. 62-67.
3. Nozkhina AA.V., Kolchemanov N.A., Kardanov A.A. and etc. Physico-chemical properties of diamond dynamical synthesis // Superhard materials. - N 1. – 2000. – P. 78-84.

# MODERN METHODS OF SYNTHESIS OF A SUPERCONDUCTIVE MATERIAL AND ITS PROPERTIES

**Flis A.A.**
Frantzevich Institute for Materials Science Problems NAS of Ukraine, Kiev, Ukraine

The yttrium ceramics is used for manufacturing volumetric products more often in comparison with other superconductive materials. The yttrium ceramics has a number of advantages: temperature of superconductive transition is above than boiling point of liquid nitrogen, rather easily it is possible to receive a single-phase charge, [ 1 ].

It is known, that volumetric superconductive high-temperature products (the targets for laser and magnetron of the equipment) receive from a plenty of a single-phase powder. For the manufacturers of high-temperature superconductive products it is important to have the authentic and reproduced information on properties of a material from which they are made and about properties of the product. The properties of products depend on a method of reception of powders and from properties of the powder.

The purpose of the present work was to receive a single-phase yttrium high-temperature powder. To investigate properties of the received powder.

In work the physical and technological properties of a yttrium superconductive powder (form, granulometric composition, bulk weight, fluidity, compressibility) are investigated. The structure of a powder is investigated.

Certification of powders carried out with the help of X-ray method on «Dron-3M» equipment. The sizes, form of particles of a powder, topography of their surface investigated on the raster electronic microscope of type "JSM – T", on the device "Superprobe – 733" and optical microscope "Neophot-2". Granulometric composition of powders determined by a method of calculation on optical microscope "MIM-7" and sift of a powder on standard sifter. The study of technological properties of a yttrium superconductive powder was carried out with use of standard techniques: bulk density, fluidity, compressibility [ 2,3 ].

In the present work the basic methods of reception single-phase HTS of powders of system Y-Ba-Cu-O: a chemical method, ceramic technology, method of explosive compression are considered.

At manufacturing yttrium HTS of powder on chemical technology as initial components used water solutions: nitrates of yttrium $Y(NO_3)_3$ and copper $Cu(NO_3)_2$ and hydroxide of a barium $Ba(OH)_2$, precipitator - hydroxide of a potassium KOH. At reception of a powder HTS ceramic method and method of explosive compression as initial components chose of yttrium $Y_2O_3$, copper CuO and barium BaO oxides.

At use of ceramic technology the initial components carefully mixed and have annolen at temperatures 150 - 400 $^0$C i 800 $^0$C during 4 - 24 h. Thus through everyone 4 h of an annealing a synthesized charge repeatedly mixed and sifted through a sieve. Thus, line of interannealings, millings have allowed to receive a homogeneous powder with a high yield ratio 85-100 % basic HTS phases $YBa_2Cu_3O_{7-\delta}$

At use of chemical technology the ambassador a joint deposition of a yttrium and the coppers as hydroxides $Y(OH)_3$, $Cu(OH)_2$ in received washed from intermediate products of reaction a deposit, entered stochiometric amount of soluble connection of barium as a water solution $Ba(OH)_2$. The received mix have steamed up to a thickening, dried up to constant weight, carried out the appropriate heat treatment.

At use of technology of explosive compression the initial components mixed in the ratio, providing ambassador of heat treatment formation of a superconductive phase $YBa_2Cu_3O_{7-\delta}$ and added the condensed explosive substance. After explosion the powders separated in depositings tank and on a centrifuge, dried in air at temperature 350 $^0$C during 0,45 - 1 h. The optimum and restrictive parameters established experimentally. The bottom limit of concentration of a mix in explosive substance - 15 %, top - 40 %. Is established, that during explosive compression of an initial powder mix the superconductive phase "123" is not formed. Therefore received powder passed heat treatment on a mode: the first stage - T- 920 - 950 $^0$C, t - 6 h, the second stage - T – 350 $^0$C, t - 10 h.

Is shown, that the powder made by a chemical method, consist from fine-dyspersated particles, which formed conglomerates of the different sizes. The particles of fineer fractions have filled space between large conglomerates.. The particles of a powder received on ceramic

technology, represented polyhedrons with the precisely expressed edges. Their surface smooth also has small quantity of ledges. As a result of explosive influence are formed nanopowders, which form conglomerates of the different sizes. The form of such particles is close to spherical.

Is established, that at comparison of technological properties of the investigated powders, the powder received on ceramic technology, has the highest fluidity for the given class of materials. The presence of different fractions provides high enough density of stacking owing to filling with fine particles of emptiness between large conglomerates, as determines high enough for the given class of materials bulk weight - up to 3,4 g/sm$^3$.

Powders received on a chemical method are fine-dyspersated. Due to presence of a plenty of ledges, accrete of a particle, complicate an opportunity easily to slide and to move in a mix. The fluidity and bulk weight of such powder is much lower, than powder received on ceramic technology. It is experimentally revealed, that the presence of a fine fraction (> 16 %) considerably is worsened fluidity of a mix as a whole and reduces its bulk weight.

On technological properties the powder received by a method of explosive compression, differed from other investigated powders. This powder very friable. It is easy crumble up to fineer fractions. Besides it is necessary to take into account, that the formation of structure "of a explosive" powder passed in conditions of a shock and detonation wave, ($t < 10^{-10}$s). In these conditions arise high imperfect structural condition, which influence on the basic physics and chemical characteristics of yttrium HTS powder. Though the particles of this powder are close to spherical, and bulk weight of spherical particles high enough and can change from 53 up to 74 %, determine fluidity "of a explosive" powder it was not possible. The advanced structure of spherical particles complicates drain of a powder from a funnel.

For researched powders the factors of fluidity were designed and the limits of a formability are established. Estimated a formability by definition of the minimal pressure of pressing at which pressed sample was not scattered, and edges remained steady, maximal - before occurrence of cracks or exfoliation in a sample.

Is shown, that the powders received by a chemical method and a method of explosive compression to be formed better, than powders received on ceramic technology. These powders begin to be compacting at pressure of pressing 1т/sm$^2$. "Ceramic" powders begin to be compacting at pressure of pressing 1,5 т/sm$^2$.

At a good formability of a powder not always it is possible to receive a final product with high density.

The dependence of porosity of samples from HTS materials from specific pressure of pressing is investigated.

Is established, that "the ceramic" powders are condensed better, than other investigated powders. "The explosive" powder has low compacting. At specific pressure of pressing 8 т/sm$^2$ the porosity in briquettes "of a explosive" powder is equal - 18 %. At specific pressure of pressing 6 т/sm$^2$ the porosity in briquettes of "ceramic" powder is equal - 17 %.

As a result of work the conclusion is made, that the physical and technological properties of powders on the basis of a phase "123", different technologies, received at use, of their manufacturing, influence properties of the pressed preparations. The powders consisting from fine-dyspersated of particles with an advanced surface, are form better, than large-dyspersated powders. However at pressing they are worse condensed also density of the pressed briquettes from these powders below.

From received yttrium HTS of powders the targets for sputtering of films were made. The superconductive properties are investigated. Temperature of superconductive transition is $T_c$= 89 - 92 K, width of superconductive transition is $\Delta T_c$= 4 - 5 K..

References

1. Achiba Shin-Ichi. Developments in the studies of high temperature superconductors // Kubutsuri. - 1991. - 60, N 5 - With 422 - 432.

2. Procceding of the workshop on chemical designing and processing of high - $T_c$ superconductor / H.Komatsu, Y. Kato, S. Miyashita et al. // Ranazawa Japan, July 27 - 29, 1991, 20c.

A.I.Raitchtnko, A.A.Flis, L.I.Cyernenko, N.I.Kryuchkova .Influence of pulsed electric current on the structure and superconducting properties of high-temperature superconductors // Superconductivity, high-temperature superconductivity. Low temperature physics, v.24, N 6? H 401- 404.

# MELT-SINTERING PROCESSING OF HYDROXYAPATITE BIOCOMPOSITES

**L.A.Ivanchenko, T.I.Fal`kovs`kaja[(1)], N.D.Pinchuk, O.V.Blyznuk[(1)]**
Institute for Problems of Materials Science of NAS, Kyiv, Ukraine
[(1)]National engineering university of Ukraine "KPI", Kyiv, Ukraine

Use of biostuffs in practical medicine for regeneration of defective fields of an osteal tissue presents them series of the demands:

1) biocompatibility of a biostuff with an osteal tissue, i.e. absence of negative responses of an organism by the way of inflammatory processes or casting-off;

2) availability of porous frame for an acceleration of processes of an intussusception of a new osteal tissue in a stuff of an implant;

3) mechanical hardness comparable to hardness of an osteal tissue;

4) economic technology for wide use providing accessibled prices of implants.

The first development of biostuffs on a basis hydroxyapatite show, that they quite answer the above indicated demands. Thus among the most perspective biostuffs there are composites on the basis of biological hydroxyapatite[1]. Biological hydroxyapatite - closed-grained stuff, which represents a mineral of a bone and can be utilized for deriving composites by the way of particles of the different dimensions with a natural porosity. Biological hydroxyapatite can be utilized in technological processes together with organic amounting (native bone) and without it (trademark "Osteoapatite"). At deriving biostuffs by the way of separate particles can be utilized "Osteoapatite" in the particles which have saved a natural porosity.

For rising mechanical hardness of separate particles was utilized their interaction with low-melting glasses based of oxides of silicon, sodium and boron in process a melt-sintering.

The technological process of deriving of composites consist of two stages with temperatures of a preliminary and final sintering $T_1$ and $T_2$. Temperature of a preliminary sintering $T_1$ were varied in limits 750-1300 °C. Temperature of a final sintering $T_2$ was saved invariable and did not exceed 800 °C. The time of a preliminary sintering also was varied in limits from about 0,25 till 2 hours.

The dimensions of particles of row mixture before a preliminary sintering did not exceed 160 micron. And the dimensions of particles of row mixture before a final sintering had different limits. For a final sintering samples formed by a method of cold pressing by the way of cylinders by a diameter 6 and 15 mm.

If into structure of row mixture was introduced biological hydroxyapatite by the way "Osteoapatite", the obtained samples of ceramics had mainly white color, sometimes with shades. At introduction biological hydroxyapatite by the way of native bone the obtained samples of ceramics had mainly grey color of different intensity. According to results of a chemical analysis in white samples of composites obtained on different technological regimens, the general common carbon content did not exceed 0,1 % (mas.). For grey composites the general common carbon content was in limits 0,06-0,21 % (mas.). Fixed, that after a preliminary high-temperature and short-term sintering in structure of mixture of composites can contain more than 12 % (mas.). Carboneum, which is significant decreases as a result of a final sintering. However, the residual amount of Carboneum also causes grey color of the obtained composites.

As the basic parameters of composites were are chosen pycknometric density, total amount of pores and mechanical compression hardness (table 1).

As it is visible from the table, white samples of composites with high temperature of a preliminary sintering (are higher 1000 °C) have the least porosity and maximum mechanical hardness. It is stipulated by various character of interaction biological hydroxyapatite with glassforming oxides at high and low temperatures of a preliminary sintering. At enough high temperatures low-melting oxides of a sodium and boron take part in interaction not only with oxide of silicon, forming a liquid phase, but also with surface layers particles biological hydroxyapatite. And at low temperatures there is mainly formation glass phase, which by the way fluid amounting inpours between grains biological hydroxyapatite, clamping them thus. It is possible, that the process of penetration of a liquid phase between particles of a solid phase at high temperatures is more intensive, that results

in the greater strengthening of samples in a final phase of a sintering. In case of introduction biological hydroxyapatite by the way of native bone in fusion mixture of composites there is a transformation of an organic component to Carboneum at a stage of a preliminary sintering.

Table 1. Some parameters of composites keeping(45-50) % (mas.) biological hydroxyapatite

a) white samples of composites

| Parameter | $T_1$=1150 °C | $T_1$=1300 °C |
|---|---|---|
| Density, g/sm$^3$ | 2,750-2,770 | 2,690-2,710 |
| Volume of pores, % | 20-43 | 15-20 |
| Hardness on compression, MPa | 20-95 | 122-173 |

b) grey samples of composites

| Parameter | $T_1$=900 °C | $T_1$=1100 °C |
|---|---|---|
| Density, g/sm$^3$ | 2,745-2,750 | 2,508-2,585 |
| Volume of pores, % | 50-58 | 31-32 |
| Hardness on compression, MPa | 36-37 | 61-87 |

At the following stage there is a burnup of Carboneum, that results in formation of the much greater formation of an amount of pores in grey samples of composites in comparison with white.

Thus, we guess, that the process of building of composites descends including liquid phases, which is saved before the terminal of a sintering. Therefore termination products remain diphasic, keeping a crystalline phase biological hydroxyapatite and amorphous glass phase. The ultimate analysis of samples structure specifies availability of ions of calcium, phosphorus, silicon and sodium both in glass phase, and in crystalline fields with predominance of ions of silicon and sodium in glass phase. At high temperatures of a preliminary sintering such allocation of elements in different fields of composites confirms, that the process of particulate dissolution and depositions glass phase on a surface of particles of a crystalline phase biological hydroxyapatite takes place.

At low temperatures of a preliminary sintering this process demands the considerable temporary costs in case the mass amount glass phase considerably exceeds an amount biological hydroxyapatite in structure of composites. At a short-term low-temperature sintering the process of strengthening is not finished completely, the sample form is in this case lost.

References

1. Pinchuk N.D., Sulima V.S. Biomaterialy dlja osteoplastiki / Problemy osteologii. - T.3, № 4, 2000. - P.37-41.

# FEATURES OF THE FORMATION OF SOLID SOLUTIONS OF TITANIUM CARBIDE WITH CARBIDES OF SOME TRANSITION METALS

**Prilutskii E.V., Makarenko G.N., Kud' I.V., Fedorus V.B., Likhoded L.S., and Eremenko L.I.**
Institute for Problems of Materials Science, National Academy of Sciences of Ukraine, Kiev, Ukraine

It has been known that the introduction of carbides of some transition metals into titanium carbide, which is a component of hard alloys, causes the comminution of the structure and provides high values of hardness, wear resistance, and resistance to deformation.

The temperature of formation of titanium carbide-based solid solutions is about 2000 °C. Since further application requires highly disperse powders of the solid solutions with a particle size of ≤0.5-1 μm, prolonged grinding is used.

In this connection, an investigation of the possibility of the formation of the titanium carbide-based solid solutions at lower temperatures and the development of a rational technology for synthesizing TiC-MeC (Me - Ta, Nb, and Sc) powders without grinding are of interest.

In the present work, the mechanism of formation of solid solutions in the TiC-TaC, TiC-NbC, TiC-ScC systems in the process of simultaneous carbothermal reduction of oxides in hydrogen and vacuum at a carbon excess and during the interaction of the intermediate product ($TiC + C_{excess}$) with oxides of the corresponding metals was investigated.

The interaction was studied in the temperature range 1600-2000 °C. In this case, the carbon excess was varied in the range 10-15 mass %.

Mixtures were prepared by mixing titanium oxide with carbon black in a planetary mill at a speed of 4800 rev/min for 30 s in in ethyl alcohol. Then the mixtures were briquetted and heated in vacuum (temperature was raised from room temperature to each set value at a rate of 100 °C/min) or in a Tamman furnace in a hydrogen atmosphere.

Interaction products were assessed by chemical and X-ray analysis.

According to the chemical analysis data, in all investigated systems, the content of excess carbon in interaction products practically coincides with its calculated content. In samples obtained in hydrogen, the presence of oxygen (0.1 - 0.7 mass %) and nitrogen (0.1 - 2.3 mass %) is due to the adsorption of the gases on the surface of highly disperse powders. The $TiO_2$-$Sc_2O_3$ system, in which the oxygen and nitrogen content exceed 4.3 and 3.9 mass %, respectively, is an exclusion. This can be due to the susceptibility of scandium carbide to binding oxygen and nitrogen with the formation of oxycarbides and oxynitrides and the high degree of incompleteness of the d-electron shell of scandium. The X-ray analysis data, indicating that, during interaction of the mixture of titanium and scandium oxides with carbon in hydrogen, a pronounced decrease in the lattice constant of the TiC-based phase takes place, confirm this assumption.

The X-ray analysis data of the interaction products are presented in the Table.

The reference data of the lattice constants: are as follows: for TiC a = 432(4) nm; for NbC a = 0.446(9) nm; and for TaC a = 0.445(9) nm.

Table. X-ray analysis data of the interaction products with a 10% carbon excess (the time of reduction is 1 h)

| No | Mixture composition | $T_{int.}$°C | X-ray data, lattice constants, nm |
|---|---|---|---|
| 1 | $TiO_2$-$Sc_2O_3$ + C | 1700 | TiC, a=0.433(3); $ScTiO_3$, $ScTiO_5$ |
| 2 | the same | 1800 | TiC, a=0.433(7); $ScTiO_3$, $ScTiO_5$ |
| 3 | the same | 1900 | TiC, a=0.433(6) |
| 4 | the same | 1900* | TiC, a=0.430(5); $ScTiO_3$, $ScTiO_5$ |
| 5 | the same | 2000 | TiC, a=0.433(7); $C_{graph.}$(traces) |
| 6 | $TiC_{i.p.}$ + $Sc_2O_3$ + C | 2000 | TiC, a=0.433(9); $C_{graph.}$(traces) |
| 7 | $TiO_2$-$Nb_2O_5$ + C | 1700 | TiC, a=0.433(5); NbC, a=0.447(5) |
| 8 | the same | 1800 | TiC, a=0.433(4); NbC, a=0.447(4) |
| 9 | the same | 1900 | TiC, a=0.433(4); NbC, a=0.446(2) |
| 10 | the same | 1900* | TiC, a=0.433(4); NbC, a=0.446(2) |
| 11 | the same | 2000 | TiC, a=0.433(5); NbC, a=0.443(2) |
| 12 | $TiC_{I.P.}$+ $Nb_2O_5$ + C | 2000 | TiC, a=0.433(3); NbC, a=0.441(5) |
| 13 | TiC + $Ta_2O_5$ + C | 1700 | TiC, a=0.433(3); TaC, a=0.446(0) |
| 14 | the same | 1800 | TiC, a=0.433(2); TaC, a=0.445(8) |
| 15 | the same | 1900 | TiC, a=0.433(4); TaC, a=0.441(1) |
| 16 | the same | 1900* | TiC, a=0.431(0); TaC, a=0.443(0) |
| 17 | the same | 2000 | TiC, a=0.433(6); TaC, a=0.438(8) |
| 18 | $TiC_{I.P.}$ + $Ta_2O_5$ + C | 2000 | TiC, a=0.433(2); TaC, a=0.439(4) |

*Synthesis was performed in a hydrogen for 2 h.

The subscript i.p. corresponds to intermediate products

According to the X-ray analysis data, in the $TiO_2$-$Nb_2O_5$ and $TiO_2$-$Ta_2O_5$ systems, the carbide phases TiC, NbC, TiC, and TaC form during carbothermal reduction in vacuum in the presence of the excess carbon even at 1700 °C. The fact that these phases are close in composition to the stoichiometric ones is confirmed by their lattice constants, that are close to the reference data (TIC = 0.433 nm, a NbC = 0.447 nm, TaC = 0.446 nm), and by the shape of their diffraction maxima.

Beginning from 1800 °C, the formation of solid solutions on the base of NbC and TaC, accompanied by the broadening of the diffraction maxima of niobium and tantalum carbides and by changes in their lattice constants, is noted. A rise in the reduction temperature up to 2000 °C did not result in the formation of homogeneous solid solutions, and only an increase of the process time enabled us to obtain the solid solutions of specified composition.

Thus, the investigation performed shows that the carbothermal reduction of oxides in vacuum in the presence of excess carbon proceeds via the formation of the individual carbide phases TiC, NbC, and TaC followed by the dissolution of TiC in the crystal lattice of NbC (TaC).

The X-ray analysis data show that, during carbothermal reduction of the $TiO_2$-$Sc_2O_3$ mixture in vacuum, the formation of the solid solution proceeds by another mechanism. In the temperature range 1700-1800 °C, titanates of scandium and titanium carbide are in equilibrium. The homogeneous solid solution (Ti, Sc)C with a lattice constant a = 0.433(9) nm was not obtained at 2000 °C.

# FINE BORON CARBIDE POWDERS AND WHISKERS FOR CERAMIC

**Prilutskii E.V., Liashenko V.I., and Tkachenko Yu.G.**
Frantsevich Institute for Problems of Materials Science, National Academy of Sciences of Ukraine, Kiev, Ukraine

Boron carbide-based and $B_4C$-containing ceramics are rather extensively used in industry, which, in turn, causes considerable demand for high-quality starting powders. The conception of high quality for boron carbide powders employed in ceramics includes a list of the following properties:

- a high degree of dispersion of powders;
- a narrow range of the granulometric composition;
- the absence of even isolated very large particles (that are by an order of magnitude larger than medium-sized ones);
- a small amount of impurities of incidental character and those connected with the production of just this powder;
- the possibility of obtaining boron carbide in the range of its homogeneity, i.e., with a lower content of bound carbon;
- the possibility of preparing powders containing a specified (tens of percents) amount of filamentary fibers, that form a high-strength reinforced system.

Conventional production technologies of fine boron carbide powders are connected with the carbothermal process of interaction between boric anhydride and carbon reducers of different origin. It has been known that the carbide formation process proceeds just on carbon particles, and their state, especially their size, plays a determining role. For instance, in the case of commercial-purity carbon, namely carbon black with a specific surface of 50-75 $m^2/g$, the temperature of carbide formation, providing the completion of this process, is above 2000 °C. This, in turn, leads to the severe sintering of briquettes obtained and requires their durable force grinding. Due to the abrasive capability of boron carbide grains, the grinding process causes the severe contamination of the powder obtained by the material of grinding bodies and equipment. Moreover, during grinding and removal of contaminants appeared as a result of grinding, the severe oxidation of the powder is observed. The values of consumption of energy and human labor required for the grinding of briquettes to micron sizes and classifying the powder constitute 50% of the total ones in the production of fine boron carbide powder. Nevertheless, in grinding, it is practically impossible to achieve a level of dispersion above 1-0.5 μm. In the conventional process, filamentous boron carbide crystals, that can be an interesting reinforcing filler owing to their high strength and low density, do not form.

We developed and tried out a solution technology for preparing fine boron carbide powder without grinding at temperatures of carbide formation ranging from 1600 to 1650 °C. This precise technology provides the monocrystalline structure of all grains, i.e., boron carbide particles, a high purity of the powder with a total content of impurities of no more than $5*10^{-2}$ mass %.

It should be noted that there exist conditions under which boron carbide powder contains about 30% of filamentous crystals. Two morphologic types of filamentous crystals form, namely the plate-like (sword-like) and prismatic one. In our opinion, this is connected with the manifestation of different mechanisms of formation of crystals. These are:

- the VLS mechanism;
- the rotation of a screw dislocation.

The ratio of the length of crystals to their thickness (diameter) is not smaller than 20-30, and, in some cases, exceeds 100. In an optical microscope, at a magnification of about 100x, some plate-like crystals are optically transparent, which points to their small thickness and the perfectness of their crystal structure. In the assessment of the strength of filamentous crystals, the following ratio is used: the strength of such crystals practically approaches the maximum possible strength of this material and can constitute 0.1 of their modulus of elasticity. For boron carbide, this value is about 4-5 $kg/mm^2$. At such a high strength and the good wetting of crystals by the matrix material, for instance aluminum, the presence of even 10 mass % of crystals in the composition can provide a strength of about 400 $kg/mm^2$ and a modulus of elasticity of no less than $2*10^3$ $kg/mm^2$.

The use of filamentous boron carbide crystals for self-reinforcement in ceramic compositions of different application is of great interest. In such

materials, one can expect a significant increase in the crack resistance of the composition, which is of the utmost importance for brittle ceramics. Electron micrographs show filamentous boron carbide crystals. Their plate-like «sword-like» structure is clearly seen.

The electron microscopic studies of two batches of boron carbide powder obtained by the solution grinding-free method has shown the following:
- the powder ensemble has two morphologic forms of particles, namely the isometric (equiaxial) and needle-like one;
- the fraction of needle-like crystals over the surface of a thin layer (practically a monolayer of particles) constitutes about 30%, which, at equal densities of particles and crystals correspond to their content in the powder ensemble;
- needle-like crystals of two types, namely plate-like ones with a width of 5-10 μm at the base and prismatic crystals, whose width and thickness are equal and ranges from 1 to 2 μm;

- equiaxial particles have a distribution close to the Gaussian distribution with a mean size of about 8 μm. The maximum size of particles is 20 μm (isolated), and the fraction of particles with a size of 2 μm and under is about 5%. A particle-size distribution obtained by the calculation of all particles on several visual fields with an assessment of their size is presented below.

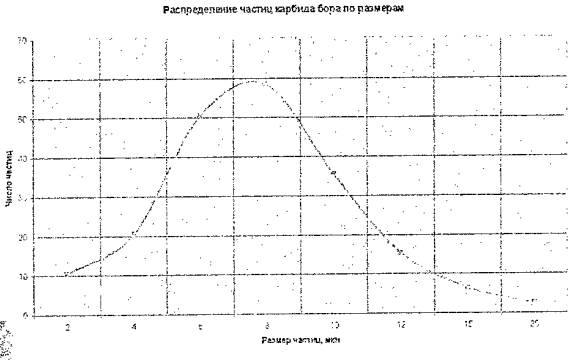

# THE APPLICATION OF CONCENTRATED LIGHT RADIATION FOR DEVELOPMENT OF TECHNOLOGICAL METHODS OF THE HIGH-TEMPERATURE MELTING OF OXIDE COMPAUNDS

**Frolov Alexander A., Andrievskaja Elena R., Lopato Lydia M.**
Frantsevich Institute for Problems of Materials Science, NAS of Ukraine, Kiev, Ukraine

The elevated power optical furnace "Crystal-M" with xenon radiation sources was developed in the IPMS of NAS of Ukraine on the basis of the equipment described in [1]. The furnace optical scheme and dependence of average magnitude of the light energy flux density in a focal zone in diameter of 10 mm versus a current intensity E (I), are shown on fig.1.

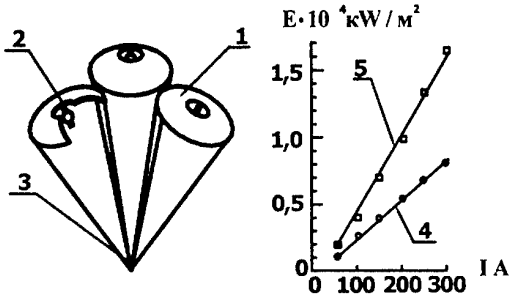


Fig.1. The optical scheme of furnace and dependence of magnitude of the average light energy flux density in the focal zone: 1- ellipsoidal reflectors; 2- xenon lamps ДКСШРБ-10000; 3- general focal zone of the light emitters; 4- dependence E (I) for one emitter; 5- dependence E (I) for three emitters.

The optical furnace is consists from three ellipsoidal reflectors. The ДКСШРБ-10000 lamps are disposed in one focus of every ellipsoidal reflector. Thus, it is concentrates over 2 kW of light energy in the general focal spot of 10 mm in diameter. The magnitude of the average light energy flux density in the focal spot at I = 300A reaches $E=1,4\cdot10^4$ kW/m$^2$. This corresponded to equilibrium radiation of absolute black body temperature $T_{a.b.b.}$ = 4000 K. The maximal magnitude of the average light energy flux density in a focal spot of a diameter of 6 mm at I=300A is $E=1,6\cdot10^4$ kW/m$^2$, $T_{a.b.b.}$= 4100 K.

The fusion experiments for high-melting oxide-coated compound, such as $HfO_2$ ($T_{melt}$ = 3103 K) and $ZrO_2$ ($T_{melt}$ = 2973 K) were carried out. It was shown that the majority of high-melting oxides could be melted in this optical furnace, under condition of the sufficiently level of a heat insulation of melt zone. Thus, the appropriate convenient laboratory installation for study of the high temperatures physicochemical processes was developed in IPMS of NAS of Ukraine. It is possible to develop various methods high-temperature treatment of materials.

The concentrated optical irradiation has the following properties: locality, one side heating, ideal cleanliness and high temperatures. The developed optical furnace was used for synthesis of homogeneous and uncontaminated solid solutions by melting on the powder blends of starting materials. As an intensive heat removal is exists toward the melting layer, under one-sided heat in the optical furnace, the thickness of the melted layer for high-melting oxides can not be higher 0,5 - 1 mm. Therefore a variant of Verneil's method was used to produce the massive ingots.

The upper butt-end of cylindrical samples with a diameter of 25 mm was pre-melted. Then the new portions of a powder of the same composition was feed to melt zone. The process was continued up to formation the melted layer thickness of 5 - 6 mm on a surface of a sample. The obtained ingots were sluggishly cooled to ambient temperature. The samples without defects regions of 2 x 5 x 7 mm were cut out from these ingots. The samples were used for carrying out of electro-physical and radiographic examinations.

The samples of the systems $HfO_2$-$Y_2O_3$-CaO, $ZrO_2$-$Y_2O_3$–CaO, $CaHfO_3$-$Y_2O_3$, $CaZrO_3$-$Y_2O_3$, $HfO_2$–$Al_2O_3$–$TiO_2$, $ZrO_2$–$Al_2O_3$–$TiO_2$, $HfO_2$–$Y_2O_3$–$Eu_2O_3$ were obtained through the described manipulation [2,3]. The X-ray phase analysis data have shown, that reception of solid solutions by melting method provides rapid and complete homogenization of mixtures due to an intensive convection and major diffusion rates in a melt. The X-ray diffraction and chemical analyses has shown that the composition of the melted samples was not deviates from of solid solutions and corresponded to the initial composition of mixtures.

It is necessary to underline, that it was not possible to produce the applicable samples for electro-physical investigations by another way then melt in the optical furnace.

The optical furnace was used to obtained the melted granules of oxide-coated materials. The high cleanliness of the process has allowed to development palletizing methods of high clear compounds, for example, such as $Nb_2O_5$ and $LiNbO_3$. These compounds were used for production of optical fiber materials and in microelectronics. There is interest for development of such processes in the technology of crystals growth. The problems of efficient filling of a crucible before the crystal growth process exists on the initial stage and delivery of raw mixture in a crucible for maintenance a melt level in accordance with elongation of a crystal. This phenomenon occurs due to contraction of a material volume during melting as source loose of a powder is in 3-3,5 times less then density of a melted material.

For palletizing the material was positioned in focus of the optical furnace and melted under concentrated light flux. The fusion process was carried out in a crucible from the sintered powder of the most material due to a locality of a heating process. Thus it completely prevented pollution from an external crucible material. Then the melt was poured out on the palletizing cone.

The designed palletize method of the high purity material have some specific features. The palletizing cone was manufactured from ceramics with protective coating from the palletizing material. Thus, was used a palletizing cone fabricated from quartz ceramics with protective coating from $Nb_2O_5$ for palletize the $Nb_2O_5$ melt. For palletizing the $LiNbO_3$ melt was superimposed an additional stratum from $LiNbO_3$ on the surface of palletizing cone [4,5]. After accumulation, a melt was poured out on a rotary palletizing cone. The cooled granules were agglomerated in the container from stainless steel. The spectrum analysis of obtained granules has shown that the content of all controlled impurities remained unchanged during in palletizing process. The impurity concentration made about $1 \cdot 10^{-3}$ - $5 \cdot 10^{-3}$ masses. % in a starting material.

In addition to these experiments the granules of compounds $Nb_2O_5$ and $CaO\text{-}Al_2O_3\text{-}CaSO_4$ were obtained by pouring out melt in to water. The pieces of melted material blocs of irregular geometrical shape were obtained. This blocs can be used the melted coats technology. Ball-shaped granules were obtained at pulsing (droplet mass) feeding of a melt in a vessel with water. But it was quite difficult to provide cleanliness of process in this case. Therefore it is not possible to recommend this process for pre-treatment of mixture to obtained high pure termination products.

The high cleanliness of an optical heating allowed us to use the developed optical furnace for development of protective ceramic coatings technology. The particular requirements to a substrate and a coat material for this process are the following:

1 - the physicochemical properties of a substrate ceramics should be corresponded with the coat material properties;

2 – the materials of substrate and coats should have the high heat resistance in order to keep the processing conditions in a local focal zone with heavy gradients of temperatures.

This problem was successfully solved for protective coatings from $Nb_2O_5$ and $LiNbO_3$. The large sizes products were obtained from such materials by scanning a handled surface in a focal zone. Thus, the dishes from $Nb_2O_5$ by volume of up to 5 litres and a series of other products were obtained. These products have passed successful trials in the production requirements at thermochemical treatment of high purity niobium compounds.

REFERENCES

1. Балбашов А.М. Коротун М.М. Условия выращивания монокристаллов тугоплавких веществ методом Чохральского с радиационным нагревом // Изв. АН СССР. Сер. Физическая - 1975. – Т. 39. - №1.-С. 222-224.

2. Андриевская Е.Р., Фролов А.А., Рагуля А.В. Физико-химические и электрофизические свойства фаз в системах гафнат (цирконат) кальция-окись иттрия // Физическое материаловедение и физико-химические основы создания новых материалов.- Киев, ИПМ, 1989.- с. 124-129.

3. Andrievskaya E.R., LopatoL.M., Red'ko V.P., Frolov A.A., Shevchenko A.V. Characterization and Properties Phases in the $HfO_2$–$Y_2O_3$–$Eu_2O_3$ Ternary System // Abstract of Paper 5-th International School "Phase Diagrams in Materials Science"JSP DMS'96, Katsyvely, Crimea, Ukraine, September, 1996.- P.14-15.

4. Фролов А.А., Пасичный В.В., Балабанов Ю.И., Агулянский А.И. Керамические материалы для технологии высокочистых оксидов ниобия и тантала // Всокочистые вещества.- 1989.-№1.-С. 102-105.

5. Фролов А.А. Керамические материалы для получения высокочистых соединений ниобия и тантала // Стекло и керамика. - 1992.- №7. - С. 14-15.

# THE USAGE OF TITANIUM HYDRIDE FOR THE PREPERATION WEAR RESISTANCE COMPOSITE COATING

**Guslienko Y. A., Luchka M. V., Kostenko V. K., Meduch R. M.**
Fransevich Institute for Problem of Materials Science,
National Academy of Science of Ukraine, Kyev, Ukraine

Lately the development of technique has dealt with the creation of materials with high temperature end composite coating with heterogeneous structure consisting of such materials. The methods of the preparation such coatings heave been worked out at the Institute for Problem of Material Science. These technologies have such peculiarity as simplicity, economic: the possibility to control of coatings thickness and uniformly deposition upon the part of complicated form.

The studding Ni-$TiH_2$ and Ni-B-$TiH_2$ system prepared by the co-deposition Ni and $TiH_2$ or Ni, B and $TiH_2$ from clorouse electrolyte of nickel plating. This is interesting from the point of view of formarion disperse-strengthening structure, whish have been achieved as a result of hard solution strengthening by means of second phase disperse distribution after the following heat treatment.

The main attention have been paid for the disperse particles content in electrolyte solution/ it have been determined the increasing particles content in coating from their increasing particles content in electrolyte solution/ As a rule this concentration reaches some maximal vale and then it changes unconsiderebly (fig. 1). The maximal amount of $TiH_2$ powder (10 % Mass.) is deposited

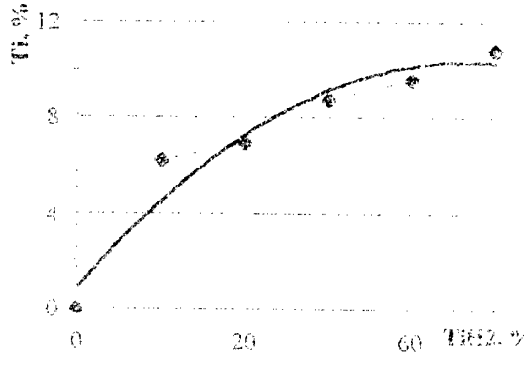


Fig. 1. $TiH_2$ particles content in CEC in dependence from their quantity in electrolyte solution.

when 10 g/l of $TiH_2$ powder is introduced in to electrolyte. The addition of the second components of amorphous boron with the particles size less then 1 mkm is leaded to the decreasing as B so $TiH_2$ content in coating.

The composite electrolytic coating (CEC) Ni-$TiH_2$ have been subjected to heat treatment in vacuum at various temperatures (200-1000 °C) and time of process (1-12 h).

The studding of coatings phase composition and measuring of crystal grating parameters at different conditions of heat treatment have shown that the formation of solid solution Ti in Ni and intermetallide $Ni_3Ti$ had taken place at all the investigated temperatures.

The chaining of crystal grating parameter essentially depends on temperature and time of heat treatment and it usually starts at temperature 400-500°C.The microstructure of first samples before the heat treatment have shown the uniform particles distribution intermetallide inclusions in the matrix of γ-solid solution after heat treatment (fig. 2). The microhardness of coating is practically unchained during heat treatment and it is found about 300-400 $Kg/mm^2$.

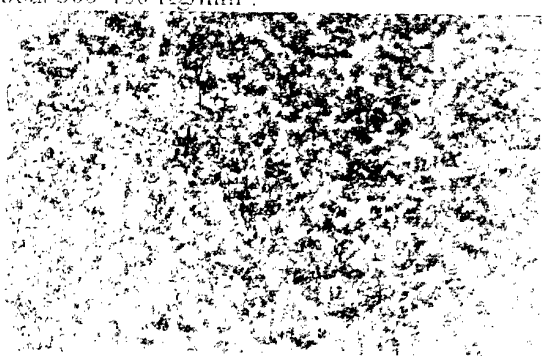

Fig. 2. Microstructure CEC Ni-Ti after heat treatment (400 °C). ×300 .

The CEC Ni-B-$TiH_2$ heat treatment at the temperature of eutectic lead to the formation of framework $Ni_3B$-$Ni_3Ti$-Ni with the microhardness about 600-1100 $kg/mm^2$ and the soft component (solid solution of boron, titanium in nickel) is accommodated in its interval.

The preparation of heterogeneous coating with the higher content of high temperature melting components and with the considerably bigger thickness (till 300-500 mkm) have been

achieved by the combination of two methods – electrolytic and electroforetic.

The necessary structure is formed by means of definite correlation between the components, which can be easy regulate be technological parameters and following heat treatment [2].

The electroforetic coating have high porosity (about 50 % for $TiH_2$) and law adhesion to foundation and therefore it demons a strengthening heat treatments.

The preparation galvanoforetic coatings (GPC) consists of a studies: 1) the deposition of previous layer CEC Ni-B with amorphous boron content near 4 % mass. which thickness is easy regulated and it determines the quantity of liquid phase at the temperature of eutectic formation; 2) the deposition of phoretic layer $TiH_2$; 3) the liquid phase sintering at the eutectic temperature.

The microstructure GPC Ni - B- TiH (fig 3) has good correlation with the phase analyze data with the presence of eutectic $Ni+Ni_3B$ through the all layer depth, Ni (Ti) solid solution and lines of intermetallide $Ni_3Ti$.

The test for the determinations of relative wear resistance of costing has been made using a special method [3]. Steel 45 have been choused as etalon. These investigations have shown high coating resistance in abrasive medium.

The corrosion testing of CEC Ni- $TiH_2$ in the mediums of concentration and dilute chloride, sulfuric and nitride acids have shown their high resistance in the medium of heat treatment. Influences essentially on the corrosion resistance, which deals with the formation of solid solution Ni

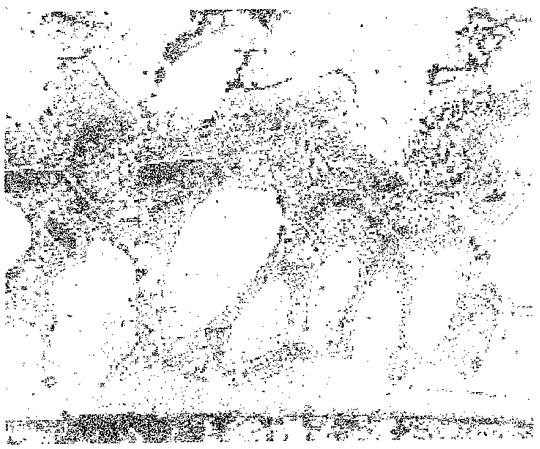

Fig. 3. Microstructure GPC Ni-B-Ti. ×300

(Ti) and decreasing of defect in coatings crystal structure.

The strengthening phase $Ni_3Ti$ increases the coating wear resistance and therefore such coating can be recommended for the protection of pert from wear corrosion mediums.

References.

1. Fedorchenko I. M., Danilenko V. A., Guslienlo Y. A. Wear Resistance Composite Costing on Ni and Fe bases Powder Metal. 1977.-5.- P. 70-72.
2. Electroporetic deposition and structure coating. Guslienlo Y. A., Furman V.V., Kostenko V. K., Shmatko I. O., Savina L.G. Powder Metal., 1988.-7.- P. 38-40
3. Kuala P.A. Methods and. Tallinn politechn. Institutes. 1976. - 7 P. 44-48.

# STRUCTURE AND PROPERTIES OF MAGNETRON FILMS USING ADVANCED COMPOSITE AlN-$TiCrB_2$ CERAMICS

**M.A. Teplenko, A.D. Panasyuk, I.A. Podchernyaeva, N.S. Boltovets[(1)], V.N. Ivanov[(1)]**
Institute for Problems of Materials Science of NAS, Kiev, Ukraine
[(1)] State plant "Scientific-research the institution "Orion", Kiev, Ukraine

Magnetron sputtering being one of the version of PVD method is widely applied for coating deposition on tools. Hereby it is necessary to use wear- and corrosion resistant materials with the higher temperature (>700°C) and enough heat conductivity. The magnetron coatings are also applied in electronics to suppress of diffusion on the "coating–substrate" boundary. The goal of this study is to research the structure, composition, mechanical characteristics and resistance to high temperature oxidation (HTO) of magnetron films using the AlN-$TiCrB_2$ (1:1) targets manufactured by powder metallurgy. As substrates the monocrystalline Si, $Al_2O_3$ (110) and GaAs (100) were used.

The magnetron films obtained were characterised by ultra-dispersion structure. The film phase composition may be differed from the target one due to AlN oxidation under conditions of ion bombardment during spraying even in the cleaned Ar environment. The main film phases were, side by side with double titanium-chromium boride, alumina and aluminum nitride. The film ultra-dispersion structure and high adhesion to the substrate were preserved after the HTO up to 1500°C. Hereby the structure reinforced with $Al_2O_3$ grains as fibres formed. The $Al_2O_3$-$TiO_2$, $Al_2O_3$-$Cr_2O_3$ and $Al_2O_3$-$B_2O_3$ solid solutions and corresponding β-tialite and aluminum borates, ensuring the material high resistance to high resistance to high temperature corrosion, formed during HTO. The AlN-$TiCrB_2$/$Al_2O_3$ (110) and AlN-$TiCrB_2$/GaAs (100) films were thermostable up to 1000°C and had enough high both microhardness (30GPa) and toughness coefficient (3.3–4.7 $MN/m^{3/2}$). As an example, the dependences of cracks length on the load for AlN-$TiCrB_2$/$Al_2O_3$ (110) sample at different annealing temperatures were presented in Fig. The structural and phase transformations took place in the films at the annealing temperatures higher than 1000°C. Hereby the mechanical properties was made worse (Table) and the adhesion strength increased. The AlN-$TiCrB_2$ target material may be recommended for the deposition of wear- and corrosion-resistant films on tools and parts working under extreme conditions.

Table

Effect of annealing on microhardness ($H_\mu$, GPa) and toughness coefficient ($K_{1c}$, $MN/m^{3/2}$) ($t_{an}$=30 min)

| Sample | | AlN-$TiCrB_2$/$Al_2O_3$ (110) | AlN-$TiCrB_2$/GaAs (100) |
|---|---|---|---|
| 25°C | $H_\mu$ | 30.0 | 30.0 |
| | $K_{1c}$ | 4.7 | 3.3 |
| 500°C | $H_\mu$ | – | 29.5 |
| | $K_{1c}$ | – | 3.1 |
| 600°C | $H_\mu$ | 30.0 | – |
| | $K_{1c}$ | 3.3 | – |
| 800°C | $H_\mu$ | 30.0 | – |
| | $K_{1c}$ | 2.9 | – |
| 900°C | $H_\mu$ | – | 24.2 |
| | $K_{1c}$ | – | 1.2 |
| 1000°C*) | $H_\mu$ | 10.0 | – |
| | $K_{1c}$ | 1.6 | – |

*) $t_{an}$=45 min.

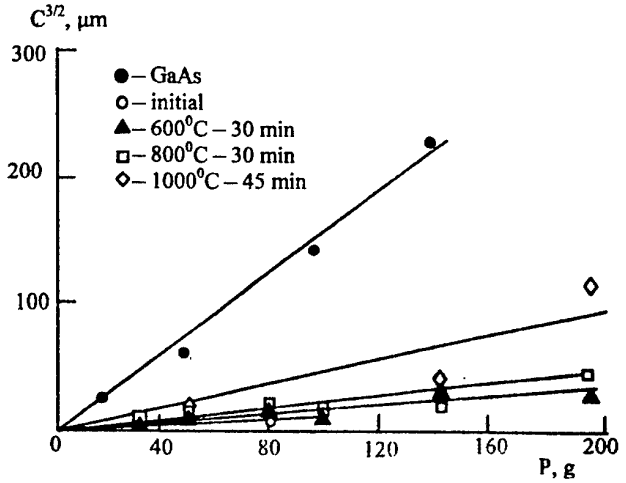


Fig. Dependences of cracks length on the load for AlN-$TiCrB_2$/$Al_2O_3$ (110) sample

# STUDY OF INFLUENCE OF BORON STATE AS INITIAL REAGENT ON MODE OF BORON SUBOXIDE SYNTHESIS AND ITS PROPERTIES

**Kharlamov A.I., Khotynenko N.G., Kirillova N.V.[1], Trapalis Ch.[2], Fomenko V.V.[3], Goydina S.V., Shatscikh C.K., Gubareni N.I.**

Institute for Problems of Materials Science NAS of Ukraine, Kiev, Ukraine

[1]National Taras Shevchenco University, Kiev, Ukraine

[2]Institute of Materials Science, Athens, Greece

[3]National University of Food Technologies, Kiev, Ukraine

In the last year, growing interest to suboxide phases of boron could be explained regarding, first of all, their high hardness (diamandand CBN are better of some phases only) and lightness. In the present paper results of study of boron anhydride interaction with powderous boron of two different modifications are reported. The aim of the investigation is to study the nucleation and growth mechanisms in heterogeneous system of suboxide boron phase and find out nature of inheriting by the yield of properties of one of precursors, in particular, boron. In the investigation the most spread commercial powders of two modification of boron, black amorphous ($B_{am}$) and rhombohedrical (Br) were used. It is common practice to suppose that their difference in reaction capabilities is great. But the most important is that this two powderous borons were chosen because of their significant difference of their particles morphology. Characterisation of as initial boron powders as products of their synthesis was carried out by means of crystal-optical, X-Ray, chemical, electron microscopy and IR-spectroscopy methods.

It was found out that $B_{am}$ obtained through crecking of borines and $B_r$ obtained through magnium thermal reduction of $B_2O_3$ differs not only by the order of crystallity. Boron powders TEM images (fig.1,a) show $B_{am}$ consist of homogenous in shape (like balls) particles but significantly various in size, diameter of which is from 30 to 150 nm. Specific surface ($S_S$) of $B_{am}$ measured by means of the BET method employing an ASAP-2000M device is 9,3 $m^2/g$. In IR transmission spectra of $B_{am}$ the characteristic lines of the lattice absorption are absent. Powder of $B_{cr}$ consist of homogenous enough particles in shape of splinters (fig.1,b) with the size of which is 0,5-1 mkm. In the yield there are also individual bigger particles in shape of rods and 3-5 mkm in length and particles in shape of right rectangles with size less than 0,5mkm. Specific surface of $B_{cr}$ powder is 3,4 $m^2/g$. Thus, initial boron reagents significantly differ not only in its inner structure (X-Ray, IR-spectra) but also apparently (dispersity and morphology of particles) that obviously has to affect on properties of products synthesized. Temperature and kinetic functions of $B_2O_3$ interactions with as $B_{am}$ as $B_{cr}$ boron were investigated at 1000-1500°C using a vacuum furnace with the tungsten heaters and carbon free crucibles. Reaction capabilities of boron modifications under investigation with $B_2O_3$ were compared and studied as in vacuum as in the medium of inert gas by means of high-temperature derivatogroph. In conditions comparable temperature at which reactions with $B_{am}$ starts is approximately 160 °C lower within all heating rates than that when $B_{cr}$ was used and at 20 degree/min rate of heating is 1260 and 1420°C, respectively. Temperature of the reaction start practically does not depend on nature of reaction medium but its decreasing is observed when rate of heating was lowered. Derivatograms of boron interaction with $B_2O$# contain two (endo- and exothermal) peaks which characterize $B_2O_3$ melting (T=340°C) and boron suboxid phase formation, respectively. Influence of initial boron state is performed not only on temperature-time parameters of $B_2O_3$ reduction process but also on chemical composition of powderous suboxide boron, its dispersity and what is the most important, morphology of its particles (fig.1,c,d). According to results of chemical analysis, the phase with composition $B_{6,3}O$ is formed from $B_{am}$ whereas when Bcr is used the phase of $B_{6,5}O$ composition is obtained. X-ray spectra of products obtained of $B_{am}$ and $B_{cr}$. are similar

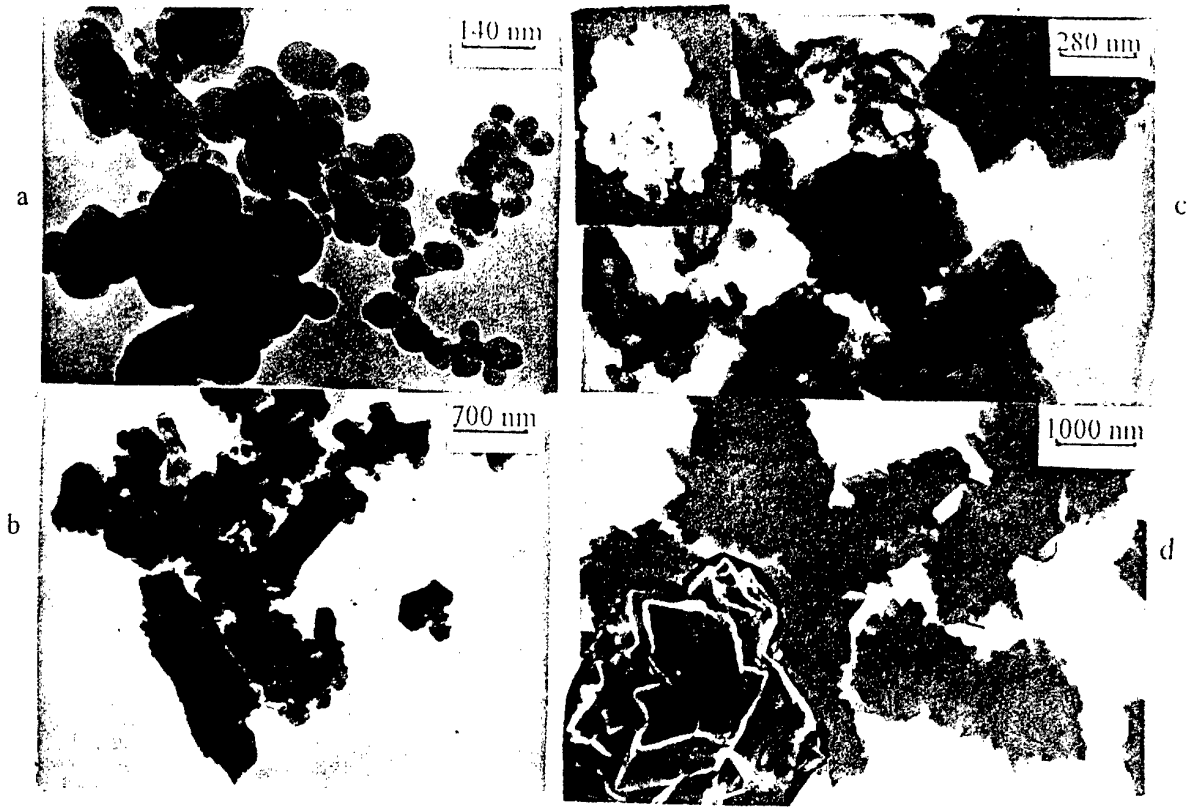


Fig.1. TEM and SEM (adhered) images of boron powders (a-$B_{am.}$, b-$B_{cr}$) and boron suboxide (c-$B_{6.3}O$, d-$B_{6.5}O$)

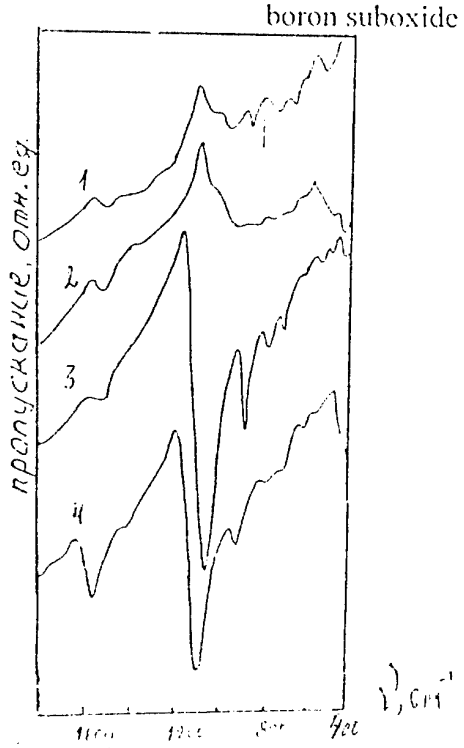


Fig.2. IR-transmission spectra powder-like boron (1-$B_{cr}$, 2-$B_{am}$) and boron suboxide (3- $B_{6.5}O$, 4- $B_{6.3}O$).

and correspond $B_6O$ phase. However, respect of relative intensities of main peaks in X-ray patterns of both products is remarkably different. IR transmission spectra of $B_{6.3}O$ and $B_{6.5}O$ powders also differ when the absorption lines are considered (fig.2). But the most interesting fact is that varying in dispersity, powder-like $B_{6.3}O$ and $B_{6.5}O$ are remarkably different when their particles surface morphology observed. Moreover, morphology of both products particles clearly enough resembles morphology of appropriate initial boron reagents. For example, $B_{6.3}O$ particles are a bit circular in shape. It is worth noticing that some of $B_{6.3}O$ particles have passing through hollows which are of right shape.

Thermostability in air of $B_{am}$, $B_{cr}$, $B_{6.3}O$ and $B_{6.5}O$ investigated in non isothermal mode testifies on considerably higher temperatures of boron suboxide oxidation. It is that $B_{6.5}O$ oxidation occurs at temperature as low as 535°C, whereas $B_{6.3}O$ is already oxidized at T=445°C.

Therefore, obtained results undoubtedly proves that boron suboxide also gets in some extent the reaction capability of initial boron, when inheriting the morphology of initial boron during process of its synthesis.

# STRUCTURE AND PROPERTIES OF RAPIDLY COOLED FIBRES PRODUCED BY EXTRACTION FROM A MELT OF METALS

**Smetkin A.A., Haidarshin A.F.**
Research Centre of Powder Materials Science, Perm, Russia

Development of materials of fibrous structure causes the huge interest due to an opportunity to combine physical and mechanical properties into complex unusual for other materials.

Representing one of traditional objects of powder metallurgy the materials made of metal fibres surpass the powder materials almost in all parameters, they are much stronger then powder materials both in pressed and in sintered condition, and their plasticity and the resistance to impact loads much higher compared to similar powder materials.

As to producing the metal fibres, the greatest attention of the researchers is attracted to various methods of Melt-Quench Solidification (MQS) due to an opportunity to form disperse structure or amorphous condition in materials and control their properties.

Method of Melt Extraction from Suspended Drop (SDME) with electron-beam heating was used in the present work for producing the rapidly cooled fibres from pure Al metals (A99 purity), Ni (H1), BT3-1 titanium alloy, D16 and 12X18H9 alloys.

In this process the metal filament is extended from a drop hanging freely at the end of melted core of initial material, by edge of rotating disk-crystallizer.

As a result of an extraction, the rapidly cooled product is formed as continuous and discrete fibres.

Cooling rate of the process is about 105-106 °C/s.

It has been established that, when extracting on a copper disk-crystallizer with 60° angle of sharpening, the cross section of rapidly cooled fibres has a shape of segment.

Structure of aluminum and nickel fibres is shown in figures 1-2.

The structure of rapidly cooled fibres of BT3-1alloy has a dendritic pattern and consists of martensite-like alpha- and beta-phases (fig. 3).

Depending on extraction process parameters the size of cross section of a fibre was in average from 120 up to 40 microns.

The ultimate tensile strength of the recovered fibres has been determined.

The results are shown in the table 1.

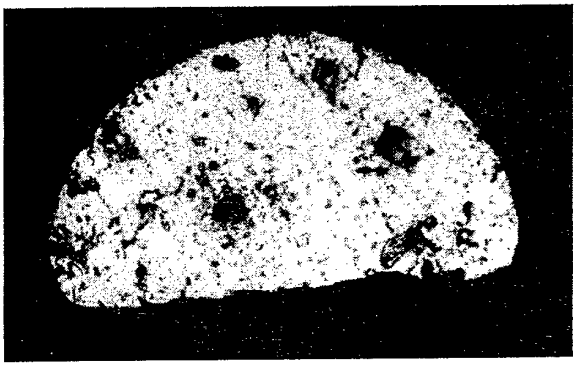

Fig. 1. Microphoto of cross section of Al-fibre

Fig. 2. Microphoto of cross section of Ni-fibre

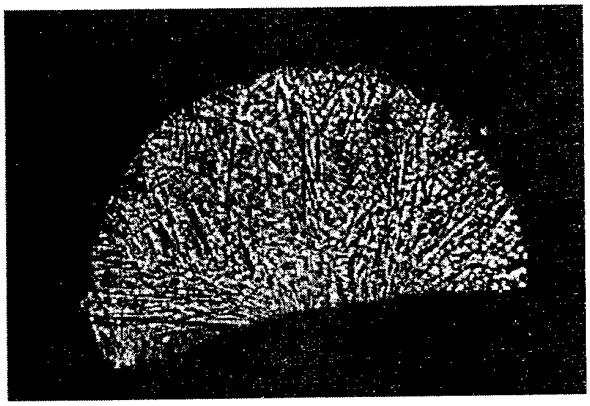

Fig. 3. Microphoto of cross section of Ti-fibre

Table 1 - Diameter and ultimate strength of rapidly cooled fibres

| Material | Fibre diameter *d*, micron | Ultimate strength $\sigma_в$, MPa |
|---|---|---|
| Nickel | 86 | 434 |
| Aluminum | 66 | 61 |
| Д16 | 123 | 118 |
| ВТ3-1 | 55 | 578 |
| 12Х18Н9 | 49 | 280 |

It has been experimentally determined, that the reduction of effective diameter of formed fibres (*d*) depends both on increase of linear speed (*v*) on a Disk-Crystallizer (DC) surface (Fig.4), and configuration of the working edge of disk.

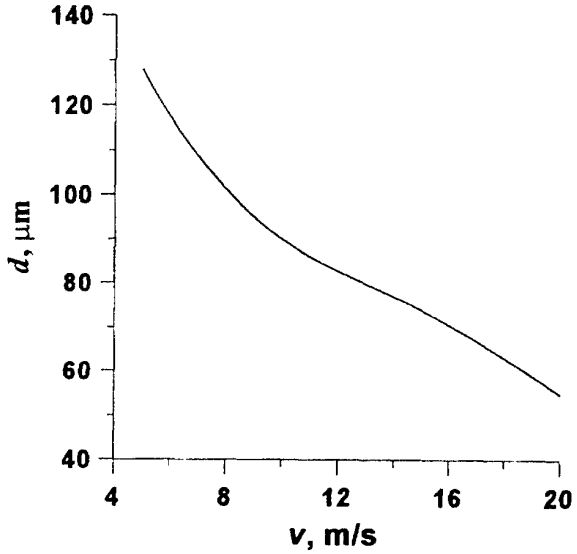


Fig.4. Dependence of Ti-fibre thickness on surface speed of disk-crystalliser

When increasing the speed of bar feed into extraction zone and reducing the linear speed on a DC surface the cross section gradually gets a crescent-type form.

Thickness change of fibres on their length is characteristic that resulted in caterpillar shape (fig. 5)

This feature is explained, on the one hand, by DC radial and axial runout, and, on the other hand, by properties of a melt.

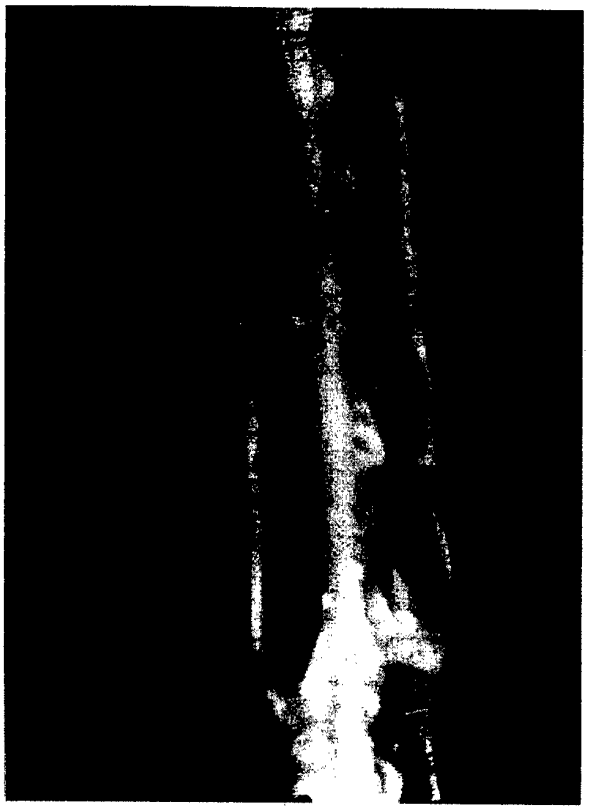

Fig.5. Appearance of Al-fibre

The recovered rapidly cooled metal fibres are a basis for the further manufacturing of filtering and composite materials having special properties.

The work has been performed in accordance with the theme of the RF Ministry of Education TOO-5.3 -2904 Grant.

# SYNTHESIS OF NANOCRYSTALLINE $ZrO_2$-X MOL.% $Y_2O_3$ POWDER

**Kobylinska O.V., Labunets T.F., Karpetz M.V., Ragulya A.V.**
Frantzevich Institute for Problems in Materials Science, Ukrainian National Academy of Sciences, Kiev, Ukraine

$ZrO_2$ –based powders are usually undergone calcination at high temperatures ~ 600-1000 °C. However, this results in hard agglomeration and particle growth [1]. From DTA data it was found, that the crystallization of the amorphous precipitate has occurred at temperatures higher, that 400 °C .

This fact allows decrease the annealing temperature compared to conventional 600 °C and, therefore, more flexible size and strength control of agglomerates. The volume ratio of tetragonal (t) to monoclinic (m) phases in the partially stabilized zirconia drastically depends on particle size and concentration of dopant [2].

The present study is about particle size control during low-temperature crystallization of amorphous zirconia doped by yttria. Nanosized powders of yttria stabilized zirconia have been obtained by co-precipitation and following calcination. The range of dopant concentration was selected as (1,2 and 3) mol.% $Y_2O_3$.

The zirconyl chloride octahydrate and yttrium oxide were selected precursors for this method. Both compounds were dissolved in HCl. The detailed procedure can be described with the flow chart presented in Fig 1.

The precursor solution was added dropwise to an excess of a 25% ammonia solution (dissolved in ethanol) at pH=9. This method is called the "chloride" method [3]. The obtained gel was then thoroughly washed with water/ammonia mixture with a gradually decreasing amount of ammonia to remove $Cl^-$ ions. Subsequently, free water was removed by washing with ethylalcohol. The replacement of water by ethanol significantly lowers the capillary forces acting on the gel during drying. Furthermore, ethoxygroups attach to the surface of the hydroxide–particles and prevent the formation of strong interparticle bonds during caltination [4]. The gel was dried in air for 15 h at 130 °C and calcined at 450 °C for 2-3 h.

The crystallization of amorphous precipitate was studied by differential thermal analysis (DTA), thermogravimetry (TG) (Derivatograph Q-100). True concentration of impurities in the calcined powder was carred out by luminescent spectroscopy.

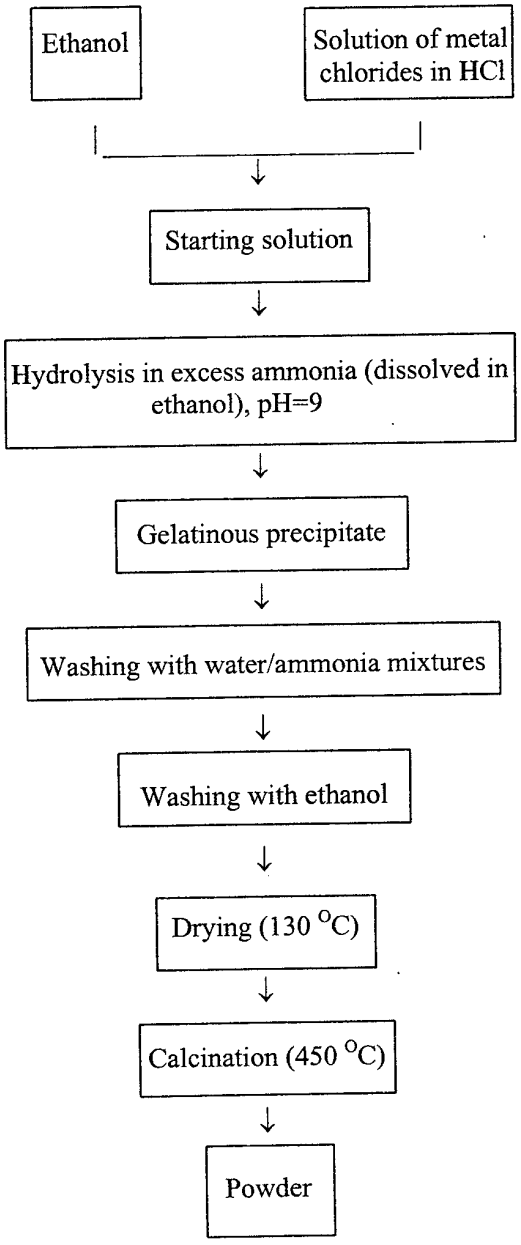


Fig. 1 Flow chart of the synthesis of yttria doped zirconia powders.

BET and X-ray diffraction in Cu $K_\alpha$ radiation with Ni filter were used for powder characterization. DTA has revealed that the crystallization occurs in the temperature range of 415-425 °C at heating rate of 10 °C/min.

The impurity content was as follows:
$Fe_2O_3 \approx 0.001$ %, $MgO \approx 0.0001$ %,
$Cu_2O_3 \approx 0.001$ %, $Cr_2O_3 \approx 0{,}0001$ %,
$SiO_2 \approx 0.1$% and $B_2O_3$ traces.

A specific surface area of the as-crystallized powders was around ~ 100 $m^2$ /g. Tetragonal zirconia doped with 3 mol.% $Y_2O_3$ was found to remain stable in the temperature range of 450 – 1200 °C. Zirconia doped by 1 and 2 mol.% $Y_2O_3$ contained 48 and 19 vol.% of m-$ZrO_2$, respectively. The m-$ZrO_2$ volume increases with annealing temperature and duration, due to particle size increase on heat treatment of as-crystallized powders.

References

1) I.A. Danilenko, T.E. Konstantinova, N. Pilipenco, A.A. Dobrikov , "Application of Phisical Action to Processes of Production of Zirconiaa Based Powder and Ceramics", *9th Cintec World Ceramics Congress* Techna Srl. 1999.

2) J. Luo and R. Stevens, "Tetragonality of Nanosized 3Y-TZP Powders", *J. Am. Ceram. Soc.*, **82** [7] 1922-24 (1999).

3) W.F.M. Groot Zevert, A.J.A. Winnubst, G.A.M. Theunissen, A.J. Burgraaf, "Powder preparation and compaction behaviour of fine-grained Y-TZP", *J. Mater. Sci.* **25** 3449-3455 (1990).

4) M.S. Kaliszewski and A.H. Heuer, *J.Am. Ceram. Soc.*, **73** [6] 1504-1509 (1990).

# COMBINATION OF SHS AND MECHANOCHEMICAL ACTIVATION FOR NANOPOWDER TECHNOLOGIES

**Grigorieva T.F., Korchagin M.A., Lyakhov N.Z.**
Institute of Solid State Chemistry SB of RAS, Novosibirsk, Russia

Mechanochemical synthesis and mechanical alloying are in wide use as experimental methods for production of highly dispersed powders and nanocomposites. Using mechanical activation we have managed to prepare the nanocomposites in immiscible systems such as Cu-Bi, Fe-Bi, Fe-In. It is possible to get supersaturated solid solutions in many other intermetallic systems (Cu-Ga, Cu-In, Cu-Sn, Ni-In, Ni-Bi, Ni-Sn, Ni-Ge, Ni-Al). But from technological point of view mechanical activation put a lot of problems which can not be easily solved. The most difficult are the low productivity of techniques available now, and the contamination of products thus obtained by the materials of mills. The energy consumption should also be taken into consideration in some large scale processes. One of the alternatives to mechanochemistry may be self propagating high temperature synthesis (SHS) which is energy saving and can be applied to a large scale production of many intermetallic compounds or complex oxides (nitrides, carbides). Nevertheless, this method include combustion stage which requires the very high temperatures. As a result the final products can be obtained only in the form of dense sintered or solidified products when SHS goes through the melting of reagents and/or products. To transform such products into commercially interesting powders one need to use milling as an unavoidable step. The grinding leads to a contamination again and to additional energy consumption which may be comparable with that which is required for mechanochemical synthesis itself. Another disadvantage of SHS in many cases is a non uniform phase composition of products obtained due to high temperature gradients in a combustion wave resulting in quenching of some non equilibrium phases. We have applied a preliminary mechanical activation to some SHS reactions. It has been shown that a very short mechanical activation of mixtures capable to react in SHS regime, provides a significant acceleration of combustion wave propagation and, at the same time, a decrease of the maximum combustion temperature. At some activation conditions the maximum temperature of SHS may be as low as *no one component of reactive mixture is melt.* This leads directly to a finely dispersed (nanosized) powders as a products of SHS. This combination of two methods can be efficient for intermetallic compounds and for some complex oxides synthesis via SHS when peroxides and metals can be chosen as a precursors for SHS. We have shown also that the *after* SHS mechanical activation can be extremely useful from the point of view of single phase powder products formation. All these advantages are illustrated in this paper on a numerous examples such as Ni-Al or Ni-Ti intermetallic compounds, or synthesis of $BaTiO_3$ from $BaO_2$ and metallic Ti, etc.

# STAGE SEQUENCE IN MECHANOCHEMICAL SYNTHESIS OF NANOMETRIC SOLID SOLUTIONS IN METAL SYSTEMS

**Grigorieva T.F., Barinova A.P., Boldyrev V.V.**
Institute of Solid State Chemistry and Mechanochemistry SB RAS, Novosibirsk, Russia

Mechanochemical obtaining of solid solutions in metal systems with negative mixing enthalpy is characterized by the formation of intermediate intermetallic phases. Mechanical alloying process (MA) in high-energy activators of planetary type with the participation of a low-melting component starts as follows: this component melts and wets the surface of solid particles; intermetallic compounds are formed at the interface. Good wetting of solid metals by metal melt simplifies and accelerates dispersing of solid metals because the liquid phase penetrates and gets adsorbed along intergrain boundaries and defects formed during plastic deformation in course of MA. The liquid metal forms intermetallic compounds on the surface of newly formed particles of a high-melting metal. Typically, an intermetallide with very high content of low-melting component is formed at this stage of the process; the synthesis of this intermetallic phase lasts till complete consumption of low-melting component.

This type of MA behaviour is also observed in the systems with higher melting points, in which metals differ in their plasticity. Rapid broadening of diffraction reflections of a more plastic component and their disappearance, along with the formation of intermetallic compound with high content of this component, allows assuming that at this stage of mechanochemical mixing of the components the more plastic one passes into liquid-like state and coats the particles of less plastic component thus accelerating dispersion similarly to what happens during liquid metal embrittlement.

The increase of the content of newly formed intermetallic compound is also observed till practically complete consumption of the plastic component; only after this, the formation of solid solution starts in course of mechanochemical interaction between the solvent metal and intermediate intermetallides.

# PROPERTIES OF ULTRAFINE SUPERSATURATED SOLID SOLUTIONS OBTAINED BY MECHANICAL ALLOYING

**Grigorieva T.F., Barinova A.P., Belykh V.D., Boldyrev V.V., Lyakhov N.Z.**
Institute of Solid State Chemistry and Mechanochemistry SB RAS, Novosibirsk, Russia

Needs of modern industry require new materials, both chemically inert ones and those with high chemical reactivity. Highly active metal and alloy powders are used in industry to obtain frame catalysts, diffusion-hardening solders, metal cements, materials for hydrogen energetics, and for some other applications. The excess free energy in the system, provided by the increased concentration of non-equilibrated defects, such as non-equilibrated stoichiometric defects (substituting atoms, vacancies) or/and plastic deformation defects (dislocations, intergrain boundaries) creates enhanced reactivity of the material. Mechanochemical synthesis is the most promising method of obtaining non-equilibrated phases in which both types of the above-mentioned defects are present.

Supersaturated solid solutions based on copper, nickel and iron were synthesized in the systems: Cu-Sn, Cu-In, Cu-Hg, Ni-Ge, Ni-Al, Ni-Bi, Ni-Sn, Ni-In, Fe-Sn.

The fact that the supersaturated solid solutions obtained by mechanochemical synthesis have the excess free energy is confirmed by calorimetric measurements. It is known that the ordering temperatures of solid solutions are usually 0.6 of melting point; the decrease of ordering temperature is promoted by high concentration of defects. For supersaturated solid solutions obtained mechanochemically, this process starts at much lower temperature. For example, in the case of the solid solution of indium in nickel, ordering should start at a temperature of above 600°C, while in the samples obtained mechanochemically it starts at ~ 460°C; for the solid solution of aluminium in nickel, the corresponding temperature points are 700 and 300°C, respectively. It is typical that ordering temperatures decrease with increasing concentrations of doping element; for solid solutions of tin in nickel, the difference is more than 100°C. For the sample with the highest tin concentration, the heat of ordering is 7.5 kJ/mole. A similar correlation between the decrease of the temperature at which ordering starts and the increase of the concentration of a second element was observed also in the Cu-Hg system. Exo-effect is also increased with increasing mercury concentration. At 10 wt.%, it is 6.18 kJ/g, while at 30 wt.% Hg it is 18.35 kJ/g.

During annealing, all the non-equilibrated solid solutions obtained mechanochemically are decomposed to form the equilibrium phases characteristic of a given concentrational range of the equilibrium state diagram. The heat effect that characterized the ordering of mechanochemically obtained supersaturated solid solutions relates both to the non-equilibrium non-stoichiometry defects and to high concentration of inter-phase boundaries due to the nanometer size of the blocks comprising the particles of these solutions.

# FUSIBLE UNDERLAYERS DURING DEPOSITION OF THERMAL COATINGS

**Kuprianov I.L.**
Institute of improvement of professional skill, Minsk, Belarus

Relaxation of stresses, reduction of defects of boundary between a coating and a substrate and increase of adhesion strength cause grounded interest to fusible underlayers for deposition of thermal coatings for heavy loading applications.

Tin, zinc, cadmium and eutectic alloy Sn–Pb were chosen as underlayer materials in the paper under presentation. Investigations were carried out on samples from thermal-treated carbon steel 45. Steel 65Г (wire) was chosen as the material for upper coating layer. The coatings wee deposited by flame spraying. Investigations of structure, phase composition and elements distribution in transformation zones were carried out. Coatings adhesion strength was also measured.

During spraying without underlayers micropores and iron oxide inclusions are clearly seen on boundaries, microstructure of separate big coating particles is not homogeneous and consists of martensite and products of bainite transformation. There are practically no pores in the transformation zone during deposition of coatings in fusible underlayers. Coating microstructure with tin underlayer can be characterized by tin filling in micro-roughnesses in the substrate material and forms a transformation zone with upper coating layer. Composition of transformation zone with Sn-Pb underlayer has much in common with the one with tin underlayer. At the same time thickness of diffusion zone in the substrate metal is 8-10 mkm, and in the upper coating layer - up to 20 mkm. Thickness of pure tin layer is within the range of 15...20 mkm. Phase composition of transformation zones is characterized by a number of iron - tin compositions. When using zinc as the fusible underlayer material, which diffusion mobility in iron is maximal, thickness of transformation zones is also maximal, and phase composition is characterized by a number zinc - iron compositions. Thickness of non-alloying zinc layer is 10...15 μm. When using cadmium as underlayer material, mutual element dissolution or formation of compositions were not observed, there is practically no transformation zone. Results of investigations of coatings adhesion showed that minimal adhesion strength during spraying without any underlayer is 20,3 MPa, and maximal with Sn–Pb underlayer – 40,4 MPa.

To summarize data of the investigations we can assume that metals or alloys with minimal melting temperature (within a reasonable range) and maximal hardness and plasticity, higher solubility of substrate in the metal without intermetallide phase formation should be chosen as metals for fusible underlayers.

# ELECTRODEPOSITION OF MOLYBDENUM CARBIDE ON THE SUFACE OF SEMICONDUCTORS FROM IONIC MELTS

**Gab A.I., Uskova N.N. Malyshev V.V.**[(1)]
V.I. Vernadskii Institute of General and Inorganic Chemistry, NAS of Ukraine, Kiev, UKRAINE
[(1)]National Technical University of Ukraine "Kyiv Polytehnical Institute", Kyiv, UKRAINE

It is well known that the deposition of metal-containing coatings on the surface of electrically conducting abrasive materials (silicon and boron carbides, zirconium and titanium diborides) in an efficient method of increasing its performance. Metallized abrasives are characterized by increased mechanical strength and adhesion to the substrate and are, therefore, consumed in smaller amounts [1].

For coating electrodeposition to be possible, it is important for the corrosion potential of the substrate to be higher than the deposition potential. To find out whether diamond, boron nitride, silicon carbide, and boron carbide can be coated with molybdenum carbide, we measured their stationary potentials relative to the $Na_2WO_4$–$0.2WO_3|O_2$,Pt half-cell (Table 1). The deposition potential of molybdenum carbide is lower than the corrosion potential of the materials examined, making possible the deposition of high-quality coatings [2].

Table 1.Corrosion potentials ($E_{corr}$) of SiC and $B_4C$, and the deposition potentials ($E_{dep}$) of $Mo_2C$ for the following melt composition (Wt%): $Na_2WO_4$(85)–$MoO_3$(5)–$Li_2CO_3$(10). T = 1073 K.

| Semiconductor | $E_{corr}$, V | $E_{dep}$, V |
|---|---|---|
| SiC | -1.05÷1.09 | -1.35÷-1.55 |
| $B_4C$ | -1.14÷-1.17 | -1.35÷-1.55 |

In this work, investigations were carried out on the high-temperature electrochemical deposition of molybdenym carbide from ionic melts in relation to temperature, cathodic current density, and electrolysis duration. An attention was also given to the relationship of these parameters with the deposition rate and with the strength and service properties of abrasive materials. In electrochemical metallizing, grains of abrasive materials (silicon and boron carbides) are held in melts of an equimolar mixture of sodium and potassium tungstates with additions of molybdenum oxide (VI) and lithium carbonate at 1073-1173 K under the cathodic current density 10-200A/$m^2$. Under these conditions electrical conductivity of the surface of abrasive marerials increases and the surface plays the role of an active substrate for high-temperature electrochemical synthesis. At temperatures less then 1073 K, metallizing does not take place because powder deposits of the molybdenum carbide forms.

The extent of metallizing was determined as the difference in the mass of initial and metallized materials. Phase composition of the coatings was studied by means of X-ray diffractometer DRON-3.0 equipement. The external appearance of coatings and their integrity were evaluated qualitatively by microscopic analysis of specimens. The coating consists of a light-gray, finely crystalline, continuous deposit. Its integrity can be clearly seen on cleaves. X-ray diffraction patterns of the surface layer of specimens with coatings contains strong lines of molybdenum carbide.

The molybdenum carbide was deposited on the grain of silicon and boron carbides 40 and 16 μm in size, respectively, at 1173 K. The extent of metallizing the grains depends strongly on the cathodic current density and electrolysis time (Fig. 1a,b). With an increase of these parameters the deposition rate increases. The maximum attained thickness of obtained coating was 5 μm.

Tests of the grains of silicon and boron carbides for fracture were carried out in accordance with GOST 9206-81 at DA-2 equipment. The coefficient of the fracture load was represented by the ratio of fracturing loads of the metallized and initial grains. Capillary, characterizing the wetting or abrazing of materials by a specific binder, was determined using generally recognized procedure [3] from the height of water level lifting in glass tubes filled with initial and metallized grains.

As the result of deposition of molybdenum carbide the coefficient of the fracture load of silicon and boron carbides grains was equal to 1.5-2.5, and the capillary of SiC grains increased 3.4-4-fold,

whereas that of boron carbide increased 2.3-2.5-fold.

Thus, electrochemical metallizing of abrasive materials with molybdenum carbide in ionic melts increases the fracture load of the grains and their wetting.

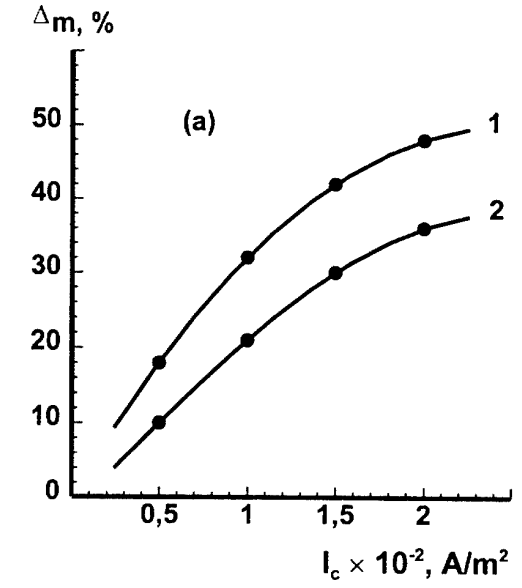


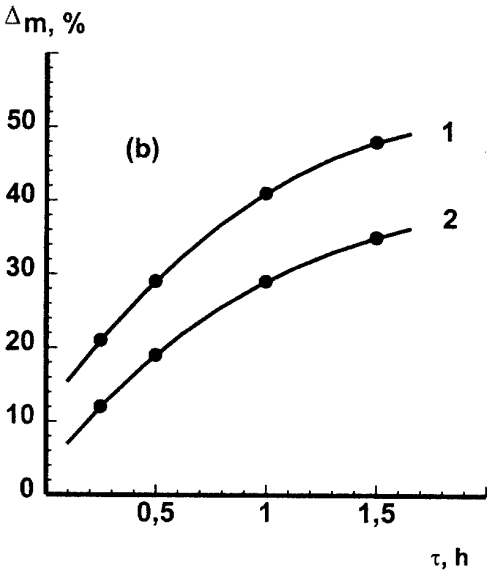


Fig. 1. Dependence of metallization degree of SiC (1) and $B_4C$ (2) by $Mo_2C$ on cathode current density ($\tau$ = 1 h) (a) and on electrolysis duration ($i_K$ = 100 A/m$^2$) (b) T = 1173 K.

LITERATURE

[1] Naidich Yu.V., Lavrinenko I.A., and Volk G.G. *Sverhtverdye Materialy* (Superhard Materials), Kyiv: Naukova Dumka, 1993.

[2] Malyshev V.V., Novoselova I.A., Gab A.I., Pisanenko A.D., Shapoval V.I. Theoretical Foundations of Galvanic Treatement of Dielectrics and Semiconductors in Ionic Melts // *Theoretical Foundations of Chemical Engineering*. – 2000. – V. 34, No. 4. – P. 391-402.

[3] Yakubovskii E.S., Eidel'shtein F.I., and Lopova A.A. Methods of surface treatment of abrasive materials and synthetic diamonds for improving their wetting // Abrasivy – 1966. – No. 2. – P. 9-14.

# CHARACTERIZATIONS OF THERMAL SPRAYED BRONZE COATINGS FOR BEARING APPLICATIONS

**Ilyuschenko A.Ph., Koval V.A., Beliaev A.V.**
Powder Metallurgy Institute, Minsk, Belarus

One of the main technical problems is improvement of reliability and service life of machines and mechanisms. Statistics prove that more than 80% of machines and mechanisms suffer failures due to worn engines working in friction conditions (bearings, journals, seals, etc.). Technical development resulting first of all in increasing speed and loadings for friction assemblies, requires introduction of new wear-resistant materials. That's why development of antifriction and wear-resistant materials and technologies for their production and also spraying of coatings on their base is an up-to-date problem.

The majority of antifrictional parts based on iron and copper (plain bearings first of all) are produced by PM methods. But quite cheap sintered alloys based on aluminium bronze are also quite interesting. They may show high operational properties in conditions of friction at high loadings.

Antifriction aluminium bronze powder material and plasma coatings on its base were chosen in the paper under presentation.

Powder produced based on copper were studied according to their X-ray-structural, microstructural analyses and microhardness. The powder was produced in the regime of technological combustion.

X-ray-structural phase analysis was carried out with the help of general purpose diffractometer ДРОН-3.0 in $CoK_\alpha$ monochrome radiation with automatic control device including a goniometer and database with software for collection, processing and analysis of data «X-ray» (versions 1.0 and 2.0) and «Aist» and also a special software GOR for automatic investigation of fine structure including program for splitting lines «SPLITLINE» realized on IBM PC/AT.

Results of comparative X-ray diffraction analysis showed that phase composition of synthesized powder materials is similar to sprayed aluminum bronze БРАЖ 9-4.

Herewith, spectra of the powder have too high background with tendency to increase to back angles.

All lines of copper solid solution are shifted to the increase of lattice parameter comparing to the standard, at the same time the shift increases with growth of the angle $2\Theta$ reaching maximum on back angles.

Results of the lattice parameter calculation and its micro-deformations showed that powder under synthesis is characterized by increased lattice parameter a=3,6483 Å...3,6511 Å and micro-deformation of about 10,03...10,78 $10^{-3}$.

Also there was observed high shift of lines of copper and high background – for the second line – line (200) $\Delta 2\Theta$ reaches 0,88° and 2,77° on line (400), which proves of strong over-saturation of copper solid solution with alloying elements.

Method plasma напыления on standard modes have received samples of coverings

Spray optimization has been processed by APS technique. Powder with fraction of 50...160 μm and with microhardness above $285HV_{50}$ was used for spraying.

For an estimation of friction forces of coatings the method based on determination of torque was used, and its realization was carried out by the machine of friction 2070 CMT-1 at speed of sliding 0,5 m/s under the "disk - disk" circuit, at liquid greasing conditions. One of disks from thermal-treated carbon steel 45 was used as contrbody. A range of examined loadings 200...1300N. With the purpose of reception of the

minimal error of measurements, 5 samples with similar parameters were tested.

It is established, that in a range of loadings 300...1100N even wear is observed, and the coefficient of friction did not exceed value 0,04, the temperature in a contact zone did not exceed 60°C. To increase of loading there is give rise in temperature up to 100...120°C and wear is considerably increased.

Thus plasma coatings from investigated material may be used for manufacturing new and restoration of the worn out details working in units of friction with constant loading up to 1100N that corresponds low and moderate trybotechnical loads. Besides, these materials are quite interesting as structure materials and matrixes for composites.

References

1. Y.S. Umansky Physical Bases for Metal Science // «Metallurgizdat» Publishers, 1955, p.199 (in Russian).

# STRUCTURE AND PROPERTIES OF $Al_2O_3$ AND $Al_2O_3$+$Cr_2O_3$ COATINGS DEPOSITED TO STEEL 3 (0.3wt.%C) SUBSTRATE USING PULSED DETONATION TECHNOLOGY

**Pogrebnjak A.D.**[(1)], **Tyurin Y.N., Zadkevich M.L.**
Paton Institute of Electric Welding, Kiev, Ukraine
[(1)]Institute of Surface Modification, Sumy, Ukraine

Coatings of aluminum oxide, which are produced by gas-thermal, plasma detonation deposition find their wide application due to their high wear resistant, corrosion resistant, heat protecting, electro-isolating, etc. properties. When the powder $Al_2O_3$ is deposited by the plasma-detonation way, it undergoes phase transformations, which ratio depends both on the characteristics of initial material, and on the way and conditions of deposition, substrate temperature, the thickness of the deposited layer, the velocity of the incident plasma jet, its temperature, and, probably, other factors. In this connection, the servicing characteristics of the aluminum oxide coating seem to be determined by a quantitative content of various modifications of $Al_2O_3$ in it. As is known, in the process of exploitation under high temperatures, the phase composition may change. Therefore, one may assume that this change of phase ratio may influence the protecting properties of aluminum oxide and, naturally, affect the life of these coatings.

Modern techniques of deposition of high quality coatings have been developing now in such a way that to provide high rate deposition of materials. In spite of evident advantages of gas-detonation way of coating deposition, application of these coatings in industry is limited because the devices for proportioning and feeding of powders are complicated and there exist power limitations of a pulsed jet.

This paper proposes to apply non-stationary detonation burning processes of combustible gas mixtures in the device for deposition to increase the pulse power. Realization of detonation of the combustible gas mixture in an electromagnetic field, which is formed between two coaxial electrodes in the reaction chamber seems to be an efficient way.

Therefore, the purpose of the presented paper was to investigate physical and chemical properties and phase composition of coatings of aluminum oxide and $Al_2O_3$ + $Cr_2O_3$ mixture, which were deposited using the plasma detonation technique (under high temperatures and high rates of the plasma jet) to the substrate of steel 3 (0.3wt.%C).

A plasmotron "Impulse-3" [1] purposed to deposit coatings has been applied. This plasmotron has a changeable pipe and a gas-dynamic combustion chamber, where the components of combustible gas mixture are mixed and their detonation with to 20 Hz frequency is initiated. Initiation of detonation is realized using a sparking plug, feeding of combustion mixture components and cooling of water are realized from the backside of the plasmotron through pipelines. Total expenditures of the combustion mixture components are 2 $m^2$ per hour, the initiation frequency being 4 Hz. The energy of charging unit is 400 mF under 3.5 kV voltage. The length of the gas-powder jet limited by the cylindrical pipe was 350 nm, and a distance of deposition was 40mm. The velocity of plasma jet may be given in advance, it can reach 600 m/s to 8 km/s, plasma temperature in the jet being 2 x $10^3$ to 3 x $10^4$ K, and the power density of pulsed plasma can reach 5 x $10^7$ W/$cm^2$. To investigate the element composition, we applied a beam of protons (1.744 MeV), using Elastic resonance on protons and Rutherford back scattering of $He^+$ ions of 2 MeV energy. To investigate the phase composition and structure, we applied X-ray phase analysis (XRD) with diffraction (the apparatus DRON-3, USSR) and transmission electron microscopy with diffraction (TEM) using the Electron microscope EM-125 (Electron, Selmi, Sumy, Ukraine) under accelerating voltage of about 125 kV. The surface morphology was studied using the raster electron microscope (REM 102 EM, Selmi, Sumy, Ukraine) and Atomic Force Microscope (AFM). Hardness was measured using PMT-3 apparatus with a pyramid KNUPA, adhesion was determined using sclerometry with indention of the diamond pyramid into a coating and its motion over it.

Presents the schematic of RBS analysis and elastic resonance on protons (an angular cross-section of $Al_2O_3$ coating with a steel 3 substrate).

As it is seen, that the measurements have been performed at three different points of the coating: near the surface, in the coating depth, and near the phase boundary of the film and the substrate. The energy RBS spectra and elastic resonance on protons show an evident surface peak of C (as a result of resonance) in the vicinity of 1.755 MeV. Also, one can see steps corresponding to O, Al, and Fe. Stoichiometry of the ceramic layer near the surface, which was averaged over the thickness of 1.6 mm, was as $Al_{35}O_{53}Fe_{0.5}$; carbon concentration was about 11at.%. Near the phase boundary, the stoichiometry of ceramic composition significantly changed and was $Al_{38}O_{58}Fe_3$. Iron concentration increased almost by a factor of 6, and the ratio of oxygen to aluminum was close to a classic one -- $Al_{40}O_{60}$. Fe was present all over the whole thickness of coating, which evidenced some erosion (evaporation) of the electrode into the plasma jet. The coating, which was composed only by aluminum oxide, had an average density of $\rho$ = 3.9 g/cm$_3$ (this was close to the value for $\alpha$-$Al_2O_3$, i.e. $\rho$ = 3.98 g/cm$^3$). Micro-hardness of some regions reached 1.95 x $10^4$ H/mm$^2$, its minimum value being about 1.4 x $10^4$ K. Measurements of heat conductivity of $Al_2O_3$ coating demonstrated a value of 38 W/m x K, which was close to that for the pure $Al_2O_3$ (40 W/m x K). One should note that the coating, which was produced from the mixture of $Al_2O_3$ + $Cr_2O_3$ powders, had higher value of hardness $\geq$ (2.1 to 2.2) x $10^4$N/mm$^2$. However, the preliminary tests for adhesion demonstrated that under the same thickness of coating (about 0.8 mm), $Al_2O_3$ had better adhesion than that of the mixed one (composed of aluminum oxide and chromium oxide).

A phase composition of $Al_2O_3$ coating, which was determined by TEM with diffraction, demonstrated the presence of such phases as: $\alpha$-$Al_2O_3$; $\beta$-$Al_2O_3$; $\gamma$-$Al_2O_3$; $\eta$-$Al_2O_3$; AlFe. $\alpha$-$Al_2O_3$ was a poly-crystal with average crystal dimensions of about 250 nm. Crystallites were without defects, had a regular cut. $\beta$-$Al_2O_3$, $\alpha$-$Al_2O_3$, and ; $\eta$-$Al_2O_3$ were poly-crystals, dimensions of their crystals were from 100 to 300 nm. A defect structure was observed inside the crystallites. It consisted of dislocations (as a contrast showed). The region of a transition layer, which was contiguous with the substrate, consisted of FeAl poly-crystals, their average dimensions being about 20 nm. This transition layer consisting of FeAl had high dislocation density. One also should know that because of high deposition rate and high temperature of the plasma jet being incident on the substrate, some discrepancy of parameters of crystal lattices of the coating and table values was noticed (which was revealed in studies of electron diffraction). XRD analysis of the same coating demonstrated good correlation of these results with TEM analysis. In spite of the fact that XRD information was obtained from a thicker layer, it was revealed that $\alpha$-phase constituted about 60% of coating, $\gamma$-phase constituted about 30%, meta-stable phases as $\beta$- and $\eta$-, which could hardly be revealed in the XRD spectrum without special thermal annealing were the rest.

Phase analysis, which was performed using TEM with diffraction, demonstrated the following phases: $\alpha$-$Al_2O_3$; $\beta$-$Al_2O_3$; $\gamma$-$Al_2O_3$; $Cr_2O_3$, and $Cr_3O$. $\alpha$-$Al_2O_3$, and $\beta$-$Al_2O_3$ crystallites are of average dimensions (about 150 nm) and have no defects. $\gamma$-phase was the region of coating with crystallites, which dimensions were scores of nano-meters (20 $\pm$ 30 nm). Micro-electron patterns showed a ring-like structure. The regions of the coating containing $Cr_2O_3$ had crystallites of average dimensions of about 150 nm, dislocations-like defects were absent. $Cr_2O_3$ regions of coatings contained very large crystals of 0.5 mm dimensions.

Conclusion: In such a way, the presented work has shown that the plasma-detonation way of deposition from $Al_2O_3$ and $Al_2O_3$ + $Cr_2O_3$ allows one to produce coatings of good quality, in which crystal dimensions are from 20 to 250 nm. They consist of $\alpha$-, $\beta$-, $\gamma$-, $\eta$- phases and the transition layer of 15 $\mu$m thickness, which contains FeAl and has high dislocation density. Coatings of aluminum oxide are of high hardness to 1.95 x $10^4$ N/mm$^2$, those of $Al_2O_3$ + $Cr_2O_3$ are of (2.1 to 2.2) x $10^4$ N/mm$^2$. Heat conductivity of $Al_2O_3$ coatings was 38 W/m x K, which was close to that of $\alpha$-$Al_2O_3$ (40 W/m x K). One should note that adhesion of the Steel 3 substrate with $Al_2O_3$ coating was higher than that of the coating deposited from the mixture of $Al_2O_3$ + $Cr_2O_3$ powders.

References

1. Yu.N.Tyurin and A.D.Pogrebnjak. Surf. and Coat. Tech. 111 (1999) p.269.

# INVESTIGATION OF IMPULSE-PLASMA TREATMENT PROCESSES FOR THERMAL SPRAYED PROTECTIVE COATINGS

**Ilyuschenko A., Shevtsov A., Okovity V., Astashynski V.[(1)], Chivel Yu.[(1)], Steinhauser S.[(2)]**
Institute of Powder Metallurgy, Minsk, Belarus
[(1)]Institute of Molecular and Atomic Physics, Minsk, Belarus
[(2)]Technical University, Chemnitz, Germany

Plasma impulse as an energy source has its own peculiarities and advantages when treating a part's surface:
- high concentration of the fed energy and locality enable to treat only the surface area of the material without heating the rest bulk and distorting its structure and properties, that results in minimum part's buckling;
- high concentration of the fed energy enables to heat and to cool the treated bulk of the material with high rates, the effect period being small. As a result it is possible to make unique structures and properties of the treated surface;
- possibility to control the parameters of impulse-plasma effect enables a structure regulation of the surface layer, its hardness, roughness, wear-resistance, geometrical sizes of the treated areas etc.

The researches and optimisation of effect of impulses of a plasma jet on thermal barrier and wear-resistant coatings obtained by plasma spraying are carried out. The equipment for deriving impulses is the quasistationary high-current plasma accelerator in an vacuum chamber. The parameters of a compression plasma stream are: length ~0.5 m, diameter in the field of maximal squeezing ~0.03 m, velocity of flow stream – $(1... 2)\cdot 10^5$ m/sec, temperature of plasma ~$3x10^4$ K.

At a research and optimisation of impulse processing varied a distance of effects and amount of impulses of a cycle. The measure of optimisation was served required structure of processed coatings $ZrO_2$+7%$Y_2O_3$, NiCr+50(80)%$Cr_3C_2$, NiCr-Fe+50%SiC. The researches of structure are supplemented with the analysis of a generalised index of porosity of the deposited materials and crumbled hard particles of carbide phase at preparation microsections. The researches of wear-resistant coatings containing a carbide phase were accompanied also with measuring of a microhardness of materials sprayed and processed by plasma impulses. The circumstantiation of the information about elements of obtained structures was carried out by X–ray diffraction analysis.

The results of researches display, that at processing the thermal barrier coating $ZrO_2$+7%$Y_2O_3$ the optimal distance of pulse-plasma effect is 0,52...0,56 m, optimal amount of impulses is 1. Thus the starting surface of sprayed ceramic with a developed relief is noticeably aligned and fissured, being disparted on large fragments, which size are 20... 30 μm. The starting structure of an oxidic coating from a surface acquires an aspect of the stiffened melt with width no more than 15...20 μm. The basic phases of a powder material $ZrO_2$+7%$Y_2O_3$ which is identifying functionality of a thermal barrier coating are saved in last. The obtained transformed layer able to deform without destruction by alms of fragmentation of a surface is uniformly place on a coating closing exits of pores and decreasing gas permeability of a coating which effectiveness is increase.

At a research of wear-resistant coatings NiCr+50(80)%$Cr_3C_2$ and NiCr-Fe+50%SiC is established, that the optimal distance of pulse-plasma effect for materials containing $Cr_3C_2$, SiC, accordingly is 0,38 and 0,40 m, optimal amount of impulses is 5. Thus the vitrification of a surface and underlying layers on whole width of sprayed materials is reached. The density and cohesive strength of sprayed materials are rises, decrease on 15...20 % its a generalised index of porosity and crumbled hard particles of carbide phase is argumentatives about that. Such transformation of structure promotes resistance of a coatings against mechanical destruction during friction.

At the same time residual porosity and crumbled hard particles of carbide phase take place, that is apparently linked with fugacity of thermal and dynamic impulse effects (~200 μsec).

The comparison of the X–raygrams of starting powders and coatings after impulse effects displays that an essential modification of phase

composition does not happen. However intensive heat by impulse of plasma with local vitrification and superfast cooling of layer of sprayed material causes modification of carbide phase and increase of presence of amorphous phases, which, as is known, create premises of wear–resistance of coatings. More random distribution of carbide phase and microhardness of coatings is linked with application of powders with composition particles NiCr+50(80)%$Cr_3C_2$. To mechanical mixture of powders NiCr-Fe+50%SiC are correspond noticeable oscillations of a microhardness of coatings, on which surface as likely as not the presence of separate extended segments from a bonded material NiCr-Fe. The indicated segments with low hardness easily distort by contrbody of tribocoupling with formation of skin-tight to each other conjugate belts, on which the propensity to microcontact grip and scratch at friction is exhibited. Investigations are made on samples from steel 45(1.0503), which were plasma sprayed with protective coatings. Spraying was made on «Plasma-Technik» (Switzerland) unit. The two stage quasi-stationary high- current plasma accelerator (QHPA) with coaxial system of electrodes served as a source of impulse effect on coatings.

# FORMATION OF GRADIENT STRUCTURE-PHASE STATES AT CRYSTALLIZATION OF FERRITE STEEL DURING WELDING

**Gagauz V.P., Kovalenko V.V., Tsellermaer V.Ya., Gromov V.E., Kozlov E.V.[(1)], Konovalov S.V.**

Siberian State University of Industry, Novokuznetsk, Russia

[(1)]Tomsk State University of Architecture and Construction, Tomsk, Russia

The structure-phase state of metal forming during crystallization pays attention of researchers since it effects significant influence on mechanical and physics-chemistry characteristics of a products. The crystallization of metal in conditions of welding has a number of the features appreciablly distinguishing it from crystallization of the big ingots.

The purpose of the present work is the research of structure and phase composition of a welded seams of steel 09G2S with thickness >30 mm, used in casings of blast furnaces.

The metallographic researches of structure and the phase composition of a welded seams have shown, that a method and a way of welding in a melted zone form the gradient structure having following characteristic features. In the centre of a seam the biphase structure consisting of grains of ferrite and pearlite is forming. The grains of ferrite have the anisotropy with factor of anisotropy k=L/D~2. The dispersion of a vector of a structural texture (a relative position the longitudinal axes of grains of ferrite on the surface of grinding) is rather significant and reaches 90%. The pearlite has lamellar morphology. Its grains (a volume fraction of them is of ~10-15%) form the complex structure, settling down along boundaries of grains of ferrite or embracing them. The given zone of a welded seam is characterized by the slow kinetics of crystallization with the subsequent full division of phases into stages of $\gamma \rightarrow \alpha$ transformation.

The layer, adjoining to the given one, has similar phase composition, however the morphology of pearlite in it changes strikingly. The lamellar structure pearlite does not come to light, the pearlite grains are broken into colonies of the submicronic sizes. The interphase boundaries have a gear (fragmentary) structure. The grains of ferrite thus change a little bit. The revealed features of a structure-phase state of the given layer allow to voice the assumption about the incompleteness of phases division and process coagulation.

The further structure formation of the steel seam is carried out by recrystallization of grain structures. The nuclei of steel recrystallization are formed along boundaries of initial grains. In process of removal from the centre of a seam the volume fraction of recrystallization a material grows, the formed grains are increased in the sizes.

The transitive zone forming in the field of contact of melting with solid material, is characterized by the third type of structure consisting of large grains, with plates. Such structure due to the morphological attribute may be referred as widmannstatten ferrite. Pearlite in the given area of a material is not found out. It is possible to assume, that carbon available in steel, forms disperse particles of carbide phases which are settling down on interphase boundaries. Hence, the given area of the welded seam is characterized by absence of division of phases that is caused, obviously, by the high speed of cooling.

The seam structure formed during crystallization is gradient structure - in process of removal from the centre of a seam the average sizes of grains of ferrite and pearlite, a volume pearlite fraction and morphology of cementite develop in conformity to certain laws. It is established that in process of removal from the centre of a seam the noneguilibrium degree of structures is increacing.

Table 1. Dependence of grains parameters from number of a zone of a welded seam

| Parameter № of zone | a, mcm | b, mcm | c, mcm |
|---|---|---|---|
| 1 | 23,5 | - | 15,0 |
| 2 | 21,8 | 2,7 | 7,5 |
| 3 | 19,7 | 6,8 | 6,2 |
| 4 | - | 7,5 | 5,0 |

The note: a - the average sizes of initial grains of ferrite, b - the average sizes of secondary grains of ferrite, c - the average sizes of pearlite grains.

It follows from the established dependences, that with increase of distance (number N of an analyzed zone) from the centre of a seam the average sizes of initial grains of ferrite and pearlite are decreased, and secondary grains of ferrite are increased. According to this, the volume fraction of initial grains of ferrite and pearlite is reducing and secondary ferrite grains is growing. The process of getting smaller of ferrite grains in a welded is caused by recrystallization to such effect. The thermal stresses arising in a material owing to constrained conditions of crystallization lead to such effect. The decrease of pearlite volume fraction is most likely connected with the high density of formed interphase boundaries. The energy of connection of carbon atoms with defects of crystal steel structure (vacancy, dislocations) is higher than for cementite particles. Hence, the ferrite grain boundaries formed in the recrystallization process will be the effective traps for carbon which in process of cooling a material may form disperse particles of carbide phase.

# FORMATION OF GRADIENT STRUCTURE–PHASE STATES AT ROLLING OF BIG DIAMETER ARMATURES

**Yuriev A.B., Gromov V.E., Kovalenko V.V., Kozlov E.V.[(1)], Plevkov A.V.[(1)], Konovalov S.V.**
Siberian State University of Industry, Novokuznetsk, Russia
[(1)]Tomsk State University of Architecture and Construction, Tomsk, Russia

The armature of low-alloy steel of various diameters strengthened by a method of interrupted quenching in a stream of high-speed mills of West-Siberian Metallurgical Works. In a building industry during the process of manufacture of building and ferro-concrete designs is widely used. The given way of thermal hardening allows to make lower the utilization of ferromanganese and also to exclude additional technological operations [1]. Thus building steel has structure of a natural composite [2].

The purpose of the present work is the investigation of the laws of plastic deformation and fracture of armature of big diameter from steel 18G2S alongside with detailed research of their defect structure and phase composition.

The researched material at the certain way of etching of face section of rod reveals the concentric zones differing by a degree of etching and the various colors. The macrostructure and the amount of zones and their parameters depend on the diameter of armature. Zones are not equivalent on the sizes. As a rule, the greatest volume is occupied by the intermediate zone. The central and undersurface zones are rather insignificant and have the similar character.

The metallographic structure analysis revealed the qualitative and quantitative distinctions in the structure of zones. The etching picture of undersurface zones is characteristic for the martensitic similar structure. In the central zone the areas of the pearlite structure are observed and we can see also the structure characterized by the fine undergraine chaotically located particles of carbide phases. The intermediate zone contains elements the both zones considered above.

The analysis of grain structures has revealed two types of grains: the large grains with the sizes of 30-40 microns, having an equilibrium configuration of boundaries and the fine grains having sizes of 3-5 microns and located along boundaries. The sizes of fine grains practically do not depend on a site in a material. The sizes of large grains grow at moving from a surface to the centre of a core. As it was marked above, the zone structure of armature depends on the heat treatment. The analysis of grain structures of the central area of samples of big diameters show that at thermal hardening the given area has ferrito-pearlite structure.

The ferrite (C solid solution in a crystal lattice of α-iron) has some morphological versions owing to the various speed of cooling of a core from temperature of rolling.

The structure formed on martensitic mechanism. On morphological type the given type concerns to the massive matrensite. It represents the crystals of α-iron parallel located to each other. The average cross sizes of crystals are 1,5-2 microns. In one pack it is totaled up to 20 soparalleled crystals having the form of strips. Packages laying by a line are disordered from each other and therefore divide an initial grain of ferrite into some areas. In one grain it may be totaled on speed of cooling of a material at training up to several tens packages. The average sizes of packages are the units of micrometers.

The bainite structure is close to structure of the above described martensite according the mechanism of formation and to morphological attributes. The bainite has the form of crystals (lenses) having units of microns in cross sizes the longitudinal – the tens of microns. The bainite structure is formed at the higher temperatures than the martensite. The mechanism of the bainite formation is the diffusion-shift. It results, in the precipitation the $Fe_3C$ carbide particles in them and in – the formation of the defect (dislocation) substructures. The density of dislocations in the

bainite crystals is lower, than in the martensite and equals to $2\text{-}3x10^{10}cm^2$. The deformation strength of the bainite should be lower than the martensitic layer.

The pearlite structure is the other type of the structures observed in researched steel. The colony of pearlite (block of pearlite) represents the ferrite grain with the ordered cementite particles located in it. In the central zone there are sites of lamellar pearlite, globular pearlite. In the researched steel the grains of ferrite, free from cementite precipitates are observed. In this case the ferrite grain has not defects, the particles of cementite as spheres or layers settle down in a joint of boundaries or along boundaries of a grain.

Undoubtedly, that the central part of a sample was expoced to softer processing, than its surface. The sizes of particles cementite on boundaries of crystals a-phase grow and far range fields of stresses decrease from the surface. Behavior of the size of grains, density of dislocations and of some other structural and mechanical characteristics are not monotonously. The martensite component has the highest, and bottom bainite has the least strength to deformation. Such pearlite and the top bainite have the similar properties.

The different structure of the investigated samples of armature steel along the section is caused by the action of the various mechanisms of fracture and leads to the formation of various structures of a failure. At the section there are zones with the various mechanisms of the failure. The external martensite layer shows the mixed surface of a fracture. The character of the fracture in an external layer is anisotropic one.

It is possible to investigate in more details a picture of fracture on samples cut out from the separate layers. The martensite fracture has basically the viscous character. The mixed fracture is observed in bainite structure. Thus, from the point of view of the fracture physics the steel armature failure as a whole and the samples which have been cut out from separate layers, show a similar picture.

References

1. Madatian S.A., Frosts S.I., Demchenko L.M. New welded armature of class A400C. // Concrete and ferro-concrete. - 1995. -No 2., - p.10.
2. Odesskii P.D., Chernenko V.T. Shaped hire of high durability with constructive anisotropy. // Metal science and thermal treatment of metals. - 1992. -No8. -pp.13-18.

# THE EFFECT OF MECHANICAL ACTIVATION ON THE PHASE FORMATION PROCESSES DURING SELF-PROPAGATING HIGH-TEMPERATURE SYNTHESIS OF BARIUM HEXAFERRITE

**Vityaz P.A., Talako T.L., Okatova G.P., Beliaev A.V., Letsko A.I., Kuznetsov M.V.[(1)], Morozov Yu.G.[(1)]**

Powder Metallurgy Research Institute with Pilot Plant, Minsk, Belarus

[(1)]Institute of Structural Macrokinetics and Materials Science, RAS, Chernogolovka, Russia

Results of investigation of phase formation peculiarities during self-propagating high-temperature synthesis of barium hexaferrite with preliminary mechanical activation of charge mixture are presented.

Mechanical treatment of reaction mixture ($BaO_2$+2,4$Fe_2O_3$+4,8Fe) was carried out in an attritor at ball-powder ratio of 25:1 and 450 rpm using ethyl alcohol as a milling media.

Relative importance of specific surface area and crystal structure defects on reaction capacity of charge mixture and conversion degree is discussed.

Dependence of specific surface area of charge mixture on the time of its treatment in an attritor is not monotonous. Its increase is connected with prevailing of milling and deformation, and reduction - with agglomeration of powder particles. Significant increase of specific surface area on the first treatment stage (within the first 90 minutes) is a result of intensive milling of brittle $Fe_2O_3$ oxides. The following growth of specific surface area with increase of treatment time up to 2 hours is mainly due to plastic deformation and development of iron particles surface. Abrupt reduction of specific surface area resulted from development of agglomeration processes takes place after 2 hours of treatment.

Comparative analysis of X-ray diffraction patterns after mechanical activation did not reveal monotonous accumulation of defects within the crystal volume. Non-systematic variations of shape, angle positions and width of reflections, as well as full scale, with the increase of activation time, prove of periodical appearing and annihilation of crystal structure defects. Changing of diffraction pattern parameters, depending on the treatment time, is complex describing many processes in operation and their mismatching in time. At the same time the most significant changes are observed for the full scales and angle positions of main reflections, while character of variations of the last is the same for all the phases, despite differences in their nature (brittle $Fe_2O_3$ and ductile Fe). These changes characterize atomic offsets on the surface, disordering as well as adsorption and dissolution of the impurities. Maximum concentration of these defects is reached for the 2 hours' activation (minimum full scale and minimum reflections angle positions), which correlates well to the maximum value of specific surface area, achieved at this mode.

The SHS process is driven by the oxidation of iron metal from Fe $_{(0)}$ to Fe $_{(III)}$ in $BaFe_{12}O_{19}$. That is why fine crystal structure parameters of iron were investigated in detail. It should be noted that integral width of alpha-iron lines in the non-activated mixture is bigger comparing to mechanically treated powder mixtures. Apparently, it is connected with partial annealing of defects and some interaction between components of charge mixture during activation. It is obviously, from comparing values of physical broadening, effective size of crystallites ($D_{eff.}$ according to Selyakov), relative average-square micro-deformations of the lattice (micro-strains) and lattice parameter of α-Fe, that narrowing of the lines for the 2 hours' activation mode is generally connected with the increase of $D_{eff.}$ at insignificant growth of micro-strains. It can be connected with oxygen adsorption on the iron particle surface and formation of Fe-FeO solid solution. Narrowing of the lines for the 3 hours' activation is mostly due to an abrupt removal of micro-strains resulted primarily from precipitation of fine inclusions of interaction products out of alpha-iron based solid solution. These speculations accord well with phase composition investigations.

According to the results of X-ray analysis, phase composition of charge mixture is very close to the specified but even during mixing (without activation) a slight interaction between the components is observed. The main interaction product is a non-equilibrium compound with hexagonal structure, which composition corresponds to $Ba_3Fe_{32}O_{51}$ formula. Structure of

this composition is close to barium hexaferrite, the difference is just in shortage of molecules of iron oxide ($BaO{\cdot}5{,}3Fe_2O_3$). Mechanical activation of the charge mixture enables to increase significantly relative concentration of non-equilibrium hexagonal phase from 2-3% up to 10-13%, with abrupt growth for 3 hour's treatment.

A synthesis product is a sinter of homogeneous composition with grain size less than 1 mkm. In accordance with X-ray analysis, the product consists of the following phases (in the order of their importance).

The main phase formed during combustion is $Fe_3O_4$ based solid solution with magnetite structure and slightly lowered crystal lattice parameters a and d. The last feature can be connected with imperfection of its structure, formed in non-equilibrium conditions. The total content of this phase is about 15-30%.

The second phase, typical for the synthesis product, produced from mechanically activated mixtures, is $Ba_3Fe_{32}O_{51}$. Its content depending on the treatment time can vary within 3-17%. This composition is characterized by the low stability. When following heating the product within temperature range of 600-800°C, percentage of this phase reduces after minor holding. At the same time amorphous halo of hexagonal structure is observed.

The synthesis product also contains some $BaFe_{12}O_{19}$ in amorphous-crystal state. It is not identified by X-ray-analysis, as it is difficult to determine halo from not very intense phase against significantly broadened lines of the other phases. Nevertheless, presence of amorphous-crystal barium hexaferrite in the synthesis product is proved by transmission electron microscopy.

It should be noted that content of $BaFe_2O_4$ that is the main intermediate phase in other processes of barium hexaferrite production in this case is not more than 10%, and its maximum percentage is obtained for a non-activated charge mixture.

Finally, the SHS product can contain up to 8% of FeO and up to 10% of other intermediate compounds of Ba-Fe-O system, in particular $BaFe_{0,72}Fe_{0,28}O_{2,64}$; $BaFeO_{2,5}$; $BaFe0_{2,78}$ and others, proving stage mechanism of barium hexaferrite formation, and also some quantity of non-reacted initial components, which, nevertheless, are uniformly distributed within the material volume in such a way that the synthesis product is characterized by high composition homogeneity and quickly transforms into a one-phase hexaferrite during the following heating.

To generalize the achieved results, the following important moments can be mentioned.

Mechanical and chemical transformations taking place during preliminary mechanical treatment of charge mixture significantly influence the processes of structure- and phase-formation during SHS.

Generally, the product of mechanically activated systems synthesis is characterized with more fine and homogeneous structure and contains more hexagonal phase than product of a non-activated mixture.

Influence of mechanical activation on the phase-formation mechanism is obviously connected with formation of active centers, which are at the same time centers of adsorption. These centers can be disordered clusters of $Fe_{(II)}$ atoms. As the development of specific surface area during activation results in an increase of a number of broken bonds, density of active centers regarding to oxygen also increases. When achieving a certain value of specific surface area, abrupt intensification of oxidation of plastically deformed iron with air oxygen adsorbed on the active centers takes place. An experimental evidence of a possibility of oxidation of alpha-iron to hematite ($Fe_2O_3$) is shown. Besides, oxygen dissolution in the deformed iron is more than a number of magnitudes higher than in the cast one, resulting in increase of output of synthesized ferrites.

Apart from that, in the result of solid-phase reactions and local melting taking place during mechanical treatment of reaction mixture, some content of non-equilibrium compounds of $BaO{\cdot}xFe_2O_3$, $BaO{\cdot}Fe_{1-x}O$ and $BaO{\cdot}xFeO{\cdot}yFe_2O_3$ types form, promoting further crystallization of ferrites with magnetoplumbite structure.

At quite a high degree of disordering of initial components structures an amorphous-crystal barium hexaferrite can be formed.

A summarized scheme of possible reaction pathways is discussed.

The work was carried out under the support of Belorussian Republican Fund of Fundamental Research (Joint Russian-Belorussian Program, grant X99P-120).

# SOME FEATURES OF FORMING THE DETONATION COATINGS VK-15 IN ROTOR PARTS OF HIGH-DUTY GTES

**Sergeyev V.V., Spiridonov Yu.L., Lunyov A.N.**[(1)]
Scientific-Industrial Complex ZAO "Yuna", Kazan, Russia
[(1)]Kazan State Technical University, Kazan, Russia

Experience gained in the field of domestic and foreign GTEs service showed that their characteristics are deteriorated as time period to the first failure increases. One of the causes of such deterioration of GTE characteristics is the ever-increasing wear of parts, especially most vital parts such as the compressor blades and the turbine. To avoid autooscillations and ruptures, the compressor fan blades are equipped with the antivibration flanges that wear out in service due to constant contact in-between. To eliminate this wear-out, the compact powder VK-15 is sprayed on the flanges using thereby the method of detonation-gas spraying.

Service of GTEs with operational age of up to 2000 hours showed that the detonation coatings VK-15 provide sufficient resistance to wear and do not influence on the mechanical characteristics of the metal the blades are made of. In most part of GTEs the fan blades are manufactured from titanium alloys. Nonetheless, in practice a large number of blades with traces of wear, spallation of coatings is revealed as the time period of service increases; with increase of operational age of up to more than 1500 hours, one reveals very often the blades with fatigue breakdown of flanges; the site of origin for such failures is at the "metal base-coating" boundary.

In the course of studies, we have established that the detonation coatings diminish the fatigue resistance of titanium alloys by 40-60% deteriorating simultaneously the base plasticity. Adhesion of coatings reached its maximum value of 120-160 MPa. Microhardness of coatings was also maximal. A decrease of adhesion value gave rise to fatigue resistance and plasticity in specimens made of titanium alloys. To provide the reliable serviceability of detonation coatings on GTE fan blades, it is necessary to ensure optimal relations between adhesion and strength- and plastic properties of coatings. The above-mentioned characteristics are specified by temperature and kinetic parameters of detonation products. As compared with conventional powders, with increase of temperature and velocity of detonation products efflux, the coatings undergo significant structural and phase changes; most part of carbon is being lost and we observe brittle $\eta$-phase and intermetallides; free binding cobalt is fully absent. In the course of studies we revealed that there occurs the maximum possible deterioration of fatigue resistance in the base, and also in the strength and plastic characteristics of coatings; structure of a coating is inhomogenuous.

Decrease of temperature and efflux velocity of detonation products that heat up and accelerate the sprayed particles results in an increase of fatigue resistance and plasticity; the structure of coatings becomes more uniform and the phase composition also undergoes significant changes, that is, the content of tungsten carbide and free cobalt increases, while the number of brittle phases decreases. Improvement of fatigue and plastic characteristics of a coating takes place to the largest degree when adhesion reaches its value of 50-60 MPa; during fatigue tests we observe however the exfoliation of coatings.

Wear resistance of coatings is influenced significantly by regimes of detonation-gas spraying. Maximal wear resistance, and, hence, GTE service life, is observed when adhesion reaches its value of 50-60 MPa. The optimal spraying regime is specified thus by the conditions at which the blades operate. The coatings that operate at heavy-duty conditions of fretting corrosion and cyclic loads on the fan blades must be sufficiently plastic, and capable to relax stresses appearing due to external loads. For this reason, the regimes of coatings spraying must provide their maximal plastic properties even at the sacrifice of cohesive (between particles) and adhesive (between the coating and base) strength of bonds. So, it is necessary to classify the technological regimes of detonation spraying using as the base the temperature and kinetic parameters of detonation products. In this connection, we divided the regimes of detonation spraying into "soft", "moderate", and "severe" regimes.

At "soft" regimes when deformation of sprayed particles and force of their collision with the base are sufficiently low, the number of structure defects in a coating is smaller as compared with that obtained at other regimes. Nonetheless, the insufficient adhesive and cohesive bonds may result in coatings exfoliation and fragmentary failures at when coatings are used at heavy-duty conditions (fretting corrosion, tension, bending, and fatigue). At "severe" regimes (when the temperature and kinetic parameters of detonation products are maximal in magnitude), there develop active processes of plastic component deformation that accompany by its break-up. At interparticle and interlayer boundaries, a great number of hydrocarbon and oxide inclusions is observed; they make coating brittle and decrease the plasticity of the system as a whole. Intensive structural and phase transformations at "severe" spraying regimes give rise to high internal stresses; very often, longitudinal and lateral cracks (concentrators of stresses and sources of failures) are being formed. These coatings are distinguished by high adhesion and hardness, low plasticity, wear resistance, cyclic strength, and resistance to crack formation.

Most preferable seem to be "moderate" regimes; they ensure coatings with reasonable properties that make it possible to withstand effectively to the action of external loads. The structure and phase composition of such coatings occupy intermediate position, since the number of defects in them is larger than that obtained at "soft" regimes; at the same time, adhesion increases in magnitude. As to the "moderate" regime that makes it possible to create qualitative coatings, it is characterized by rather narrow range of temperature and kinetic parameters. Most stringent requirements are imposed on gas mixture composition, spraying distance, position of powder cloud, and the degree of filling-in the pistol gun bore by working gases.

Long-term tests of heavy-duty GTEs and their service showed that detonation coatings created at "moderate" regimes make it possible to ensure the proper GTE operation.

Based on the results of the herein-presented studies, we revealed that coatings, that suffer for a very long period of time from fretting corrosion and cyclic loads that are inherent to operating conditions of GTE fan blades, must be sufficiently plastic and capable to relax stresses appearing due to external loads even at the sacrifice of decrease in adhesion and cohesion links. The "moderate" regime meets all these conditions and requirements to the largest degree. The long-term test-bench tests and service have confirmed the reliability of the results obtained.

# DENTAL IMPLANTS FABRICATED BY SELECTIVE LASER PROCESSING OF TITANIUM POWDERS

**Tolochko N.K., Savich V.V.[1], Artushkevich A.S.[2], Laoui T.[3], Froyen L.[4], Kruth J.-P.[4], Onofrio G.[5], Signorelli E.[5]**

Institute of Technical Acoustics, NASB, Vitebsk, Belarus
[1]Powder Metallurgy Research Institute, NASB, Minsk, Belarus
[2]Belarusian Institute for Postgraduate Medical Education, Minsk, Belarus
[3]University of Wolverhampton, Wolverhampton, United Kingdom
[4]Department of Metallurgy & Materials Engineering, K.U. Leuven, Leuven, Belgium
[5]Istituto per la Technologia dei Materiali e dei Processi Energetici, Milano, Italy

Tooth's root implants used in dentistry must correspond to natural dental roots by their shape. In this case it is possible to carry out the so-called «direct» implantation. Besides the implants must posses a rough surface with macroscopic grooves and threads or a porous surface. Thus, the primary mechanical retention of the implants is provided and sufficient bone in-growth is ensured for subsequent mechanical stabilisation. Moreover, the implants must have a dense core in order to provide the strong mechanical joint between dental root implant and dental crown implant. However, the implants manufactured traditionally of Ti or Ti-alloys by machining, casting or powder metallurgy have as a rule a homogeneous (dense or porous) structure. Using these methods, it is difficult or impossible at all to fabricate implants with a graded structure possessing a comparatively high porosity at the surface and a high density in the core. The aim of this study is to investigate the possibility of producing dental root implants, which almost correspond to natural dental roots by their geometrical, structural and mechanical characteristics. To achieve this aim, a novel processing approach based on the combined Selective Laser Sintering (SLS) and Selective Laser Melting (SLM) of Ti powders was suggested [1,2]. Some physical regularities and mechanisms of the processes formed the basis for the methods developed were investigated before [3-6].

The test specimens of tooth's root implants were fabricated by selective laser processing of Ti powders. In different experiments the powders consisted of 160-200, 200-315 or 315-400 μm spherical particles and 160-315 μm shapeless particles. Nd:YAG laser was used in the study. New technical approaches to produce the implants were suggested. These are: (a) depositing the powder in small discrete portions using special feeding systems in which the powder flow is initiated by means of vibration; (b) processing the powder layers deposited by motionless collimated beam uninterruptedly (during all the process of powder deposition); (c) varying the powder layers' thickness as well as laser radiation parameters in the course of the process. The experiments have been shown that both SLS and SLM processes can take place depending on the energetic contribution of laser radiation.

The samples obtained had a rod shape with 15-20 mm in height and 5-9 mm in diameter. The diameter of the sample varied by changing the processing parameters. The structure of the implant processed by SLS/SLM consisted of two different zones: a core having a molten compact structure (porosity 0-5%) and a shell having a sintered porous structure (porosity 40-45% and pores' size 100-200 μm) (Figure 1). The dimensions of both porous and melted zones can be modified and increased by increasing the laser radiation power. In general, the porous zone has a rather homogeneous structure with a uniform density.

Figure 1. Sintered/remelted structure of rod (cross

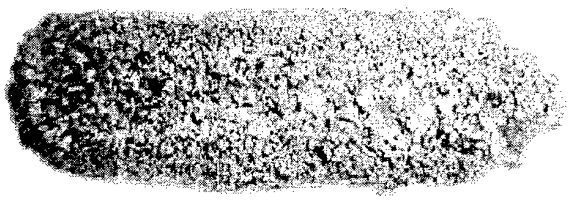

section). Rod diameter is about 7.5 mm

Due to varying the processing conditions it was possible to fabricate the samples correspond to alveolus in shape (Figure 2). Under certain processing conditions, it was possible to achieve and exceed the threshold compression force of 1000 N for the part processed by laser processing (the maximum value of real force for food

fragmentation equal to 323 N). A further post-sintering of the laser-processed samples (e.g. a heat treatment in a furnace) resulted in the improvement of their characteristics.

Figure 2. Fresh dead body sample of lower jaw with natural tooth, alveolus without tooth and dental root implant (test sample) put into alveolus (on the left) (X-ray photograph)

Dental implant surgery was performed along with local anesthesia. The implant was placed in the dog jaw using a gentle surgical technique. The one stage implanting technique was used. One stage implants were placed such that the implant was exposed at all times after surgery. Implants required the expertise of two distinct dental professional, an oral and maxillofacial surgeon and the restoring dentist. The two worked together to customize the dental implant • treatment program. The standard clinical 3 months *in vivo* investigations as applied to the dogs (at the age of ~ 6 years and weighing ~20 kg) showed the following results: all the cross sectional specimens possessed the advanced osseous structure with a conically spread bone plates and *osteons* (haversian systems). There were observed oriented advanced bone bridges along all the bone-implant interfaces as well as inside the porous implants' structures (Figure 3). Neither inflammation nor degenerative/dissolving tissue changes were observed at the interface thus proving the high rate of the implant biocompatibility.

Thus, the experimental results obtained in the present study demonstrate clearly the feasibility of producing dental root implants with required operating properties by selective laser processing of Ti powders.

Figure 3. Cross-section of bone tissue with porous titanium implant.$^{x}$50 (a) implant globules; (b) boundary zone; (c) inter-globule

## References

1. Tolochko N.K., Titov V.I., Artushkevich A.S., Laoui T., Onofrio G., Signorelli E., Manufacturing of Tooth's Root Implants by Selective Laser Processing of Titanium Powders, 4th INTAS Interdiscipl. Symp. on Phys. And Chem. Methods in Biology, Medicine and Environment (Grant Monitoring Conf.), Moscow, 30 May - 3 June 2001, Moscow Univ. and INTAS Secretariat, Proc. Book, MAX Press, Moscow, 2001, pp. 56-57.

2. Tolochko N.K., Laoui T., Froyen L., Onofrio G., Signorelli E., Titov V.I., Manufacturing of Titanium Parts for Medical Purposes by Combined Selective Laser Sintering/Melting of Powders, Conf. Abstr. EUROMAT 2001, 7th Europ. Conf. on Advanced Materials and Processes, Rimini, Italy, 10-14 June 2001, p. 16

3. Tolochko N.K., Yadroitsev I.A., Mozzharov S.E., Michailov, V.B., Selective laser sintering: some questions of physics and technology. Proc. PM World Congress, Granada, Spain, October 18-22 1998, 5, pp. 407-412.

4. Tolochko N.K., Mozzharov S.E., Yadroitsev I.A., Titov V.I., Ignatiev M.B., Structure of sintered materials fabricated by laser beam, Science of Sintering, 1999, 31 (2), 91-96.

5. Tolochko N.K., Michailov V.B., Laoui T., Froyen L., Ilyuschenko A.Ph., Steinhauser S., Ignatiev M.B. Laser sintering of single-component metal and two-component metal/ceramic powders, Science of Sintering, 2000, 32 (2), 53-59.

# SYNTHESES OF NEW COMPOSITE CERAMIC AND METAL-CERAMIC MATERIALS IN COMBUSTION MODE

**Okrostvaridze O., Tavadze G., Khvadagiani A., Lekishvili K., Sahvadze D.**
State scientific-technical center "Delta", Tbilisi, Georgia

Development of modern techniques is impossible without development and perfection of the technology of ceramic materials. However, high sensibility of these materials to stress microconcentrators as well as hard-controlled process of failure is impediment for large application. At the same time, the greatest achievement of the materials science in last few decades is a creation and application in technique the materials of a new class-composites. Modern composites, among them **Composite Ceramic Materials (CCM)**, play important role not only in civil industry, but also in construction of different kinds of ammunition and military techniques, especially in space and aircraft branches, in armor productions, etc. All the above mentioned is a great encouragement for fast development of the so called "ceramic-technology". One of the most perspective and effective methods to obtain complex CCM is a technology of **Self-propagating High–temperature Syntheses (SHS)**, which is based on a principle of maximum use of chemical energy of the reacting systems. Because of high temperatures and high speed of chemical transformation, SHS is attributed to extremal technologies; the final products advantageously differ from their traditional analogs by high values of physical-mechanical properties and other exploitation characteristics.[1,2]

In the present article are given the results of long-term scientific technological investigations of SHS-syntheses of complex three-, four-, five-component composites. A whole group of a new CCM with phase constituents of refractory compounds $TiB_2$, TiC, $Al_2O_3$, $B_4C$, $CaB_6$, SiC and etc.,and metals Ti, Cu, Ni, Co and their compounds NiAl, TiN, Ti00000Ni, Ti-Al was synthesized.
New materials were obtained in the form of:

a) composite powders;
b) composite consolidates materials;
c) layered or functional - gradient materials (FGM).

Where:
1.Powder CCM were obtained from refractory compounds of $B_4C$, $TiB_2$, $Al_2O_3$, SiC, TiC of different dispersion (5-100mkm).
2.One layered CCM, with phase constituents of $B_4C$, $TiB_2$, $Al_2O_3$, SiC, TiC and etc. constructed so that a structure of material could provide the given level of physical-mechanical properties.
3.Layered CCM were constructed by the following structural scheme:

- first layer – CCM from $B_4C$, $TiB_2$, $Al_2O_3$, SiC, TiC, Cu, Ni, Ti and etc.;
- transition layer from exothermic or inert mixture;
- second layer – metal-ceramic $TiB_2$·Ti, TiC·Ti, TiAl, NiAl and etc;
- transition layer from exothermic or inert mixture;
- third layer – metals Ti, Cu, Ni and etc.

4.FGM were constructed:
- with symmetric distribution of the bunch. The FGM surface is from $B_4C$, $TiB_2$, $Al_2O_3$, SiC, TiC and etc; back layer – metals: Cu, Ni, Co, Ti and compounds: TiNi, Ni-Al, Ti-Al. Concentration of metal changes smoothly from surface to the other side. On the boundary of layered composites: composite ceramics, metal-ceramic, pressed by SHS -compacting method, the main factors, which define good cohesion, are metal layers, composed of Ni, Al, Fe, Co, Ti compounds in various combinations. On boundaries occur stress relaxations, caused by difference in CTE of phase constituents of ceramic and metal-ceramic layers.
Structures of some compositions are given below:

- $TiC{\cdot}TiB_2{\cdot}Al_2O_3$;
- $B_4C{\cdot}$ TiC$\cdot$ $Al_2O_3$;
- SiC$\cdot$ TiC$\cdot$ $TiB_2 \cdot Al_2O_3$;
- $B_4C$ ·SiC · $Al_2O_3$·NiAl;
- SiC$\cdot$ $TiB_2\cdot$ $Al_2O_3$·TiAl;
- TiC$\cdot$ ·$Al_2O_3$·NiCo;
- $B_4C \cdot TiB_2 \cdot Al_2O_3$·Co;Cu;Ni;
- $TiB_2\cdot$ $CaB_6\cdot$ $Al_2O_3$·Fe;Ni;Co;
- In SHS-compacted samples could be largely changed characteristics of :
- macrostructure–distribution of composition, macroscopic defects;

- microstructures – relative position of phases and structures, grain structure;
- crystal structure-defectiveness, type and parameters of crystal lattice.

The concentration of phase constituents in above mentioned compositions may be changed over a wide range.

Scientific and technological bases of "construction" of materials with advanced complex of physical-mechanical properties were elaborated. This was achieved by "construction" of composite structure from refractory compound, metals and alloys, using correlation dependencies of the "technology-structure-property" and distinctive features of technological character.

Synthesized powders, layered composites and FG-materials have better technological, economic and qualitative characteristics than their traditional analogs.

This was achieved by:

a) composition building of micro-, as well as macrostructure of multi-phase materials;
b) realization of the SHS–technology advantages, such as: small energetic expenditures, high speed and extremity of the process, which provide good conditions for the formation of microstructure, simplicity of technological equipment, one-staginess of the article manufacturing process.[3]

For synthesized materials correlation dependencies between parameters of initial burden, burning parameters and compacting were determined. Physical properties and structure of powder compositions; structure, morphology and phase composition of SHS –compacted layered composites of CCM, metal and functional gradient materials were investigated.[4]

Physical-mechanical properties (hardness, strength, crack resistance, density distribution) of these materials were investigated.

Some physical-mechanical characteristics of composites:

- modulus of elasticity – 350-430 MPa
- hardness of phase constituents – 200-4800 kg/mm$^2$
- coefficient of failure viscosity –10 ÷13 MPa
- fragile strength – 2,5 ÷4 GPa
- porosity of SHS-compacting samples - 3 ÷6 %
- cutting capacity –0,58 ÷0,96 gr/min.

High values of failure power-consuming, in particular, coefficient of failure viscosity $K_{1c}$, which reaches 11-13MPa·m$^{0,5}$ are provided by formation matrix type structure, during the syntheses of composite ceramic, strengthened phases, which in its turn provide effective braking action of a crack with dispersive elements of the structure and internal stresses, caused by differences of coefficients of Thermal Expansion(CTE) of phase components in fine-grained medium.

Possible areas of application of SHS-composite materials may become:
-for powder CCM-abrasives, abrasive pastes and tools, initial material for plating manufacturing of tool and constructive ceramic by hot - pressing and hot isostatic pressing methods;
-for layer CCM, layered and FG-composite materials-heatproof and armor materials for aircrafts, materials for cutting tools, tribotechnique, constructive materials for new generation engines, engineering protection of banks and special transport of collections.

Using of elaborated compositions and technology of their manufacturing must considerably increase exploitation characteristics of the articles, at the same time decreasing their cost on the account of low powder expenditure, simplicity of high temperature equipment and high-speed of manufacture process.

References:

1.A.G.Merjanov. Ten Research Directions in the Future of SHS. Int. I. of SHS, 1995, v.4, №4, p.323-350.
2.В.И.Вершинников, С.С.Мамян, А.А.Ширяев и др. Закономерности синтеза композиционного порошка Ti $B_2$·$Al_2O_3$. Материал на основе (Препринт).-Черноголовка,1992,39с.
3.O.Okrostsvaridze, A.Khvadagiani, G.Tavadze, K.Lekishvili./Fabrication of Two and Multylayered Composite Materials by SHS and Compacting Method./Proceedings of the Symposium on Boron, Borides and Related Compound/Baden,Austria-1996,pp.126-127.
5.О.Окросцваридзе, К.Лекишвили, Г.Тавадзе, А.Хвадагиани – Многофазные композиции, полученные методом СВС.-научно-техническая конференция по сварке, металлургии и родственным технологиям. - Тбилиси, 2000, с.92-96.

# ZIRCONIUM DODECABORIDE SINGLE CRYSTAL GROWTH

**Paderno Yu.B., Layshchenko A.B., Filippov V.B., Duhnenko A.V**
I.N.Frantsevich Institute for Problems of Material Sciences of NASU, Kiev, Ukraine

Due to their unique combination of properties, such as high melting point, hardness, thermal and chemical stability metal-boron refractory compounds are widely applied in modern technique [1-2]. Moreover, these compounds can be used as model materials for a number of physical investigations, since, for example, it is possible to evaluate the influence of the construction of the boron sublattice in borides with different boron content - $MeB_2$, $MeB_4$, $MeB_6$, $MeB_{12}$ and $MeB_{66}$ phases for a definite metal onto the properties of these materials. On the other hand, the influence of a nature of the metallic ion onto the properties of boride phases can be evaluated as well.

For instance, the electrical conductivity of $MeB_6$ phases can vary form the values corresponding to an insulator ($CaB_6$) to a material with a typical metallic conductivity ($LaB_6$ and some others). The hardness, chemical resistance in boride phases usually is growing with boron content increase.

Recently, after the discovering of comparatively high temperature of superconductivity in one of the long before known magnesium diboride, the all boride phases, particularly not very widespread attracted the big attention of scientists.

From this point of view a big interest draw the zirconium dodecaboride, $ZrB_{12}$. This phase was synthesized comparatively long ago, but the knowledge related to its properties, apart crystal structure, up today is very limited [3-6]. Moreover, there are very much contradictions in the question of the temperature range of its existence - from very large, including room and melting temperatures, to very limited one [7-8]. Massalski presented the constitutional diagram of Zr - B binary system, where it exists only between 1696 - 2082°C and has peritectic melting character [9].

The fall of the crystal structure of $ZrB_{12}$ to the $UB_{12}$ type permits to suppose that its properties may be similar to such interesting compounds as $YbB_{12}$, $UB_{12}$, $REB_{12}$, which are characterized by unusual fundamental physical features, as mixed valence, heavy fermions, specific magnetic transitions etc.

The most of physical properties research demand having high purity and perfect structure samples. Many experiments need in sufficiently large single crystals. For today the information about producing of big $ZrB_{12}$ single crystals is absent.

In the present work for the first there was studied the possibility to obtain sufficiently large $ZrB_{12}$ single crystals using induction zone melting method. This technology successfully was applied for many boride phases' single crystals. Where as this method may be realized comparatively easy for congruent melting materials, for materials having incongruent melting character it demands some contrivances.

The source $ZrB_{12}$ was prepared by different using for boride synthesis methods - by synthesis from metal and boron, by reducing of $ZrO_2$ with boron or boron carbide, from the mixture of $ZrB_2$ and boron. All mixtures were heated in vacuum at temperature in limits 1500 - 1600 °C during 1 hour. In all cases there were obtained any amount $ZrB_{12}$ simultaneously with $ZrB_2$ and boron. The amount of $ZrB_{12}$ was in limits 50 - 95 %. Obtained materials were subjected to crucibleless zone induction melting in argon atmosphere. The most stable melting process was achieved by using as a source material the zirconium and boron mixture. It is interesting to note that just this material contained after sintering less $ZrB_{12}$ phase - only near 50 %. It may be explained by the combination of zone crystallization and flux processes, due the excess of boron in material. The produced rod is shown in the Figure. It has diameter near 6 mm and up to 40 mm length.

X-ray diffraction analyses of crushed rod revealed only $ZrB_{12}$ phase and had shown the absence of any additional phases. The cell parameter 0.74072±5 nm is very close to the known value (0.7408 nm [4]). The measured specific density of the rod is 3.60 gr/cm$^3$, which practically coincide with the computed density. Metallographic investigation of the cross section had not detected any grain boundaries; the X-ray epigram confirmed that obtained rod is single crystalline.

There were investigated some properties of obtained $ZrB_{12}$ single crystal. The microhardness is 36-38 GPa, that is any more than for other $MeB_{12}$ phases. The elastic module, calculated from measured hypersonic oscillations along the rod is

near 390 GPa, that gives the Debay temperature 1040 K.

$ZrB_{12}$ single crystal.

**REFERENCES**

1. T Serebriakova, V.Neronov, P.Peshev, Refractory borides. Metalurgia, M., 1991 (in Russian).

2. Boron and Refractory Borides. Ed. V.I.Matkovich. Berlin-Heidelberg-New York: Springer-Verlag. 1977.

3. B.Post, F.Glaser, J.Metals, 4, 631, 1952.

4. V.Matkovich, J.Economy, R.Giese, R.Barrett, Acta Cryst, 19, 1056, 1965.

5. Yu.Paderno, B.Odintsov, I.Timofeeva, L.Klochkov, Teplofizika vysokich temperatur, 9, 200, 1971 (in Russian).

6. M.Arbusov, A.Adamovsky, A.Liashchenko, Powder Metallurgy, #1, 50, 1979 (in Russian).

7. K.Portnoi, V.Romashov, L.Burobina, Powder Metallurgy, #7, 68, 1970 (in Russian).

8. F.Glaser, B.Post, Trans.AIME, 197, 1117, 1953.

9. H.Okamoto, J.of Phase Equilibria Vol.14, No.2, 1993 p. 261-262.

# OBTAINING OF MONO- AND BIMETAL DISPERSE POWDERS BY ELECTROLYSIS AND CEMENTATION

**Kunty O.I., Sribny V.M.[1], Minakova R.V.[2], Kozak S.I.**
National University «Lviv politechnik», Lviv, Ukraine
[1] State enterprise «Argentum», Lviv, Ukraine
[2] Frantsevich Institute for Problems of Materials Science NAS of Ukraine, Kyiv, Ukraine

The authors carried out works on obtaining of highly dispersed mono- and bimetallic powders in the aqueous solutions and medium of aprotic solvents. In the aqueous solutions it is investigated: 1) the precipitation of monometallic powders by electrolysis with the undissolved anodes; 2) the precipitation of monometallic powders by cementation on magnesium; 3) the electrochemical application of coatings on the monometallic powders with obtaining of bimetallic; 4) obtaining bimetallic powders by cementation. In this case possibility of using of recoverable nonferrous and noble metals (direction 1 and 2) and obtaining the wide spectrum of bimetallic powders (direction 3 and 4) was studied; 5) electrolysis with the precipitation of dispersed powdered metal in the aprotic solvents was investigated.

1. Electrolysis with the insoluble anodes is studied of the nickel powder precipitation as the example. Accordingly to experimental dates, conditional dispersed nickel can be obtained in the range of ion concentrations of metal 0,1... 0,8 mol/l and pH = 4...10 in the presence of buffer additive – ammonium salt. Electrolysis in the potentiostatic regime during a constant circulation of electrolyte is most technologically effective. On the base of nickel leaching process according to [1], technological cycle was proposed by following scheme: the leaching of metal → the cathodic precipitation of dispersed powder → the leaching of metal with step-by-step correction of the solutions for operations and their number. The concentration of metal in the electrolyte, temperature and voltage in the electrolyzer (or cathodic current density) are the basic parameters, which substantially influence on the electrochemical deposition of conditional dispersed nickel. The values indicated and the fundamental characteristics of nickel powder (dispersivity, granulometric composition, bulk density) are interrelated. They are amenable to the mathematical simulation and must take account into automatization of the separate stages of technological process. The given technological cycle of dispersed nickel powder obtaining, during the electrolysis with the insoluble anodes, gives the possibility to use the nickel-containing solutions, which are formed during processing of spent catalysts, electrolytes of nickel plating, electrodes of storage batteries, etc. To fig.1 is given the morphology of the nickel powder, received from recoverable raw materials.

2. Cementation on magnesium under the conditions of metal powder precipitating with of high dispersivity is studied. The very low value of the standard electrode potential of magnesium ($E^0_{Mg^{2+}/Mg} = -2{,}363$ V) leads to the high values of current density on the micro-cathodes during the cementation. This favorably influences completeness of the deposition of metals [2] and obtaining the highly dispersed powders of the quite a number of metals. It is shown based on the example of electronegative (zinc, cadmium, nickel, cobalt, lead) and electropositive (copper, silver, platinum) metals that the dispersivity of powders strongly depends on nature of the precipitated metal. Its most significant characteristics are next: the value of standard electrode potential, overvoltage of its cathodic isolation and overvoltage of the isolation of hydrogen on its surface. The following regularity is revealed: the higher the cathodic overvoltage of the metal isolation and the lower the overvoltage of the electrochemical hydrogen isolation on its surface, the higher the dispersivity of precipitated of metal powder during the cementation by magnesium. The magnitudes of these two values can have more essential influence than the magnitude of standard electrode potential. Thus, during the cementation by magnesium of cadmium ($E^0_{Cd^{2+}/Cd} = -0{,}4029$V) on surface of which the overvoltage value of the hydrogen isolation very high, dispersed powders precipitate out only for the low concentrations of metal ions. Cobalt and nickel, are distinguished little from cadmium by magnitude of the standard electrode potential values, ($E^0_{Co^{2+}/Co} = -0{,}277$V; $E^0_{Ni^{2+}/Ni} = -0{,}25$V), but these metals characterized by high overvoltage of cathodic isolation and the very low overvoltage of hydrogen isolation on their surface. In this case powders with the high

dispersivity precipitate out even from the concentrated solutions of metals salts. With an increase in the values of standard electrode potential the tendency toward an increase in the dispersivity of the precipitated metal powder under other identical characteristics of metal and conditions of cementation is observed.

3. Obtaining the bimetallic powders of metals is studied on the systems Cu-Ag, Ag-Cd, Ag-Ni, C-Ni, W-Ni. The possibility of obtaining the uniform electrochemical coatings with the high adhesion is shown. In this case it is noted, that the last parameter favorably influences the ultrasonic field. To fig.1 is given the morphology of the nickel-plated powder of tungsten.

High adhesion to the base metal permits implementation of chemical modification of coatings. Thus, during the heating in air of bimetallic powder Ag-Cd occurs the surface oxidation of cadmium with the formation of system Ag-CdO with good adhesion phase boundaries. Thus, the electrochemical coating of dispersed powders can be used for obtaining the compositions with the nonmetallic components.

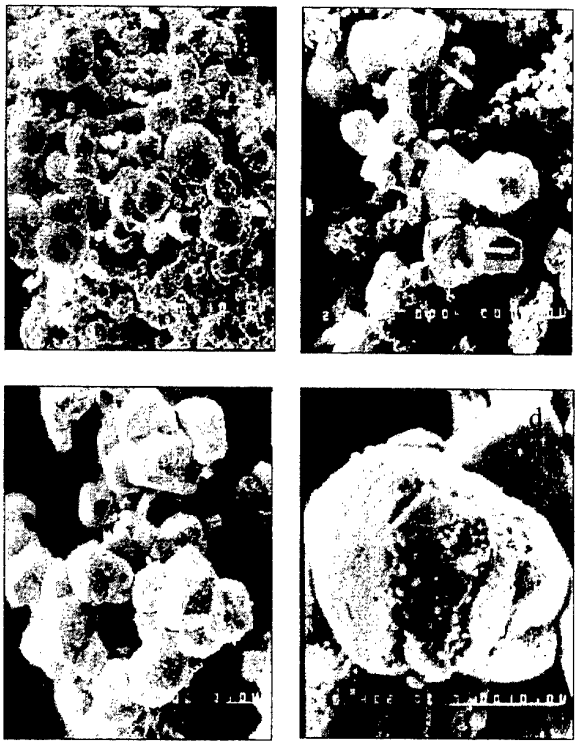

Fig.1. Morphology monometallic powders Ni-W (a,b) and bimetallic powder W-Ni (c, d) received from recoverable raw materials

Obtaining bimetallic dispersed powders was based on maximum by the use of second raw material so, as raw material for the dispersal system W-Ni served the tungsten-bearing raw materials of electric-lamp production (for obtaining the dispersed tungsten) and the second nickel-containing raw material (for obtaining anodic nickel).

4. Obtaining bimetallic powders by cementation is in detail studied on the system Cu-Ag It is shown that the morphology of copper powder changes in the process of the deposition of silver and the greater it is, the higher the content of the second component. The uniformity of coating strongly depends on nature of electrolyte. Thus, in the complex electrolytes it is considerably higher than in the simple. On the base of the powders Cu-Ag, analysis it is noted that the cementation is effective in obtaining of dispersed bimetallic systems with the small content of the second component.

5. It is shown that during the electrolysis of salts of the row of d-metals in the aprotic solvents (DMFA, DMAA, DMSO) the tendency toward the cathodic precipitation of dispersed powders even at the low current densities is observed. It is noted, that high tendency toward the adsorption of the metal: increased of cathodic polarization; contributes to the formation of new crystal nuclei, which leads to an increase in the dispersivity of the precipitated metal powder; stabilized highly dispersed powders. Based on the example of the cathodic precipitation of nickel and cobalt is shown the possibility of obtaining by the ultra- dispersed powders with the high current efficiency. Dendrites growth on the surface of cathode during the electrolysis in the aprotic solvents has local nature in comparison with the frontal in the aqueous solutions. Therefore to initial process of electrolysis with the formation of the crystallization centers significant influence has nature and state of cathodic surface. The distinctive special feature of the medium of aprotic solvents is also the absence of the hydrogen absorption of metal powder during their cathodic precipitation.

REFERENCES

1.Демидов А.И., Красовицкая О.А. Извлечение никеля из отработанных электродов никель-железных аккумуляторов в аммиачных растворах // ЖПХ. – 2000. – №10. – С.1656-1659.

2.Patent of Ukraine № 39018A C 22B 11/00. 15.05.2001.

# DEVELOPMENT OF TECHNOLOGY OF COHESION OF METALLIC DENTAL BODY WITH POLYMERS AND CERAMICS

**Besov A.V.**
National Technical University of Ukraine "KPI", Kiev, Ukraine

In orthopedic stomatology a great attention is being given issues related to the mechanism of a facing cover cohesion with metallic body of a crown due to the wide application of polymer-metallic dentures. Cohesion strength of crown's metal achieved with a polymer facing material when traditional methods of denture mounting have been used often does not meet proposed requirements [1]. Moreover, the large thickness of traditional metal-polymer and metal-ceramic covers that is on order of 1.5-2 mm makes dental orthopedist to prepare significant volume of hard tissue of a tooth, which is undesirable from medic point of view.

As conversion processes as well as integration of various branches of science develop, new technologies, namely, the plasma spraying among them, have been employed for solving urgent medical issues, for instance, in orthopedic stomatology. The plasma spraying method showing practically unlimited possibilities allows depositing high-quality covers of different materials regardless shape and dimensions of an object to be sprayed on. Nowadays, there is a great demand in manufacturing of high-quality dentures that is due to tends in patient's welfare and culture level growth. This put higher requirements on esthetics and reliability of both temporary and fixed dentures. Employing of this method permits us to make significant contribution to development of modern orthopedic stomatology.

The present work is devoted to development and implementation of a plasma technology for retension covers to be sprayed on permanent denture's constructions made of metal (crowns and bridge-like dentures) which is followed by facing with polymers or ceramics. Finishing off of spraying modes in dependence on current of plasmatron, range of spraying and dispersity of powders used was carried out on a handy plasma unit electrically supplied from the ordinary main. Optimal spraying modes allowed depositing covers of nickel-aluminum, nickromium, stainless steel and titanium on different substrates [2]. The covers were up to 50-200 mkm thick.

Bonding of a sprayed cover with a substrate, for example, metallic body of a fixed denture was realized due to mechanical adhesion of sprayed material particles with unevenness of the surface of a denture. The surface was previously treated in a stream of sand. Besides it, diffusion of components into a material of the substrate as well as alloying and chemical interaction of conjugating materials also appears to play a great role for cohesion. It results in formation of a plasma sprayed cover with characteristics and properties determined by conditions of the spraying process on a body-substrate. Plasma spraying is performed on both single stamped and cast crowns and solder and cast bridge-like dentures or different parts of their surface. To suppress color of crown's metallic body it also possible to carry out depositing of oxide ceramic covers, for instance, aluminum, zirconium, and yttrium. Materials such as polymers, photo composites, various kinds of porcelain and sitals are used for a body facing with plasma sprayed retention covers.

Analysis of the cohesion mechanism of plasma sprayed covers with facing materials was made using results of electron microscopic investigations on cover structure and conjugated areas. Characteristics on strength of covers were obtained for test-samples by studying their bending and tension properties. Thus, significant growth of the surface area under plasma spraying conditions facilitates to improve cohesion of a facing cover with a retention layer of micro pearls. Strength of cohesion in samples was measured by the normal detachment method. Results of tests have shown that the usage of plasma sprayed retention layers of micro pearls increases strength of cohesion 3-5 times in comparison with traditional methods [3,4]. Fabricated dental crowns with plasma sprayed covers were investigated on resistance to affections of destructive loads. The value of destructive pressure was measured using ZIP R-0,5 device and a hydraulic following convenient methods. Tests showed crowns remained stable under load ranging from 6 to 260 kg that exceeds the required Denis's chewing efforts value [5].

New technology of manufacturing of both fixed and temporary dentures based on the plasma spraying of retention covers of various stomatologic materials (metals, alloys and ceramics) was developed. Technological investigations of the plasma spraying process and its further optimization in purpose to apply for different stomatological items were carried out. Physical-mechanical properties of plasma sprayed covers were investigated. It was shown that the technology developed provides tighter cohesion of plasma covers with material s of a body as well as facing covers.

References:

1. Копейкин В.Н. Ошибки в ортопедической стоматологии//М.: Медицина,1986.-174с.
2. Бесов А.В. Способ изготовления порошковых материалов для плазменного напыления ретенционных покрытий //Патент РФ №2151668 от 27.06.2000г.
3. Бесов А.В. Исследование прочности сцепления плазмонапыленных композиций с облицовочным покрытием//Вестник национального технического университета Украины "Киевский политехнический институт". Машиностроение.-2001 вып.41.-С.246-250.
4. Гальченко В.В., Бесов А.В., Павленко А.В. и др. Улучшение качества эстетических покрытий несъемных зубных протезов// Український стоматологічний альманах. 2002.-№1-С.41-43.
5. Жулев Е.Н. Несъемные протезы. Теория, клиника и лабораторная техника//-Н.Новгород. Изд-во НГМА. 1995.-356с.

# К ВОПРОСУ О ПРОИЗВОДСТВЕ ПОЛУПРОВОДНИКОВОГО КРЕМНИЯ: АНАЛИЗ ОТХОДОВ И ВАРИАНТЫ ИХ ПЕРЕРАБОТКИ

Ж.Н.Галиева[1], Н.В.Степаненко[2], О.Н.Бондарук[1]

1 – УП «Минский НИИ радиоматериалов»
2 – Белорусский государственный университет информатики и радиоэлектроники

На первом Международном научно-техническом семинаре в Новополоцке в мае 2000 г. были представлены технико-экономические предпосылки создания в Республике Беларусь производства полупроводникового кремния и первые результаты анализа энергетики отдельных технологических процессов [1,2].

В течение 1999-2001 гг. Минским НИИ радиоматериалов, Белорусским государственным университетом информатики и радиоэлектроники (БГУИР) и Новополоцким заводом «Измеритель» в рамках проекта «Разработать технологию производства полупроводникового кремния из побочного продукта переработки апатитов Гомельского химического завода» были проведены укрупненные лабораторные испытания технологии получения поликристаллического кремния (ПКК).

В основу технологии получения ПКК положена реакция термического разложения кремнефторида натрия ($Na_2SiF_6$) с получением газообразного тетрафторида кремния ($SiF_4$) [3], восстанавливаемого затем до моносилана ($SiH_4$) и ПКК.

Технологическая схема получения кремния включает следующие основные стадии:

*Стадия 1* – термическое разложение кремнефторида натрия (КФН):
отход – твердый продукт термического разложения КФН, представленный фторидом натрия, остатками неразложившегося КФН и примесями, содержавшимися в исходном сырье. Годовой объем отходов составляет 1800 т из расчета предполагаемой производительности производства ПКК – 500 т в год.

*Стадия 2* – восстановление тетрафторида кремния до моносилана:
отход – фторид кальция, отработанный плав эвктектической смеси LiCl + KCl с включением не вступившего в реакцию избытка гидрида кальция. Годовой выход отработанного плава около 5000 т.

*Стадия 3* – получение ПКК:
отход – водород с примесью непрореагировавшего моносилана. Годовой объем отходов – 880 тыс.м$^3$.

Анализ балансовой технологической схемы показывает, что количество твердых отходов, которые будут образовываться на заводе при реализации указанной технологии с заданной производительностью 500 т ПКК в год, составляет около 7 тыс.т в год, количество газообразных отходов – около 1 млн.м$^3$. При этом во всех отходах присутствуют фтористые соединения [4].

При разработке той или иной технологии учитываются в первую очередь экономический и экологический факторы.

Как показывает предварительный экономический анализ [1], предлагаемая технология позволит получить ПКК по цене 17 долл.США за 1 кг вместо 50 долл.США по традиционной технологии. Такой экономический эффект является стимулом для поиска путей решения сопутствующих проблем, включая экологическую.

Фтористые соединения относятся к 1-2 и 3 классу опасности по ГОСТ 12.1.005. Наибольшей токсичностью обладает фтористый водород. Токсическое действие тетрафторида кремния и кремнефтористоводородной кислоты выражено слабее. Для КФН ПДК в воздухе рабочей зоны в пересчете на фтор составляет 0,005 мг/м$^3$ [3].

При реализации предлагаемой технологии все газовые и жидкие отходы должны подвергаться очистке от фтора до достижения соответствующих санитарных норм. Твердые отходы должны быть нейтрализованы до безопасного состояния либо пере-

работаны в продукцию народнохозяйственного назначения.

Наиболее перспективной в плане экологии и экономики выглядит технология с замкнутым циклом.

**Целью** настоящей работы явилось исследование проблемы отходов предполагаемого производства ПКК, установление их истинного состава и проведение предварительных изысканий по возможным направлениям их переработки и использования.

**Методика экспериментов**

Исследования проводились на образцах отходов, полученных на Новополоцком заводе «Измеритель» при проведении укрупненных лабораторных испытаний технологии получения ПКК. Пробы предварительно измельчали и усредняли. Изучение фазового химического состава проводили на рентгеновском дифрактометре ДРОН-4-13 (Со-излучение с железным фильтром), количественный элементный состав определяли на атомно-абсорбционном спектрометре Spectr AA 250 фирмы Varian. Содержание гидрида кальция определяли обратным титрованием соляной кислотой.

После уточнения состава отходов проводились эксперименты по их переработке до товарной продукции.

**Результаты экспериментов**

В таблице приведены результаты анализа усредненных проб отходов и состав продуктов, полученных при их переработке.

**Обсуждение результатов**

Результаты проведенных исследований показали, что:

1. Исследуемые образцы отходов предполагаемой технологии получения ПКК представляют собой технические смеси высокотоксических продуктов, относящиеся по ГОСТ 12.1.005 ко 2 и 3 классу опасности и подлежащие нейтрализации.

2. По предложенному методу карбонизации (обработка горячим содовым раствором) отходы от термического разложения КФН были переработаны до фторида натрия квалификации ч.д.а. по ГОСТ 4463. Области использования NaF – производство антисептиков, алюминия, фторированных лечебно-профилактических продуктов для народно-хозяйственного потребления (зубных паст, питьевой и минерализованной воды) и др., в том числе в качестве сорбентов газообразных фторсодержащих продуктов в рассматриваемой технологии ПКК.

3. Обработка отходов от восстановления тетрафторида кремния до моносилана горячей водой позволила выделить из отработанного плава в раствор хлориды лития и калия, которые будут возвращены на стадию восстановления кремния после некоторой переработки. Твердый отход, представляющий собой гидрооксид кальция и фторид кальция, перерабатывали методом гидрофазного фторирования до фторида кальция. Область использования $CaF_2$ – производство плавиковой кислоты и фторида аммония, изготовление специальных оптических изделий для микроэлектроники и др. Большой интерес к материалу как к заменителю флюоритового концентрата для сварочных работ проявили производители электродов для сварочных работ. Предварительные испытания материала в составе флюсов, используемых в качестве защитного покрытия электродов, показали большие перспективы использования отходов в данном производстве. Объем потребления для стран СНГ, включая Россию, Беларусь и Украину, составляет около 1,5-2,0 тыс.т., что подтверждает возможность полной утилизации отходов производства ПКК из КФН.

Работа выполнена при содействии программы НАТО «Наука для мира».

Составы отходов предполагаемого производства ПКК.
Результаты эксперимента и составы продуктов, полученных при переработке отходов

| Стадия процесса | Характеристика пробы | Состав, % | Примечание |
|---|---|---|---|
| 1. Отходы от термического разложения КФН | Неоднородный спек серого цвета с включениями белого цвета | $Na_2SiF_6$ – 15,7<br>NaF – 84,4<br>$SiO_2$ – 0,4 | |
| 2. Отходы от восстановления тетрафторида кремния до моносилана | Плав эвтектической смеси LiCl-KCl, содержащий $CaF_2$ и $CaH_2$ в виде прослоек белого цвета | LiCl, KCl –32,0<br>$CaF_2$ - 26,0<br>$CaH_2$ – 42,0 | Проба с предельным содержанием $CaH_2$ |
| 3. Продукт карбонизации отходов стадии 1 | Однородный порошок светло-серого цвета | NaF – 99,7<br>$SiO_2$ – 0,3 | Соответствует ГОСТ 4463 |
| 4. Продукт гидратации отхода со стадии 2 технологии ПКК | Серый однородный порошок | $Ca(OH)_2$ – 74,0<br>$CaF_2$ – 26,0 | Выход сухого составляет 26 % от исходного сырья |
| 5. Продукт гидрофазного фторирования отхода со стадии 2 (после предварительной гидратации) | Серый однородный порошок | $CaF_2$ – 90,8<br>$AlF_3$ - 1,74<br>Ba $F_2$ – 0,01<br>Pb $F_2$ – 0,02<br>Fe $F_3$ – 6,1<br>Co $F_2$ - 0,02<br>Cr $F_3$ – 0,46<br>Mg $F_2$ – 0,14<br>Mn $F_2$ – 0,07<br>Ni $F_2$ – 0,63 | В продукте содержатся примеси от коррозии материала оборудования установки. Гидрофазное фторирование проводили на фторопластовом оборудовании |
| 6. Отход кремнефтористоводородной кислоты (стадия получения КФН) | Водный раствор | $H_2SiF_6$ – 12,8<br>HF – 1,5 | |
| 7. Продукт нейтрализации отхода КФН известью | Белый порошок | $CaF_2$ – 97,5<br>$SiO_2$ – 2,5 | Соответствует ГОСТ 4421 Концентрат плавикового шпата для сварочных работ марки ФКС-95А |

## Литература

1. Василевич В.П., Васюков А.В., Котов Д.А., Степаненко Н.В., Степаненко В.Н. Технико-экономические предпосылки создания в Республике Беларусь производства полупроводникового кремния // Современные проблемы проектирования и производства радиоэлектронных средств: Материалы Международного научно-технического семинара. – Новополоцк: ПГУ, 2000. – С.42-45.

2. Поляченок О.Г., Степаненко В.Н., Васюков А.В., Варанкова Н.В., Дудчик Г.П., Степаненко Н.В. Энергетика некоторых процессов получения кремния из фторсодержащего сырья // Там же – С.92-95.

3. Зайцев В.А., Новиков А.А., Родин В.И. Производство фтористых соединений при переработке фосфатного сырья. – М.: Химия. 1982. – 246 с.

4. Галиева Ж.Н., Степаненко Н.В., Бондарук О.Н. К вопросу о производстве полупроводникового кремния: анализ отходов и варианты их переработки // Проблемы проектирования и производства радиоэлектронных средств: Материалы II Международной научно-технической конференции. – Новополоцк: ПГУ, 2002. – Т.1. – С.45-50.